

**BIOTRANSFORMATIONS EMPLOYING NITRILE  
HYDROLYSING ENZYMES TOWARDS THE  
ENANTIOSELECTIVE SYNTHESIS OF  $\beta$ -AMINO ACIDS**

Being a thesis submitted for the degree of

DOCTOR OF PHILOSOPHY

in

Chemistry

To Waterford Institute of Technology

By

**Tatenda M. Mareya**



Based on research carried out under the supervision of

Dr. Claire M Lennon Ph.D,

And

Dr. Lee V Coffey Ph.D,

Dr. Michael Kinsella Ph.D.

Department of Chemical and Life Sciences,  
Waterford Institute of Technology.

Waterford, Ireland.

July 2020

## **DECLARATION**

I hereby certify that this material is entirely my own work and has not been taken from the work of others, save and to the extent that such work has been cited and acknowledged within the text. It is based on research carried out within the department of Chemical and Life Science at Waterford Institute of Technology.

Signed: \_\_\_\_\_

Date: \_\_\_\_\_

## ACKNOWLEDGEMENTS

Firstly, I would like to express my appreciation to my supervisors, Dr Claire Lennon, Dr Mike Kinsella, and Dr Lee Coffey. Thank you all for your support and guidance throughout my time in this project. I am grateful for the opportunity I have been fortunate to have.

This research was funded by the WIT PhD Scholarship scheme, and I am sincerely grateful to WIT for granting me this opportunity that would have otherwise been out of my reach. All the staff in WIT have proven invaluable: from the supportive team in the RSU; the technicians in both chemistry and biology who were always ready to come to my rescue; cleaning staff who, with a smile, were willing to work around me when I was in at odd hours; and finally my superhero porters who would open up on Saturdays for me in the long summers and made sure I didn't get locked in late at night!

My fellow Postgrads and Postdocs in the PMBRC and department, past and present, you have helped to make this PhD journey easier. Thank you for all the laughs and memories, and to my international crew, thank you for all the meals shared. Triona, you were amazing taking me under your wing. Whilst I am a long way from being a fully-fledged microbiologist, all your training and assistance, along with Lee's incredible patience and hands-on approach truly helped make me confident in that B19 lab.

To my church family in Maranatha, your support has been incredible. Special thanks to the Worship Team and all those who knew to give me a hug at just the right time. Epaphrases, only eternity will tell what you have meant to me. I love you ladies.

Sy, I can't imagine my life now without you. You didn't let me give up, thank you. It's been challenging for both of us, especially as we prepare to become three, and I'm so grateful for your love and support. Here's to the rest of lives together – college free.

Finally, to my family, thank you for your patience, even when you didn't quite understand what was going on. Thank you for your prayers and check-ins. I dedicate this thesis to you Mom and Dad, this was for you. Your last baby is finally done with school. I hope I've made you proud.

## ABSTRACT

Nitrile hydrolysing enzymes continue to be of great interest particularly for their pharmaceutical applications. This work set out to utilise novel bacterial isolates containing nitrile-metabolising enzyme systems in the synthesis of a series of chiral  $\beta$ -amino acids and amines with key goals to achieve high enantioselectivity and reaction efficiency. Biocatalysis offers many advantages as an alternative to traditional chemical synthetic methods employed in the production of fine chemicals such as pharmaceuticals with improved productivity, higher yields, shortened synthetic sequences, and reduced costs. In addition, the use of biocatalysts in synthesis adheres to many of the “green chemistry principles” which have become core values of pharmaceutical production.

Initial work focussed on further assessing the functional group tolerance and mechanistic action of bacterial isolate SET1 with a view to the production of  $\beta$ -amino acids. A series of model  $\beta$ -aminonitriles, structurally related to the  $\beta$ -hydroxynitriles previously studied were synthesised and evaluated. Whilst the synthesis of the aliphatic unprotected nitrile, 3-aminobutyronitrile, was unsuccessful and led to its purchase, the remaining seven nitriles were successfully synthesised. The corresponding acid and amide standards were also synthesised. Additionally, work was carried out to develop analytical methods to assess yield and purity of the reaction products. Some of this work entailed derivatisation of the products to allow for successful analysis.

Bacterial isolate SET1 unfortunately has shown to be disappointingly poor at selectively hydrolysing the unprotected  $\beta$ -amino nitriles, 3-aminobutyronitrile and 3-amino-3-phenylpropionitrile. The acid yields were extremely low, with the highest being <1% at pH 7 and steadily decreased as pH increased. The ee results again were very low, with the highest ee being 29% at pH 7 and this steeply dropped again as pH increased, and by pH 9 the ee was 5%. Studies on protected variants of 3-aminobutyronitrile gave more promising results, in particular with the *N*-Benzyl group which gave the overall best result of acid product with 75% ee and 6% yield.

Screening was carried out on five bacterial isolates from the PMBRC bank to identify possible other isolates to work with. They were screened on 3-aminobutyronitrile and 3-phenyl-3-propionitrile at pH 7 and 9. The best results were seen from bacterial isolates 6 and 39. Both isolates 6 and 39 gave excellent ee's of 99% at pH 9 and ee's of 89% and 87% respectively at



pH 7. For 3-phenyl-3-propionitrile, isolate 39 was the only one to show activity giving an ee of >99% at pH 7 with no activity at pH 9. Bacterial isolate 39 was thus selected for further investigations and to screen it against the *N*-protected amino nitriles.

Contamination was unfortunately discovered with isolates 6 and 39, and this placed on hold further work with these isolates. A novel nitrilase enzyme Nit1, was then acquired from the PMBRC isolate bank. Nit1 showed improved results with 3-ABN from the initial screen with 76% yield and 24 % (*S*) ee being observed. As for the *N*-protected variants, it only showed activity with the benzyl aliphatic nitrile. It encouragingly achieved ee's of 43% (*S*) at pH 7 and 4% (*S*) at pH 9 for this substrate. Some issues were experienced however with the presence of solvent and buffer from the biotransformations, possibly interfering with the HPLC results and extensive method development had to be carried. More robust HPLC methods were successfully developed which allowed for high throughput screening and would enable future work to be carried out with Nit1 more efficiently.

## ABBREVIATIONS

Ar	Aryl
Bn	Benzyl
<i>t</i> -Bu	<i>tert</i> -Butyl
Cbz	<i>N</i> -carbobenzyloxysuccinimide
DEPT	Distortionless Enhancement by Polarization Transfer
DMAP	4-Dimethylaminopyridine
ee	Enantiomeric excess
ESI	Electrospray ionisation
EtOAc	Ethyl acetate
GITC	2,3,4,6-Tetra-O-acetyl- $\beta$ -D-glucopyranosyl Isothiocyanate
Hex	Hexane
HPLC	High-Performance Liquid Chromatography
IPA	Isopropanol
LC-MS	Liquid Chromatography – Mass Spectroscopy
Me	Methyl
NMR	Nuclear Magnetic Resonance
Ph	Phenyl
rt	Room temperature
TFA	Trifluoroacetic acid
THF	Tetrahydrofuran
TLC	Thin Layer Chromatography
TMS	Trimethylsilyl
Ts	<i>p</i> -Tolylsulfonyl

# CONTENTS

DECLARATION .....	2
ACKNOWLEDGEMENTS .....	3
ABSTRACT.....	4
ABBREVIATIONS .....	6
CHAPTER 1	
LITERATURE REVIEW .....	1
1.1 Introduction.....	1
1.2 Methodology for the synthesis of single enantiomers .....	2
1.3 Enzymes in synthesis: structure and application .....	6
1.4 Nitrile Hydrolysing Enzymes .....	11
1.4.1 Nitrile hydratases .....	12
1.4.2 Amidases.....	21
1.4.3 Nitrilases .....	25
1.4.4 Nitrilase catalysed synthesis of single enantiomer $\beta$ -amino acids.....	33
1.5 Conclusion .....	39
REFERENCES .....	40
CHAPTER 2	
SUBSTRATE SYNTHESIS & HPLC METHOD DEVELOPMENT .....	46
2.1 Synthesis of Substrates .....	47
2.1.1 Background.....	47
2.1.2 Synthesis of the aliphatic $\beta$ -amino nitriles.....	48
2.1.3 Synthesis of the aromatic $\beta$ -amino nitriles.....	54
2.2 Synthesis of Racemic and Single Enantiomer Acid and Amide Standards and Derivatisation of Nitriles.....	65
2.2.1 Standards for compound <b>124</b> .....	66
2.2.2 Standards for compound <b>125</b> .....	72
2.2.3 Standards for compound <b>126</b> .....	75
2.2.4 Standards for compound <b>127</b> .....	77
2.2.5 Standards for compound <b>122</b> .....	81
2.2.6 Standards for compound <b>128</b> .....	82
2.2.7 Standards for compound <b>129</b> .....	84

2.2.8 Standards for compound <b>45</b> .....	86
2.3 Summary of Chapter 2 .....	88
REFERENCES .....	91
CHAPTER 3	
SCREENING OF ISOLATES SET1, 6, & 39 WITH $\beta$ -AMINONITRILES.....	94
3.1 Enantioselectivity Screening of SET1 with 3-aminobutyronitrile.....	95
3.1.1 Background.....	95
3.1.2 Initial screening studies.....	98
3.1.3 Additional studies to improve acid yield .....	107
3.1.4 Induction Investigations for Isolate SET1 .....	113
3.1.5 Summary from enantioselectivity screening of SET1 with 3-aminobutyronitrile ( <b>124</b> ).....	114
3.2 Enantioselectivity Screening of SET1 with the <i>N</i> -protected nitriles .....	114
3.2.1 SET1 and compound <b>125</b> .....	114
3.2.2 SET1 and compound <b>126</b> .....	116
3.2.3 SET1 and compound <b>127</b> .....	118
3.2.4 Summary from SET1 and <i>N</i> -protected nitriles .....	120
3.3 Enantioselectivity Screening of SET1 with Aromatic $\beta$ -Amino Nitriles .....	122
3.4 Enantioselectivity Screening of Additional Isolates .....	124
3.4.1 Additional studies using Isolates 6 and 39.....	126
3.5 Summary for Chapter 3.....	130
REFERENCES .....	131
CHAPTER 4	
ISOLATES PURIFICATION & ANALYSIS .....	135
4.1 Selection and Enantioselectivity Screening of Additional Isolates .....	136
4.2.2 Phase 2: Culturing.....	138
4.2 Purification Protocol .....	138
4.2.1 Phase 1: Streaking.....	138
4.2.3 Phase 3: Activity screening.....	142
4.2.4 Phase 4: Identification.....	142
4.3 Final Results of Purification .....	144
REFERENCES .....	148

## CHAPTER 5

### EVALUATION OF PURIFIED ENZYME NIT1 WITH AMINONITRILE SUBSTRATES

.....	150
5.1 Background.....	151
5.2 Activity Check for Nit1 .....	154
5.3 Screening of Nit1 with 3-aminobutyronitrile ( <b>124</b> ).....	157
5.3.1 Optimisation of GITC derivatisation for quantitation .....	157
5.3.2 Initial Screening of 3-aminobutyronitrile ( <b>124</b> ).....	161
5.3.3 Time Study.....	164
5.3.4 Solvent effects and analytical variation and substrate/product recovery .....	167
5.3.5 Troubleshooting of HPLC analytical method .....	173
5.3.6 Optimisation of Nit1 Concentration.....	176
5.3.7 pH 9 investigation .....	177
5.4 Screening of <i>N</i> -protected nitriles .....	178
5.5 Summary .....	181
REFERENCES .....	182

## CHAPTER 6

### CONCLUSIONS & FUTURE WORK.....

6.1. Conclusions.....	185
6.2. Future Work.....	187
REFERENCES .....	190

## CHAPTER 7

### EXPERIMENTAL.....

7.1 General Experimental Conditions.....	193
7.2 Screening of Bacterial Isolates.....	194
7.3 Media and Buffer Preparation.....	194
7.3.1 M9-Minimal media preparation .....	194
7.3.2 Potassium phosphate buffer preparation .....	195
7.4 Optical Density of Isolates.....	195
7.5 Induction of Cells.....	196
7.6 Preparation of Nitriles.....	196
7.7 Preparation of Racemic and Single Enantiomer Standards for Chiral HPLC Method Development.....	202

7.7.1	GITC Derivatisations .....	211
7.8	HPLC Analysis of $\beta$ -aminonitrile Substrates and Products .....	215
7.9	Screening of SET1 Towards 3-aminobutyronitrile hydrochloride ( <b>124</b> ).....	217
7.9.1	Initial enantioselectivity screening studies .....	217
7.9.2	Larger-scale biotransformations .....	217
7.9.3	Enantioselectivity screening of other bacterial isolates towards 3-aminobutyronitrile hydrochloride ( <b>124</b> ) .....	218
7.9.4	Standard curves .....	219
7.10	Biotransformations of <i>N</i> -Benzyl Protected Nitriles with SET1 – General Procedure .....	221
7.11	Biotransformations on <i>N</i> -Tosyl and <i>N</i> -Boc Protected Nitriles .....	221
7.12	Purification and Identification of Contaminated Isolates .....	222
7.12.1	Agar plates preparation and cell culture .....	222
7.12.2	Procedure for PCR .....	223
7.12.3	Procedure for electrophoresis .....	223
7.12.4	Procedure for sequencing .....	224
7.13	Screening of The Purified Enzyme Nit1 with Unprotected and <i>N</i> -Protected Nitriles.....	224
7.13.1	Nessler’s microscale ammonia assay for determination of Nit1 activity .....	224
7.13.2	Standard curve for Nessler’s colorimetric assay for HPAN activity determination .....	225
7.13.3	Procedure for Nit1 screening with nitriles .....	225
REFERENCES	.....	229
APPENDIX I		
	HPLC chromatograms of synthesised $\beta$ -aminonitrile substrates and products .....	231
	$^1\text{H}$ and $^{13}\text{C}$ NMR spectra.....	240
APPENDIX II		
	Publications.....	278



# **CHAPTER 1**

## **LITERATURE REVIEW**



## LITERATURE REVIEW

### 1.1 Introduction

Since the release of “Silent Spring” by Rachel Carson in 1962, a controversial book seeking to alert the public at the time of the extensive use of pesticides and herbicides<sup>1</sup>, the importance of green chemistry and the development thereof have rapidly increased. Ultimately this resulted in the formation of the 12 principles of Green Chemistry by Anastas and Warner shown in Table 1.1<sup>2</sup>.

**Table 1.1: The 12 principles of Green Chemistry**

	<b>Principle</b>
1.	Prevention
2.	Atom Economy
3.	Less Hazardous Chemical Synthesis
4.	Designing Safer Chemicals
5.	Safer Solvents and Auxiliaries
6.	Design for Energy Efficiency
7.	Use of Renewable Feedstocks
8.	Reduce Derivatives
9.	Catalysis
10.	Design for Degradation
11.	Real-time Analysis for Pollution Prevention
12.	Inherently Safer Chemistry for Accident Prevention

Many processes and methods are constantly being evaluated to try to fulfil these principles. For pharmaceutical drug development, ten of the principles can be fulfilled by employing biocatalysis. The only exceptions are principles 4 and 10 which relate to the products formed<sup>3</sup>. Biocatalysis has thus quickly risen to the forefront over the years for the pharmaceutical industry.

Biocatalysis uses enzymes in their whole cell or isolated form to catalyse a reaction. Particularly in the case of whole cell isolates, less harsh conditions often must be used, such as close to neutral pH, mostly ambient temperature, and water-based solvents are necessary to maintain the cell culture. It should be noted that extremophiles can be utilised however to carry out reactions requiring beyond ambient conditions. The work described in this thesis lies in the

investigation of both whole cell and isolated enzyme biocatalytic processes for the synthesis of pharmaceutically relevant amino acids.

The focus of Chapter 2 of this Thesis describes the synthesis of the amino nitrile substrates required for investigation in this work. It will also describe the synthesis of the corresponding acid and amide standards, and HPLC method development for analysis of biocatalytic mixtures and product characterisation.

In Chapter 3, the substrate scope of *Rhodococcus Erythropolis* SET1 is examined, utilising the synthesised  $\beta$ -amino nitriles presented in Chapter 2. Screening to identify other possible bacterial isolates suitable for transforming the substrates and the findings thereof are also discussed.

It became necessary during the work to carry out purification techniques on some of the bacterial isolates. Descriptions of the work involved, and the required subsequent analysis to confirm activity and purity is discussed in Chapter 4.

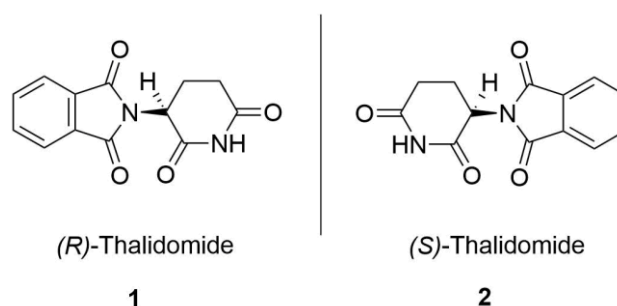
In Chapter 5, substrate screening of a newly isolated nitrile metabolising enzyme NIT1 made available through the Pharmaceutical and Molecular Biotechnology Research Centre at WIT is reported along with associated high throughput method development.

This review Chapter will present a brief history and background of biocatalysis in the pharmaceutical industry, showcasing its importance. The specific class of enzymes utilised in this project, namely nitrile hydrolysing enzymes will be presented and current advances with these enzymes will be detailed thus highlighting the relevance of the research of this thesis outlined in the further chapters.

## 1.2 Methodology for the synthesis of single enantiomers

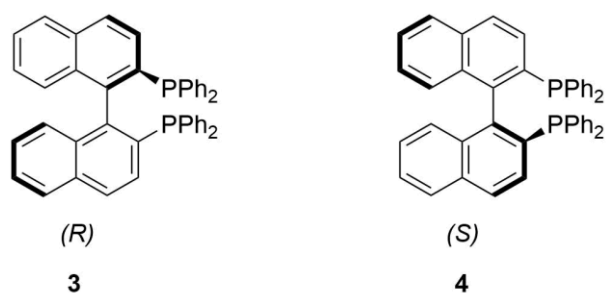
The use of biocatalysis as a synthetic methodology as mentioned above offers significant advantages in the production of pharmaceuticals and has since been applied to many industrial applications, for example, lipases, proteases, and esterases, for selective hydrolysis and esterification/transesterification<sup>4-9</sup>. The first example of the use of biocatalysis in industry was in the production of acetic acid from ethanol employing the use of the *Acetobacter* strain, which was immobilised on wood shavings<sup>10</sup>.

Of significant relevance to the pharmaceutical industry is the ability of biocatalysis to allow for the isolation of single enantiomers of chiral products. This is extremely important as it is common for the two enantiomeric forms of a chiral compound to have different pharmacological profiles and toxicities<sup>11,12</sup>. The FDA thus generally requires that in a case where a drug has a chiral centre, the stereoisomeric composition needs to be known<sup>13</sup>. The release of Thalidomide for example, as a racemate resulted in toxic side effects (see Figure 1.1). It was originally marketed as a morning sickness drug however the (*S*)-Thalidomide form (**2**) led to numerous birth defects.



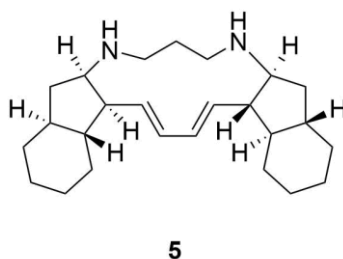
**Figure 1.1: The two enantiomers of Thalidomide. (*R*)-Thalidomide is the therapeutic form, marketed initially to treat morning sickness. (*S*)-Thalidomide however, exhibits teratogenic effects.**

Traditional chemical synthetic methods without a chiral influence always produce racemic mixtures of enantiomers. Stereoselective synthesis of APIs is thus of great importance and can be achieved with synthetic catalysts or biocatalysts<sup>3,14,15</sup>. Some synthetic catalysts are either transition metal catalysts or organocatalysts. Transition metal catalysts employ a chiral ligand along with a transition metal (TM) to influence reaction selectivity. Metals such as Ru, Rh and Pd can act as coordination sites for substrates. By using ligands which are chiral and single enantiomers the catalysis can be enantioselective by influencing the substrate approach to the TM-ligand complex and subsequently the transition state during the reaction. A class of transition metal catalysts that has experienced success in the area of catalytic asymmetric synthesis are those developed by Noyori which are involved in chiral hydrogenation reactions. The most famous ligand developed by Noyori is BINAP a chelating diphosphine shown in Figure 1.2, and when used in catalysis the metal sits between the two phosphorous atoms in the chiral environment.



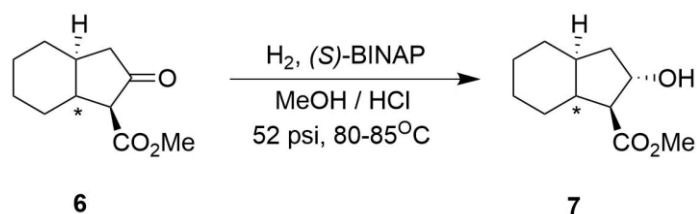
**Figure 1.2: Structure of BINAP**

It is notable that BINAP is an atropisomer and has no chiral centres and its chirality arises from the fact that the bond between the two naphthalene cannot rotate. One example in particular in which this type of catalyst is applied is in the synthesis of (-)-Haliclونadamine, an alkaloid which exhibits antibiotic and antifungal properties from the marine sponge *Haliclona* sp., the structure of which is shown in Figure 1.3<sup>16,17</sup>.



**Figure 1.3: Structure of (-)-Haliclونadamine**

Taber *et al* were the first to report the stereocontrolled synthesis of (-)-Haliclونadamine with 43% yield<sup>18</sup>. The use of a Ru-BINAP hydrogenation was employed to selectively hydrogenate a racemic  $\beta$ -keto ester to an enantiomerically pure  $\beta$ -hydroxy ester (7), as shown in Scheme 1.1, which was subsequently converted to (-)-Haliclونadamine *via* a series of steps.



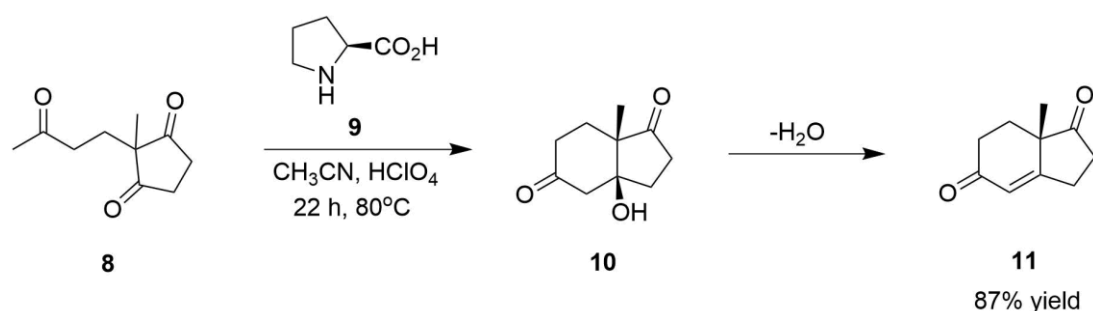
**Scheme 1.1: Hydrogenation of the  $\beta$ -keto ester using RuCl<sub>2</sub>-BINAP<sup>18</sup>**

In optimising the addition of HCl to the reaction, 100% ee of the desired enantiomer was achieved<sup>18</sup>. This was a critical step in the total synthesis which allowed the pentacyclic alkaloid to be achieved.

Some further examples of the applications of Noyori's system are in the synthesis of (-)-Roxaticin, a polyene macrolide with antibiotic activity, Pestalotioprolide C, a macrolide

with cytotoxic activity on the murine lymphoma cell line L5178Y, and most recently the synthesis of 5,7,8-trioxygenated-3-benzylchroman-4-ones which are homoflavonoids with pharmacological applications<sup>19-22</sup>. It is notable that Noyori shared the Nobel prize for his work on catalytic asymmetric hydrogenation in 2001 with Knowles and Sharpless. Transition metal catalysts can be highly effective however, the reactions tend to be overall relatively expensive to run, often require inert atmosphere, difficult to recycle the catalyst and can generate toxic by-products.

Organocatalysts on the other hand, small organic metal-free catalysts are less expensive and less toxic in comparison to transition metal catalysts and they are also less sensitive to moisture and oxygen<sup>23</sup>. The key discovery in the development organocatalysis was the proline-catalysed intramolecular aldol reaction that was reported simultaneously by Eder *et al* during the early 1970's<sup>24</sup>. Since then, the development and use of proline and its derivatives in the synthesis of pharmaceuticals has been significant. Scheme 1.2 illustrates the application of proline (compound **9**) by Eder *et al* in the synthesis of compound **11** which is an example of an essential starting compound in the synthesis of steroids<sup>24</sup>.



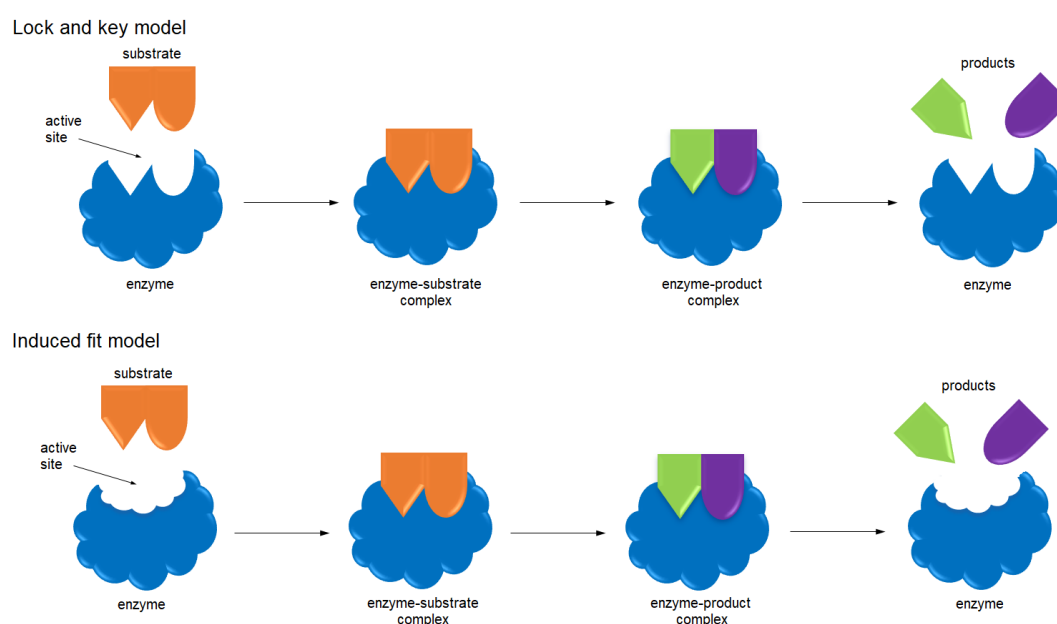
**Scheme 1.2: Application of (S)-proline in the synthesis of (S)-7a-Methyl-2,3,7,7a-tetrahydro-1H-indene-1,5-(6H)-dione**<sup>24</sup>

Central to the success of proline and its derivatives in reactions such as aldol transformations is thought to be hydrogen bonding between the catalyst and the carbonyl electrophile which both activates and introduces spatial effects to influence the enantioselectivity of the reaction.

The application of enzymes to influence reactions will be presented in the following section.

### 1.3 Enzymes in synthesis: structure and application

Enzymes are naturally occurring catalysts that regulate the rate of chemical reactions in cells without being altered. The majority are made of protein sub-units, but few are comprised of RNA molecules, such as ribozymes<sup>25-28</sup>. Some will also have a non-protein unit attached which is referred to as a cofactor which aids in the reaction being undertaken. Within an enzyme is an active site which consists of a binding site and a catalytic site. Initially it was thought the active site functioned with a lock and key mechanism proposed by Emil Fischer but later Koshland proposed that the mechanism occurred alternatively *via* an induced fit theory and hence developed the induced fit theory<sup>29-31</sup>. The lock and key mechanism proposes that only a precisely sized key (the substrate) will exactly fit into the key hole (active site) of the specific lock (the enzyme). The Induced fit theory on the other hand suggests that a specific substrate induces a change in the protein structure of the enzyme as the 3-dimensional relationship of the amino acids in the active site adjust to fit the substrate, as illustrated in Figure 1.4<sup>29</sup>.



**Figure 1.4: Comparison of the lock and key model to the induced fit model**

There are six main classes of enzymes according to the International Union of Biochemistry and Molecular Biology<sup>32</sup>. These are shown in Table 1.2 and classified according to the reaction which they influence.

**Table 1.2: Classification of enzymes**

<b>Classification</b>	<b>Reaction</b>
1. Oxidoreductases	Redox reaction
2. Transferases	Transfer of a group from one substrate to another
3. Hydrolases	Hydrolytic cleavage
4. Lyases	Cleavage of bonds not by hydrolysis or oxidation
5. Isomerases	Geometric or structural change
6. Ligases	Joining two molecules

Whole cells have long been the traditional format of biocatalysts. They allow the enzymes to be in their native environment, giving them physical protection. This is also one of the more affordable options as whole cells are relatively easily grown and stored. Having mentioned the relative ease of growing whole cells biocatalysts, the growth process however, can often give way to long lead times. There is also a need to constantly replenish the cells in some cases thus creating a fermentation process which again, increases the length of time in the workflow and begins to increase the costs. There is also the possibility of observing variations in yield and selectivities as other enzyme pathways within the cell may potentially interfere with each other. Of late, recombinant whole-cell biocatalysts are growing in application to combat this<sup>33</sup>. An example of this is a lipase isolated from bacterium K107 of *Proteus* sp. from soil samples in China. This was cloned and expressed in *Escherichia coli* BL21 (DE3) and used in the production of biodiesel<sup>34</sup>.

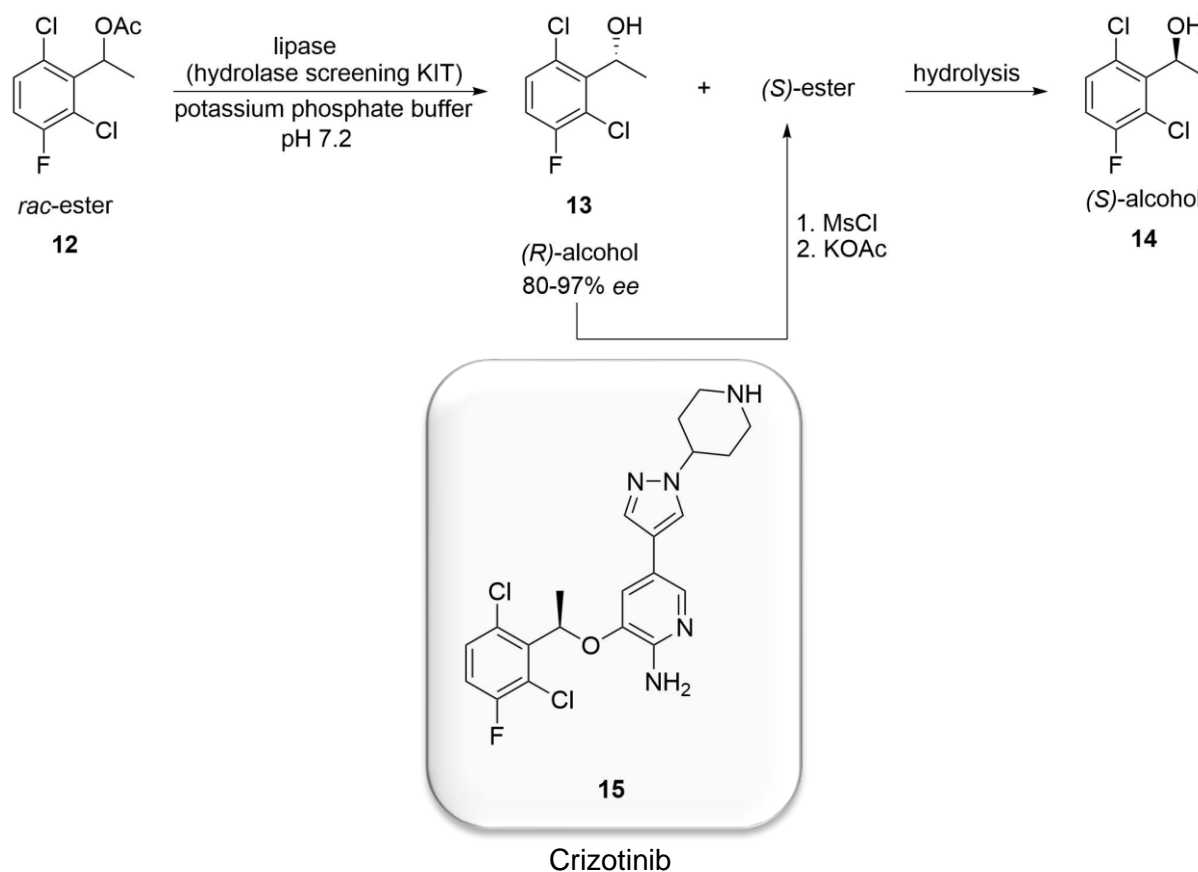
An alternative to whole cell biocatalysts is to isolate the enzymes such that the purified enzyme may be utilised without the additional enzymes which may be present in the cell. There is an option also to immobilise the enzyme on a natural or synthetic polymer, or on an inorganic material such as zeolites or ceramics. This is so that they are handled in a solid form or for them to be in an inactive cell thus still simulating a whole cell scenario. The main methods of immobilisation are adsorption or cross-linkage to the support particle, and encapsulation. Utilising immobilised enzymes allows for a reduction in production costs, increased stability of the enzyme, and it allows for easier re-usage of the enzyme<sup>35</sup>. The choice in method of immobilisation, however, exposes the weaknesses with immobilised enzymes. Enzymes which are adsorbed on the particle surface can easily be leached and are also prone to degradation<sup>35</sup>. Cross-linked enzymes have greater stability but may exhibit lower enzyme activity as the degree of freedom is limited for the active site. Encapsulated enzymes face a similar dilemma

to cross-linked enzymes in that enzyme activity is decreased as the polymer used for encapsulation can hinder the amount of substrate that reaches the enzyme.

The most important aspect of enzymes relevant to the synthesis of pharmaceuticals is their ability to act on one enantiomer of a racemic mixture and thus produce a specific single enantiomer product. This ability to be selective due to exact chiral recognition in the enzyme is referred to as enantioselectivity and can be quantified and expressed as enantiomeric excess (ee)<sup>36</sup>. The ability to produce only a specific enantiomer product from a racemic substrate, however, is referred to as enantiospecificity<sup>37</sup>. Where an enzyme can work on both enantiomers of the substrate, kinetic resolution may become a factor. This is where one enantiomer has a faster rate of reaction than the other<sup>38</sup>. The influence of these different properties; enantioselectivity, enantiospecificity, and kinetic resolution, can all affect the successful outcome of a biotransformation.

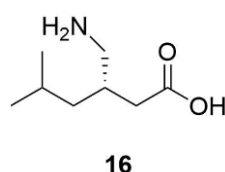
An example demonstrating the enantioselective synthetic utility of lipase enzymes is the synthesis of an intermediate of Crizotinib, an antitumor drug, (*S*)-1-(2,6-dichloro-3-fluorophenyl)ethanol, which is prepared by the highly enantioselective hydrolysis of an ester precursor using a lipase as shown in Scheme 1.3<sup>5,39,40</sup>. The lipases screened for this work were *Candida antarctica* lipase B (CAL-B), Pig liver esterase, *Rhizopus delemar* lipase, Porcine kidney acylase, cholesterol esterase, Bovine intestinal protease, sigma protease P6 type VIII, and *Candida rugosa* lipase in purified or isolated form. The pig liver esterase gave the best rate of reaction and was used for this work. This enzyme is also known to be selective for similar type substrates that have an (*R*)-configuration<sup>41</sup>. The (*R*)-alcohol was achieved in 97.0% ee with 51% conversion and the (*S*)-ester was achieved with 97.5% ee. The final (*S*)-alcohol was achieved in 87% yield with 99% ee<sup>39</sup>.





**Scheme 1.3:** Synthesis of (*S*)-1-(2,6-dichloro-3-fluorophenyl)ethanol, the intermediate to Crizotinib using a lipase enzyme in potassium phosphate buffer at pH 7.2. The (*R*)-alcohol and (*S*)-ester were separated by silica gel chromatography and reacted to give an (*S*)-acetate. This (*S*)-acetate was hydrolysed with lithium methoxide in methanol to give the (*S*)-alcohol<sup>5</sup>

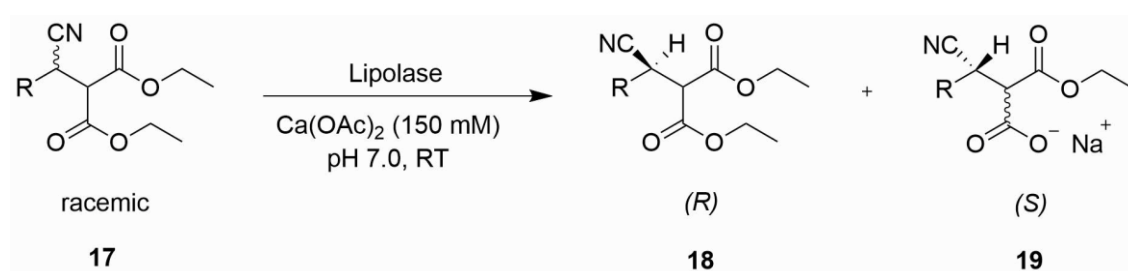
Another example of the application of enzymes in the synthesis of single enantiomers is in the synthesis of Pregablin shown in Figure 1.5, the active ingredient in Lyrica, which is an anticonvulsant and is also used to treat anxiety symptoms<sup>5,42</sup>. It is a  $\beta$ -substituted  $\gamma$ -amino acid and its synthesis includes the enzymatic resolution of a  $\beta$ -cyanodiester with a lipase<sup>43</sup>.



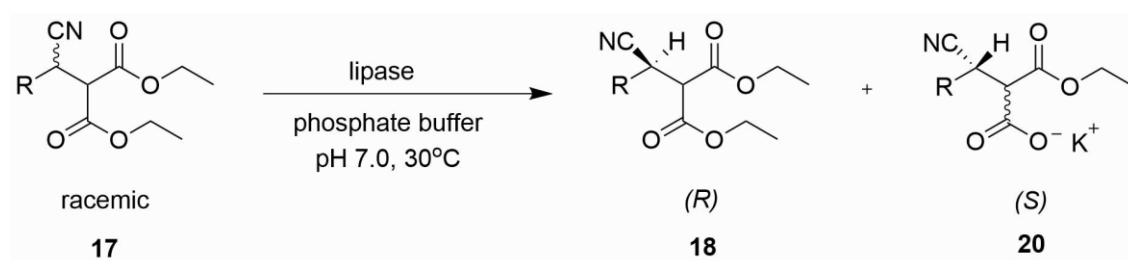
**Figure 1.5:** Structure of (*S*)-Pregablin

Martinez *et al* screened several enzymes and discovered that Lipolase from *Thermomyces lanuginosus* had the best activity and enantioselectivity<sup>44</sup>. This was thus chosen to carry out the reaction, shown in Scheme 1.4. The reaction was carried out in calcium acetate at pH 7.0 at room temperature. The (*S*)-product was acquired with >98% ee and 45-50% conversion. This

work was further investigated by Mukherjee *et al* who found that in their case *Mucor miehei* lipase (Palatase 20000 L) and *Rhizopus delemar* lipase (Lipase D “Amano”) were the best enzymes and their optimised reaction was conducted at 30°C in phosphate buffer at pH 7.0 shown in Scheme 1.5<sup>45</sup>. For their work, the (*S*)-product was achieved with 84.8% ee and >99% ee for Lipase D “Amano” and Palatase 20000 L respectively, with both having a 52% conversion.

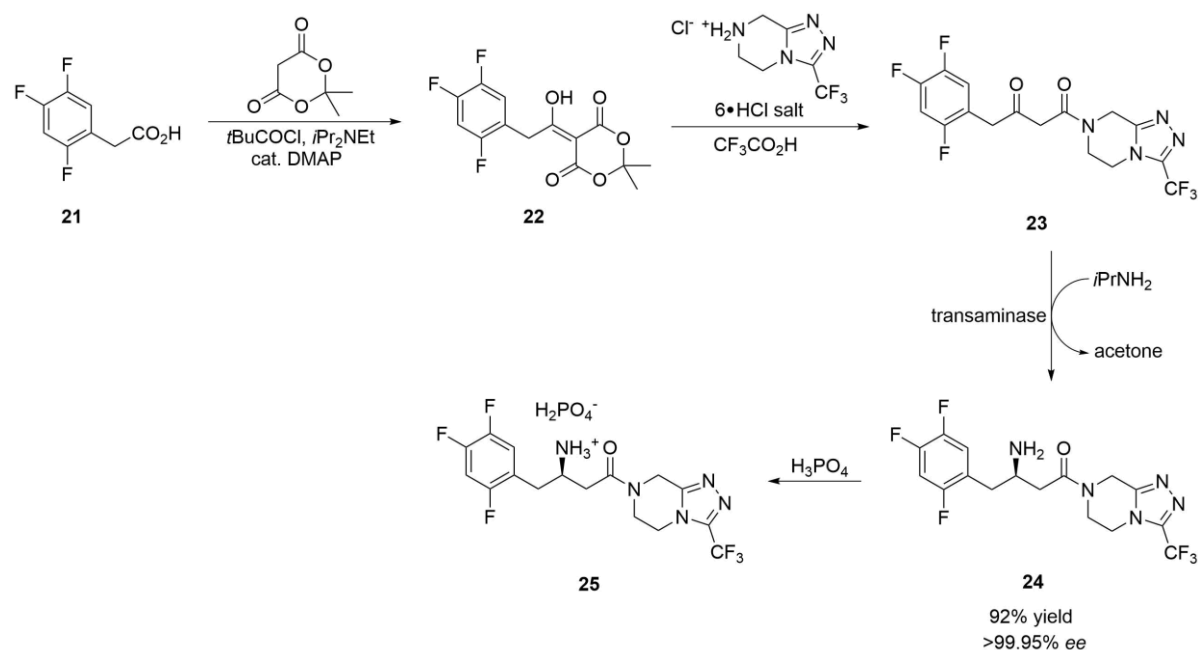


**Scheme 1.4:** The enzymatic resolution of the  $\beta$ -cyanodiester by Martinez *et al*<sup>44</sup>



**Scheme 1.5:** The enzymatic resolution of the  $\beta$ -cyanodiester by Mukherjee *et al*<sup>45</sup>

It is also possible for enzymes to generate a single enantiomer from a prochiral substrate. In this case the enzyme will be selective to generate only one enantiomer of the specific product during the chiral centre bond-forming reaction. An example of this is in the synthesis of Sitagliptin. Sitagliptin has shown great success as the API in Januvia®, a once-daily tablet for Type 2 diabetes marketed by Merck & Co<sup>46,47</sup>. In the place of using transition metal catalysts during synthesis, as earlier synthetic routes required, a highly evolved transaminase was engineered and applied as illustrated in Scheme 1.6<sup>48</sup>. An (*R*)-selective transaminase underwent directed evolution and 6 g L<sup>-1</sup> was used with 200 g L<sup>-1</sup> of the substrate in DMSO (50%). The reaction was carried out at 40°C.

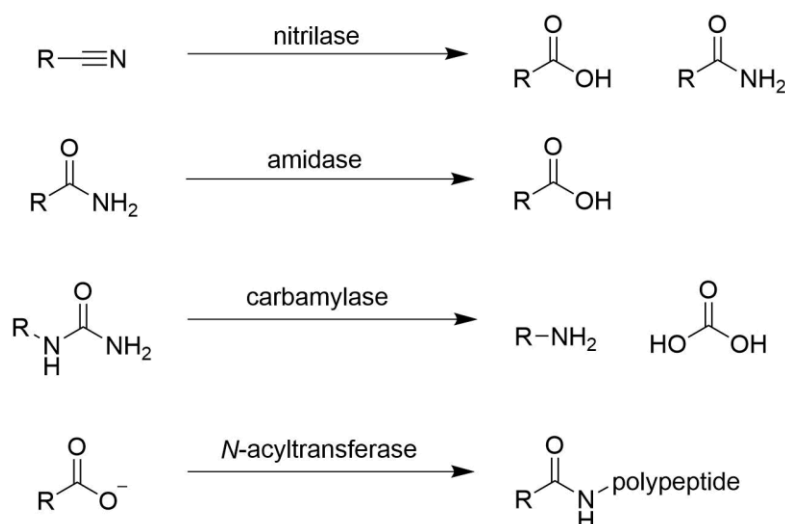


**Scheme 1.6: Synthetic route to achieve Sitagliptin phosphate<sup>48</sup>**

This route shown in Scheme 1.6 led to a 13% increase in overall yield, a 53% increase in productivity, and a 19% reduction in the total waste produced<sup>7</sup>.

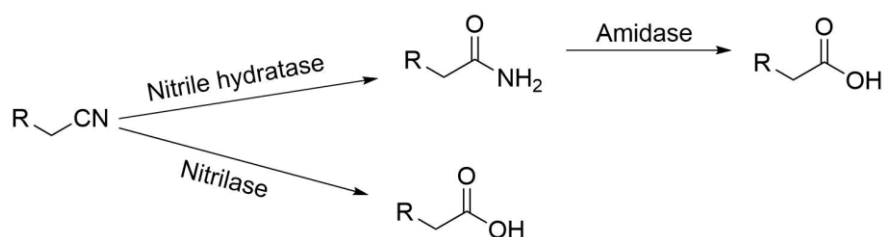
## 1.4 Nitrile Hydrolysing Enzymes

Nitriles as substrates are highly useful precursors to acid and amide and can be effectively hydrolysed to these by members of the nitrilase superfamily and nitrile hydratases. A significant advantage of using nitrile hydrolysing enzymes for synthesis in this way is the avoidance of the use of strongly acidic or basic conditions and elevated temperatures. Hence if the substrate has a labile group present this may be impacted under standard chemical synthetic methods. The nitrilase superfamily was defined by Brenner *et al* which in addition to nitrilases includes *N*-acyltransferases, carbamylases, amidases, and presumptive amidases, illustrated in Scheme 1.7.<sup>49,50</sup>



**Scheme 1.7: Nitrilase superfamily general reaction pathways<sup>49</sup>**

The superfamily consists of 13 branches, of which only Branch 1 exclusively contains enzymes which act on only nitriles. The remaining branches contain varying amidase activity. Nitrile hydratases, amidases, and nitrilases, are the most significant enzymes in nitrile metabolism, frequently employed in biocatalysis and will be focussed on for the remainder of this Section. The general pathways for nitrilases, nitrile hydratases, and amidases are shown in Scheme 1.8.

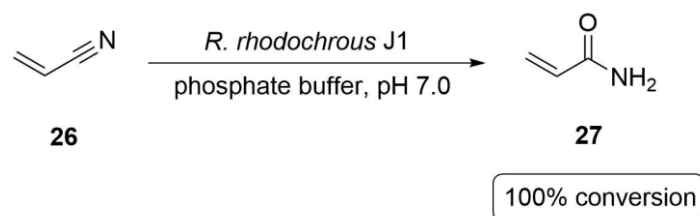


**Scheme 1.8: General pathways for enzymatic nitrile hydrolysis using nitrile hydratase/amidase and nitrilase**

### 1.4.1 Nitrile hydratases

Nitrile hydratases are metalloenzymes, containing either cobalt or iron as a cofactor at their active sites, which hydrolyse nitriles to amides only and not completely to the carboxylic acid. Nitrile hydratases (NHases) were first reported and named by Yamada *et al* utilising first *P. chlororaphis* then later *R. rhodochrous* J1 in their investigations to produce acrylamide<sup>51</sup>. In contrast to nitrilases, NHases are found solely in bacteria and in order to ensure active expression of NHase when culturing, cobalt or iron salts need to be present in the culture media. For the iron NHase, its structure is composed of serine and threonine at the third and eighth amino acid residues of the octahedral active site<sup>52</sup>. This differs from the cobalt NHase which

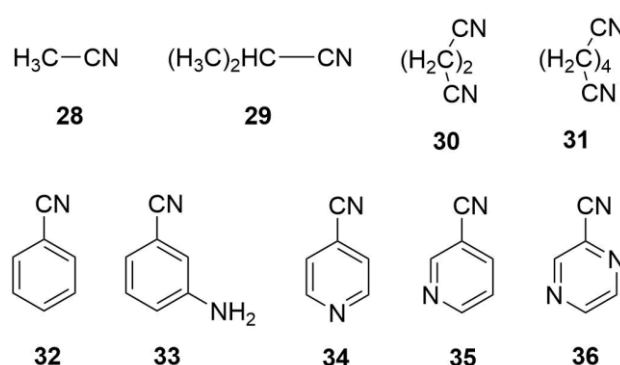
has threonine and tyrosine at the same corresponding positions. Interestingly, *Rhodococci* species can also contain a competing nitrilase as well as the NHase and amidase which can make whole cell work complex<sup>53</sup>. The first successful industrial example of the application of NHase in biocatalysis was in the synthesis of acrylamide as reported by Yamada *et al*, which is illustrated in Scheme 1.9<sup>51,54</sup>.



**Scheme 1.9: General scheme of industrial production of acrylamide using a NHase**

Another example is the production of nicotinamide which is useful for agricultural applications, as a drug intermediate, and a precursor of nicotinic acid<sup>55</sup>.

In the last decade, work has been carried out to seek optimisation of biotransformations involving NHase by immobilising the whole cells or enzymes which allows for a reusable catalyst system to be achieved<sup>56</sup>. This is desirable for industrial applications as it will be a more cost-effective approach compared to the standard protocol of conducting biotransformations. One such example is from the work of Kamble *et al* who took immobilised whole cells containing NHase for the biotransformations of the aliphatic and aromatic nitriles in Figure 1.6<sup>57</sup>. The NHase was of a cobalt-type and it was acquired from the bacterium *Rhodococcus erythropolis* MTCC 1526.

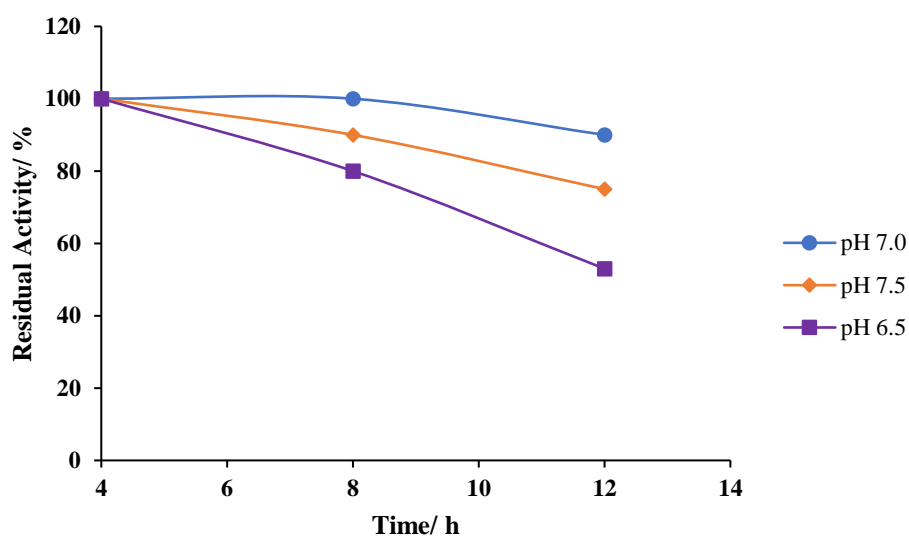


**Figure 1.6: Nitriles used for the investigation of immobilised whole cell catalysts<sup>57</sup>**

An activity assay was carried in phosphate buffer (10 mM, pH 7.0) with the nitriles (5 mM, 400  $\mu\text{L}$ ) and amide production was determined by HPLC. The enzyme purification was carried out using fast protein liquid chromatography (FPLC). Reactions were conducted at 4°C in

phosphate buffer at pH 6.8 with sodium butyrate (20 mM). The purification factor achieved was 10.8 and the total initial activity that was recovered was 18%.

The activity profile of the NHase enzyme was characterised with variations of temperature and pH. It was found that the peak activity was at 20°C and 7.0 was the optimum pH. This can be observed in the graph in Figure 1.7 produced from the study conducted with varying incubation pHs at 20°C.



**Figure 1.7: Residual activity of nitrile hydratase versus time at various values of the incubation pH, at 20°C<sup>57</sup>**

The effect of the presence of metal ions and inhibitors was also examined as well as thermostability and pH stability. Metal ions were found to enhance the activity, with Cobalt (II) giving the strongest effect. The enzyme showed the greatest thermostability at 20°C and pH stability was determined to be at 7.0. Substrate specificity was also investigated with nine substrates in phosphate buffer (20 mM, pH 7.0) at 20°C. Relative to 3-cyanopyridine, which experienced 100% conversion, good activity was observed for aromatic nitriles apart from 3-aminobenzonitrile. Better activity, however, was seen with the aliphatic nitriles except for acetonitrile. No activity was observed for the dinitriles, as shown in Table 1.3.

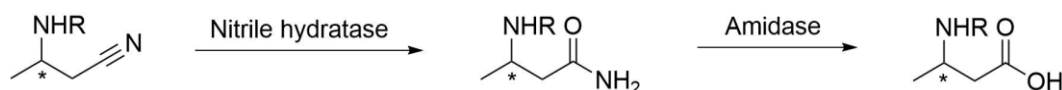
**Table 1.3: Results of substrate screening of *R. erythropolis* MTCC 1526<sup>57</sup>**

Nitrile	Relative activity/ %
<b>Aliphatic nitriles</b>	
Acetonitrile	54
Isobutyronitrile	110
<b>Aromatic nitriles</b>	
Benzonitrile	105
3-aminobenzonitrile	56
4-cyanopyridine	104
3-cyanopyridine	100
pyrazinonitrile	94
<b>Dinitriles</b>	
Succinonitrile	0
Adiponitrile	0

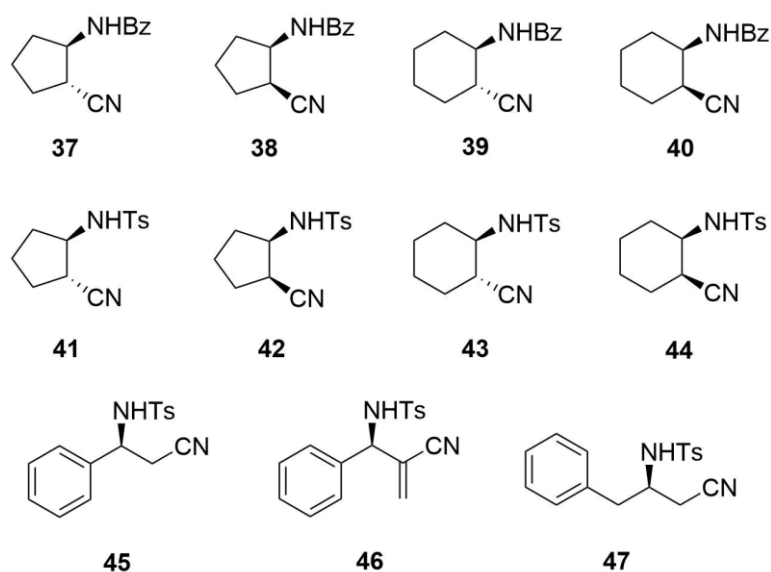
Biotransformations were carried out by incubating substrate (2 mM) in a suspension of *Rhodococcus erythropolis* in phosphate buffer (pH 7.0) at 20°C for 30 min

The cells were immobilised on sodium alginate beads and reactions were compared between those run with free whole cells and those with immobilised cells. Optimum conditions for the immobilised cells were established to be in a packed bed reactor at 25°C and a substrate flow rate of 2.5 mL h<sup>-1</sup> for benzonitrile and 4-cyanopyridine and 5 mL h<sup>-1</sup> for isobutyronitrile. Freely suspended cells gave a substrate conversion of 93% but lost activity rapidly with each cycle when tested for reusability giving a conversion of approximately 40% by the sixth cycle but the immobilised cells gave a substrate conversion initially of approximately 95% and by the sixth cycle it had only dropped to 85%.

In whole cells it is common to find NHases working with amidases and such systems were investigated by Winkler *et al* using cells from *Rhodococcus equi* A4, *Rhodococcus* sp. R312, and *Rhodococcus erythropolis* NCIMB 11540 which all contained both NHase and amidase<sup>58</sup>.

**Scheme 1.10: Conversion of nitrile to amide by nitrile hydratase, then to acid by amidase**

The synthesis of 11 nitriles, shown in Figure 1.8, for the investigations was carried out and the synthesis of 15 new compounds was also reported.



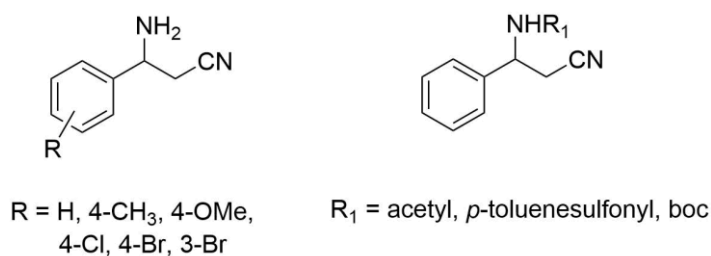
**Figure 1.8: Racemic  $\beta$ -amino nitriles synthesised for the biotransformations with only the single enantiomer depicted<sup>58</sup>**

All the strains were cultivated on BSB medium at 30°C using acetonitrile as the sole nitrogen source. Initial screening experiments were carried out in an inductive medium at 32°C which yielded less biomass but better activity. It was observed that the *trans*-nitriles were hydrolysed faster in comparison to the *cis*-nitriles. The *cis*-benzoates however, were rejected as substrates. Large scale biotransformations were carried out in phosphate buffer (pH 7.5) at 30°C for 24 h.

The five-membered alicyclic 2-amino nitriles were hydrolysed much faster than the six-membered ring. The *trans* acid and amide products were produced faster than the *cis* products. The only exception was with  $\alpha$ -methylene- $\beta$ -amino carbonitrile which exclusively gave the amide. It was interestingly observed that the enantioselectivity was dependent on the structure. For the *trans*-five-membered nitriles, the amide products gave the best enantioselectivity of 94 – 99%. This contrasts the *trans*-six-membered nitriles which showed excellent enantioselectivity for the acid instead (87 – 99%). The *cis*-nitriles unfortunately all gave poorer enantioselectivities. It is of note that the products in this study can be converted to  $\beta$ -amino acids. Such products are highly interesting and offer significant potential for use in novel pharmaceuticals .

The selective synthesis of  $\beta$ -amino amides using the cobalt NHase found in *Rhodococcus rhodochrous* ATCC BAA-870 was investigated by Chhiba *et al*<sup>59</sup>. The substrates used were various protected and unprotected 3-amino-3-phenylpropanenitriles which were synthesised and are illustrated in Figure 1.9.





**Figure 1.9: Substrates of interest for *R. rhodochrous* ATCC BAA-870<sup>59</sup>**

The cells were cultured in rich medium, TSB, before induction in a defined media with benzamide as the inducer. The biotransformations were carried out in Tris buffer (100 mM, pH 7 or 9) at 5°C or 30°C and the substrates were solubilised in 1 mL of methanol. The *N*-boc and *N*-tosyl protected nitriles showed negligible conversion. This was hypothesised as being due to the steric hindrance presented by the bulky protecting groups to the active site of the NHase. The *N*-acetyl nitrile however gave amide in 19% yield at 30°C and pH 7.0, as shown in Table 1.4.

**Table 1.4: Main results of substrate screening of *R. rhodochrous* ATCC BAA-870<sup>59</sup>**

R	R <sub>1</sub>	Conversion/ %	( <i>R</i> )-nitrile ee/ %	( <i>S</i> )-amide ee/ %
H	H	46 <sup>a</sup>	8	7
H	acetyl	ND <sup>b</sup>	ND	19
H	boc	ND <sup>b</sup>	ND	negligible <sup>c</sup>
H	tosyl	ND <sup>b</sup>	ND	negligible <sup>c</sup>
4-CH <sub>3</sub>	H	39 <sup>a</sup>	21	3
4-OMe	H	62 <sup>a</sup>	39	24
4-Cl	H	0 <sup>a</sup>	0	0
4-Br	H	55 <sup>a</sup>	32	43

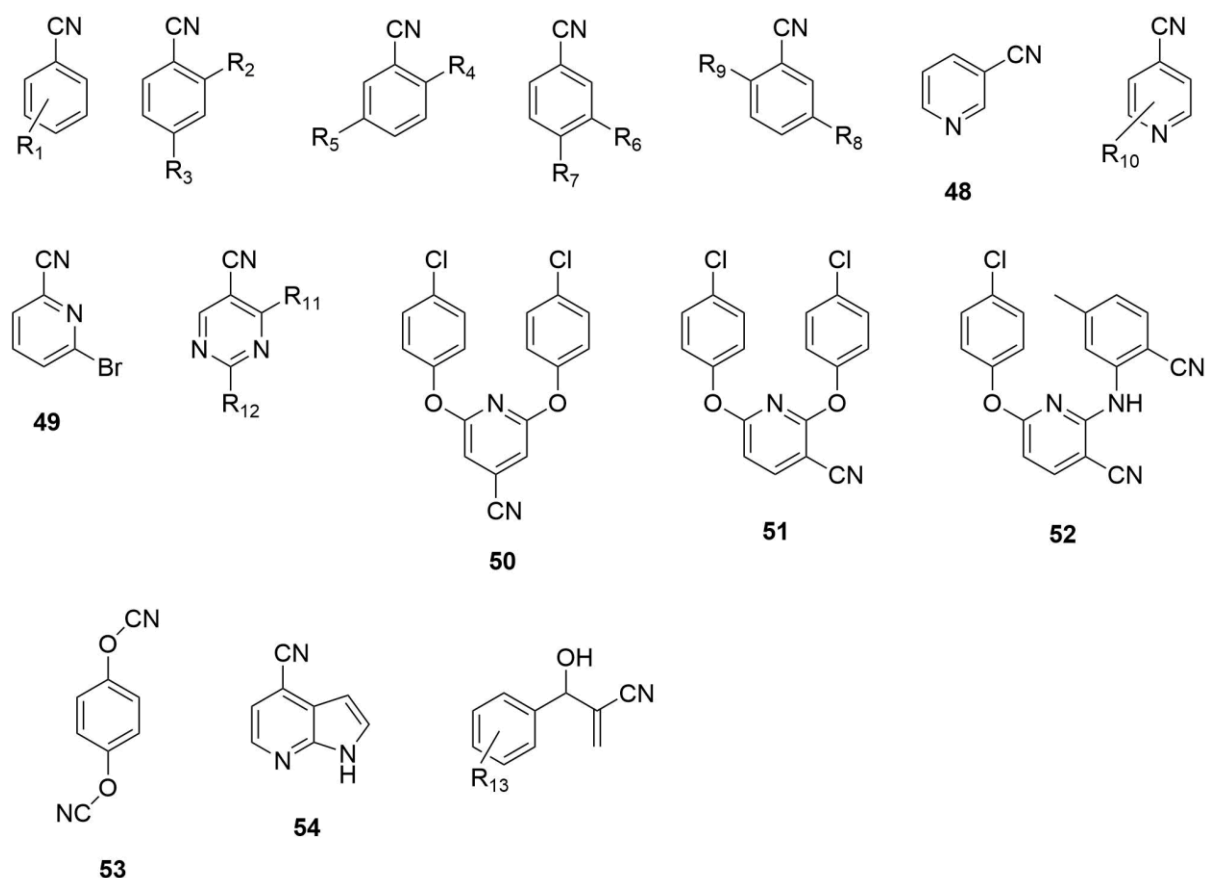
Biotransformations were carried out by incubating the nitrile in a suspension of *Rhodococcus rhodochrous* at 30°C <sup>a</sup>phosphate buffer at pH 9. <sup>b</sup>phosphate buffer at pH 7. <sup>c</sup>exact values not given. ND = Not Disclosed.

The unprotected 3-amino-3-phenylpropionitrile failed to be hydrolysed at pH 7 and so subsequent experiments for it and the aryl substituted unprotected nitriles were carried out at pH 9. The substrate, 3-amino-3-phenylpropionitrile was hydrolysed at pH 9 but with very poor enantioselectivity (7%). The aryl substituted nitriles gave similar poor enantioselectivities with the chloro-substituted nitrile being the exception, which gave no amide product.

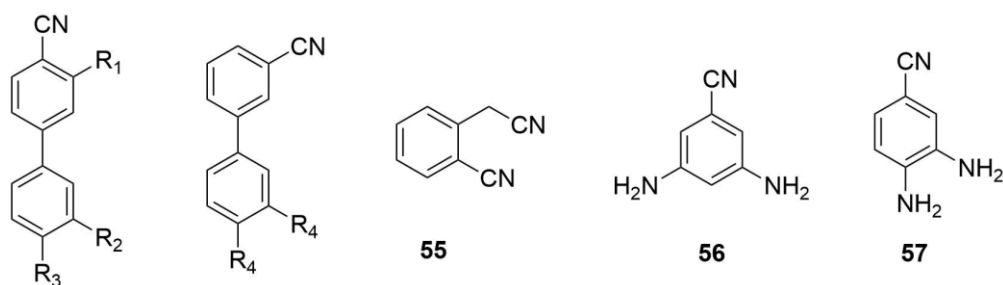
It was observed that the (*S*)-enantiomer of the amide was formed preferentially. The enantioselectivity of the enzyme was found to not be static, as complete conversion of the nitrile transpired with time, thus the reaction was determined to be kinetic resolution. It was concluded that it was achievable to asymmetrically synthesise β-amino amides using NHase

from the unprotected  $\beta$ -amino nitriles. The *N*-protected nitriles were not as successful but gave insight as to the selectivity of the active site. For this particular NHase it was found that steric hindrance and a charged primary amine led to no reaction occurring and thus a critical parameter to address.

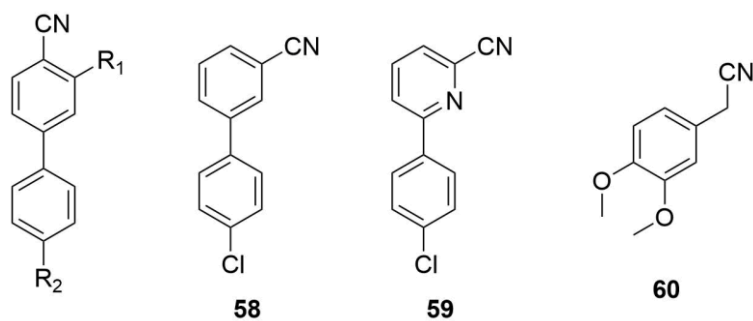
A cobalt nitrile hydratase was evaluated against aromatic substrates by Mashweu *et al*<sup>53</sup>. The nitrile hydratase was isolated and purified from *Rhodococcus rhodochrous* ATCC BAA 870. Alongside aromatic nitriles, biaryl substrates were also successfully synthesised and assessed. The biotransformations were carried out in Tris buffer (pH 7.6) at 30°C with 10% solvent (acetone or methanol). The substrates which were screened, and a summary of the results observed are shown in Figures 1.10 to 1.13.



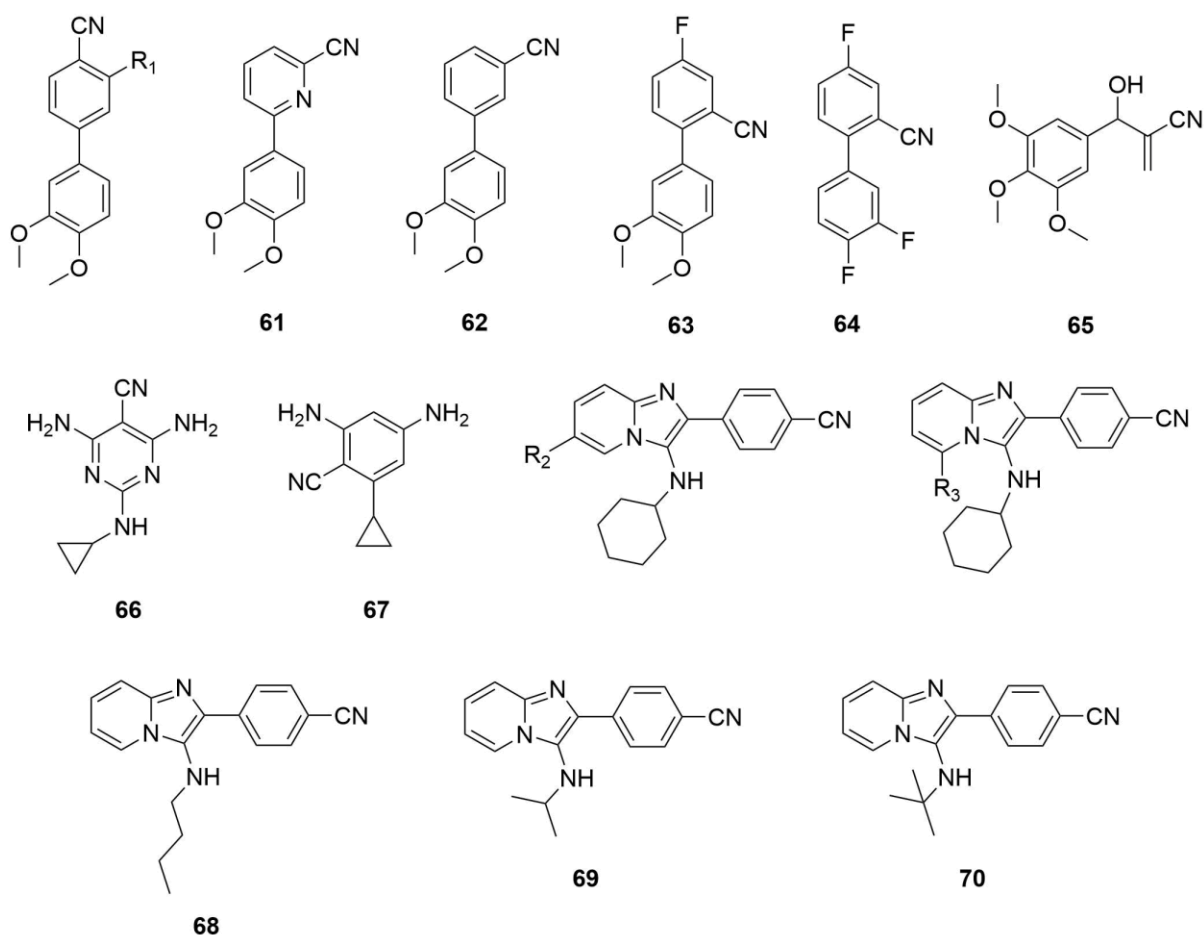
**Figure 1.10: Compounds which showed 50 – 100% conversion. Biotransformations carried out in Tris buffer (pH 7.6) with 10% acetone or methanol, at 30°C. R<sub>1</sub> = H, 4-Cl, 4-Br, 4-OMe, 3-Cl, 2-NH<sub>2</sub>, 2-OH. R<sub>2</sub> = F, NH<sub>2</sub>. R<sub>3</sub> = Br, Me. R<sub>4</sub> = F, Br. R<sub>5</sub> = Me, I, F. R<sub>6</sub> = Br. R<sub>7</sub> = Me. R<sub>8</sub> = Br. R<sub>9</sub> = NH<sub>2</sub>. R<sub>10</sub> = H, 2-NH<sub>2</sub>. R<sub>11</sub> = H, NH<sub>2</sub>. R<sub>12</sub> = NH<sub>2</sub>, OMe, Br. R<sub>13</sub> = H, 2-Br, 3-Br, 4-Cl, 4-OMe<sup>53</sup>**



**Figure 1.11: Compounds which showed 16 – 50% conversion. Biotransformations carried out in Tris buffer (pH 7.6) with 10% acetone or methanol, at 30°C. R<sub>1</sub> = H, F. R<sub>2</sub> = H, F. R<sub>3</sub> = H, F, Cl. R<sub>4</sub> = H, F<sup>53</sup>**



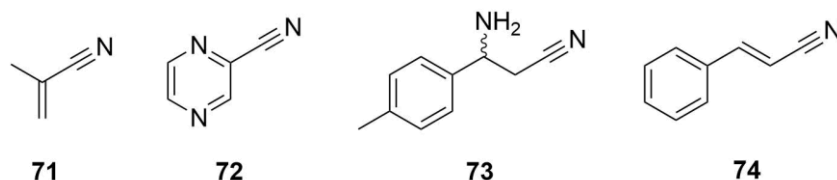
**Figure 1.12: Compounds which showed 5 – 15% conversion. Biotransformations carried out in Tris buffer (pH 7.6) with 10% acetone or methanol, at 30°C. R<sub>1</sub> = F. R<sub>2</sub> = H, Cl<sup>53</sup>**



**Figure 1.13: Compounds which showed 0 – 5% conversion. Biotransformations carried out in Tris buffer (pH 7.6) with 10% acetone or methanol, at 30°C.  $R_1 = H, F$ .  $R_2 = H, Me, Cl$ .  $R_3 = Me, Br$ <sup>53</sup>**

It was found that the electronic properties and the steric hindrance of the nitrile were the two main influences on if hydrolysis occurred and on the conversion rate. Highly sterically hindered substrates were seen to not be tolerated by the enzyme and experienced low, and in some cases no conversion. Substrates with electron-donating groups attached to the aromatic ring were found to have a lower rate of conversion. Of all the 67 diverse substrates evaluated however, the enzyme was only unable to hydrolyse three of them, indicating an accommodating active site.

Recently, Grill *et al*, carried out work to express and characterise NHases<sup>60</sup>. They looked to express novel proteins which exhibit a similar sequence to NHases. The substrates used in this study are shown in Figure 1.14.



**Figure 1.14: Substrates for screening NHases<sup>60</sup>**

The best expression levels in the presence of CoCl<sub>2</sub> and FeSO<sub>4</sub> were seen for *Paenibacillus chondroitinus*, *Microvirga iotononidis*, *Rhodococcus erythropolis*, *Gordonia hydrophobica*, *Caballeronia jiangsuensis*, and *Bacillus* sp. RAPc8. Methacrylonitrile was used to assess the hydrolysis capability of the NHases which were presented in the form of cell free extracts. It was found that there was little correlation with expression levels and activity. The iron-dependant *R. erythropolis* and *P. kilonensis* NHases and the cobalt-dependent *K. oxytoca* and *C. testosterone* were observed to have the best activity towards methacrylonitrile. The general optimum reaction temperature and pH were found to be 37°C and 8.0 respectively. The Fe-dependent NHases were observed to show activity between pH 6.0-8.0 whilst Co-dependent NHases were able to work up to pH 9.5.

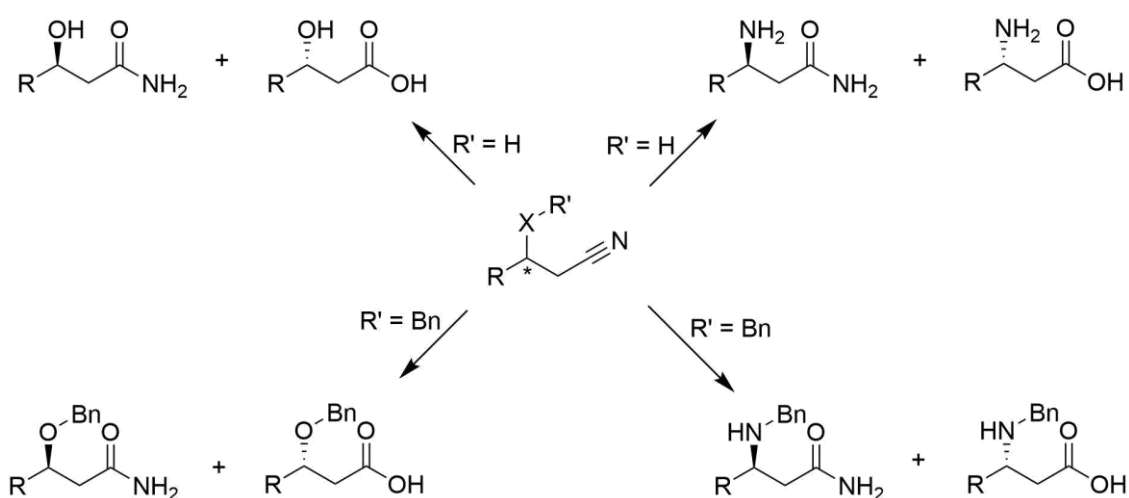
When the remaining substrates were screened with the NHases differing activities were observed. The cinnamic acid nitrile was best hydrolysed by *C. jiangsuensis* NHase whereas the  $\beta$ -amino nitrile revealed good activity from Co-dependent *Comamonas testosterone*, *Pseudonocardia thermophila*, *Roseobacter* sp. MedPE-SWchi NHases and Fe-dependent *Pseudomonas marginalis* NHase. Seven NHases, both Fe- and Co-dependent, were able to hydrolyse the pyrazine nitrile. Overall, it was observed that both the Fe- and the Co-dependent NHases had a broad affinity for the given substrates.

### 1.4.2 Amidases

Amidases are enzymes which convert amides to the corresponding carboxylic acid and in metabolic pathways usually work in tandem with NHases. Their multimeric structures, which are strong and compact, make amidases resistant to denaturation at pH and temperature extremities<sup>61</sup>. Except for one amidase found in *Brevundimonas diminuta*, amidases, like nitrilases, are not metalloenzymes<sup>62</sup>. The four general types of reactions catalysed by amidases are acid transferase, ester transferase, amidotransferase, and acyltransferase activity. Most bacterial amidases exhibit high therapeutic value and one particular example is that of L-

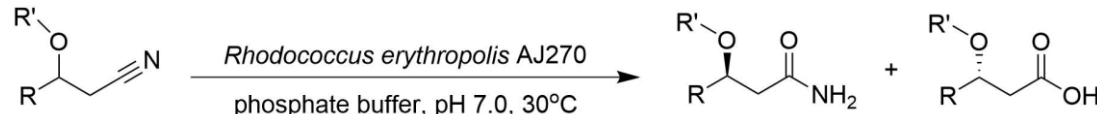
asparaginase which was approved by the Food and Drug Administration (FDA) and World Health Organization (WHO) for treating acute lymphoblastic leukemia<sup>63</sup>.

The synthesis of enantiopure  $\beta$ -hydroxy and  $\beta$ -amino acids and amides was investigated by Ma *et al* using the whole cell catalyst *Rhodococcus erythropolis* AJ270<sup>64</sup>. This system contained both the NHase and the amidase pathway. In their work they aimed to test the hypothesis that the chiral recognition site may be far from the catalytic centre and so a decrease in enantioselectivity should not be observed with the movement of the stereocenter in the substrate. Investigations were also targeted at exploring nitrile biotransformations to acquire the desired products. A summary of their target products is shown in Scheme 1.11.



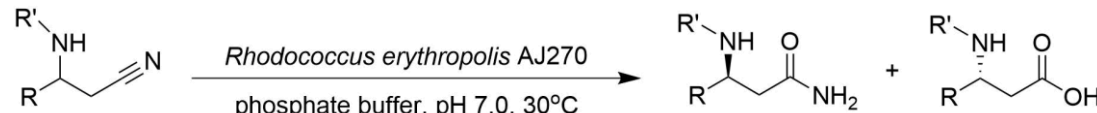
**Scheme 1.11: Biotransformation target products for the work of Ma *et al*<sup>64</sup>**

The first nitriles to be investigated were 3-hydroxy alkanenitriles in phosphate buffer at 30°C at pH 7.0. The biotransformations proceeded rapidly but gave poor enantioselectivity and poor yield for both acid and amide. This suggested that both the NHase and amidase exhibited low enantioselectivity towards the hydroxy acid and amide products. These poor results led to the implementation of a docking strategy by the addition of a removable protecting group. This was thought it would enhance the chiral recognition of the enzyme and thus increase the enantioselectivity results. It was indeed observed that there was a drastic increase in enantioselectivity and a considerable increase in yield as shown in Table 1.5.

**Table 1.5: Comparative results of biotransformations on racemic  $\beta$ -hydroxy and  $\beta$ -benzyloxy nitriles with *R. erythropolis* AJ270, phosphate buffer, pH 7.0, 30°C<sup>64</sup>**


Unprotected hydroxy nitriles				Benzyl protected hydroxy nitriles			
Amide		Acid		Amide		Acid	
ee (%)	Yield (%)	ee (%)	Yield (%)	ee (%)	Yield (%)	ee (%)	Yield (%)
2.0 – 12.0	13 – 41	3.0 – 17.8	12 – 32	>99.5	41 – 50	≤94.4	47 – 50

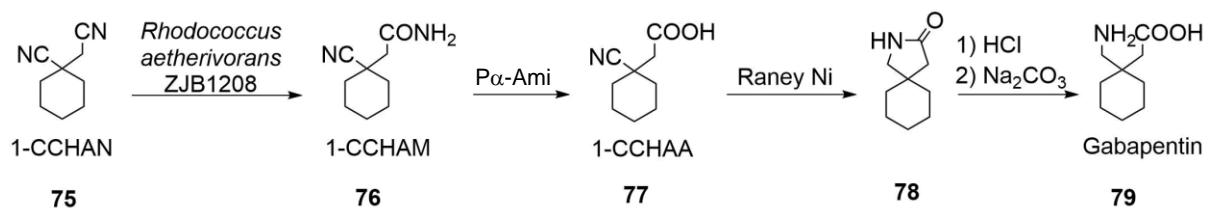
The docking strategy was applied also to the  $\beta$ -amino nitriles. Similar considerable improvements in the enantioselectivity and yield were seen with the addition of the benzyl protecting group as seen in Table 1.5. The unprotected amino amide and acid products were analysed as *N*-Cbz protected derivatives as the Cbz aided in the recovery of the products and attached a chromophore for HPLC analysis.

**Table 1.6: Comparative results of biotransformations on racemic  $\beta$ -amino and  $\beta$ -benzylamino nitriles with *R. erythropolis* AJ270, phosphate buffer, pH 7.0, 30°C<sup>64</sup>**


Unprotected amino nitrile				Benzyl protected amino nitrile			
Amide		Acid		Amide		Acid	
ee (%)	Yield (%)	ee (%)	Yield (%)	ee (%)	Yield (%)	ee (%)	Yield (%)
56.2	30	20.8	43	93.2	46	61.4	53

Overall, it was observed from this work the considerable effect a protecting group can have on the enantioselectivity and yield of nitrile hydrolysis.

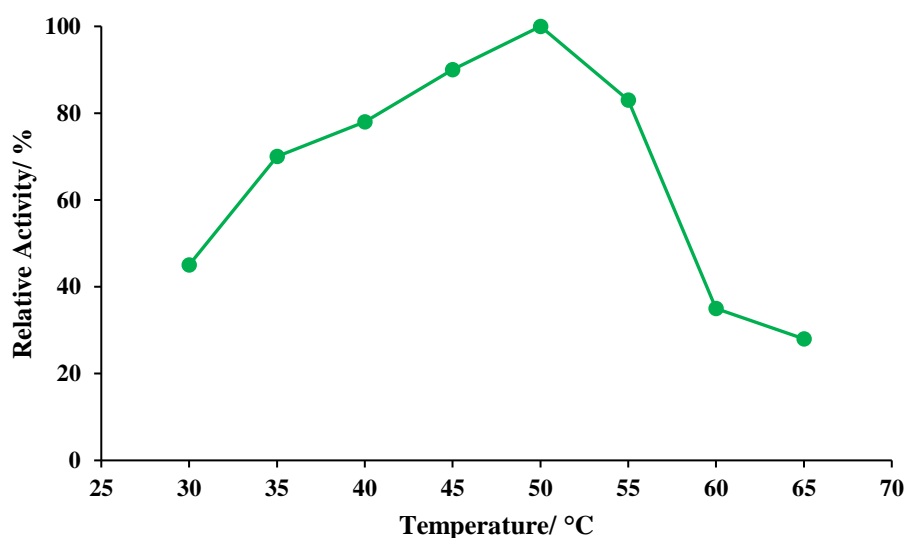
A study carried out by Wu *et al* looked to use a recombinant amidase in the synthesis of Gabapentin, as shown in Scheme 1.12<sup>65</sup>. Gabapentin is a drug that is the structural analogue of  $\gamma$ -aminobutyric acid (GABA), an inhibitory neurotransmitter. The focus of the research was in synthesising the key intermediate, 1-cyanocyclohexaneacetic acid (1-CCHAA) from 1-cyanocyclohexaneacetamide (1-CCHAM). The amide was produced as a result of hydrolysis of the nitrile by NHase from *Rhodococcus aetherivorans* ZJB1208 as reported by Zheng *et al* previously<sup>66</sup>.



**Scheme 1.12: Biocatalytic synthesis of Gabapentin<sup>65</sup>**

The enzyme P $\alpha$ -Ami was the amidase chosen for its excellent catalytic efficiency. An activity assay was carried out at 45°C in Tris-HCl buffer (20 mM, pH 8.0) with 1-CCHAM (20 mM).

The effects of temperature and pH were also assessed. The temperature studies were carried out in Tris-HCl buffer (20 mM, pH 8.0) at temperatures 30 – 65°C. The pH studies were done under the activity assay conditions utilising three buffers: phosphate buffer (pH 6.0 – 7.5), Tris-HCl (pH 7.5 – 9.0), and Gly-NaOH (pH 9.0 – 10.0). In terms of temperature, the maximum activity was observed at 50°C, as seen in Figure 1.15.



**Figure 1.15: Temperature effect on P $\alpha$ -Ami activity. Studies carried out in Tris-HCl buffer at pH 8.0<sup>65</sup>**

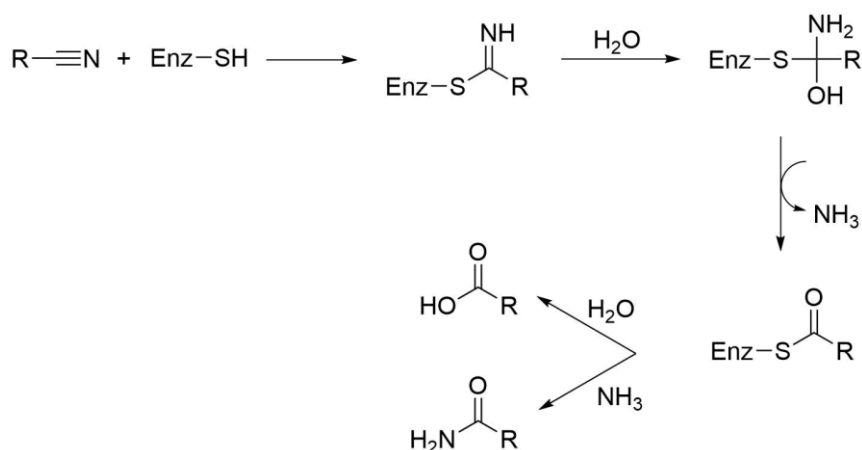
The pH that gave the highest activity of >90% was 8.5 in Tris-HCl buffer. It was also observed that P $\alpha$ -Ami was robust enough to still show activity at high substrate concentrations of up to 100 g L<sup>-1</sup>.

Biotransformations were carried out at 35°C in Tris-HCl buffer (100 mM, pH 8.5) which afforded the desired product, 1-CCHAA with a yield of 5794.7 g<sub>product</sub> L<sup>-1</sup> d<sup>-1</sup>. Overall, it was observed that P $\alpha$ -Ami exhibited high activity as well as a desirable strong tolerance against the presence of high substrate concentration.



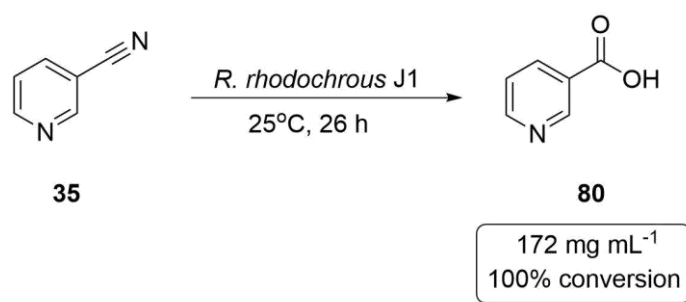
### 1.4.3 Nitrilases

Nitrilase enzymes hydrolyse nitriles directly to carboxylic acids and ammonia. They are found in numerous sources, but bacteria such as *Rhodococcus* are the major producers of nitrilases<sup>67</sup>. Nitrilases sourced from *Rhodococcus* species show diverse substrate affinity as well as a wide tolerance to solvents<sup>67</sup>. The nitrilase protein structure is comprised of a  $\alpha$ - $\beta$ - $\beta$ - $\alpha$  sandwich fold and its active site contains the Glu-Lys-Cys triad<sup>68</sup>. The generally accepted proposed pathway of hydrolysis is illustrated in Scheme 1.13. It can be observed that an imine forms with the sulphur of the cysteine residue to give the enzyme complex. Hydrolysis leads to a keto structure with a loss of ammonia. Further addition of water gives the acid. Where the second addition of water does not occur quickly enough, ammonia is added and the amide forms.



**Scheme 1.13: Current proposed pathway for the nitrilase biocatalytic pathway<sup>68</sup>**

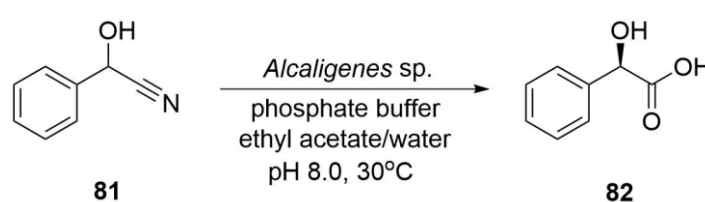
Nitrilases have been applied in numerous examples for the synthesis of carboxylic acids. Nicotinic acid or Vitamin B3 is one such example as shown in Scheme 1.14.



**Scheme 1.14: 100% conversion of 3-cyanopyridine by *R. rhodochrous* J1**

Synthesis of nicotinic acid using the whole cell catalyst *R. rhodochrous* J1 was reported by Matthew *et al* with 100% conversion<sup>69</sup>. Nicotinic acid plays an important role in metabolism such as being a component of coenzymes when converted to its active form and also because it exhibits antihyperlipidemic activity.

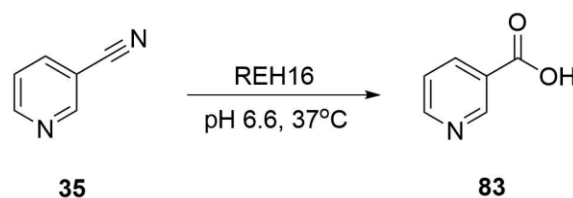
The extremely useful chemical, acrylic acid, can be produced using *A. nitroguajacolicus* as reported by Shen *et al*<sup>70</sup>. Acrylic acid is widely used in the polymer industry and the development of a novel more environmentally friendly approach is thus of great interest as traditional synthetic routes produce several by-products. Another example is the synthetic utility of nitrilase particularly in the synthesis of single enantiomer chiral acids in the production of mandelic acid as shown in Scheme 1.15. The nitrilase present in *Alcaligenes* sp. was found to produce mandelic acid from the batch hydrolysis of mandelonitrile with great specificity of >99.9% ee (*R*), a productivity of 40.9 g L<sup>-1</sup> h<sup>-1</sup>, and a relative production of 38.9 g mandelic acid g<sup>-1</sup> cell<sup>71</sup>.



**Scheme 1.15: Hydrolysis of mandelonitrile to give R-(-)-mandelic acid by *Alcaligenes* sp.<sup>71</sup>**

Mandelic acid is a very useful chiral building block for agricultural and pharmaceutical applications.

Recently, a novel nitrilase from *Ralstonia eutropha* H16 (REH16) was applied to the production of nicotinic acid by Fan *et al* as shown in Scheme 1.16<sup>72</sup>.



**Scheme 1.16: Hydrolysis of 3-cyanopyridine to give nicotinic acid using REH16<sup>72</sup>**

This nitrilase was cloned then overexpressed in *Escherichia coli* BL21 (DE3). In this investigation, several studies were carried out to ascertain the optimal parameters for REH16 in the biocatalytic reaction. The Berthelot method was used to determine the formation of ammonia and the quantification of 3-cyanopyridine along with nicotinic acid were carried out by HPLC. Temperature and pH studies were carried out at different levels. To investigate the optimal temperature, the reactions were carried out in sodium phosphate buffer (pH 7.0, 100 mM) and different temperatures were applied from 10 – 70°C. The optimal temperature was determined as 37°C and above 50°C it was found that the activity of REH16 sharply decreased. For the pH study, the temperature was kept constant at 25°C. In order to cover a range of pH

5.0 – 9.0, three buffers were used; sodium citrate (pH 5.0 – 6.0, 100 mM), sodium phosphate (pH 6.0 – 8.0), and Tris-HCl buffer (8.0 – 9.0, 100 mM). The pH that gave the highest activity was determined to be 6.6.

The thermal stability of REH16 was investigated by carrying out incubations at various temperatures (20, 30, 37, and 50°C) for various periods of time. The best stability was observed at 25°C with merely a 5% loss of activity after 120 h of incubation. In addition, REH16 was assessed for the impact of various metal ions would have on it and also in particular, how ethylenediaminetetraacetic acid (EDTA) would affect it. EDTA was found to have little to no effect but thiol-binding metal ions inhibited the nitrilase activity. A total of 28 nitriles were used to study the substrate specificity of REH16 and are shown in Figure 1.16.

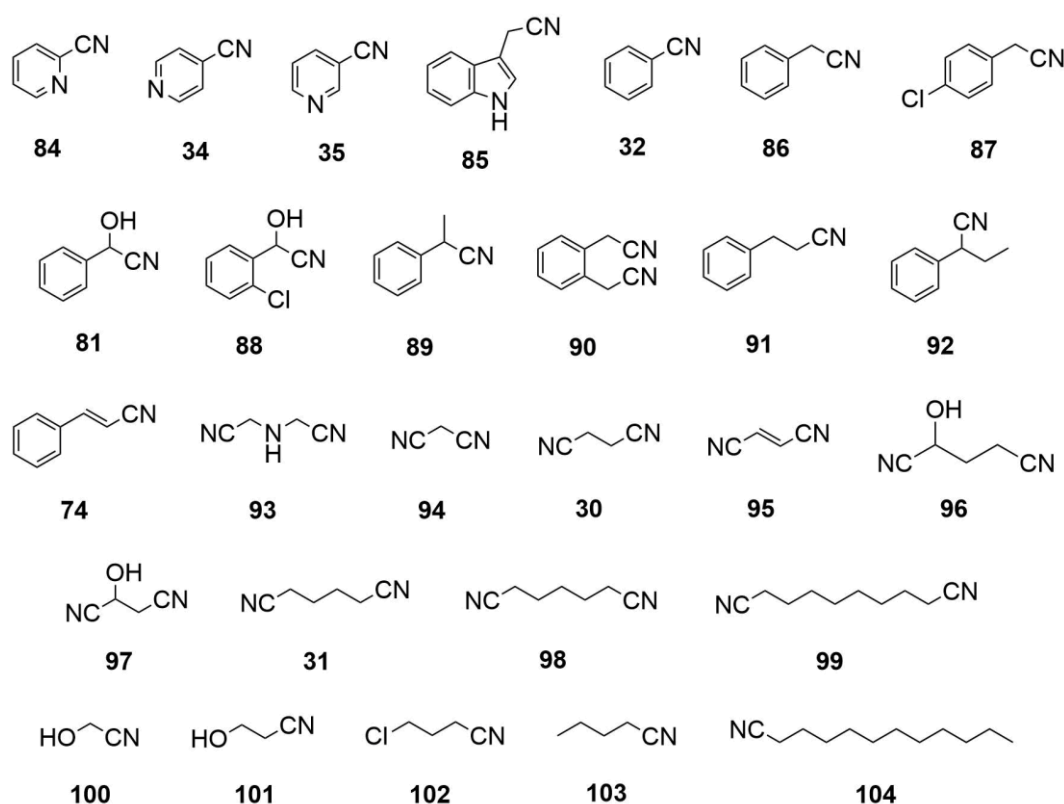
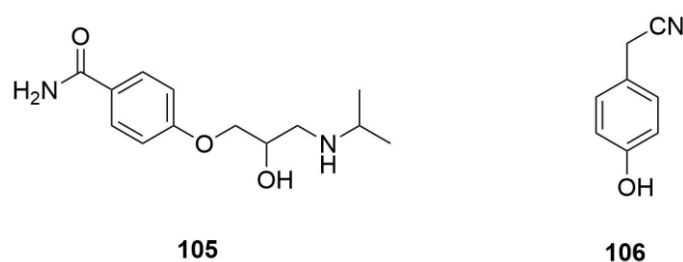


Figure 1.16: The nitriles used to test REH16 for substrate specificity<sup>72</sup>

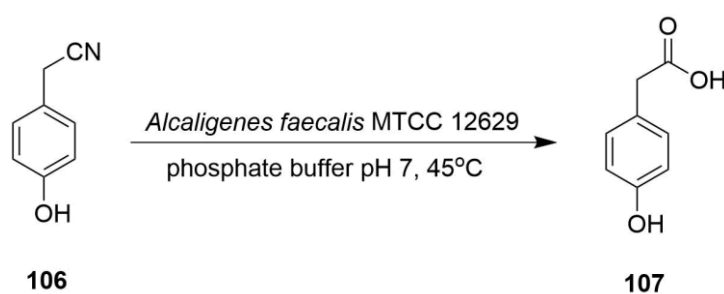
The nitrilase showed a wide range of activity across the aliphatic and heterocyclic nitriles which was influenced by the length of the carbon chain. The highest activity was observed for fumaronitrile (**95**), whilst no hydrolysis was observed for dodecanenitrile (**104**) and malononitrile (**94**). The hydrolytic activity of REH16 was not detected however for most of the aromatic nitriles, with the exception of cinnamitrile (**74**), 2-phenylbutanenitrile (**92**), and 3-phenylpropanenitrile (**91**).

The effects of co-solvents on REH16 was assessed in sodium phosphate buffer (pH 6.6, 100 mM) using a concentration range of 5 – 25% of various solvents. The solvents DMSO, acetone, and THF were shown to significantly inhibit the activity of REH16. While methanol, ethanol, and isopropanol, on the other hand, were observed to enhance the activity, with 100% conversion being achieved with 5 – 10% methanol or ethanol. The potential of REH16 to have industrial application was observed through fed-batch reactions which were carried out. It was found that in a 20.8 h period, a total of 1050 mM 3-cyanopyridine was completely hydrolysed, producing 129.2 g/L of nicotinic acid.

Amidst the rise of research utilising purified enzymes, there is still reported success with whole cell enzymes. This was favoured by Thakur *et al* due to the cell's ability to stabilise the enzyme and provide it a natural environment in which to work in<sup>73</sup>. Thakur *et al* are the first in literature to successfully report the process development of the synthesis of 4-hydroxyphenylacetic acid (4-HPAA) (**107**), an intermediate in the synthesis of atenolol, shown in Figure 1.17, using a nitrilase on 4-hydroxyphenylacetonitrile (4-HPAN) (**106**), shown in Scheme 1.17.



**Figure 1.17: Structure of Atenolol (105) and 4-HPAN (106)**



**Scheme 1.17: Hydrolysis of 4-HPAN to 4-HPAA<sup>73</sup>**

The bacteria chosen in the study by Thakur *et al* was *Alcaligenes faecalis* MTCC 12629 which was kept on nutrient agar. The nitrilase assay was carried out in a 1 mL volume with potassium phosphate buffer (100 mM, pH 7.0), resting cells (0.32 mg dcw), and 4-hydroxyphenylacetonitrile (1 mL). This was incubated at 30°C. The reaction was quenched after 30 min by the addition of HCl (0.1 N, 1 mL). The phenyl-hypochlorite method was used

to measure the ammonia produced<sup>19</sup>. The best *A. faecalis* MTCC 12629 nitrilase inducer was selected by screening different nitriles, acids, and amides at 40 mM for 24 h. Aliphatic nitriles were shown to be the best nitrilase inducer with relatively high biomass. Growth was inhibited by the aromatic nitriles, aryl nitriles,  $\epsilon$ -caprolactum, mandelic acid, and acetonecyanohydrin. Some of the amides such as 2-cyanopyridine, *N*-methylacetamide, acrylamide did support growth but the nitrilase was not induced. The leading inducer from the screening was determined to be isobutyronitrile.

Hyperinduction of the nitrilase was achieved by varying the concentration of isobutyronitrile in 15 sets, shown in Table 1.7.

**Table 1.7: Isobutyronitrile feeding schedule to achieve hyperinduction of the nitrilase<sup>73</sup>**

SET	Isobutyronitrile concentration/ mM	Time intervals added/ h
1 (control)	0	-
2	25	0
3	50	0
4	75	0
5	100	0
6	200	0
7	50	4, 8, 12
8	50	4, 8, 12
9	50	4, 8, 12
10	50	0, 4
11	50	0, 8
12	50	0, 12
13	50	0, 4, 8
14	50	0, 4, 8, 12
15 (exponential level)	25, 50, 75, 100	0, 4, 8, 12

There was negligible induction with Set 1. For sets 4, 5, and 6, the high concentration of the inducer at 0 h was toxic. Induction was increased for Set 7 at 4 h, Set 8 at 8 h, and Set 9 at 12 h. Inhibition was observed for Set 15 because of toxicity of the inducer to the cells at the high concentrations. Maximum induction was achieved with 50 mM of the inducer in SET 7 at 4 h. Nitrilase production increased by 1.2-fold.

The reaction conditions were optimised by varying different parameters. Different buffer systems were evaluated. These were citrate (pH 4.0-6.0), tris-HCl (pH 5.0-8.0), potassium

phosphate (pH 6.0-8.0), sodium phosphate (pH 6.0-8.0), borate (pH 7.0-9.0), sodium carbonate (pH 9.0-10.0), and borax (pH 10.0-11.0). Potassium phosphate buffer at pH 7.0 and 50 mM concentration was revealed to be the optimum buffer system. Nitrilase activity was shown to decline as the strength of the buffer was increased or decreased from 50 mM.

Temperature effects were studied within the range of 25 – 60°C to ascertain the thermal stability of the enzyme. The substrate specificity of the nitrilase was also evaluated. The optimum temperature was determined to be 45°C. Above 55°C, a significant loss was noted for the nitrilase activity, with deactivation occurring at 60°C after an hour. The maximum activity and operational stability for the nitrilase were determined to be 45°C. Aliphatic, aromatic, heterocyclic, and arylacetonitriles were all screened using nitrilase induced on isobutyronitrile. Arylacetonitriles emerged as the preference of the nitrilase. The best substrates were 4-hydroxyphenylacetonitrile, 4-aminophenylacetonitrile, mandelonitrile, and phenylglycinonitrile. Screening against various amides as a substrate gave no activity.

The effect of the presence of the product, 4-HPAA on the nitrilase activity was evaluated. Activity loss was observed on the addition of 4-HPAA at time 0 h at 10-40 mM. This differed however from the observations of the gradual formation of the product in a reaction which did not result in inhibition at the same concentrations tested.

The bioprocess was developed for further optimisation. The substrate, 4-HPAN had its concentration varied from 5 mM to 150 mM in a 1 mL reaction mixture. This was assayed at 30 min intervals for 160 min. Higher concentrations of the substrate began to show inhibition of the nitrilase, with complete inhibition occurring at 150 mM. Product formation was observed to slowly increase between 10 – 40 mM. Beyond 50 mM however, there was a notable decrease in product formation.

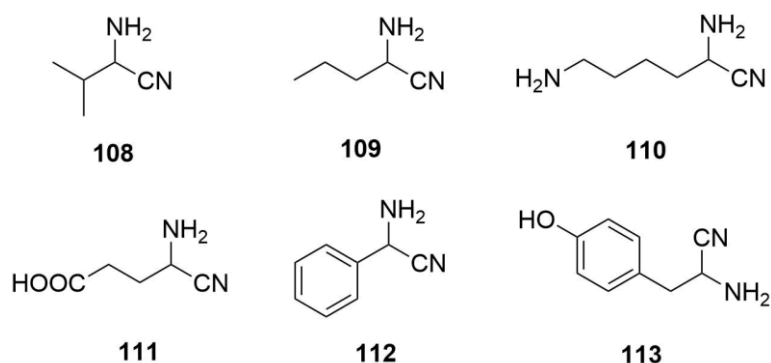
The effect of the enzyme concentration was evaluated with 40 mM substrate and a range of 6 U/mL – 21 U/mL. Samples were taken at 30 min intervals for 120 min and analysed by HPLC. As the amount of biocatalyst increased, there was an increase also in product formation with a decrease in incubation time. It was found that 18 U/mL whole cell enzyme with 40 mM 4-HPAN yielded the maximum substrate conversion in 30 min.

The effect of the nitrilase to substrate ratio on product formation was investigated. This was assessed at 45°C for 160 min and analysis by HPLC was carried out at the 30 min time point. Increasing the nitrilase amount along with the substrate concentration did not yield greater

conversion as high substrate loading led to inhibition. The best ratio was thus determined to be 40 mM substrate and 18 U/mL nitrilase.

Fed batch reactions were carried out at a 50 mL scale under the optimised conditions which were 40 mM substrate, 18 U/mL whole cell enzyme, and 5 successive feedings at 30 min intervals. A steady decline was observed in the conversion after the first feeding due to inhibition occurring after the third feeding at 40 mM. The 5 feedings were thus adjusted to reflect this, and this resulted in 100% conversion to give 150 mM of 4-HPAA. The batch feeding reaction was then increased to a 500 mL scale under the optimum conditions. The product was recovered by decreasing the pH and filtering to obtain the white precipitate. The 4-HPAA recovered was 96% pure. The volumetric productivity and the catalytic productivity were determined to be 23 g/L and 4.13 g/g dcw/h respectively.

As there is a constant need to discover new nitrilases with high-throughput screening, Bordier *et al* investigated the discovery of new  $\alpha$ -aminonitrilases that can be used to produce chiral  $\alpha$ -amino acids with a focus on developing a high-throughput screening method which is of great interest<sup>74</sup>. A collection of 588 enzymes were screened against the  $\alpha$ -aminonitriles in Figure 1.18 with the aim of producing  $\alpha$ -amino acids.



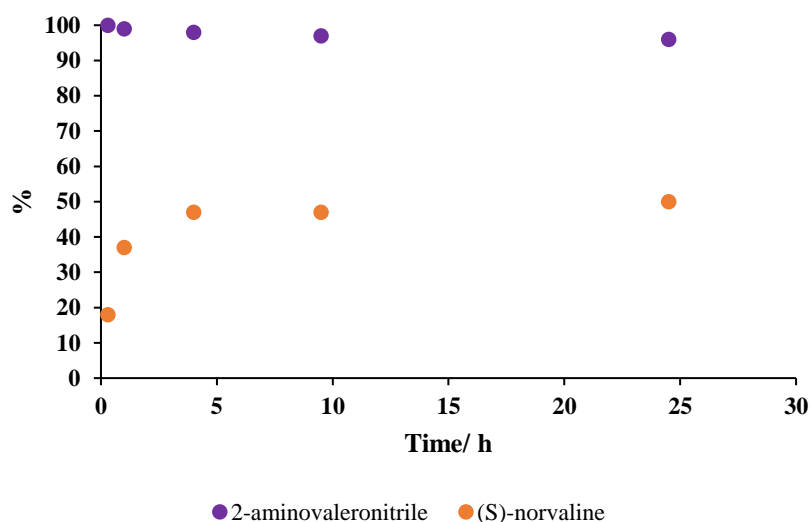
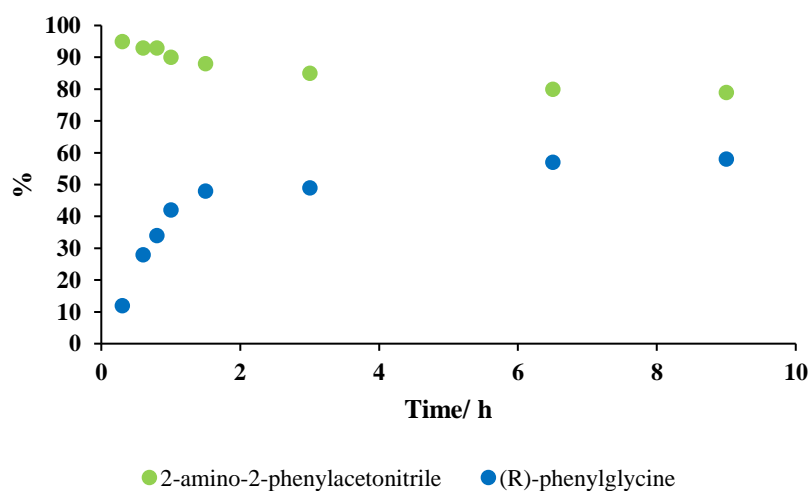
**Figure 1.18: Substrates used to screen the isolates<sup>74</sup>**

Five nitrilases were obtained from the screening and only three were purified and carried forward. Only two of the substrates were found to be suitable, 2-aminobutanenitrile (**109**) and 2-amino-2-phenylacetonitrile (**112**), the precursors to norvaline and phenylglycine respectively. The results of the activity screening are shown in Table 1.8.

**Table 1.8: Activity screening results. Substrate 109 – AN-norvaline, substrate 112 – AN-phenylglycine<sup>74</sup>**

NIT	Substrate	Conversion (%)	ee (%)
191	109	53	94 ( <i>S</i> )
09	112	7	95 ( <i>R</i> )
28	112	63	9 ( <i>R</i> )
29	112	5	95 ( <i>R</i> )
158	112	11	95 ( <i>R</i> )
191	112	64	5 ( <i>S</i> )

The biotransformations were carried out in potassium phosphate buffer, at pH 7.3, at 30°C. Analysis was carried out using LC-MS/MS and (*S*)-NIFE was used as the derivatisation agent for ee analysis.

**Figure 1.19: Conversion of 2-aminovaleronitrile (109) (10 mM) by NIT191 and enantiomeric excess of (*S*)-norvaline formed after derivatization of the reaction medium with (*S*)-NIFE<sup>74</sup>****Figure 1.20: Conversion of 2-amino-2-phenylacetonitrile (112) (10 mM) by NIT28 and enantiomeric excess of (*R*)-phenylglycine formed<sup>74</sup>**



In Figure 1.19, the conversion of 2-aminovaleronitrile to (*S*)-norvaline is observed. This was monitored by HPLC-UV. It shows NIT191 to be quite stereospecific for the (*S*)-enantiomer, giving an ee of 96% for (*S*)-norvaline. In Figure 1.20, the conversion of 2-amino-2-phenylacetonitrile by NIT28 is shown. This was monitored by HPLC and the ee's were determined after derivatisation with Marfey's reagent. NIT28 was found to be stereospecific for the (*R*)-enantiomer. However, 8% of (*S*)-phenylglycine was detected. This result was in conflict with the original screening results the authors observed, and they saw inconsistent results in terms of ee. Interestingly, they cited the reasons to be the instability of the medium during the acid quench and the consequent weak re-basification to only pH 7.5 in preparation for the (*S*)-NIFE derivatisation.

The mass spectrometry was run in the positive ESI ion mode and the MS/MS experiments were done using multiple reaction monitoring scanning. The LC-MS method that was developed monitored the reaction using three parameters: retention time, and the abundance of two daughter ions for each substrate and for the corresponding product. This allowed for a highly sensitive method to be developed which detected nitrilase activity and rapidly discriminated high enantiospecific nitrilases from poor ones. Consequently, it was only five enzymes that exhibited  $\alpha$ -aminonitrilase activity with none of the original collection displaying nitrile hydratase activity.

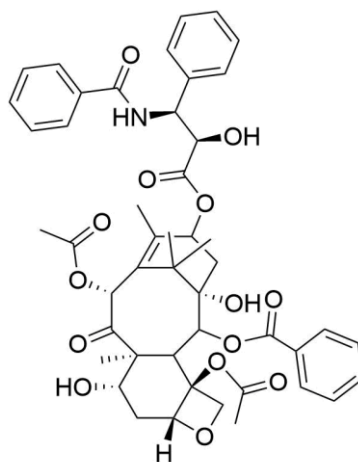
#### 1.4.4 Nitrilase catalysed synthesis of single enantiomer $\beta$ -amino acids

The synthesis of  $\beta$ -amino acids is highly interesting and  $\beta$ -amino acids offer significant potential for use in novel pharmaceuticals. In contrast to  $\alpha$ -amino acids,  $\beta$ -amino acids are not native to the human body, with only one natural  $\beta$ -amino acid,  $\beta$ -alanine, occurring in nature. The structural difference of  $\beta$ -amino acids to  $\alpha$ -amino acids is shown in Figure 1.21. Many  $\beta$ -amino acids are abundant in nature, and they can be found as part of numerous active natural products.



**Figure 1.21: Structural comparison of alpha and beta amino acids**

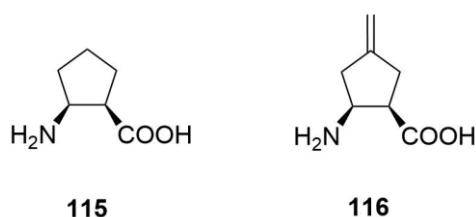
One such example shown in Figure 1.22 is Taxol (Paclitaxel), which is acquired from the bark of the Pacific Yew tree and is important in the treatment of breast cancer<sup>75,76</sup>.



114

**Figure 1.22: Chemical structure of Taxol**

Compared to  $\alpha$ -peptides,  $\beta$ -peptides exhibit a higher *in vivo* stability<sup>77</sup>. This is partly because of the predictable folding of  $\beta$ -peptides which gives rise to stable secondary structures and also, they are resistant to cleavage by peptidases. This means drugs based on  $\beta$ -amino acids will have a greater chance at being more stable in the human body. They have been applied as building blocks in drugs demonstrating hypoglycaemic, antiketogenic, and antifungal properties<sup>78</sup>. For example BAY 10-8888 as presented by Ziegelbauer *et al* has antifungal activity against *Candida* spp. similar to cispentacin which was released within the same era<sup>79</sup>. Both are illustrated in Figure 1.23.

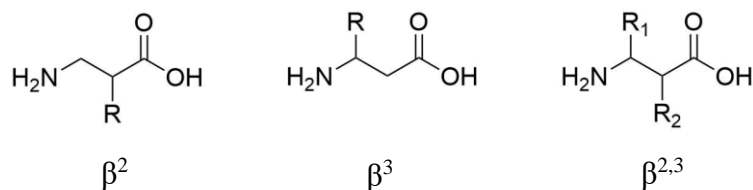


115

116

**Figure 1.23: Comparison of cispentacin (115) to BAY 10-8888 (116)**

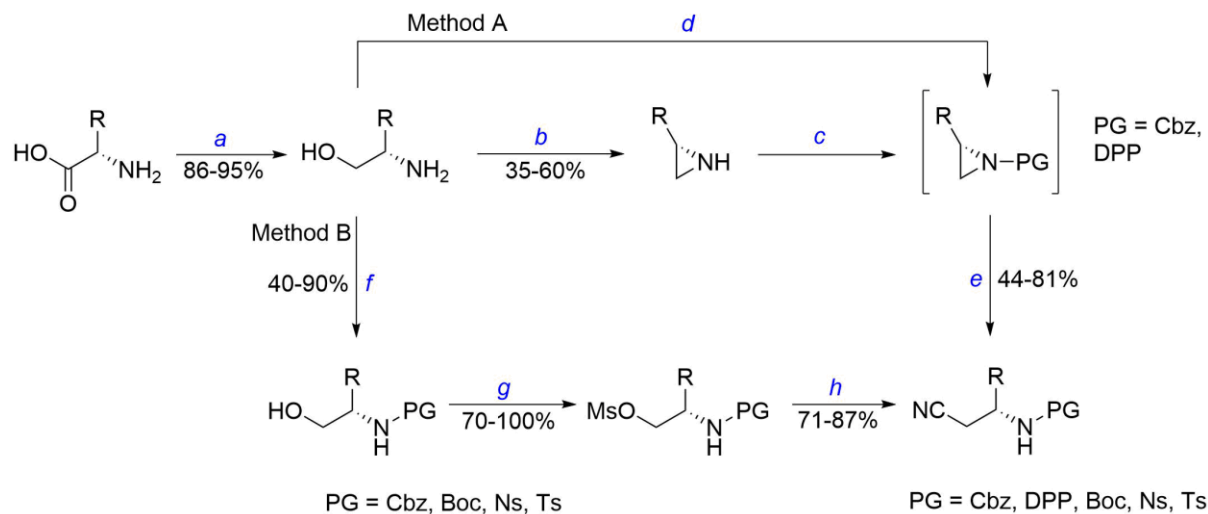
In addition,  $\beta$ -amino acids fold in a predictable way to give their secondary structures and they also allow for greater variation as compared to  $\alpha$ -amino acid scaffolds.  $\beta$ -amino acids can be subdivided into three categories, namely  $\beta^2$ ,  $\beta^3$ , and  $\beta^{2,3}$ , determined by the positioning of the side chain (R), also attached to the scaffold, as illustrated in Figure 1.24<sup>77</sup>.



**Figure 1.24: Differentiation of  $\beta^2$ ,  $\beta^3$ , and  $\beta^{2,3}$  amino acids**

In this work,  $\beta^3$ -amino acids were of interest and of the three sub-types, are often the most readily available.

As the use of NHase/amidase systems for the enantioselective synthesis of  $\beta$ -amino acids as outline above has been developing, so have investigations into the use of nitrilases for such syntheses. Veitía *et al* conducted investigations to expand the application of nitrilases to substrates containing an *N*-protected starting nitrile which is necessary for peptidomimetic synthesis applications<sup>80</sup>. The effect of these protecting groups on the nitrilases was the focus. Purified nitrilases were employed to circumvent the use of whole cell biotransformation systems. Initial attention was placed on the synthesis of the *N*-protected  $\beta^3$ -amino nitriles. This was to be done from the corresponding  $\alpha$ -amino acids as illustrated in Scheme 1.18. Both aliphatic and aromatic L-amino acids were used for this work.

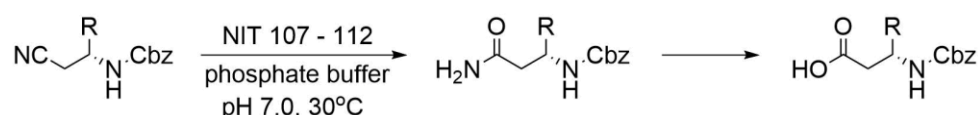


**Scheme 1.18: Synthetic routes for the  $\beta$ -amino nitriles. Reagents and conditions (a)  $\text{NaBH}_4$ ,  $\text{ZnCl}_2$ , THF; (b):  $\text{PPh}_3/\text{DEAD}$ , THF or toluene (c)  $\text{CbzCN}$ ,  $\text{CH}_3\text{CN}$ ; (d):  $\text{DppCl}$ , TEA, THF,  $0^\circ\text{C}$ ; (e)  $\text{NaCN}$ ,  $\text{CH}_3\text{CN}/\text{H}_2\text{O}$  9:1, reflux; (f)  $\text{CbzCl}$ , TEA  $\text{CH}_2\text{Cl}_2$  (or THF) or  $\text{Boc}_2\text{O}$ ,  $\text{NaOH}$ , dioxane or  $\text{TsCl}$  (or  $4\text{NsCl}$ ),  $\text{NaHCO}_3$ , THF (g)  $\text{MsCl}$ , TEA, THF; (h)  $\text{NaCN}$ ,  $\text{DMF}$ <sup>80</sup>**

Two strategies were developed to prepare the nitriles. Method A involved the preparation of *N*-H aziridines, the activation thereof with a benzyloxycarbonyl group, and subsequently using a cyanide ion for the regioselective ring-opening to give the *N*-Cbz- $\beta^3$ -amino nitriles. Only modest yields were obtained and greater than 50% of product was lost after work-up due to instability of the *N*-H aziridines, which could have led to polymerisation, and their volatile

unstable nature making their true yield difficult to determine. Method B comprised of protection of the amine group, mesylation of the alcohol group for its activation, then S<sub>N</sub>2 displacement by a cyanide ion. This was ultimately the chosen strategy as it employed inexpensive reagents with easier workups and was cleaner and faster. It also lent itself to be applicable to large-scale applications.

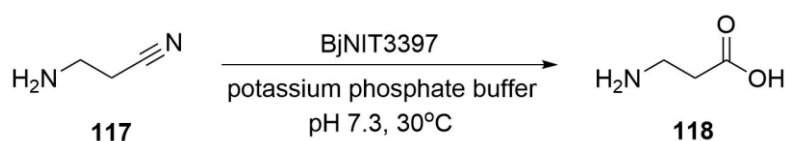
The biotransformations were carried out with 12 nitrilases in phosphate buffer at pH 7 at 30 – 32°C and HPLC was used to monitor conversion, as shown in Scheme 1.19.



**Scheme 1.19: General scheme of the hydrolysis of the  $\beta$ -amino nitriles with the 12 nitrilases<sup>80</sup>**

Nitrilase NIT-107 was highlighted as the best performer, producing a yield of 98% of the *N*-Cbz- $\beta$ -amino acid based on alanine, with no amide production. Some of the other *N*-Cbz protected nitriles gave rise to the formation of the corresponding amide as well the acid, whilst others displayed poor solubility giving rise to decreased activity and thus required co-solvents. The nitriles that were *N*-protected with sulphonamide-like or diphenylphosphinyl-like groups were not hydrolysed by the nitrilases thus alluding to the influence of the *N*-protecting group on the substrate specificity of the nitrilase.

The preparation of  $\beta$ -alanine using microorganisms from 3-aminopropionitrile has been reported in literature previously however the industrial applications were limited due to the restriction on the substrate concentration. Han *et al* set out to discover other nitrilases which could hydrolyse 3-aminopropionitrile exhibiting high activity and tolerating high substrate concentration<sup>81</sup>. Selection of the appropriate nitrilase was carried out by screening nitrilase genes expressed in *Escherichia coli* with 3-aminopropionitrile. At the substrate concentration of 50 mM, the only nitrilase to still exhibit activity was that from *Bradyrhizobium japonicum* USDA110 (BjNIT3397), so this was selected for the remainder of the investigations, as shown in Scheme 1.20.



**Scheme 1.20: Hydrolysis of 3-aminopropionitrile by BjNIT3397 to give  $\beta$ -alanine<sup>81</sup>**

Conversion was determined using HPLC following derivatisation of both the substrate and product with 1-fluoro-2,3-dinitrophenyl-5-L-alanine amide (FDAA). The effect of pH was studied by carrying out reactions from pH range 5.0 – 10.0. The strong alkalinity of the substrate meant the pH could not be adjusted conventionally using different buffers such as potassium phosphate or sodium citrate and concentrated hydrochloric acid (12M) was used. The optimal pH was determined to be 7.0. Investigations into the effect of temperature were carried out over a temperature range of 20 to 60°C at pH 7.0. It was found that 40°C was the optimal temperature.

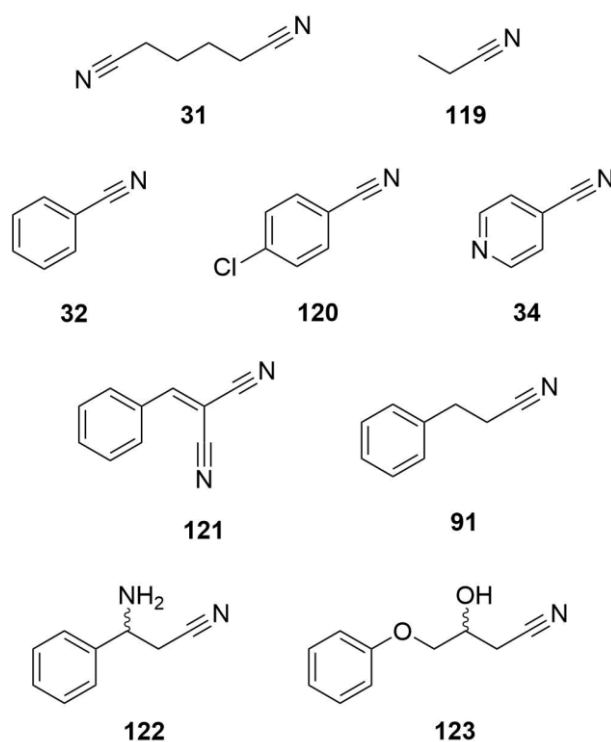
A study was then carried out to ascertain the effect of substrate concentration using a range of 0.7 – 3.5 M at the optimal temperature and pH. A substantial amount of 3-aminopropanamide was produced as the substrate concentration increased which competed with the production of  $\beta$ -alanine. This led to investigations to reduce the formation of 3-aminopropanamide by the removal of ammonia. This was achieved by the addition of aspartate ammonia-lyase with fumaric acid, which would produce L-aspartic acid, in reactions with varying substrate concentrations (0.6 – 3.0 M) at pH 7.3 at 25°C). It was observed that the percentage of 3-aminopropanamide present in the product reduced from 33% to 3%.

Finally, a time study was conducted for the biotransformation with 3 M substrate at 30°C, pH 7.3, for 8 h. This was done with and without the addition of ammonia-lyase and fumaric acid. Samples were taken at half hour intervals for the first 4 h, then hourly subsequently. Without ammonia-lyase, observations indicated that 3-aminopropanamide was formed within the first 2 h. With ammonia-lyase, production of 3-amino-propanamide was observed to have been inhibited from the start. Overall, this tandem strategy was seen to hold potential for both  $\beta$ -alanine and L-aspartic acid to be produced in one process however, the issues concerning the separation of the two products would need to be investigated and solved. Finally, it was noted by the authors that the only nitrilase which could exhibit high enough activity with a high substrate concentration was BjNIT3397.

Novel nitrilases are continually being discovered and applied alongside investigations into the distribution and specificity of nitrile-hydrolysing micro-organisms. Rapheeha *et al* recently sought to expand the existing information on the aforementioned as well as increase information on the environment in which they are found by isolating soil bacteria from where nitrile-producing plants were cultivated and also from uncultivated soil, including industrial land<sup>82</sup>. Samples were collected from 11 sites over approximately 1000 km from central to the

south-west coast of South Africa. Nine nitriles, shown in Figure 1.25 were utilised as sole sources of carbon and/or nitrogen; adiponitrile, propionitrile, benzonitrile, 4-chlorobenzonitrile, 4-cyanopyridine, benzylidenemalononitrile, and hydrocinnamonitrile. Three isolation methods were applied:

1. Solid minimal medium utilising a nitrile as the source of both carbon and nitrogen
2. Solid minimal medium employing the nitrile as solely the nitrogen source
3. Liquid culture enrichment medium using the nitrile as the nitrogen source



**Figure 1.25: Nitrile compounds utilised for isolation of the bacteria: (31) adiponitrile, (119) propionitrile, (32) benzonitrile, (120) 4-chlorobenzonitrile, (34) 4-cyanopyridine, (121) benzylidenemalononitrile, (91) hydrocinnamonitrile and for the biotransformations: (122) 3-amino-3-phenylpropionitrile, (123) 3-hydroxy-4-phenoxybutyronitrile<sup>82</sup>**

To validate the viability of the cells, nutrient agar plates were used as the control. The negative control was *E. coli* whilst *R. rhodochrous* ATCC BAA-870 served as the positive control. Biocatalytic activity was assessed using the  $\beta$ -amino nitrile 3-amino-3-phenylpropionitrile (**122**) and the  $\beta$ -hydroxynitrile 3-hydroxy-4-phenoxybutyronitrile (**123**). Biotransformations were carried out with Tris or phosphate buffer at pH 9 and 7, respectively. Incubations were carried out 30°C with samples taken at 0.5, 2, 4, and 24 h. The bacterial isolates were also identified using 16S rRNA. The isolation method which required the nitrile to be the sole

source of both carbon and nitrogen lead to the least number of isolates being acquired as compared to the other methods with a supplemented carbon source. It was observed for uncultivated soil samples, that the geographical location gave minimal influence on the isolates. For agricultural and mined soil, isolates were identified which were able to grow on aliphatic, aromatic, and aryl-aliphatic nitriles.

Fewer isolates were acquired from the liquid medium approach as compared to direct plating. The liquid medium approach consisted of the soil sample being inoculated into a minimal medium with a nitrile as the nitrogen source and after being incubated, the cultures were transferred and streaked onto agar. The direct plating approach however, consisted of the nitrile being streaked onto either agar containing a nitrile as both the carbon and nitrogen source or agar containing a nitrile as just the nitrogen source. The concentration of the nitrile also had an effect. Isolates grown on 0.5 mmol/L nitrile failed to grow afterward on 5 mmol/L nitrile plates. From 613 isolates, only 14 showed the ability to utilise 3-amino-3-phenylpropionitrile (**122**) and/or 3-hydroxy-4-phenoxybutyronitrile (**123**). Earlier observations by the same research group (Chhiba *et al*) confirmed that 3-amino-3-phenylpropionitrile (**122**) requires pH 9 for hydrolysis to occur as at lower pHs, the protonated form dominates<sup>59</sup>. When the biotransformation for 3-amino-3-phenylpropionitrile (**122**) was repeated at pH 9.0, poor results were unfortunately observed of 46% conversion, (*R*)-nitrile 8% ee, and (*S*)-amide 7% ee. Gene sequencing with 16S rRNA revealed that the majority of the isolates were from *Rhodococcus erythropolis* or *Rhodococcus* sp.

## 1.5 Conclusion

The literature has thus shown the viability of biotransformations on  $\beta$ -amino nitriles. An important parameter to control that is evident is pH, particularly for unprotected amino nitriles, which could lead to no reaction happening if the amino nitrile is in its protonated form. In some cases, it may be also necessary to add protecting groups which have been shown to greatly improve enantioselectivity and yield. In scenarios where the amino nitrile contains no chromophore or presents extraction issues due to high water solubility, derivatisation will be necessary for analysis to occur. Chapter 2 will now describe the synthesis and HPLC method development for the  $\beta$ -amino nitrile substrates and corresponding acid and amide standards.

## REFERENCES

1. Carson, Rachel. *Silent Spring*. (Fawcett Publications, 1962).
2. Anastas, Paul. T. & Warner, John. C. *Green Chemistry: Theory and Practice*. (Oxford University Press, 1998).
3. Sheldon, Roger. A. & Brady, Dean. *Broadening the Scope of Biocatalysis in Sustainable Organic Synthesis*. *ChemSusChem*, 2019, **12**, (13), 2859-2881
4. Lee, Hyuk. *et al.* *Expression of a Lipase on the Cell-Surface of Escherichia coli Using the OmpW Anchoring Motif and its Application to Enantioselective Reactions*. *Biotechnology Letters*, 2013, **35**, (10), 1677-1683
5. Carvalho, Ana. Caroline. *et al.* *Recent Advances in Lipase-Mediated Preparation of Pharmaceuticals and Their Intermediates*. *International Journal of Molecular Science*, 2015, **16**, (12), 29682-29716
6. Zheng, Ren-Chao. *et al.* *Enzymatic Production of (S)-3-cyano-5-methylhexanoic Acid Ethyl Ester With High Substrate Loading by Immobilized Pseudomonas cepacia Lipase*. *Tetrahedron: Asymmetry*, 2012, **23**, (22-23), 1517-1521
7. Dong, Hua-Ping. *et al.* *Enantioselective Hydrolysis of Diethyl 3-hydroxyglutarate to Ethyl (S)-3-hydroxyglutarate by Immobilized Candida antarctica Lipase B*. *Journal of Molecular Catalysis B: Enzymatic*, 2010, **66**, (1-2), 90-94
8. Atalah, Joaquín. *et al.* *Thermophiles and the Applications of Their Enzymes as New Biocatalysts*. *Bioresource Technology*, 2019, **280**, 478-488
9. Pätzold, Magdalena. *et al.* *Deep Eutectic Solvents as Efficient Solvents in Biocatalysis*. *Trends in Biotechnology*, 2019, **37**, (9), 943-959
10. Christian., Wandrey *et al.* *Industrial Biocatalysis: Past, Present, and Future*. *Organic Process Research & Development*, 2000, **4**, (4), 286-290
11. Eichelbaum, M. in *Toxicology in Transition. Archives of Toxicology (Supplement) Vol. 17 Side Effects and Toxic Reactions of Chiral Drugs: A Clinical Perspective* (eds Gisela. H. Degen *et al.*) 514-521 (Springer, Berlin, 1995).
12. Chhabra, Naveen. *et al.* *A Review of Drug Isomerism and its Significance*. *International Journal of Applied & Basic Medical Research*, 2013, **3**, (1), 16-18
13. FDA. *Development of New Stereoisomeric Drugs*, <<https://www.fda.gov/regulatory-information/search-fda-guidance-documents/development-new-stereoisomeric-drugs>> (2018).
14. Patel, Ramesh. N. in *Biocatalysis for Green Chemistry and Chemical Process Development Chapter 5: Biocatalytic Routes to Chiral Intermediates for Development*



- of Drugs 5* (eds Junhua. Alex. Tao & Romas. Kazlauskas) 91-149 (John Wiley & Sons, Inc., 2011).
15. Adams, Joseph P. *et al.* *Biocatalysis: A Pharma Perspective*. *Advanced Synthesis & Catalysis*, 2019, **361**, (11), 2421-2432
  16. Abdjul, Delfly. B. *et al.* *Anti-mycobacterial Haliclonadamine Alkaloids from the Okinawan Marine Sponge Haliclona sp. Collected at Iriomote Island*. *Phytochemistry Letters*, 2018, **26**, 130-133
  17. Fahy, Eoin. *et al.* *Haliclonadamine, An Antimicrobial Alkaloid from the Sponge Haliclona sp.* *Tetrahedron Letters*, 1988, **29**, (28), 3427-3428
  18. Taber, Douglass. & Wang, Yanong. *Synthesis of (-)-Haliclonadamine*. *Journal of the American Chemical Society*, 1997, **119**, (1), 22-26
  19. Rychnovsky, Scott. D. & Hoye, Rebecca. C. *Convergent Synthesis of the Polyene Macrolide (-)-Roxaticin*. *Journal of the American Chemical Society*, 1994, **116**, (5), 1753-1765
  20. Reddy, K. Siva. Nagi. & Sabitha, Gowravaram. *First Total Synthesis of Pestalotioprolide C and its C7 Epimer*. *Tetrahedron Letters*, 2017, **58**, (12), 1198-1201
  21. Liu, Shuai. *et al.* *Cytotoxic 14-Membered Macrolides from a Mangrove-Derived Endophytic Fungus, Pestalotiopsis microspora*. *Journal of Natural Products*, 2016, **79**, (9), 2332-2340
  22. Kwon, Sangil. *et al.* *Total Synthesis of Naturally Occuring 5,7,8-Trioxxygenated Homoisoflavonoids*. *ACS Omega*, 2020, **5**, (19), 11043-11057
  23. Ricci, Alfredo. *Asymmetric Organocatalysis at the Service of Medicinal Chemistry*. *ISRN Organic Chemistry*, 2014, **2014**
  24. Eder, Ulrich. *et al.* *New Type of Asymmetric Cyclization to Optically Active Steroid CD Partial Structures*. *Angewandte Chemie International Edition*, 1971, **10**, (7), 496-497
  25. Liu, Shijie. in *Bioprocess Engineering (Third Edition) Chapter 7: Enzymes* (ed Shijie. Liu) 229-290 (Elsevier, 2020).
  26. Tsujiuchi, Takashi. *et al.* in *Gene Therapy of Cancer Chapter 27 - RNA Interference Therapeutics for Tumor Therapy: Promising Work in Progress* (eds Edmund. C. Lattime & Stanton. L. Gerson) 393-408 (Academic Press, 2014).
  27. James, Helen. A. in *Encyclopedia of Cancer Ribozymes and Their Applications* (ed Joseph. R. Bertino) 179-188 (Academic Press, 2002).
  28. Robertson, Michael. P. & Joyce, Gerald. F. *Highly Efficient Self-Replicating RNA Enzymes*. *Chemistry & Biology*, 2014, **21**, (2), 238-245

29. Koshland, Daniel E., Jr. *The Key-Lock Theory and the Induced Fit Theory*. Angewandte Chemie International Edition in English, 1995, **33**, 2375-2378
30. Fischer, Emil. *Einfluss der Configuration auf die Wirkung der Enzyme*. Berichte der deutschen chemischen Gesellschaft, 1894, **27**, (3), 2985-2993
31. Fischer, Emil. *Ueber die optischen Isomeren des Traubenzuckers, der Gluconsäure und der Zuckersäure*. Berichte der deutschen chemischen Gesellschaft, 1890, **23**, (2), 2611-2624
32. McDonald, Andrew. G. *et al.* in Encyclopedia of Life Sciences *Enzyme Classification and Nomenclature* 1-11 (John Wiley & Sons, Ltd, 2015).
33. Gröger, Harald. *et al.* in Green Biocatalysis *Chapter 23: Asymmetric Synthesis with Recombinant Whole-Cell Catalysts* 23 (ed Ramesh. N. Patel) 557-585 (John Wiley & Sons, Inc., 2016).
34. Gao, Bei. *et al.* *Development of Recombinant Escherichia coli Whole-cell Biocatalyst Expressing a Novel Alkaline Lipase-coding Gene From Proteus sp. for Biodiesel Production*. Journal of Biotechnology, 2009, **139**, (2), 169-175
35. Minteer, S. D. in Biotechnology for Biofuel Production and Optimization *Chapter 16: Cell-Free Biotechnologies* (eds Carrie. A. Eckert & Cong. T. Trinh) 433-448 (Elsevier, 2016).
36. Nakamura, Kaoru. & Matsuda, Tomoko. in Enantiomer Separation: Fundamentals and Practical Methods *Chapter 8: Enzymatic Kinetic Resolution* (ed Fumio. Toda) 231-266 (Springer Netherlands, 2004).
37. Uzir, Mohamad. Hekarl. in Encyclopedia of Membranes *Enantiospecificity* (eds Enrico. Drioli & Lidietta. Giorno) 702-703 (Springer Berlin Heidelberg, 2016).
38. Koskinen, Ari. M. P. in Asymmetric Synthesis of Natural Products *Chapter 3: Asymmetric Synthesis* 55-113 (John Wiley & Sons, Ltd, 2012).
39. Martinez, Carlos. A. *et al.* *Biotransformation-mediated Synthesis of (1S)-1-(2,6-dichloro-3-fluorophenyl)ethanol in Enantiomerically Pure Form*. Tetrahedron: Asymmetry, 2010, **21**, (19), 2408-2412
40. Cui, Jean. J. *et al.* *Structure Based Drug Design of Crizotinib (PF-02341066), a Potent and Selective Dual Inhibitor of Mesenchymal-Epithelial Transition Factor (c-MET) Kinase and Anaplastic Lymphoma Kinase (ALK)*. Journal of Medicinal Chemistry, 2011, **54**, (18), 6342-6363
41. Izumi, Taeko. *et al.* *Chemoenzymic Synthesis of Optically Active 3-methyl- and 3-butylphthalides*. Journal of Chemical Technology & Biotechnology, 1996, **67**, (1), 89-95
42. Tao, Junhua. & Xu, Jian-He. *Biocatalysis in Development of Green Pharmaceutical Processes*. Current Opinion in Chemical Biology, 2009, **13**, (1), 43-50

43. Winkler, Christoph. K. *et al.* *Chemoenzymatic Asymmetric Synthesis of Pregabalin Precursors via Asymmetric Bioreduction of  $\beta$ -Cyanoacrylate Esters Using Ene-Reductases*. *The Journal of Organic Chemistry*, 2013, **78**, (4), 1525-1533
44. Martinez, Carlos. A. *et al.* *Development of a Chemoenzymatic Manufacturing Process for Pregabalin*. *Organic Process Research & Development*, 2008, **12**, (3), 392-398
45. Mukherjee, Herschel. & Martinez, Carlos. A. *Biocatalytic Route to Chiral Precursors of  $\beta$ -Substituted- $\gamma$ -Amino Acids*. *ACS Catalysis*, 2011, **1**, (9), 1010-1013
46. Preskar, Maja. *et al.* *Pharmaceutical Composition of Sitagliptin*. United States patent (2012).
47. Kim, Doseop. *et al.* *(2R)-4-Oxo-4-[3-(Trifluoromethyl)-5,6-dihydro[1,2,4]triazolo[4,3-a]pyrazin-7(8H)-yl]-1-(2,4,5-trifluorophenyl)butan-2-amine: A Potent, Orally Active Dipeptidyl Peptidase IV Inhibitor for the Treatment of Type 2 Diabetes*. *Journal of Medicinal Chemistry*, 2005, **48**, (1), 141-151
48. Desai, Aman. A. *Sitagliptin Manufacture: A Compelling Tale of Green Chemistry, Process Intensification, and Industrial Asymmetric Catalysis*. *Angewandte Chemie International Edition in English*, 2011, **50**, (9), 1974-1976
49. Pace, Helen. C. & Brenner, Charles. *The Nitrilase Superfamily: Classification, Structure and Function*. *Genome Biology*, 2001, **2**, (1), 1-9
50. Brenner, Charles. *Catalysis in the Nitrilase Superfamily*. *Current Opinion in Structural Biology*, 2002, **12**, (6), 775-782
51. Yamada, Hideaki. & Kobayashi, Michihiko. *Nitrile Hydratase and its Application to Industrial Production of Acrylamide*. *Bioscience, Biotechnology, and Biochemistry*, 1996, **60**, (9), 1391-1400
52. Prasad, Shreenath. & Bhalla, Tek. Chand. *Nitrile Hydratases (NHases): At the Interface of Academia and Industry*. *Biotechnology Advances*, 2010, **28**, (6), 725-741
53. Mashweu, Adelaide. *et al.* *Substrate Profiling of the Cobalt Nitrile Hydratase from *Rhodococcus rhodochrous* ATCC BAA 870*. *Molecules*, 2019, **25**, (1), 238
54. Kobayashi, Michihiko. & Shimizu, Sakayu. *Metalloenzyme Nitrile Hydratase: Structure, Regulation, and Application to Biotechnology*. *Nature Biotechnology*, 1998, **16**, (8), 733-736
55. Wang, Zhe. *et al.* *Establishment of Bioprocess for Synthesis of Nicotinamide by Recombinant *Escherichia coli* Expressing High-Molecular-Mass Nitrile Hydratase*. *Applied Biochemistry and Biotechnology*, 2017, **182**, (4), 1458-1466
56. Pawar, Sandip. V. & Yadav, Ganapati. D. *PVA/chitosan–glutaraldehyde Cross-linked Nitrile Hydratase as Reusable Biocatalyst for Conversion of Nitriles to Amides*. *Journal of Molecular Catalysis B: Enzymatic*, 2014, **101**, 115-121

57. Kamble, Ashwini. L. *et al.* *Nitrile Hydratase of Rhodococcus erythropolis: Characterization of the Enzyme and the Use of Whole Cells for Biotransformation of Nitriles*. *3 Biotech*, 2013, **3**, (4), 319-330
58. Winkler, Margit. *et al.* *Synthesis and Microbial Transformation of  $\beta$ -amino Nitriles*. *Tetrahedron*, 2005, **61**, (17), 4249-4260
59. Chhiba, Varsha. *et al.* *Enantioselective Biocatalytic Hydrolysis of  $\beta$ -aminonitriles to  $\beta$ -Amino-amides Using Rhodococcus rhodochrous ATCC BAA-870*. *Journal of Molecular Catalysis B: Enzymatic*, 2012, **76**, 68-74
60. Grill, Birgit. *et al.* *Functional Expression and Characterization of a Panel of Cobalt and Iron-Dependent Nitrile Hydratases*. *Molecules*, 2020, **25**, (11), 2521
61. Sharma, Monica. *et al.* *Amidases: Versatile Enzymes in Nature*. *Reviews in Environmental Science and Biotechnology*, 2009, **8**, (4), 343-366
62. Komeda, H. *et al.* *L-Stereoselective Amino Acid Amidase with Broad Substrate Specificity from Brevundimonas diminuta: Characterization of a New Member of the Leucine Aminopeptidase Family*. *Applied Microbiology and Biotechnology*, 2006, **70**, (4), 412-421
63. Mario, Sanches. *et al.* *Structure, Substrate Complexation and Reaction Mechanism of Bacterial Asparaginases*. *Current Chemical Biology*, 2007, **1**, (1), 75-86
64. Ma, Da-You. *et al.* *Nitrile Biotransformations for the Synthesis of Highly Enantioenriched  $\beta$ -Hydroxy and  $\beta$ -Amino Acid and Amide Derivatives*. *Journal of Organic Chemistry*, 2008, **73**, (11), 4087-4091
65. Wu, Zhe-Ming. *et al.* *Enzymatic Production of Key Intermediate of Gabapentin by Recombinant Amidase from Pantoea sp. with High Ratio of Substrate to Biocatalyst*. *Process Biochemistry*, 2016, **51**, (5), 607-613
66. Zheng, Ren-Chao. *et al.* *Highly Regioselective and Efficient Production of 1-cyanocyclohexaneacetamide by Rhodococcus aetherivorans ZJB1208 Nitrile Hydratase*. *Journal of Chemical Technology & Biotechnology*, 2016, **91**, (5), 1314-1319
67. Busch, Hanna. *et al.* *Rhodococcus as a Versatile Biocatalyst in Organic Synthesis*. *International Journal of Molecular Sciences*, 2019, **20**, (19), 4787
68. Gong, Jin-Song. *et al.* *Nitrilases in Nitrile Biocatalysis: Recent Progress and Forthcoming Research*. *Microbial Cell Factories*, 2012, **11**, (142), 1-18
69. Mathew, Caluwadewa. Deepal. *et al.* *Nitrilase-Catalyzed Production of Nicotinic Acid from 3-Cyanopyridine in Rhodococcus rhodochrous J1*. *Applied and Environmental Microbiology*, 1988, **54**, (4), 1030-1032

70. Shen, Mei. *et al.* Isolation and Characterization of a Novel *Arthrobacter nitroguajacolicus* ZJUTB06-99, Capable of Converting Acrylonitrile to Acrylic Acid. *Process Biochemistry*, 2009, **44**, (7), 781-785
71. Ni, Kefeng. *et al.* Efficient Production of (R)-(-)-Mandelic Acid in Biphasic System by Immobilized Recombinant *E. coli*. *Journal of Biotechnology*, 2013, **167**, (4), 433-440
72. Fan, Haiyang. *et al.* A Novel Nitrilase from *Ralstonia eutropha* H16 and its Application to Nicotinic Acid Production. *Bioprocess and Biosystems Engineering*, 2017, **40**, (8), 1271-1281
73. Thakur, Neerja. *et al.* Biotransformation of 4-hydroxyphenylacetonitrile to 4-hydroxyphenylacetic Acid Using Whole Cell Arylacetonitrilase of *Alcaligenes faecalis* MTCC 12629. *Process Biochemistry*, 2018, **73**, 117-123
74. Bordier, Franck. *et al.* Large  $\alpha$ -Aminonitrilase Activity Screening of Nitrilase Superfamily Members: Access to Conversion and Enantiospecificity by LC-MS. *Journal of Molecular Catalysis B: Enzymatic*, 2014, **107**, 79-88
75. Ji, Yuan. *et al.* Taxol-producing Fungi: A New Approach to Industrial Production of Taxol. *Chinese Journal of Biotechnology*, 2006, **22**, (1), 1-6
76. Ran, Ningqing. *et al.* Recent Applications of Biocatalysis in Developing Green Chemistry for Chemical Synthesis at the Industrial Scale. *Green Chemistry*, 2008, **10**, (4), 361-372
77. Lelais, Gérald. & Seebach, Dieter.  $\beta$ -Amino acids—Syntheses, Occurrence in Natural Products, and Components of  $\beta$ -peptides. *Biopolymers*, 2004, **76**, (3), 206-243
78. Riaz, Nagina. Naveed. *et al.*  $\beta$ -Amino Acids: Role in Human Biology and Medicinal Chemistry - A Review. *Medicinal Chemistry*, 2017, **7**, (10), 302-307
79. Ziegelbauer, Karl. *et al.* Molecular Mode of Action of the Antifungal  $\beta$ -Amino acid BAY 10-8888. *Antimicrobial Agents and Chemotherapy*, 1998, **42**, (9), 2197-2205
80. Veitía, Maité. S. *et al.* Synthesis of Novel N-protected  $\beta$ 3-Amino Nitriles: Study of Their Hydrolysis Involving a Nitrilase-Catalyzed Step. *Tetrahedron: Asymmetry*, 2009, **20**, (18), 2077-2089
81. Han, Chao. *et al.* Nitrilase-catalyzed Hydrolysis of 3-aminopropionitrile at High Concentration with a Tandem Reaction Strategy for Shifting the Reaction to  $\beta$ -alanine Formation. *Journal of Molecular Catalysis B: Enzymatic*, 2015, **115**, 113-118
82. Rapheeha, O. K. *et al.* Hydrolysis of Nitriles by Soil Bacteria: Variation With Soil Origin. *Journal of Applied Microbiology*, 2017, **122**, (3), 686-697

## **CHAPTER 2**

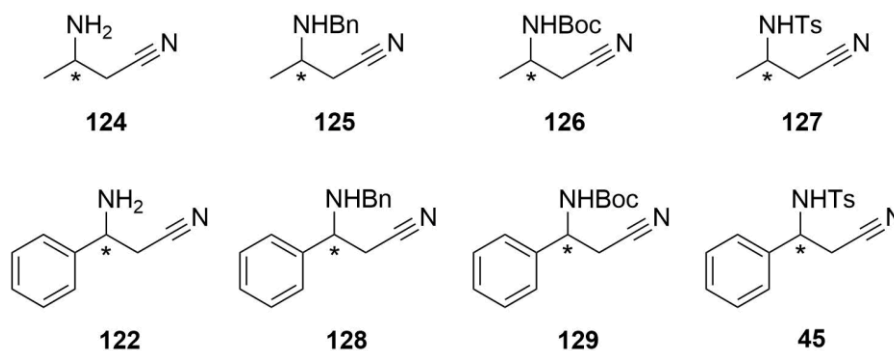
### **SUBSTRATE SYNTHESIS & HPLC METHOD DEVELOPMENT**

## SUBSTRATE SYNTHESIS & HPLC METHOD DEVELOPMENT

### 2.1 Synthesis of Substrates

#### 2.1.1 Background

Work carried out by Coady *et al* demonstrated that whole cell catalyst, bacterial isolate SET1 could selectively hydrolyse  $\beta$ -hydroxy nitriles to carboxylic acids and amides with 3-hydroxybutyronitrile (3-HBN) (**131**) in particular, yielding an ee of 99% (*S*) acid in 42% yield<sup>1</sup>. This bacterial isolate was thus thought to be promising for replicating that work using  $\beta$ -amino nitriles in order to acquire  $\beta$ -amino acids. The structures in Figure 2.1 are the range of amino nitriles proposed as substrates for this work.

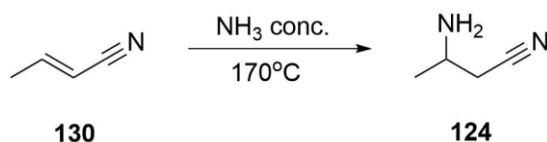


**Figure 2.1: Structures of  $\beta$ -amino nitrile substrate targets**

Firstly, both aliphatic and aromatic substrates were included to mimic the work of Coady *et al* and thus offer comparisons to the known preferences of Isolate SET1<sup>1</sup>. In this research, Isolate SET1 was shown to more selectively and efficiently hydrolyse aliphatic over aromatic structures. Aromatic hydroxynitriles took much longer to be hydrolysed, in some cases days, compared to the aliphatic hydroxynitriles which took hours. Secondly, the protecting groups were chosen as they are commonly used in amine protection and would help provide possibly some insight into the conformation of the active sites of the enzymes<sup>2</sup>. In the work of Klempier *et al*, it was noted that the boc and tosyl groups offer synthetic advantages in that they are much easier to synthesise<sup>3</sup>. However, the addition of these groups reduces aqueous solubility meaning the addition of a solvent may be necessary to allow biotransformations to proceed effectively. This same poor aqueous solubility serves an advantage nonetheless in terms of recovery of the products<sup>4</sup>.

### 2.1.2 Synthesis of the aliphatic $\beta$ -amino nitriles

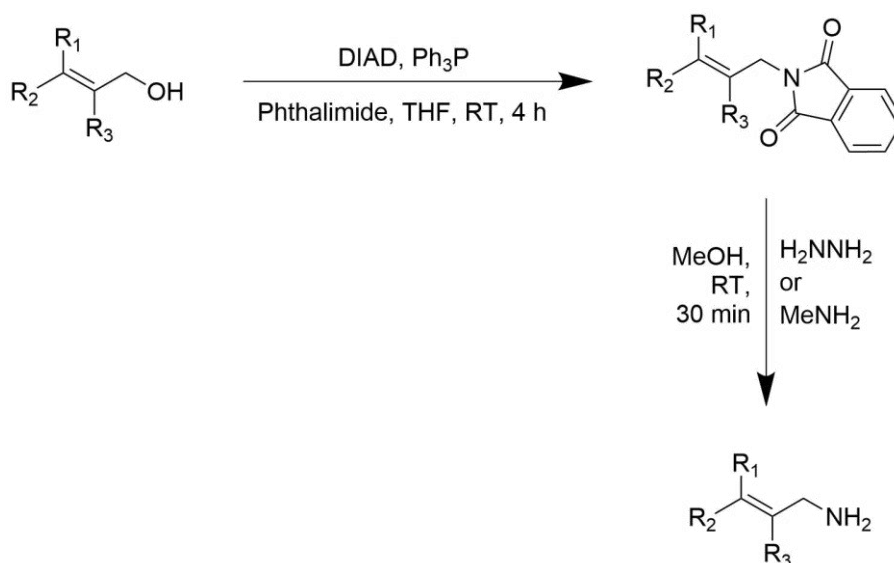
The first substrate of interest for our investigations was 3-aminobutyronitrile (**124**). It was anticipated that the synthetic approach to prepare (**124**) described by Wang *et al* would be replicable, as shown in Scheme 2.1<sup>5</sup>.



**Scheme 2.1:** Reaction of crotonitrile with ammonia as described by Wang *et al*<sup>5</sup>

This involved the conjugate addition of ammonia to crotonitrile. The experimental method however presented some challenges as a closed system with an applied heat of 170°C was detailed, which could not be reproduced. Investigations were made into conducting a microwave-assisted synthesis of substrate (**124**) but instrumental restrictions prevented this from being undertaken in a safe manner. An attempt was made using crotonitrile and ammonia in ethanol (2M) at reflux for a 24 h reaction time. The mixture was evaporated down, and water was added. The mixture was then extracted with chloroform, dried over Na<sub>2</sub>SO<sub>4</sub> and the solvent removed *in vacuo*. The product acquired was a pale-yellow oil with a crude yield of 1%. The relatively small molecular weight of the product (84.12 g mol<sup>-1</sup>) and its high water affinity possibly had an impact on extraction and thus gave a low yield. This was not purified as the TLC showed the product to be highly impure.

A two-step synthetic route to (**124**) was then evaluated inspired by Sen *et al* who used a Mitsunobu/Gabriel synthesis method to reach their targets shown in Scheme 2.2<sup>6</sup>.

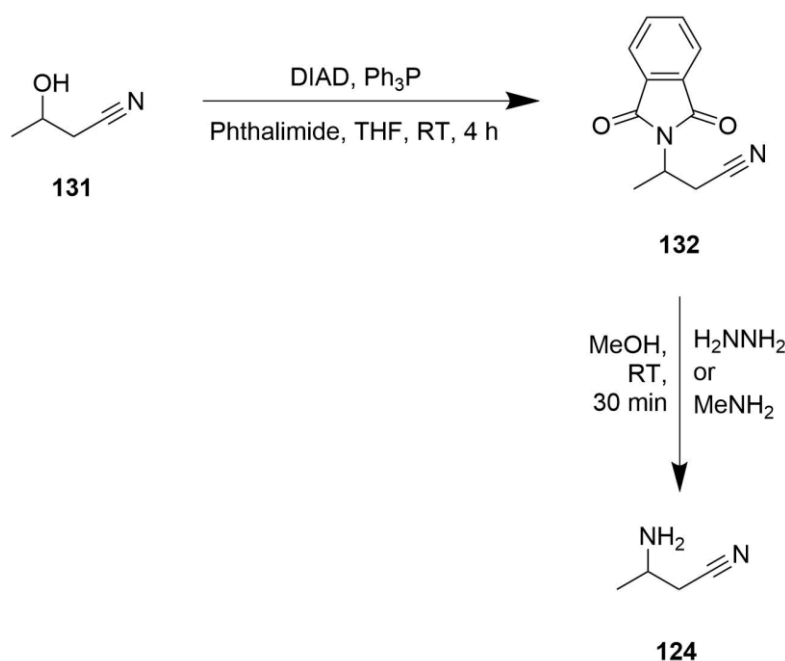


**Scheme 2.2:** General reaction scheme of the synthesis of allylic amines from tri-substituted allylic alcohols<sup>6</sup>



In their case, the combination of these two reactions allowed for exceptional yields of primary amine products. In the mechanism, diisopropyl azodicarboxylate (DIAD) forms a zwitterionic intermediate with triphenylphosphine. This intermediate reacts with phthalimide to form a 1,3-dioxoisindol-2-yl derivative. This then undergoes a mild deprotection with hydrazine or methyl amine to give the allylic amine.

To acquire our desired compound, the starting material chosen was 3-hydroxybutyronitrile (3-HBN) (**131**) which would be converted using DIAD/Ph<sub>3</sub>P into the intermediate, 3-(1,3-dioxoisindol-2-yl)butanenitrile (see structure **132** in Scheme 2.3). Deprotection could afford 3-aminobutyronitrile (structure **124**).



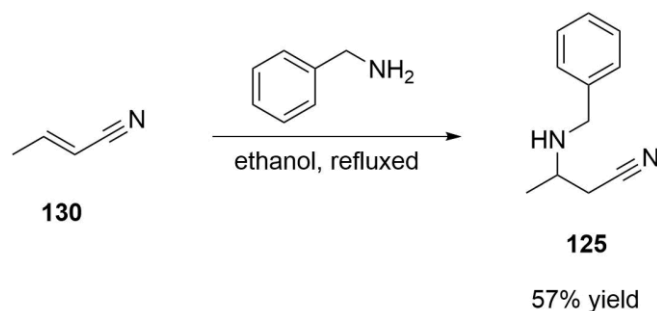
**Scheme 2.3: Mitsunobu/ Gabriel synthesis on 3-hydroxybutyronitrile to give 3-aminobutyronitrile**

The initial reaction was attempted as described by Sen *et al*<sup>6</sup>. To a solution of 3-HBN, phthalimide, and triphenylphosphine in THF, DIAD was added dropwise. This was left to stir at room temperature for 4 h. Water was then added, and the aqueous phase was extracted with hexane. The reaction was unsuccessful as no product was detected by LC-MS. Next, staggered additions of the starting material, in order to improve reactivity was evaluated. Here, DIAD was added dropwise to a solution of triphenylphosphine in dry THF and stirred for 5 min, 3-HBN was then added and the mixture stirred for 5 min. Finally, phthalimide was added and reaction stirred for 4 h. No product was observed by mass spectrometry and in a further attempt the phthalimide was added before the 3-HBN and the mixture was stirred for 10 min. Finally, 3-HBN was added and the mixture was left to stir overnight. Again, no product was observed

by mass spectrometry and the starting material, 3-HBN, was also not observed in any of the reactions by mass spectrometry. Ultimately, the lack of an easily scalable synthetic method led to the decision to purchase the expensive substrate (**124**), in this case it was supplied predominantly as the hydrochloride (HCl) salt. The supplier chosen (Enamine), offered the nitrile HCl salt existing as 70% free nitrile at pH 7. Their observations also showed that the nitrile has greater stability at pHs lower than 7. This characteristic would later be of importance regarding the biotransformations which would be required to run at pH 7 and above.

Once this starting nitrile was acquired, we then set out to synthesise the amine protected derivatives. Revisiting the Michael addition protocol from Wang *et al*, allowed us to achieve the *N*-benzyl derivative (**125**)<sup>5</sup>.

The conjugate addition protocol was followed to acquire substrate (**125**), using benzylamine. However, in this case, the reaction was found to proceed under reflux conditions, as shown in Scheme 2.5. Crotonitrile was heated to reflux with benzylamine in ethanol overnight and the solvent was removed *in vacuo*. The product was purified by silica flash chromatography using gradient elution (100% Hex to 40% EtOAc) to give a colourless oil in 57% yield.

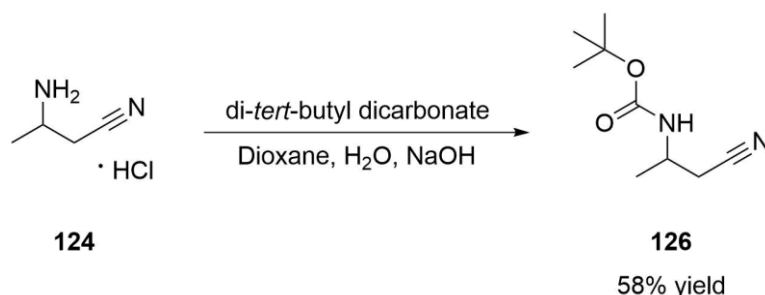


**Scheme 2.5: Synthesis of 3-(benzylamino)butyronitrile (**125**)**

This reaction yielded the protected amine which was proved by observations in the <sup>1</sup>H NMR with the aromatic protons at 7.41 – 7.30 ppm and the CH<sub>2</sub> group present in the benzyl protecting group as a doublet at 3.81 ppm. The LC-MS showed an m/z of 196.5 for the M+Na<sup>+</sup> adduct and 174.6 for the M+H<sup>+</sup> ion. This product, however, could not be separated satisfactorily by HPLC for ee determination on the available Chiralpak columns within the group under both normal and reverse phase conditions. A solution to this was found using a GITC derivatisation process which is described in the next section.

To acquire the *N*-boc derivative (**126**), an amino protection method from Chhiba *et al* was implemented, as seen in Scheme 2.6<sup>7</sup>. The HCl salt of (**124**), dioxane, sodium hydroxide (NaOH) and water were stirred together at 0°C, after which di-*tert*-butyl dicarbonate was

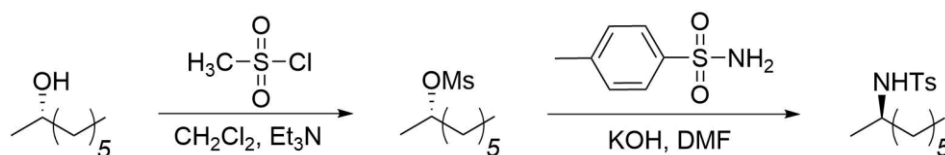
added. This was stirred at room temperature for 6 h. The solution was concentrated *in vacuo*. An acid workup was carried out, the organic solution was dried over Na<sub>2</sub>SO<sub>4</sub> and the solvent removed *in vacuo* to give a white solid in 58% yield.



**Scheme 2.6:** Boc protection of 3-aminobutyronitrile (**124**) to give 2-methyl-2-propanyl(1-cyano-2-propanyl)carbamate (**126**)

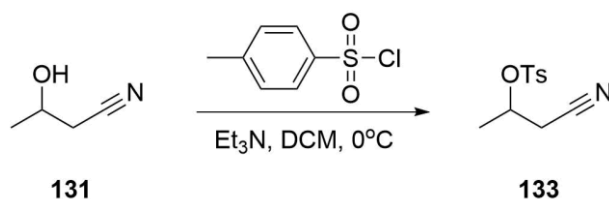
The product was positively identified by observing in the <sup>1</sup>H NMR the *tert*-butyl CH<sub>3</sub> protons integrating for 9 hydrogens at 1.52 – 1.33 ppm in addition to the expected peaks for the main aliphatic skeleton. The LC-MS also showed an m/z of 206.9 for the M+Na<sup>+</sup> adduct and 185.1 for the M+H<sup>+</sup> ion. This product, however, again could not be separated by HPLC for ee determination on the available Chiralpak columns as well as on chiral GC with a  $\beta$ -cyclodextrin column.

Two attempts were made to prepare the *N*-tosyl protected substrate (**127**), the tosyl protected derivative. The approach of Marcotullio *et al* was first applied<sup>8</sup>. Here, an alcohol was used to prepare a mesylate which was then converted with inversion to the tosyl amide directly as seen in Scheme 2.7.



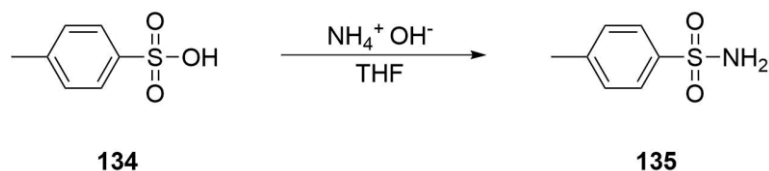
**Scheme 2.7:** Synthesis scheme of tosylamides as outlined by Marcotullio *et al*<sup>8</sup>.

Instead of initially forming a mesylate, it was decided to prepare a tosylate (**133**) from 3-HBN (**131**), shown in Scheme 2.8.



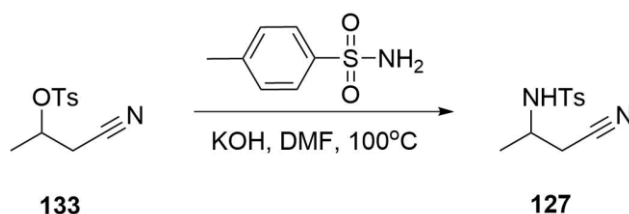
**Scheme 2.8:** Synthesis of the 3-HBN tosylate (**133**)

For the 3-HBN tosylate synthesis, 3-HBN was reacted with *p*-toluenesulfonyl chloride in DCM. This was stirred at 0°C, triethylamine was added, and the mixture was left to stir for 1 h at 0°C. The solution was then diluted with water and after an extractive workup, dried over Na<sub>2</sub>SO<sub>4</sub>, and the solvent removed *in vacuo*. The product was a pale-yellow residue with a 55% yield. This was confirmed by an observation in the LC-MS of *m/z* 240.1 for the M+H<sup>+</sup> adduct.



**Scheme 2.9: Synthesis of *p*-toluenesulfonamide<sup>9</sup>**

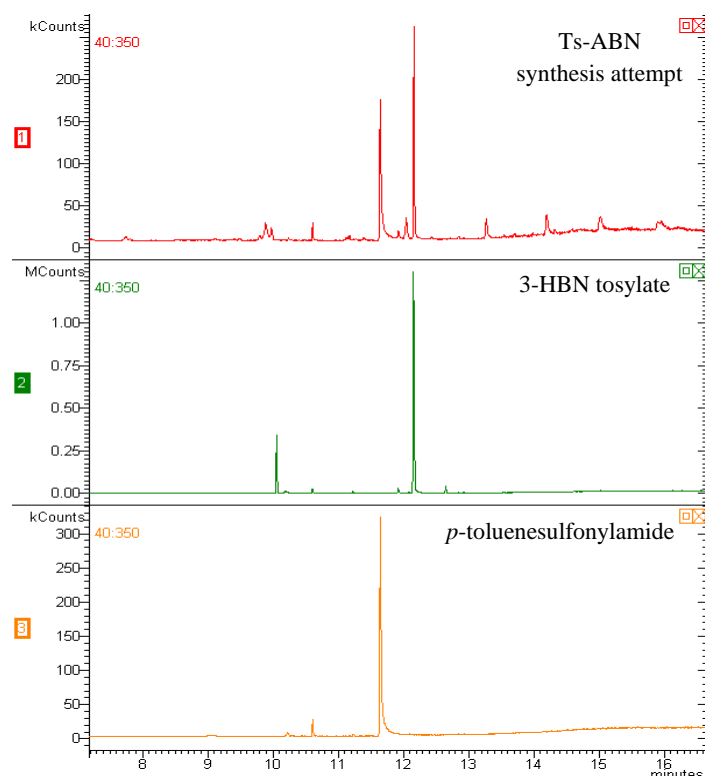
The *p*-toluenesulfonamide, for the substitution reaction, was synthesised following a method developed by Guo *et al* (Scheme 2.9) which reacted *p*-toluenesulfonyl chloride with ammonium hydroxide in THF at room temperature<sup>9</sup>. The reaction was set-up as defined in the procedure with Guo *et al*. Ammonium hydroxide (6.1 eq) was added slowly to a solution of *p*-toluenesulfonyl chloride in THF at room temperature. The reaction was stirred until no starting material could be detected by TLC. After an extractive workup, the solution was dried over Na<sub>2</sub>SO<sub>4</sub>, and the solvent removed *in vacuo*. The product was recrystallised from hexane to give a white solid in 59% yield. Successful reaction was confirmed by observations in the <sup>1</sup>H NMR of the aromatic protons at 7.80 and 7.30 ppm, the CH<sub>3</sub> protons at 2.42 ppm, and the NH<sub>2</sub> protons at 4.94 ppm. LC-MS also showed an *m/z* of 169.8 for the M-H<sup>+</sup> adduct.



**Scheme 2.10: Synthesis attempt of *N*-(1-cyano-2-propanyl)-4-methylbenzenesulfonamide (127)**

Finally, to attempt to make substrate (127), both fragments were brought together in the substitution reaction, as shown in Scheme 2.10. Here potassium hydroxide was dissolved in DMF at 100°C and the *p*-toluenesulfonamide was added. This was stirred for 30 min before 3-HBN tosylate in DMF was added. The mixture was stirred for 1 h and after an extractive workup, this was dried over Na<sub>2</sub>SO<sub>4</sub>. The solvent was then removed *in vacuo* to give a white residue. The product, however, could not be detected by mass spectrometry. From the GC-MS shown in Figure 2.2 it can be observed that the starting materials were still present at the end

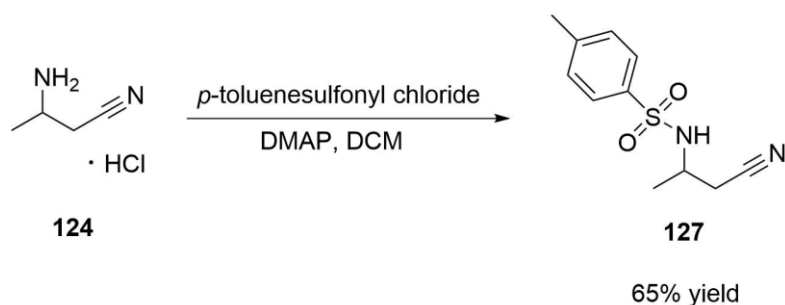
of the reaction, and it is the presence of *p*-toluenesulfonylamide that most likely gave rise to the white residue observed.



**Figure 2.2:** GC-MS chromatogram comparing the attempt to make substrate (**127**) with its starting materials, 3-HBN tosylate and *p*-toluenesulfonylamide

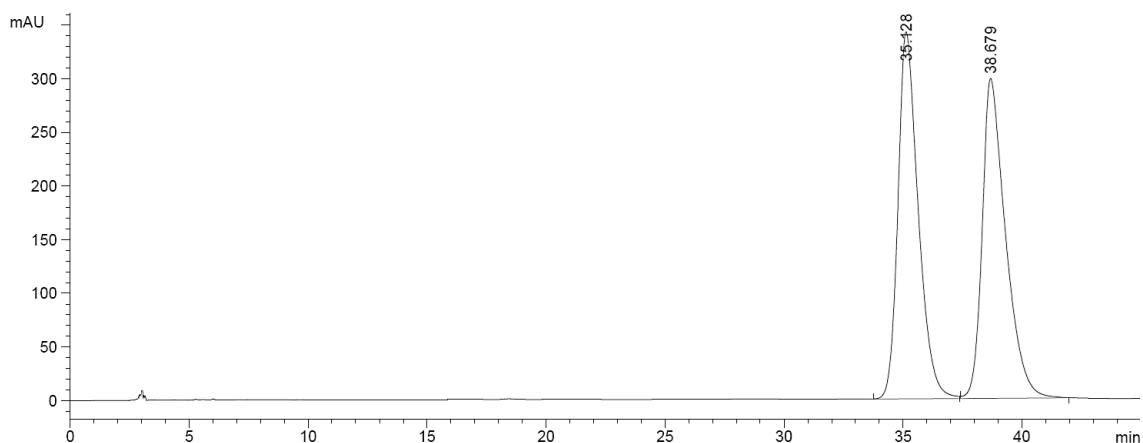
Further investigation into this method was not carried out as a decision was made to purchase 3-ABN which would yield a more facile and shorter route to the tosyl protected amine.

Once amine (**124**) was purchased, substrate (**127**) was synthesised per Chhiba *et al*'s method, as shown in Scheme 2.11, by dissolving (**124**) along with 4-Dimethylaminopyridine (DMAP) (1.3 eq) in dichloromethane and stirring that at room temperature for 5 mins to break the nitrile salt<sup>7</sup>. Following that, *p*-toluenesulfonyl chloride (1.2 eq) was added. The reaction was left to stir at room temperature over 2 days before completing an acid workup. The product was purified by silica flash chromatography using gradient elution (100% hexane to 60% EtOAc) to give a white solid in 65% yield.



**Scheme 2.11: Tosyl protection of 3-aminobutyronitrile to give *N*-(1-cyano-2-propanyl)-4-methylbenzenesulfonamide (127)**

The product was positively identified from  $^1\text{H}$  NMR observations of aromatic proton doublets at 7.76 and 7.33 ppm as well as the  $\text{CH}_3$  protons in the tosyl group as a singlet at 2.43 ppm. The LC-MS also showed  $m/z$  of 260.9 for the  $\text{M}+\text{Na}^+$  adduct and 238.9 for the  $\text{M}+\text{H}^+$  ion. This was successfully separated by HPLC for ee determination on a Chiralpak IA, mobile phase Hex:IPA 90:10,  $1.0\text{ mL min}^{-1}$ , 35.1 and 38.7 min. Baseline resolution was achieved. The HPLC chromatogram of substrate (127) is shown in Figure 2.3.



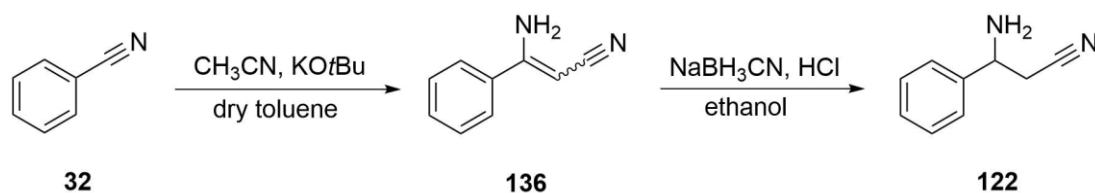
**Figure 2.3: HPLC chromatogram showing the separation of substrate (127) on an IA column. Mobile phase Hex:IPA 90:10 at a flow rate of  $1\text{ mL}\cdot\text{min}^{-1}$ .  $t_{\text{R}} = 38.7\text{ min}$  (major) and  $35.1\text{ min}$  (minor)**

### 2.1.3 Synthesis of the aromatic $\beta$ -amino nitriles

With the synthesis of the aliphatic substrates completed, the synthesis of the corresponding aromatic substrates was initiated. Analogous protecting groups to the aliphatic derivatives were used in this work.

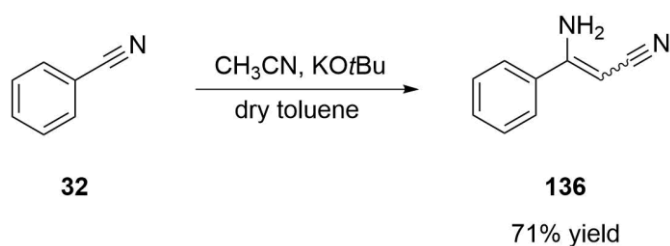
The synthesis of 3-amino-3-phenylpropionitrile (**122**) is described in a paper by Chhiba *et al* as shown in Scheme 2.12<sup>7</sup>. It was decided to adapt the method as they employ the use of sodium

cyanoborohydride, for the reduction, which is a source of cyanide and necessitates the use of highly controlled conditions. Therefore, an alternative reducing agent was necessary.



**Scheme 2.12: Reaction scheme for the full synthesis of 3-amino-3-phenylpropionitrile<sup>7</sup>**

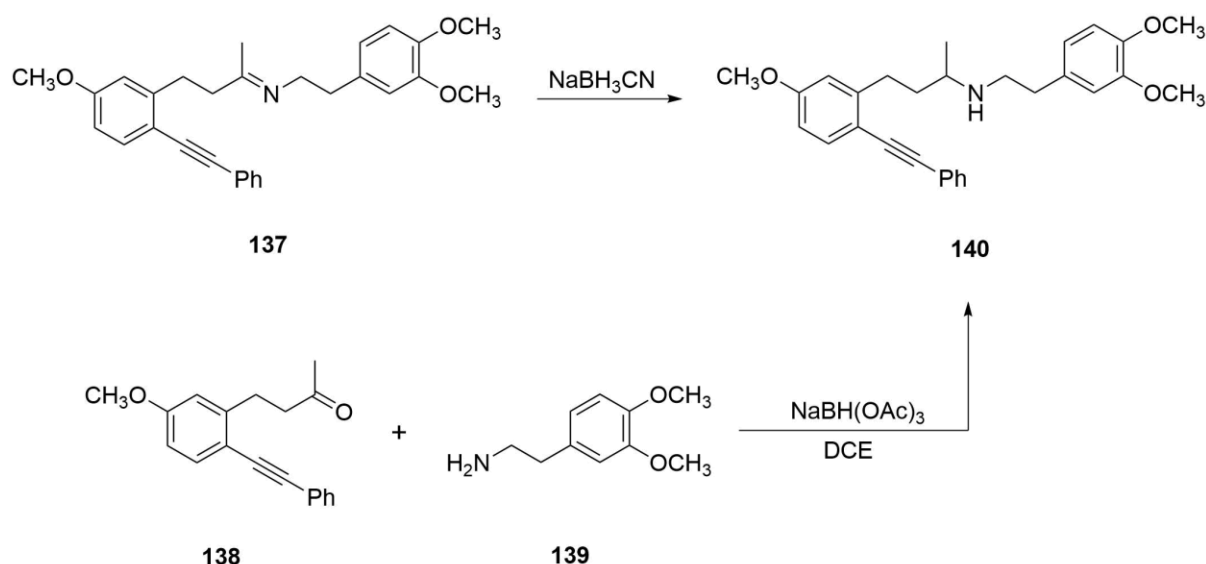
The method for synthesis of the enamine was however followed from Chhiba *et al*, as shown in Scheme 2.13<sup>7</sup>. Benzonitrile, acetonitrile (2 eq), and potassium *tert*-butoxide (2.3 eq) were dissolved in dry toluene and the mixture was stirred overnight. After an extractive workup, the organic solution was dried over Na<sub>2</sub>SO<sub>4</sub> and the solvent removed *in vacuo*. The product was purified by silica gel flash chromatography (Hex:EtOAc 70:30) to give a white solid with 71% yield.



**Scheme 2.13: Synthesis of 3-amino-3-phenylacrylonitrile**

The enamine, 3-amino-3-phenylacrylonitrile, was positively identified by observations in the <sup>1</sup>H NMR of aromatic protons at 7.53 – 7.37 ppm, the NH<sub>2</sub> protons at 4.98 ppm, and the CH vinylic proton at 4.23 ppm. LC-MS showed m/z of 166.5 for the M+Na<sup>+</sup> adduct and 144.6 for the M+H<sup>+</sup> ion.

An alternative reducing agent was investigated for the reduction in place of sodium cyanoborohydride. Here sodium triacetoxyborohydride (STAB-H, NaBH(OAc)<sub>3</sub>) was investigated which has been demonstrated to be effective in the completion of reductive amination reactions<sup>10</sup>. Literature research found the use of STAB-H was successful for the synthesis of a precursor for the then new class of calcium entry blockers, 2-ethynylbenzenealkaniamines<sup>11</sup>. This involved the formation of an imine (**137**) which was successfully reduced in high yield to give the precursor as shown in Scheme 2.14.



**Scheme 2.14: Reductive amination with STAB-H as conducted by Carson *et al*<sup>11</sup>**

In this case of our work, enamine reduction was required. Two types of attempts were made following methods adapted from the detailed review provided by Abdel-Magid *et al* on STAB-H mediated reductions<sup>10</sup>. A summary of reaction conditions for reductive amination with STAB-H on ketones and aldehydes as reviewed by Abdel-Magid *et al* is shown in Table 2.1.

**Table 2.1: Summary of reductive amination reaction methods in the review of Abdel-Magid *et al* contrasted with any modifications for our work<sup>10</sup>**

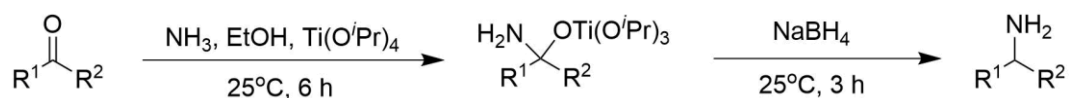
Original method	Reagents and conditions	Our modification	Reference
<b>I</b> The reagent	STAB-H purchased or prepared <i>in-situ</i> in benzene, toluene, or <i>N,N</i> -dimethylacetamide	Prepared <i>in-situ</i> in ethyl acetate	Evans <i>et al</i> <sup>12</sup>
<b>II</b> Solvent	1,2-dichloroethane, THF, acetonitrile, DMF	Ethyl acetate and acetic acid	Abdel-Magid <i>et al</i> <sup>13</sup>
<b>III</b> Stoichiometry	1.4 – 4 eq of STAB-H	1.4 eq	Abdel-Magid <i>et al</i> <sup>10</sup>
<b>IV</b> Acid effect	1 eq acetic acid	No additional acid added	Abdel-Magid <i>et al</i> <sup>10</sup>
<b>V</b> Temperature	Room temperature, 20 – 25°C	None	Abdel-Magid <i>et al</i> <sup>10</sup>
<b>VI</b> Isolation	Extraction after basification with NaOH (1 N)	None	Abdel-Magid <i>et al</i> <sup>10</sup>

The first type of attempt was in forming STAB-H *in situ* with sodium borohydride and acetic acid in EtOAc to avoid working with the more toxic benzene, toluene, or *N,N*-dimethylacetamide. The enamine, 3-amino-3-phenylacrylonitrile (1 eq) was then added to the newly formed STAB-H (1.4 eq) and the mixture was left to stir for 24 h. The reaction was

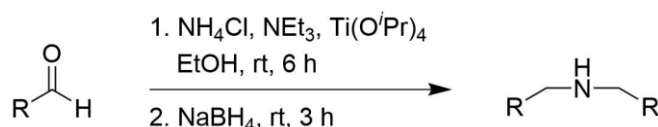


quenched with NaOH then extracted with diethyl ether. Disappointingly, no reduced product was identified by LC-MS using this approach. The second type of attempt made was as the first, but pre-formed STAB-H (1.4 eq) purchased from Sigma-Aldrich was used, and variations were made between using standard EtOAc and lab-dried EtOAc, to see if water content in the solvent would affect the STAB-H. The lab-dried EtOAc was prepared using pre-dried molecular sieves. Again, there was no evidence of reduction and no product could be detected by LC-MS using either form of solvent. The original protocol from Abdel-Magid *et al* was also tried using purchased STAB-H (1.4 eq) and dissolving the enamine (1 eq) in 1,2-dichloroethane and acetic acid (1 eq). Starting materials were recovered for both types of attempts.

At this point a modified approach to synthesise the aminonitrile was also undertaken following Miriyala *et al*'s method which involved the reductive alkylation of ammonia with various carbonyl compounds, namely ketones and aldehydes<sup>14</sup>. They employed the use of Ti(O<sup>*i*</sup>Pr) which in their case acts as a Lewis acid catalyst. The general reaction scheme for the reduction of the ketones and aldehydes is shown in Scheme 2.15 and 2.16.

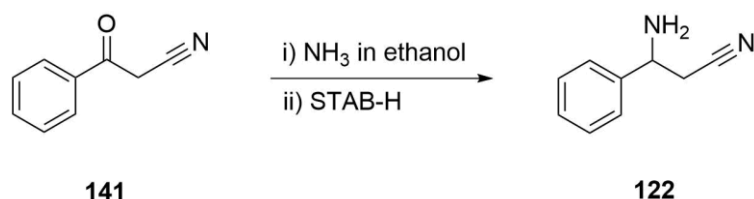


**Scheme 2.15: General reaction scheme of reduction of ketones to give primary amines**



**Scheme 2.16: General scheme of reduction of aldehydes to give the secondary amines**

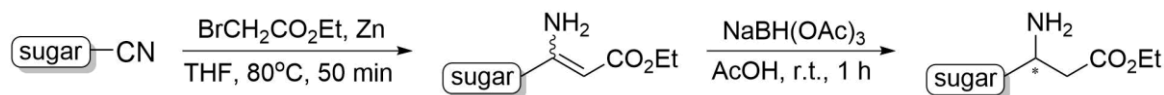
For our attempt, benzoyl acetonitrile was reacted with ammonia in ethanol (5 eq) for 6 h and initially without the Ti(O<sup>*i*</sup>Pr) stated in the method. Pre-formed STAB-H (2 eq) was added, and the mixture was reacted for a further 4 h, as shown in Scheme 2.17. The reaction was quenched with ammonium hydroxide and extracted into EtOAc. An acid workup was then carried out, followed by a basic workup.



**Scheme 2.17: Attempted synthesis of 3-amino-3-phenylpropionitrile (122) from benzoyl acetonitrile with ammonia in ethanol.**

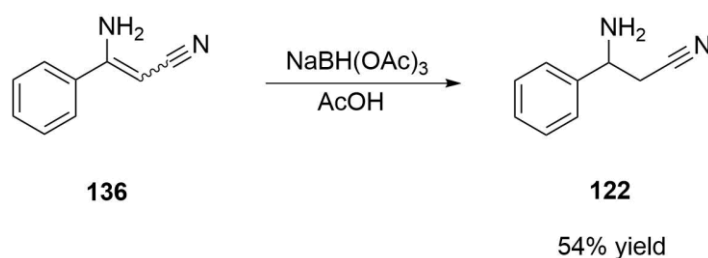
Disappointingly as before, no product was detected by LC-MS after the reaction with only starting material being recovered.

Finally, the approach from Dondoni *et al* was applied, as shown in Scheme 2.18<sup>15</sup>. In their work,  $\beta$ -enamino esters were reduced by STAB-H prepared *in situ* to  $\beta$ -amino esters. The synthesised  $\beta$ -amino esters served as intermediates to  $\beta$ -amino acids.



**Scheme 2.18:** General synthesis of (*R*) and (*S*)- $\beta$ -amino esters as described by Dondoni *et al*<sup>15</sup>

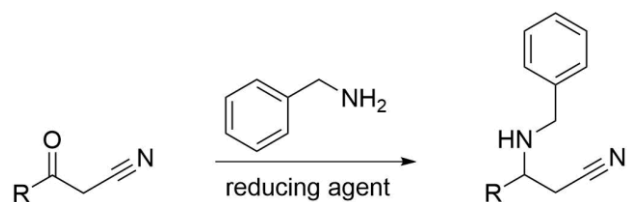
Attempts were made with minor adjustments to the workup with this method. A solution of STAB-H was prepared *in situ* by the addition of NaBH<sub>4</sub> (3 eq) to glacial acetic acid (52 eq) at 10°C. The mixture was stirred for 30 min. A solution of 3-amino-3-phenylacrylonitrile (1 eq) in glacial acetic acid was then added and the mixture was stirred for 2 h. The mixture was concentrated *in vacuo* then NaOH was added. Extraction was carried out with EtOAc and the product was purified by silica flash chromatography (Hex:EtOAc 70:30) to give a pale-yellow oil in 54% yield, as shown in Scheme 2.19.



**Scheme 2.19:** Synthesis of 3-amino-3-phenylpropionitrile (**122**)

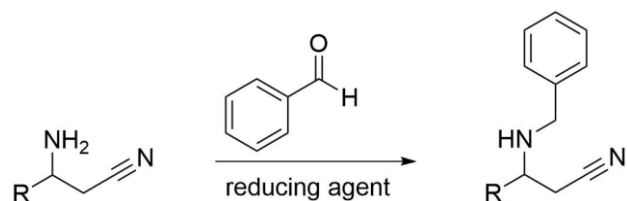
The product was confirmed by observations in the <sup>1</sup>H NMR of the absence of vinylic protons, the presence of the CH proton at 4.31 ppm and the CH<sub>2</sub> protons at 2.75-2.58 ppm. LC-MS showed m/z of 168.9 for the M+Na<sup>+</sup> adduct and 147.0 for the M+H<sup>+</sup> ion.

In order to synthesise substrate (**128**), the benzyl aromatic derivative, a series of methods were applied to generate the protected product, with modifications in each case to try to promote the reduction. There are two main reductive amination approaches which were used. The first approach is with benzylamine and a ketonitrile, as shown in Scheme 2.20.



**Scheme 2.20: General reaction of a ketonitrile with benzylamine**

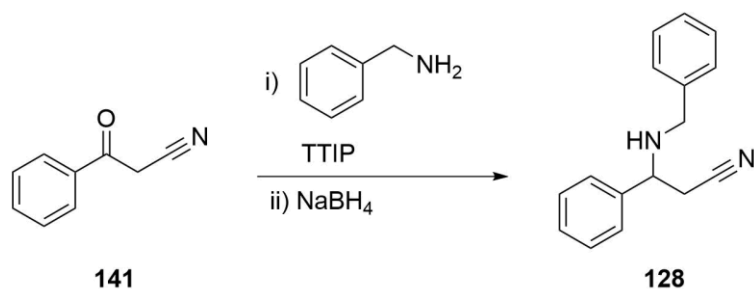
The second approach is to react an aminonitrile with benzaldehyde, as seen in Scheme 2.21.



**Scheme 2.21: General reaction of an aminonitrile with benzaldehyde**

The addition of a reducing agent is necessary in both cases as an imine forms as an intermediate with both reactions and requires reduction to reach the product. The applications of these approaches to our work are described sequentially in the following section.

The reductive amination approach from Miriyala was first applied, as shown in Scheme 2.22<sup>14</sup>.

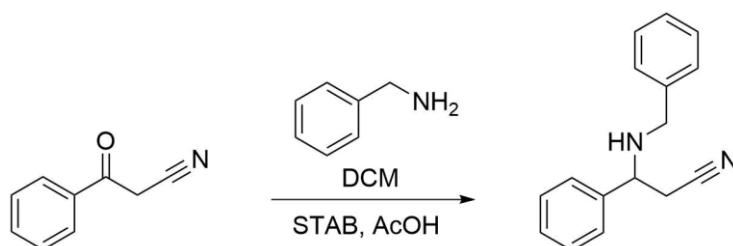


**Scheme 2.22: Synthetic approach from Miriyala *et al* to synthesise substrate (128)<sup>14</sup>.**

Benzoyl acetonitrile, titanium (IV) isopropoxide (2 eq), and benzylamine (2.3 eq), were stirred together at room temperature for 6 h under nitrogen. Sodium borohydride (1.5 eq) was added, and the mixture was stirred for an additional 3 h after which the reaction was quenched with ammonium hydroxide. The mixture was filtered, and the precipitate was washed with EtOAc. After extraction, an acid/base workup was carried out and the organic solution was dried over Na<sub>2</sub>SO<sub>4</sub>, then concentrated *in vacuo* to give a yellow liquid. This reaction was however unsuccessful as no product was detected by mass spectrometry using both GC-MS and LC-MS.

The reaction was repeated using STAB-H. Again, no product was detected by mass spectrometry in both GC-MS and LC-MS. An attempt was then made using Abdel-Magid's

approach as described previously and shown in Scheme 2.23<sup>10</sup>. This would again form the imine to be reduced *in situ*.



**Scheme 2.23: Synthesis attempt following Abdel-Magid *et al* to achieve substrate (128)<sup>10</sup>**

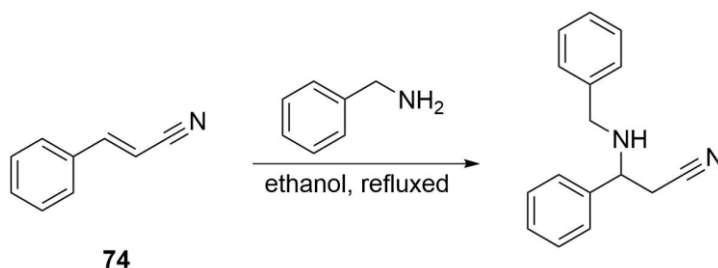
Benzoyl acetonitrile and benzylamine (1 eq) were mixed in dichloromethane. STAB-H (1.4 eq) and acetic acid (1 eq) were then added. The mixture was stirred at room temperature under nitrogen for 24 h. The reaction was quenched with NaOH and extracted with diethyl ether. The combined organic extracts were washed with brine, dried over Na<sub>2</sub>SO<sub>4</sub>, and the solvent removed *in vacuo* to give a dark yellow oil. This was also disappointingly unsuccessful with no product being detected by mass spectrometry with both GC-MS and LC-MS.

In this reaction however it did appear from analysis of the mass spectrometry from LC-MS that the imine had formed from observations of *m/z* of 235.0 for the M+H<sup>+</sup> ion and 256.9 for the M+Na<sup>+</sup>. The crude product was dissolved in methanol and treated with an additional aliquot of sodium borohydride in an attempt to reduce it. The mixture was stirred for a further 52 h. The reaction was quenched with NaOH and extracted with diethyl ether. The combined organic extracts were washed with brine, dried with Na<sub>2</sub>SO<sub>4</sub>, and the solvent was removed *in vacuo* to give a dark yellow oil. No product was detected by mass spectrometry even after this additional reaction time with only the unreacted imine being detected.

In another attempt, adjustments were made by using Method VI from Abdel-Magid *et al*<sup>13</sup>. A solution of benzoyl acetonitrile (1 eq) and benzylamine (0.3 eq) in dichloromethane was treated with STAB-H (0.6 eq) at 0°C and then the mixture was stirred at room temperature for 24 h. Additional STAB-H (0.3 eq) was then added at this timepoint, and the mixture was stirred for an additional 24 h. The mixture was then diluted with EtOAc and quenched with water. A workup at pH 7 was carried out, the organic solution was dried over Na<sub>2</sub>SO<sub>4</sub>, and the solvent removed *in vacuo* to give a dark yellow oil. The reaction was also disappointingly unsuccessful as no product was detected by mass spectrometry using both GC-MS and LC-MS.

A further modification was made again from the same paper by Abdel-Magid *et al*, which took benzoyl acetonitrile and benzylamine (1 eq) and mixed them in methanol at room temperature

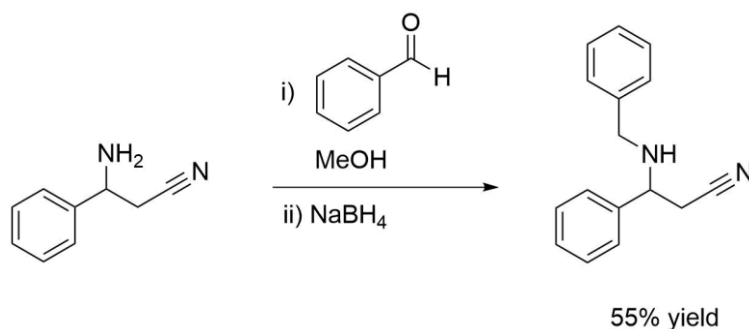
under nitrogen for 52 h<sup>13</sup>. The mixture was then treated with sodium borohydride (1.6 eq) and left to stir at room temperature for 2 h. The reaction was quenched with NaOH then extracted with diethyl ether. The combined organic extracts were washed with brine, dried over Na<sub>2</sub>SO<sub>4</sub>, and the solvent removed *in vacuo* to give a dark yellow oil. No product was detected by mass spectrometry with both GC-MS and LC-MS.



**Scheme 2.24: Michael addition approach to synthesise substrate (128)**

Up to this point, attempting to carry out reductive aminations was unsuccessful. A conjugate addition approach from Wang *et al* was then investigated and applied, as shown in Scheme 2.24<sup>5</sup>. Cinnamionitrile was heated to reflux with benzylamine (1.6 eq) in ethanol overnight and the solvent was removed *in vacuo* to give a yellow liquid. This reaction was however unsuccessful as no product was detected by mass spectrometry using both GC-MS and LC-MS.

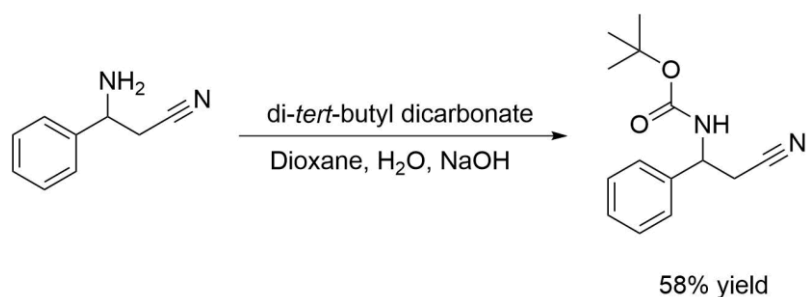
Finally, the reductive amination method of Abdel-Magid *et al* was revisited using the alternative approach of amino nitrile (**122**) and benzaldehyde as the starting material, as shown in Scheme 2.25<sup>13</sup>. The substrate 3-amino-3-phenylpropanenitrile and benzaldehyde (0.8 eq) were stirred in methanol under nitrogen for 3 h. Sodium borohydride (1.4 eq) was added, and the mixture was stirred for 2 h. This was then quenched with NaOH and extracted with diethyl ether. The combined organic extracts were washed with brine, dried over Na<sub>2</sub>SO<sub>4</sub>, and the solvent was removed *in vacuo*. The product was purified by silica flash chromatography using gradient elution (100% Hexane to 30% EtOAc) to give a colourless oil in 55% yield.



**Scheme 2.25: Successful synthesis of 3-(benzylamino)-3-phenylpropanenitrile (128)**

The product was successfully identified from observing in the  $^1\text{H}$  NMR aromatic protons integrating for 10 at 7.58 – 7.14 and the  $\text{CH}_2$  protons from the benzyl group at 2.70 ppm. LC-MS showed  $m/z$  of 258.9 for the  $\text{M}+\text{Na}^+$  adduct and 236.9 for the  $\text{M}+\text{H}^+$  ion. This could not be separated by HPLC on the available Chiralpak columns and was derivatised with GITC as will be described shortly.

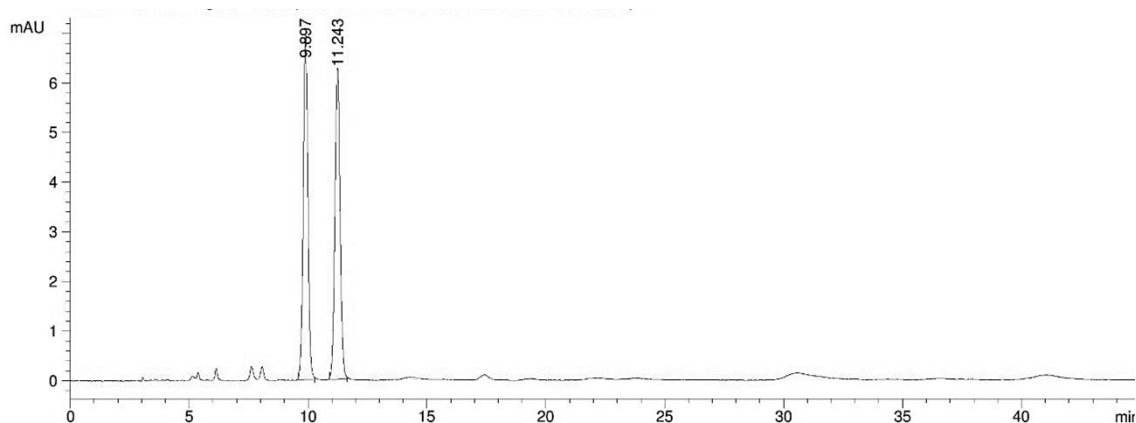
To obtain substrate (**129**), the *N*-*tert*-butyl aromatic derivative, the method by Chhiba *et al* was followed, as seen in Scheme 2.26<sup>7</sup>.



**Scheme 2.26: Synthesis of *tert*-Butyl (2-cyano-1-phenylethyl)carbamate (**129**)**

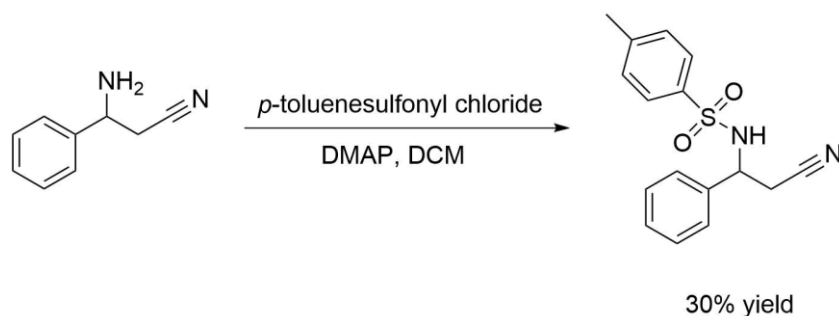
Unprotected nitrile (**122**) (1 eq) was dissolved in dioxane, water, and NaOH. Di-*tert*-butyl dicarbonate (1.1 eq) was added at 0°C and the mixture was stirred for 6 h. Solvent was removed *in vacuo* and following an extractive acid/base work up the combined organic extracts were washed with brine, dried over  $\text{Na}_2\text{SO}_4$ , and the solvent removed *in vacuo* to give a pure white solid in 58% yield.

The product was positively identified from the  $^1\text{H}$  NMR from the additional observations of the *tert*-butyl  $\text{CH}_3$  protons as a singlet integrating for 9 at 1.48 ppm. LC-MS showed  $m/z$  of 268.9 for the  $\text{M}+\text{Na}^+$  adduct and 246.9 for the  $\text{M}+\text{H}^+$  ion. This was separated by HPLC for ee determination on a Chiralpak IA, mobile phase Hex:IPA 90:10, 1.0  $\text{mL min}^{-1}$ , 9.9 and 11.2 min. Baseline resolution was achieved, as shown in Figure 2.4.



**Figure 2.4:** HPLC chromatogram showing the separation of substrate (**129**) on an IA column. Mobile phase Hex:IPA 90:10 at a flow rate of 1 mL min<sup>-1</sup>.  $t_R$  = 9.9 min (major) and 11.2 min (minor)

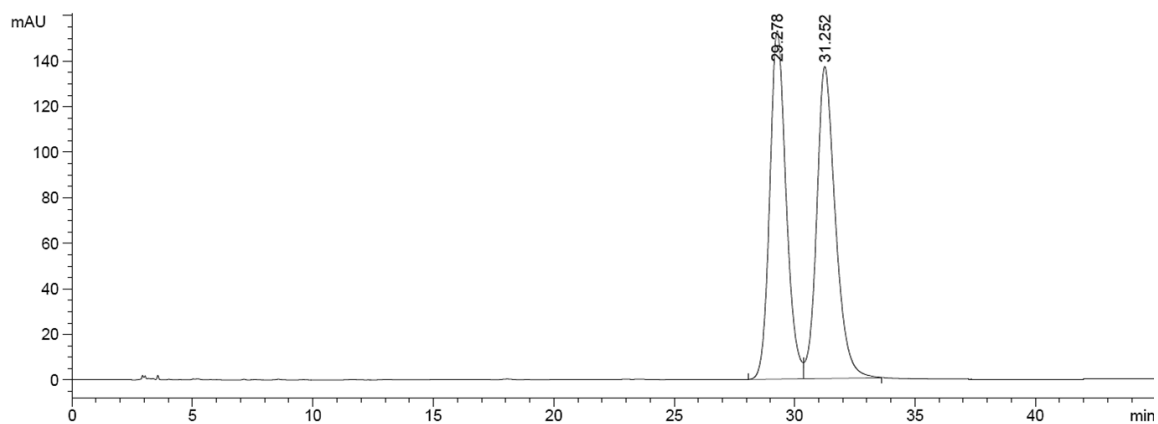
Substrate (**45**), the *N*-tosyl derivative, was synthesised following the previously described protocol by Chhiba *et al.*, as shown in Scheme 2.27<sup>7</sup>.



**Scheme 2.27:** Synthesis of *N*-(2-cyano-1-phenylethyl)-4-methylbenzenesulfonamide (**45**)

The unprotected aromatic nitrile (**122**) was dissolved in DCM, and DMAP and *p*-toluenesulfonyl chloride were added. The reaction was stirred at room temperature for 48 h. After an acid workup, the organic layer was dried over Na<sub>2</sub>SO<sub>4</sub> and the solvent removed *in vacuo*. The product was purified by silica flash chromatography using gradient elution (100% hexane to 30% ethyl acetate) to give a white solid with 30% yield.

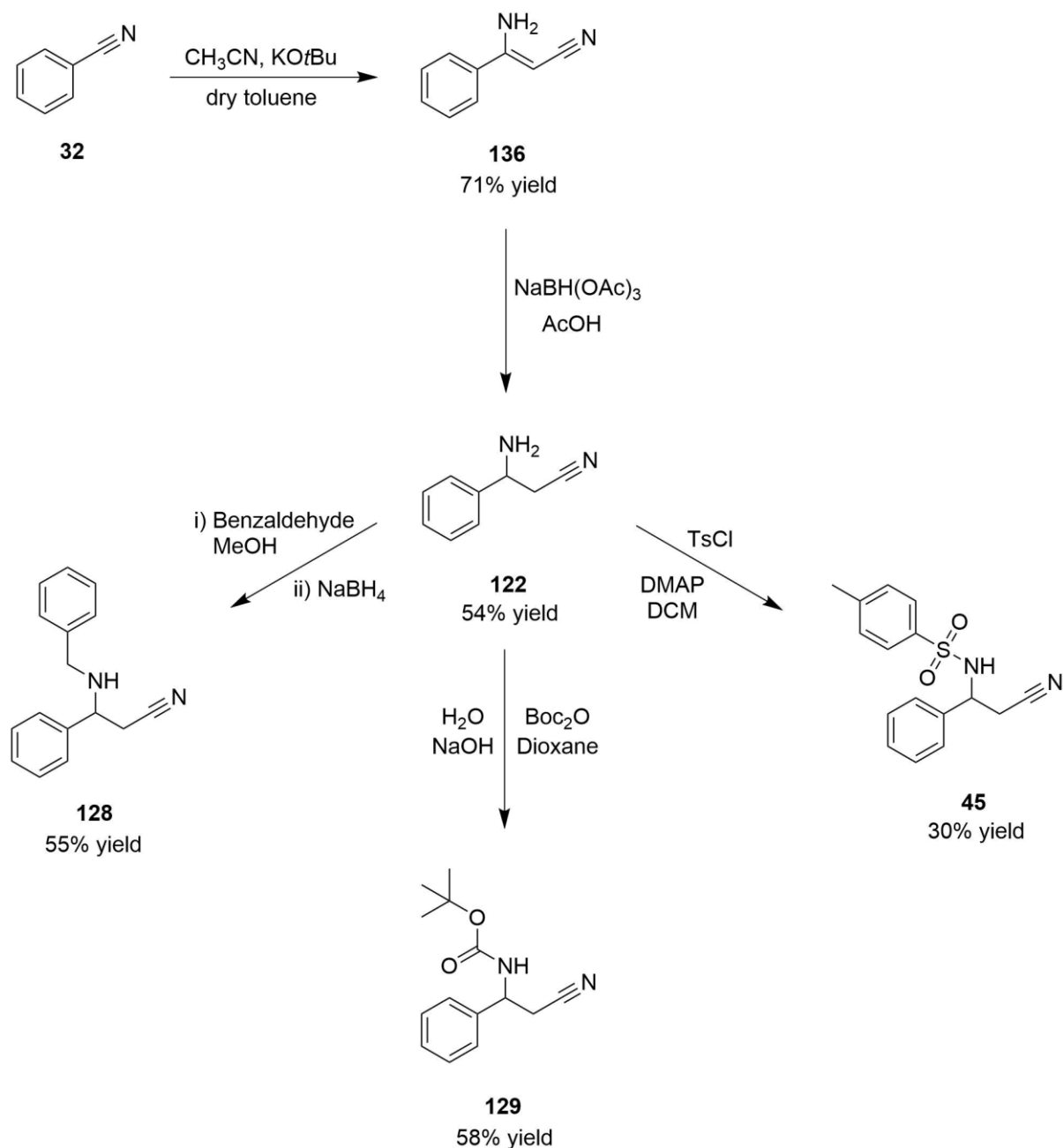
The product was identified from <sup>1</sup>H NMR observations of aromatic protons at 7.69 – 7.62, 7.29 – 7.21, and 7.12 ppm as well as the CH<sub>3</sub> protons in the tosyl group as a singlet at 2.40 ppm. LC-MS showed a *m/z* of 298.7 for the M-H<sup>+</sup> ion. This was separated by HPLC for ee determination on a Chiralpak IA, mobile phase Hex:IPA 90:10, 1.0 mL min<sup>-1</sup>, 30.2 and 32.4 min. Baseline resolution was achieved as shown in Figure 2.5.



**Figure 2.5:** HPLC chromatogram showing the separation of substrate (**45**) on an IA column. Mobile phase Hex:IPA 90:10 at a flow rate of 1 mL.min<sup>-1</sup>.  $t_R = 30.2$  min (major) and 32.4 min (minor)

A summary of the successful synthesis of the *N*-protected substrates **128**, **129**, and **45**, from benzonitrile (**32**) is shown in Scheme 2.28.



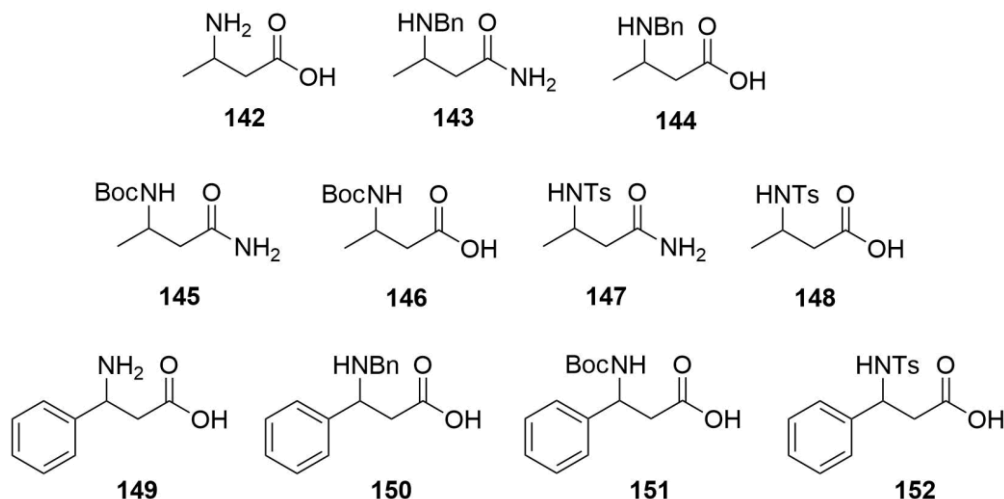


**Scheme 2.28:** Synthesis summary of the generation of the aromatic *N*-protected substrates from benzonitrile (32)

## 2.2 Synthesis of Racemic and Single Enantiomer Acid and Amide Standards and Derivatisation of Nitriles

The biotransformation products, acid and/or amide, and the nitrile substrate, needed to be separated and analysed during and after biotransformation studies thus the development of their

respective HPLC methods was necessary and will now be described. The racemic and single enantiomer nitriles, amide, and acid standards for HPLC method development required are shown in Figure 2.6. In each case the appropriate amide and acid was synthesised except for acids **142** and **149** which were purchased from TCI Chemicals.



**Figure 2.6: Proposed amide and acid standards required for HPLC method development**

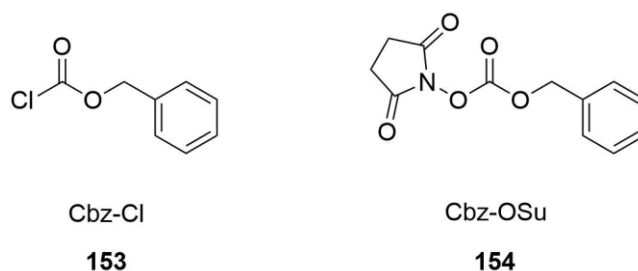
In developing HPLC methods for ee determination, the majority of these, including the starting nitriles themselves, could not be analysed in their native form for various reasons which will be described, and thus derivatisation methods were developed. It was also necessary to analyse single enantiomers of the acid standards in order to assign stereochemistry. The columns available for method development within the group were Chiralpak columns IA, AD-H, OJ-H, and AS-H, and Crownpak CR(+) and Waters Symmetry C18 columns.

### 2.2.1 Standards for compound 124

As mentioned earlier, the unprotected nitrile (**124**) was purchased as a salt which exists in its free form at 70% at pH 7. To investigate the potential recovery of the free amine form of the substrate after biotransformation salt breaks were attempted using NaOH saturated with NaCl. This entailed saturating NaOH with NaCl, adding nitrile (**124**) HCl with stirring then extracting with EtOAc. This proved unsuccessful with little to no nitrile (**124**) detected by LC-MS alluding that the recovery on extraction was problematic due to nitrile (**124**) being water soluble. This extreme water solubility coupled with nitrile (**124**) being a relatively small molecule, presenting problems with extraction, meant recovery after the biotransformation would also be particularly challenging. The molecule thus had to be modified by a protecting

group to make extraction after the biotransformation easier. The choice in protecting group should be dictated by ease of protection and removal of the group, improvement in analytical reaction monitoring and in product detection, and substrate solubility is also a factor<sup>4</sup>.

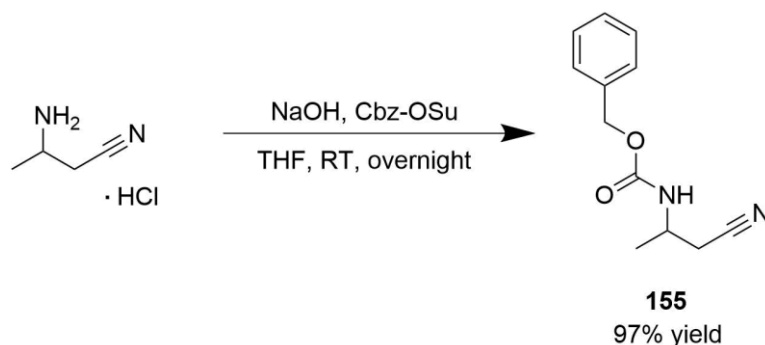
In terms of UV detection and the development of analytical methods, nitrile (**124**) also lacks a sufficient chromophore and this made the addition of a protecting group necessary. Following the work of Wang *et al*, the Cbz protecting group was added to address this<sup>5</sup>. The method calls for Cbz-Cl to be used but this is a lachrymator and is carcinogenic. At low temperatures, in the presence of moisture, it undergoes HCl degradation to give carbon dioxide. Our procedure was thus modified to use Cbz-OSu in the place of Cbz-Cl and the comparison in their structures can be seen in Figure 2.7. Cbz-OSu is less hazardous to handle and forms either an *N*-hydroxysuccinimide sodium salt or *N*-hydroxysuccinimide as by-product depending on the pH. In comparison, the use of Cbz-Cl is a relatively cleaner reaction as it mainly produces NaCl as a by-product.



**Figure 2.7: Structural comparison of Cbz-Cl to Cbz-OSu**

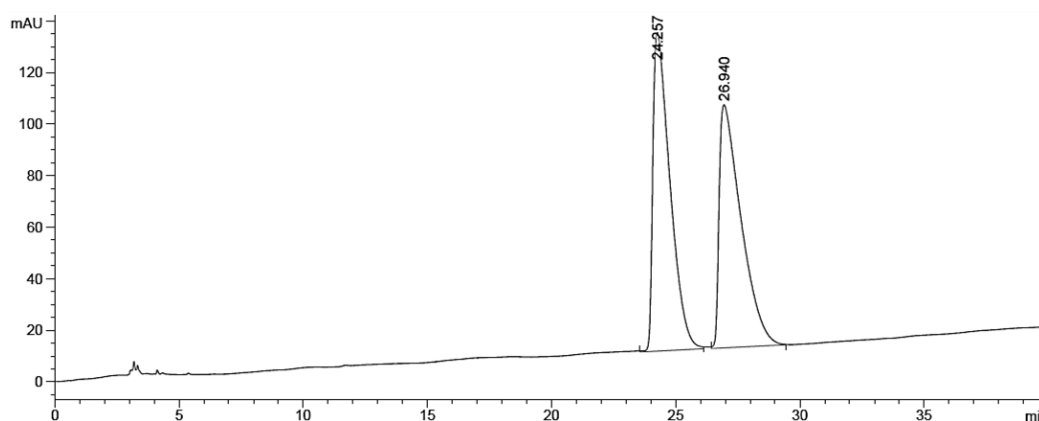
The main difference in reaction conditions is that a strong base such as NaOH is used for Cbz-Cl, whilst a weaker base like NaHCO<sub>3</sub> can be used for Cbz-OSu. More commonly in literature, the use of Cbz-Cl is reported than Cbz-OSu to add a Cbz protecting group<sup>16-18</sup>. As mentioned earlier, working with Cbz-Cl gives a cleaner reaction but Cbz-OSu is more preferable as it is less hazardous.

The protection was carried out by reacting 3-ABN.HCl dissolved in NaOH with Cbz-OSu pre-dissolved in THF, as shown in Scheme 2.29. After a basic workup, the organic layer was dried over Na<sub>2</sub>SO<sub>4</sub> and the solvent removed *in vacuo*. The product was purified by silica flash chromatography (Hex:EtOAc 80:20) to give a colourless oil in 97% yield. The product (**155**) was confirmed by additional observations in the <sup>1</sup>H NMR of aromatic protons at 7.35 ppm, and the CH<sub>2</sub> protons in the Cbz group at 5.18 – 5.03 ppm.



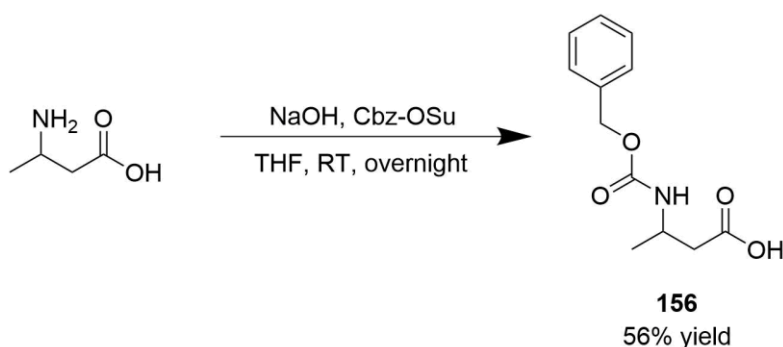
**Scheme 2.29:** Cbz protection of substrate (**124**) to give the protected nitrile standard (**155**), Benzyl (1-cyano-2-propanyl)carbamate

The protected nitrile **155** offered much improved extraction availability for analysis and could be separated by HPLC for ee determination on a Chiralpak OJ-H column with mobile phase of Hexane:IPA 80:20 and flow rate 1.0 mL min<sup>-1</sup> to give retention times of 24.3 and 26.9 min as is evidenced in Figure 2.8. Baseline resolution was achieved, as shown in Figure 2.8.



**Figure 2.8:** HPLC chromatogram showing the separation of Benzyl (1-cyano-2-propanyl)carbamate (**155**) on an OJ-H column. Mobile phase Hex:IPA 80:20 at a flow rate of 1 mL.min<sup>-1</sup>.  $t_R = 24.3$  min (major) and 26.9 min (minor)

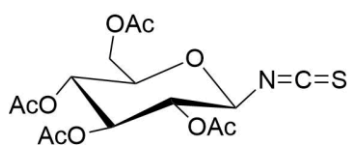
The corresponding acid standard, 3-aminobutyric acid (**142**), was purchased from TCI Chemicals and the acid was then treated the same way as the nitrile by adding on the Cbz protecting group using Cbz-OSu. The product was acquired with an acidic workup and was purified by silica flash chromatography (Hex:EtOAc 70:30) to give a colourless oil in 56% yield as shown in Scheme 2.30. The product was confirmed by observations in the <sup>1</sup>H NMR of aromatic protons at 7.40 – 7.27 ppm, the Cbz CH<sub>2</sub> protons at 5.16 – 5.01 ppm, and the acid proton at 9.93 ppm.



**Scheme 2.30: Cbz protection of 3-aminobutyric acid (142) to give the Cbz protected acid, 156**

While Cbz protection helped to solve product extraction issues, the Cbz protected acid could not be separated on the available columns (IA, OJ-H, AS-H, and CR(+)). Separation was attempted under both normal phase and reverse phase conditions as per the column requirements with varying mobile phase ratios. This meant this method would be unsuitable to determine ee and would only serve to acquire the concentration of acid in isolated product mixtures and hence determine yield. It is worth mentioning that compound **156** was found to not be very stable as degradation could be observed quickly over time as evidenced by increased spots appearing on the TLC analysis.

In order therefore, to acquire the acid ee, derivatisation was attempted using 2,3,4,6-Tetra-*O*-acetyl- $\beta$ -D-glucopyranosyl Isothiocyanate (GITC), illustrated in Figure 2.9, following the work of Mitsukura *et al* where their biotransformation product 2-methylpyrrolidine was derivatised<sup>19</sup>.



**157**

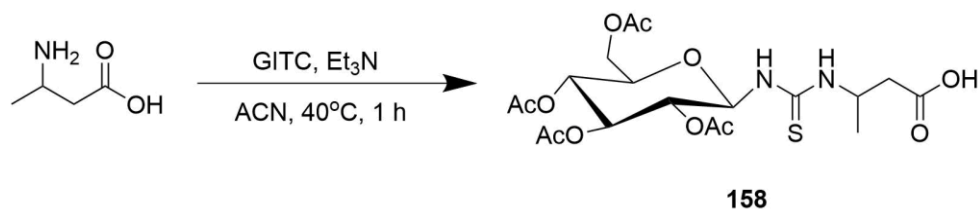
**Figure 2.9: Structure of GITC**

By adding the GITC group, this allowed them to ascertain the concentration and the optical purity of their expected product by HPLC. They reacted their sample (50  $\mu$ L) with GITC (100  $\mu$ L), and triethylamine (50  $\mu$ L, 0.2% w/v) in acetonitrile at 40°C for 1 h. No workup was done, and this was injected directly onto the HPLC.

GITC is an effective derivatising agent in HPLC analysis, particularly for amino acids<sup>20-22</sup>. There are other derivatising agents which can be used in the HPLC analysis of amino acids which have been extensively reviewed by Ilisz *et al*, such as Marfey's reagent (FDAA) or (*S*)-

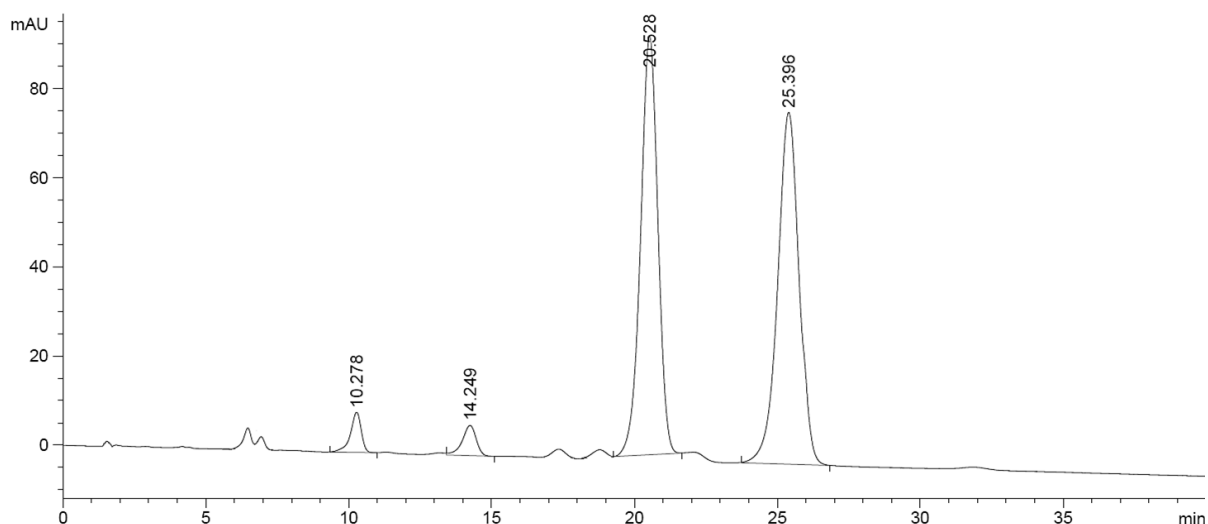
NIFE<sup>23</sup>. The use of GITC is one of the most straightforward, in comparison to Marfey's reagent which requires the reaction to be quenched with HCl before analysis can occur. Marfey's reagent also generally requires a higher wavelength for detection of 340 nm, unlike GITC which can be adequately detected around 250 nm<sup>23</sup>. The concentration of GITC can be seen to affect the diastereomers formed as observed by Nguyen *et al*<sup>24</sup>. We briefly investigated this for our latter work to determine the optimum GITC concentration and this is reported later on in Chapter 5. The reaction temperature has also been shown to possibly effect the HPLC peak areas observed as well as the production of any by-products<sup>24</sup>. This would be of merit to investigate in our future work to try and eliminate the by-product peaks we observed in our analyses.

Mitsukura's GITC method was applied directly to acid product (**142**) of interest as illustrated in Scheme 2.31. Triethylamine and GITC were added to a solution of 3-aminobutyric acid (**142**) in ACN. The mixture was left to stir at 40°C for 1 h. The mixture was injected directly into the HPLC. The product was confirmed by observations in the LC-MS of  $m/z$  493.1 for  $M+H^+$ , 515.1 for  $M+Na^+$ , and 1005.2 for  $2M^++Na^+$ .



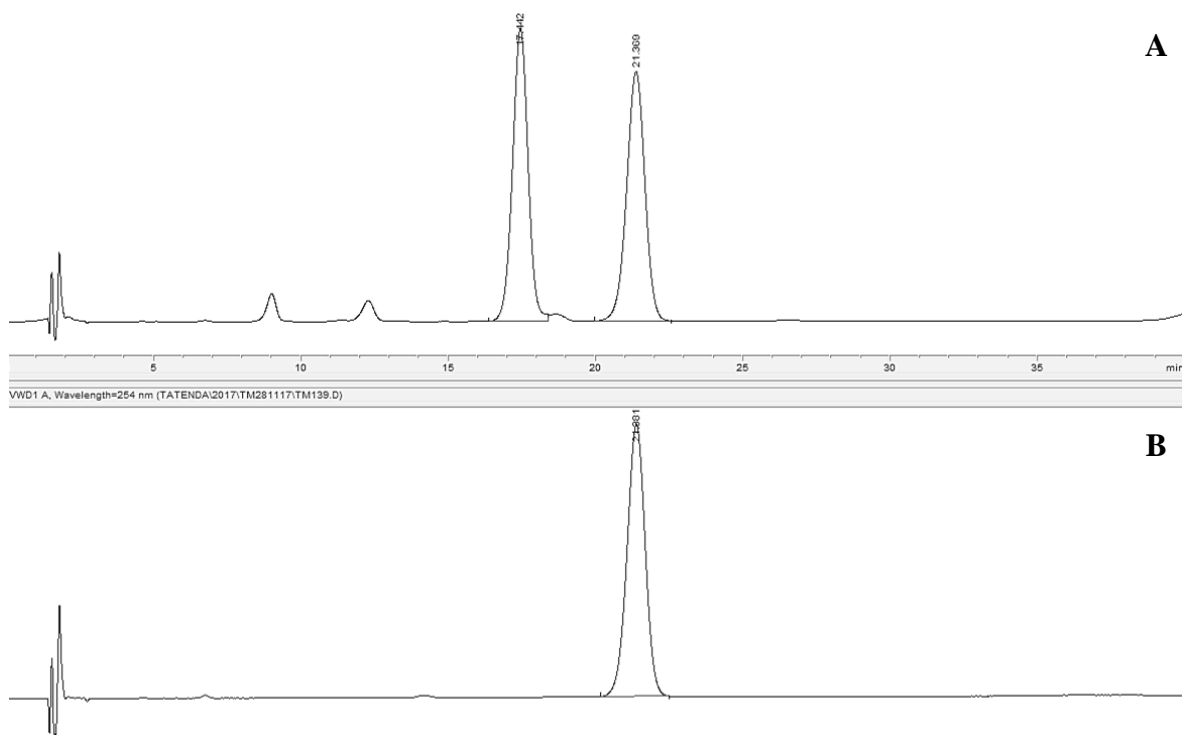
**Scheme 2.31: GITC derivatisation of acid 142 to give GITC standard 158**

This proved successful for chiral separation by HPLC as seen in Figure 2.10, and compound **158** was separated by HPLC on a Waters Symmetry C18 column, mobile phase MeOH:H<sub>2</sub>O 35:65 + 0.1% TFA, flow rate 1.0 mL min<sup>-1</sup>, to give retention times of 20.5 and 25.4 min. A single HPLC injection was carried out. Baseline resolution was achieved, as shown in Figure 2.10.



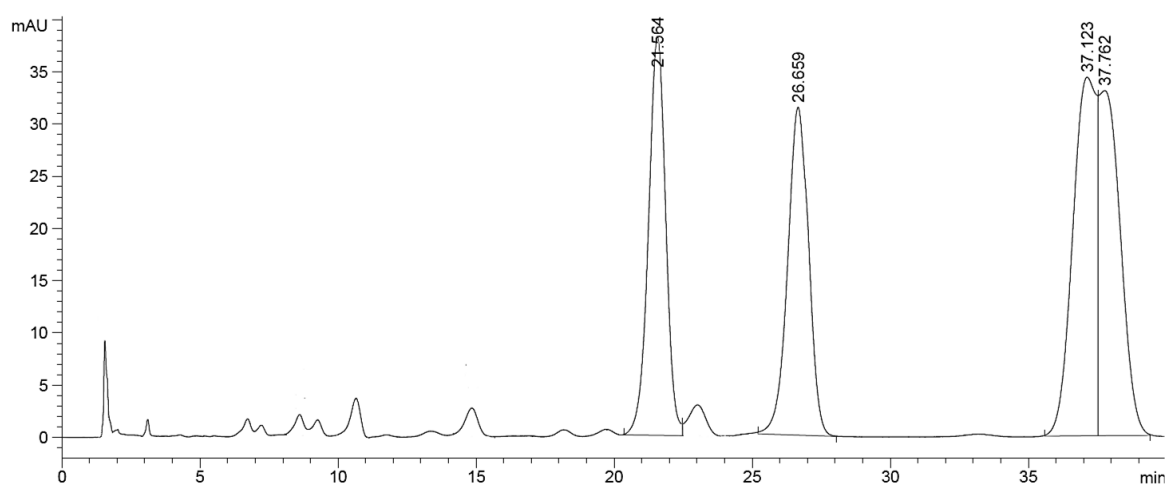
**Figure 2.10:** HPLC chromatogram showing the separation of the GITC acid standard (**158**) on a C18 column. Mobile phase MeOH:H<sub>2</sub>O 35:65 + 0.1% TFA at a flow rate of 1 mL.min<sup>-1</sup>.  $t_R$  = 20.5 min (major) and 25.4 min (minor)

The (*R*)-enantiomer of the GITC derivatised 3-aminobutyric acid (**158b**) was also prepared to facilitate configuration assignment for the biotransformations. The starting acid, (*R*)-3-aminobutyric acid was purchased from Sigma. The standard was prepared following Mitsukura's method described previously. The mixture was injected directly into the HPLC as a single injection. This allowed for configuration to be assigned to biotransformations as the acid elutes in order (*S*) then (*R*) enantiomer, as seen in Figure 2.11.



**Figure 2.11:** Comparison HPLC chromatograms of A – GITC-ABA (**158**) and B – GITC-(*R*)-ABA (**158b**) on a C18 column. Mobile phase MeOH:H<sub>2</sub>O 35:65 at a flow rate of 1 mL.min<sup>-1</sup>

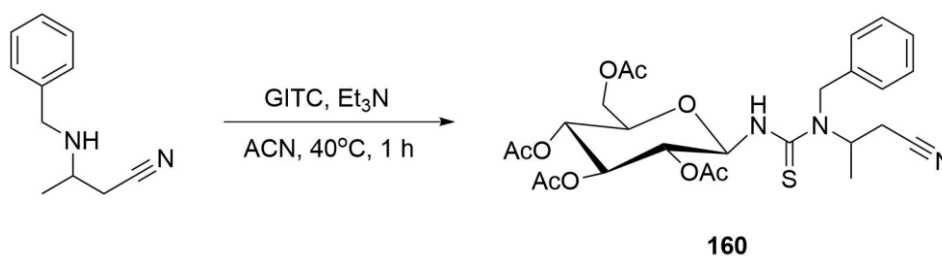
The nitrile salt (**124**) was also treated with GITC as described to allow for detection in aliquots from the biotransformations. This successfully produced the GITC derivatised nitrile (**159**) which was positively identified by observations in the LC-MS of  $m/z$  474.1 for  $M+H^+$  and 496.1 for  $M+Na^+$  adducts. The compound could not be separated on the Waters Symmetry C18 column, but its retention time was noted as 37.5 min with mobile phase 35:65 + 0.1% TFA, a flow rate of  $1.0 \text{ mL min}^{-1}$ , as a single injection, under the same conditions for the GITC acid derivative. This allowed for a mixed standard of the GITC derivatised acid and nitrile to be analysed as shown in Figure 2.12 to check for potential retention time overlap.



**Figure 2.12:** HPLC chromatogram of the mixed standard of GITC-ABA (**158**) and GITC nitrile (**159**) on a C18 column. Mobile phase MeOH:H<sub>2</sub>O 35:65 + 0.1% TFA at a flow rate of  $1 \text{ mL} \cdot \text{min}^{-1}$ . Acid  $t_R = 21.6 \text{ min}$  (major) and  $26.7 \text{ min}$  (minor), nitrile  $t_R = 37 \text{ min}$

### 2.2.2 Standards for compound 125

Unfortunately, substrate (**125**), the benzyl *N*-protected nitrile, could also not be separated satisfactorily on the available columns thus it was treated with GITC as previously described to achieve the derivatised substrate (**160**) as shown in Scheme 2.32. The product was confirmed by observations in the LC-MS of  $m/z$  for 564.2 for the  $M+H^+$  adduct and 586.2 for the  $M+Na^+$  adduct.

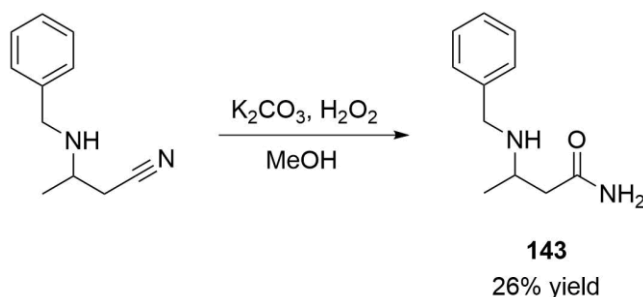


**Scheme 2.32:** GITC derivatisation of nitrile **125** to give standard **160**



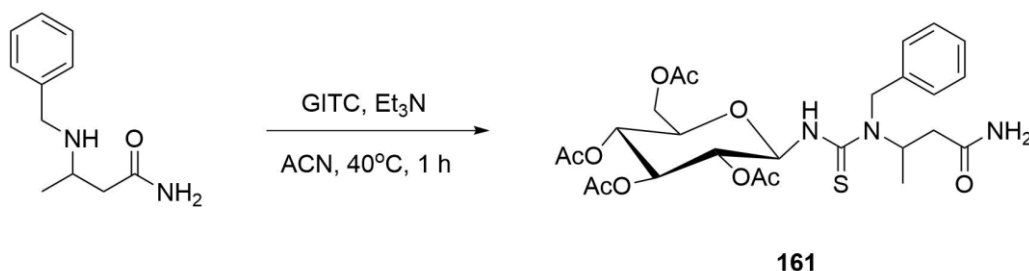
This was separated by HPLC for ee determination on a Waters Symmetry C18 column, mobile phase MeOH:H<sub>2</sub>O 50:50 + 0.1% TFA, flow rate 1.0 mL min<sup>-1</sup> to give retention times of 16.6 and 22.3 min. The resolution was 10.4 and the separation factor was 1.3.

The benzyl protected amide standard (**143**) was made by the hydrolysis of the corresponding nitrile implementing the method of Winkler *et al* as shown in Scheme 2.33<sup>25</sup>. 3-(benzylamino)butyronitrile (1 eq) was dissolved in methanol and to it, potassium carbonate (5 eq) and hydrogen peroxide (35%, 1 mL) were added. The reaction was stirred at room temperature and monitored by TLC. The product was extracted into DCM, dried over Na<sub>2</sub>SO<sub>4</sub> and the solvent removed *in vacuo*. The product was purified using C18 endcapped silica flash chromatography using gradient (100% H<sub>2</sub>O to 50% MeOH) to give a colourless oil in 26% yield. The success of the reaction was confirmed by observations in the LC-MS of m/z of 193.1 for the M+H<sup>+</sup> adduct and 215.0 for the M+Na<sup>+</sup> adduct. The product was also confirmed by observations in the <sup>1</sup>H NMR of the amide protons at 5.58 ppm, and in the <sup>13</sup>C NMR the benzyl carbons at 132.1 and 128.9 ppm for the aromatic carbons and at 67.21 ppm for the benzyl CH<sub>2</sub> carbon.



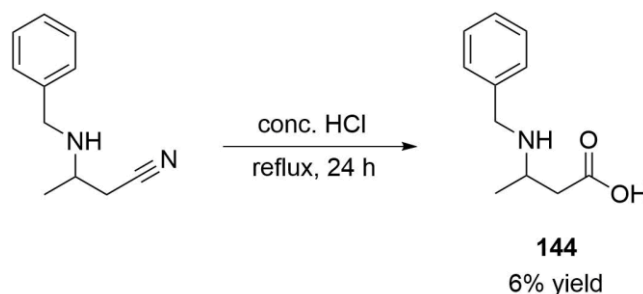
**Scheme 2.33: Synthesis of 3-(Benzylamino)butanamide (143)**

This product was again not however separable by HPLC using the available columns. It was thus treated with GITC as described previously, which allowed for successful analysis for ee determination on a Waters Symmetry C18 column, mobile phase MeOH:H<sub>2</sub>O 55:45 + 0.1% TFA, flow rate 1.0 mL min<sup>-1</sup> to give retention times of 20.7 and 24.1 min respectively. Baseline resolution was achieved.



**Scheme 2.34: GITC derivatisation of amide 143 to give GITC amide standard 161**

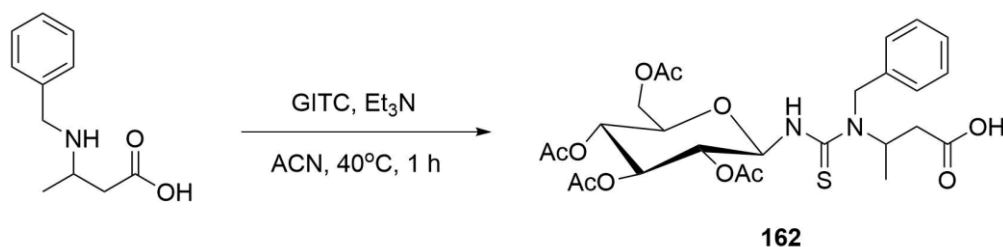
The presence of the GITC derivative was confirmed by observations in the LC-MS of  $m/z$  582.3 for  $M+H^+$  and 604.3 for  $M+Na^+$ .



**Scheme 2.35: Synthesis of 3-(Benzylamino)butanoic acid (144)**

The Benzyl protected acid standard (**34**) was formed by applying the hydrolysis method of Winkler *et al* as rendered in Scheme 2.35<sup>25</sup>. Here, 3-(benzylamino)butyronitrile was suspended in concentrated HCl and heated to reflux for 24 h. The pH was adjusted to 6 and the mixture was concentrated *in vacuo*. The product was purified by semi-preparatory HPLC (Phenomenex Jupiter C18 10  $\mu\text{m}$  column, gradient elution  $\text{H}_2\text{O}:\text{ACN} + 0.1\%$  formic acid, flow rate  $5 \text{ mL min}^{-1}$ ). The success of the formation of product was verified by observations in the LC-MS of  $m/z$  of 194.0 for the  $M+H^+$  adduct and 216.1 for the  $M+Na^+$  adduct. The product was also confirmed by observations in the  $^{13}\text{C}$  NMR of the disappearance of the CN group previously seen at 118.2 ppm for the nitrile. Unfortunately, only a very low yield of the purified product could be obtained (6%).

This could not be separated by HPLC for ee determination and was derivatised with GITC to give standard **34.1** shown in Scheme 2.35. The GITC derivative was successfully separated on a Symmetry C18, mobile phase  $\text{MeOH}:\text{H}_2\text{O} 45:55 + 0.1\%$  TFA, flow rate  $1.0 \text{ mL min}^{-1}$ , to give retention times of 11.5 and 22.6 min. Baseline resolution was achieved.



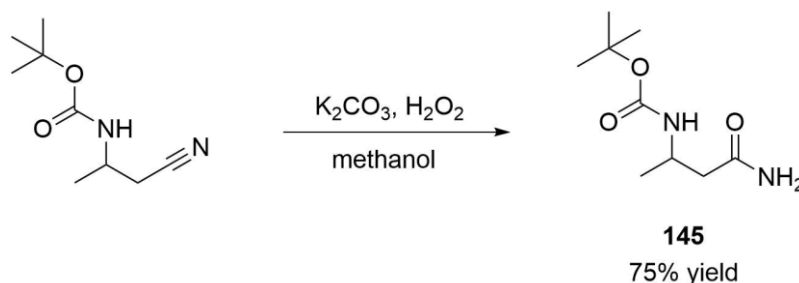
**Scheme 2.36: GITC derivatisation of acid 144 to give GITC standard 162**

The presence of the GITC derivative was confirmed by observations in the LC-MS of  $m/z$  583.3 for the  $M+H^+$  adduct and 605.2 for the  $M+Na^+$  adduct.

The single enantiomer of the *N*-benzyl protected acid could not be synthesised as the method required the starting single enantiomer nitrile, which was not purchased.

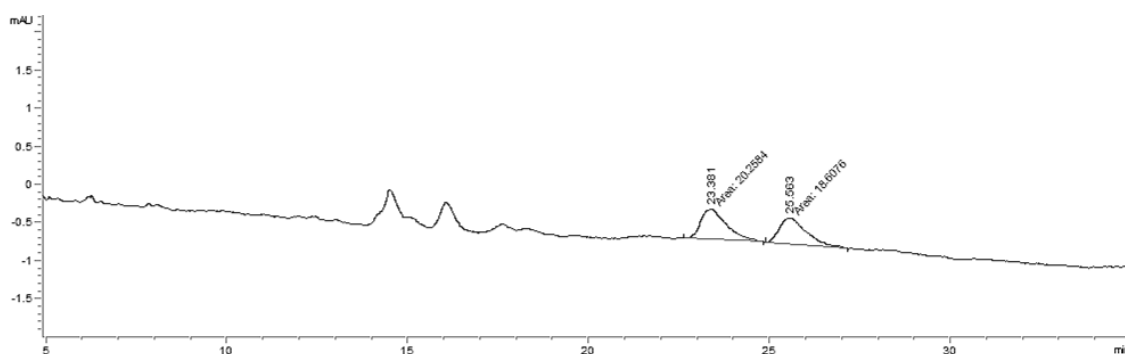
### 2.2.3 Standards for compound 126

The boc protected amide standard (**145**) was synthesised by hydrolysing the nitrile using the method of Winkler *et al*, as shown in Scheme 2.37<sup>25</sup>. The starting nitrile was dissolved in methanol and to it, potassium carbonate (5 eq) and hydrogen peroxide (35%, 1 mL) were added. The mixture was stirred at room temperature and monitored by TLC. The product was worked up using extraction, dried over Na<sub>2</sub>SO<sub>4</sub> and the solvent removed *in vacuo*. The product was purified by silica flash chromatography Hex:EtOAc (70:30) to give a white solid in 75% yield.



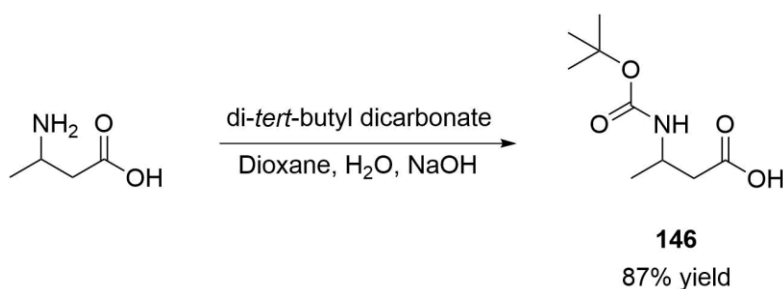
**Scheme 2.37: Synthesis of *tert*-butyl 1-carbamoylpropan-2-ylcarbamate (**145**)**

This was successfully separated without derivatisation for ee determination on the Chiralpak IA column, mobile phase Hex:IPA 97:3 + 0.1% TFA, flow rate 1.0 mL min<sup>-1</sup>, with retention times of 23.4 and 25.6 min. Adequate resolution was achieved, as shown in Figure 2.10



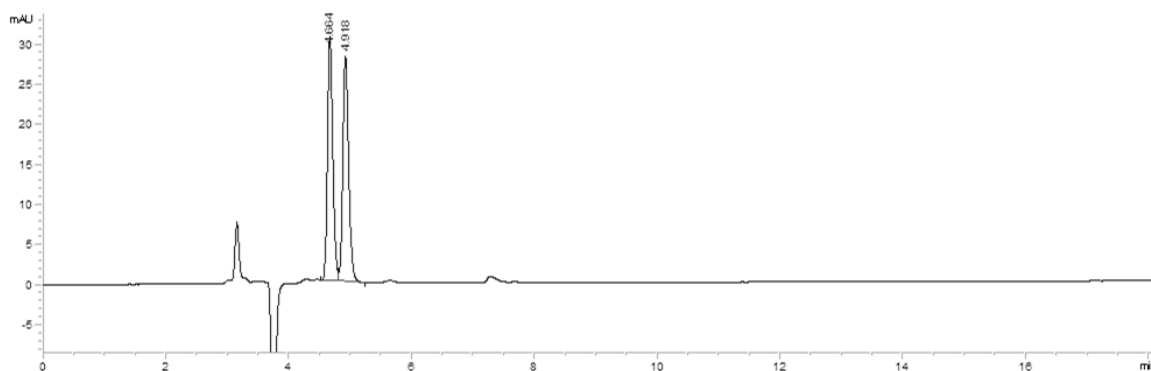
**Figure 2.10: HPLC chromatogram showing the separation of amide standard 145 on an IA column. Mobile phase Hex:IPA 97:3 at a flow rate of 1 mL.min<sup>-1</sup>.  $t_R = 23.4$  min (major) and 25.6 min (minor). Low peaks due to dilute sample**

The corresponding boc protected acid standard (**146**) was produced implementing the method of Chhiba *et al* as discussed previously and shown in Scheme 2.38<sup>7</sup>. The product was obtained as a white solid in 87% yield without purification being necessary.



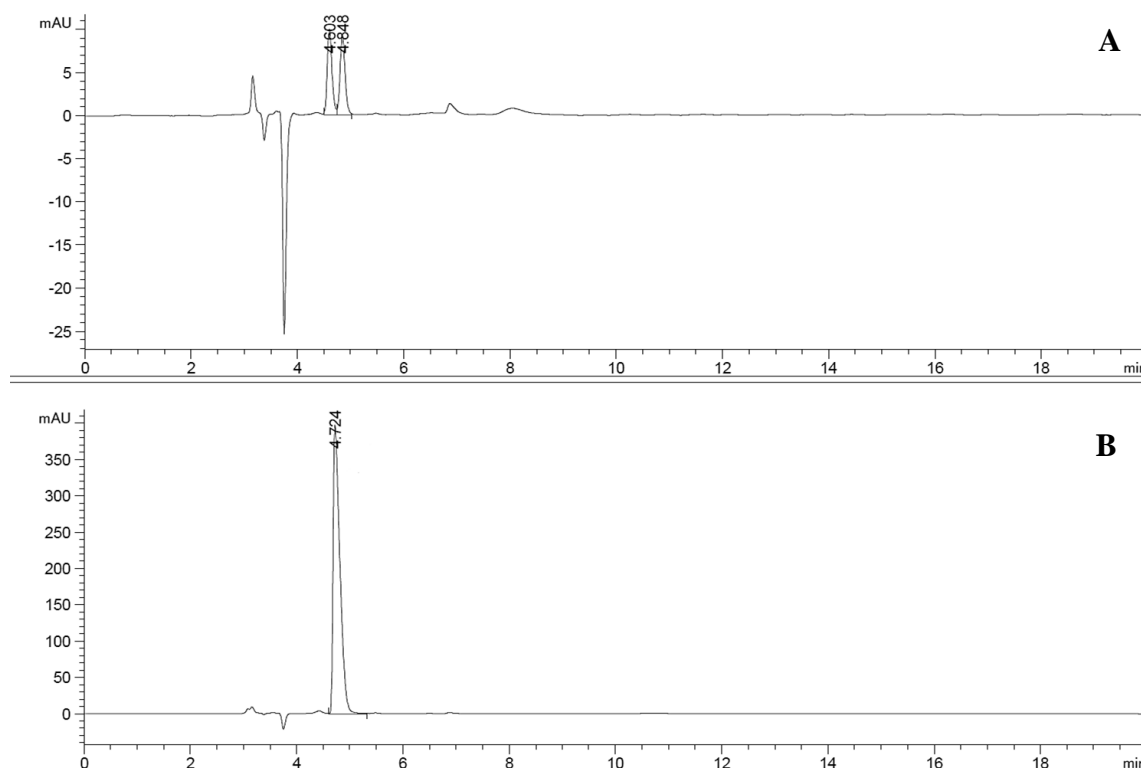
**Scheme 2.38: Synthesis of 3-((*tert*-Butoxycarbonyl)amino)butanoic acid (146)**

The acid product was confirmed by observations in the  $^1\text{H}$  NMR of *tert*-butyl protons at 1.43 ppm and the broad singlet acid proton,  $-\text{COOH}$ , at 8.44 ppm. LC-MS also showed  $m/z$  of 201.4 for the  $\text{M}-\text{H}^+$  adduct. This was successfully separated by HPLC for ee determination on the Chiralpak OJ-H column, mobile phase Hex:IPA 90:10 + 0.1% TFA,  $1.0\text{ mL min}^{-1}$ , 4.7 and 4.9 min. Adequate baseline resolution was achieved, as shown in Figure 2.11.



**Figure 2.11: HPLC chromatogram showing the separation of acid standard 36 on an OJ-H column. Mobile phase Hex:IPA 90:10 at a flow rate of  $1\text{ mL}\cdot\text{min}^{-1}$ .  $t_{\text{R}} = 4.7\text{ min}$  (major) and  $4.9\text{ min}$  (minor)**

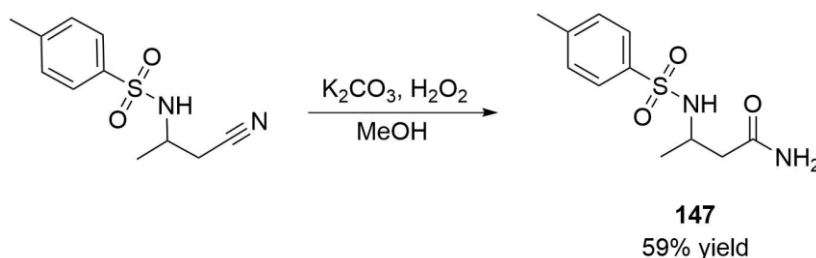
The (*R*)-enantiomer of the boc acid (**146b**) was also prepared. This was synthesised following the boc protection method of Chhiba *et al* as described previously using 3-((*tert*-Butoxycarbonyl)amino)butanoic acid in this instance, without purification<sup>7</sup>. Quite tentatively, it can be assigned from Figure 2.12 that the boc acid elutes (*S*) then (*R*) enantiomer based on previous findings with the other *N*-protected acids however, further method development would be necessary to acquire better separation of the enantiomers and thus more confidently give assignments.



**Figure 2.12:** Comparison HPLC chromatograms of A – racemic boc acid,  $t_R = 4.6$  min (major) and 4.9 min (minor), and B – boc-(*R*)-acid,  $t_R = 4.7$  min

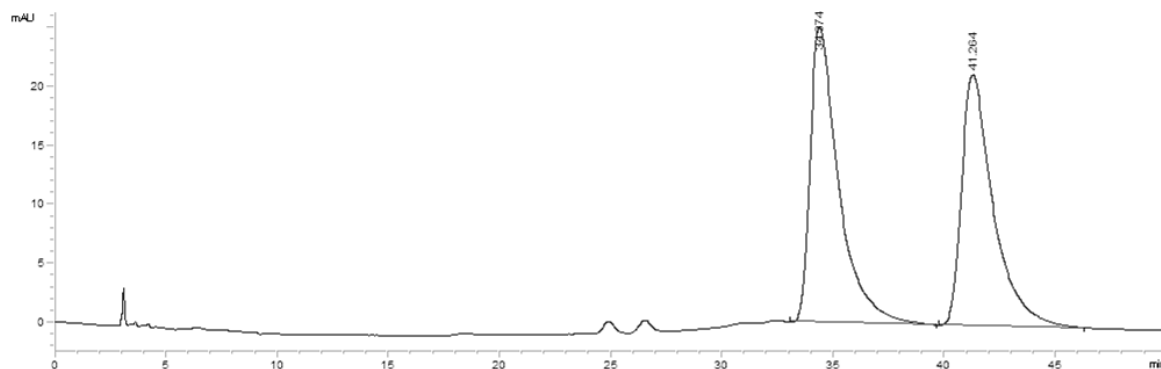
#### 2.2.4 Standards for compound 127

The tosyl protected amide standard (**147**) in Scheme 2.39, was synthesised following the hydrolysis method of Winkler *et al* as outlined previously<sup>25</sup>. The product was purified by silica flash chromatography (Hex:EtOAc 60:40) to give a white solid in 59% yield. The success of the reaction was proved by observations in the LC-MS of  $m/z$  of 256.6 for the  $M+H^+$  adduct and 278.6 for the  $M+Na^+$  adduct.



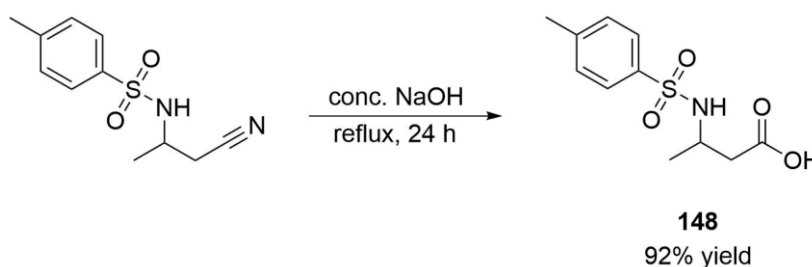
**Scheme 2.39:** Synthesis of 3-(4-methylphenylsulfonamido)butanamide (**147**)

This successfully separated on an OJ-H column, mobile phase Hex:IPA (90:10) + 0.1% TFA,  $1.0 \text{ mL min}^{-1}$ , 34.4 and 41.3 min. Baseline resolution was achieved as shown in Figure 2.13.



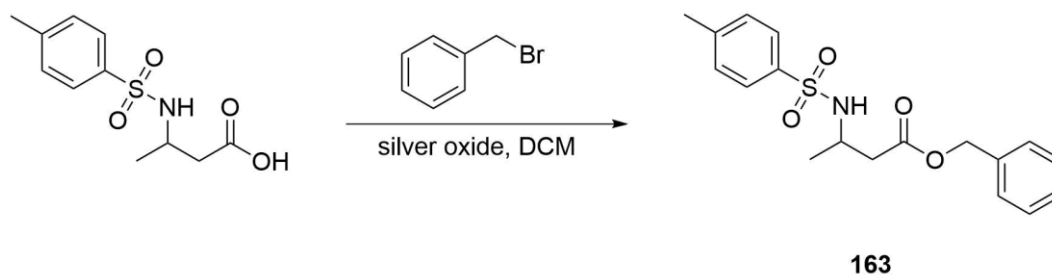
**Figure 2.13:** HPLC chromatogram showing the separation of amide standard **147** on an OJ-H column. Mobile phase Hex:IPA 90:10 + 0.1% TFA at a flow rate of 1 mL.min<sup>-1</sup>.  $t_R = 34.4$  min (major) and 41.3 min (minor).

The tosyl protected acid standard (**148**) was also synthesised as per Winkler *et al*'s method, as shown in Scheme 2.40<sup>25</sup>. The product was purified by semi-preparatory HPLC (Phenomenex Jupiter C18 10  $\mu$ m column, gradient elution H<sub>2</sub>O:ACN + 0.1% formic acid, flow rate 5 mL min<sup>-1</sup>), to give a white solid in 92% yield.



**Scheme 2.40:** Synthesis of 3-[[4-methylphenyl]sulfonyl]aminobutanoic acid (**148**)

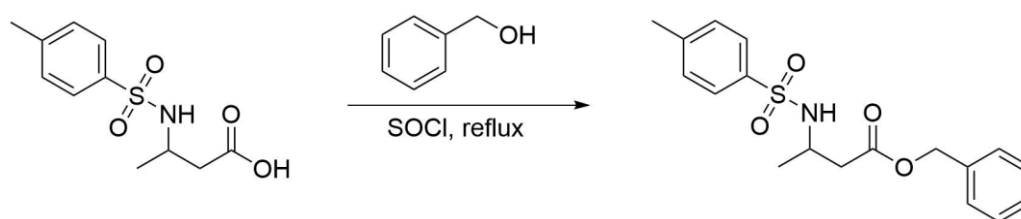
The product was confirmed by observations in the <sup>1</sup>H NMR of a broad singlet for the acid proton at 5.69 ppm and the disappearance of CN in the <sup>13</sup>C NMR which was replaced by the detection of the acid carbonyl at 172 ppm. This product was not however separable by HPLC for ee determination at the time on the available columns. Esterification procedures were then investigated to acquire a product which would be separable by HPLC. The first attempt was using the method followed by Wang *et al* in the treatment of the  $\beta$ -hydroxynitrile biotransformation products, as shown in Scheme 2.41<sup>26</sup>.



**Scheme 2.41:** Esterification attempt with benzyl bromide

3-[[4-methylphenyl)sulfonyl]amino}butanoic acid (1 eq), benzyl bromide (4 eq), silver oxide (1 eq), were dissolved in DCM and the mixture was stirred in the dark for 24 h. No product was detected by LC-MS.

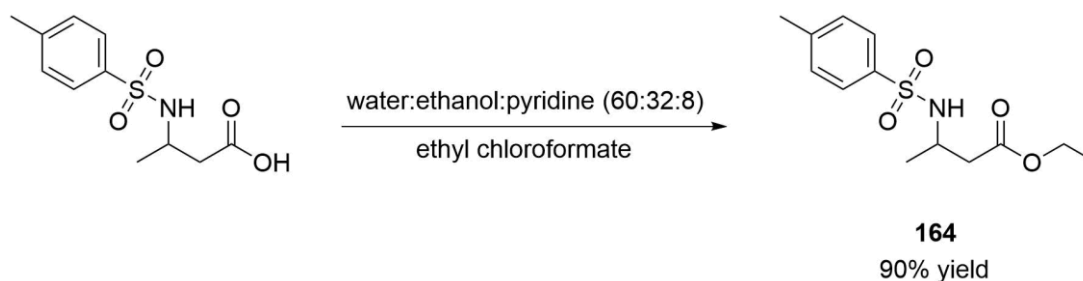
The second attempt made was with the method of Alexander *et al* who employed an esterification protocol during the synthesis of MK2 inhibitors<sup>27</sup>. Adapting this method, the tosyl acid (1 eq), thionyl chloride (2 eq), and benzyl alcohol (25 eq), were added together and heated to reflux for 24 h, as shown in Scheme 2.42.



**Scheme 2.42: Esterification attempt with benzyl alcohol**

Unfortunately, no product was detected again by LC-MS.

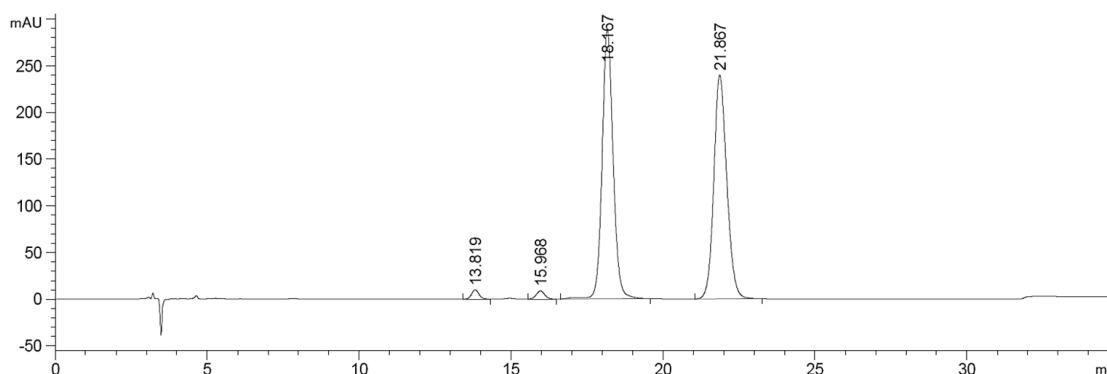
Finally, the method of Husek *et al* was employed as shown in Scheme 2.43<sup>28</sup>. They sought to develop a high throughput analysis method of native amino acids with gas chromatography. They successfully developed a rapid method to analyse all the amino acids, with the exception of arginine. More commonly in literature it is the Fischer esterification method that is applied<sup>29</sup>. In this method, a simple alcohol such as methanol or ethanol is reacted with the acid under acidic conditions. In application of the procedure, the racemic acid was dissolved in a mixture of water:ethanol:pyridine (60:32:8). Ethyl chloroformate was added and the reaction mixture was stirred for 5 min. The mixture was extracted with chloroform including 1% ethyl chloroformate. The solvent was removed *in vacuo* to give a colourless residue in 90% yield.



**Scheme 2.43: Synthesis of ethyl 3-[[4-methylphenyl)sulfonyl]aminobutanoate (164)**

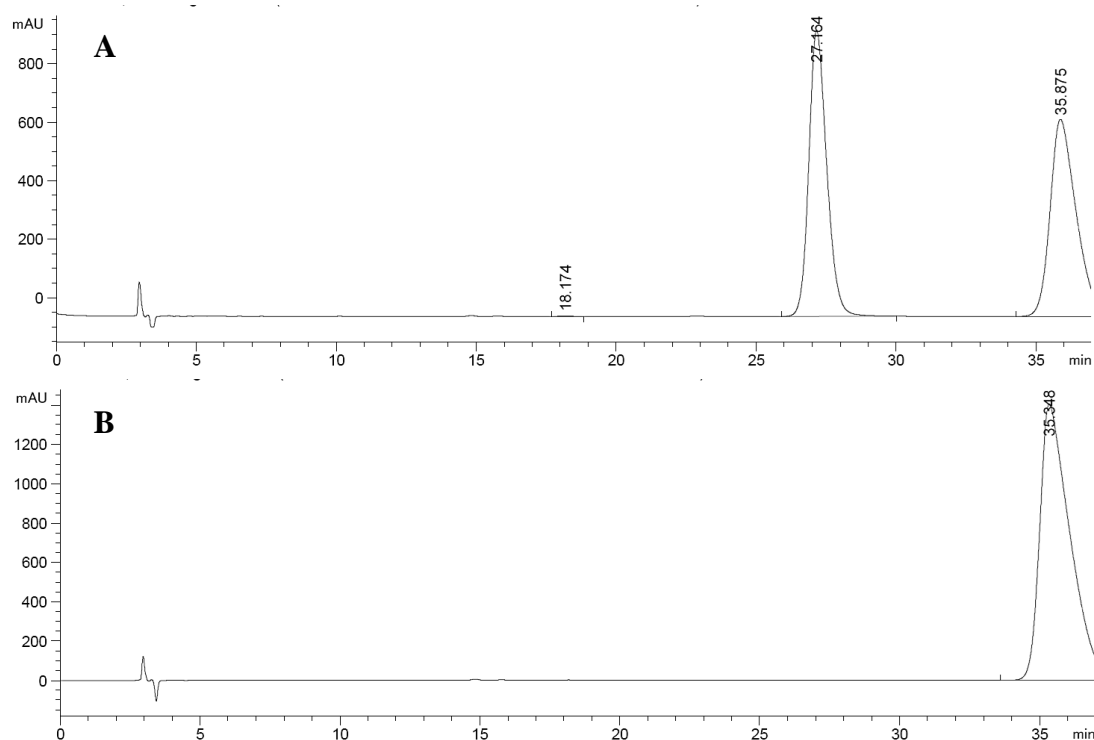
The product was confirmed by observations in the <sup>1</sup>H NMR of CH<sub>2</sub> protons in the ethyl group as a sharp quartet at 4.05 – 3.91 ppm and the CH<sub>3</sub> protons in the ethyl group as a sharp doublet at 0.98 ppm. In the LC-MS there were also observations of m/z of 286.0 for the M+H<sup>+</sup> adduct

and 308.0 for the  $M+Na^+$  adduct. This successfully separated by HPLC for ee determination on an IA column, mobile phase Hex:IPA (90:10) + 0.1% TFA,  $1.0 \text{ mL min}^{-1}$ , 18.2 and 21.9 min. Baseline resolution was achieved, as shown in Figure 2.14.



**Figure 2.14:** HPLC chromatogram showing the separation of acid standard 38.1 on an IA column. Mobile phase Hex:IPA 90:10 + 0.1% TFA at a flow rate of  $1 \text{ mL.min}^{-1}$ .  $t_R = 18.2 \text{ min}$  (major) and  $21.9 \text{ min}$  (minor).

The single enantiomer of the tosyl acid was prepared following the method of Chhiba *et al* on (*R*)-3-amino-3-phenylpropionic acid<sup>7</sup>. Near the end of our studies, it was discovered that it was now possible to separate the free racemic acid on the IA column (Hex:IPA 90:10 + 0.1% TFA). The comparison spectra of the free racemic acid to the free single enantiomer are shown in Figure 2.15. Under the same HPLC conditions, it can be observed that the (*S*)-enantiomer elutes first, followed by the (*R*)-enantiomer.



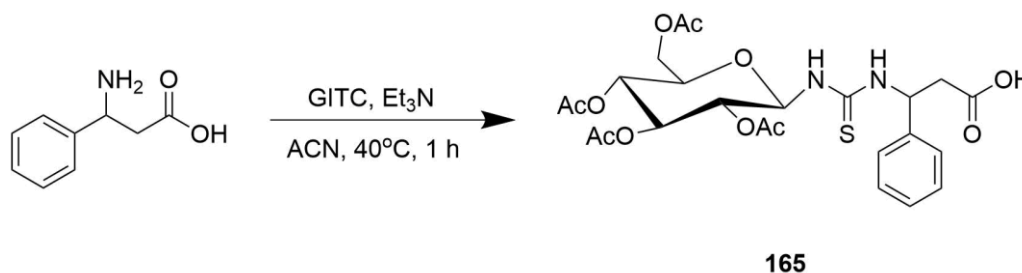
**Figure 2.15:** HPLC comparison of A – racemic Ts-ABA (27.2 and 35.9 min) to B – (*R*)-Ts-ABA (35.5 min)



### 2.2.5 Standards for compound 122

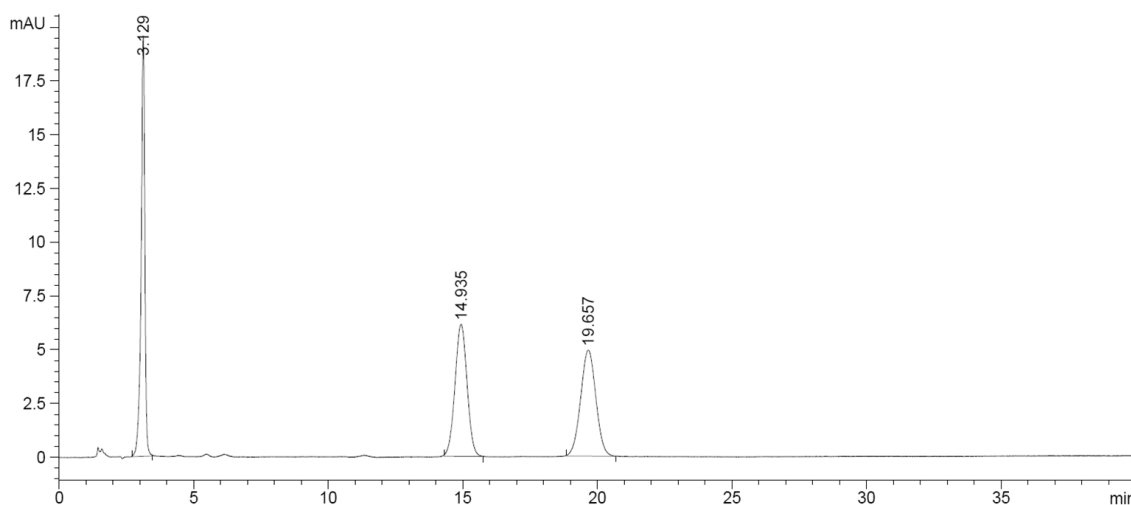
As outlined in the previous section, a series of derivatisation, protection, and hydrolysis methods were employed to obtain nitrile, acid, and amide standards and hence develop analytical standards and methods for the aromatic protected and unprotected substrates. The methods will not be described in detail in the following section to avoid repetition, but results are presented and discussed.

The acid **149**, 3-amino-3-phenylpropionic acid (3-APPA), which would be formed from 3-amino-3-phenylpropionitrile upon reaction was purchased from TCI Chemicals, but could not be separated by HPLC on the available columns in both normal and reverse phase. The GITC derivative was thus synthesised and analysed implementing the work of Bea *et al* as shown in Scheme 2.44, with evidence from LC-MS of derivatisation<sup>30</sup>.



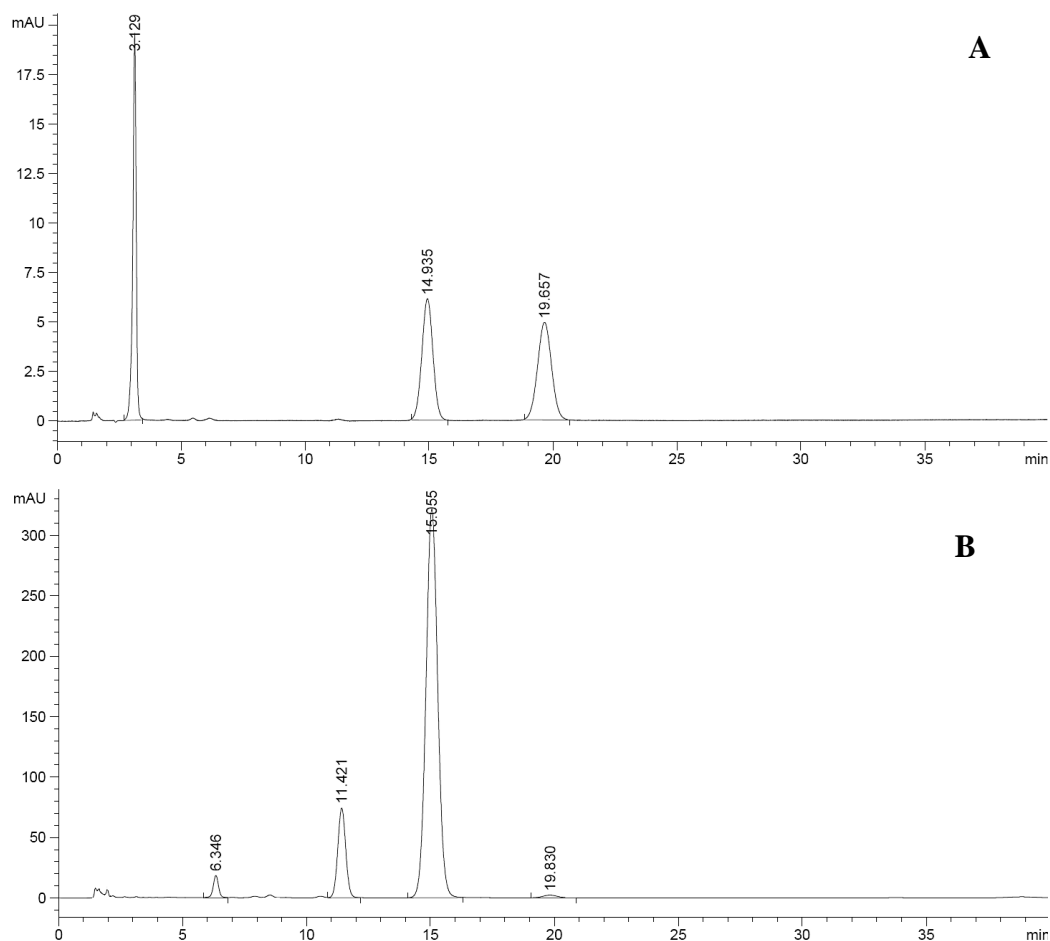
**Scheme 2.44:** Synthesis of GITC standard 165 by GITC derivatisation

This gave separation on a Waters Symmetry C18 column, mobile phase MeOH:H<sub>2</sub>O 47:53 + 0.1% TFA, 1.0 mL min<sup>-1</sup>, 14.9 and 19.7 min. Baseline resolution was achieved, as shown in Figure 2.16.



**Figure 2.16:** HPLC chromatogram of the separation of GITC acid standard 165 on a C18 column. Mobile phase MeOH:H<sub>2</sub>O 47:53 + 0.1% TFA at a flow rate of 1 mL.min<sup>-1</sup>.  $t_R = 14.9$  min (major) and 19.7 min (minor).

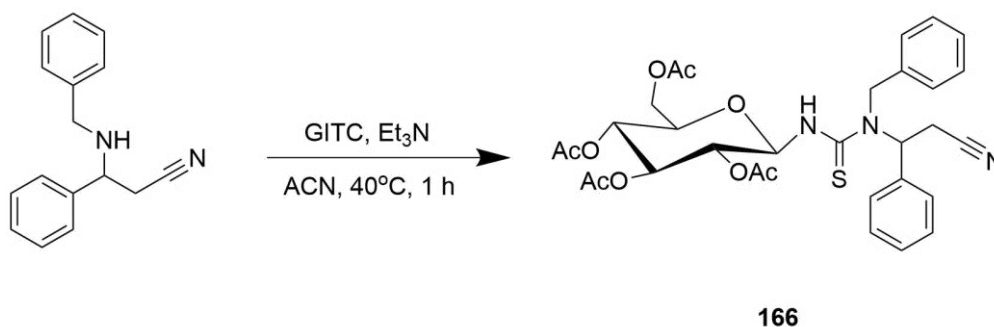
The (*R*)-enantiomer of the GITC derivatised 3-APPA was also prepared. This was synthesised following the GITC protocol of Bea *et al* as described previously using (*R*)-3-APPA as the starting material<sup>30</sup>. The comparison in spectra of the racemic acid to the single enantiomer, run under the same conditions, can be seen in Figure 2.17. It can be observed that for the aromatic unprotected acid, the (*R*)-enantiomer elutes first, followed by the (*S*)-enantiomer.



**Figure 2.17: HPLC comparison of A – racemic GITC-3-APPA to B – GITC-(*R*)-3-APPA**

### 2.2.6 Standards for compound 128

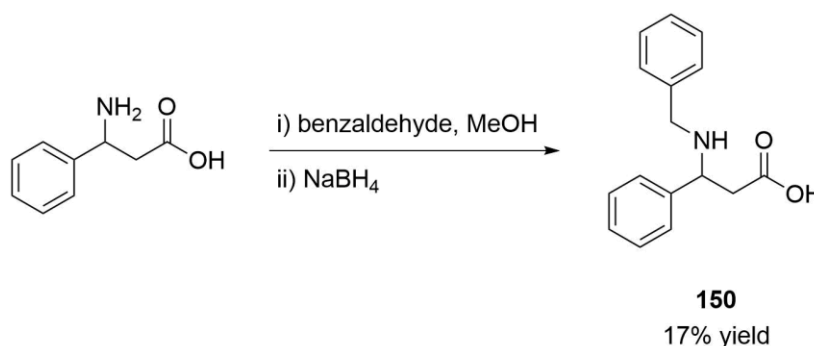
The benzyl protected nitrile (**128**) could not be separated by HPLC and was thus derivatised by GITC to give standard (**166**), as shown in Scheme 2.45.



**Scheme 2.45: GITC derivatisation of standard 128 to give standard 166**

The GITC derivative was successfully separated on a C18 Symmetry column, mobile phase MeOH:H<sub>2</sub>O (55:45 + 0.1% TFA), flow rate 1.0 mL min<sup>-1</sup>, which gave retention times of 22.6 min and 28.6 min.

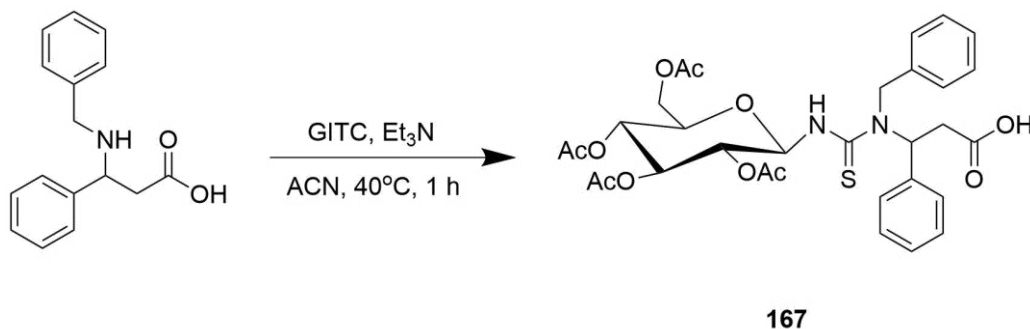
The benzyl protected acid (**150**) was prepared following the method by Abdel-Magid *et al*, as shown in Scheme 2.46<sup>13</sup>. Benzaldehyde (0.8 eq) and 3-amino-3-phenylpropanoic acid (1 eq) were stirred together in MeOH at room temperature under nitrogen for 3h. Sodium borohydride (1.4 eq) was added portion-wise and the mixture was stirred for a further 2h. The reaction was quenched with NaOH. The mixture was extracted with diethyl ether. The combined organic extracts were washed with brine, dried over Na<sub>2</sub>SO<sub>4</sub>, and the solvent removed *in vacuo*. The product was purified by silica flash chromatography using gradient elution (100% Hex to 30% EtOAc) to give a colourless oil in 17% yield.



**Scheme 2.46: Synthesis of 3-(benzylamino)-3-phenylpropanoic acid (150)**

The product was confirmed by observations in <sup>1</sup>H NMR of the CH<sub>2</sub> protons in the benzyl protecting group at 3.95 ppm and the aliphatic CH<sub>2</sub> protons separately at 3.26 and 2.92 ppm. In the <sup>13</sup>C NMR, the carbonyl carbon was observed at 184.7 ppm. The LC-MS also showed a m/z of 255.6 for the M+H<sup>+</sup> ion.

This could not be separated by HPLC for ee determination on any of the available columns and was thus derivatised with GITC to give standard (**167**) shown in Scheme 2.47. The GITC derivative was successfully separated on a Symmetry C18, mobile phase MeOH:H<sub>2</sub>O + 0.1% TFA gradient, flow rate 1.0 mL min<sup>-1</sup>, to give retention times of 11.4 and 12.6 min. Baseline resolution was achieved, as shown in Figure 2.18.



Scheme 2.47: GITC derivatisation of acid **150** to give standard **167**

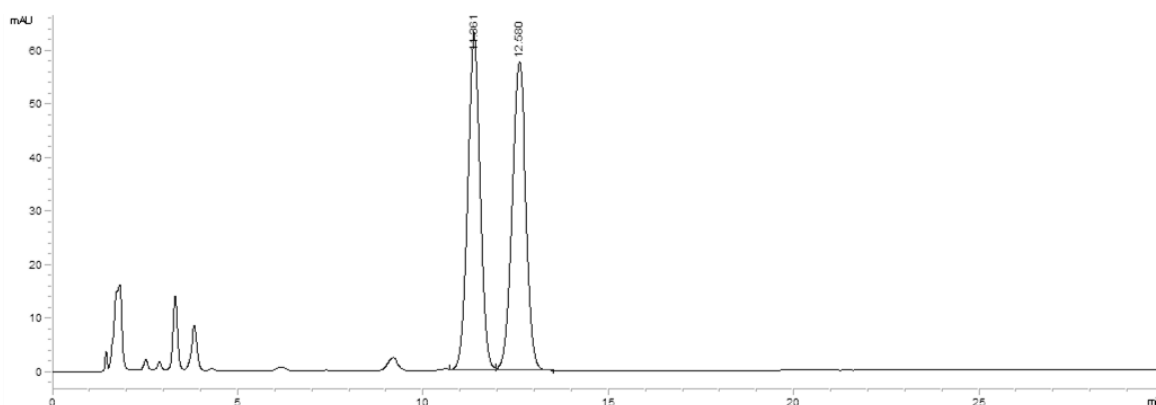


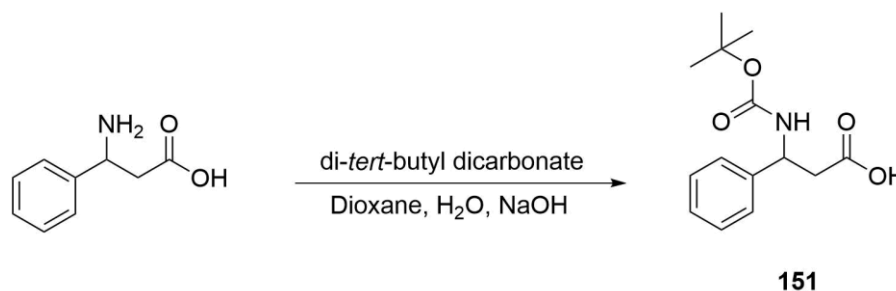
Figure 2.18: HPLC chromatogram of the separation of acid standard **167**

The single enantiomer for this acid could not be synthesised at the time as the method would have required the single enantiomer acid which had not yet been purchased.

### 2.2.7 Standards for compound 129

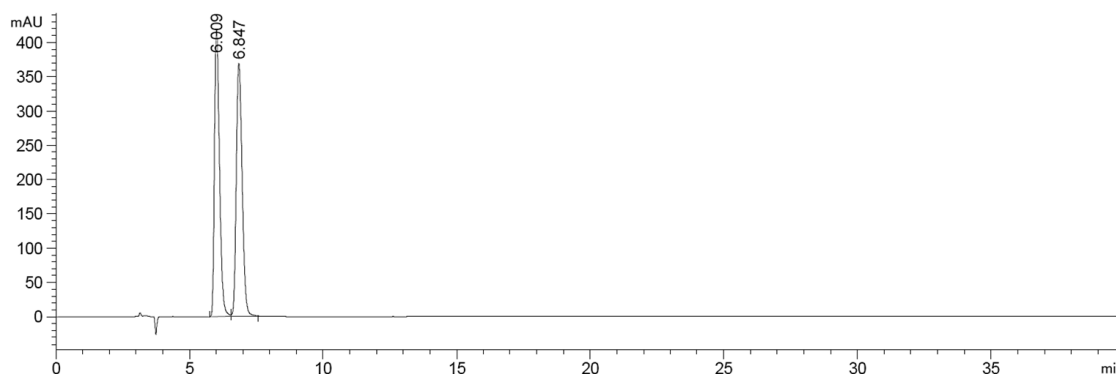
The boc protected acid standard (**151**) was produced implementing the method of Chhiba *et al* starting from the unprotected acid, as shown in Scheme 2.48<sup>7</sup>. The product was purified by silica flash chromatography (Hex:EtOAc 60:40) to give a white solid with 70% yield. The reaction was confirmed by observations in the <sup>1</sup>H NMR of the *tert*-butyl protons at 1.42 – 1.26

ppm and in the  $^{13}\text{C}$  NMR, the carbonyl in the boc group was observed at 80.1 ppm as well as the central carbon in the *tert*-butyl group at 28.36 ppm.



**Scheme 2.48: Synthesis of 3-(((2-Methyl-2-propanyl)oxy})carbonylamino)-3-phenylpropanoic acid (151)**

This successfully separated by HPLC for ee determination on an OJ-H column, mobile phase Hex:IPA (90:10) + 0.1% TFA, 1.0 mL min<sup>-1</sup>, 6.0 and 6.8 min. Adequate resolution was achieved, as shown in Figure 2.19.



**Figure 2.19: HPLC chromatogram of the separation of acid standard 151 on an OJ-H column. Mobile phase Hex:IPA 90:10 + 0.1% TFA at a flow rate of 1 mL.min<sup>-1</sup>.  $t_R$  = 6.0 min (major) and 6.8 min (minor).**

The single enantiomer boc protected acid was prepared following the amino protection outlined by Chhiba *et al* as described earlier, using (*R*)-3-amino-3-phenylpropionic acid<sup>7</sup>. Comparison HPLC spectra of the racemic acid to the single enantiomer can be seen in Figure 2.20. From this it can be observed that under the same HPLC conditions, the (*R*)-enantiomer elutes first followed by the (*S*)-enantiomer.

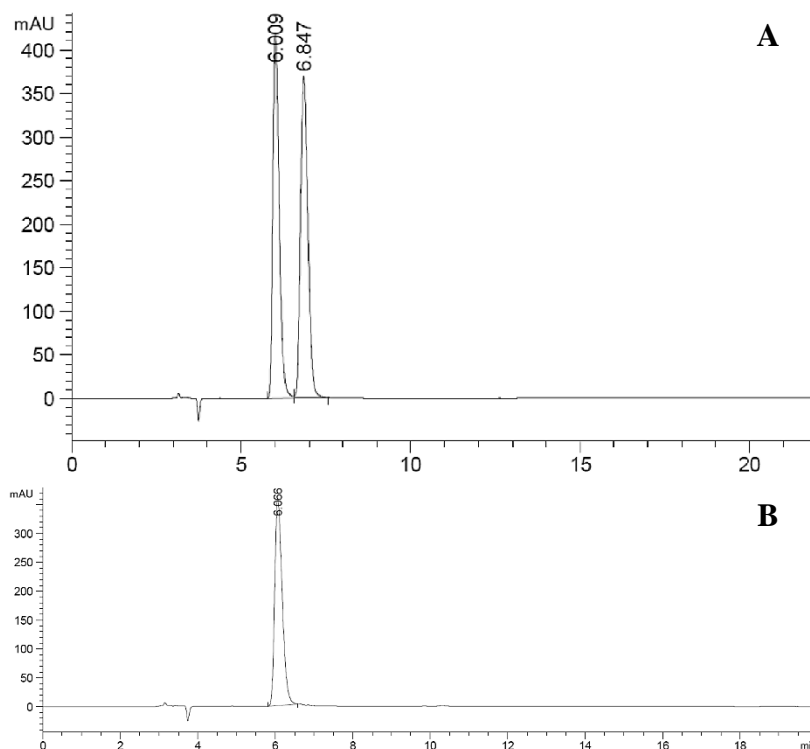
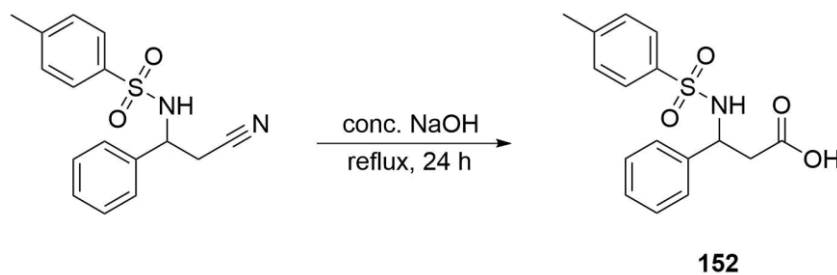


Figure 2.20: HPLC comparison spectra of A – racemic Boc-APPA to B – (R)-Boc-APPA

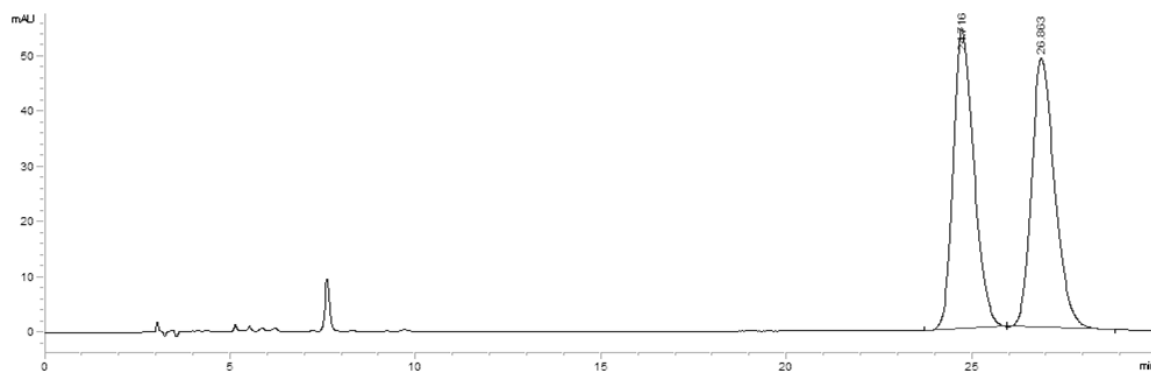
### 2.2.8 Standards for compound 45

The tosyl protected acid standard (**152**) was produced implementing the method of Winkler *et al.*, as shown in Scheme 2.49<sup>25</sup>. *N*-(2-cyano-1-phenylethyl)-4-methylbenzenesulfonamide was suspended in concentrated NaOH and the mixture was heated to reflux overnight. The acid was released by the addition of HCl and the mixture was diluted. The product was extracted into DCM, dried over Na<sub>2</sub>SO<sub>4</sub> and the solvent removed *in vacuo*.



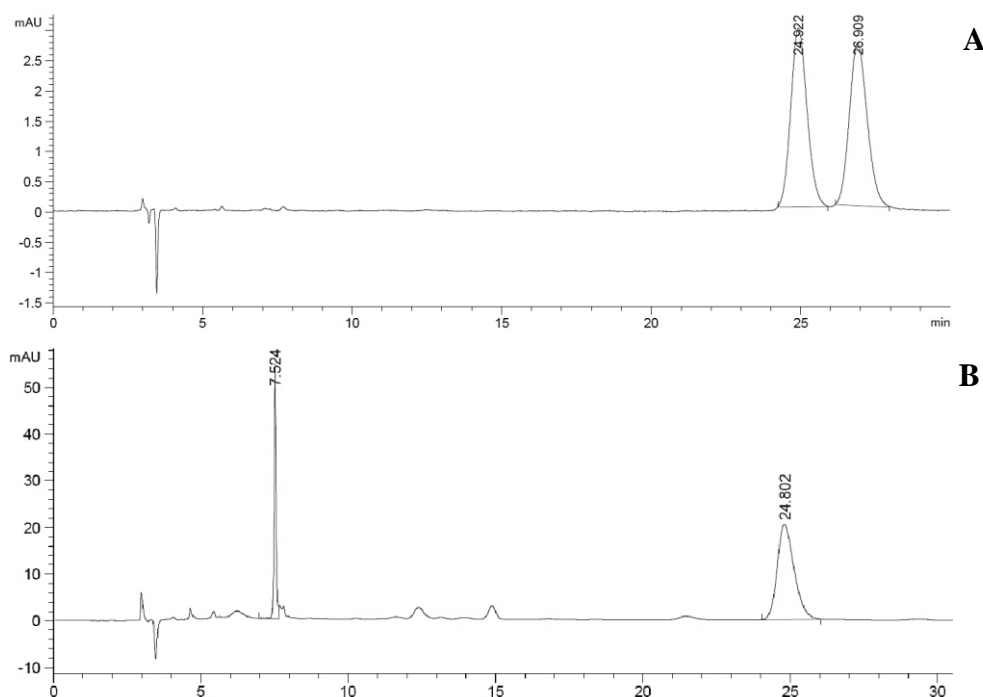
Scheme 2.49: Synthesis of 3-[[[4-Methylphenyl]sulfonyl]amino]-3-phenylpropanoic acid (**152**)

This was successfully separated on the OJ-H column, mobile phase Hex:IPA 90:10 + 0.1% TFA, flow rate 1.0 mL min<sup>-1</sup> to give retention times of 24.7 and 26.7 min. Baseline resolution was achieved, as shown in Figure 2.21.



**Figure 2.21:** HPLC chromatogram of the separation of acid standard **152** on an OJ-H column. Mobile phase Hex:IPA 90:10 + 0.1% TFA at a flow rate of 1 mL.min<sup>-1</sup>.  $t_R = 24.7$  min (major) and 26.7 min (minor)

The single enantiomer of the tosyl acid was prepared following the method of Chhiba *et al* on (*R*)-3-amino-3-phenylpropionic acid (**152b**)<sup>7</sup>. The comparison spectra of the racemic acid to the single enantiomer are shown in Figure 2.22. Under the same HPLC conditions, it can be observed that the (*R*)-enantiomer elutes first, followed by the (*S*)-enantiomer.



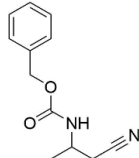
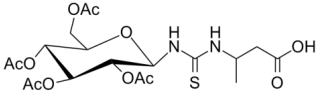
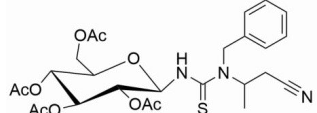
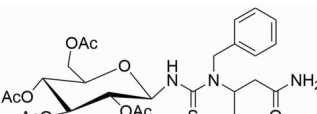
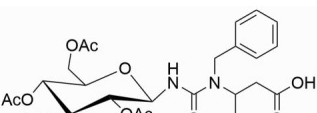
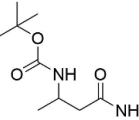
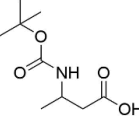
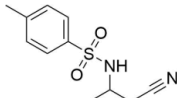
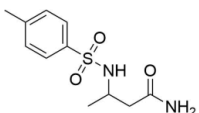
**Figure 2.22:** HPLC comparison spectra of A – racemic Ts-APPA to B – (*R*)-Ts-APPA

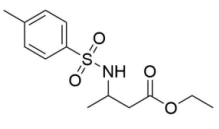
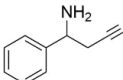
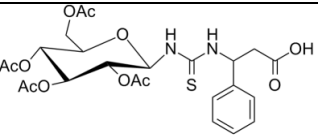
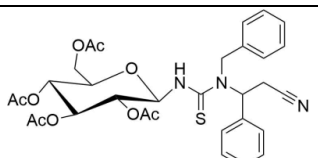
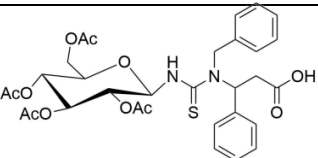
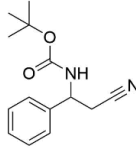
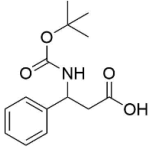
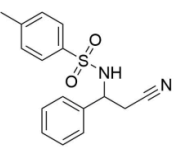
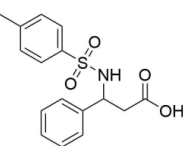
### 2.3 Summary of Chapter 2

In summary, all the starting  $\beta$ -amino nitriles were successfully synthesised and HPLC methods were developed for them. The acid and amide standards where necessary, were also successfully synthesised and HPLC methods were developed for ee determination. The complete summary of method developed is outlined in Table 2.2. With these methods in place, this allowed for work to occur on screening the bacterial isolates which will be described in Chapter 3.



Table 2.2: Summary of HPLC conditions and retention times for the nitrile, acid, and amide standards

Compound	Column	Mobile Phase	Flow Rate (mL/min)	t <sub>1</sub> (min)	t <sub>2</sub> (min)
 <b>155</b>	OJ-H	Hex:IPA 80:20	1.0	24.3	26.9
 <b>158</b>	C18	MeOH:H <sub>2</sub> O 35:65 + 0.1% TFA	1.0	20.5	25.4
	C18	MeOH:H <sub>2</sub> O + 0.1% TFA Gradient	1.0	14.1	17.1
 <b>160</b>	C18	MeOH:H <sub>2</sub> O 50:50 + 0.1% TFA	1.0	16.6	22.3
	C18	MeOH:H <sub>2</sub> O + 0.1% TFA Gradient	1.0	21.9	29.7
 <b>161</b>	C18	MeOH:H <sub>2</sub> O 55:45 + 0.1% TFA	1.0	20.7	24.1
 <b>162</b>	C18	MeOH:H <sub>2</sub> O 55:45 + 0.1% TFA	1.0	22.9	28.5
	C18	MeOH:H <sub>2</sub> O + 0.1% TFA Gradient	1.0	19.7	22.9
 <b>145</b>	IA	Hex:IPA 97:3 + 0.1% TFA	1.0	23.4	25.6
 <b>146</b>	OJ-H	Hex:IPA 90:10 + 0.1% TFA	1.0	4.7	4.9
 <b>127</b>	IA	Hex:IPA 90:10	1.0	30.9	34.9
 <b>147</b>	OJ-H	Hex:IPA 90:10 + 0.1% TFA	1.0	34.4	41.3

Compound	Column	Mobile Phase	Flow Rate (mL/min)	t <sub>1</sub> (min)	t <sub>2</sub> (min)
 <b>164</b>	IA	Hex:IPA 90:10 + 0.1% TFA	1.0	18.2	21.9
 <b>122</b>	AD-H	Hex:IPA 90:10	0.8	16.1	18.9
 <b>165</b>	C18	MeOH:H <sub>2</sub> O 47:53 + 0.1% TFA	1.0	14.9	19.7
 <b>166</b>	C18	MeOH:H <sub>2</sub> O 55:45 + 0.1% TFA	1.0	22.6	28.6
 <b>167</b>	C18	MeOH:H <sub>2</sub> O 35:65 + 0.1% TFA	1.0	11.4	12.6
 <b>129</b>	IA	Hex:IPA 90:10	1.0	9.9	11.2
 <b>151</b>	OJ-H	Hex:IPA 90:10 + 0.1% TFA	1.0	6.0	6.8
 <b>45</b>	IA	Hex:IPA 90:10	1.0	29.3	31.3
 <b>152</b>	OJ-H	Hex:IPA 90:10 + 0.1% TFA	1.0	24.7	26.7

## REFERENCES

1. Coady, Tracey. M. *et al.* *Substrate Evaluation of Rhodococcus erythropolis SET1, a Nitrile Hydrolysing Bacterium, Demonstrating Dual Activity Strongly Dependent on Nitrile Sub-Structure.* European Journal of Organic Chemistry, 2015, **2015**, (5), 1108-1116
2. Veitía, Maité. S. *et al.* *Synthesis of Novel N-protected  $\beta$ -Amino Nitriles: Study of Their Hydrolysis Involving a Nitrilase-Catalyzed Step.* Tetrahedron: Asymmetry, 2009, **20**, (18), 2077-2089
3. Preiml, Margit. *et al.* *A New Approach to  $\beta$ -amino Acids: Biotransformation of N-protected  $\beta$ -amino Nitriles.* Tetrahedron Letters, 2003, **44**, (27), 5057-5059
4. Preiml, Margit. *et al.* *Biotransformation of  $\beta$ -amino Nitriles: The Role of the N-protecting Group.* Journal of Molecular Catalysis B: Enzymatic, 2004, **29**, (1-6), 115-121
5. Ma, Da-You. *et al.* *Nitrile Biotransformations for the Synthesis of Highly Enantioenriched  $\beta$ -Hydroxy and  $\beta$ -Amino Acid and Amide Derivatives.* Journal of Organic Chemistry, 2008, **73**, (11), 4087-4091
6. Sen, Stephanie. E. & Roach, Steven. L. *A Convenient Two-Step Procedure for the Synthesis of Substituted Allylic Amines.* Synthesis, 1995, **1995**, (07), 756-758
7. Chhiba, Varsha. *et al.* *Enantioselective Biocatalytic Hydrolysis of  $\beta$ -aminonitriles to  $\beta$ -Amino-amides Using Rhodococcus rhodochrous ATCC BAA-870.* Journal of Molecular Catalysis B: Enzymatic, 2012, **76**, 68-74
8. Marcotullio, Maria. *et al.* *A New, Simple Synthesis of N-Tosyl Pyrrolidines and Piperidines.* Synthesis, 2006, **2006**, (16), 2760-2766
9. Guo, Hongchao. *et al.* *Phosphine-Promoted [3 + 3] Annulations of Aziridines With Allenolates: Facile Entry Into Highly Functionalized Tetrahydropyridines.* Journal of the American Chemical Society, 2009, **131**, (18), 6318-6319
10. Abdel-Magid, Ahmed F. & Mehrman, Steven J. *A Review on the Use of Sodium Triacetoxyborohydride in the Reductive Amination of Ketones and Aldehydes.* Organic Process Research & Development, 2006, **10**, 971-1031
11. Carson, J. R. *et al.* *2-Ethynylbenzenealkanamines. A New Class of Calcium Entry Blockers.* Journal of Medicinal Chemistry, 1988, **31**, (3), 630-636
12. Evans, David. A. *et al.* *Directed Reduction of  $\beta$ -hydroxy Ketones Employing Tetramethylammonium Triacetoxyborohydride.* Journal of the American Chemical Society, 1988, **110**, (11), 3560-3578
13. Abdel-Magid, Ahmed F. *et al.* *Reductive Amination of Aldehydes and Ketones with Sodium Triacetoxyborohydride.* Journal of Organic Chemistry, 1996, **61**, (11), 3849-3862

14. Miriyala, Bruhaspathy. *et al.* *Chemoselective Reductive Alkylation of Ammonia With Carbonyl Compounds: Synthesis of Primary and Symmetrical Secondary Amines.* Tetrahedron, 2004, **60**, (7), 1463-1471
15. Dondoni, Alessandro. *et al.* *A Facile and General Entry to C-Glycosyl (R)- and (S)- $\beta$ -Amino Acid Pairs from Glycosyl Cyanides Through Enamino Ester Intermediates.* Synlett, 2006, (4), 0539-0542
16. Pehere, Ashok. D. & Abell, Andrew. D. *An Improved Large Scale Procedure for the Preparation of N-Cbz Amino Acids.* Tetrahedron Letters, 2011, **52**, (13), 1493-1494
17. Oba, Makoto. *et al.* *Synthesis of Both Enantiomers of Cyclic Methionine Analogue: (R)- and (S)-3-aminotetrahydrothiophene-3-carboxylic Acids.* Tetrahedron: Asymmetry, 2013, **24**, (8), 464-467
18. Bora, Pranja. P. *et al.* *Amberlyst-15 Catalyzed Cbz Protection of Amines Under Solvent-Free Conditions.* Synthetic Communications, 2011, **41**, (18), 2674-2683
19. Mitsukura, Koichi. *et al.* *Asymmetric Synthesis of Chiral Amine From Cyclic Imine by Bacterial Whole-cell Catalyst of Enantioselective Imine Reductase.* Organic & Biomolecular Chemistry, 2010, **8**, (20), 4533-4535
20. Péter, A. *et al.* *High-performance Liquid Chromatographic Enantioseparation of  $\beta$ -amino acids.* Journal of Chromatography A, 2001, **926**, (2), 229-238
21. Mathew, Sam. *et al.* *Asymmetric Synthesis of Aromatic  $\beta$ -amino Acids Using  $\omega$ -transaminase: Optimizing the Lipase Concentration to Obtain Thermodynamically Unstable  $\beta$ -keto Acids.* Biotechnology Journal, 2016, **11**, (1), 185-190
22. Péter, Antal. *et al.* *High-performance Liquid Chromatographic Separation of the Enantiomers of Unusual  $\alpha$ -amino Acid Analogues.* Journal of Chromatography A, 2000, **871**, (1-2), 105-113
23. Ilisz, István. *et al.* *Application of Chiral Derivatizing Agents in the High-performance Liquid Chromatographic Separation of Amino Acid Enantiomers: A Review.* Journal of Pharmaceutical and Biomedical Analysis, 2008, **47**, (1), 1-15
24. Nguyen, Ngoc-Van. Thi. *et al.* *Development of a UPLC Method with Chiral Derivatization for the Determination of Atenolol and Metoprolol Enantiomers in Tablet Preparations.* Pharmaceutical Sciences Asia, 2018, **45**, (2), 66-76
25. Winkler, Margit. *et al.* *Synthesis and Microbial Transformation of  $\beta$ -amino Nitriles.* Tetrahedron, 2005, **61**, (17), 4249-4260
26. Ma, Da-You. *et al.* *Dramatic Enhancement of Enantioselectivity of Biotransformations of  $\beta$ -Hydroxy Nitriles.* Organic Letters, 2006, **8**, (15), 3231-3234
27. Alexander, Matthew. D. *et al.* *MK2 Inhibitors And Uses Thereof.* United States patent (2014).
28. Husek, Petr. *Rapid Derivatization and Gas Chromatographic Determination of Amino Acids.* Journal of Chromatography, 1991, **552**, 289-299

29. Markworth, Christopher. John. *et al.* Benzamide Derivatives. United States patent (2010).
30. Bea, Han-Seop. *et al.* *Kinetic Resolution of Aromatic  $\beta$ -Amino Acids by  $\omega$ -Transaminase*. Chemical Communications, 2011, **47**, (20), 5894-5896

## **CHAPTER 3**

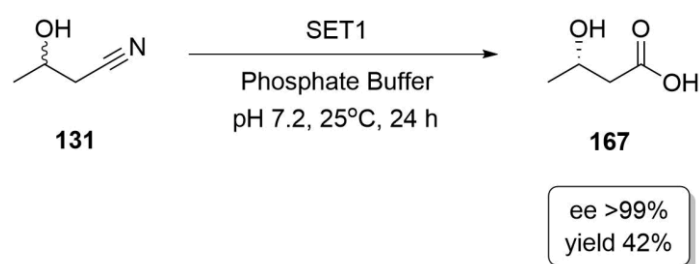
### **SCREENING OF ISOLATES SET1, 6, & 39 WITH *β*-AMINONITRILES**

SCREENING OF ISOLATES SET1, 6, & 39 WITH  $\beta$ -AMINONITRILES

## 3.1 Enantioselectivity Screening of SET1 with 3-aminobutyronitrile

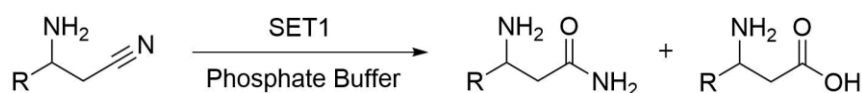
## 3.1.1 Background

Previous investigations by Coady *et al* as highlighted in Chapter 2, had identified the whole cell catalyst bacterial isolate SET1 to be selective for hydroxynitriles, particularly 3-hydroxybutyronitrile (3-HBN) (**131**), with enantioselectivity greater than 99.9%, shown in Scheme 3.1<sup>1</sup>.



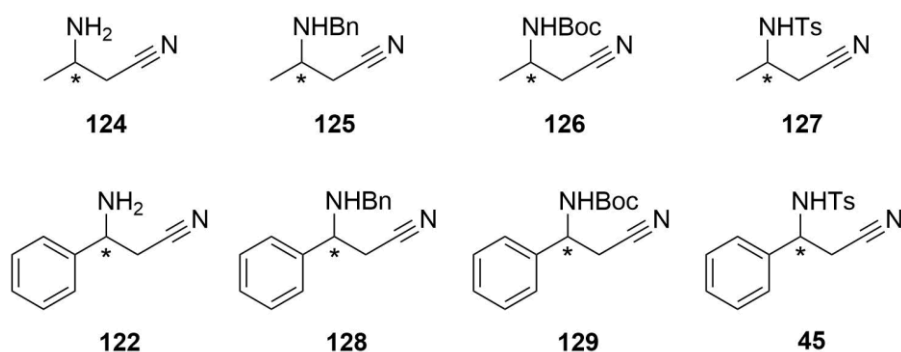
**Scheme 3.1:** Isolate SET1's hydrolysis of 3-hydroxybutyronitrile

It was thus of great interest to observe isolate SET1's behaviour towards aminonitriles in order to attempt to prepare  $\beta$ -amino acids, as shown in Scheme 3.2.



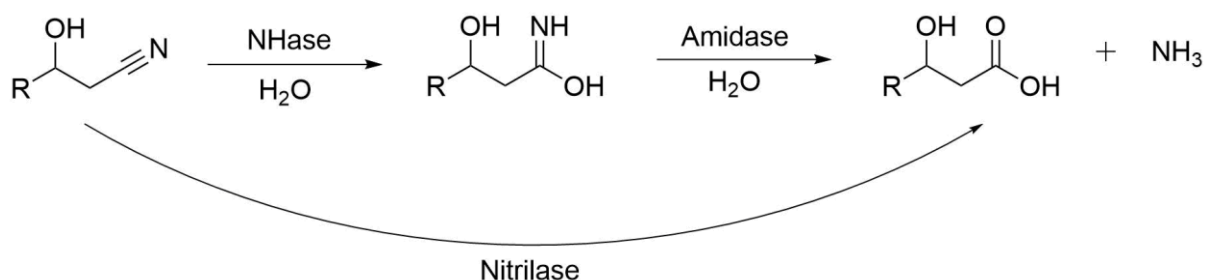
**Scheme 3.2:** Proposed action of Isolate SET1 on  $\beta$ -amino nitriles

In prior work, Isolate SET1 was shown to be selective towards aliphatic hydroxynitriles. Whilst the same response was anticipated for the aminonitriles it was still decided to attempt to screen against both aliphatic and aromatic aminonitriles as shown in Figure 3.1 in case the change to an amino group would facilitate acceptance of the aromatic structures.



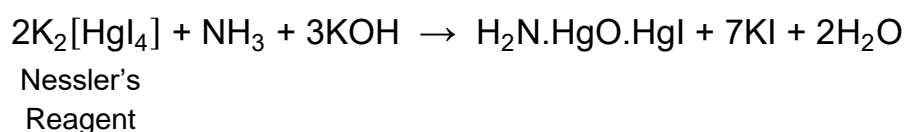
**Figure 3.1:** Structures of the  $\beta$ -amino nitrile substrate to be screened against isolate SET1

Protocols and methods for working with Isolate SET1 from the prior aforementioned work were used as a starting point for investigation conditions using the aminonitriles. Some parameters taken on board were that optimum temperature and pH for Isolate SET1 with 3-hydroxybutyronitrile were 25°C and 7 respectively<sup>1</sup>. In terms of the pH however, being aware that substrate (**124**) existed as a HCl salt, it would require a higher pH for the free form to be available. It was thus decided to run the biotransformations at both pH 7 and 9 to evaluate the pH effect with this substrate. The M-9 minimal media used to grow isolate SET1 in previous work was maintained, as well as the phosphate buffer for running the biotransformations. Cultures of isolate SET1 would also be induced on 3-HBN (**131**) before proceeding to biotransformations on the substrates. What could not be transferred was the use of the Nessler's colorimetric activity assay to indicate enzyme activity<sup>2,3</sup>. A schematic of the hydrolysis of  $\beta$ -hydroxynitriles in Scheme 3.3 shows ammonia is produced which then reacts with the Nessler's reagent<sup>4</sup>.



**Scheme 3.3: General hydrolysis of  $\beta$ -hydroxynitriles which produces ammonia**

The subsequent reaction of the produced ammonia with the Nessler's reagent is shown in Scheme 3.4 which gives rise to the observed yellow brown soluble product.



**Scheme 3.4: Reaction of ammonia with Nessler's reagent**

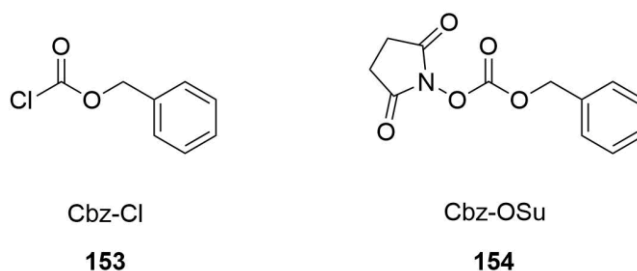
An issue arises therefore since the amino group on the aminonitriles would also react with Nessler's reagent causing additional precipitation and thus the results would be unreliable<sup>5</sup>. Also, there is a possibility that any ammonia produced can be taken up in side reactions in the cell and furthermore, any amide reactions which occur will not be detected<sup>2</sup>. Therefore, HPLC and isolated yields were the determining method of enzyme activity for this work. For biotransformations carried out on a small scale (less than 50 mg of substrate), where isolated yield in some cases could not be captured, HPLC analysis was used to determine ee and yields



employing standard curves for both nitrile and acid where applicable. During the studies, HPLC standards were run with the biotransformation samples to allow for positive identification. Developed HPLC methods for the substrates and products are described in detail in Chapters 2 and 7. Where possible, products were additionally confirmed by LC-MS and NMR. Enantioselectivity of the products was determined by comparing to single enantiomer standards prepared and analysed as described in Chapters 2 and 7.

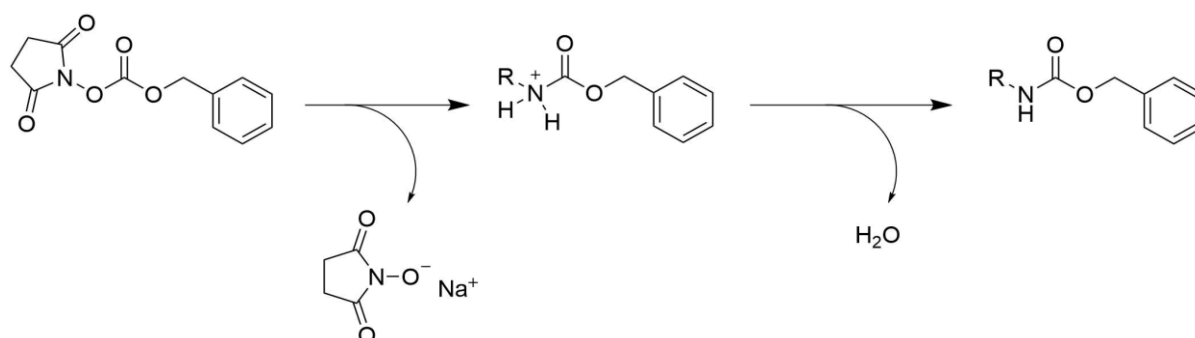
The volume of cells to add to each biotransformation was determined by measuring the optical density of each batch of cells. This was done with a NanoDrop® spectrophotometer ND1000 at 600 nm. The recorded optical density was multiplied by a factor of 10 then the volume of cells required to reach a final concentration of 1 was calculated.

Workup procedures were implemented from Wang *et al* who used AJ270 to hydrolyse 3-aminobutyronitrile as described in Chapter 1. In their workup, they used Cbz chloride to protect the acid and amide products to isolate them<sup>6</sup>. The adjustment made for this research was that Cbz-OSu (**154**), see Figure 3.2, was used in the place of the more toxic Cbz-Cl (**153**) which is more hazardous to handle.



**Figure 3.2: Structure of Benzyl chloroformate (Cbz-Cl) in comparison to N-(Benzyloxycarbonyloxy)succinimide (Cbz-OSu)**

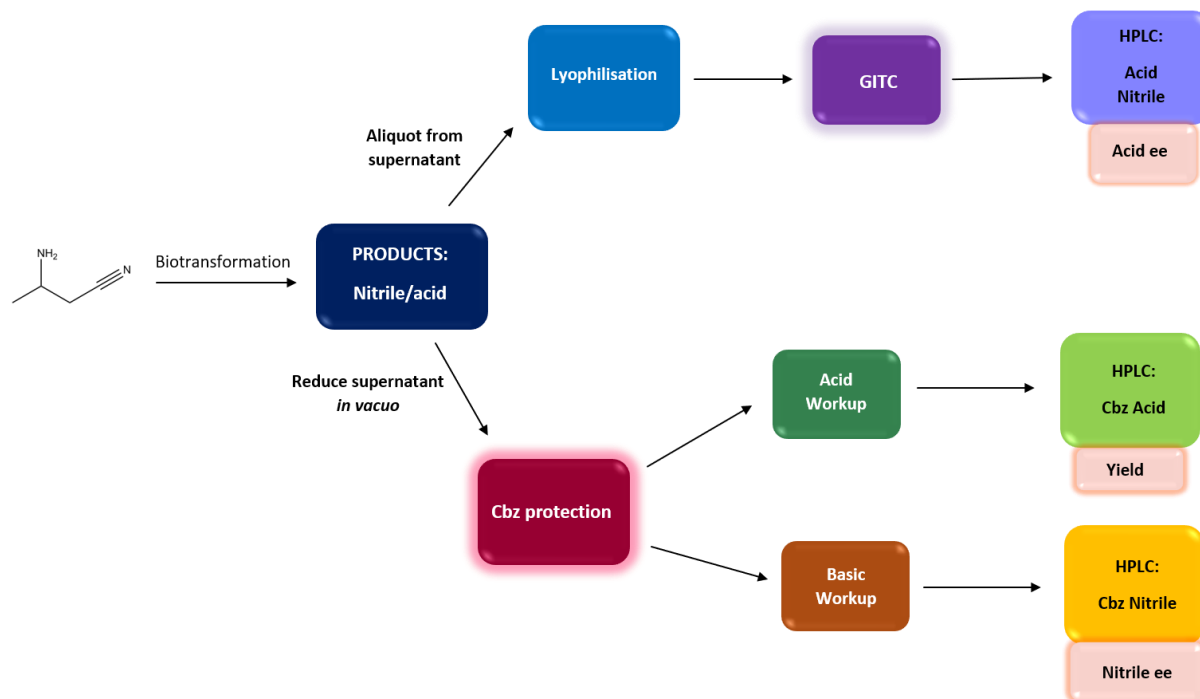
The mechanism for Cbz protection is illustrated in Scheme 3.5. The starting amino nitriles are readily water soluble but once the Cbz group is added, polarity of the products decreases, and the products can be extracted using an organic solvent such as ethyl acetate at the appropriate pH.



**Scheme 3.5: Mechanism of Cbz N-protection in a NaOH solution**

## 3.1.2 Initial screening studies

A flow chart depicting the complete workflow strategy for analysis and workup of the biotransformations of 3-aminobutyronitrile, substrate (**124**), is shown in Scheme 3.6.



**Scheme 3.6:** Flow chart for the biotransformation of 3-aminobutyronitrile, substrate (**124**)

An initial investigation to verify the validity of this work was carried out on a small scale of 6 mL, requiring 10.4 mg of substrate (**124**). The biotransformations were carried out in a suspension of phosphate buffer (0.1 M) at pH 7, 8, or 9, adjusted with NaOH, containing induced cells ( $OD_{600nm} = 1$ ). Racemic 3-aminobutyronitrile (10 mM) was added to the flasks and the mixture was incubated at 25°C for 3 days with mechanical shaking (200 rpm). The reactions were quenched by removal of the biomass by centrifugation. The supernatants were concentrated *in vacuo* then NaOH was added. A solution of Cbz-OSu in THF was added and the mixtures were stirred for 24 h. After pH adjustments and workup by extraction, the products were obtained in their Cbz protected forms. No nitrile was observed by HPLC for all pHs. This was also observed in the work of Coady *et al*, where the nitrile, 3-hydroxybutyronitrile (**131**), failed to be recovered<sup>1,7</sup>. At this stage a HPLC method was yet to be developed for the acid however, the presence of the acid was confirmed by LC-MS observations of  $m/z$  of 237.9 for the  $M+H^+$  adduct and 259.9 for the  $M+Na^+$  adduct.

## 3.1.2.1 Effect of pH

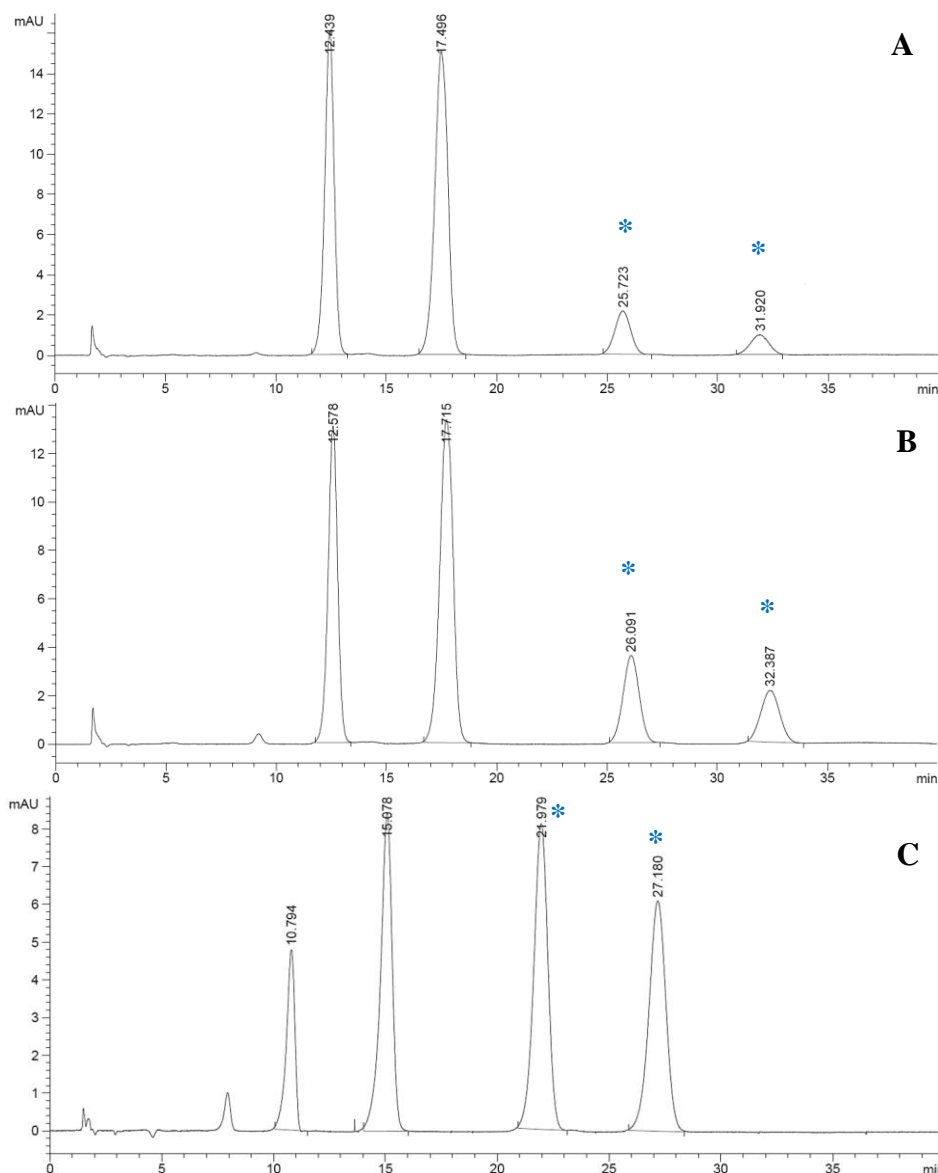
The biotransformation procedure was then scaled up to a larger scale, requiring 50 mg (10 mM) of substrate (**124**) at pHs 7, 8, and 9. Acid ee's were acquired by taking a 1 mL aliquots of the supernatants after centrifugation, freezing them overnight, lyophilising them, then derivatising with GITC for reverse phase HPLC as discussed in Chapter 2. For analysis HPLC was carried out as single injections. Isolated yields were acquired on products purified by prep TLC (Hex:EtOAc 70:30). The acid products were confirmed by LC-MS by observations of  $m/z$  259.6 ( $M+Na^+$ ) and 237.5 ( $M+H^+$ ). The only exception was at pH 9 where the crude Cbz product was confirmed by peaks in the  $^1H$  NMR of the aromatic protons from the Cbz protecting group at 7.33 ppm and the NH proton at 5.25 ppm.

A summary of the results from the larger scale biotransformations is shown in Table 3.1 and HPLC chromatograms are shown in Figure 3.3.

**Table 3.1: Effect of pH on the biotransformation of Isolate SET1 with 3-aminobutyronitrile (**124**) at a 50 mg scale**

Entry	pH	Time (h)	Nitrile	Acid	
				Yield (%) <sup>[b]</sup>	ee (%) <sup>[c]</sup>
1	7	72	ND	<1	29 ( <i>S</i> )
2	8	72	ND	<1	18 ( <i>S</i> )
3	9	72	ND	<1	5 ( <i>S</i> )

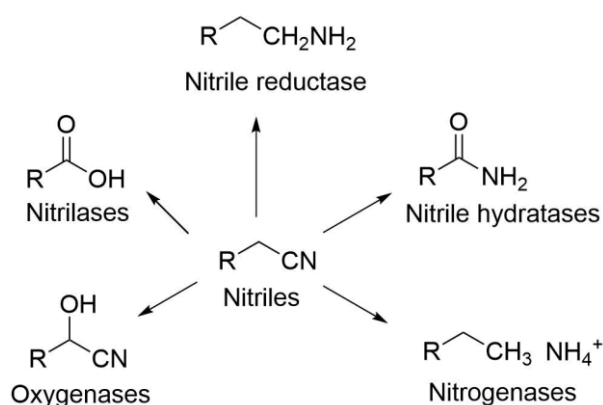
<sup>a</sup>Biotransformations were carried out by incubating 3-aminobutyronitrile (10 mM) in a suspension of *Rhodococcus erythropolis* SET1 ( $OD_{600nm}=1$ ) in phosphate buffer (pH 7, 8, or 9) at 25°C. <sup>b</sup>Isolated yield after prep TLC upon Cbz protection. <sup>c</sup>Determined by HPLC analysis using a chiral column. ND = Not Detected



**Figure 3.3:** HPLC chromatograms of the SET1 biotransformation GTC derivatised acid products. A – carried out at pH 7, B – carried out at pH 8, C – carried out at pH 9 (shift in retention times due to unknown reasons but standards were used for peak confirmation). Asterix denote acid peaks of interest. Analysis carried out on a C18 column. Mobile phase MeOH:H<sub>2</sub>O 35:65 + 0.1% TFA, at a flow rate of 1 mL.min<sup>-1</sup>

It can be observed that as pH increases that the enantioselectivity of isolate SET1 towards substrate (**124**) falls rapidly. This result mimics observations noted in prior work with 3-hydroxybutyronitrile (**131**)<sup>1</sup>. The yield of the acid was extremely poor. The pH may be a considerable hinderance in this case as SET1 cannot tolerate high pH's whilst  $\beta$ -amino nitriles are known to be in a protonated form at and below pH 7 thus rendering them potentially incompatible with the active site of the enzyme<sup>1,8</sup>.

Nitrile was not recovered or detected in any of the cases. It is worth noting that in the work of Coady *et al* with the analogous 3-HBN (**131**), no nitrile was recovered either<sup>1</sup>. This could be because the nitrile becomes trapped within the cell or in its outer membrane and thus does not make it back into the buffer for recovery<sup>9</sup>. Another possibility is the presence of another enzymatic pathway that is employing and thus possibly competing for the nitrile. Scheme 3.7 illustrates the various enzymatic pathways that can potentially make use of a nitrile and could thus possibly be found at work in a bacterial whole cell. It is uncommon to find oxygenases which contribute to nitrile conversion and there are few reports attributing activity to nitrogenases, so it may be a nitrile reductase or alternative metabolising enzyme that would compete for the nitrile if present<sup>10-12</sup>.



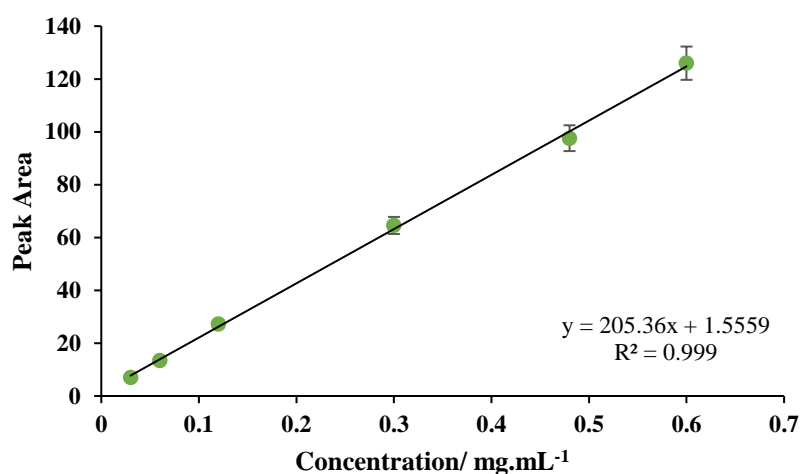
**Scheme 3.7: Enzymatic pathways utilising nitriles as a substrate**

The possible presence of nitrile reductase in *Rhodococcus* sp. was made plausible by Sehajpal *et al*, who discovered novel enzymes in *Rhodococcus ruber* and *Bacillus subtilis* whose activity strongly suggests that they are most likely nitrile reductases and ketoreductases<sup>13</sup>.

### 3.1.2.2 Mass loss investigation, nitrile study

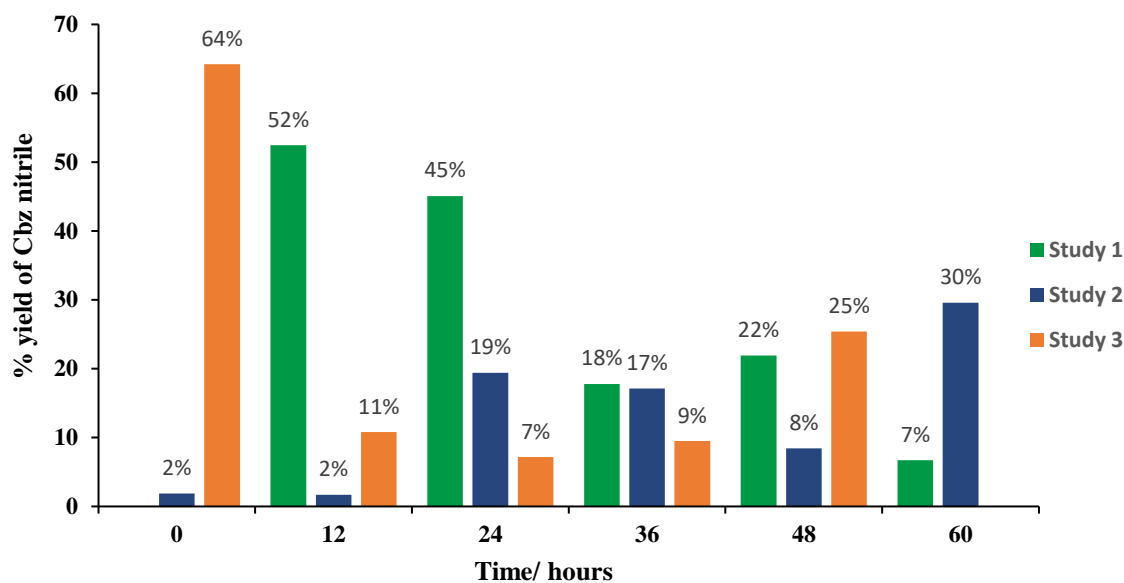
In order to investigate the mass loss in the biotransformation, cell blank studies on nitrile and acid standards were carried out. Three biological replicate cell blank studies were carried out for the nitrile at pH 7 over 60 hours, with sampling over that period to review recovery. The difference in the studies was that sampling for Study 1 commenced at the 12 h time point and ended at 60 h, Study 2 sampling commenced at the 0 h time point and ended at 60 h, and sampling for Study 3 sampling commenced at 0 h and ended at 48 h. The disparities in sampling times were due to time restrictions. Reactions were carried out at a 6 mL scale with racemic 3-

aminobutyronitrile (10 mM, 0.0025 g) in phosphate buffer (0.1 M) at pH 7. The reactions were incubated at 25°C with mechanical shaking (200 rpm). The supernatant was concentrated *in vacuo* then NaOH was added. A solution of Cbz-OSu in THF was added and the mixture was stirred for 24 h. After pH adjustments and workup by extraction, the acid and nitrile were obtained in their Cbz protected forms. Samples were carried out without replicates and the HPLC was also carried out as a single injection as it was an exploratory screening. A standard curve with an  $R^2$  of 0.999 was used to calculate yields of the nitrile. This was prepared using Cbz protected nitrile (**155**) and was analysed in duplicate by HPLC as shown in Figure 3.4.



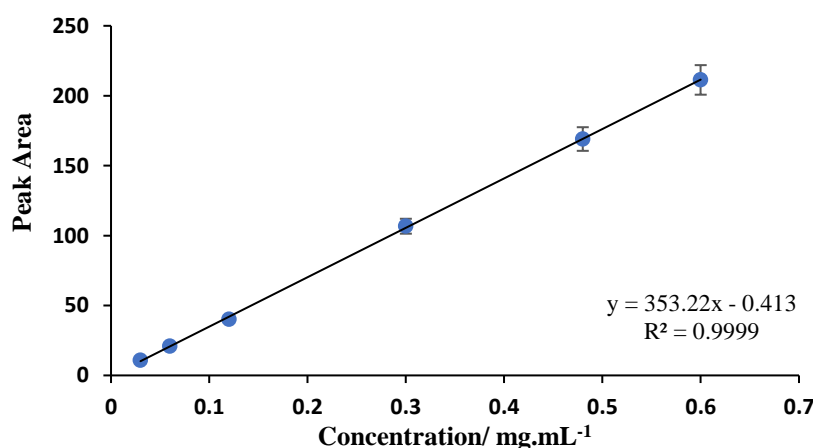
**Figure 3.4:** HPLC standard curve of Cbz protected nitrile (Benzyl (1-cyano-2-propanyl)carbamate). Analysis carried out on an OJ-H column. Mobile phase Hex:IPA 80:20 at a flow rate of 1 mL.min<sup>-1</sup>. Error bars represent the error across the mean of the HPLC duplicates

It was noted that the amount of protected nitrile recovered at the different time points varied greatly as seen in Figure 3.5. It was also observed that at no point was 100% of the Cbz protected nitrile recovered. This is in contrast to the synthesis of the Cbz nitrile standard (Benzyl (1-cyano-2-propanyl)carbamate) (**155**) which was produced at 97% yield. All conditions for the synthesis and workup of the Cbz nitrile were precisely the same. The only exception was the presence of the phosphate buffer in the samples from the biotransformation. These studies could indicate, in addition to the reasons suggested earlier, that the phosphate buffer system may interfere with the recovery and possibly the integrity of the nitrile.



**Figure 3.5: Cell blank studies of 3-aminobutyronitrile HCl salt in phosphate buffer at pH 7 over a 60 h period at 25°C. Nitrile detected after workup by HPLC. Yields acquired from standard curve**

In addition to mass loss during these studies, analysis of the Cbz protected acid product also proved difficult. This was observed particularly during purification as the acid product appeared to degrade somewhat, even in cold storage conditions. New spots on TLC analysis would appear over time. This made acquiring yields difficult and eventually HPLC was used to determine yield by comparison to a standard curve with a  $R^2$  of 0.9999, generated by prepared Cbz acid which is shown in Figure 3.6. This was prepared using Cbz protected acid and was analysed in duplicate by HPLC.

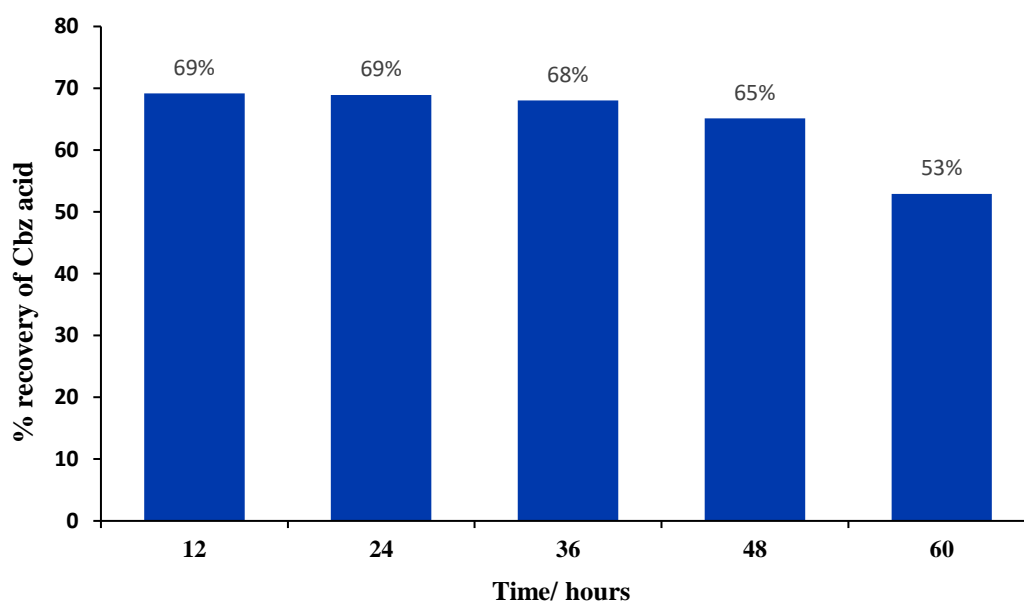


**Figure 3.6: HPLC standard curve of Cbz protected acid (3-[(Benzyloxy)carbonyl]amino)butanoic acid). Analysis carried out on an IA column. Mobile phase Hex:IPA 90:10 + 0.1% TFA at a flow rate of 1 mL.min<sup>-1</sup>. Error bars represent the error across the mean of the HPLC duplicates**

In terms of determining ee, HPLC separation could not be achieved with the available columns within the group (Chiralpak IA, AD-H, OJ-H, and AS-H), therefore an alternative protocol for ee determination before protection was employed.

### 3.1.2.3 Mass loss investigation, acid study

A cell blank study was also carried out for the acid to investigate mass loss. Single reactions (no duplicates or replicates) were completed without enzyme and single injection HPLC (no duplication) was done on samples immediately after the workup procedure. A small decrease in recovery was observed over the 60 h period from 69% to 53% which is shown in Figure 3.7. It should be noted that 100% recovery was not achieved at any time point. This is comparable however to the synthesis of the Cbz acid standard from free acid which achieved a 56% yield. In this case, losses in general for the acid may have occurred in a few places; during the Cbz protection as the acid may degrade during the overnight reaction, during the extraction, and during reduction *in vacuo* of the organic extracts.

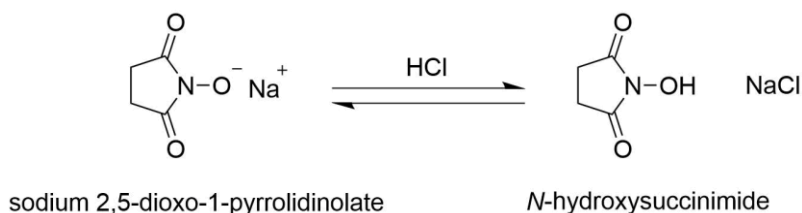


**Figure 3.7:** Cell blank study of 3-aminobutyric acid in phosphate buffer at pH 7 over a 3-day period at 25°C. Acid detected after workup by HPLC. % recovery acquired from standard curve.

As discussed earlier, the *N*-protection procedure was altered from using Cbz-Cl which Wang *et al* used to using Cbz-OSu for safety reasons<sup>6</sup>. The use of Cbz-Cl would possibly give a much cleaner reaction overall as NaCl would be the main by-product. In contrast, Cbz-OSu gives rise



to a salt, sodium 2,5-dioxo-1-pyrrolidinolate which can become *N*-hydroxysuccinimide as pH is decreased during the workup procedures as shown in Scheme 3.8.

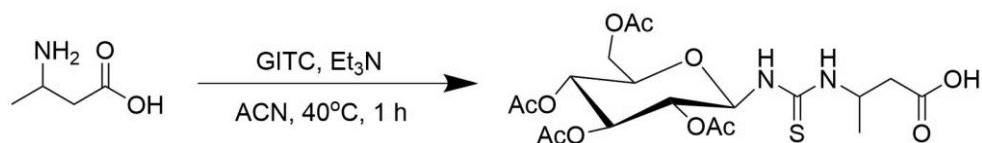


**Scheme 3.8: By-products of the Cbz-OSu protection during the workup**

These by-products may interfere with the extractions and indeed the integrity of the desired biotransformation protected products and starting protected nitrile.

### 3.1.2.4 Enantioselectivity determination

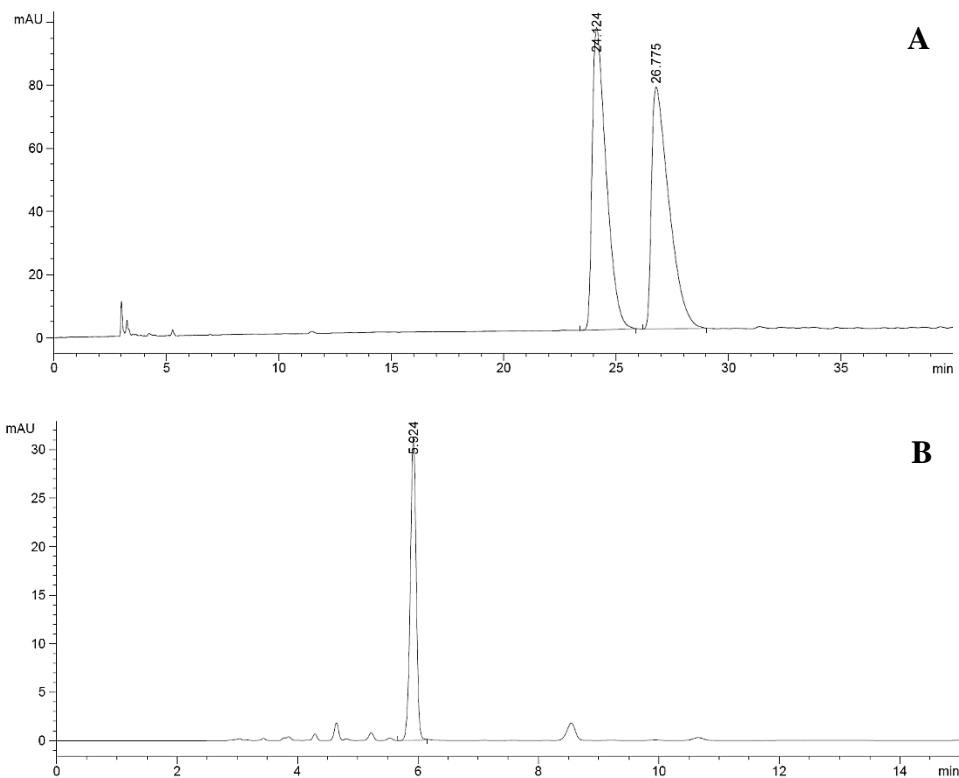
As we found issues with separation of the acid on available chiral columns within the PMBRC the Cbz protection method was thus solely used as a method to acquire isolated acid product and hence determine yield for this body of work. Enantioselectivity therefore had to be determined differently. The method chosen was that of derivatisation with GITC by Mitsukura *et al* as discussed in Chapter 2 as shown in Figure 3.8<sup>14</sup>. The derivatisation reagent GITC, along with a few other agents such as Marfey's agent, have been successfully used and reported in literature to derivatise amino acids for HPLC analysis<sup>15-17</sup>. In this case, GITC added a necessary chromophore to 3-aminobutyric acid and formed diastereomers which could easily be separated on a C18 column.



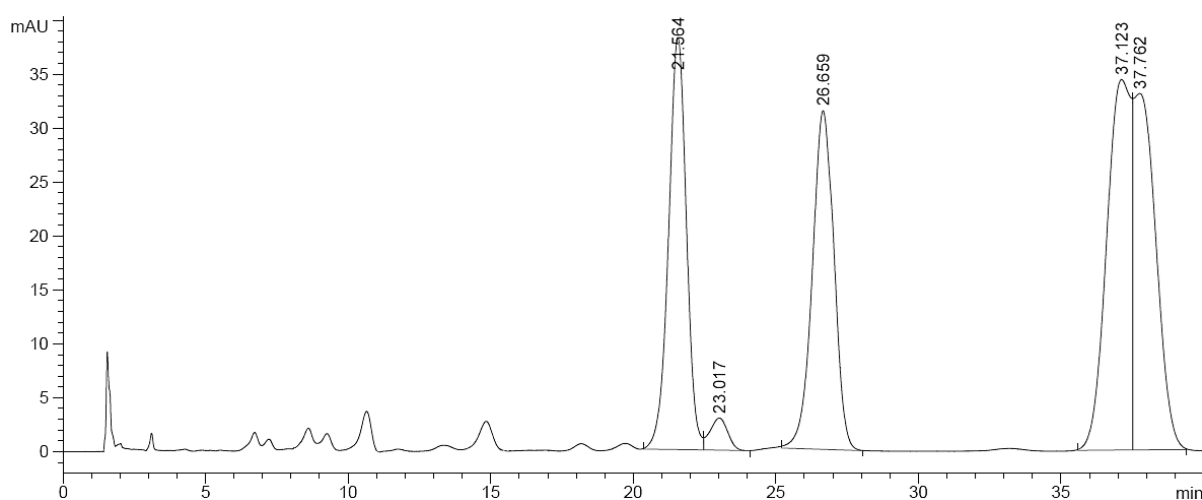
**Figure 3.8: GITC derivatisation of 3-aminobutyric acid**

To develop an *in-situ* reaction monitoring and product determination procedure, a 1 mL aliquot of the supernatant at the end of the biotransformation, prior to Cbz derivatisation, was lyophilised for 24 h. Following this, a solution of GITC in ACN was added with triethylamine and the reaction stirred for 1 h, at 40°C and this allowed derivatisation of acid and nitrile, and possibly amide product also. Separation was achieved on a Waters Symmetry C18 column, with a mobile phase of MeOH:H<sub>2</sub>O 35:65 + 0.1% TFA, and a flow rate of 1.0 mL.min<sup>-1</sup>. Comparative chromatograms of Cbz protected nitrile and acid are shown in Figure 3.9 where

the non-separation of the acid can be observed. A chromatogram of a mixed standard of GITC derivatised nitrile and acid is shown in Figure 3.10. The resolution of the acid peaks is 8.2 which is greater than 1.5 and thus means the peaks are now fully resolved.



**Figure 3.9: HPLC chromatograms of Cbz derivatised nitrile and acid. A – Cbz nitrile separated on chiral OJ-H column, mobile phase Hex:IPA 80:20 at a flow rate of 1 mL.min<sup>-1</sup>. B – Cbz acid run on chiral IA column, mobile phase Hex:IPA 90:10 + 0.1% TFA at a flow rate of 1 mL.min<sup>-1</sup>**



**Figure 3.10: HPLC chromatogram of a mixed standard of GITC derivatised nitrile and acid. Acid peaks at 21.6 and 26.7 min. Nitrile peaks at 37 min. Analysis carried out on a C18 column. Mobile phase MeOH:H<sub>2</sub>O 35:65 + 0.1% TFA, at a flow rate of 1 mL.min<sup>-1</sup>**

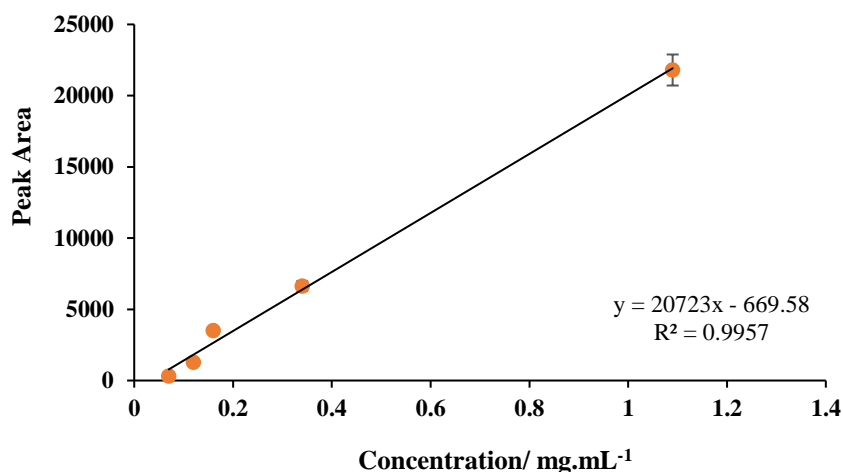
### 3.1.2.5 Summary

In summary, from the initial studies with the 3-HBN analogue 3-ABN and the isolate SET1, no nitrile was detected in any of the biotransformations. Acid was detected but in disappointing yields and poor ee which were worsened with increasing pH. It was observed that the acid produced was the (*S*) enantiomer and this is consistent with other work using *Rhodococcus* species<sup>18,19</sup>.

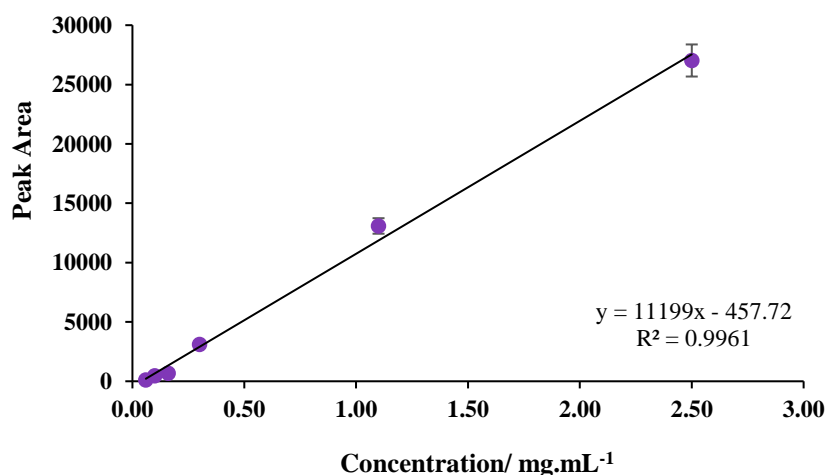
### 3.1.3 Additional studies to improve acid yield

#### 3.1.3.1 Time study

Further investigations were carried out to try and improve the yield of acid and efficiency of the biotransformation. In some cases, the concentrations of the products were low so exact absolute values must be treated with caution as value sample responses were below the calibrated response range in many cases. The first consideration in the investigations was that of the length of time of the biotransformations. The reactions were carried out over a period of 3 days with no intermittent testing and so it was possible that any product generated could be lost before then by metabolism by the whole cell. To test this, a timed experiment was carried out over 24 h with HPLC testing at 4 h, 8h, and 24 h, including a cell blank left for 24 h. Reactions were carried out at a 6 mL small scale with racemic 3-aminobutyronitrile (10 mM). The biotransformations were carried out in a suspension of phosphate buffer (0.1 M) at pH 7, containing induced cells ( $OD_{600nm} = 1$ ). The reactions were incubated at 25°C with mechanical shaking (200 rpm). Samples were put on with a biological replicate for each time point and the HPLC was completed in duplicate for each sample. Yields were calculated using generated standard curves of GITC derivatised nitrile and acid. Standard curves were produced using standards run in duplicate on the HPLC, giving  $R^2$  values of 0.9957 and 0.9961 for the nitrile and acid respectively. Curves are shown in Figures 3.11 and 3.12.



**Figure 3.11: HPLC standard curve of GITC-3-aminobutyronitrile. Analysis carried out on a C18 column. Mobile phase MeOH:H<sub>2</sub>O 35:65 at a flow rate of 1 mL.min<sup>-1</sup>. Error bars represent the error across the mean of the HPLC duplicates**



**Figure 3.12: HPLC standard curve of GITC-3-aminobutyric acid. Analysis carried out on a C18 column. Mobile phase MeOH:H<sub>2</sub>O 35:65 at a flow rate of 1 mL.min<sup>-1</sup>. Error bars represent the error across the mean of the HPLC duplicates**

Chromatograms of the results are shown in Figure 3.13. A representative calculation of how the acid yields were determined is shown below, using the 4 h time point as an example:

$$\begin{aligned}
 \text{Acid yield} &= \left( \frac{14.85 + 457.72}{11199} \right) \times 10 \\
 &= \frac{0.42198 \text{ mg mL}^{-1}}{1000} \times 1 \text{ mL} \\
 &= \frac{0.000422 \text{ g}}{0.00616} \\
 &= 7\%
 \end{aligned}$$

4 h sample acid peak areas: 19.7 and 10 = **14.85 average**

4 h sample HPLC repeat acid peak areas: 20.3 and 10.1 = 15.20 average

4 h biological repeat sample peak areas: 39.1 and 20.1 = 29.60 average

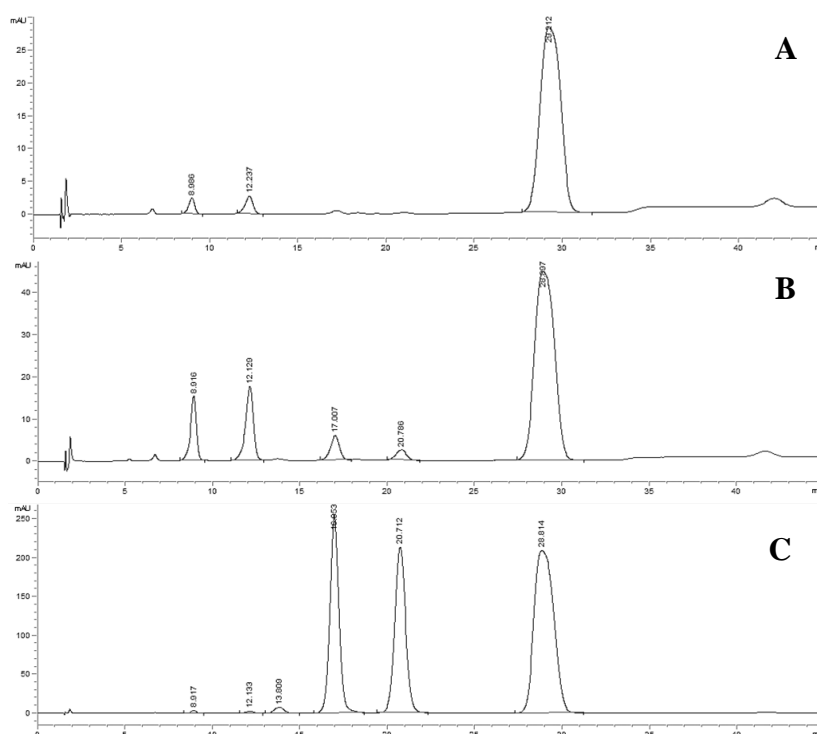
4 h biological repeat sample HPLC repeat peak areas: 38.1 and 18.4 = 28.25 average

Dilution factor = 10

1 mL sample analysed by HPLC

Nitrile added = 0.0072 g

Theoretical yield = 0.0062 g



**Figure 3.13:** HPLC chromatograms of SET1 with 3-ABN monitored over 24 h. A – 4h, B – 24 h, C – mixed standard of GITC-ABA and GITC-ABN at 1 mg.mL<sup>-1</sup>. Acid peaks at 17.0 and 20.7 min. Nitrile peak at 28.8 min. Analysis carried out on a C18 column. Mobile phase MeOH:H<sub>2</sub>O 35:65 + 0.1% TFA, at a flow rate of 1 mL.min<sup>-1</sup>

During these studies it was discovered that at the 4 h time point, acid could already be detected with an average yield of 7% and an average ee of 33%, the highest that had been detected thus far. Values slightly increased to 9% yield and 35% ee by the 24 h time point as seen in Table 3.2.

**Table 3.2:** Time study of SET1 with 3-aminobutyronitrile

Entry	Time (h)	Nitrile	Acid	
		% recovered	Yield (%) <sup>[b]</sup>	ee (%) <sup>[c]</sup>
<b>1</b>	4	26	7	33 ( <i>S</i> )
<b>2</b>	8	30	8	34 ( <i>S</i> )
<b>3</b>	24	26	9	35 ( <i>S</i> )

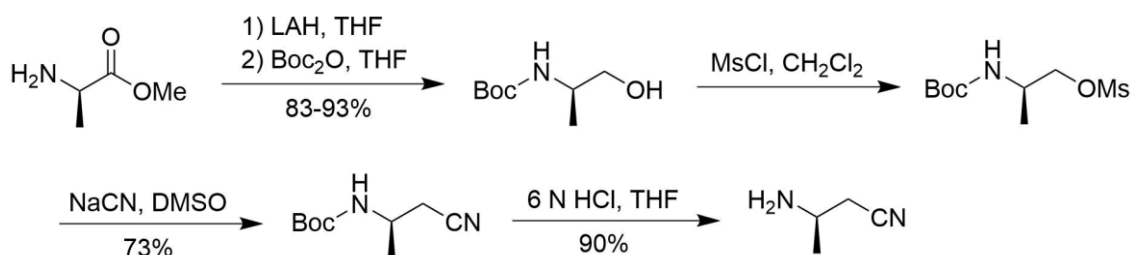
<sup>a</sup>Biotransformations were carried out by incubating 3-aminobutyronitrile (10 mM) in a suspension of *Rhodococcus erythropolis* SET1 (OD<sub>600nm</sub>=1) in phosphate buffer (pH 7) at 25°C. <sup>b</sup>Calculated yields using GITC standard curves in Fig 3.11-3.12. <sup>c</sup>Determined by HPLC analysis using a C18 column following chiral derivatisation

Interestingly, nitrile was detected for the first time from the 4 h time point, right up to 24 h but in relatively small quantities (26%) for that stage of the reaction. This is comparable to the cell blanks carried out at the same time, which indicated a 30% recovery of nitrile after 24 h. This

study served to inform future studies with 3-aminobutyronitrile so that they would be carried out over shorter periods of time with periodic monitoring where possible.

### 3.1.3.2 Free nitrile or HCl salt

The next consideration was that the nitrile was supplied in a 30% HCl salt form and this may have an effect on yield. The supplier stated the nitrile is 70% free at pH 7 and is most stable at pHs below this point. This clearly posed a challenge as biotransformations in this work are thought to work optimally at pH 7 and above<sup>8,20,21</sup>. Generation of the free base for biotransformation was explored. Attempts to isolate this by salting extraction were thus carried out followed by biotransformations with SET1 to see if this could lead to improved product yield. Firstly, a salt break was attempted following the approach of Crawford *et al* to isolate (*R*)-3-aminobutyronitrile from their synthesis shown in Scheme 3.8<sup>22</sup>.



**Scheme 3.8: Synthesis of (*R*)-3-aminobutyronitrile intermediate by Crawford *et al*<sup>22</sup>**

In their procedure, which followed a *N*-boc deprotection, tetrahydrofuran was removed *in vacuo*. The mixture was then cooled to 10°C. Sodium hydroxide (40%) was added slowly. Sodium chloride was added, and the mixture was extracted with methanol:dichloromethane (1:9), dried over Na<sub>2</sub>SO<sub>4</sub> and reduced *in vacuo* to give an orange oil.

Our attempt was carried out at a small scale. A solution of 3-aminobutyronitrile HCl (10 mM, 0.0072 g) was prepared with 40% NaOH which was added slowly over a 10°C water bath. Sodium chloride was added, and the solution was extracted with a mixture of methanol:dichloromethane (1:9). The combined organic extracts were dried over Na<sub>2</sub>SO<sub>4</sub> and reduced *in vacuo* to give a colourless residue of theoretically free 3-aminobutyronitrile. This was transferred to the biotransformation which was carried out at a 6 mL scale. The biotransformation was carried out in a suspension of phosphate buffer (0.1 M) at pH 7, containing induced cells (OD<sub>600nm</sub> = 1). The reaction was incubated at 25°C with mechanical

shaking (200 rpm) for 24 h. A replicate reaction was carried out for 48 h and both reactions were analysed by HPLC in duplicate. Yields were calculated from HPLC GITC standard curves.

**Table 3.3: Effect on the biotransformation of using the generated free nitrile**

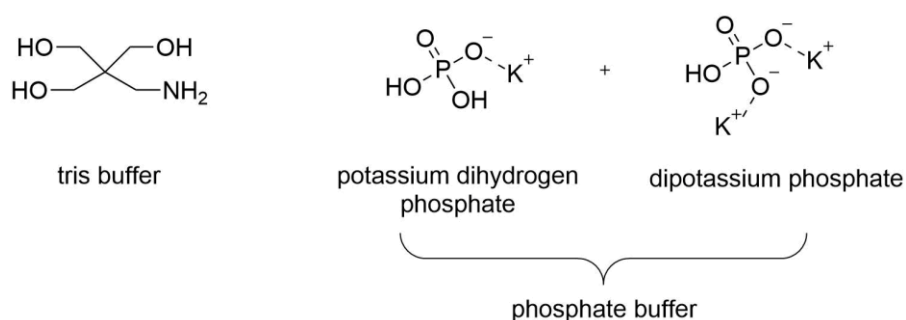
Entry	Time (h)	Nitrile	Acid	
		% recovered	Yield (%) <sup>[b]</sup>	ee (%) <sup>[c]</sup>
1	24	5	7	8 ( <i>S</i> )
2	48	5	7	11 ( <i>S</i> )

<sup>a</sup>Biotransformations were carried out by incubating 3-aminobutyronitrile (10 mM) in a suspension of *Rhodococcus erythropolis* SET1 (OD<sub>600nm</sub>=1) in phosphate buffer (pH 7) at 25°C. <sup>b</sup>Calculated yields using GITC standard curves in Fig 3.11-3.12. <sup>c</sup>Determined by HPLC analysis using a C18 column following chiral derivatisation

Whilst the acid yield remained comparable to previous studies, the ee had dropped significantly for these time points as seen in Table 3.3. The amount of nitrile recovered was also substantially less. This perhaps indicated that the free amino could have possibly been more accessible to be metabolised by competing enzymatic pathways as suggested previously. Another possibility is that at pH 7, the free amino may have been re-ionised thus making it less compatible with the nitrilase active site.

### 3.1.3.3 Buffer system

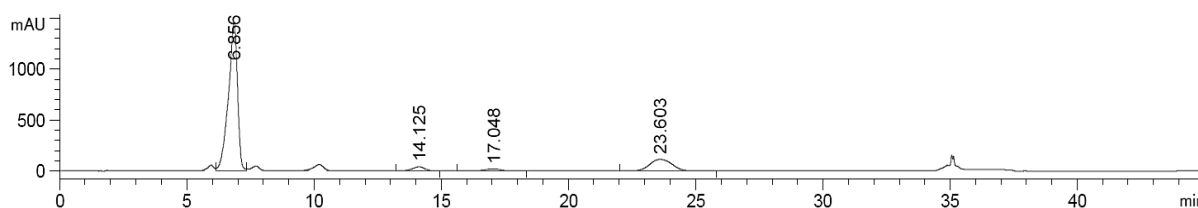
The final investigation was into the buffer system of the biotransformations and effect on yield and ee. This was of importance as the buffer system can possibly affect the substrate binding action of the enzyme<sup>23</sup>. Previously biocatalytic studies were carried out in phosphate buffer at pH 7, 8, and 9. Phosphate buffer is classed as having a working range of 5.8-8 and required the addition of sodium hydroxide to alter buffer to the required pH. Tris(hydroxymethyl)aminomethane (Tris) buffer in comparison, could prove better as it is best for biotransformations within a pH range of 7-9<sup>2,24,25</sup>.



**Scheme 3.9: Chemical composition of Tris buffer and Phosphate buffer**

From Scheme 3.9, the difference in composition between Tris buffer and phosphate buffer can be observed. The pKa of phosphate buffer is approximately 7.2 and that of Tris buffer is approximately 8.1. Phosphate buffer therefore has a poorer buffering capacity when over pH 7.5 whilst Tris buffer is poorer below pH 7.5<sup>26,27</sup>. This would make tris buffer more ideal for working from pH 8 upwards.

Small scale experiments were thus carried out utilising Tris buffer at pH 7, 8, 9 (0.1 M) with 3-aminobutyronitrile HCl (10 mM), containing induced cells ( $OD_{600nm} = 1$ ). The reactions were incubated at 25°C with mechanical shaking (200 rpm) for 24 h. A repeat experiment was carried out at pH 7 to facilitate comparison when running a cell blank experiment at pH 7 under the same conditions. All samples were run with biological duplicates. HPLC was carried out in duplicate on 1 mL aliquots of each reaction which were GITC derivatised. Yields were calculated from standard curves. A representative HPLC chromatogram is shown in Figure 3.14 and the results are shown in Table 3.4.



**Figure 3.14:** HPLC chromatogram of the biotransformation replicate of SET1 with 3-ABN in Tris buffer (pH 7) for 24 h. GITC acid peaks at 14.1 and 17.0 min. GITC nitrile peak at 23.6 min. Analysis carried out on a C18 column. Mobile phase MeOH:H<sub>2</sub>O 35:65 + 0.1% TFA, at a flow rate of 1 mL.min<sup>-1</sup>

**Table 3.4:** Effect of Tris buffer on the biotransformation of SET1 with 3-aminobutyronitrile

Entry	pH	Time (h)	Nitrile		Acid	
			% recovered	Yield (%) <sup>[b]</sup>	Yield (%) <sup>[b]</sup>	ee (%) <sup>[c]</sup>
1	7	24	40	23	25 (S)	
2	8	24	13	28	25 (S)	
3	9	24	13	23	12 (S)	
4	7 replicate	24	28	16	21 (S)	
5	7 cell blank	24	56	ND	ND	

<sup>a</sup>Biotransformations were carried out by incubating 3-aminobutyronitrile (10 mM) in a suspension of *Rhodococcus erythropolis* SET1 ( $OD_{600nm}=1$ ) in Tris buffer (pH 7, 8, or 9) at 25°C. <sup>b</sup>Calculated yields using GITC standard curves in Fig 3.11-3.12. <sup>c</sup>Determined by HPLC analysis using a C18 column following chiral derivatisation. ND = Not Detected



The change in buffer appeared to significantly increase the yields of acid observed whilst ee's were comparable to previous studies. The ee's are seen to again decrease as pH increases. A small increase in acid yield at pH 8 without the loss of ee may indicate this may have been the best pH to work with for the Tris buffer. The nitrile was recovered at its highest percentage thus far at 40% for pH 7 but dropped sharply for pH 8 and 9. The experiments were only carried out at a small scale and so further work would be needed at a larger scale to acquire isolated product for analysis and isolated nitrile to assess its ee. Although ee remained low, the *N*-protected variants may offer more potential in the Tris buffer system. Whilst these preliminary results were positive, they did not yield a great enough improvement in acid ee to warrant further investigations with this substrate within the given time.

#### 3.1.4 Induction Investigations for Isolate SET1

Enzyme induction on the substrate of interest can often yield high ee and recovery. This may occur because when the cells are exposed specifically to a substrate which the enzyme can metabolise, the rate of synthesis of that particular enzyme increases<sup>28</sup>. Nitrilases are known to be mostly inducible by substrates, products and also by their analogs<sup>10,29</sup>. In our case, 3-HBN (**131**) was used to induce isolate SET1 following on from Coady *et al*<sup>1</sup>. An attempt was made therefore to induce isolate SET1 on 3-aminobutyronitrile hydrochloride (**124**). Cells were inoculated into M9 minimal media containing racemic 3-aminobutyronitrile (10 mM) at a final cell density of  $OD_{600nm} = 1$ . The culture was incubated at 25°C for 3 days with mechanical shaking (200 rpm). The cells were pelleted, washed with phosphate buffer (pH 7), then resuspended in phosphate buffer (pH 7). The biotransformation was then carried out at a 6 mL scale in phosphate buffer (pH 7) with substrate (**124**) and induced SET1 cells ( $OD_{600nm} = 1$ ) at 25°C for 3 days with mechanical shaking (200 rpm). In this instance, only 8% nitrile was recovered with 2% ee. The ee of the acid decreased significantly in comparison to when induced on 3-HBN, down to 5% (*S*) from 29% (*S*) but the yield increased to 5%. These results meant it was not a viable option to induce isolate SET1 on 3-aminobutyronitrile (**124**) for biotransformations.

### 3.1.5 Summary from enantioselectivity screening of SET1 with 3-aminobutyronitrile (124)

In summary, while progress was made to detect and improve the recovery of product from the biotransformation mixture, the relatively poor results of isolate SET1 with 3-aminobutyronitrile lead us to screen SET1 with *N*-protected nitrile variants to determine if this would yield an improvement in the scope of SET1 with  $\beta$ -aminonitriles.

## 3.2 Enantioselectivity Screening of SET1 with the *N*-protected nitriles

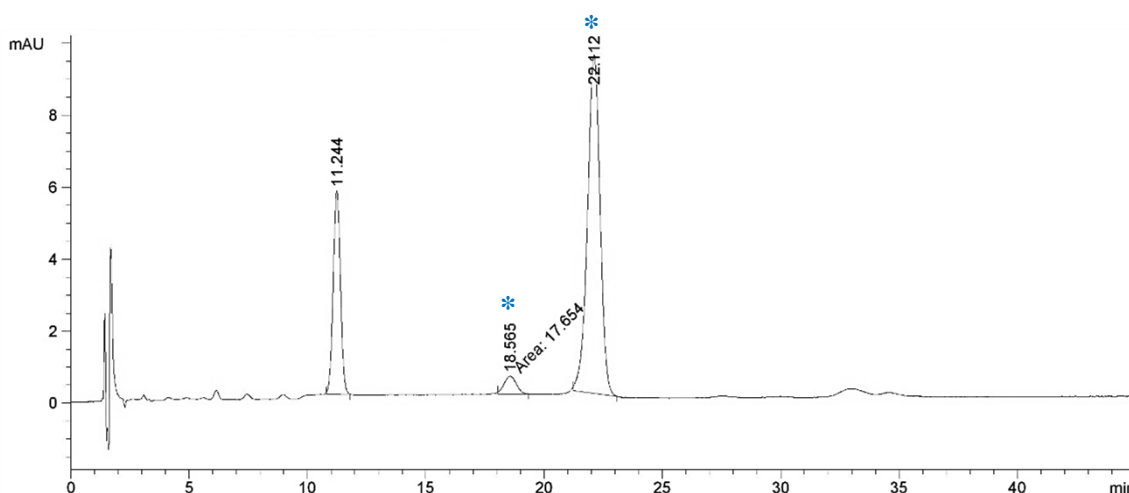
The *N*-protected nitriles chosen for screening SET1 were those shown previously in Figure 3.1 and are discussed in depth in Chapter 2. The addition of the protecting groups was anticipated to result in a possible increase in yield and ee. It was also anticipated that some of the *N*-protected nitriles would exhibit poor solubility in phosphate buffer, so measures were taken to ensure 100% availability of the substrate to the bacterial isolate. Organic solvent studies and their effect on isolate SET1's performance, carried out by Coady *et al*, showed the best activity results of isolate SET1 were with the addition of 5% DMSO<sup>30</sup>. IPA also produced excellent activity results at 35% up to 50% IPA. While activity studies were carried out, the effect on enantioselectivity was not determined in both cases. A conservative approach was chosen however, as to not risk overwhelming the bacterial isolate with solvent and 20% IPA or 5% DMSO was selected to enhance solubility of the substrate in this work. For this stream of research, the pH was kept at 7 for all the biotransformations as isolate SET1 had demonstrated loss of enantioselectivity at higher pH's, with already poor yields and ee only decreasing rapidly with increasing pH.

### 3.2.1 SET1 and compound 125

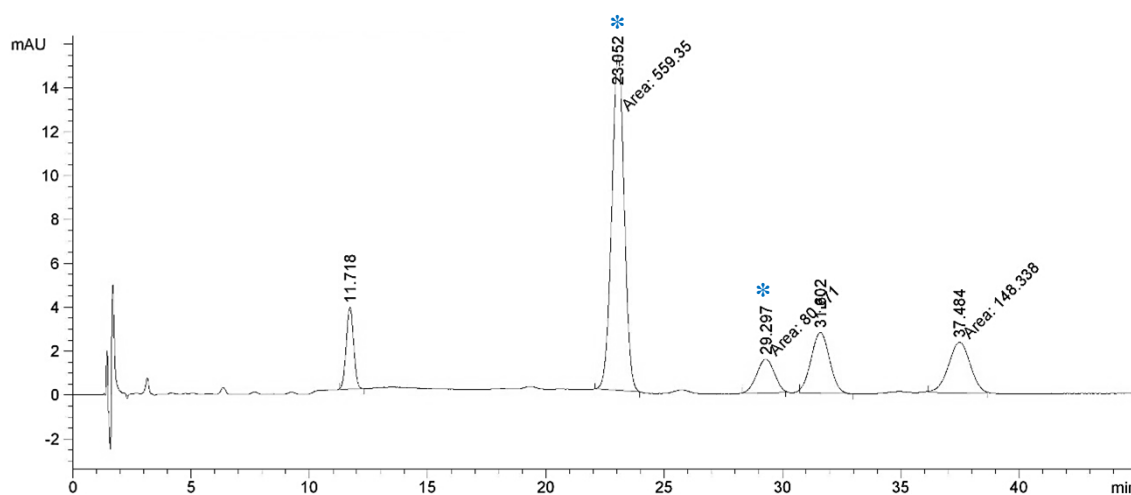
The first protected substrate to be evaluated was 3-(benzylamino)butyronitrile, substrate (**125**). The workup method applied was that by Wang *et al*<sup>6</sup>. The solvent of choice was DMSO as the oily substrate best dissolved in DMSO in comparison to IPA. The biotransformation was carried out in a suspension of phosphate buffer (0.1 M, pH 7) with 5% DMSO, containing induced cells ( $OD_{600nm} = 1$ ). Racemic 3-(benzylamino)butyronitrile (10 mM) was added to the

flask and the mixture was incubated at 25°C for 24 hours with mechanical shaking (200 rpm). The reaction was quenched by removal of the biomass by centrifugation. The acidified supernatant was passed through a cation exchange Amberlite® resin and the ammonia eluent was concentrated and purified on a semi-preparatory C18 HPLC (Phenomenex Jupiter C18 10 µm column, gradient elution H<sub>2</sub>O:ACN + 0.1% formic acid, flow rate 5 mL.min<sup>-1</sup>). The products could not be separated on the available HPLC columns to determine ee, so they were derivatised with GITC to acquire ee data. Yields were acquired as isolated yields.

As with 3-ABN, no nitrile was detected post work-up, but amide was detected in 3% yield with 90% ee, and acid was present in 6% yield with 75% ee (*S*). The presence of acid was verified by observations in the LC-MS of *m/z* 216.0 (M+Na<sup>+</sup>) and 194.1 (M+H<sup>+</sup>). Representative HPLC chromatograms of the biotransformation are shown in Figures 3.16 and 3.17 and a summary of the data is shown in Table 3.5.



**Figure 3.16: HPLC chromatogram showing the amide product of the biotransformation of SET1 with the Benzyl protected nitrile. Asterix denote peaks of interest. Chiral analysis carried out on a C18 column. Mobile phase MeOH:H<sub>2</sub>O 55:45 + 0.1% TFA, at a flow rate of 1 mL.min<sup>-1</sup>**



**Figure 3.17:** HPLC chromatogram showing the acid product of the biotransformation of SET1 with the Benzyl protected nitrile. Asterixis denote peaks of interest. Chiral analysis carried out on a C18 column. Mobile phase MeOH:H<sub>2</sub>O 55:45 + 0.1% TFA, at a flow rate of 1 mL.min<sup>-1</sup>

**Table 3.5:** Biotransformations of SET1 with 3-(benzylamino)butyronitrile

Co-solvent	pH	Time	Nitrile	Amide		Acid	
				Yield (%) <sup>[b]</sup>	ee (%) <sup>[c]</sup>	Yield (%) <sup>[b]</sup>	ee (%) <sup>[c]</sup>
5% DMSO	7	24 h	ND	3	90	6	75 (S)

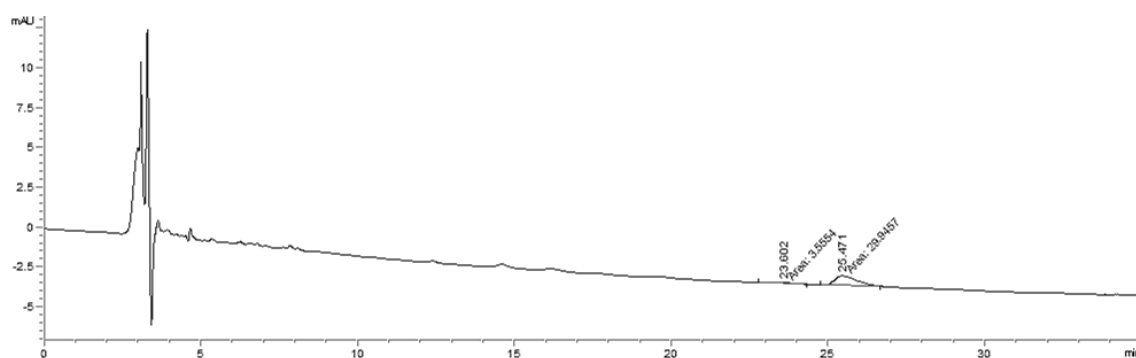
<sup>a</sup>Biotransformations were carried out by incubating 3-(benzylamino)butyronitrile (10 mM) in a suspension of *Rhodococcus erythropolis* SET1 (OD<sub>600nm</sub>=1) in phosphate buffer (pH 7) at 25°C. <sup>b</sup>Isolated yield after semi-prep HPLC. <sup>c</sup>Determined by HPLC analysis using a C18 column following chiral derivatisation. ND = Not Detected

Despite the low yield, the ee of the acid had dramatically increased. This was surprising as at pH 7, the substrate would highly likely be protonated<sup>8,20</sup>. Another interesting observation was the first-time appearance of amide with a high ee of 90%.

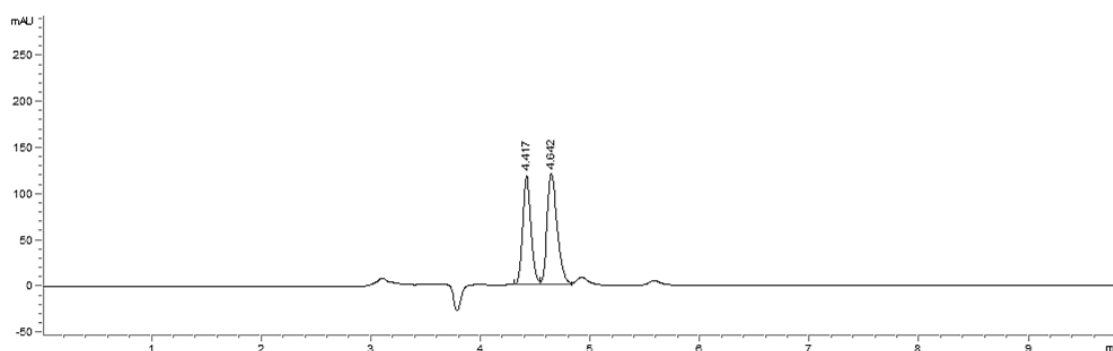
### 3.2.2 SET1 and compound 126

The next substrate to be evaluated was 2-methyl-2-propanyl(1-cyano-2-propanyl)carbamate, substrate (**126**). The workup method implemented was that of Chhiba *et al*<sup>8</sup>. Two biotransformations were carried out in suspensions of phosphate buffer (0.1 M, pH 7), one with 5% DMSO and the other with 20% IPA, both containing induced cells (OD<sub>600nm</sub> = 1). Racemic 2-methyl-2-propanyl(1-cyano-2-propanyl)carbamate (10 mM) was added to each flask and the

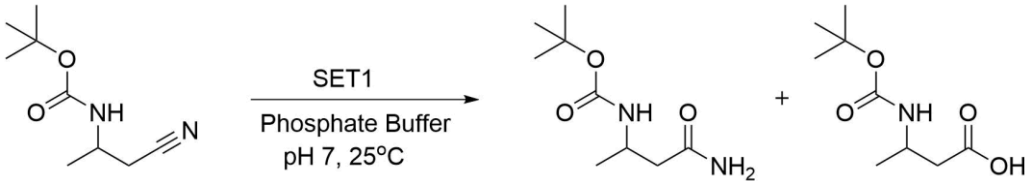
mixtures were incubated at 25°C for 3 days with mechanical shaking (200 rpm). The reactions were quenched by removal of the biomass by centrifugation. An acid/base workup allowed for the products to be acquired. The nitrile could not be separated by HPLC with any of the chiral columns available (IA, AD-H, OJ-H, AS-H). Chiral GC with a  $\beta$ -cyclodextrin column was attempted and no separation was achieved. The nitrile product was thus hydrolysed to the amide and ee was reported using the developed method for the amide standard (IA column, Hex:IPA 97:3 + 0.1% TFA). The nitrile was dissolved in MeOH and potassium carbonate and aqueous hydrogen peroxide (35%) were added. The reaction was stirred at room temperature with monitoring. On completion, the MeOH was removed under reduced pressure and the aqueous phase was diluted with water. This was extracted with DCM, dried over Na<sub>2</sub>SO<sub>4</sub>, and reduced *in vacuo* to give the amide. This was analysed by LC-MS to verify the presence of amide. Representative HPLC chromatograms of the biotransformations are shown in Figures 3.18 and 3.19 and a summary of the data is shown in Table 3.6.



**Figure 3.18:** HPLC chromatogram of the recovered nitrile hydrolysed to amide of the biotransformation of SET1 with the boc protected nitrile with 5% DMSO. Analysis carried out on a chiral IA column. Mobile phase Hex:IPA 97:3 + 0.1% TFA, at a flow rate of 1 mL.min<sup>-1</sup>



**Figure 3.19:** HPLC chromatogram of the acid of the biotransformation of SET1 with the boc protected nitrile with 5% DMSO. Analysis carried out on a chiral OJ-H column. Mobile phase Hex:IPA 90:10 + 0.1% TFA, at a flow rate of 1 mL.min<sup>-1</sup>

**Table 3.6: Biotransformation of boc *N*-protected substrate (126) with isolate SET1**


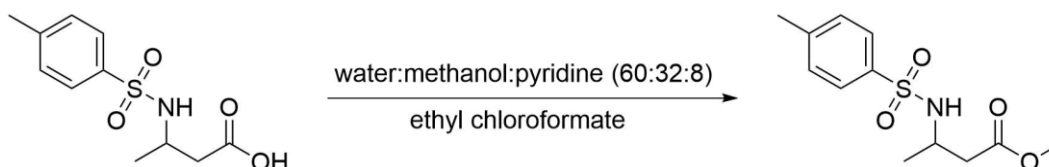
Co-solvent	pH	Nitrile		Amide	Acid	
		Yield (%) <sup>[b]</sup>	ee (%) <sup>[c]*</sup>	Yield (%)	Yield (%) <sup>[b]</sup>	ee (%) <sup>[c]</sup>
5% DMSO	7	55	79	ND	1	10 ( <i>S</i> )
20% IPA	7	97	0.1	ND	ND	ND

<sup>a</sup>Biotransformations were carried out by incubating 2-methyl-2-propanyl(1-cyano-2-propanyl)carbamate (10 mM) in a suspension of *Rhodococcus erythropolis* SET1 (OD<sub>600nm</sub>=1) in phosphate buffer (pH 7) at 25°C. <sup>b</sup>Isolated yields after flash column. <sup>c</sup>Determined by HPLC analysis using a chiral column following chiral derivatisation. \*Analysed as amide

It was evident that IPA was not a suitable co-solvent in this case with no amide or acid being detected and 97% nitrile recovered from the reaction. The biotransformation conducted with 5% DMSO produced a poor yield of acid however and a disappointing ee of 10%.

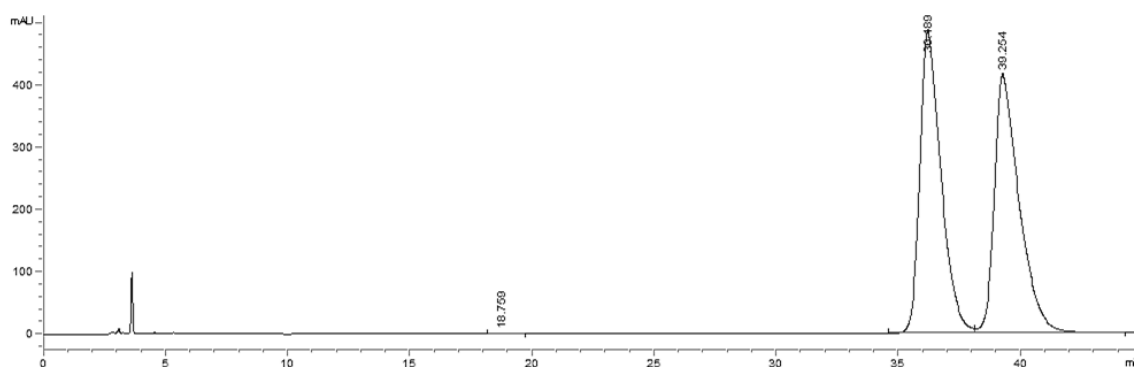
### 3.2.3 SET1 and compound 127

Finally, the last 3-ABN protected substrate to be evaluated with isolate SET1 was the tosyl derivative *N*-(1-cyano-2-propanyl)-4-methylbenzenesulfonamide, substrate (127). The workup method followed was adapted from Chhiba *et al*<sup>8</sup>. Two biotransformations were carried out in suspensions of phosphate buffer (0.1 M, pH 7), one with 5% DMSO and the other with 20% IPA, both containing induced cells (OD<sub>600nm</sub> = 1). Racemic *N*-(1-cyano-2-propanyl)-4-methylbenzenesulfonamide (10 mM, 0.050 g) was dissolved in the required amount of either DMSO or IPA separately and was added to each flask and the mixtures were incubated at 25°C for 3 days with mechanical shaking (200 rpm). It is worth mentioning that the solubility of the nitrile remained poor even in the presence of 5% DMSO, with the substrate crashing out into the buffer solution upon contact. The reactions were quenched after reaction by removal of the biomass by centrifugation and the pellet was washed with ethyl acetate to maximise recovery. An acid/base workup allowed for the acid, amide, nitrile products to be acquired. As the acid enantiomers cannot be separated by chiral HPLC as discussed in Chapter 2, the acid product was esterified to the methyl ester at the time, to allow determination of selectivity as shown in Scheme 3.10.

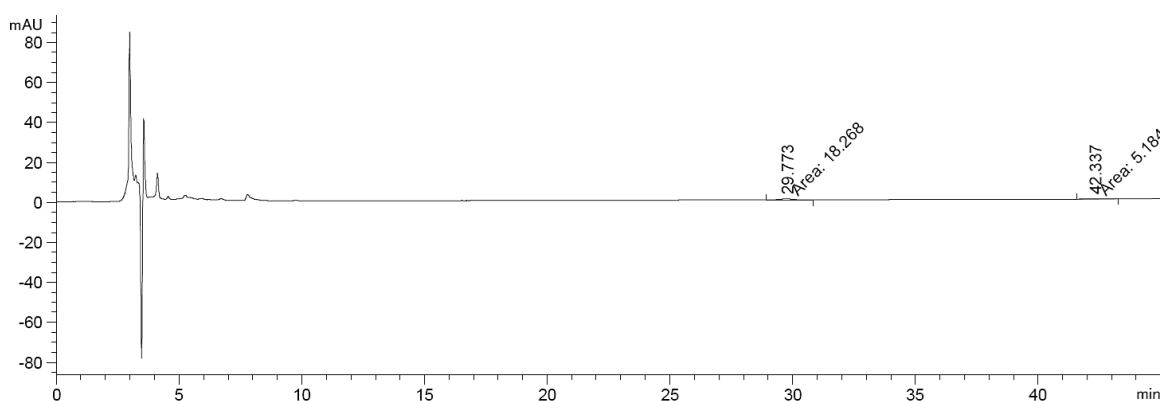


**Scheme 3.10: Esterification of tosyl protected acid to the methyl ester**

The acid was dissolved in a mixture of water:methanol:pyridine (60:32:8). Ethyl chloroformate was added and the reaction mixture was stirred for 5 min. The mixture was extracted with chloroform including 1% ethyl chloroformate. The solvent was removed *in vacuo* to give the methyl ester and this was analysed on an IA column. The presence of the acid and nitrile were confirmed by LC-MS. HPLC chromatograms of the biotransformations are shown in Figures 3.20 and 3.21.



**Figure 3.20: HPLC chromatogram showing the recovered nitrile of the SET1 biotransformation with the tosyl nitrile with 5% DMSO. Analysis carried out on a chiral IA column. Mobile phase Hex:IPA 90:10, at a flow rate of 1 mL.min<sup>-1</sup>**



**Figure 3.21: HPLC chromatogram showing the acid product of the SET1 biotransformation with the tosyl nitrile with 5% DMSO. Analysis carried out on a chiral IA column. Mobile phase Hex:IPA 90:10 + 0.1% TFA, at a flow rate of 1 mL.min<sup>-1</sup>**

**Table 3.7: Results of biotransformation of tosyl *N*-protected substrate (127) with isolate SET1**

Co-solvent	pH	Nitrile		Amide		Acid	
		Yield (%) <sup>[b]</sup>	ee (%) <sup>[c]</sup>	Yield (%) <sup>[b]</sup>	ee (%) <sup>[c]</sup>	Yield (%) <sup>[b]</sup>	ee (%) <sup>[c]</sup>
5% DMSO	7	74	0	9	1	<1	>99 ( <i>S</i> )
20% IPA	7	86	0.2	ND	ND	ND	ND

<sup>a</sup>Biotransformations were carried out by incubating *N*-(1-cyano-2-propanyl)-4-methylbenzenesulfonamide (10 mM) in a suspension of *Rhodococcus erythropolis* SET1 (OD<sub>600nm</sub>=1) in phosphate buffer (pH 7) at 25°C. <sup>b</sup>Isolated yields after flash column. <sup>c</sup>Determined by HPLC analysis using a chiral column

In this case again, IPA was not an appropriate co-solvent for the biotransformation with no amide or acid being produced as seen in Table 3.7 and starting substrate recovered. With 5% DMSO, high acid ee was observed. The acid was observed in very low yield, however. Apart from the *N*-benzyl protected biotransformation, this was the other protected variant where amide was detected after the reaction, albeit with low yield and ee. Despite very poor yield of acid product, there was interest to see if further investigations could be carried out to improve acid yield by variation of quantity solvent additive to enhance the solubility of the starting nitrile. The fact that SET1 was able to even tolerate such a bulky protecting group was of great interest as this was not observed in previous work by Coady *et al*<sup>7</sup>.

### 3.2.4 Summary from SET1 and *N*-protected nitriles

In the studies of protected variants of 3-ABN the boc and tosyl *N*-protected substrate biotransformations were the only cases where nitrile was observed, with the highest ee observed for the *N*-boc protected nitrile at 79% which is surprising and it is disappointing that similar enhancement in ee of the product acid was not obtained. In this case, the presence of the *N*-boc and *N*-tosyl groups may offer the substrate protection from degradation *in situ* as well as increasing recovery from the aqueous reaction phase hence these results were observed. Both the *N*-boc and *N*-tosyl protections gave poor acid yields however, in the case of the tosyl protection, the acid was in a high ee, >99%. The *N*-tosyl protection also yielded amide albeit in poor yield and ee whereas no amide was detected for the *N*-boc derivative. Similar



observations can be found in the work of Chhiba *et al* who saw negligible results upon the addition of the *N*-boc and *N*-tosyl groups, and Preiml *et al* who also detected amide for their *N*-tosyl protected nitrile derivatives using *Rhodococcus* sp<sup>8,31</sup>. In the findings of Preiml *et al*, they mostly recovered nitrile with low yields for the amide and acid of 3% and 2% respectively for *Rhodococcus* sp. R312, and 7% and 3% respectively for *Rhodococcus erythropolis* NCIMB 11540<sup>31</sup>. This is comparable to our results where we observed 9% amide and <1% acid. Preiml *et al* also noted the difficulty in solubilising the bulkier protecting groups in aqueous media which we also experienced<sup>31</sup>.

The best overall results were observed for the benzyl *N*-protected nitrile, which gave no nitrile but high ee's of 90% and 75% for the amide and acid respectively within 24 h. Such improvement in results by the addition of the benzyl group were also observed in the work of Wang *et al* which alludes to isolate SET1 possible need of a docking group for interaction to occur with  $\beta$ -amino nitrile substrates<sup>6</sup>. Wang *et al* postulated that a docking group would lead to the enzyme's chiral recognition being heightened thus resulting in higher enantioselectivities being seen. They did indeed observe higher ee's with the added benzyl group however the reaction time increased also. In their case much higher yields were obtained. In our case, the *N*-benzyl protecting group allowed relatively high ee's to be achieved in a much shorter time i.e. 24 h versus the 72 h needed for the *N*-boc and *N*-tosyl protecting groups but with poor yields. A summary of the results can be seen in Table 3.8.

**Table 3.8: Summary of *N*-protected biotransformations with SET1**

Entry	R	Co-solvent	Nitrile		Amide		Acid	
			Yield (%) <sup>[b]</sup>	ee (%) <sup>[c]</sup>	Yield (%) <sup>[b]</sup>	ee (%) <sup>[c]</sup>	Yield (%) <sup>[b]</sup>	ee (%) <sup>[c]</sup>
1	Bn	5% DMSO	ND	ND	3	90	6	75 ( <i>S</i> )
2	Boc	5% DMSO	55	79 <sup>*a</sup>	ND	ND	1	10 ( <i>S</i> )
3	Boc	20% IPA	97	0.1 <sup>*a</sup>	ND	ND	ND	ND
4	Ts	5% DMSO	74	0.03	9	1	<1	>99 <sup>*b</sup> ( <i>S</i> )
5	Ts	20% IPA	86	0.2	ND	ND	ND	ND

<sup>a</sup>Biotransformations were carried out by the nitrile (10 mM) in a suspension of *Rhodococcus erythropolis* SET1 (OD<sub>600nm</sub>=1) in phosphate buffer (pH 7) at 25°C. <sup>b</sup>Isolated yields after purification. <sup>c</sup>Determined by HPLC analysis using a chiral column

### 3.3 Enantioselectivity Screening of SET1 with Aromatic $\beta$ -Amino Nitriles

Having observed interesting results screening the aliphatic substrates against SET1, the analogous aromatic substrates were also screened. The isolate SET1 was observed to prefer aliphatic substrates in prior work so it was expected to not perform well with the aromatic substrates<sup>7</sup>. The reactions were all carried out at a 50 mg nitrile scale and 5% DMSO was added in cases to facilitate solubility of the nitriles. The first aromatic substrate to be evaluated was 3-amino-3-phenylpropionitrile (**122**). Reactions were carried out at a 50 mg small scale with racemic 3-amino-3-phenylpropionitrile (10 mM). The biotransformations were carried out at 25°C in a suspension of phosphate buffer (0.1 M) at pH 7, containing induced cells ( $OD_{600nm} = 1$ ) with mechanical shaking (200 rpm). The reaction was quenched by removal of the biomass by centrifugation. An acid/base workup allowed for the acid and nitrile products to be acquired. Products were purified by prep TLC to acquire isolated yields. The acid fraction was derivatised with GITC to obtain ee. The biotransformation was put on as a single sample and the HPLC was completed as single injections. Acid products were verified by comparison to analysed standards. Again, disappointingly poor recovery of nitrile was obtained at pH 7 (17%) and no acid was observed, however. This substrate was also evaluated under pH 9 conditions and another biotransformation was carried out with the same protocol with the exception of using phosphate buffer at pH 9. No nitrile or acid was observed.

Screening of the *N*-protected aromatic nitriles saw no acid or amide products, but the starting nitrile was recovered in each case as indicated in Table 3.9. This may be because the protected aromatic substrates are too bulky, and the enzyme faces steric hinderance. The pH may also be a factor as below pH 9 the amino group may be protonated and thus will react poorly with the enzyme active site. This was the case for Chhiba *et al* when they screened 3-APPN and saw no results at pH 7 but they observed acid with 7% ee at pH 9 in their study<sup>8</sup>.

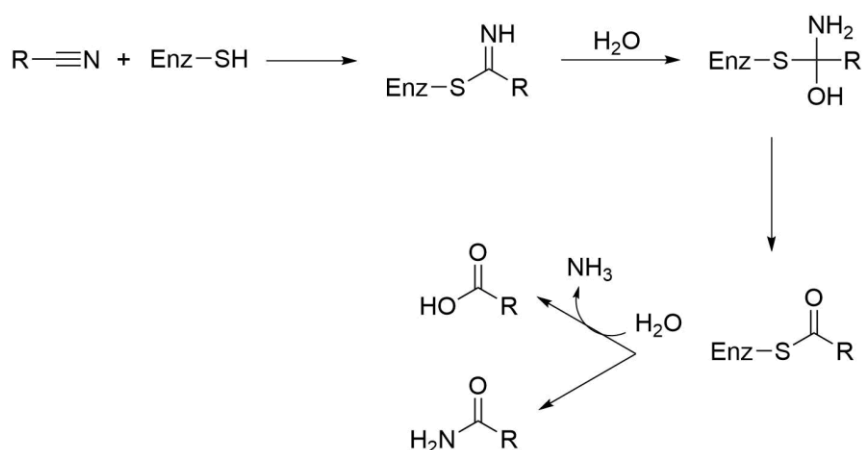
Many of the aromatic nitriles were difficult to synthesise especially since the protected variants required 3-amino-3-phenylpropionitrile (3-APPN) (**122**) as a starting point. This nitrile, 3-APPN (**122**), was particularly challenging to synthesise and thus created a bottle neck to producing the protected analogues. This meant that further investigations with these substrates were limited.

**Table 3.9: Summary of biotransformations for SET1 with the aromatic  $\beta$ -amino nitriles**

Entry	R	Time (h)	pH	Nitrile		Amide		Acid	
				Yield (%) <sup>[b]</sup>	ee (%) <sup>[c]</sup>	Yield (%) <sup>[b]</sup>	ee (%) <sup>[c]</sup>	Yield (%) <sup>[b]</sup>	ee (%) <sup>[c]</sup>
1	H	72	7	17	11	ND	ND	2	3 ( <i>R</i> )
2	H	72	9	ND	ND	ND	ND	ND	ND
3	Bn	72	7	78	0.6	ND	ND	ND	ND
4	Boc	72	7	66	0.5	ND	ND	ND	ND
5	Ts	72	7	96	0.8	ND	ND	ND	ND

<sup>a</sup>Biotransformations were carried out by incubating the nitrile (10 mM) in a suspension of *Rhodococcus erythropolis* SET1 ( $OD_{600nm} = 1$ ) in phosphate buffer at pH 7 with 5% DMSO, at 25°C. <sup>b</sup>Isolated yields after purification. <sup>c</sup>ee determined by HPLC. ND = not detected

As it became apparent that isolate SET1 was not a suitable isolate for the transformation of these substrates with the required yield and ee for an industrial setting, effort was put into identifying other possible isolates for the work which may offer more potential to transform the class of substrate. It would appear that SET1 may possibly be working with a dual mechanism from the results observed with the  $\beta$ -amino nitriles. The suggestion of a dual pathway is prompted by the detection of both acid and amide products. The nitrilase contains a Glu-Lys-Cys triad at its active site and the thiol group in cysteine proves particularly critical for the pathway, as shown in Scheme 3.10.

**Scheme 3.10: Proposed pathway of a nitrilase with the thiol functionality of the active site triad highlighted**

### 3.4 Enantioselectivity Screening of Additional Isolates

In order to identify more suitable isolates to work on the specific  $\beta$ -aminonitriles in this research, five bacterial isolates were acquired which were originally screened and isolated within the PMBRC group in WIT<sup>32</sup>. These were namely Isolates 3, 6, 12, 39, and 46 and will be detailed further in Chapter 4. The activity screening showed them to be active against both aliphatic and aromatic hydroxynitriles. Small scale preliminary enantioselectivity screening (6 mL) was carried out on the 5 isolates for both the 3-HBN (**131**) and 3-hydroxy-3-phenylpropionitrile (3-HPPN) analogues, 3-ABN (**124**) and 3-APPN (**122**) respectively at both pH 7 and 9 using the same procedures outlined earlier. The biotransformations were carried out, in a suspension of phosphate buffer (0.1 M, 6 mL, pH 7 and 9) containing induced cells ( $OD_{600nm} = 1$ ) at 25°C for 3 days with mechanical shaking (200 rpm). The reaction was quenched by removal of the biomass by centrifugation. The reactions were carried out as single reactions i.e. not duplicated and HPLC was also conducted as single injections without duplication. The ee's were determined by GITC derivatisation for both the nitrile and acid. The focus of this initial study was on ee screening.

**Table 3.10: Biotransformations of 3-aminobutyronitrile (1) with Isolates 3, 6, 12, 39, and 46**

Entry	Isolate	pH	Nitrile ee (%)	Acid ee (%) <sup>[b]</sup>
<b>1</b>	3	7	ND	69 ( <i>R</i> )
<b>2</b>	3	9	ND	20 ( <i>R</i> )
<b>3</b>	6	7	ND	>99 ( <i>R</i> )
<b>4</b>	6	9	ND	8 ( <i>R</i> )
<b>5</b>	12	7	ND	58 ( <i>R</i> )
<b>6</b>	12	9	ND	10 ( <i>R</i> )
<b>7</b>	39	7	ND	77 ( <i>R</i> )
<b>8</b>	39	9	ND	81 ( <i>R</i> )
<b>9</b>	46	7	ND	37 ( <i>R</i> )
<b>10</b>	46	9	ND	30 ( <i>R</i> )

<sup>a</sup>Biotransformations were carried out by incubating 3-aminobutyronitrile (10 mM) in a suspension of cells ( $OD_{600nm}=1$ ) in phosphate buffer (pH 7 or 9) at 25°C. <sup>b</sup>Determined by HPLC analysis using a C18 column following chiral derivatisation. ND = Not Detected

Excellent preliminary enantioselectivity results were seen from bacterial isolates 6 (*Klebsiella* sp.) and 39 (*Rhodococcus* sp.). Isolate 6 produced an acid ee of >99% (*R*) at pH 7 however a considerable drop in ee to 8% (*R*) at pH 9, whilst isolate 39 gave 77% (*R*) and 81% (*R*) ee at

pH 7 and 9 respectively. It was interesting to note the overall tolerance of isolates 6 and 39 to the higher pH conditions. This may allude to these bacteria possibly preferring alkaline soil conditions in their native environment. In general, nitrilases are reported to prefer pH 7 – 9, such as *Rhodococcus rhodochrous* NCIMB 11216 whose optimum pH is 8.0<sup>33-35</sup>. Only a few are reported to work in more acidic conditions such as *R. rhodochrous* K22 which is active against crotononitrile at pH 5.5<sup>36</sup>. The ability of these bacteria to tolerate alkaline conditions was of great interest due to the nature of the substrates of this study.

While ee appeared to be excellent and this was the primary focus of this initial work, the peak area on the HPLC appeared very low in comparison to standards, indicating possible a low yield of acid. In the next set of studies, the biotransformations were repeated containing a higher concentration of induced cells ( $OD_{600nm} = 5$ ) which was a 5-fold increase than the standard concentration of  $OD_{600nm} = 1$ . An increase in cells was hoped to increase the turnover of product and thus give a greater response by HPLC and overall yield. Separation was achieved on a Waters Symmetry C18 column, mobile phase MeOH:H<sub>2</sub>O 35:65 + 0.1% TFA, flow rate 1.0 mL.min<sup>-1</sup>. The summary of the results from making a 5-fold increase in the concentration of cells is shown in Table 3.11. Whilst the HPLC response did not appear to increase, indicating low yields, it can be seen from the results that the acid ee increased in all cases to give excellent results.

**Table 3.11: Biotransformations of 3-aminobutyronitrile (124) with Isolates 6 and 39 at  $OD_{600nm} = 5$**

Entry	Isolate	pH	Nitrile ee (%)	Acid ee (%) <sup>[b]</sup>
1	6	7	ND	89 (R)
2	6	9	ND	99 (R)
3	39	7	ND	87 (R)
4	39	9	ND	99 (R)

<sup>a</sup>Biotransformations were carried out by incubating 3-aminobutyronitrile (10 mM) in a suspension of cells ( $OD_{600nm}=5$ ) in phosphate buffer (pH 7) at 25°C. <sup>b</sup>Isolated yields after flash column. <sup>c</sup>Determined by HPLC analysis using a C18 column following chiral derivatisation. ND = Not Detected

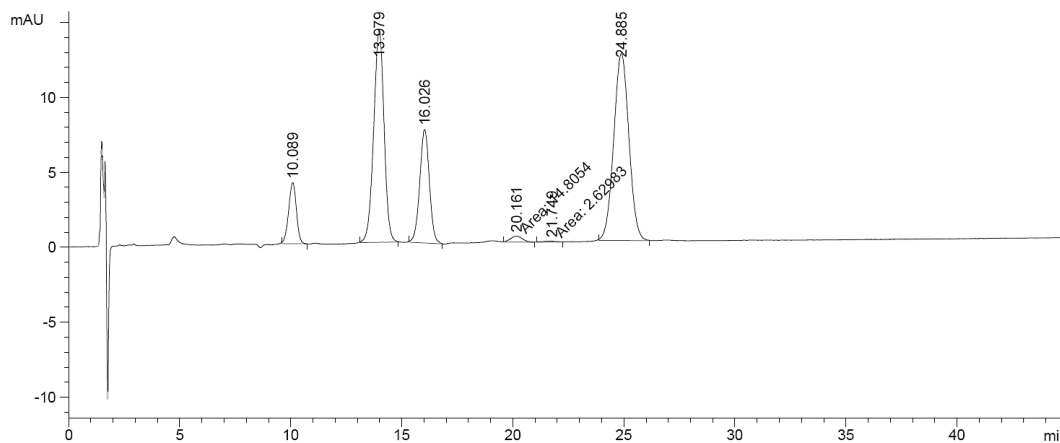
The five isolates were also subjected to a preliminary enantioselectivity screen with 3-APPN. The biotransformations were carried out, in a suspension of phosphate buffer (0.1 M, 6 mL, pH 7 and 9) containing induced cells ( $OD_{600nm} = 1$ ) and the nitrile and the mixture was incubated at 25°C for 3 days with mechanical shaking (200 rpm). The reaction was quenched by removal of the biomass by centrifugation. Biotransformations were carried out as single

reactions i.e. not duplicated and HPLC was also conducted as single injections without duplication. The ee's were determined by GITC derivatisation. The HPLC conditions were: Waters Symmetry C18 column, mobile phase 35:65 + 0.1% TFA, and flow rate 1.0 mL min<sup>-1</sup>. Samples were put on as single reactions i.e. not duplicated and HPLC was completed as single injections without duplication. No nitrile was detected in all cases and acid was only observed with isolate 39 at pH 7 which gave an ee of >99% (*R*). This was interesting to note as SET1 was completely unable to convert 3-APPN at pH 7 in the given time.

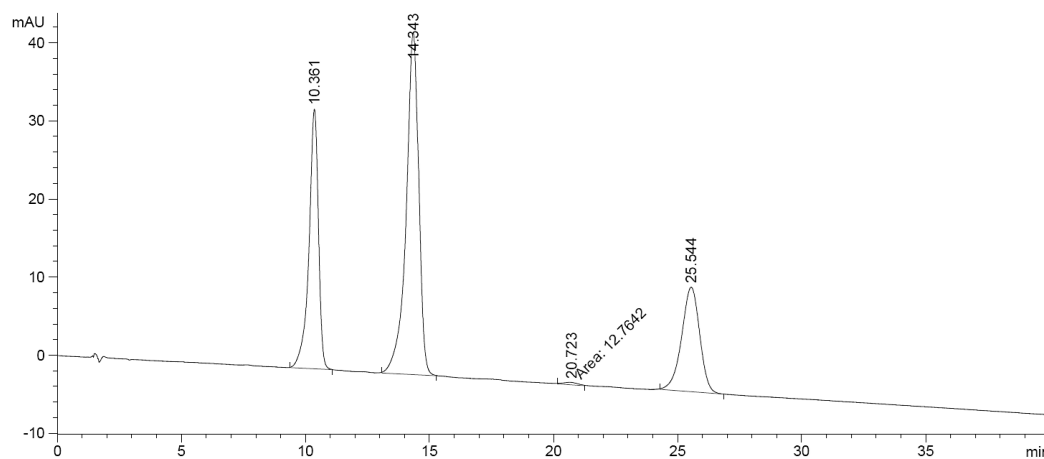
### 3.4.1 Additional studies using Isolates 6 and 39

#### 3.4.1.1 pH study using Isolates 6 and 39

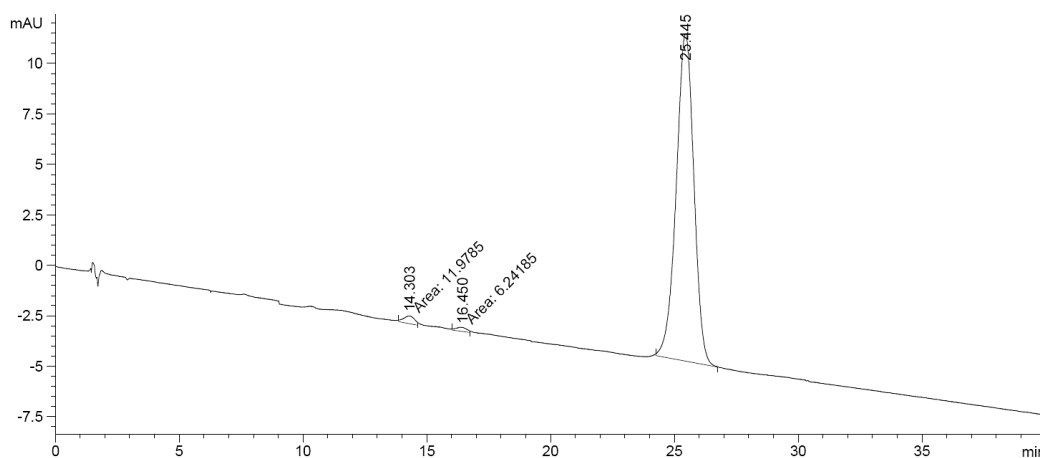
The two isolates selected for further work with 3-ABN (**124**) were thus isolate 6 and isolate 39, with isolate 39 showing the most promise as it appeared to show potential selectivity for both 3-ABN (**124**) and 3-APPN (**122**). Biotransformations at a larger scale (50 mg nitrile) were carried out for isolate 6 at pH 7 and 9, and for isolate 39 at pHs 7, 8, 9, and 10. The reactions were conducted in phosphate buffer and incubated at 25°C with mechanical shaking (200 rpm). An aliquot of the supernatant (1 mL) was lyophilised and derivatised with GITC to acquire the acid ee and yield. The remainder of the supernatant was concentrated *in vacuo* then NaOH was added. A solution of Cbz-OSu in THF was added and the mixture was stirred for 24 h. After pH adjustments and workup by extraction, the acid and nitrile were obtained in their *N*-Cbz protected forms. Singular reactions and HPLC injections without duplication were carried out. The GITC HPLC standard curve as shown earlier in Figure 3.12 was used to determine the acid yields. A summary of the results can be found in Table 3.13. The best result for isolate 6 was at pH 9, where acid ee was observed at 95% (*R*) however, the yield was extremely low. For isolate 39, it can be observed that the maximum selectivity was reached at pH 8 however, the maximum yield was at pH 9. It is interesting to note that the yield dropped drastically at pH 10 whilst maintaining a high ee. Representative HPLC spectra are shown in Figures 3.22-3.24.



**Figure 3.22:** HPLC chromatogram of the acid product of the biotransformation of Isolate 6 with 3-ABN at pH 9. GITC acid peaks at 20.2 and 24.9 min. Analysis carried out on a C18 column. Mobile phase MeOH:H<sub>2</sub>O 35:65 + 0.1% TFA, at a flow rate of 1 mL.min<sup>-1</sup>



**Figure 3.23:** HPLC chromatogram of the acid product of the biotransformation of Isolate 39 with 3-ABN at pH 7. GITC acid peaks at 20.7 and 25 min. Analysis carried out on a C18 column. Mobile phase MeOH:H<sub>2</sub>O 35:65 + 0.1% TFA, at a flow rate of 1 mL.min<sup>-1</sup>



**Figure 3.24:** HPLC chromatogram of the acid product of the biotransformation of Isolate 39 with 3-ABN at pH 9. Acid peak at 25.4 min. Analysis carried out on a C18 column. Mobile phase MeOH:H<sub>2</sub>O 35:65 + 0.1% TFA, at a flow rate of 1 mL.min<sup>-1</sup>

**Table 3.13: Biotransformations of Isolates 6 and 39 with 3-aminobutyronitrile**

Entry	Isolate	pH	Time (h)	Nitrile Yield (%)	Acid Yield (%) <sup>[b]</sup>	ee (%) <sup>[c]</sup>
1	6	7	72	ND	<1	89 ( <i>R</i> )
2	6	9	72	ND	<1	95 ( <i>R</i> )
3	39	7	72	ND	1	96 ( <i>R</i> )
4	39	8	72	ND	8	>99 ( <i>R</i> )
5	39	9	72	ND	15	>99 ( <i>R</i> )
6	39	10	72	ND	2	>99 ( <i>R</i> )

<sup>a</sup>Biotransformations were carried out by incubating 3-aminobutyronitrile (10 mM) in a suspension of *Rhodococcus* sp. Isolate 39 (OD<sub>600nm</sub>=1) of *Klebsiella* sp. Isolate 6 (OD<sub>600nm</sub>=1) in phosphate buffer (pH 7, 8, 9, or 10) at 25°C.

<sup>b</sup>Calculated from standard curve in Fig 3.12. <sup>c</sup>Determined by HPLC analysis using a C18 column following chiral derivatisation. ND = Not Detected

An investigation into the induction of bacterial isolate 39 on 3-aminobutyronitrile HCl (**124**) was also carried out at pH 7 in phosphate buffer. The isolate was able to grow but upon conducting the biotransformation with the same nitrile, no nitrile was detected. Acid was produced in 1% yield with 97% ee (*R*), a slight improvement to the 96% ee obtained with uninduced cells. The lack of observation of nitrile was disappointing as with SET1, nitrile could be detected upon induction with 3-ABN (**124**).

#### 3.4.1.2 Time study using Isolates 6 and 39

A time study was carried out to monitor the production and ee of acid product. This was carried out using isolate 39, which provided the best ee at pH 9. Biotransformations were conducted on a small scale of 6 mL. Reactions were carried out in a suspension of phosphate buffer (0.1 M) at pH 9, adjusted with NaOH, containing induced cells (OD<sub>600nm</sub> = 1) and racemic 3-aminobutyronitrile (10 mM). The reactions were quenched by removal of the biomass by centrifugation. Biotransformations were run in duplicate with a biological replicate which also had a duplicate. Aliquots (1 mL) of the supernatant were lyophilised and derivatised with GITC for HPLC analysis. Two separate experiments were conducted with the first taking samples at time points 3, 6, 17, and 20 h. The second experiment took samples at 13, 36, 46, and 60 h. GITC derivatised samples were run in duplicate on HPLC for ee determination.

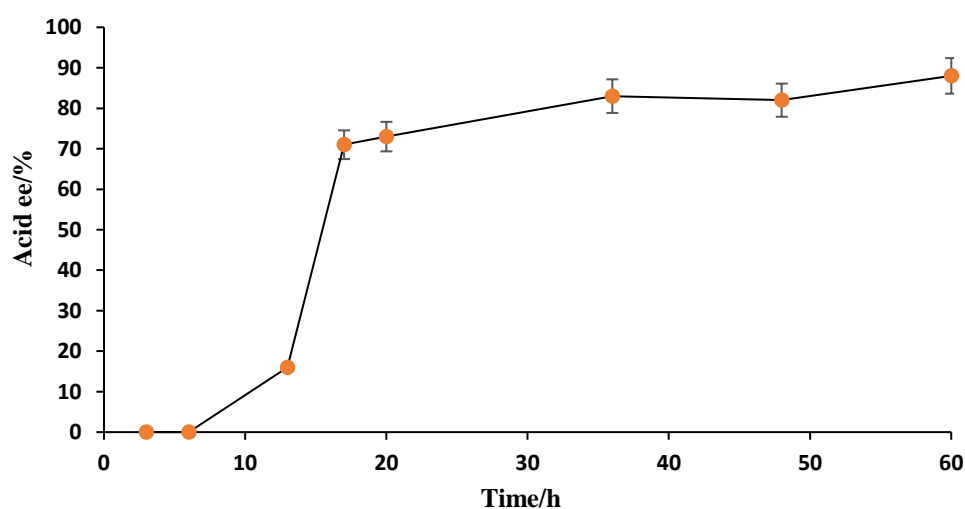


**Table 3.14: Time study of Isolate 39 with 3-ABN (124) at pH 9. Acid results shown.**

Time (h)	3	6	13	17	20	36	48	60
ee (%) <sup>[b]</sup>	0	0	16 (R)	71 (R)	73 (R)	83 (R)	82 (R)	88 (R)

<sup>a</sup>Biotransformations were carried out by incubating 3-aminobutyronitrile (10 mM) in a suspension of *Rhodococcus* sp. Isolate 39 ( $OD_{600nm}=1$ ) in phosphate buffer (pH 9) at 25°C. <sup>b</sup>Determined by HPLC analysis using a C18 column following chiral derivatisation

Observation of the ee produced interesting insight to the possible inner workings of isolate 39 as shown in Figure 3.25. Isolate 39 appeared to require at least 17 h to reach an ee of 71%. After this, over the time remaining, the ee steadily rose to 88%. In terms of yield, the peak area was seen to generally increase in the first 20 h but then began to decrease. This may allude to the possibility of degradation of the acid product over time or the involvement of the acid product in another metabolic pathway of the bacterial isolate.



**Figure 3.25: Enantioselectivity study of the acid product, 3-aminobutyric acid, over time for isolate 39 with 3-aminobutyronitrile. Analysis carried out on a C18 column. Mobile phase MeOH:H<sub>2</sub>O 35:65 + 0.1% TFA at a flow rate of 1 mL.min<sup>-1</sup>. Error bars represent the error across the mean of the HPLC duplicates**

Attempts were made to follow the conversion and yield at various time points for 3-ABN (**124**) with HPLC using a standard curve. Unfortunately, the area for nitrile varied significantly mostly due to recovery issues from the aqueous layer, and an accurate mass balance could not be obtained.

### 3.4.1.3 Summary of Isolates 6 and 39

Further detailed study of the reaction work-up was planned to be a part of the focus for future work on increasing the recovery of 3-aminobutyronitrile (**124**) and the corresponding acid. Further studies to acquire optimum conditions for isolate 39 were also planned. The biotransformations were to be scaled up with 3-ABN (**124**) so as to acquire sufficient product for full analysis. Isolate 39 was to be screened against both the protected aliphatic and aromatic substrates to assess its potential. The best substrate would thus be determined, and measures were to be taken to optimise the reaction. Contamination of the isolates was unfortunately discovered before all the aforementioned work could take place and ultimately prevented this work from continuing altogether and so other work was focussed on as a result. The contamination and purification issues are discussed in the subsequent Chapter.

## 3.5 Summary for Chapter 3

The results observed from this body of work are summarised in Table 3.15, with the most promising observations highlighted. Whilst SET1 exhibited difficulties in effectively acting on the unprotected substrate 3-ABN (**124**) it showed a greater affinity for the *N*-benzyl protected variant. These results for SET1 may allude to a dual mechanism present in isolate SET1 which was referred to in the work of Coady *et al* on  $\beta$ -hydroxy nitriles<sup>1,6,7</sup>. The effort made to identify other isolates which could work on this substrate class proved productive as isolate 39 returned promising results with the unprotected nitrile 3-ABN (**124**) at the higher pH, pH 9. Overall difficulties experienced in recovering nitrile may be due to other competing pathways which may exist in the whole cells such as a nitrile reductase, which was discussed earlier. Another possibility is the presence of an amidase, which could utilise what amide is formed and converts it into acid. The acid product could also be a substrate for another metabolic pathway. The presence of such unknown variables is a common hindrance to working with whole cell catalysts, making work with isolated enzymes more desirable.

Table 3.15: Summary of biotransformation data for isolates SET-1, 6, and 39 on  $\beta$ -amino nitriles

Isolate	R	R'	pH	Co-solvent	Nitrile		Amide		Acid	
					Yield (%)	ee (%) <sup>[b]</sup>	Yield (%)	ee (%) <sup>[b]</sup>	Yield (%)	ee (%) <sup>[b]</sup>
SET1	H	Me	7	-	ND	ND	ND	ND	<1	29 (S)
SET1	H	Me	8	-	ND	ND	ND	ND	<1	18 (S)
SET1	H	Me	9	-	ND	ND	ND	ND	<1	5 (S)
SET1 induced on 3-ABN	H	Me	7	-	8	2	ND	ND	5	7 (S)
SET1	Bn	Me	7	5% DMSO	ND	ND	3	90	6	75 (S)
SET1	Boc	Me	7	5% DMSO	55	79 <sup>*a</sup>	ND	ND	1	10 (S)
SET1	Boc	Me	7	20% IPA	97	0.1 <sup>*a</sup>	ND	ND	ND	ND
SET1	Ts	Me	7	5% DMSO	74	0.03	9	1	<1	>99 <sup>*b</sup> (S)
SET1	Ts	Me	7	20% IPA	86	0.2	ND	ND	ND	ND
SET1	H	Ph	7	5% DMSO	17	11	ND	ND	ND	ND
SET1	H	Ph	9	5% DMSO	ND	ND	ND	ND	ND	ND
6	H	Me	7	-	ND	ND	ND	ND	0.5	89 (R)
6	H	Me	9	-	ND	ND	ND	ND	0.5	95 (R)
39	H	Me	7	-	ND	ND	ND	ND	1	96 (R)
39	H	Me	8	-	ND	ND	ND	ND	8	>99 (R)
39	H	Me	9	-	ND	ND	ND	ND	15	>99 (R)
39	H	Me	10	-	ND	ND	ND	ND	2	>99 (R)
39 induced on 3-ABN	H	Me	7	-	ND	ND	ND	ND	1	97 (R)

<sup>a</sup>Biotransformations were carried out by incubating nitrile (10 mM) in a suspension of cells ( $OD_{600nm=1}$ ) in phosphate buffer (pH 7, 8, 9, or 10) at 25°C. <sup>b</sup>Determined by HPLC analysis using a chiral column. <sup>\*a</sup> analysed as amide, <sup>\*b</sup> analysed as Me ester. ND = Not Detected

## REFERENCES

1. Coady, Tracey. M. *et al.* A High Throughput Screening Strategy for the Assessment of Nitrile-hydrolyzing Activity Towards the Production of Enantiopure  $\beta$ -hydroxy Acids. *Journal of Molecular Catalysis B: Enzymatic*, 2013, **97**, 150-155
2. Martínková, Ludmila. *et al.* Selection and Screening for Enzymes of Nitrile Metabolism. *Journal of Biotechnology*, 2008, **133**, (3), 318-326

3. Molins-Legua, C. *et al.* *A Guide for Selecting the Most Appropriate Method for Ammonium Determination in Water Analysis*. *TrAC Trends in Analytical Chemistry*, 2006, **25**, (3), 282-290
4. Vanselow, A. P. *Preparation of Nessler's Reagent*. *Industrial & Engineering Chemistry Analytical Edition*, 1940, **12**, (9), 516-517
5. Liebhafsky, Herman. A. & Bronk, Lester. B. *Action of Nessler's Reagent on Amines*. *Analytical Chemistry*, 1948, **20**, (6), 588-589
6. Ma, Da-You. *et al.* *Nitrile Biotransformations for the Synthesis of Highly Enantioenriched  $\beta$ -Hydroxy and  $\beta$ -Amino Acid and Amide Derivatives*. *Journal of Organic Chemistry*, 2008, **73**, (11), 4087-4091
7. Coady, Tracey. M. *et al.* *Substrate Evaluation of *Rhodococcus erythropolis* SET1, a Nitrile Hydrolysing Bacterium, Demonstrating Dual Activity Strongly Dependent on Nitrile Sub-Structure*. *European Journal of Organic Chemistry*, 2015, **2015**, (5), 1108-1116
8. Chhiba, Varsha. *et al.* *Enantioselective Biocatalytic Hydrolysis of  $\beta$ -aminonitriles to  $\beta$ -Amino-amides Using *Rhodococcus rhodochrous* ATCC BAA-870*. *Journal of Molecular Catalysis B: Enzymatic*, 2012, **76**, 68-74
9. Schüürmann, Jan. *et al.* *Bacterial Whole-cell Biocatalysts by Surface Display of Enzymes: Toward Industrial Application*. *Applied Microbiology and Biotechnology*, 2014, **98**, (19), 8031-8046
10. Banerjee, A. *et al.* *The Nitrile-degrading Enzymes: Current Status and Future Prospects*. *Applied Microbiology and Biotechnology*, 2002, **60**, (1-2), 33-44
11. Yang, Lifeng. *et al.* *Nitrile Reductase as a Biocatalyst: Opportunities and Challenges*. *Catalysis Science & Technology*, 2014, **4**, (9), 2871-2876
12. Suyal, Deep. Chandra. *et al.* *Differential Protein Profiling of Soil Diazotroph *Rhodococcus qingshengii* S10107 Towards Low-temperature and Nitrogen Deficiency*. *Scientific Reports*, 2019, **9**, (1), 20378
13. Sehajpal, Pallvi. *et al.* *Generation of Novel Family of Reductases from PCR based Library for the Synthesis of Chiral Alcohols and Amines*. *Enzyme and Microbial Technology*, 2018, **118**, 83-91
14. Mitsukura, Koichi. *et al.* *Asymmetric Synthesis of Chiral Amine From Cyclic Imine by Bacterial Whole-cell Catalyst of Enantioselective Imine Reductase*. *Organic & Biomolecular Chemistry*, 2010, **8**, (20), 4533-4535
15. Kwon, Yun. *et al.* *Depsidomycins B and C: New Cyclic Peptides from a Ginseng Farm Soil-Derived Actinomycete*. *Molecules*, 2018, **23**, (6), 1266

16. Péter, Antal. *et al.* High-performance Liquid Chromatographic Separation of the Enantiomers of Unusual  $\alpha$ -amino Acid Analogues. *Journal of Chromatography A*, 2000, **871**, (1-2), 105-113
17. Péter, Antal. *et al.* A Comparison of the Direct and Indirect LC Methods for Separating Enantiomers of Unusual Glycine and Alanine Amino Acid Analogues. *Chromatographia*, 2002, **56**, (1-2), S79-89
18. Ma, Da-You. *et al.* Nitrile Biotransformations for the Synthesis of Enantiomerically Enriched  $\beta$ 2-, and  $\beta$ 3-hydroxy and -alkoxy Acids and Amides, A Dramatic O-substituent Effect of the Substrates on Enantioselectivity. *Tetrahedron: Asymmetry*, 2008, **19**, (3), 322-329
19. Kinfé, Henok. Hadgu. *et al.* Enantioselective Hydrolysis of  $\beta$ -hydroxy Nitriles Using the Whole Cell Biocatalyst *Rhodococcus rhodochrous* ATCC BAA-870. *Journal of Molecular Catalysis B: Enzymatic*, 2009, **59**, (4), 231-236
20. Rapheeha, O. K. *et al.* Hydrolysis of Nitriles by Soil Bacteria: Variation With Soil Origin. *Journal of Applied Microbiology*, 2017, **122**, (3), 686-697
21. Zhang, Z. J. *et al.* Characterization of a New Nitrilase from *Hoeflea phototrophica* DFL-43 for a Two-step One-pot Synthesis of (S)- $\beta$ -amino acids. *Applied Microbiology and Biotechnology*, 2018, **102**, (14), 6047-6056
22. Crawford, Jason. B. *et al.* Practical Convergent Laboratory-Scale Synthesis of a CCR5 Receptor Antagonist. *Organic Process Research & Development*, 2012, **16**, (1), 109-116
23. Metrick, Michael. A. *et al.* The Effects of Buffers and pH on the Thermal Stability, Unfolding and Substrate Binding of RecA. *Biophysical Chemistry*, 2013, **184**, 29-36
24. Chhibha-Govindjee, Varsha. P. *et al.* Dimethylformamide is a Novel Nitrilase Inducer in *Rhodococcus rhodochrous*. *Applied Microbiology and Biotechnology*, 2018, **102**, (23), 10055-10065
25. Wilding, Birgit. *et al.* An Investigation of Nitrile Transforming Enzymes in the Chemo-enzymatic Synthesis of the Taxol Sidechain. *Organic & Biomolecular Chemistry*, 2015, **13**, (28), 7803-7812
26. Good, Norman. E. *et al.* Hydrogen Ion Buffers for Biological Research. *Biochemistry*, 1966, **5**, (2), 467-477
27. Good, Norman. E. & Izawa, Seikichi. in *Methods in Enzymology* Vol. 24 Chapter 3: *Hydrogen Ion Buffers* 3 (ed San. Anthony. Pietro) 53-68 (Academic Press, 1972).
28. Hayes, A. Wallace. *et al.* in *Loomis's Essentials of Toxicology Chapter 4: Chemical Factors that Influence Toxicity* (eds A. Wallace. Hayes *et al.*) 45-59 (Academic Press, 2020).

29. Gong, Jin-Song. *et al. Nitrilases in Nitrile Biocatalysis: Recent Progress and Forthcoming Research*. Microbial Cell Factories, 2012, **11**, (142), 1-18
30. Coady, Tracey. M. *Biotransformations Using Nitrile Hydrolysing Enzymes for Stereoselective Organic Synthesis*, Doctor of Philosophy thesis, Waterford Institute of Technology, (2014).
31. Preiml, Margit. *et al. A New Approach to  $\beta$ -amino Acids: Biotransformation of N-protected  $\beta$ -amino Nitriles*. Tetrahedron Letters, 2003, **44**, (27), 5057-5059
32. Bragança, Caio. Roberto. Soares. *Development of Recombinant Enzymes Towards the Production of Pharmaceutical Intermediates Using Biotransformations*, Doctor of Philosophy thesis, Waterford Institute of Technology, (2020).
33. Yamamoto, K. *et al. Production of S-(+)-ibuprofen From a Nitrile Compound by Acinetobacter sp. Strain AK226*. Applied and Environmental Microbiology, 1990, **56**, (10), 3125-3129
34. Hoyle, Alison. J. *et al. The Nitrilases of Rhodococcus rhodochrous NCIMB 11216*. Enzyme and Microbial Technology, 1998, **23**, (7), 475-482
35. Yamamoto, Keizou. & Komatsu, Ken-ichi. *Purification and Characterization of Nitrilase Responsible for the Enantioselective Hydrolysis from Acinetobacter sp. AK 226*. Agricultural and Biological Chemistry, 1991, **55**, (6), 1459-1466
36. Kobayashi, Michihiko. *et al. Monohydrolysis of an Aliphatic Dinitrile Compound by Nitrilase From Rhodococcus rhodochrous K22*. Tetrahedron, 1990, **46**, (16), 5587-5590

## **CHAPTER 4**

### **ISOLATES PURIFICATION & ANALYSIS**

## ISOLATES PURIFICATION & ANALYSIS

### 4.1 Selection and Enantioselectivity Screening of Additional Isolates

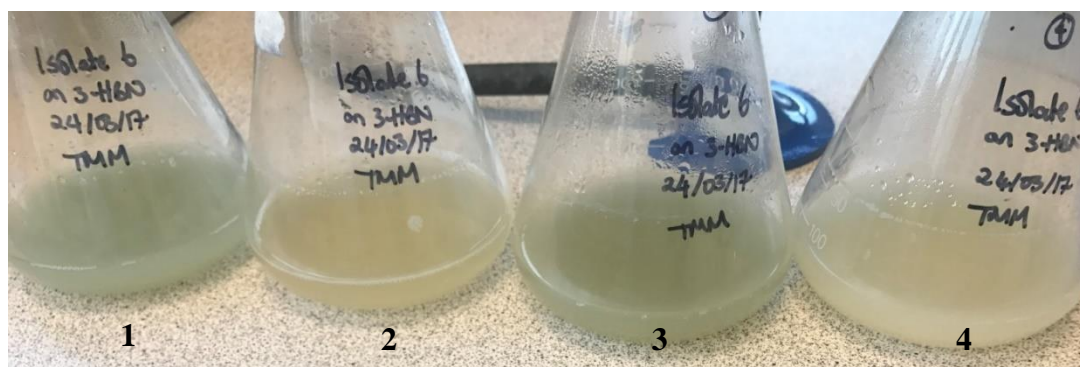
As demonstrated in Chapter 2 isolate SET1 showed limited selectivity towards  $\beta$ -aminonitrile substrates. The *N*-benzyl protected 3-amino substrate 3-(benzylamino)butyronitrile (**125**) gave the optimum enantioselectivity of 75% (*S*) acid in 6% yield and 90% ee amide with 3% yield. In an effort to improve the production of  $\beta$ -aminoacids alternate bacterial isolates were sought.

Five novel bacterial isolates obtained from the PMBRC Molecular Biology Group were chosen for screening with the  $\beta$ -aminonitrile substrates. These were named for reference as Isolates 3, 6, 12, 39, and 46. The bacterial isolates were sourced from soil samples previously collected by the research group Coffey *et al*<sup>1</sup>. These soil samples were collected from a range of sites (e.g. suburban, forest, estuaries) from Ireland, England, Wales, France, Poland, South Africa, Germany, Spain and Australia. The isolation of bacteria from these soils in this study was carried out according to Coffey *et al* with some modifications: M9 minimal media was used for all isolations, with 0.5 g of soil sample and 10 mM nitrile<sup>2</sup>. Of note is that these soil samples were mixed together for selective isolation media instead of incubating the soils separately.

Bragança *et al* carried-out toxicity screening, activity assays, genetic identification, gene screening and ee screening on the five isolates<sup>3</sup>. Detailed results for these studies can be found in the work of Bragança *et al*<sup>3</sup>. Isolates 3, 6, 39, and 46 were isolated as 3-hydroxybutyronitrile (3-HBN) degraders and showed 68-99.99% (*S*) ee for the acid. Isolate 12 was isolated as a 3-hydroxyglutaronitrile (3-HGN) degrader however no %ee for the acid was tested. Bragança *et al* identified the isolates as: isolate 3 (*Nocardia coeliaca*), 6 (*Klebsiella oxytoca*), 12 (*Rhodococcus jialingiae*), 39 (*Rhodococcus erythropolis*), and 46 (*Nocardia coeliaca*)<sup>3</sup>.

These isolates underwent screening with the unprotected  $\beta$ -aminonitriles which is described in depth in Chapter 3 and isolates 6 and 39 were identified as potential isolates for further work. Contamination was observed unfortunately during the next stage of working with the isolates 6 and 39, after several experiments and sub-culturing rounds of the isolates had taken place. Figure 4.1 is an example of the difference first observed in the growth broth cultures inoculated from the same glycerol stock for Isolate 6 grown in replicate M9 broth containing 3-HBN.





**Figure 4.1:** M9 3-day broth cultures of isolate 6 grown with 3-HBN as the nitrogen source. Broths prepared from the same glycerol stock. Broths 2 and 4 represent a typical broth, whilst broths 1 and 3 are atypical

This representation shows how upon visual inspection, different colours for the broths could be observed. This could suggest different organisms being present in the flasks. Another possibility could be varying amounts of a mixed culture, containing perhaps two or more different microbes. This would then have a subsequent effect on the biotransformations as activity and selectivity would be shown to decrease drastically.

This is not an uncommon observation when working with liquid cultures of bacterial isolates, which are prone to contamination and require rigorous aseptic conditions. Some bacteria are also known to have a symbiotic relationship thus making them extremely difficult to separate. What that can also imply is that any activity observed is as a result of symbiotic metabolic pathways and so individual activity observed would be far below that which is expected.

The most common example of symbiosis of bacteria in nature involves the relationship of nitrogen-fixing bacteria and plants, in particular rhizobia<sup>4-6</sup>. The relationship between bacteria and other microbes is also apparent, with some relationships having recently been found to be a source of novel antibiotics as reviewed by Gogineni *et al*<sup>7,8</sup>. Some of the symbiosis sources they found are amongst bacteria themselves, bacteria with marine invertebrates, and marine sponges and bacteria. Another example is the symbiosis of bacteria and other organisms such as nematodes<sup>9,10</sup>. One of the uses of this particular relationship has been shown to be as an alternative to pesticides<sup>9</sup>. Bacteria in themselves can exist symbiotically in a form of synergy to bring benefits to all the bacteria involved. It has also been observed that earthworms secrete mucous which among other things can affect the soil pH and can be metabolised by soil bacteria<sup>11,12</sup>.

### 4.2.2 Phase 2: Culturing

When visually, it appeared the colonies were pure, an attempt was made to grow the cells in a broth culture. Two broths selected for growth were LB broth and M9 broth containing 3-HBN. The LB broths would provide reserve stocks which could be re-visited and starved out on M9 plates if needed. The broths were inoculated with a sample of a pure colony from the plates and the broths were incubated at 25°C with shaking for 2 days (LB broth) or 4 days (M9 broth). It was at this stage that many of the colonies failed to grow in the M9 broth. Those which were successful were glycerol stocked for activity screening.

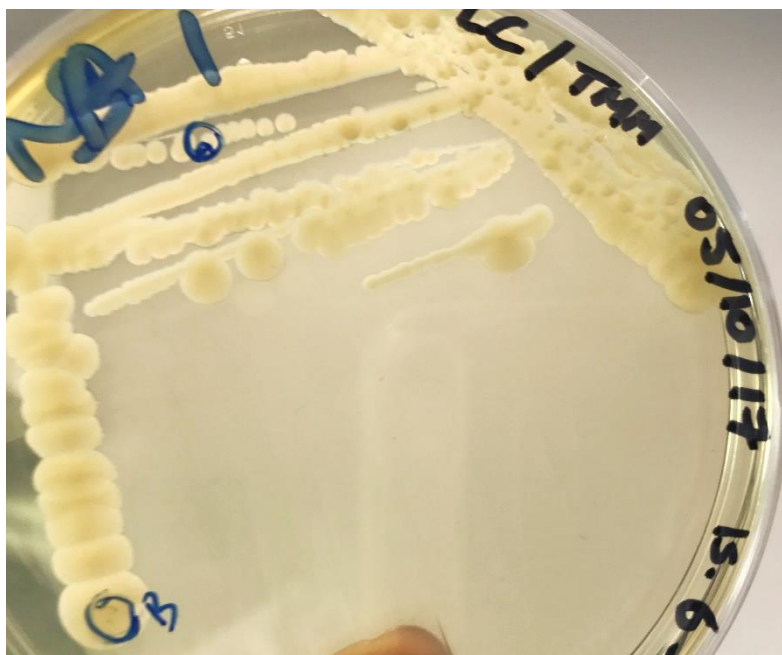
## 4.2 Purification Protocol

It had been established through inoculating broths from the originally provided glycerol stocks of the isolates that these stocks were possibly contaminated, along with subsequent glycerol stocks made from the originals. It was therefore necessary to attempt to purify the original stocks. In order to assess the level of contamination, the first step would be to streak out the isolates onto M9 and nutrient agar plates. The results from these would inform how many more iterations of streaks would be necessary to acquire pure colonies of bacteria. These pure colonies would be then cultured, and preliminary activity testing would be carried out. Those pure colonies which show promising results would then undergo further purification and an identification process to match them back to what was originally provided from the PMBRC group library and final activity testing would be conducted. In total, this work was carried out over a period of nine months and will now be described in detail.

### 4.2.1 Phase 1: Streaking

Five glycerol stocks, three of isolate 6 and two of isolate 39, were streaked out onto nutrient agar plates, which enables most bacteria to grow, and M9-minimal media agar plates which contained 3-HBN, on which only microbes able to use 3-HBN as a nitrogen source will grow. These were incubated at room temperature for three days initially, and due to slow growth being observed in some cases for the M9 plates, was adjusted to four days. The plates were then visually assessed then placed into cold storage. It was observed that additional growth

occurred after the plates had been stored in a cold room at 4°C for at least two nights. The protocol was therefore modified to include incubation at room temperature followed by two-night storage at 4°C prior to re-streaking on further plates. An example of an initial nutrient agar plate from an original glycerol stock of isolate 6 is shown in Figure 4.2. In this case, two distinct colonies could be observed so a pure sample, as pure as could be acquired, of each colony was streaked on to fresh nutrient agar plates and incubated. If mixed colonies were still observed, they would be re-streaked separately onto new plates until the entire plate contained only one colony. Each re-streak onto a new plate has been called a tier in this work for convenience.



**Figure 4.2:** Isolate 6 streaked and incubated on nutrient agar. Circled portions in the image identify the different colonies present

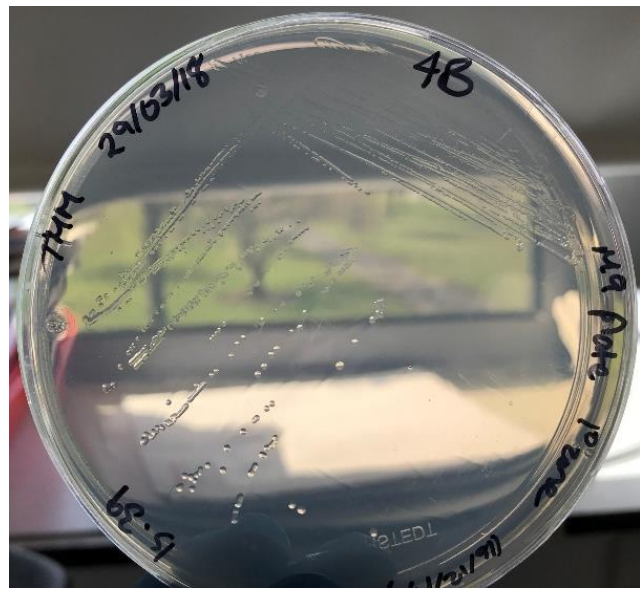
The different colonies present in the isolate 6 and 39 stocks could be observed visually due to their differing morphologies. A trend that was observed was that colonies observed after room temperature incubation mostly had sharp defined edges and were circular in shape. The second colony which grew under the colder conditions tended to spread out on the plates with soft edges.

In Figure 4.3 (3) the severity of some of the contamination can be seen. Here it can be observed that the different colonies grew on top of each other and these were noted to appear after cold storage. Figure 4.3 (2) is a representative of how most of the plates appeared at the end of the purification protocol. The majority were no longer opaque, and the cultures struggled to grow

in the minimal media with 3-HBN. In these cases, it would appear that it was a contaminant or pre-existing colony that could not work on 3-HBN.



(1)



(2)



(3)

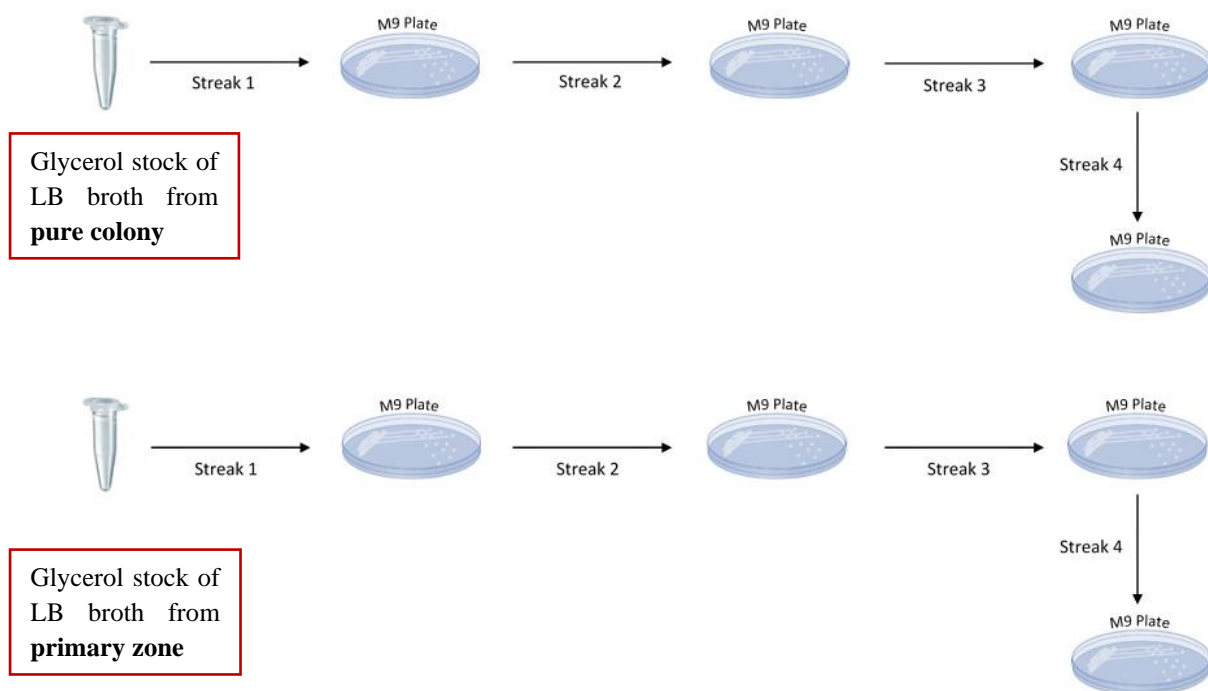


(4)

**Figure 4.3: M9 agar plates of Isolates 6 and 39. (1) – Isolate 39, Tier 1 colonies separated. (2) – Isolate 39, representative of a pure colony. (3) – Isolate 6. (4) – Isolate 6, representative of a pure colony.**

For isolates 6 and 39, the plates were re-streaked on new plates three consecutive times to create a total of four tiers. It became necessary at this point to preserve the cells to allow for long term storage. Two methods were used. Method 1: a sample of pure colonies from all the Tier 4 M9 plates was inoculated into Luria-Bertani (LB) broth, a nutrient rich broth in which most bacteria grow, and these were incubated at 25°C with shaking for two days. The broths were centrifuged, the cell pellets washed with NaCl (0.85%) and stored with M9 media and glycerol (70%). Method 2: a sample of pure colonies from the primary zones of the Tier 4 M9 plates was also inoculated into LB broths and these were incubated at 25°C with shaking for two days. These broths were also centrifuged, the pellets washed with NaCl (0.85%), and stored with M9 media and glycerol (70%).

This created two branches of the tiers named, Tiers 5A and 5B. Since the cells had been grown in LB broth, they needed to be starved of the provided nutrients which would still be present in the cells so that they would only grow with the provided nitrogen source, 3-HBN. The Method 1 Tier 4 glycerol stocks were streaked out onto M9 plates to begin the starvation process. This became Tier 5A. The Method 2 Tier 4 glycerol stocks were also streaked out onto M9 plates, to give Tier 5B. These were then streaked on to a further four tiers as shown in Figure 4.4.

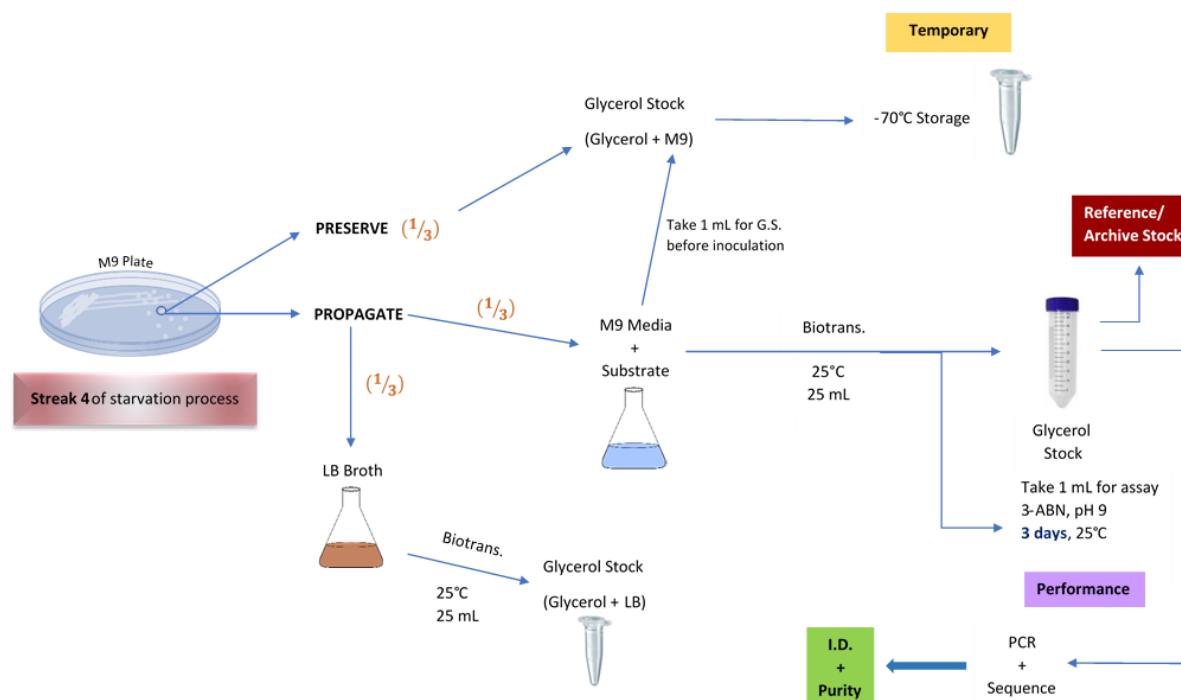


**Figure 4.4: Starvation protocol during the isolate purifications**



### 4.2.3 Phase 3: Activity screening

The nitrile 3-ABN was used for the activity screening in order to make a comparison with the data attained at the initial screening of the isolates. The screening was carried out under similar conditions i.e. phosphate buffer at pH 7, 25°C, for three days at a 6 mL scale. Biotransformations were carried out as single reactions, without duplicates. Testing was focused solely on acquiring enantioselectivity by HPLC. An overview of the workflow is shown in Figure 4.5.



**Figure 4.5: Workflow of isolate purifications**

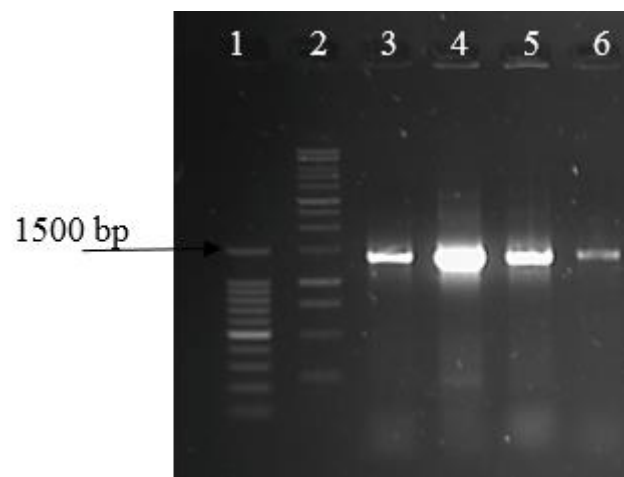
### 4.2.4 Phase 4: Identification

Identification of the isolates was achieved by carrying out a PCR amplification and gene sequencing of the 16S rRNA genes from the purified isolates, as per Marchesi *et al*<sup>13</sup>. A Polymerase Chain Reaction (PCR) is a method of amplifying target DNA. This step was necessary to ensure sufficient quantities of the 16S rRNA gene would be present for the gene sequencing stage. The three major stages in PCR are denaturation, annealing, and elongation. Denaturation is where the double stranded DNA separates into single strands as the bonds between are broken under the high temperature. During annealing, the complementary primers

anneal to the DNA. The polymerase enzyme then adds bases to the primer thus extending the DNA sequence in the elongation stage. PCR is thus an effective way to amplify DNA.

In order to prepare the samples for PCR, the glycerol stocks were centrifuged, and the supernatant was decanted. Sterile de-ionised water (1 mL) was added to resuspend the cells. The optical density was measured and adjusted to an  $OD_{600nm} = 1$ . Components of the PCR recipe were assembled as outlined: The primer mix was made using forward primer 63f (5  $\mu$ L of 100 $\mu$ M stock) and reverse primer 1387r (5  $\mu$ L of 100 $\mu$ M stock) which was diluted with sterile de-ionised water (30  $\mu$ L) to give a 25  $\mu$ M primer mix. The 2X GoTaq Green Master Mix was already pre-optimised and contained; Taq polymerase, buffer,  $MgCl_2$ , and dNTPS. The final PCR recipe was composed of 1X GoTaq Master Mix (12.5  $\mu$ L), primer mix (1  $\mu$ L, 0.5  $\mu$ M), sterile de-ionised water (10  $\mu$ L), and cells at  $OD_{600nm} = 1$  (1.5  $\mu$ L). The PCR programme was as follows: after initially holding at 95°C for 5 min for denaturation, this was followed by 30 cycles of: 95°C for 1 min for denaturation, 56°C for 1 min for annealing, and 72°C for 1.5 min for extension. This was followed by holding at 72°C for a further 8 min for final extension, then another hold step at 4°C.

Gel electrophoresis was carried out to analyse the PCR products. The gel was made with agarose (final concentration 0.8%) and TAE buffer (1X). Ethidium bromide (Sigma Aldrich) was used as the stain to visualise DNA. The ladder used for band sizing was Promega 1 kb DNA ladder. The results are shown in Figure 4.6.



**Figure 4.6: Agarose gel displaying the ~1380bp amplification products of the 16s rRNA gene PCR on isolates. Promega 100 bp ladder (lane 1), Promega 1 kb ladder (lane 2) Isolate 6 - 1 (lane 3), Isolate 6 - 3 (lane 4), Isolate 39 - 1 (lane 5), Isolate 39 - 2 (lane 6 )**

Following the gel electrophoresis, the remaining PCR product (20  $\mu$ L) together was purified prior to sequencing using the Zymo Clean and Conc 5 kit; briefly, the PCR product was mixed with DNA binding buffer (40  $\mu$ L) and were applied to a Zymo-Spin column and subjected to centrifugation at 10,000xg for 10 seconds. This column was washed twice with wash buffer and centrifuged as per manufacturer's instructions. Finally, the Zymo-Spin column was inserted into a new collection tube and the product eluted with sterile de-ionised water by centrifugation. This cleaned and concentrated DNA is what was DNA sequenced to identify the PCR product and therefore the isolate identity.

### 4.3 Final Results of Purification

Many of the purified isolates samples failed to reproduce the target enantioselectivity of >99%, with most showing less than half the selectivity. An overview of the purifications, tracking the different stocks and their final observed enantioselectivity is shown in Table 4.1.

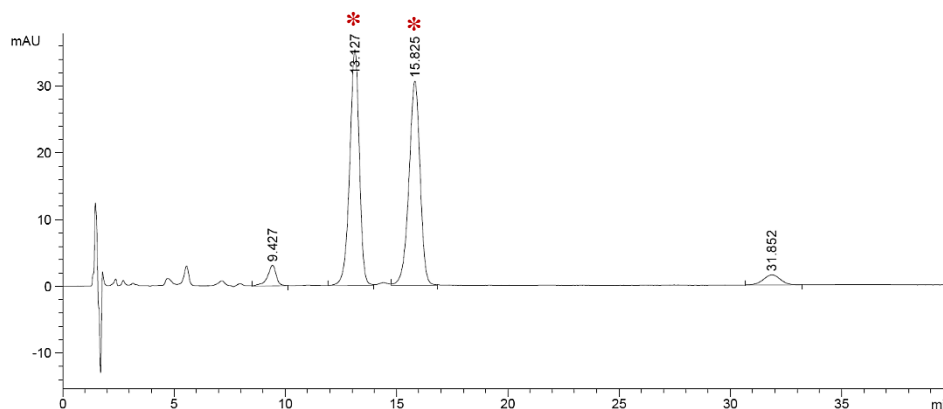
**Table 4.1: Overview of purifications protocol for isolates 6 and 39 with representative acid ee values observed. Analysed as GITC derivatives. ee determined by HPLC**

	Tier 1	Tier 2	Tier 3-9	Assay	Tiers	Identification	ee (%)
Is. 6 - 1	Streaked to NA & M9 plates. 4 days at RT. 2 nights cold room	2 colonies streaked on to NA & M9 plates. 4 days at RT. 2 nights cold room	Repeated streaking on approx. 2 colonies from each plate to NA & M9 plates	Assay of visually pure plates. 3 days to incubate broth + 3 days assay	Repeated further streaking if necessary, for PCR	Gel electrophoresis, PCR, and gene sequencing	0.2 ( <i>S</i> )
Is. 6 - 2							0.1 ( <i>S</i> )
Is. 6 - 3							0.3 ( <i>S</i> )
Is. 39 - 1							29 ( <i>R</i> )
Is. 39 - 2							28 ( <i>R</i> )

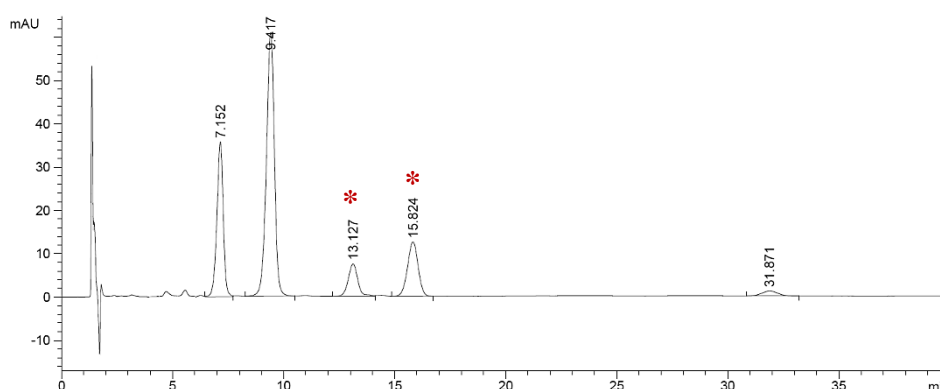
On review, it also became apparent that the selectivity of the tested bacteria was different. The original isolates showed (*R*)-selectivity whereas the latest purifications, particularly for isolate 6, were exhibiting (*S*)-selectivity. Examples of the HPLC data observed are shown in Figures 4.7 and 4.8. This was a further indicator that the isolates, whilst visually pure, were not a representative of what was tested in the beginning. This apparent difference in selectivity may be plausible as some nitrilases have been shown to exhibit (*S*)-selectivity. Prior to the work of Robertson *et al*, there were only 12 nitrilases in the sequence database<sup>14</sup>. They successfully characterised an additional 137 nitrilases which were added to the database. The nitrilases were



grouped in clades based on sequence similarity and patterns in the enantioselectivity grouping could be observed as nitrilases in the clade showed similar selectivity. It was shown to be possible that nitrilases with similar sequences and thus belonging to the same clade could exhibit different enantioselectivity. An example is with the purified enzyme, Nit1, which we used in the work discussed in Chapter 5. Nit1 is a member of the 2A clade according to its sequence similarity and thus should exhibit (*R*)-selectivity as 2A clade nitrilases predominantly show (*R*)-selectivity. We however found that it exhibited (*S*)-selectivity in our work. It is thus possible that the enzymes in our tested isolates may belong to a group such as 1B clade which shows (*S*)-selectivity. This may warrant future investigations to determine and classify these isolates for the enzyme sequence and activity in comparison to known enzymes.

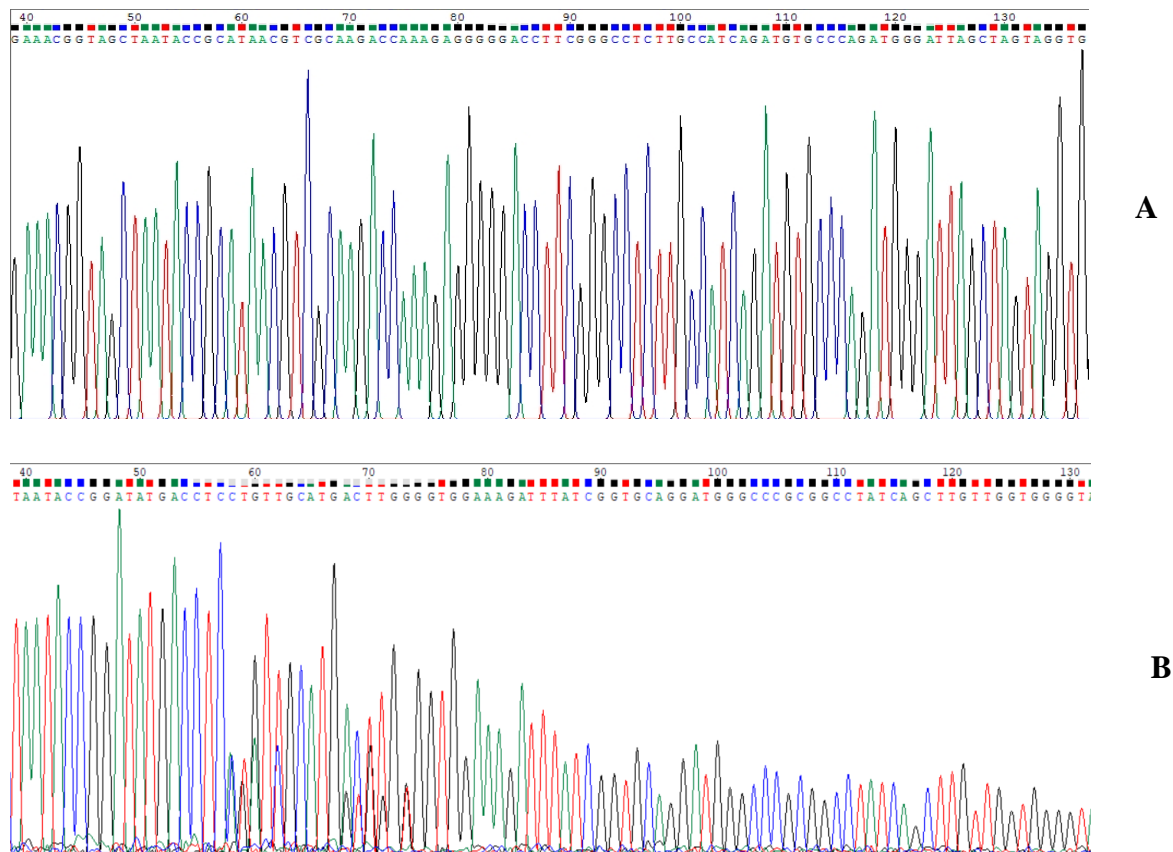


**Figure 4.7:** HPLC chromatogram of the performance check of isolate 6 – 1 with 3-ABN at pH 9 to give ee of 0.2% (*S*). Asterix denote peaks of interest (13.1 and 15.8 min). Analysis carried out on a C18 column. Mobile phase MeOH:H<sub>2</sub>O + 0.1% TFA gradient, at a flow rate of 1 mL.min<sup>-1</sup>



**Figure 4.8:** HPLC chromatogram of the performance check of isolate 39 – 1 with 3-ABN at pH 9 to give ee of 29% (*R*). Asterix denote peaks of interest (13.1 and 15.8 min). Analysis carried out on a C18 column. Mobile phase MeOH:H<sub>2</sub>O + 0.1% TFA gradient, at a flow rate of 1 mL.min<sup>-1</sup>

Gene sequencing was carried out to ensure that the isolates had indeed been purified successfully and thus could be compared to the original data on their discovery by Bragança *et al*<sup>3</sup>. Results that would be expected from gene sequencing typically are no mixing, low level mixing, or substantial mixing. A mixed sequence means that there are at least two microbes in the sample, and it is not pure. Low level mixing means that the culture is predominantly one microbe with a small amount of a contaminant present, relatively speaking. Substantial mixing means that there are equal amounts of two or more microbes in a culture. Of the five samples submitted for sequencing, two samples showed low level mixing, two had little to no apparent mixing, with only one showing a substantial amount of mixing. Representative comparison spectra are shown for the isolate 6 samples in Figure 4.9.



**Figure 4.9: DNA Sequencing chromatograms of 16S rRNA gene from isolate 6 samples. A – pure sequence with no trace contamination or overlapping sequence. B – mixed culture. Overlapping peaks present.**

A determination was needed to show if those pure samples were the original isolates. This was achieved by means of sequence analysis on the NCBI Blast platform, running a standard nucleotide BLAST. The majority of the sequences producing significant alignments for isolate 6 were *Klebsiella sp.* and for isolate 39, the genus *Rhodococcus sp.* This corresponds back to

the original identifications made by Bragança *et al* thus confirming the presence of the original isolates in the stocks<sup>3</sup>. However, the presence of *Klebsiella* sp. in isolate 39 samples and *Rhodococcus* sp. in isolate 6 samples was also noted, suggesting the possibility that cross-contamination may have occurred.

Performance testing on the purified isolates revealed decreased enantioselectivity as aforementioned as well as a reversal in selectivity. Since it has been confirmed that the original isolates are indeed present in the purified stocks, the data raises a few questions. Firstly, was contamination introduced in the lab, possibly by crossing the isolates with each other? This is feasible, resulting from a lapse in aseptic technique and would have reduced the observed enantioselectivity during the performance testing. Secondly, do the cells need different induction to activate the relevant enzymes needed?

Thirdly, was the contaminant, a second similar strain, always present from the beginning, existing in symbiosis as discussed prior, to achieve the high enantioselectivity observed initially? If so, was the initial activity based on it being present in a certain ratio or 100% of the activity observed was attributed to the contaminant? Is the reversal in selectivity due to the change in ratio after the purifications? The contaminant was observed after having kept the plates in 4°C. This could indicate that the second strain is possibly a psychrophile and in the soil would grow during colder temperatures.

It may also be possible that there could have been a pre-existing minute level of a contaminant present in the cultures which would have been impossible to detect and separate. This could have eventually grown to dominate the medium or grown to equivalent levels during the culturing on different compounds. Part of what makes separation difficult is that similar bacteria have the ability to self-bind, or autoaggregate, which makes them very difficult to separate from each other during tiered streaking<sup>15</sup>. This ability has been exhibited by *Rhodococcus erythropolis* as it can autoaggregate to form a biofilm<sup>16</sup>.

The low-level mixing observed from the gene sequencing has made it apparent that attempting to separate the isolate and its contaminant is challenging and would require much more time and investigation. What has been described in this chapter is but one of the issues with carrying out whole cell biocatalysis. Whole cell work carries many unknowns, an example of which is the uncertainty of which enzymes are at work on the given substrate. It is difficult to ascertain if it is just the one enzyme pathway or several in tandem at work. This could mean that the potentially desired product may be produced by one pathway then taken up by another pathway

for a different reaction. Another issue is the potential for the substrate and products to adhere to the cell walls thus making recovery difficult. There is a level of uncertainty as to the product release by the cell and also if the cellular activity on the substrate is strictly intercellular.

## REFERENCES

1. Coffey, Lee. V. *et al.* *Real-time PCR Detection of Fe-type Nitrile Hydratase Genes From Environmental Isolates Suggests Horizontal Gene Transfer Between Multiple Genera.* *Antonie Van Leeuwenhoek*, 2010, **98**, (4), 455-463
2. Coffey, Lee. V. *et al.* *Isolation of Identical Nitrilase Genes From Multiple Bacterial Strains and Real-time PCR Detection of the Genes From Soils Provides Evidence of Horizontal Gene Transfer.* *Archives of Microbiology*, 2009, **191**, (10), 761-771
3. Bragança, Caio. Roberto. Soares. *Development of Recombinant Enzymes Towards the Production of Pharmaceutical Intermediates Using Biotransformations*, Doctor of Philosophy thesis, Waterford Institute of Technology, (2020).
4. van der Heijden, Marcel.. G. *et al.* *Symbiotic Bacteria as a Determinant of Plant Community Structure and Plant Productivity in Dune Grassland.* *FEMS Microbiology Ecology*, 2006, **56**, (2), 178-187
5. Harman, Gary. E. & Uphoff, Norman. *Symbiotic Root-Endophytic Soil Microbes Improve Crop Productivity and Provide Environmental Benefits.* *Scientifica*, 2019, **2019**, 9106395
6. Dinnage, Russell. *et al.* *Larger Plants Promote a Greater Diversity of Symbiotic Nitrogen-fixing Soil Bacteria Associated with an Australian Endemic Legume.* *Journal of Ecology*, 2019, **107**, (2), 977-991
7. Gogineni, Vedanjali. *et al.* *Role of Symbiosis in the Discovery of Novel Antibiotics.* *The Journal of Antibiotics*, 2020
8. Brock, Debra. A. *et al.* *Endosymbiotic Adaptations in Three New Bacterial Species Associated with Dictyostelium discoideum: Paraburkholderia agricolaris sp. nov.,*

- Paraburkholderia hayleyella* sp. nov., and *Paraburkholderia bonniea* sp. nov. PeerJ, 2020, **8**, 9151
9. Salvadori, Juliana. De. Marco. *et al.* Characterization of Entomopathogenic Nematodes and Symbiotic Bacteria Active Against *Spodoptera frugiperda* (Lepidoptera: Noctuidae) and Contribution of Bacterial Urease to the Insecticidal Effect. Biological Control, 2012, **63**, (3), 253-263
  10. Liao, Chunli. *et al.* Two Symbiotic Bacteria of the Entomopathogenic Nematode *Heterorhabditis* spp. Against *Galleria mellonella*. Toxicon, 2017, **127**, 85-89
  11. Salmon, Sandrine. *Earthworm Excreta (Mucus and Urine) Affect the Distribution of Springtails in Forest Soils.* Biology and Fertility of Soils, 2001, **34**, (5), 304-310
  12. Guhra, Tom. *et al.* Earthworm Mucus Contributes to the Formation of Organo-mineral Associations in Soil. Soil Biology and Biochemistry, 2020, **145**, 107785
  13. Marchesi, Julian. R. *et al.* Design and Evaluation of Useful Bacterium-Specific PCR Primers That Amplify Genes Coding for Bacterial 16S rRNA. Applied and Environmental Microbiology, 1998, **64**, (2), 795-799
  14. Robertson, Dan. E. *et al.* Exploring Nitrilase Sequence Space for Enantioselective Catalysis. Applied and Environmental Microbiology, 2004, **70**, (4), 2429-2436
  15. Trunk, Thomas. *et al.* Bacterial Autoaggregation. AIMS microbiology, 2018, **4**, (1), 140-164
  16. Rodrigues, Carlos. J. C. & de Carvalho, Carla. C. C. R. *Rhodococcus erythropolis* Cells Adapt their Fatty Acid Composition During Biofilm Formation on Metallic and Non-metallic Surfaces. FEMS Microbiology Ecology, 2015, **91**, (12)

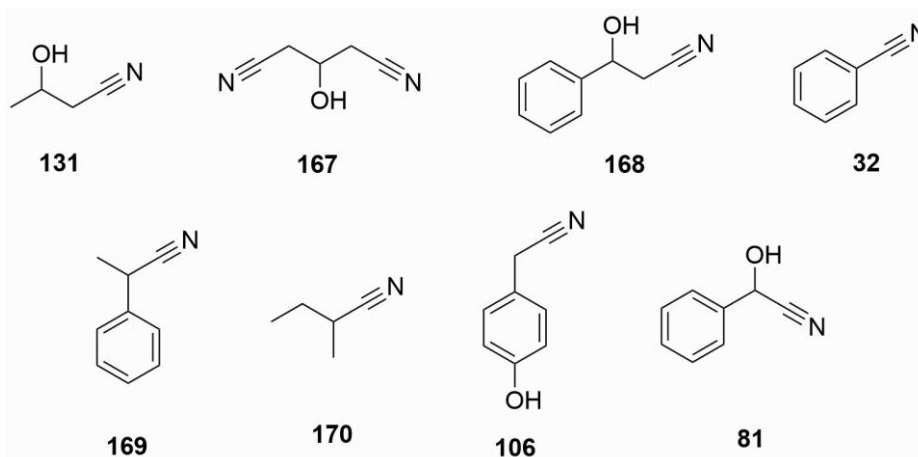
## **CHAPTER 5**

### **EVALUATION OF PURIFIED ENZYME NIT1 WITH AMINONITRILE SUBSTRATES**

## EVALUATION OF PURIFIED ENZYME NIT1 WITH AMINONITRILE SUBSTRATES

### 5.1 Background

The work in Chapters 3 and 4 highlighted some potential for the use of nitrile containing whole cells for the transformation of  $\beta$ -aminonitriles to  $\beta$ -amino acids, but it also highlighted some of the challenges associated with this series of substrates and the use of whole cells i.e. contamination product isolation and cell metabolism. The preliminary results acquired with the whole cells SET1, isolates 6, and 39, did however all support the validity of continuing to search for another nitrile metabolising enzyme which could hydrolyse  $\beta$ -amino nitriles under the required conditions. In this case we looked to find an isolated enzyme which would allow us also to contrast the effect of isolated enzyme with that of the whole cell. A novel isolated nitrilase enzyme Nit1, as identified by Coffey *et al*, was thus acquired from the PMBRC isolate bank in the form of an unsupported pure protein suspended in water<sup>1</sup>. In work conducted by Dooley-Cullinane *et al*, Nit1 was found to show activity towards both aliphatic and aromatic nitriles, with approximately 100% relative activity being observed with 4-hydroxyphenylacetonitrile (4-HPAN) (**106**)<sup>2</sup>. The substrates which Nit1 was screened against are shown in Figure 5.1 and the results obtained have been reproduced in Table 5.1.



**Figure 5.1: Substrates screened with Nit1.** 131 – 3-hydroxybutyronitrile (3-HBN), 167 – 3-hydroxyglutaronitrile (3-HGN), 168 – 3-hydroxy-3-phenylpropionitrile (3-HPPN), 32 – benzonitrile, 169 – 2-phenylpropionitrile (3-PPN), 170 – 2-methylbutyronitrile (2-MBN), 106 – 4-hydroxyphenylacetonitrile (4-HPAN), 81 – mandelonitrile

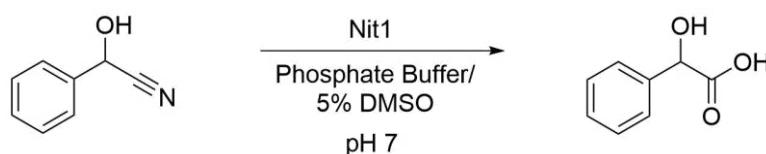
**Table 5.1: Screening results of Nit1 with selected substrates. Substrates 3-HBN to 2-MBN were analysed with a Nessler's assay, substrates 4-HPAN and mandelonitrile were analysed by HPLC to detect acid. Average results shown<sup>2</sup>**

$$\text{R}-\text{C}\equiv\text{N} \xrightarrow[\text{Phosphate Buffer}]{\text{Nit1}} \text{R}-\text{C}(=\text{O})\text{OH}$$

	3-HBN	3-HGN	3-HPPN	Benzonitrile	2-PPN	2-MBN
<b>Absorbance</b>	1.07	1.03	0.75	0.69	1.10	0.99
<b>Average Acid concentration/ mM</b>	8.02	7.72	5.65	5.19	8.37	7.47

	4-HPAN	Mandelonitrile
<b>Absorbance Average</b>	622.91	10504.75
<b>Acid concentration/ mM</b>	9.83	7.32

From Table 5.1 it can be observed that Nit1 was able to show activity towards a range of substrates. The highest acid concentration was seen with 4-HPAN which gave 9.83 mM of the acid, and it was observed for mandelonitrile that the enzyme was selective to produce (*R*)-mandelic acid with >99.9% ee. Enantioselectivity data for the other substrates were not stated. Dooley-Cullinane *et al*'s work with Nit1 discovered it had an optimum temperature of 40°C in a temperature activity assay completed with mandelonitrile at pH 7<sup>2</sup>.

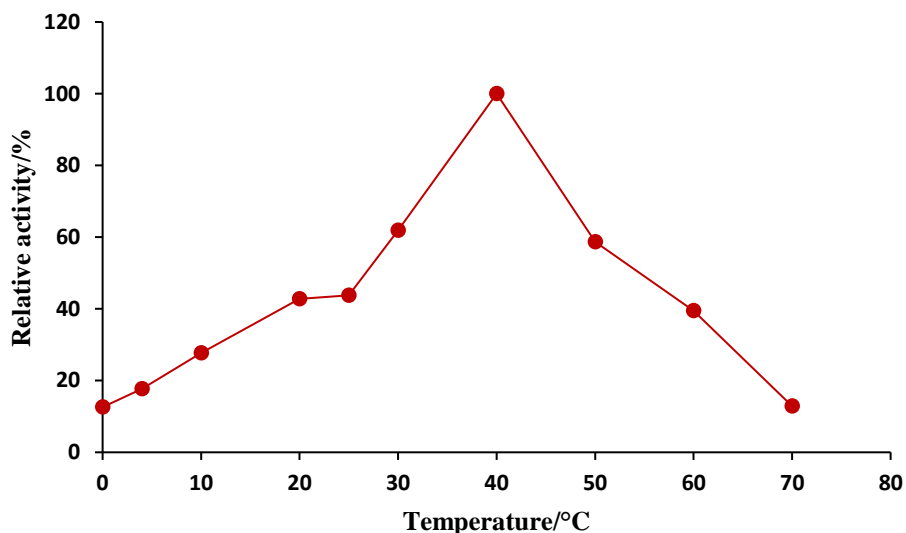


**Scheme 5.1: Hydrolysis of mandelonitrile to determine optimum temperature of Nit1**

At 25°C, the relative activity was found to be 43.8% and 61.9% at 30°C respectively. No yield data was acquired in this work.

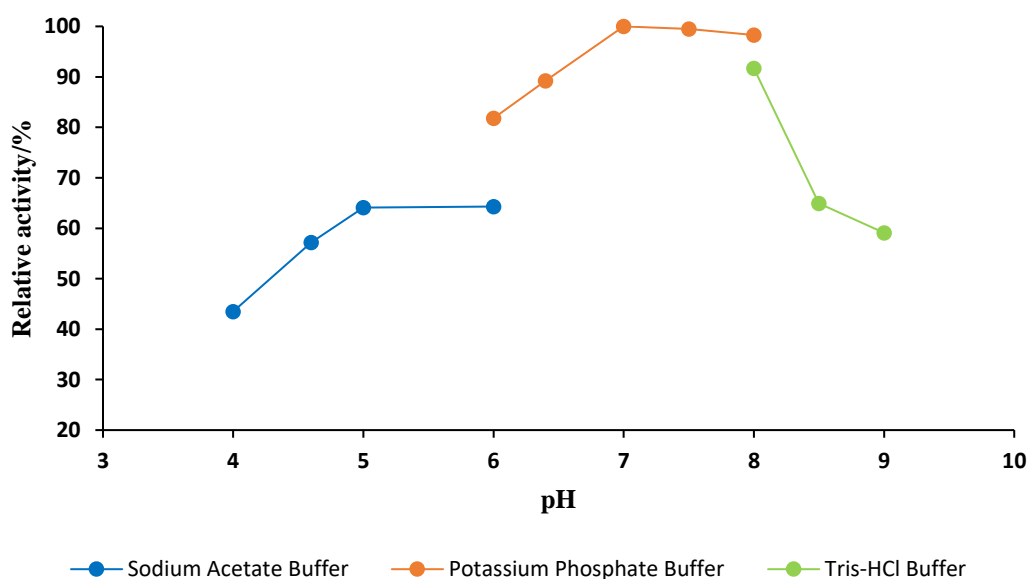
The full activity profile of Nit1 that was generated is reproduced in Figure 5.2. In order for possible enantioselectivity to be imparted by the enzyme on reactions with 3-aminobutyronitrile, we preferred to evaluate at initially the lower temperature of 25 °C and would possibly increase once activity was determined.





**Figure 5.2: Temperature activity assay of Nit1 with mandelonitrile reproduced from Dooley-Cullinane *et al*<sup>2</sup>**

The optimum pH of Nit1 was discovered through an activity assay conducted by Dooley-Cullinane *et al* on Nit1 with mandelonitrile in three different buffer solutions<sup>2</sup>. Analysis was conducted by HPLC. The optimum pH was found to be pH 7 in phosphate buffer (0.1 M), giving 100% relative activity, and the relative activity was 59.1% at pH 9 in Tris-HCl buffer. The full activity profile with pH that was made is reproduced in Figure 5.3. The use of pH 8 in both buffer systems appeared for the context of this work to be possible without significant loss of enzyme activity. It was thought to be of benefit to the work also to evaluate the pH at various pH and temperature with the synthesised aminonitriles.



**Figure 5.3: pH activity assay of Nit1 with mandelonitrile reproduced from Dooley-Cullinane *et al*<sup>2</sup>**

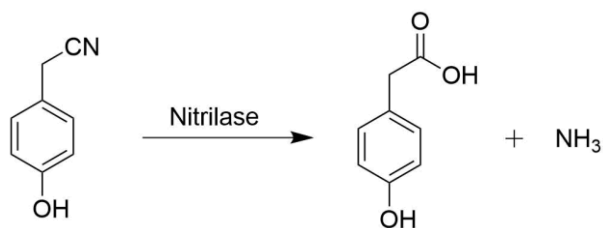
In order to obtain suitable enzyme for evaluation it was necessary to obtain significant quantities of enzyme. For this Dooley-Cullinane *et al* developed the following conditions. Here, Nit1 containing cells underwent PCR amplification and cloning. For the cloning, the *N*-terminal His-tagged expression of the enzyme was achieved with a pRSF-2 Ek/LIC vector. The clones were then transformed into *E. coli* BL21 (DE3) cells and the cells were induced to produce the His-tagged protein. The protein was purified with the Ni-NTA purification system. The purified Nit1 protein was analysed by SDS-PAGE electrophoresis to determine protein size and purity, and Native-PAGE electrophoresis was also carried out. Further detailed information on this enzyme and its activity is outlined in the findings of Coffey *et al* and Dooley-Cullinane *et al*<sup>1,2</sup>.

A limitation in the design of this work was the enzyme quantities available from each culture batch purified and the necessity for this to be quantified when the batch was prepared. It was necessary for reactions to be scaled to a 200  $\mu\text{L}$  scale to allow for preservation of the enzyme and for multiple screening biotransformations to take place. For analysis, HPLC methods thus had to be adapted to allow for high throughput screening which will be discussed subsequently. We initially chose to screen unprotected 3-aminobutyronitrile and also planned to screen the nitrilase with the protected variants synthesised and discussed in Chapter 2.

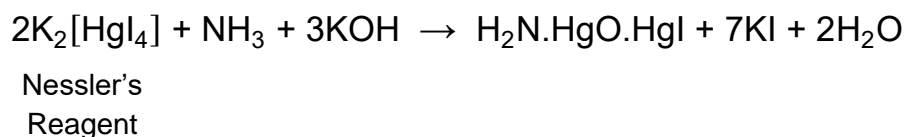
## 5.2 Activity Check for Nit1

The enzyme as obtained as a batch of approximately 20 – 40  $\mu\text{L}$  quantity, depending on the purification yield, and a biotransformation with 4-HPAN therefore became the reference activity check for every batch and also used to determine the required enzyme quantity for each reaction.

The reaction between Nit1 and 4-HPAN releases ammonia, as shown in Scheme 5.2 thus the biotransformation could be analysed using the Nesslerisation technique<sup>3</sup>. The ammonia reacts with the Nessler's reagent to give a soluble product, shown in Scheme 5.3, which can be quantitatively detected by measuring its absorbance at 425  $\text{nm}$ <sup>4</sup>. As noted earlier, unfortunately the same activity test could not be used for evaluation with the aminonitriles due to interference with the Nessler's Reagent.

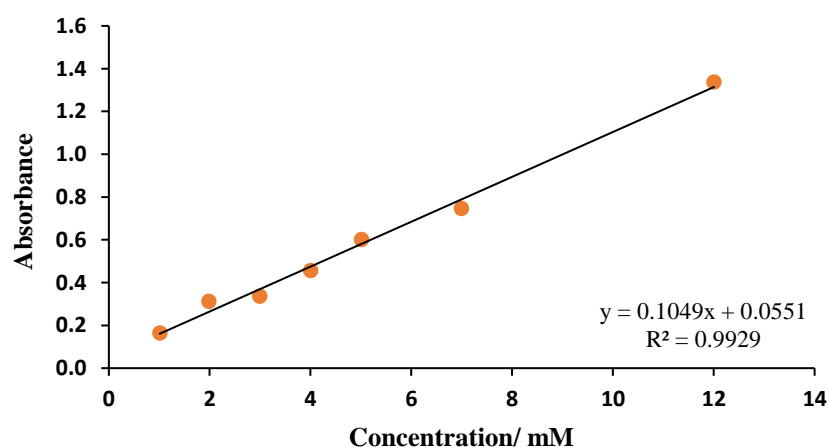


**Scheme 5.2: Enzymatic hydrolysis of 4-HPAN giving ammonia as a by-product**



**Scheme 5.3: Reaction scheme of Nessler's reaction to give the coloured product observed**

In the case of HPAN performance checking, a standard curve was prepared for the analysis of each batch of purified Nit1 and the volume of Nit1 by Nesslerisation required for a 200  $\mu\text{L}$  biotransformation with 3-aminobutyronitrile (3-ABN) was calculated. Standards were prepared of ammonium chloride with concentrations of 1 – 12 mM. Nessler's mastermix (181  $\mu\text{L}$ ) was added to the standards (20  $\mu\text{L}$ ) and the absorbance was measured at 425 nm to give a standard curve such as shown in Figure 5.4.



**Figure 5.4: Standard curve for ammonia detection using the Nessler's colorimetric assay**

For the enzyme activity assay, a stock solution of 4-HPAN in ethanol (2 mL) was prepared to give a concentration of 200 mM. The biotransformation was carried out in phosphate buffer (1.0 M, pH 7) to which 4-HPAN in ethanol was added was (10 mM), followed by the addition of Nit1. After incubation and shaking for 24 h, the addition of HCl quenched the reaction. The mixture was centrifuged, the supernatant transferred to a microtitre plate and Nessler's mastermix was added. The mixture was allowed to stand for 10 min then the absorbance was read immediately. A representative of the microtitre plate with the Nessler's samples is shown

in Figure 5.5. The absorbance results were then inputted into the standard curve to give the concentration of ammonia produced, which indicated the level of enzyme activity and thus the volume of Nit1 needed for work with the aminonitriles could be determined. A standard curve was used to determine the activity of each Nit1 batch received and thus the volume of Nit1 needed for each screening, which are summarised in Table 5.2.

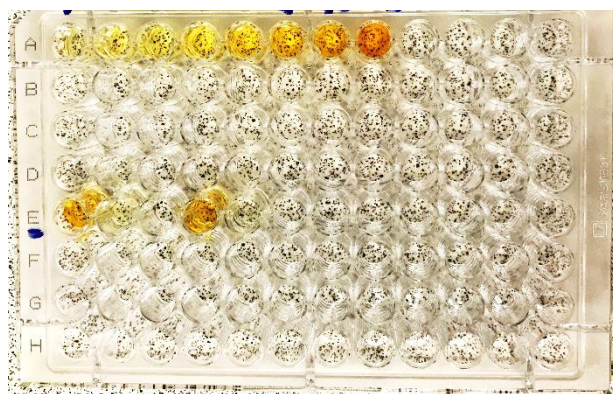
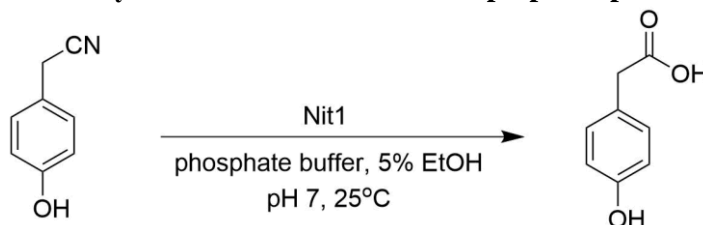


Figure 5.5: Nessler's colorimetric assay of Nit1 with 4-HPAN (row E), along with standards (row A)

Table 5.2: Summary of Nit1 batches received and reacted with 4-HPAN as a reference. Analysis carried out by Nessler's assay. Note: new standard curves prepared periodically



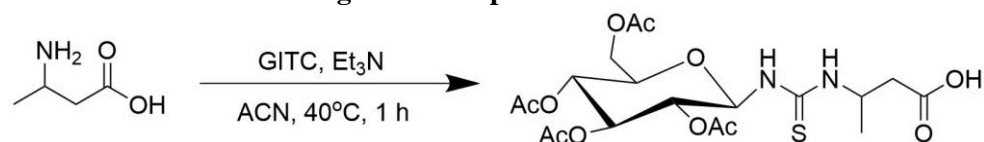
Batch	Absorbance	4-HPAA yield/ mM	Enzyme preparation volume required for screening/ $\mu$ L
1	0.953	9.105	20
2	0.124	1.357	134
3	0.671	6.679	27
4	0.885	8.230	22

### 5.3 Screening of Nit1 with 3-aminobutyronitrile (124)

#### 5.3.1 Optimisation of GITC derivatisation for quantitation

As initial screening studies planned to evaluate 3-aminobutyronitrile (**124**) with Nit1 in its unprotected form, for analysis, 2,3,4,6-tetra-*O*-acetyl- $\beta$ -D-glucopyranosyl isothiocyanate (GITC) protection would be necessary to determine the ee of acid products as discussed previously in Chapter 2. In order to ensure accurate quantitation GITC standard curves, particular since this body of work would involve very small quantities, the derivatisation method of GITC based on Mitsukura *et al* was examined<sup>5</sup>. Derivatisation of 3-aminobutyric acid was reviewed using GITC in 1.2, 1.5, and 2 mole equivalents as shown in Table 5.3.

**Table 5.3: Optimisation of GITC reaction. Reaction quantities shown. Reactions carried out at 40°C for 1 h. 3-ABA and GITC weighed on a 5-place balance**



3-ABA/ g	3-ABA/ mg mL <sup>-1</sup>	GITC/ g	Equivalent	Et <sub>3</sub> N/ $\mu$ L	ACN/ $\mu$ L
0.0001	0.1	0.00045	1.2	162	0.838
0.0001	0.1	0.00057	1.5	162	0.838
0.0001	0.1	0.00076	2.0	162	0.838

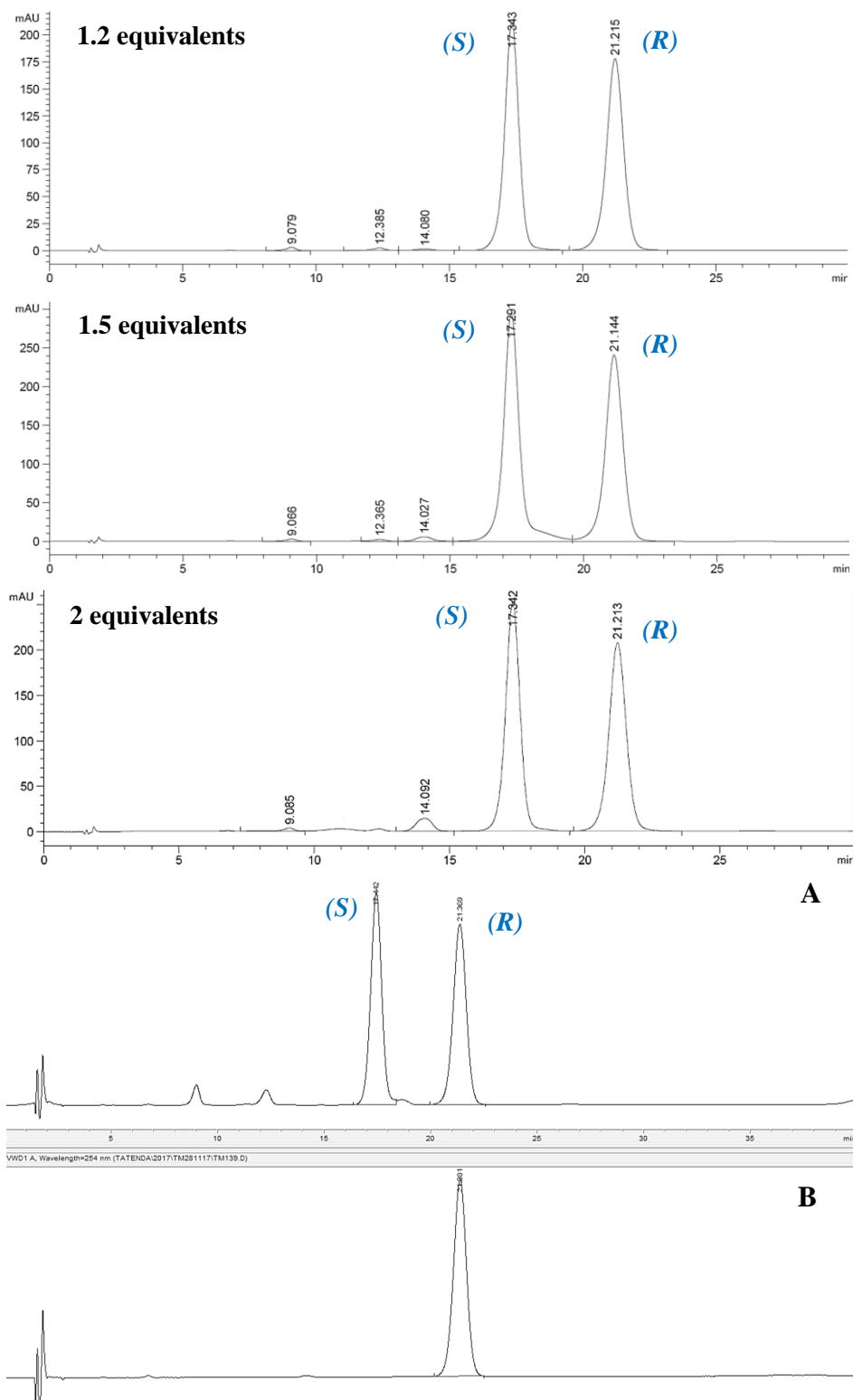
Samples were prepared then analysed in duplicate by HPLC (MeOH:H<sub>2</sub>O 35:65 + 0.1% TFA). It was discovered that the optimum amount of GITC was 1.5 mole equivalents as seen in Figure 5.6 as no further improvement in the HPLC response, i.e. peak area, was observed with higher amounts of GITC added and so this quantity was used for all the work in this study. The key HPLC results observed are detailed in Table 5.4.

**Table 5.4: HPLC parameters of the GITC derivatisation study**

GITC Equivalent	Average Peak Area	Resolution	Selectivity Factor
1.2	8338.82	6.03	1.22
1.5	11722.08	5.70	1.22
2.0	9860.65	5.74	1.22

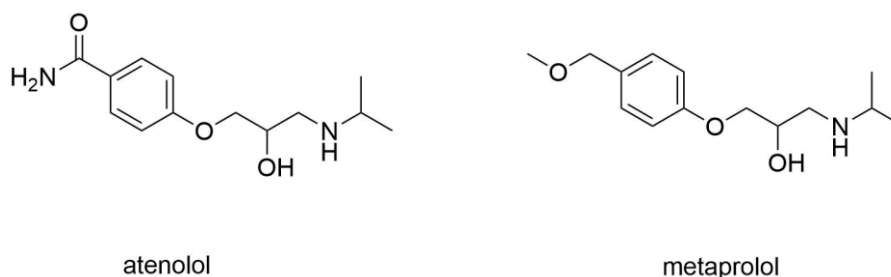
In all cases of the work with Nit1 and 3-aminobutyronitrile, the configuration of the acid product was assigned based on a prepared standard of GITC-(*R*)-3-aminobutyric acid from which it can be determined that in a chromatogram of racemic GITC-3-aminobutyric acid, the

first peak at retention time of 17 min is the (*S*)-isomer and the second peak at retention time of 21 min is the (*R*) configuration.



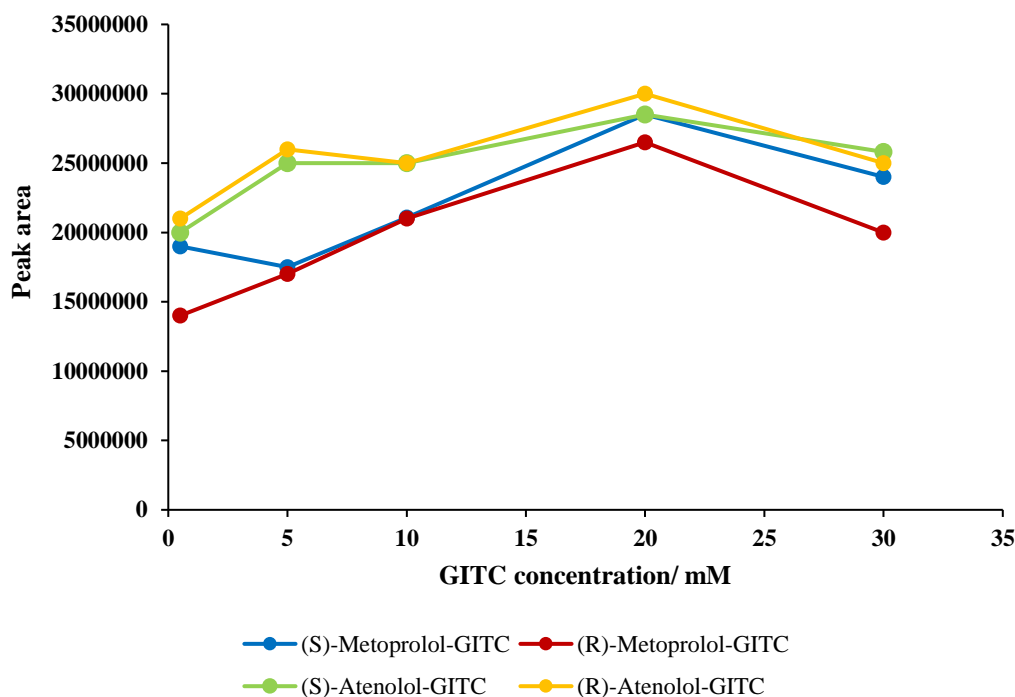
**Figure 5.6: Chromatograms showing GITC-3-aminobutyric acid prepared with 1.2, 1.5, and 2 equivalents of GITC, A – racemic GITC-3-aminobutyric acid, B – (*R*)-GITC-3-aminobutyric acid Analysis carried out on a C18 column. Mobile phase MeOH:H<sub>2</sub>O 35:65 + 0.1% TFA at a flow rate of 1 mL.min<sup>-1</sup>**

It is worth noting that the use of GITC as a derivatising agent is often employed for qualitative rather than for quantitative purposes, and in the case of  $\beta$ -amino nitriles and acids that were of interest to us, to our knowledge there are few quantitative methods employing GITC as a quantitative derivatising method. One such case is the work of Nguyen *et al* who were looking to rapidly derivatise and determine the enantiomers for atenolol and metoprolol, which are  $\beta$ -adrenoceptor blocking agents shown in Figure 5.7<sup>6</sup>.



**Figure 5.7: Structures of atenolol and metoprolol**

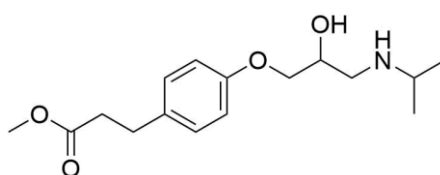
They investigated parameters of the derivatisation procedure such as the GITC concentration, the reaction time, and the reaction temperature. They also considered the RP-UPLC conditions. The samples were prepared as follows: atenolol ( $200 \mu\text{g mL}^{-1}$ ) was made up in methanol and metoprolol ( $600 \mu\text{g mL}^{-1}$ ) was prepared in ACN:HCl (0.1 M) 95:5. A solution of GITC in acetonitrile ( $100 \mu\text{L}$  of 15 mM) was added, along with triethylamine in acetonitrile ( $100 \mu\text{L}$  of 10 mM). The mixture was left to stand for 15 min at room temperature then injected directly into the UPLC. The concentration of GITC was then varied and it was observed that in general the increase in GITC concentration caused an increase in derivatisation products, as seen in Figure 5.8, with the best results being obtained with GITC in a molar excess of 20 times.



**Figure 5.8: Graph of effect of GITC concentration on the UPLC peak areas observed<sup>6</sup>**

They increased the temperature up to 60°C from room temperature, and it was found that the whilst the peak area on the UPLC increased, it was a narrow rate of change. At room temperature, it was observed that up to 20 min, the production of the derivatisation products increased. After this point, a plateau was reached. For atenolol, the LOQ and LOD were determined to be 0.35  $\mu\text{m mL}^{-1}$  and 0.18  $\mu\text{m mL}^{-1}$ , respectively. For metoprolol, the LOQ and LOD were determined to be 0.2  $\mu\text{m mL}^{-1}$  and 0.06  $\mu\text{m mL}^{-1}$ , respectively. This study showed GITC to be quite effective to analyse atenolol and metoprolol rapidly and precisely. In comparison to our work, the LOD for GITC-3-aminobutyric acid as calculated from the standard curve was 0.047  $\text{mg mL}^{-1}$  and the LOQ was 0.060  $\text{mg mL}^{-1}$ .

Another example is in the work of Tang *et al* who sought to determine the enantiomers of esmolol, shown in Figure 5.9, by HPLC utilising GITC<sup>7</sup>. Esmolol, chemically known as methyl 3-[4-(2-hydroxy-3-isopropylamino-propoxy)-phenyl]-propanoate, is an effective rapid acting  $\beta_1$ -adrenergic blocker. Originally, it was sold as the racemate however it was found that only the (*S*)-(–) enantiomer was active whilst the (*R*)-(+) enantiomer was shown to be inactive<sup>8</sup>.



**Figure 5.9: Structure of esmolol**

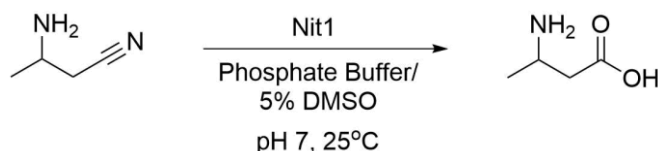


Stock solutions of  $100 \mu\text{g mL}^{-1}$  esmolol and the internal standard, (*S*)-(-)-propranolol were prepared. The esmolol stock was then used to prepare solutions of  $10$  and  $50 \mu\text{g mL}^{-1}$  in methanol. Human plasma samples were then prepared using dried standard solutions of esmolol of concentrations  $10$ ,  $50$ , and  $100 \mu\text{g mL}^{-1}$  reconstituted with human plasma to give a series of samples. An aliquot of the human plasma sample was extracted with a mixture of the internal standard, ammonia water, and dichloromethane. The organic extract was dried and derivatised with GITC at room temperature for  $15$  min. This was then dried and reconstituted in mobile phase for analysis by HPLC.

Results of the study showed it was possible to completely separate the enantiomers with a selectivity factor of  $1.27$  and a resolution of  $5.53$ , and the method showed satisfactory reproducibility. The LOD was  $0.003 \mu\text{g mL}^{-1}$  and the LOQ was  $0.035 \mu\text{g mL}^{-1}$  for each enantiomer.

### 5.3.2 Initial Screening of 3-aminobutyronitrile (**124**)

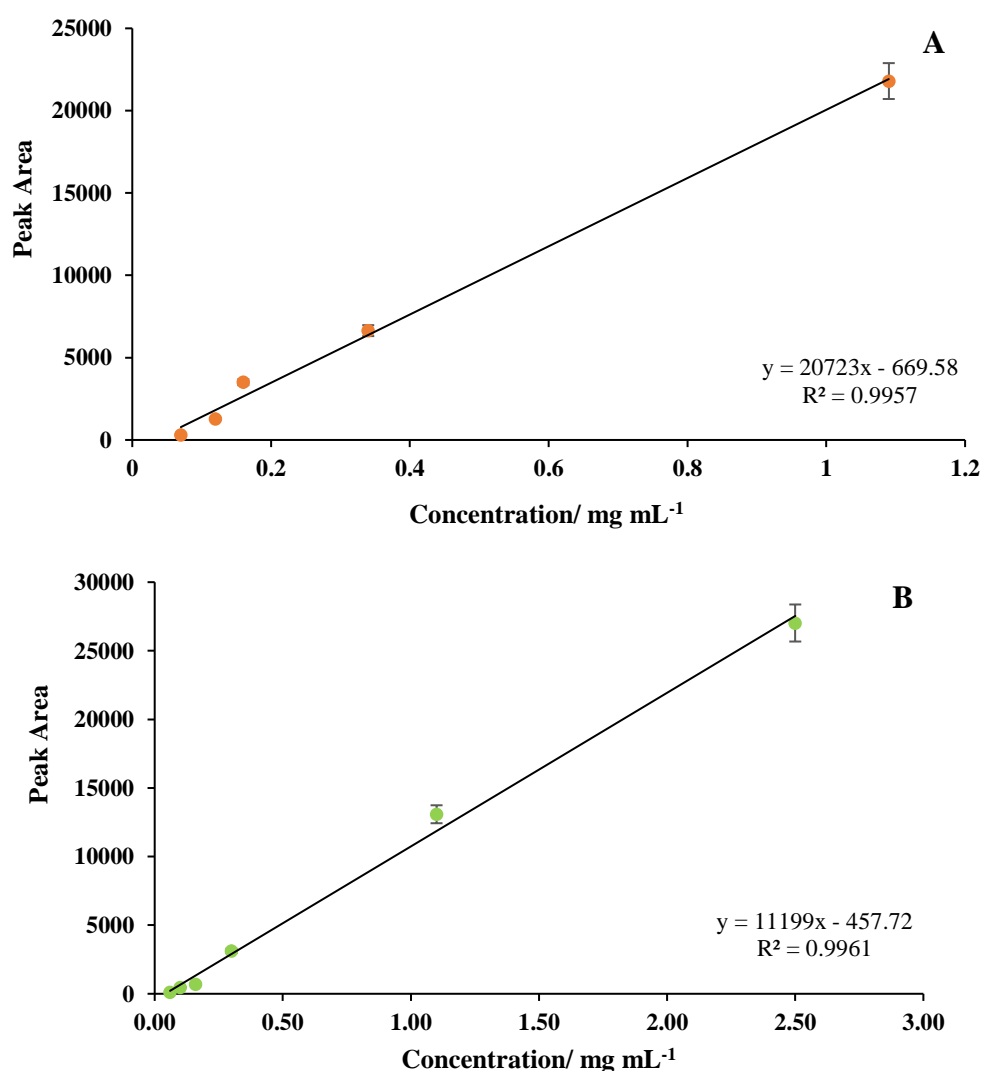
An initial investigation of the reaction of Nit1 with unprotected 3-ABN (**124**) for  $24$  h at pH  $7$  and  $25^\circ\text{C}$  was carried out to investigate activity with the substrate, as seen in Scheme 5.4.



**Scheme 5.4: Biotransformation of Nit1 with 3-aminobutyronitrile (**124**)**

Biotransformations were carried out first in phosphate buffer ( $0.1$  M,  $190 \mu\text{L}$ ) without solvent at pH  $7$  and racemic 3-aminobutyronitrile ( $10$  mM,  $0.00017$  g), measured with a  $5$ -place balance was added. A second set of reactions contained  $5\%$  DMSO ( $10 \mu\text{L}$ ) to evaluate the effect of solvent on the reaction. In their work, Dooley-Cullinane *et al* used  $5\%$  ethanol in their reaction with little effect on their results and the activity of Nit1<sup>2</sup>. The enzyme was then added ( $20 \mu\text{L}$ ). Biological replicates were completed for both reactions. The mixtures were incubated at  $25^\circ\text{C}$  with mechanical shaking ( $200$  rpm) for  $24$  h and quenched by the addition of acetonitrile and the mixtures were centrifuged to remove the biomass. A shorter reaction time was chosen as it was thought the isolated enzyme could be significantly more active and this timeframe would give an indication. To remove the solvent, the supernatants were lyophilised

for at least 24 h and treated with GITC for HPLC analysis which was conducted in duplicate. As mentioned in prior Chapters, ee for the GITC nitrile could not be determined, only yield, but yield and ee of the acid could potentially be determined by GITC derivatisation by comparison to standard curves. The standard curves were prepared using individual standards derivatised with GITC for the nitrile and acid. These curves are shown in Figure 5.10. It was necessary to calculate yields based on a standard curve as the scale of the reactions was too small to successfully acquire isolated yields. HPLC peak areas obtained from the biotransformations were thus inputted into the equation of the line of the standard curves to acquire the yields.



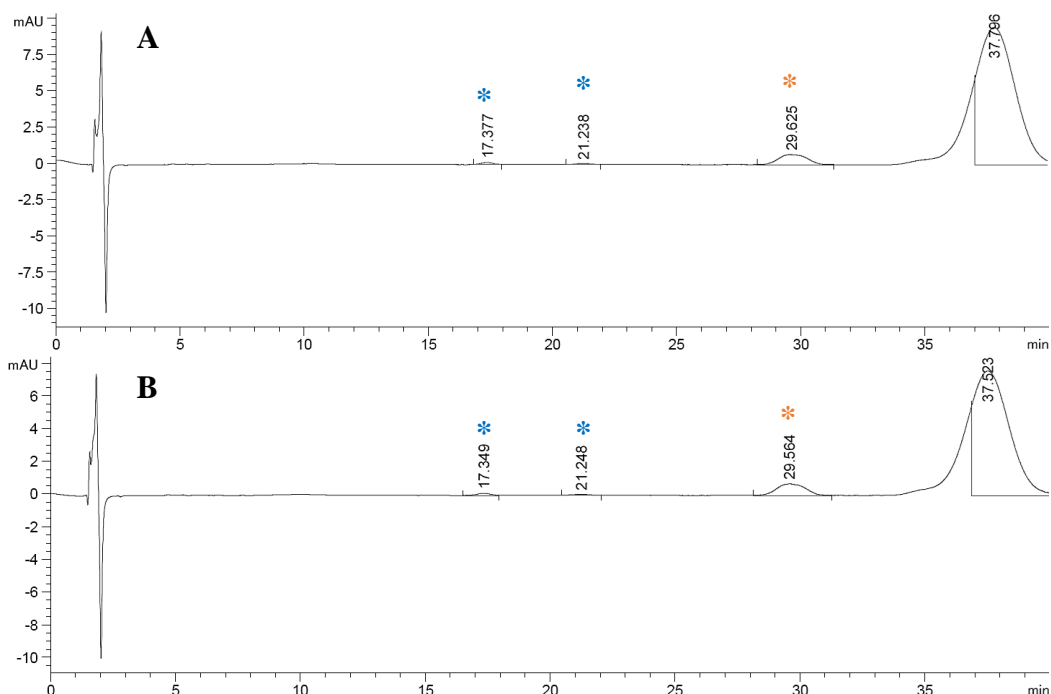
**Figure 5.10: GITC standard curves. A – GITC-3-ABN, B – GITC-3-ABA. Analysis carried out on a C18 column. Mobile phase MeOH:H<sub>2</sub>O 35:65 + 0.1% TFA at a flow rate of 1 mL.min<sup>-1</sup>. Error bars represent the error across the mean of the HPLC duplicates**

After the reaction, acid appeared to be obtained in 57% yield for reactions completed in phosphate buffer whilst it was observed in 76% yield where 5% DMSO was present. The acid

ee's were 16% (*S*) and 24% (*S*) respectively. No amide was detected for any of the samples. Although nitrile could be detected for the first time for this substrate without induction of the enzyme, the results were disappointingly inconclusive with recovery being calculated as over 100% for most of the samples as shown in Table 5.5, which does not fit with the mass balance for the process in all cases. HPLC chromatograms of the reactions are shown in Figure 5.11. This would later be shown to be possibly linked to issues with the HPLC method such as ghost peaks and by-products of the derivatisation reaction which may have inflated some of the results.

**Table 5.5: Initial screen of Nit1 with 3-aminobutyronitrile at pH 7 for 24 h. Average values shown. 8 reactions were carried out and each was analysed in duplicate on HPLC, thus n = 16. Yields acquired by HPLC standard curve. ND = not detected**

Solvent	Nitrile	Acid	
	Recovery (%)	Yield (%)	ee (%)
Phosphate buffer	112	57	16 ( <i>S</i> )
5% DMSO	95	76	24 ( <i>S</i> )
Phosphate buffer enzyme blank	108	ND	ND
5% DMSO enzyme blank	117	ND	ND



**Figure 5.11: HPLC chromatograms of Nit1 reaction with 3-ABN at pH 7 in A – 100% phosphate buffer, B – 5% DMSO. \*acid peaks (17 and 21 min), \*nitrile peak (29 min). Analysis carried out on a C18 column. Mobile phase MeOH:H<sub>2</sub>O 35:65 + 0.1% TFA at a flow rate of 1 mL.min<sup>-1</sup>**

The potential yield results obtained with Nit1 for the product 3-aminobutyric acid appeared the best thus far that had been observed in comparison to SET1, which only obtained 29% (*S*) with <1 yield at pH 7. These results are comparable, if not slightly better than those observed by Wang *et al* in their reaction on unprotected 3-ABN who generated 43% yield and 20.8% ee of (*S*)-isomer with AJ270<sup>9</sup>. The initial results with Nit1 for 3-aminobutyronitrile were therefore quite encouraging, and we wanted to explore the reaction further at small scale prior to attempting to scale up the process.

### 5.3.3 Time Study

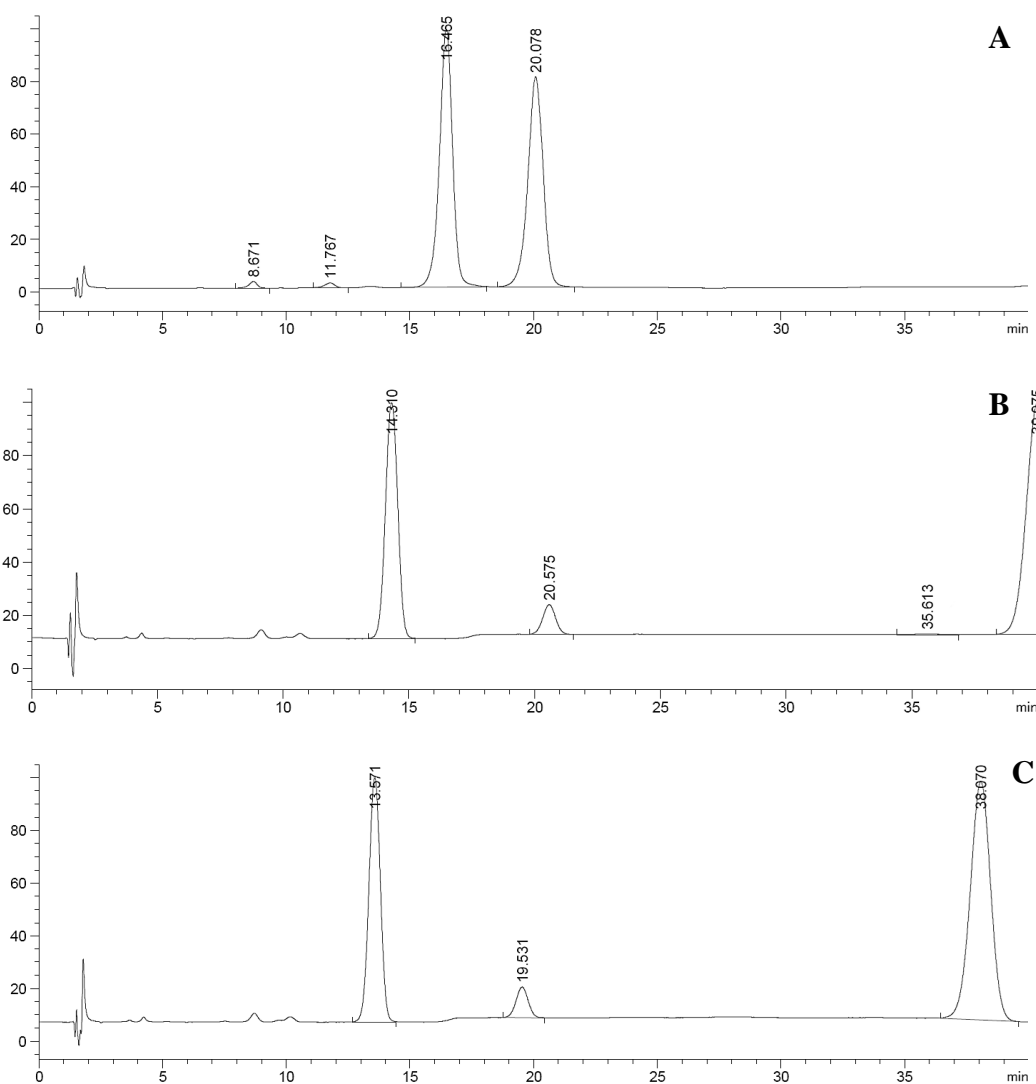
A time study of the hydrolysis of 3-ABN (**124**) by Nit1 over 48 h was carried out with testing at 0 h, 3 h, 6 h, 24 h, and 48 h to determine if the ee had reached a peak prior to 24 hours and there was a kinetic effect on the selectivity of the reaction. Biotransformations were carried out in phosphate buffer (0.1 M, 170  $\mu$ L) at pH 7 with 5% DMSO (10  $\mu$ L) and racemic 3-aminobutyronitrile (10 mM, 0.00017 g) measured with a 5-place balance was added. Biological replicates were completed for all the samples. The mixtures were incubated with enzyme at 25°C with mechanical shaking (200 rpm) for 48 h. The reactions were quenched by the addition of acetonitrile and the mixtures were centrifuged to remove the biomass. The supernatants were lyophilised for at least 24 h and treated with GITC for HPLC analysis which was conducted in duplicate i.e., two subsequent injections into the same HPLC vial.

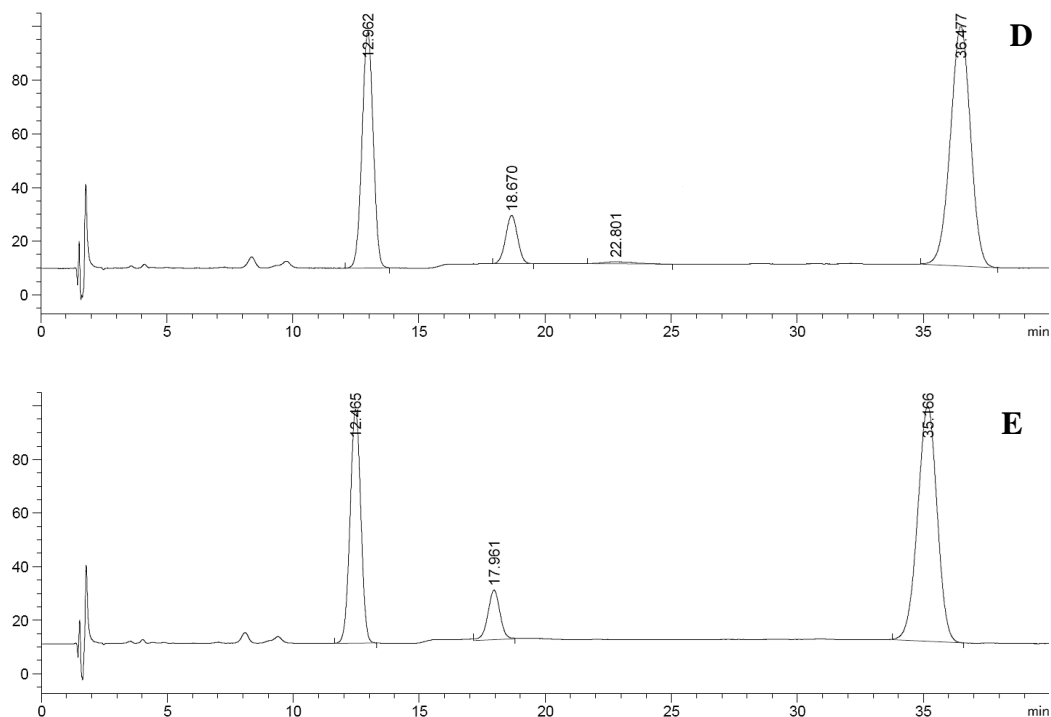
**Table 5.6: Time study of Nit1 with 3-aminobutyronitrile at pH 7 for 48 h in phosphate buffer with 5% DMSO. Average values shown. Yields acquired by HPLC standard curve. ND = not detected**

Time (h)	Nitrile	Acid	
	Recovery (%)	Yield (%)	ee (%)
0	131	ND	ND
3	204	ND	ND
6	325	ND	ND
24	231	ND	ND
48	233	77	97 ( <i>S</i> )

Again, the percentage of recovered nitrile was observed as above 100% on average, as can be seen from Table 5.6. In contrast to the earlier reaction discussed above where acid was observed

at 24 h, no acid was conclusively detected until the 48 h time point at 77% yield and 97% (*S*) ee. The 24 h time point produced unusual results. In the replicates, it would appear that acid is present but as the (*R*)-enantiomer. When compared to a standard however and tracked through the sample replicates plus the HPLC duplicates, the peak is seen to be drifting thus making it difficult to assign. The peak appears to elute at progressively earlier times until it coincides with the expected elution time of the (*S*)-enantiomer. The expected elution times of the acid based on the standard are 16 and 20 min for the (*S*)- and (*R*)-enantiomer respectively. By the point the HPLC duplicate of the sample replicate is run, peaks are observed at 12 and 17 min. These could possibly be the acid peaks, but this could not be said with certainty. The drifting may possibly be attributed to column temperature fluctuations on the day of analysis. Representative HPLC chromatograms can be seen in Figure 5.12.





**Figure 5.12:** HPLC chromatograms of the 24 h time point of Nit1 with 3-ABN. Same batch of Nit1 as 24 h experiment utilised. A – GITC-3-ABA standard, B – 24 h sample, C –HPLC duplicate of sample B, D – 24 h sample replicate, E –HPLC duplicate of sample D. Peaks at 8 and 11 min are GITC by-products. Chiral analysis carried out on a C18 column. Mobile phase MeOH:H<sub>2</sub>O 35:65 + 0.1% TFA at a flow rate of 1 mL.min<sup>-1</sup>

Had this peak at 20 min in the first sample for the 24 h time point truly been the acid product this would be peculiar as many *Rhodococci* containing nitrilase species exhibit (*S*) selectivity<sup>10-13</sup>.

This deviation in selectivity was observed later on in some of the pH study samples so this may be a point of further study in future work to understand conditions which may possibly affect the enantioselectivity of Nit1 or if different batches of purified Nit1 could exhibit variations in enantioselectivity. An additional peak was consistently observed at the 35 min point and later. This would later be confirmed to be a by-product of the GITC derivatisation.

Studies were also completed to see if an increase in temperature could enhance the enzyme activity and perhaps speed up the production of acid. It is known that temperature can affect the nature and also the structure of an enzyme and also that Nit1 had an increased activity at higher temperature<sup>14</sup>. As the optimum temperature of the enzyme is reached, the rate of the reaction increases as the molecular free energy increases, allowing for more successful collisions<sup>15</sup>. The optimum temperature of Nit1 was 40°C but it was thought that this would be

initially too high for the substrate and potential products observed so a temperature of 35°C was selected. Samples were tested at the 2 h and 6 h time point. Again, the reaction time was reduced as it was felt that any increase in activity should be clearly observed by this time-point. Biotransformations were carried out in phosphate buffer (0.1 M, 170 µL) with 5% DMSO (10 µL) at pH 7 as previously in the time study. Biological replicates were included for all the samples. The mixtures were incubated at 35°C with mechanical shaking (200 rpm) for 6 h. The reactions were quenched and analysed as previously. Again, HPLC data proved problematic as HPLC duplicates were returning the percentage of nitrile recovered as >100%. Analysing just the first HPLC injections, showed an appreciable improvement in terms of more nitrile being acted upon by the enzyme at the time point as the average nitrile recovered was 54% at 2 h and 55% at 6 h. Disappointingly, there was no acid detected by the 6 h time point.

Unfortunately, in this study it became clear that variations in the HPLC chromatograms between experiments and HPLC runs were present which inflated the nitrile recovery quantitation and possibly interfered with the acid results. This prompted investigations into the effects of solvents and the necessity for significant troubleshooting of the HPLC methodology for the GITC derivatised nitrile and acid.

#### *5.3.4 Solvent effects and analytical variation and substrate/product recovery*

During the previous studies and also a further investigation of the effect of solvent on the biotransformation it became clear that significant variations on the HPLC for quantitation of nitrile and acid were being observed. This became most clear during a study on the effect of the addition of solvent on the biocatalytic performance with significant variations between determined yields from replicates, experiments and HPLC runs leading us to question the applicability of this method for quantitation. To test the effect of variation of the solvent in the biocatalytic system on the analytical methodology the addition of 5% DMSO and 5% EtOH, to the phosphate buffer along with 100% H<sub>2</sub>O, were compared with 100% phosphate buffer at pH 7 to determine the impact on derivatisation and standard curves generation. In this case, it was possible to consider 100% H<sub>2</sub>O as a solvent system as Nit1 was supplied as the unsupported free protein in water.

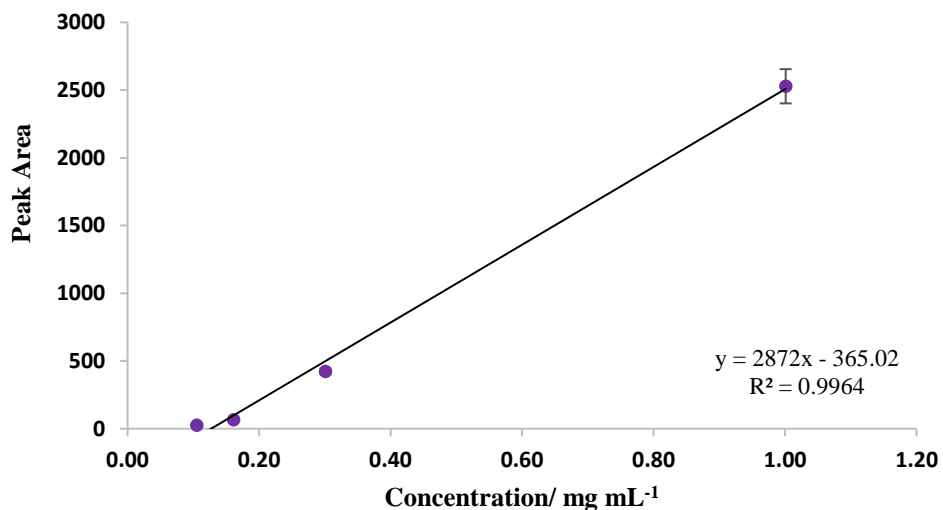
To investigate the effect of solvent on the validity of standard curves for the GITC nitrile and acid derivatisation reactions were completed on acid and nitrile standards spiked with added

solvents to simulate biotransformation conditions. The preparation of the standards was modified to the following: the nitrile or acid was dissolved in the solvent system (200  $\mu\text{L}$ ) with ACN (600  $\mu\text{L}$ ) to mimic the work-up of the reaction. The samples were then lyophilised for at least 24 h then derivatised with GITC using previously developed conditions. The standards were analysed by HPLC in duplicate.

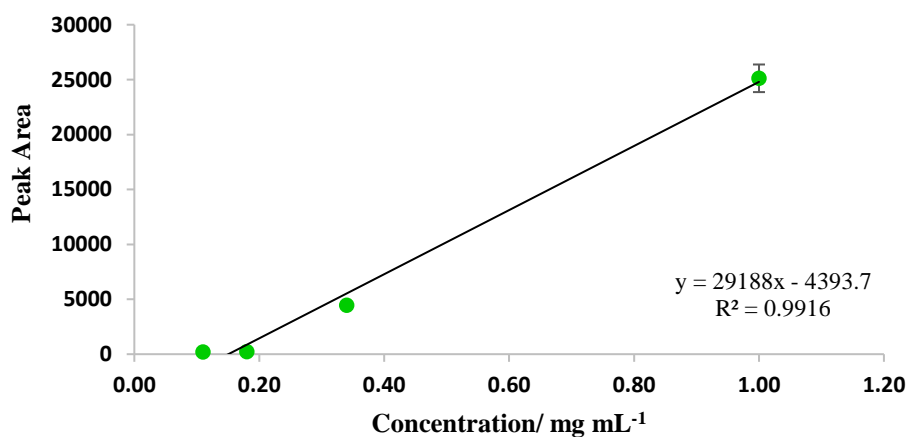
It was observed that the greater the gradient of the curve, then the greater the effect of the solvent had an effect. For the nitrile, it was found that 100% phosphate buffer gave the best curve, as it had the smallest gradient of 2872  $\text{mAU}\cdot\text{s}\cdot\text{mg}\cdot\text{mL}^{-1}$ . The addition of 5% DMSO caused the gradient to increase considerably to 29188  $\text{mAU}\cdot\text{s}\cdot\text{mg}\cdot\text{mL}^{-1}$ . The added solvent that gave the least effect was found to be 5% EtOH as it had a gradient of 6659.4  $\text{mAU}\cdot\text{s}\cdot\text{mg}\cdot\text{mL}^{-1}$ , however it also had the worst linearity with an  $R^2$  value of 0.9826. It was observed that the most affected curve was obtained with 100%  $\text{H}_2\text{O}$  which had a gradient of 32202  $\text{mAU}\cdot\text{s}\cdot\text{mg}\cdot\text{mL}^{-1}$ , which is marginally more than DMSO. The linearity was best however, with 100%  $\text{H}_2\text{O}$ , which gave an  $R^2$  value of 0.9994.

For the acid, it was found that the least solvent effect was observed for 5% EtOH, which had a gradient of 9628.4  $\text{mAU}\cdot\text{s}\cdot\text{mg}\cdot\text{mL}^{-1}$  but again it had the worst linearity with an  $R^2$  value of 0.9862. The solvent that caused the most effect was 5% DMSO, which gave a gradient of 14753  $\text{mAU}\cdot\text{s}\cdot\text{mg}\cdot\text{mL}^{-1}$  whereas 100% phosphate buffer had a slightly lesser effect, giving a gradient of 13486  $\text{mAU}\cdot\text{s}\cdot\text{mg}\cdot\text{mL}^{-1}$ . The curve with 100%  $\text{H}_2\text{O}$  gave a gradient of 11396  $\text{mAU}\cdot\text{s}\cdot\text{mg}\cdot\text{mL}^{-1}$  and again gave the best linearity with an  $R^2$  value of 0.9978. The standard curves are shown in Figure 5.13 and 5.14. It is possible that the presence of DMSO and EtOH in the reaction mix may affect the quantity of compound before GITC derivation and hence cause the standard curve variation and hence mass balance inconsistencies when the standards and samples are lyophilised. These may also alter the reagent ratios affecting the extent of GITC derivatisation. In this work it began to become apparent that the analytical methods may not be applicable for absolute quantitation.

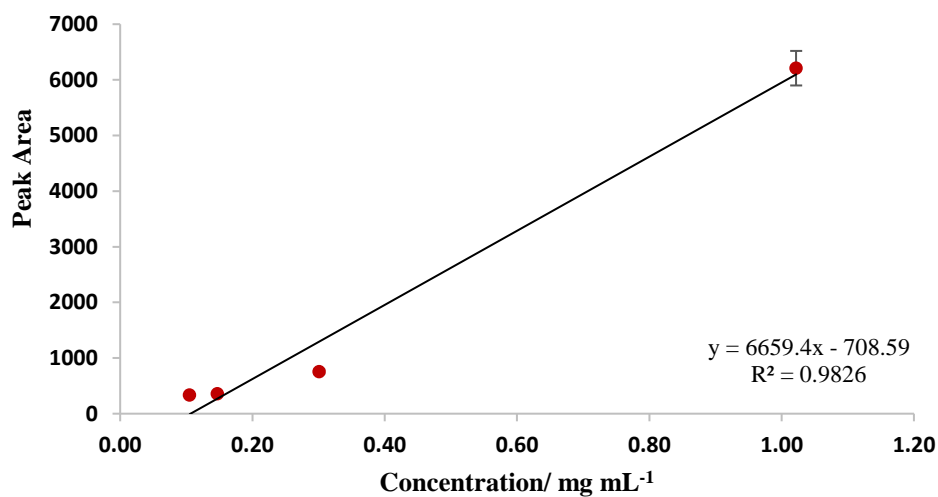




A



B



C

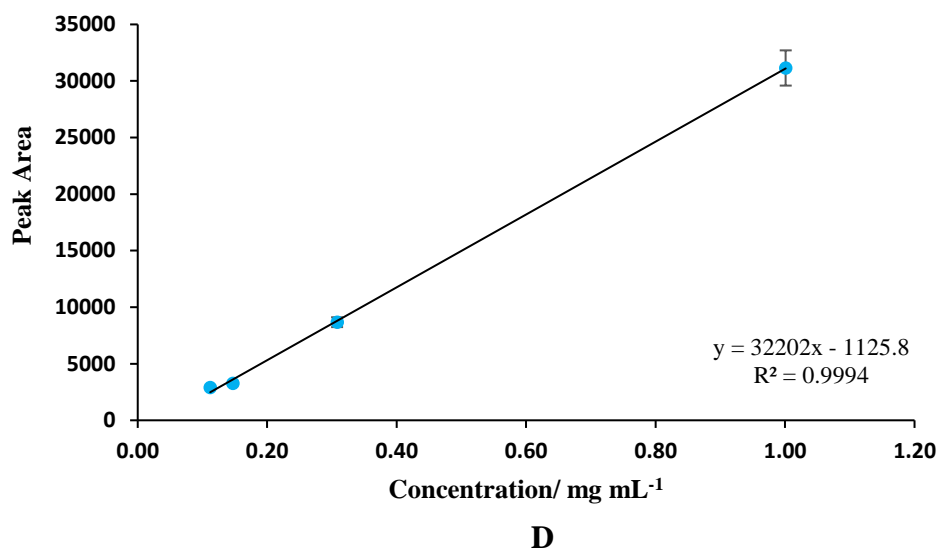
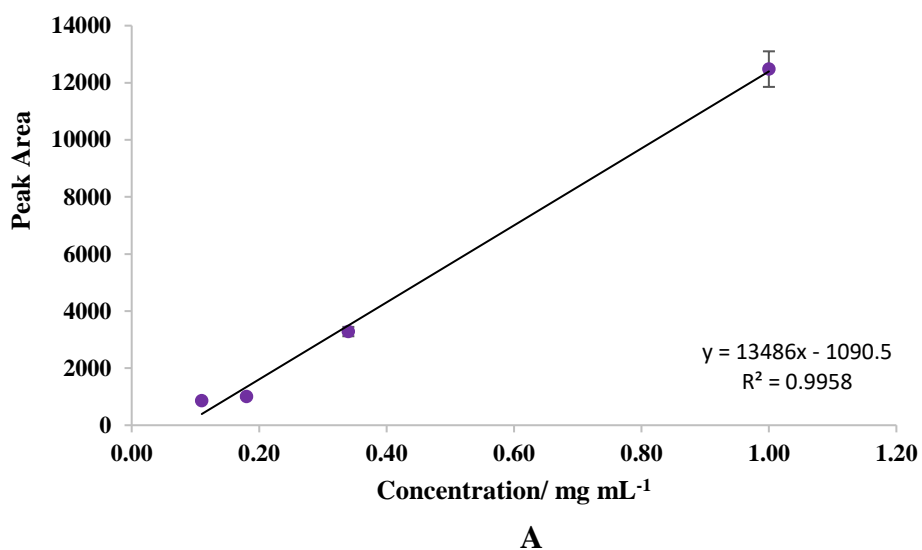


Figure 5.13: Standard curves of GITC-3-aminobutyronitrile. A – 100% phosphate buffer, B – 5% DMSO, C – 5% EtOH, D – 100% H<sub>2</sub>O. Mobile phase MeOH:H<sub>2</sub>O 35:65 +0.1% TFA, flow rate 1 mL.min<sup>-1</sup>. Error bars represent the error across the mean of the HPLC duplicates



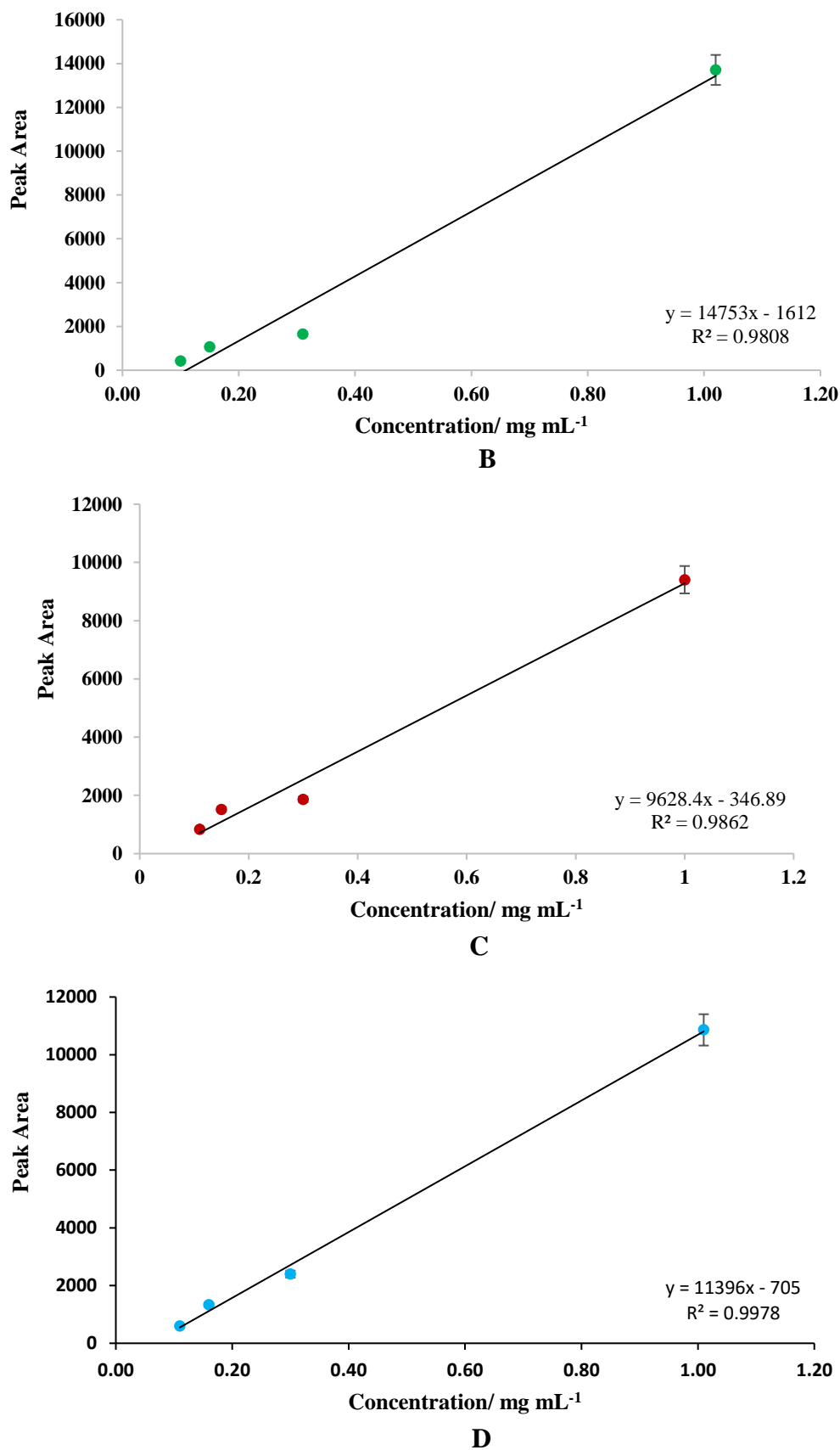
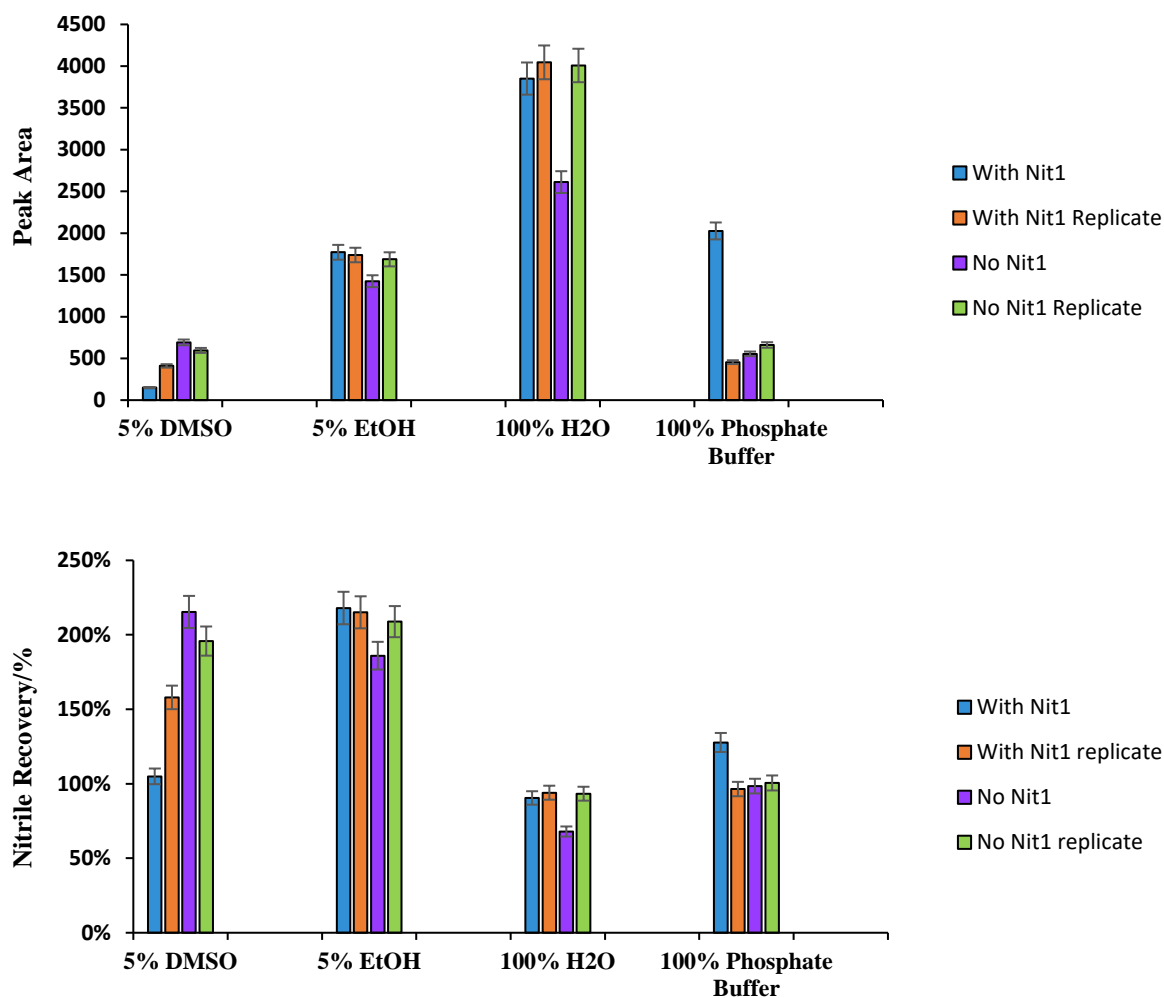


Figure 5.14: Standard curves of GITC-3-aminobutyric acid. A – 100% phosphate buffer, B – 5% DMSO, C – 5% EtOH, D – 100% H<sub>2</sub>O. Mobile phase MeOH:H<sub>2</sub>O 35:65 +0.1% TFA, flow rate 1 mL.min<sup>-1</sup>. Error bars represent the error across the mean of the HPLC duplicates

In order to determine further if the solvent additive affected the recovery and analysis of nitrile, biotransformations were carried out and stopped and evaluated at time 0. Biotransformation reactions were prepared in phosphate buffer as previously at pH 7 with 5% DMSO or EtOH (10  $\mu$ L) and racemic 3-aminobutyronitrile (10 mM). Additional biotransformation reactions were carried out in 100% phosphate buffer (0.1 M, 180  $\mu$ L) or 100% H<sub>2</sub>O (180  $\mu$ L). Biological replicates were completed for all the samples. Enzyme blanks for each solvent system were also prepared. The mixtures were lightly vortexed to ensure even mixing then the reactions were immediately quenched by the addition of acetonitrile and worked up as previously described including lyophilisation to remove the water.

In all cases of the study, as expected, no acid was detected. Whilst it was still difficult to achieve consistency between replicates due to HPLC issues which were yet to be dealt with and caused some peaks to be amplified during a sequence run, some trends could still be observed. As no internal standard was used, peak area was expected to vary slightly as there can be slight variations in injection volumes by the HPLC injector. Peak area responses were highest overall for 100% H<sub>2</sub>O, followed by 5% EtOH. The greatest nitrile recovery was observed for 5% EtOH and 5% DMSO but these were well over 100% so the most accurate nitrile recovery percentage was actually for 100% H<sub>2</sub>O. From the data it would appear the best solvent system to run the biotransformations would be 100% H<sub>2</sub>O with no other solvent or buffer present. The graphs are shown in Figure 5.15.

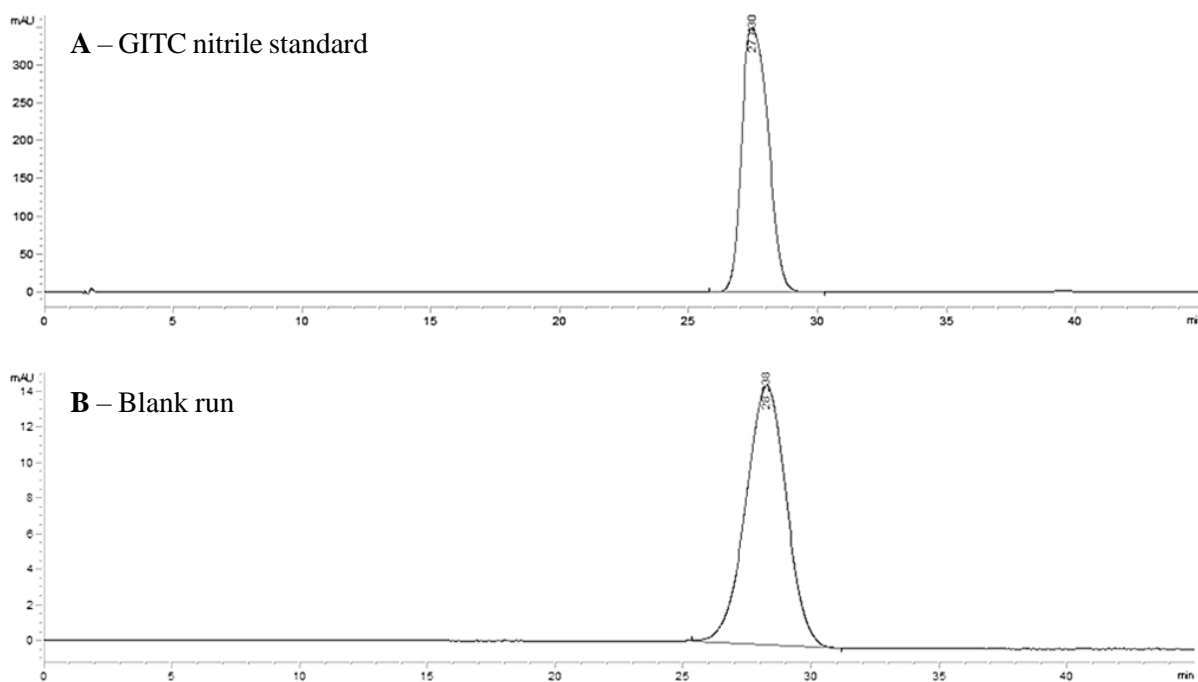


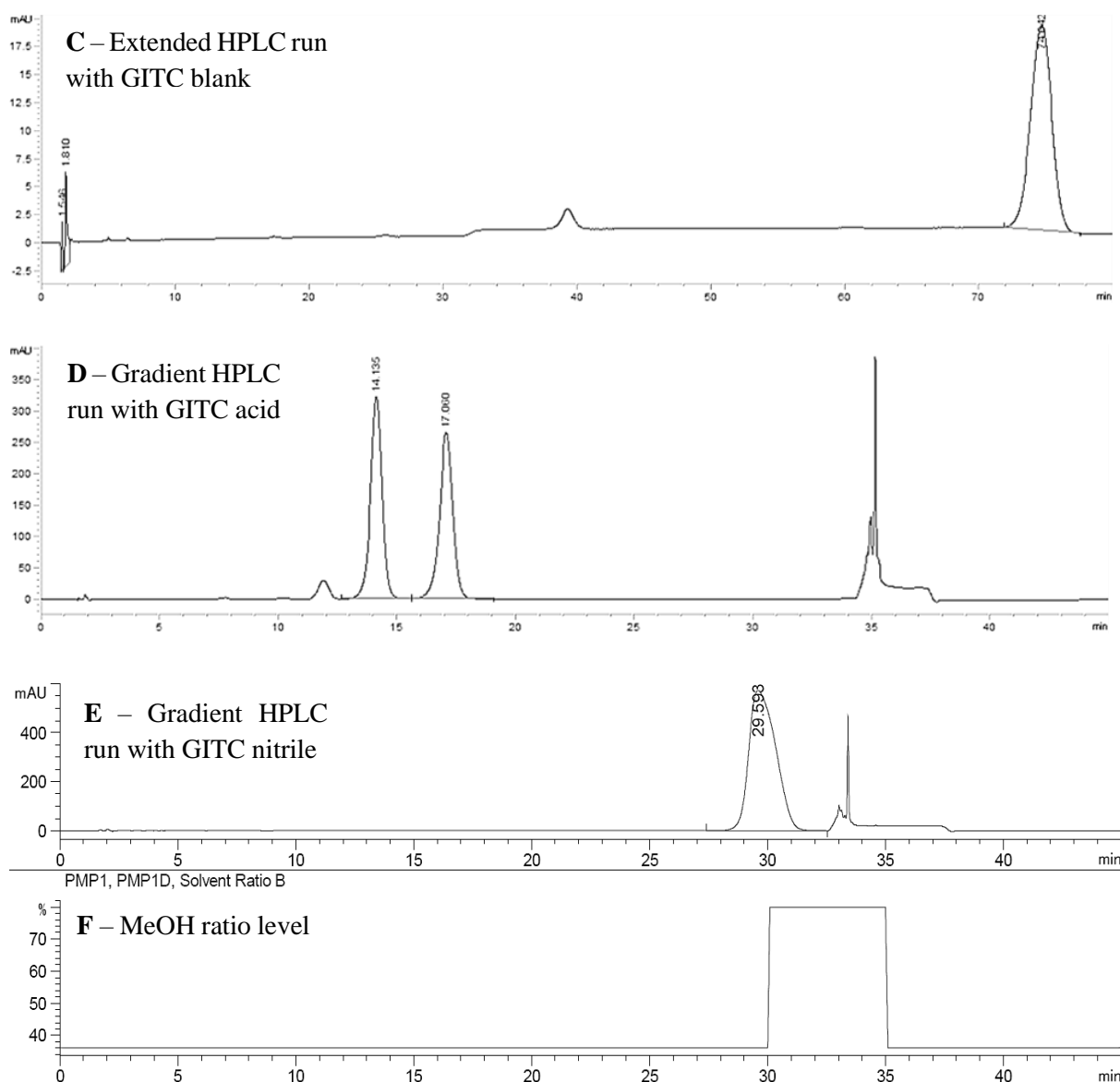
**Figure 5.15:** Graphs showing peak area and nitrile recovery for the different solvent systems after GTC derivatisation at time = 0. Error bars represent the error across the mean of the HPLC duplicates

### 5.3.5 Troubleshooting of HPLC analytical method

The HPLC method employed during the biotransformation screening and investigations into potential recovery issues during the work-up and derivatisation method, had been developed and configured to run in isocratic mode with a 45 min long HPLC run. Over time, as a significant number of samples and replicates were run, an additional peak at approximately 35 min was found to appear in samples, which would then progressively drift at times and obscure the peaks of interest. When subsequent blank runs were analysed, which were non-injection mobile phase, a peak appeared at 28 min which is close to the retention time of the nitrile, as shown in Figure 5.16B.

A longer isocratic HPLC run was carried out (Figure 5.14C) with a substrate blank of the GITC derivatisation reaction and it was discovered that there was a late eluting peak at 75 min which was most likely a by-product of the reaction. At this point, it would have been impractical and inefficient to proceed with conducting 75 min HPLC runs due to the significant number of samples. The HPLC machine and method were therefore re-configured to gradient mode in an attempt to elute compounds in a more acceptable time frame. Run times of 45 min could now be achieved and give clean spectra each time as shown in Figure 5.14D which is a representation with GITC-3-aminobutyric acid. The gradient was achieved with the same solvent system of MeOH:H<sub>2</sub>O + 0.1% TFA. The run began with an isocratic period of MeOH:H<sub>2</sub>O 36:64 + 0.1% TFA for 30 min, at which point the nitrile would be eluting, then the methanol was immediately increased to 80%, water 20% for 5 min. This allowed for everything to elute off the column. The ratio was then immediately returned to MeOH:H<sub>2</sub>O 36:64 + 0.1% TFA for 10 min to condition the column for the next run. Whilst it would still be necessary to conduct an HPLC run with only GITC to verify if the peak is GITC as it is being used in excess, the method is now valid and previously run samples could ideally be re-analysed with this new method.





**Figure 5.16: Chromatograms showing the HPLC method development for the GITC derivatisation. A – GITC-3-aminobutyronitrile with the isocratic method, B – HPLC run of a mobile phase blank immediately after the GITC nitrile run, C – An extended HPLC run of the GITC reaction containing no substrate with the isocratic method, D – Gradient HPLC for GITC-3-aminobutyric acid, E - Gradient HPLC for GITC-3-aminobutyronitrile. Acid peaks at 20.7 and 25 min. Analysis carried out on a C18 column. Mobile phase MeOH:H<sub>2</sub>O + 0.1% TFA, at a flow rate of 1 mL.min<sup>-1</sup>**

Investigations into the determination of the origin of this late eluting peak were completed. It was thought that there may be a possibility that some cell debris and proteins from *E. coli* remaining after purification of Nit1 may not have been completely removed by centrifugation and could have been the source of the interference observed by HPLC. It was thus decided to attempt to combat this with the use of an Amicon® Ultra centrifugal filter column on one of the samples to attempt to remove the cell debris and or proteins. An extra biotransformation and biological replicate were completed at the reaction time of 2 hours. One of these samples

was passed through the ultrafiltration column in a centrifuge for 5 min at 15000 rpm after the initial centrifugation process to remove the possible remaining biomass. There was no change observed in the nitrile results with the extra filtration step. The peak area for the nitrile without filtration was 22.9 and for the filtered sample, 24.8. It was therefore unlikely that any appreciable amount of cell debris or protein remained after standard centrifugation of the biotransformations that would interfere with the HPLC data.

The development of the new HPLC method could possibly cast doubt and impact the validity of initial results obtained in this work. It would be necessary to re-test samples from these earlier studies, something which was not conducted owing to time restrictions, to verify the results.

### 5.3.6 Optimisation of Nit1 Concentration

In order to try to optimise the biotransformation further a study was carried out to investigate if the addition of more enzyme added during the biotransformation reaction could increase the nitrile turnover. It was thought that in this work if all the available active sites became saturated, adding an additional quantity of enzyme could help to drive the reaction forward. A timed study was conducted over 24 h with testing at 0 h with no enzyme, 1 h, 3 h, 6 h, and 24 h with and without enzyme. Biotransformations were carried out in phosphate buffer (0.1 M, 170  $\mu$ L) at pH 7 with 5% DMSO (10  $\mu$ L) as previously with 20  $\mu$ L of Nit1 but at the 6 h time point, a duplicate sample was spiked with an additional 20  $\mu$ L. Other biotransformations were completed in 100% H<sub>2</sub>O. Biological replicates were completed for all the samples. The supernatants were lyophilised for at least 24 h and treated with GITC for HPLC analysis which was conducted in duplicate.

No acid was detected until the 24 h time point, and the sample spiked with additional Nit1 showed no significant improvement in apparent acid yield, with a 48% yield on average. A slightly increased ee of 29% (*S*) on average was obtained however in comparison to a biotransformation performed for 24 h at the lower concentration of enzyme, which had an ee of 24% (*S*).



## 5.3.7 pH 9 investigation

The effect of pH was investigated with the hope that an increase in pH would possibly improve the yield and pH of the biotransformation with 3-aminobutyronitrile. Below pH 9 most amino groups are protonated which could interfere with their interaction with an enzyme active site<sup>16</sup>. However, if biotransformation conditions are pushed beyond pH 10, this could lead to the enzyme becoming deactivated<sup>17</sup>. In light of this, pH 9 was chosen for this study and testing was carried out at 3 h, and 24 h to monitor the progress of the biocatalytic reaction. Biotransformations were carried out in 100% H<sub>2</sub>O (163  $\mu$ L) in an attempt to give the most accurate results possible as determined through the solvent study. The water was adjusted to pH 9 with NaOH and racemic 3-aminobutyronitrile from a stock solution made in H<sub>2</sub>O at pH 9 (10 mM, 10  $\mu$ l, 0.00017 g) was added. Nit1 (27  $\mu$ L) was added to all the biotransformations. Biological replicates were completed for all the samples. The mixtures were incubated at 25°C with mechanical shaking (200 rpm) for 24 h and worked up and analysed as previously. HPLC analysis which was conducted in duplicate utilising the gradient method. Yields were calculated based on standard curves as shown previously. It was thought that any increase in effect of pH on the enzyme should see improvement at the 3h timepoint.

**Table 5.7: Biotransformation of Nit1 with 3-ABN at pH 9 in 100% H<sub>2</sub>O for 24 h**

Entry	Time/ h	Nitrile yield/ %	Acid yield/ %	Acid ee/ %
1	3	54	60	22 ( <i>S</i> )
2	24	25	104	7 ( <i>S</i> )

For the first time, acid was detected from the 3 h time point as predicted with an ee of 22% of (*S*) isomer indicating a more rapid reaction, as shown in Table 5.7. The mass balance from the biocatalytic studies clearly indicate issues with the method of quantitation. A general trend could however be observed of decreasing nitrile as acid production increases along with a kinetic effect of decreasing ee as nitrile is consumed.

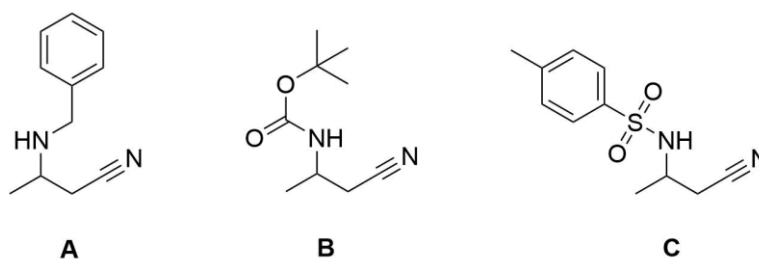
In summary, despite analytical problems for quantitation, it was clear from this work that the ee for reaction of Nit1 with 3-ABN was not viable from an industrial perspective. The enzyme did not demonstrate the same selectivity for the aminonitrile as obtained with mandelonitrile. These studies did however indicate that the enzyme was able to hydrolyse the nitrile to some extent, yielding an ee of 22% (*S*) at the optimum conditions of pH 9 and 100% H<sub>2</sub>O. These

studies also highlighted problems within the HPLC analysis, some of which still need to be addressed and led to some data being inconclusive.

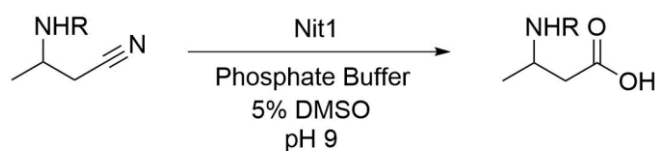
As the reaction of Nit1 with the unprotected nitrile did not generate enantioenriched acid product to the level necessary in its current state, it is not favourable for direct use. Given that the enzyme can turn the unprotected nitrile over to some extent it may be possible to improve this with rational design and directed evolution.

#### 5.4 Screening of *N*-protected nitriles

After having observed some positive results with the 3-ABN (**124**), the next stage was to evaluate the activity of Nit1 against the *N*-protected aliphatic nitriles as shown in Scheme 5.5. The same *N*-protected nitriles evaluated with SET1 were used in this study and are shown in Figure 5.17. There was insufficient time at this point in the project to produce the appropriate standard curves for the protected nitriles in order to allow for quantitation. The results in this study are of an initial screen thus reported in terms of peak areas and ee's only.



**Figure 5.17:** The *N*-protected nitriles screened against Nit1. A – 3-(benzylamino)butyronitrile, B – 2-methyl-2-propanyl(1-cyano-2-propanyl)carbamate, C – *N*-(1-cyano-2-propanyl)-4-methylbenzenesulfonamide



R = Bn, Boc, or Ts

**Scheme 5.5:** Biotransformation scheme of Nit1 against the *N*-protected aminonitriles

Biotransformations were carried out in phosphate buffer (0.1 M, 168 μL) at pH 9. Previous studies with these substrates and SET1 showed minimal activity at pH 7. Nit1 has been shown to tolerate pH 9 and so it was anticipated that the results for these substrates would be better at

pH 9 and so, in order to conserve enzyme, the initial screen was carried out at pH 9. Racemic 3-(benzylamino)butyronitrile, 2-methyl-2-propanyl(1-cyano-2-propanyl)carbamate, and *N*-(1-cyano-2-propanyl)-4-methylbenzenesulfonamide were added from a stock solution prepared in DMSO (10 mM, 10  $\mu$ l) to give a final composition of 5% DMSO to aid in solubility of the substrate. Nit1 (22  $\mu$ L) was then added to all the biotransformations. Biological replicates were put on for all the samples. The mixtures were incubated at 25°C for 24 h. The reactions were quenched by the addition of acetonitrile (600  $\mu$ L) and the mixtures were centrifuged to remove the biomass. In the case of the benzyl biotransformations, the supernatants were lyophilised for at least 24 h and treated with GITC for HPLC analysis which was conducted in duplicate. For the boc and tosyl protected biotransformations, the supernatants underwent an acid/base workup after which HPLC analysis was carried out in duplicate.

Disappointingly, acid product was only detected for the *N*-benzyl protected substrate albeit with an average ee of only 2% (*S*). The nitrile in this case was not recovered from the biocatalytic system. A summary of the screening results can be seen in Table 5.8.

**Table 5.8: Biotransformation results of initial screen of Nit1 with *N*-protected substrates carried out at pH 9 with 5% DMSO for 24 h. ND = not detected**

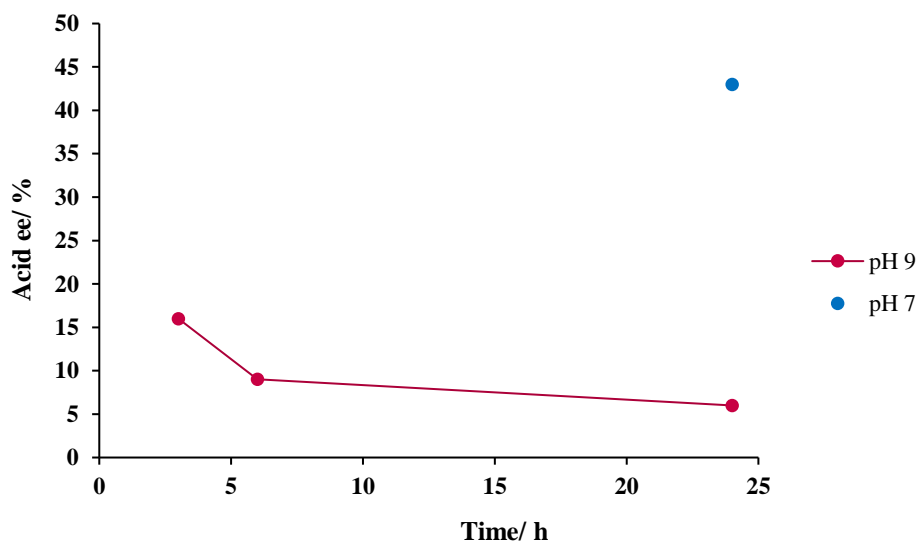
Entry	Protecting group	Nitrile peaks area	Acid peaks area	Acid ee/ %
1	<i>N</i> -Bn	ND	69.6	2 ( <i>S</i> )
2	<i>N</i> -Boc	293.5	ND	ND
3	<i>N</i> -Ts	1508.6	ND	ND

These results echo the findings of the research studies of others in which the *N*-boc and *N*-tosyl group gave poor results<sup>16,18,19</sup>. These protecting groups may prove to be too large for the active site of Nit1 and once again, the *N*-boc and *N*-tosyl substrates showed poor solubility, even with 5% DMSO present. It is, however, difficult to conclusively comment on the active site as there is little information available as few nitrilase structures have been elucidated. One attempt at structure elucidation of a nitrilase was made by Thuku *et al* who analysed the nitrilase from *Rhodococcus rhodochrous* J1 and were able to offer insight into the helical and oligomeric structure of the nitrilase<sup>20</sup>. In our case, our nitrilase is His-tagged at the end (C-terminal) on every subunit and this may interfere with substrate access, but it does allow however, for it be purified away from the cell. It is therefore only speculations that can be made in predicting substrate docking without carrying out specific studies. An example of such a specific study is

from the work of Yeom *et al* who successfully identified the amino acid 142, which determines substrate specificity, in a nitrilase from *Rhodococcus rhodochrous* ATCC 33 278<sup>21</sup>. They used metagenesis to change the nitrilase and observed the substrate changes. They completed molecular docking studies which allowed them to show the different substrates docked. This type of study could potentially be carried out on Nit1 in future.

It is also possible that the other substrates simply required more time to observe results as well as looking at different pH's and this can be investigated in future studies. Based on the 24 h results, a time study was thus carried out with the *N*-benzyl protected nitrile at both pH 7 and 9 for 24 h to investigate the Nit1 profile in the production of the acid. Testing was done at 0 h, 1 h, 3 h, 6 h, and 24 h. Biotransformations were carried out in phosphate buffer (0.1 M, 168  $\mu$ L) at pH 7 and 9 as previously with biological replicates. The supernatants were lyophilised for at least 24 h and treated with GITC for HPLC analysis which was conducted in duplicate.

For reactions completed at pH 9, acid was first detected at the 3 h time point with an average ee of 16% (*S*). The ee steadily declined over time to 9% (*S*) at 6 h, then 4% (*S*) at the 24 h end point, which can be seen in Figure 5.18. At pH 7 however, no acid was detected until the 24 h time point but it was observed in an appreciable ee of 43% (*S*).



**Figure 5.18 :** Graph tracking acid ee of the biotransformation of Nit1 with Bn-ABN at pH 7 and 9. Analysis carried out on a C18 column. Mobile phase MeOH:H<sub>2</sub>O + 0.1% TFA, at a flow rate of 1 mL.min<sup>-1</sup>

In Table 5.9, a comparison is shown of these results versus some the observations with 3-aminobutyronitrile in order to better judge the results seen by the addition of the *N*-benzyl

group. It would appear that directly comparing the performance of the two substrates at pH 7 with 5% DMSO over 24 h, Nit1 was more selective with the *N*-benzyl group present. At the higher pH however, it would appear that the unprotected nitrile performed slightly better than with the protecting group.

**Table 5.9:** Biotransformations were carried out by incubating the nitrile (10 mM) in a suspension of Nit1 in a total volume of 200  $\mu$ L at 25°C over 24 h. Analysed as GITC derivatives by HPLC

Substrate	pH	Solvent	ee (%)
3-ABN	7	100% phosphate buffer	22 ( <i>S</i> )
3-ABN	7	5% DMSO	23 ( <i>S</i> )
3-ABN	9	100% H <sub>2</sub> O	7 ( <i>S</i> )
Bn-ABN	7	5% DMSO	43 ( <i>S</i> )
Bn-ABN	9	5% DMSO	4 ( <i>S</i> )

## 5.5 Summary

Nit1 was found to be active against the unprotected 3-ABN and showed better overall selectivity in comparison to SET1 with the same substrate. There is still room to develop this reaction further, in particular since the effect of solvents on the HPLC was not completely resolved to allow for satisfactory reproducibility between reactions. Nit1 was unable to hydrolyse the boc and tosyl *N*-protected nitriles in the given time at pH 9. A longer reaction time may yield some results, but it is unlikely to give high yields and ee. The biotransformation with the *N*-benzyl protected nitrile at pH 7 gave the best selectivity observed at the 24 h time point instead of at pH 9 as expected. This is consistent with what is known at this point about Nit1, in that the best activity is observed under pH 7 conditions and by pH 9, the enzyme activity would have dropped considerably. The addition of the *N*-benzyl did give rise to greater selectivity which could allude to a docking strategy which enhances the chiral recognition of the enzyme as suggested by Wang *et al*<sup>9,22</sup>. In their work, they observed an appreciable increase in enantioselectivity but over a longer period of time. Further studies will need to be done to see if the yields are indeed better also with the *N*-benzyl group which would allow for the realisation of  $\beta$ -amino acids to be made with this promising enzyme.

## REFERENCES

1. Coffey, Lee. V. *et al.* Isolation of Identical Nitrilase Genes From Multiple Bacterial Strains and Real-time PCR Detection of the Genes From Soils Provides Evidence of Horizontal Gene Transfer. *Archives of Microbiology*, 2009, **191**, (10), 761-771
2. Dooley-Cullinane, Tríona. Marie. *The Identification of Genes and Enzymes in the Aldoxime-nitrile Metabolising Pathway*, PhD thesis, Waterford Institute of Technology, (2019).
3. Snell, David. & Colby, John. *Enantioselective Hydrolysis of Racemic Ibuprofen Amide to S-(+)-Ibuprofen by Rhodococcus AJ270*. *Enzyme and Microbial Technology*, 1999, **24**, (3-4), 160-163
4. Bzura, Justyna. & Koncki, Robert. *A Mechanized Urease Activity Assay*. *Enzyme and Microbial Technology*, 2019, **123**, 1-7
5. Mitsukura, Koichi. *et al.* Asymmetric Synthesis of Chiral Amine From Cyclic Imine by Bacterial Whole-cell Catalyst of Enantioselective Imine Reductase. *Organic & Biomolecular Chemistry*, 2010, **8**, (20), 4533-4535
6. Nguyen, Ngoc-Van. Thi. *et al.* Development of a UPLC Method with Chiral Derivatization for the Determination of Atenolol and Metoprolol Enantiomers in Tablet Preparations. *Pharmaceutical Sciences Asia*, 2018, **45**, (2), 66-76
7. Tang, Yi-Hong. *et al.* Stereoselective RP-HPLC Determination of Esmolol Enantiomers in Human Plasma After Pre-column Derivatization. *Journal of Biochemical and Biophysical Methods*, 2004, **59**, (2), 159-166
8. Wiest, Donald. *Esmolol: A Review of its Therapeutic Efficacy and Pharmacokinetic Characteristics*. *Clinical Pharmacokinetics*, 1995, **28**, (3), 190-202
9. Ma, Da-You. *et al.* Nitrile Biotransformations for the Synthesis of Highly Enantioenriched  $\beta$ -Hydroxy and  $\beta$ -Amino Acid and Amide Derivatives. *Journal of Organic Chemistry*, 2008, **73**, (11), 4087-4091
10. Bhalla, Tek Chand. *et al.* Asymmetric Hydrolysis of  $\alpha$ -aminonitriles to Optically Active Amino Acids by a Nitrilase of *Rhodococcus rhodochrous* PA-34. *Applied Microbiology and Biotechnology*, 1992, **37**, 184-190
11. Effenberger, Franz. & Böhme, Joachim. *Enzyme-catalysed Enantioselective Hydrolysis of Racemic Naproxen Nitrile*. *Biorganic & Medicinal Chemistry*, 1994, **2**, (7), 715-721
12. Lévy-Schil, Sophie. *et al.* Aliphatic Nitrilase From a Soil-isolated *Comamonas testosteroni* sp.: Gene Cloning and Overexpression Purification and Primary Structure. *Gene*, 1995, **161**, (1), 15-20

13. Effenberger, Franz. & Graef, Bernd. Walter. *Chemo- and Enantioselective Hydrolysis of Nitriles and Acid Amides, Respectively, with Resting Cells of Rhodococcus sp. C3II and Rhodococcus erythropolis MP50*. Journal of Biotechnology, 1998, **60**, (3), 165-174
14. Gong, Jin-Song. *et al. Nitrilases in Nitrile Biocatalysis: Recent Progress and Forthcoming Research*. Microbial Cell Factories, 2012, **11**, (142), 1-18
15. Shen, Mei. *et al. Isolation and Characterization of a Novel Arthrobacter nitroguajacolicus ZJUTB06-99, Capable of Converting Acrylonitrile to Acrylic Acid*. Process Biochemistry, 2009, **44**, (7), 781-785
16. Chhiba, Varsha. *et al. Enantioselective Biocatalytic Hydrolysis of  $\beta$ -aminonitriles to  $\beta$ -Amino-amides Using Rhodococcus rhodochrous ATCC BAA-870*. Journal of Molecular Catalysis B: Enzymatic, 2012, **76**, 68-74
17. Martínková, Ludmila. *et al. Biodegradation Potential of the Genus Rhodococcus*. Environment International, 2009, **35**, (1), 162-177
18. Preiml, Margit. *et al. A New Approach to  $\beta$ -amino Acids: Biotransformation of N-protected  $\beta$ -amino Nitriles*. Tetrahedron Letters, 2003, **44**, (27), 5057-5059
19. Winkler, Margit. *et al. Synthesis and Microbial Transformation of  $\beta$ -amino Nitriles*. Tetrahedron, 2005, **61**, (17), 4249-4260
20. Thuku, Robert. N. *The Structure of the Nitrilase from Rhodococcus Rhodochrous JI: Homology Modeling and Three-dimensional Reconstruction*, MSc thesis, University of the Western Cape, (2006).
21. Yeom, Soo-Jin. *et al. An Amino Acid at Position 142 in Nitrilase from Rhodococcus rhodochrous ATCC 33278 Determines the Substrate Specificity for Aliphatic and Aromatic Nitriles*. Biochemical Journal, 2008, **415**, (3), 401-407
22. Coady, Tracey. M. *et al. Substrate Evaluation of Rhodococcus erythropolis SET1, a Nitrile Hydrolysing Bacterium, Demonstrating Dual Activity Strongly Dependent on Nitrile Sub-Structure*. European Journal of Organic Chemistry, 2015, **2015**, (5), 1108-1116

## **CHAPTER 6**

### **CONCLUSIONS & FUTURE WORK**



## CONCLUSIONS & FUTURE WORK

### 6.1. Conclusions

A series of model  $\beta$ -aminonitriles, structurally related to the  $\beta$ -hydroxynitriles previously studied were successfully synthesised. The  $\beta$ -aminonitrile, 3-aminobutyronitrile (**124**) unfortunately had to be purchased as it proved difficult to synthesise. The corresponding amide and acid standards for the nitriles were also successfully synthesised. Additionally, extensive work was carried out to develop analytical methods to assess yield and enantioselectivity of the reactions. In some cases, this required derivatisation of the standards to either assist in recovery from the reaction, to add a chromophore for detection, or to enable separation on the available HPLC columns.

Bacterial isolate SET1 had shown excellent activity at hydrolysing aliphatic  $\beta$ -hydroxy nitriles in the work of Coady *et al*, the best results being with 3-hydroxybutyronitrile (3-HBN) (**131**) (>99% (*S*) ee) and was thus anticipated to exhibit a similar response to aliphatic  $\beta$ -amino nitriles<sup>1</sup>. Initial work however, on the unprotected aliphatic  $\beta$ -amino nitrile, 3-aminobutyronitrile (**124**) (an analogue of 3-HBN (**131**)), were disappointing. The acid yields were extremely low, with the highest being <1% at pH 7. The ee results again were low, with the highest ee being 29% at pH 7 and this rapidly decreased as pH increased as by pH 9 the ee was 5%. This loss in ee as pH increased was expected and observed from prior work with Coady *et al* where the effect of pH on isolate SET1 was investigated. It was found that activity decreased to 76% at pH 11 however enantioselectivity swiftly decreased to 66% at only pH 9<sup>2</sup>. This presented a limitation as the  $\beta$ -amino nitrile substrates, particularly the unprotected nitriles required for this work, perform better at higher pH's as there they exist in an unprotonated form. This is important as protonation would appear to interfere with the active site of most enzymes giving rise to poor results, as discussed in Chapter 1 from the observations of Chhiba *et al*<sup>3</sup>.

Isolate SET1 was screened with *N*-protected nitriles at pH 7. It was observed that the addition of a protecting group in general, increased the activity of SET1 towards the  $\beta$ -amino nitriles. Yield and ee for the acid products generally increased, with the best overall result being observed for the benzyl *N*-protected derivative which gave an acid yield of 6% and a

dramatically improved ee of 75%. Amide was also detected for the first time with the benzyl and tosyl *N*-protected derivatives, in 3% and 9% yield and 90% and 1% ee respectively.

Screening was then carried out on five bacterial isolates from the PMBRC bank to identify possible other isolates to work with on the  $\beta$ -amino nitriles which could tolerate pH 9. They were screened on 3-aminobutyronitrile (**124**) and 3-phenyl-3-propionitrile (**122**) at pH 7 and 9. The best results were seen from bacterial isolates 6 and 39. Both isolates 6 and 39 gave excellent ee's of 99% (*R*) at pH 9 and ee's of 89% (*R*) and 87% (*R*) respectively at pH 7. No activity was observed for either isolate against the aromatic substrates. Further studies with isolate 39 on 3-ABN (**124**) were pursued however, whilst the ee remained high at >99% (*R*), yields remained consistently low, with a maximum of 15% at pH 9.

Contamination was unfortunately discovered with isolates 6 and 39, and although much work was put into their purification, this was not achieved to a sufficient degree in time, as the original activity observed could not be duplicated. This placed on hold further work with these isolates.

Whilst the work with SET1, and isolates 6 and 39, highlighted some potential for the use of whole cells for the transformation of  $\beta$ -aminonitriles to  $\beta$ -amino acids, it also highlighted some of the challenges i.e., contamination, product isolation, and cell metabolism. The results supported the search for a purified enzyme which could hydrolyse  $\beta$ -amino nitriles under the required conditions. A novel nitrilase enzyme Nit1, was acquired from the PMBRC isolate bank. Nit1 showed improved results with 3-ABN (**124**) from the initial screen with 76% yield and 24% (*S*) ee being observed. It also tolerated pH 9 marginally better in comparison to SET1, giving an ee of 7% (*S*). As for the *N*-protected variants, it only showed activity with the benzyl aliphatic nitrile. It encouragingly achieved ee's of 43% (*S*) at pH 7 and 4% (*S*) at pH 9 for this substrate. Some issues were experienced however with the presence of solvent and buffer from the biotransformations possibly interfering with the HPLC results. Numerous attempts were made to troubleshoot this, and extensive method development was carried out. This alleviated some of the issues, but further work remains with this.

## 6.2. Future Work

Possible future work arising from the results described in Chapters 2 and 3 is that the workup of 3-aminobutyronitrile (**124**), could be revisited by investigating the use of a different protecting group to allow for complete extraction and HPLC analysis. Alternatives to Cbz are Fmoc (9-fluoromethoxycarbonyl) or Boc. The Boc group would be less likely as an HPLC method could not be developed to separate the nitrile with the available columns, making Fmoc the more likely choice. The Fmoc group has already been reported as a possible derivatisation method for amino acids and amines<sup>4,5</sup>. Similar to Cbz, Fmoc-OSu should be investigated preferentially over Fmoc-Cl for safety reasons.

While the cells and enzymes of the WIT bank are being licensed to a company for commercial purposes post-PhD projects, the following suggested future work summarises logical next steps, be they completed in academic or private company settings.

A section of future work based on the findings in Chapter 3 would be further investigations with bacterial isolate 39. The focus would particularly be on screening it against the *N*-protected amino nitriles initially on a small scale. The aliphatic *N*-protected amino nitriles will be assessed first, followed by the aromatic analogues. The enzyme activity can be monitored over time by HPLC to establish the optimum reaction times for hydrolysis to occur. Viable biotransformations resulting from this will be scaled up and tested for effects in variations of temperature and pH. Induction of the enzyme activity in the whole cells could also be investigated by growing the cells in the target substrate first before washing cells for activity assays.

Further future work could include investigations with a substrate fed-batch approach in order to increase yields. This is where a determined amount of substrate is fed into the reaction at periodic intervals over the course of the biotransformation. An example of this on a nitrilase was with the work of Fan *et al* using the aliphatic nitrilase REH16<sup>6</sup>. The substrate 3-cyanopyridine was successfully completely hydrolysed over eight feedings to give nicotinic acid. The reaction of isolate 39 with 3-aminobutyronitrile can be investigated applying this approach, along with other studies, such as temperature and pH. The temperature studies will look to propagate an activity graph over a range of 10°C up to 70°C. The pH studies will assess activity over the range of pH 2 to 10 with three different buffers, which will be carried out at the optimum temperature determined from the temperature studies. The cells will also be grown

in medium and assayed for ee, as well as then sub-culturing to the same medium for a mid-log phase or faster conversion. This will be carried out with and without inhibitors and solvent tolerance will also be analysed.

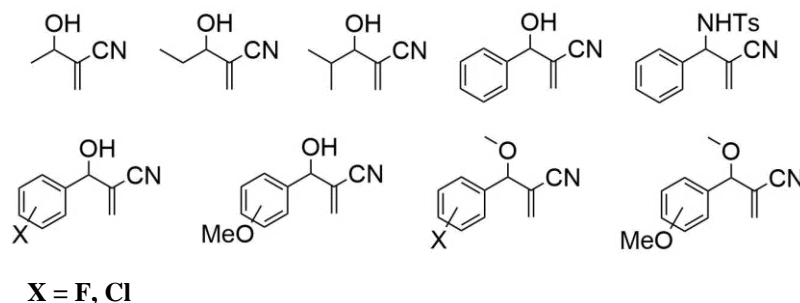
In order to carry out further work with isolate 39 however, the purification of isolates 6 and 39 will need to be completed, as highlighted from Chapter 4. Seeing as the purified stocks acquired did not exhibit the same activity as observed initially, it may be necessary to utilise stocks from earlier in the purification process and attempt to purify from that point once again, being diligent to test for activity with each re-streak to determine where activity is either gained or lost.

In terms of microbiology, the isolates have undergone gene screening with no nitrilase genes sequenced that are responsible for the activities. They have all shown partial NHase and/or potential nitrilase gene products, but these were not fully sequenced and cloned and then enzyme performance tested. This would have taken a considerable amount of time with the possibility that no enzyme could have turned out to be exceptional. Genome sequencing of the key isolates should thus be carried out to obtain the full sequences. These could then be searched for the partial nitrilase and gene sequences identified by Bragança *et al*<sup>7</sup>. These genes should then be cloned and expressed. These enzymes should then be performance tested to characterise them, and to see if they are responsible for the same activities seen in our work. Activity assays on cell-free-extracts from the isolates can also be carried out to see if removed cellular debris affects nitrile and acid recovery, as well as pH issues when working with whole cells. Purified enzyme from these isolates would also allow enzyme kinetics and definitive screening against our substrates without possible cellular interference.

Possible future work arising from the results described in Chapter 5 is further solvent studies and HPLC method development to attempt to eliminate the inflation of HPLC data and give a more accurate representation. The GITC derivatisation procedure can also be re-assessed for optimisation of the amounts of triethylamine required, as well as the temperature and reaction time. The effect of the lyophilisation process could also be investigated on if there are considerable losses being experienced at this point, thus affecting yields observed.

Another future study could include investigations of Nit1 against the  $\beta$ -aromatic nitriles to assess if any activity could be observed. Some of the other substrates on which Nit1 can be screened against are shown in Scheme 6.1. These are found in the work of Coady *et al* and

several of the most appropriate could be selected and adapted<sup>8</sup>. These include  $\beta$ -hydroxy nitriles and  $\alpha$ -methylene- $\beta$ -hydroxy nitriles.



**Scheme 6.1. Possible choice of substrates for investigation with a purified enzyme as the hydroxy and amino analogues**

It is preferable to investigate  $\alpha$ -methylene- $\beta$ -amino nitriles as substrates as well, as they offer a large degree of functionality and little work has been conducted with *N*-protected derivatives. In the work of Coady *et al*, interesting results were observed for  $\alpha$ -methylene- $\beta$ -hydroxy nitriles<sup>2</sup>. In comparison to 3-hydroxy-3-phenylpropionitrile, the  $\alpha$ -methylene- $\beta$ -hydroxy nitriles also formed amide in addition to the acid and increased yields and ee were observed. It is anticipated that similar results may be observed for the  $\alpha$ -methylene- $\beta$ -amino nitriles.

For the microbiology, future work could include the study of enzyme kinetics on the range of our unique substrates, this could also be then retested alongside solvent and metal tolerance testing. This ensures that the true enzyme performance by the minute and activity per ml is acquired rather than a total amount of product after a set period of time.

Another section of future work, which would be a major undertaking would be to further analyse the enzyme native structure via crystallography, as nitrilase structures have been very hard to elucidate. Subunit formation issues were noted in the work of Dooley-Cullinane *et al* i.e. some gels were observed with a ladder of Nit1 bands of differing sizes, therefore, what could be attempted is to separate the individual subunit protein bands from each other using size exclusion chromatography, then measuring the amount of purified enzyme in each band and testing enzyme kinetics against each one<sup>9</sup>. This study would be of use as there is a possibility that not all subunits in a purified enzyme batch were active, giving us lower activity than we potentially could have measured.

Finally, if the Nit1 gene were to undergo directed evolution (random mutagenesis) to improve enzyme characteristics in other projects, a testing strategy could be developed for screening

hundreds or even thousands of mutants for enhanced activity. This could be activity at more extreme pHs, better ee, and activity now being observed on our synthesised protected substrates. This would also allow for the amino acids in the enzyme, that are essential for activity, to be identified, as well as generation and identification of an enhanced enzyme. Such identified amino acids could become targets for site directed mutagenesis studies, after which studies on the potential effects on activity, enantioselectivity, temperature, solvent tolerance, thermal stability, substrate range/docking or pH can be analysed. The work of Liu *et al* on screening and improving recombinant nitrilases offers a strategy which could be adapted for our future work<sup>10</sup>. It would involve site directed mutagenesis of the nitrilase, performance testing, followed by homology modelling and docking using software, all with a focus on a particular substrate.

## REFERENCES

1. Coady, Tracey. M. *et al.* *A High Throughput Screening Strategy for the Assessment of Nitrile-hydrolyzing Activity Towards the Production of Enantiopure  $\beta$ -hydroxy Acids.* Journal of Molecular Catalysis B: Enzymatic, 2013, **97**, 150-155
2. Coady, Tracey. M. *Biotransformations Using Nitrile Hydrolysing Enzymes for Stereoselective Organic Synthesis*, Doctor of Philosophy thesis, Waterford Institute of Technology, (2014).
3. Chhiba, Varsha. *et al.* *Enantioselective Biocatalytic Hydrolysis of  $\beta$ -aminonitriles to  $\beta$ -Amino-amides Using *Rhodococcus rhodochrous* ATCC BAA-870.* Journal of Molecular Catalysis B: Enzymatic, 2012, **76**, 68-74
4. Gawande, Manoj. B. & Branco, Paula. S. *An Efficient and Expeditious Fmoc Protection of Amines and Amino Acids in Aqueous Media.* Green Chemistry, 2011, **13**, (12)
5. Teleha, Christopher. *et al.* *Preparation of  $\alpha$ -Hydroxy- $\beta$ -Fmoc Amino Acids from N-Boc Amino Acids.* Synthesis, 2011, **2011**, (24), 4023-4026
6. Fan, Haiyang. *et al.* *A Novel Nitrilase from *Ralstonia eutropha* H16 and its Application to Nicotinic Acid Production.* Bioprocess and Biosystems Engineering, 2017, **40**, (8), 1271-1281

7. Bragança, Caio. Roberto. Soares. *Development of Recombinant Enzymes Towards the Production of Pharmaceutical Intermediates Using Biotransformations*, Doctor of Philosophy thesis, Waterford Institute of Technology, (2020).
8. Coady, Tracey. M. *et al.* *Substrate Evaluation of Rhodococcus erythropolis SET1, a Nitrile Hydrolysing Bacterium, Demonstrating Dual Activity Strongly Dependent on Nitrile Sub-Structure*. *European Journal of Organic Chemistry*, 2015, **2015**, (5), 1108-1116
9. Dooley-Cullinane, Tríona. Marie. *The Identification of Genes and Enzymes in the Aldoxime-nitrile Metabolising Pathway*, PhD thesis, Waterford Institute of Technology, (2019).
10. Liu, Zhi-Qiang. *et al.* *Screening and Improving the Recombinant Nitrilases and Application in Biotransformation of Iminodiacetonitrile to Iminodiacetic Acid*. *PLoS ONE*, 2013, **8**, (6), e67197

## **CHAPTER 7**

### **EXPERIMENTAL**



## EXPERIMENTAL

### 7.1 General Experimental Conditions

All commercial chemicals were obtained from Enamine, Sigma, and TCI and were used as received unless otherwise stated. Nuclear Magnetic Resonance Spectroscopy (NMR) spectra were recorded on a Jeol ECX-400 spectrometer operating at 400 MHz, using deuteriochloroform as the solvent unless otherwise stated. The following abbreviations (and combinations thereof) have been used to describe signal multiplicity: b – broad, s – singlet, d – doublet, t – triplet, q – quartet, m – multiplet.

Infra-red spectra were recorded on a Shimadzu FTIR-8400s, melting points were determined using a Stuart Scientific melting point apparatus smp3 and were uncorrected. Compounds were weighed on out on an Explorer OHAUS analytical balance. GC-MS analysis was carried out on a Varian Saturn 2000 GC/MS/MS and optical rotations were measured on an AA series polar 20 automatic polarimeter. LC-MS analysis was carried out on an Agilent Technologies LC-MSD Trap XCT Ultra, ESI 6300 Series Trap. Mobile phase was ACN:H<sub>2</sub>O both with 0.1% formic acid, run in gradient mode at 500  $\mu\text{L min}^{-1}$  at 25°C.

Thin layer chromatography (TLC) was performed using silica coated aluminium plates (60 F<sub>254nm</sub>) supplied by Merck. They were visualised using ultra-violet radiation or developed in potassium permanganate solution and vanillin. Flash column chromatography was performed using flash silica (40-63  $\mu\text{m}$ ) supplied by VWR. Cation exchange chromatography was performed using Ion Exchange Amberlite® IR-120, (0.3-1.2 mm) supplied by Merck.

Preparative TLC was carried out on glass plates pre-coated with (60 GF<sub>254nm</sub>) supplied by Apex Scientific.

Preparative HPLC was performed using a semi-preparative Varian with a C18 Phenomenex Jupiter column, 10  $\mu\text{m}$ . Mobile phase was ACN:H<sub>2</sub>O both with 0.1% trifluoroacetic acid, run in gradient mode at 5  $\text{mL min}^{-1}$ .

The organic layers were continuously dried over anhydrous magnesium sulphate or sodium sulphate, and they were concentrated by rotary evaporation. The last traces of solvent were removed on a high vacuum pump. Solvents were purchased pre-dried where required.

Chiral HPLC was conducted on a HP 1050 or HP 1100 HPLC using a chiral column (Daicel Chiralpak AD-H, IA, or OJ-H). Reverse phase HPLC was conducted on a HP 1100 HPLC using a C18 column (Waters Symmetry). Samples for the reverse phase HPLC were firstly frozen with liquid nitrogen or overnight in a -20°C freezer in an Eppendorf or centrifuge tube. The opening of the tubes were then covered in tissue and the samples placed in the freeze dryer to allow lyophilisation to occur in preparation for derivatisation prior to analysis. Samples were lyophilised in a Labconco FreeZone, 2.5L, at -51°C and 0 mBar.

## 7.2 Screening of Bacterial Isolates

The bacterial isolates used for this study are SET1, described by Coady *et al*, Isolate 6 and Isolate 39, described by Bragança *et al*, and Nit1, described by Dooley-Cullinane *et al*, from the PMBRC library of isolates<sup>1-3</sup>. These isolates were previously identified as nitrile metabolisers with enantioselectivity displayed towards certain  $\beta$ -hydroxynitriles. All cultures were maintained as glycerol stocks and stored at -70°C.

## 7.3 Media and Buffer Preparation

### 7.3.1 M9-Minimal media preparation

5X M-9 Basis Preparation: Sodium phosphate dibasic dodecahydrate (86 g, 240 mM, >98% purity), potassium dihydrogen ortho-phosphate (15 g, 110 mM, >95% purity), and sodium chloride (2.5 g, 43 mM, >95% purity) were dissolved in 1000 mL deionised water. The white suspension was stirred at room temperature until fully dissolved and autoclaved at 121°C for 15 min.

Calcium chloride dihydrate (0.1 M) preparation: Calcium chloride dihydrate (1.5 g, 10 mmol, >95% purity) was dissolved in deionised water and the solution was made up to 100 mL with deionised water and autoclaved at 121°C for 15 min.

Glucose 20% (w/v) preparation: Glucose (20 g) was dissolved in deionised water and the solution made up to 100 mL with deionised water and autoclaved at 121°C for 15 min.

Iron (II) sulphate heptahydrate preparation: Iron (II) sulphate heptahydrate (0.14 g, 0.50 mmol) was dissolved in deionised water and the solution made up to 100 mL with deionised water and filtered with a sterile syringe and 0.22 µm filter disc into sterile Eppendorf tubes.

Magnesium sulphate heptahydrate preparation: Magnesium sulphate heptahydrate (25g 0.10 mol, >99% purity) was dissolved in deionised water and the solution made up to 100 mL with deionised water and autoclaved at 121°C for 15 min.

Trace elements preparation: Zinc sulphate heptahydrate (29 mg, 0.1 mmol, >99% purity), manganese chloride tetrahydrate (198 mg, 1.0 mmol, >99% purity), cobalt chloride hexahydrate (129 mg, 1.0 mmol, >98% purity), copper chloride dihydrate (17 mg, 0.1 mmol, >95% purity), and calcium chloride dihydrate (147 mg, 1.0 mmol) were dissolved in deionised water and the solution made up to 100 mL with deionised water. The solution was autoclaved at 121°C for 15 min.

To 5X M-9 basis (20 mL) was added calcium chloride dihydrate (100 µL), glucose (2 mL), iron (II) sulphate heptahydrate (100 µL), magnesium sulphate heptahydrate (100 µL), and trace elements solution (100 µL). The volume was made up to 100 mL with sterile deionised water in a sterile container.

### 7.3.2 Potassium phosphate buffer preparation

Potassium dihydrogen phosphate (5.3 g, 39 mmol) and di-Potassium hydrogen phosphate (11 g, 61 mmol) were dissolved in deionised water and the solution made up to 1000 mL with deionised water. If necessary, the pH was adjusted to the required set point using NaOH (2M). The solution was autoclaved at 121°C for 15 min.

## 7.4 Optical Density of Isolates

The optical density of all cell cultures was measured using the NanoDrop® spectrophotometer ND1000 at 600 nm. The volume needed to produce a final optical density in the biotransformation of 1 ( $OD_{600nm} = 1$ ), and in some cases,  $OD_{600nm} = 5$ , was calculated using the formula below:

$$C_1V_1 = C_2V_2$$

$C_1$  = optical density measured

$C_2$  = target optical density for biotransformation

$V_1$  = volume of suspended cells to add

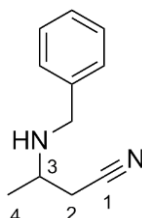
$V_2$  = total volume of biotransformation

## 7.5 Induction of Cells

Cells were inoculated into M9 minimal media containing racemic 3-hydroxybutyronitrile (10 mM, 97% purity) at a final cell density of  $OD_{600nm} = 1$ . The culture was incubated at 25°C for 3 days with mechanical shaking (200 rpm). The cells were pelleted and stored as glycerol stocks with M9-minimal media (with final glycerol concentration at 30%) ready for subsequent work.

## 7.6 Preparation of Nitriles

### 3-(benzylamino)butyronitrile (**125**)<sup>4</sup>

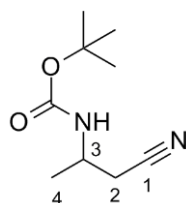


Crotonitrile (1.65 g, 2 mL, 24.6 mmol), benzylamine (2.67 g, 2.7 mL, 24.9 mmol), and ethanol (50 mL) were heated to reflux for 24 h. The solvent was removed *in vacuo*. The product was purified by silica flash chromatography (Hex:EtOAc 60:40) to give the title compound as a colourless oil (2.43 g, 13.9 mmol, 57%).

<sup>1</sup>H NMR (400 MHz, CDCl<sub>3</sub>),  $\delta$  7.38 – 7.24 (m, 5H, Ar-H), 3.82 (d,  $J = 1.4$  Hz, 2H, Ar-CH<sub>2</sub>), 3.09 – 3.04 (m, 1H, CH), 2.41 – 2.51 (m, 2H, CH<sub>2</sub>), 1.43 (s, 1H, NH), 1.26 (s, 3H, CH<sub>3</sub>) (lit.<sup>4</sup>)

<sup>13</sup>C NMR (100 MHz, CDCl<sub>3</sub>),  $\delta$  139.8 (C-Ar), 128.7 (C-Ar), 128.1 (C-Ar), 127.4 (C-Ar), 118.2 (CN), 51.2 (CH<sub>2</sub>-Ar), 49.4 (C-3), 25.1 (C-2), 20.7 (C-4) (lit.<sup>4</sup>)

ESI-MS, low res,  $m/z$  196.5 (M+Na<sup>+</sup>), 174.6 (M+H<sup>+</sup>), C<sub>11</sub>H<sub>14</sub>N<sub>2</sub>

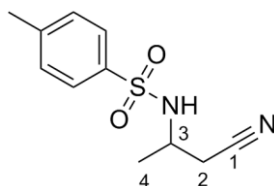
**2-methyl-2-propanyl(1-cyano-2-propanyl)carbamate (126)<sup>5</sup>**

Solid 3-aminobutanenitrile hydrochloride (0.150 g, 1.24 mmol, 95% purity) was added to a solution of dioxane (2.5 mL), water (1.2 mL), and NaOH (1M, 2 mL). Di-*tert*-butyl dicarbonate (0.298 g, 1.36 mmol) was then added at 0°C. The reaction was stirred at room temperature for 6h. Half the solvent was removed *in vacuo* and EtOAc (10 mL) was added. The aqueous layer was acidified to pH 4. This was then extracted with EtOAc (4 x 10 mL). The combined organic extracts were washed with brine, dried over Na<sub>2</sub>SO<sub>4</sub>, and solvent removed *in vacuo*. The product was purified by silica flash chromatography using gradient (100% Hex to 30% EtOAc) to give the title compound as a colourless oil (0.166 g, 0.90 mmol, 73%).

<sup>1</sup>H NMR (400 MHz, CDCl<sub>3</sub>), δ 4.75 (bs, 1H, NH), 3.94 – 3.91 (m, 1H, CH), 2.62 (dd, *J* = 6.8, 5.3 Hz, 2H, CH<sub>2</sub>), 1.45 – 1.38 (m, 9H, C(CH<sub>3</sub>)<sub>3</sub>), 1.28 (d, *J* = 6.8 Hz, 3H, CH<sub>3</sub>)

<sup>13</sup>C NMR (100 MHz, CDCl<sub>3</sub>), δ 154.9 (C=O), 117.5 (CN), 80.2 (C(CH<sub>3</sub>)<sub>3</sub>), 43.2 (C-3), 28.4 (C(CH<sub>3</sub>)<sub>3</sub>), 25.2 (C-2), 19.6 (C-4)

ESI-MS, low res, *m/z* 185.1 (M+H<sup>+</sup>), 206.9 (M+Na<sup>+</sup>), C<sub>9</sub>H<sub>16</sub>N<sub>2</sub>O<sub>2</sub>

***N*-(1-cyano-2-propanyl)-4-methylbenzenesulfonamide (127)<sup>5</sup>**

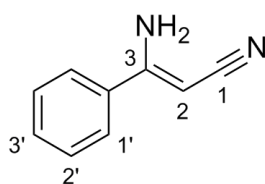
Solid 3-aminobutanenitrile hydrochloride (0.150 g, 1.24 mmol) was dissolved in dichloromethane (20 mL) and DMAP (0.228 g, 1.87 mmol) and *p*-toluenesulfonyl chloride (0.285 g, 1.49 mmol) were added. The reaction was stirred for 48 h. A solution of HCl (1M, 30 mL) was added and the organic layer was separated. The organic layer was dried (Na<sub>2</sub>SO<sub>4</sub>) and the solvent removed *in vacuo*. The product was purified by silica flash chromatography using gradient (100% Hex to 60% EtOAc) to give the title compound as a white crystalline solid (0.193 g, 0.81 mmol, 65%).

$^1\text{H}$  NMR (400 MHz,  $\text{CDCl}_3$ ),  $\delta$  7.76 (d,  $J = 8.3$  Hz, 2H, Ar-H), 7.33 (d,  $J = 8.3$  Hz, 2H, Ar-H), 5.08 (d,  $J = 7.3$  Hz, 1H, NH), 3.60 (dt,  $J = 11.4, 7.3$  Hz, 1H, CH), 2.56 (m, 2H,  $\text{CH}_2$ ), 2.43 (s, 3H, Ar- $\text{CH}_3$ ), 1.24 (d,  $J = 7.0$  Hz, 3H,  $\text{CH}_3$ )

$^{13}\text{C}$  NMR (100 MHz,  $\text{CDCl}_3$ ),  $\delta$  154.1 (C-Ar), 144.2 (C-Ar), 137.1 (C-Ar), 130.1 (C-Ar), 127.1 (C-Ar), 116.8 (CN), 46.2 (C-3), 26.4 (C-2), 21.7 (C-4), 20.4 ( $\text{CH}_3$ )

ESI-MS, low res,  $m/z$  260.9 ( $\text{M}+\text{Na}^+$ ), 238.9 ( $\text{M}+\text{H}^+$ ),  $\text{C}_{11}\text{H}_{14}\text{N}_2\text{O}_2\text{S}$

### 3-amino-3-phenylacrylonitrile (136)<sup>5</sup>

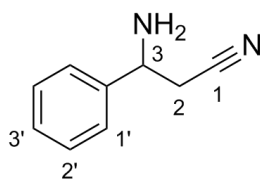


Benzonitrile (4.00 g, 38.8 mmol) was dissolved in dry toluene (100 mL) and acetonitrile (3.14 g, 4 mL, 76.5 mmol) was added. Potassium *tert*-butoxide (10.0 g, 89.2 mmol) was added in portions and the mixture was stirred for 24 h. Water (100 mL) and diethyl ether (100 mL) were added to the reaction mixture and the organic layer separated. The aqueous layer was extracted with diethyl ether (100 mL). The combined organic layers were washed with brine, dried over  $\text{Na}_2\text{SO}_4$ , and the solvent removed *in vacuo*. The product was purified by silica flash chromatography (Hex:EtOAc 70:30) to give the title compound as a white crystalline solid (2.71 g, 18.8 mmol, 49%).

$^1\text{H}$  NMR (400 MHz,  $\text{CDCl}_3$ ),  $\delta$  7.51 – 7.39 (m, 5H, Ar-H), 4.98 (s, 2H,  $\text{NH}_2$ ), 4.23 (s, 1H, CH) (lit.<sup>5</sup>)

$^{13}\text{C}$  NMR (100 MHz,  $\text{CDCl}_3$ ),  $\delta$  161.7 (C-3), 135.4 (C-Ar), 131.1 (C-3'), 129.1 (C-2'), 126.1 (C-1'), 119.7 (CN), 63.7 (C-2) (lit.<sup>5</sup>)

ESI-MS, low res,  $m/z$  166.5 ( $\text{M}+\text{Na}^+$ ), 144.6 ( $\text{M}+\text{H}^+$ ) (lit.<sup>5</sup>),  $\text{C}_9\text{H}_8\text{N}_2$

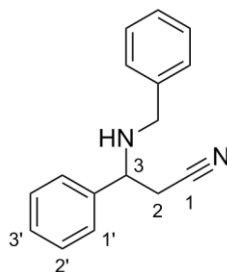
**3-amino-3-phenylpropionitrile (122)<sup>6</sup>**

Solid NaBH<sub>4</sub> (0.388 g, 10.3 mmol) was added portion-wise with stirring to glacial acetic acid (10.8 g, 10.3 mL, 0.179 mol) at 10°C. A small portion of the NaBH<sub>4</sub> was initially added at room temperature then the mixture was cooled to 10°C and the remainder of the NaBH<sub>4</sub> was added portion-wise with stirring. The mixture was stirred for 30 min. A solution of 3-amino-3-phenylacrylonitrile (0.493 g, 3.42 mmol) in glacial acetic acid (3.4 mL) was added portion-wise. The solution was left to stir at room temperature for 2h. The mixture was concentrated *in vacuo* then NaOH (1M, 40 mL) was added. The mixture was extracted with EtOAc (3 x 40 mL) and the combined organic extracts were washed with brine, dried over Na<sub>2</sub>SO<sub>4</sub>, and the solvent removed *in vacuo*. The product was purified by silica flash chromatography (Hex:EtOAc 70:30) to give the title compound as a pale-yellow oil (0.272 g, 1.86 mmol, 54%).

<sup>1</sup>H NMR (400 MHz, CDCl<sub>3</sub>), δ 7.47 – 7.25 (m, 5H, Ar-H), 4.31 (dd, *J* = 7.2, 5.7 Hz, 1H, CH), 2.71 – 2.59 (m, 2H, CH<sub>2</sub>), 1.79 (s, 2H, NH<sub>2</sub>) (lit.<sup>5</sup>)

<sup>13</sup>C NMR (100 MHz, CDCl<sub>3</sub>), δ 142.5 (CN), 129.0 (C-Ar), 128.5 (C-Ar), 126.2 (C-Ar), 118.1 (C-5), 52.8 (C-4), 28.6 (C-3) (lit.<sup>5</sup>)

ESI-MS, low res, *m/z* 168.9 (M+Na<sup>+</sup>), 147.0 (M+H<sup>+</sup>) (lit.<sup>5</sup>), C<sub>9</sub>H<sub>10</sub>N<sub>2</sub>

**3-(benzylamino)-3-phenylpropanenitrile (128)<sup>7</sup>**

Benzaldehyde (0.069 g, 66 μL, 0.65 mmol) and 3-amino-3-phenylpropionitrile (0.111 g, 0.76 mmol) were stirred together in MeOH (5 mL) at room temperature under nitrogen for 3h. Solid NaBH<sub>4</sub> (0.040 g, 1.06 mmol) was added portion-wise and the mixture was stirred for a further 2h. The reaction was quenched with NaOH (1M, 10 mL). The mixture was extracted with

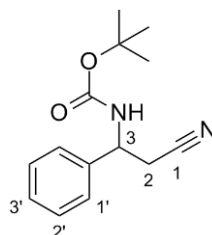
diethyl ether (3 x 20 mL). The combined organic extracts were washed with brine (20 mL), dried over Na<sub>2</sub>SO<sub>4</sub>, and the solvent removed *in vacuo*. The product was purified by silica flash chromatography using gradient (100% Hex to 30% EtOAc) to give the title compound as a colourless oil (0.098 g, 0.41 mmol, 55%).

<sup>1</sup>H NMR (400 MHz, CDCl<sub>3</sub>), δ 7.60 – 7.19 (m, 10H, Ar-H), 4.28 (dd, *J* = 10.9, 4.5 Hz, 1H, CH), 3.68 (s, 2H, Ar-CH<sub>2</sub>), 2.41 (ddd, *J* = 21.1, 10.9, 4.5 Hz, 2H, CH<sub>2</sub>), 1.25 (s, 1H, NH)

<sup>13</sup>C NMR (100 MHz, CDCl<sub>3</sub>), δ 131.3 (C-Ar), 131.0, 130.41 (C-Ar), 130.2 (C-Ar), 130.1 (C-Ar), 129.9 (C-Ar), 129.3 (C-Ar), 128.1 (C-Ar), 114.8 (CN), 59.0 (C3), 50.3 (CH<sub>2</sub>), 22.7 (C-2)

ESI-MS, low res, *m/z* 258.9 (M+Na<sup>+</sup>), 236.9 (M+H<sup>+</sup>), C<sub>16</sub>H<sub>16</sub>N<sub>2</sub>

#### ***tert*-Butyl (2-cyano-1-phenylethyl)carbamate (129)<sup>5</sup>**



The starting unprotected nitrile 3-amino-3-phenylpropanenitrile (0.107 g, 0.73 mmol) was added to a solution of dioxane (2.5 mL), water (1.2 mL), and NaOH (1M, 1.2 mL). Di-*tert*-butyl dicarbonate (0.175 g, 0.80 mmol) was then added at 0°C. The reaction was stirred at room temperature for 6h. Half the solvent was removed *in vacuo* and EtOAc (10 mL) was added. The aqueous layer was acidified to pH 4. This was then extracted with EtOAc (4 x 20 mL). The combined organic extracts were washed with brine, dried over Na<sub>2</sub>SO<sub>4</sub>, and the solvent removed *in vacuo* to give a white solid (0.105 g, 0.43 mmol, 58%).

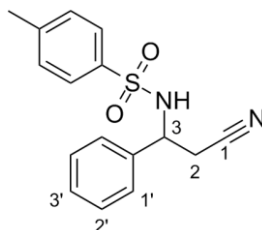
<sup>1</sup>H NMR (400 MHz, CDCl<sub>3</sub>), δ 7.45 – 7.26 (m, 5H, Ar-H), 5.11 (bs, 1H, NH), 4.97 (s, *J* = 55.6 Hz, 1H, CH), 2.98 – 2.81 (m, 2H, CH<sub>2</sub>), 1.50 (s, 9H, C(CH<sub>3</sub>)<sub>3</sub>) (lit.<sup>5</sup>)

<sup>13</sup>C NMR (100 MHz, CDCl<sub>3</sub>), δ 155.0 (C=O), 138.6 (C-Ar), 129.3 (C-Ar), 129.3 (C-Ar), 129.3 (C-Ar), 128.8 (C-Ar), 126.3 (C-Ar), 117.2 (CN), 80.7 (C(CH<sub>3</sub>)<sub>3</sub>), 51.3 (C-3), 28.4 (C(CH<sub>3</sub>)<sub>3</sub>), 25.3 (C-2) (lit.<sup>5</sup>)



ESI-MS, low res,  $m/z$  268.9 ( $M+Na^+$ ) (lit.<sup>5</sup>), 246.9 ( $M+H^+$ ),  $C_{14}H_{18}N_2O_2$

***N*-(2-cyano-1-phenylethyl)-4-methylbenzenesulfonamide (45)<sup>5</sup>**



The starting unprotected nitrile 3-amino-3-phenylpropionitrile (0.131 g, 0.90 mmol) was dissolved in dichloromethane (20 mL) and DMAP (0.143 g, 1.17 mmol) and *p*-toluenesulfonyl chloride (0.206 g, 1.08 mmol) were added. The reaction stirred for 48 h. HCl (1 M, 50 mL) was added and the organic layer was separated. The organic layer was dried ( $Na_2SO_4$ ) and the solvent removed *in vacuo*. The product was purified by silica flash chromatography using gradient (100% Hex to 30% EtOAc) to give the title compound as a white crystalline solid (0.082 g, 0.27 mmol, 30%).

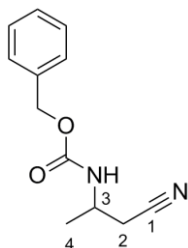
$^1H$  NMR (400 MHz,  $CDCl_3$ ),  $\delta$  7.69 – 7.62 (m, 2H, Ar-H), 7.29 – 7.21 (m, 5H, Ar-H), 7.12 (tdd,  $J = 3.7, 3.1, 0.9$  Hz, 2H, Ar-H), 5.43 (d,  $J = 7.0$  Hz, 1H, NH), 4.61 – 4.50 (m, 1H, CH), 2.98 – 2.83 (m, 2H, CH<sub>2</sub>), 2.40 (s, 3H, CH<sub>3</sub>), 1.66 (s, 2H, CH<sub>2</sub>) (lit.<sup>5</sup>)

$^{13}C$  NMR (100 MHz,  $CDCl_3$ ),  $\delta$  144.1 (C-Ar), 137.3 (C-Ar), 136.6 (C-Ar), 129.9 (C-Ar), 129.3 (C-Ar), 129.1 (C-Ar), 127.2 (C-Ar), 126.3 (C-Ar), 116.5 (CN), 54.2 (C-3), 26.4 (C-2), 21.6 (Ar-CH<sub>3</sub>) (lit.<sup>5</sup>)

ESI-MS, low res,  $m/z$  298.7 ( $M-H^+$ ),  $C_{16}H_{16}N_2O_2S$

## 7.7 Preparation of Racemic and Single Enantiomer Standards for Chiral HPLC Method Development

### Benzyl (1-cyano-2-propanyl)carbamate (155)<sup>4</sup>



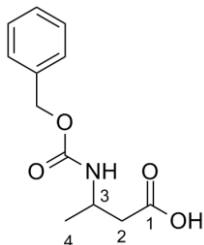
To NaOH (2M, 5 mL) was added 3-aminobutyronitrile hydrochloride (0.30 g, 2.5 mmol). A solution of Cbz-OSu (1.2 g, 4.8 mmol) in THF (5 mL) was then added at 0°C. The mixture was stirred for 24 h. The pH was adjusted to 12 then the mixture was extracted with EtOAc (3 x 50 mL). The combined organic extracts were dried over Na<sub>2</sub>SO<sub>4</sub> and the solvent removed *in vacuo*. The product was purified by silica flash chromatography (Hex:EtOAc 80:20) to give the title compound as a colourless oil (0.53 g, 2.5 mmol, 97%).

<sup>1</sup>H NMR (400 MHz, CDCl<sub>3</sub>), δ 7.35 (d, *J* = 4.4 Hz, 5H, Ar-H), 5.18 – 5.03 (m, 2H, Ar-CH<sub>2</sub>), 4.98 (s, 1H, NH), 4.11 – 3.90 (m, 1H, CH), 2.68 (dd, *J* = 16.3 Hz, 2H, CH<sub>2</sub>), 1.41 – 1.23 (m, 3H, CH<sub>3</sub>)

<sup>13</sup>C NMR (100 MHz, CDCl<sub>3</sub>), δ 155.5 (C=O), 136.1 (C-Ar), 128.7 (C-Ar), 128.4 (C-Ar), 128.3 (C-Ar), 117.3 (CN), 67.1 (CH<sub>2</sub>), 43.8 (C-3), 25.2 (C-2), 19.6 (C-4)

ESI-MS, low res, *m/z* 240.9 (M+Na<sup>+</sup>), 218.9 (M+H<sup>+</sup>), C<sub>12</sub>H<sub>14</sub>N<sub>2</sub>O<sub>2</sub>

### 3-[[[(Benzyloxy)carbonyl]amino]butanoic acid (156)<sup>4</sup>



To NaOH (2M, 5 mL) was added 3-aminobutyric acid (0.106 g, 1.03 mmol). A solution of Cbz-Osu (0.484 g, 1.94 mmol) in THF (5 mL) was then added at 0°C. The mixture was stirred for 24 h. The pH was adjusted to 4 then the mixture was extracted with EtOAc (3 x 50 mL).

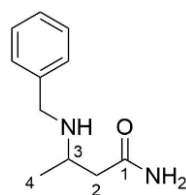
The combined organic extracts were dried over Na<sub>2</sub>SO<sub>4</sub> and the solvent removed *in vacuo*. The product was purified by silica flash chromatography (Hex:EtOAc 70:30) to give the title compound as a colourless oil (0.138 g, 0.58 mmol, 56%).

<sup>1</sup>H NMR (400 MHz, CDCl<sub>3</sub>), δ 9.90 (bs, 1H, COOH), 7.40 – 7.28 (m, 5H, Ar-H), 5.29 (d, *J* = 6.2 Hz, 1H, NH), 5.17 – 5.09 (m, 2H, Ar-CH<sub>2</sub>), 4.10 (d, *J* = 5.5 Hz, 1H, CH), 2.56 – 2.47 (m, 2H, CH<sub>2</sub>), 1.25 (d, *J* = 6.7 Hz, 3H, CH<sub>3</sub>) (lit.<sup>4</sup>)

<sup>13</sup>C NMR (100 MHz, CDCl<sub>3</sub>), δ 176.5 (C=O), 155.8 (Ar-C=O), 136.4 (C-Ar), 128.6 (C-Ar), 128.2 (C-Ar), 66.9 (CH<sub>2</sub>), 44.0 (C-3), 40.4 (C-2), 20.5 (C-4) (lit.<sup>4</sup>)

ESI-MS, low res, *m/z* 260 (M+Na<sup>+</sup>), 238 (M+H<sup>+</sup>), C<sub>12</sub>H<sub>15</sub>NO<sub>4</sub>

### 3-(Benzylamino)butanamide (143)<sup>8</sup>

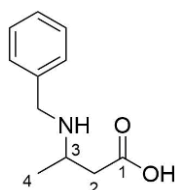


3-(Benzylamino)butyronitrile (0.05 g, 0.29 mmol) was dissolved in MeOH (5 mL) and potassium carbonate (0.20 g, 1.4 mmol) and aqueous hydrogen peroxide (35%, 1 mL) were added. The reaction was stirred and monitored by TLC. On completion, the MeOH was removed under reduced pressure and the aqueous phase was diluted with water. This was extracted with DCM (3 x 20 mL). The combined organic extracts were dried over Na<sub>2</sub>SO<sub>4</sub> and the solvent removed *in vacuo*. The product was purified by C18 silica flash chromatography using gradient (100% H<sub>2</sub>O to 50% MeOH) to give the title compound as a colourless residue (0.02 g, 0.08 mmol, 26%).

<sup>1</sup>H NMR (400 MHz, CD<sub>3</sub>CN) δ 7.32 – 7.21 (m, 5H, Ar-H), 5.58 (s, 1H, CONH), 3.75 (dd, *J* = 34.5, 13.2 Hz, 2H, CH<sub>2</sub>), 3.01 – 2.96 (m, 1H, CH), 1.24 (d, *J* = 10.8 Hz, 2H, CH<sub>2</sub>), 1.08 (d, *J* = 6.4 Hz, 3H, CH<sub>3</sub>)

<sup>13</sup>C NMR (100 MHz, CD<sub>3</sub>CN) δ 132.09 (C-Ar), 128.91 (C-Ar), 67.21 (CH<sub>2</sub>-Ar), 43.99 (C-3)

ESI-MS, low res, *m/z* 192.9 (M+H<sup>+</sup>) (lit.<sup>4</sup>), C<sub>16</sub>H<sub>18</sub>N<sub>2</sub>O

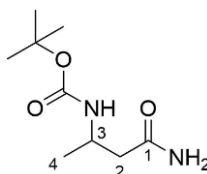
**3-(Benzylamino)butanoic acid (144)<sup>8</sup>**

The starting nitrile 3-(benzylamino)butyronitrile (0.10 g, 0.6 mmol) was suspended in concentrated HCl (10 mL). The mixture was heated to reflux for 24 h. The solution was brought up to pH 7 and the volume reduced down *in vacuo*. The purified product was obtained using semi-prep HPLC, gradient elution (ACN:H<sub>2</sub>O + 0.1% formic acid), 5 mL min<sup>-1</sup> to give the title compound as a colourless residue (0.0070 g, 0.03 mmol, 6%).

<sup>1</sup>H NMR (400 MHz, ACN-D<sub>3</sub>) δ 7.50–7.44 (m, 5H, Ar-H), 4.27 (d, *J* = 1.3 Hz, 1H, CH), 4.22 (d, *J* = 1.3 Hz, 1H, CH), 3.67–3.62 (m, 1H, CH), 2.81–2.69 (m, 2H, CH<sub>2</sub>) 1.42–1.41 (m, 3H, CH<sub>3</sub>) (lit.<sup>4</sup>)

<sup>13</sup>C NMR (100 MHz, ACN-D<sub>3</sub>) δ 131.20 (C-Ar), 129.55 (C-Ar), 129.41 (C-Ar), 129.06 (C-Ar), 78.27 (CH<sub>2</sub>-Ar), 77.95 (C-3), 77.63 (C-2), 15.55 (C-4)

ESI-MS, low res, *m/z* 194.0 (M+H<sup>+</sup>), C<sub>16</sub>H<sub>17</sub>N<sub>2</sub>O<sub>2</sub>

***tert*-butyl 1-carbamoylpropan-2-ylcarbamate (145)<sup>8</sup>**

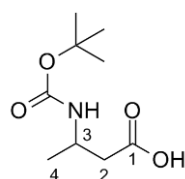
Solid 2-methyl-2-propanyl(1-cyano-2-propanyl)carbamate (0.020 g, 0.10 mmol) was dissolved in MeOH (3 mL) and potassium carbonate (0.075 g, 0.54 mmol) and aqueous hydrogen peroxide (35%, 1 mL) were added. The reaction was stirred at room temperature with monitoring. On completion, the MeOH was removed under reduced pressure and the aqueous phase was diluted with water. This was extracted with DCM (3 x 20 mL). The combined organic extracts were dried over Na<sub>2</sub>SO<sub>4</sub> and the solvent removed *in vacuo* to give the title compound as a white solid (0.016 g, 0.080 mmol, 75%).

$^1\text{H}$  NMR (400 MHz,  $\text{CDCl}_3$ ),  $\delta$  6.04 (bs, 1H, NH), 5.59 (bs, 1H, CONH), 5.11 (bs, 1H, CONH), 4.08 – 3.95 (m, 1H, CH), 2.43 (d,  $J = 5.8$  Hz, 2H, CH<sub>2</sub>), 1.42 (s, 9H, C(CH<sub>3</sub>)<sub>3</sub>), 1.24 (d,  $J = 6.7$  Hz, 3H, CH<sub>3</sub>)

$^{13}\text{C}$  NMR (100 MHz,  $\text{CDCl}_3$ ),  $\delta$  173.75 (C-1), 155.73 (C=O), 79.79 (C(CH<sub>3</sub>)<sub>3</sub>), 44.16 (C-3), 42.46 (C-2), 28.46 (C(CH<sub>3</sub>)<sub>3</sub>), 20.88 (C-4)

ESI-MS, low res,  $m/z$  225.0 ( $\text{M}+\text{Na}^+$ ),  $\text{C}_9\text{H}_{18}\text{N}_2\text{O}_3$

### 3-((*tert*-butoxycarbonyl)amino)butanoic acid (**146**)<sup>5</sup>



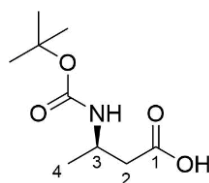
Solid 3-aminobutyric acid (0.15 g, 1.2 mmol) was added to a solution of dioxane (5 mL), water (2.4 mL), and NaOH (1M, 2.4 mL). Di-*tert*-butyl dicarbonate (0.35 g, 1.6 mmol) was then added at 0°C. The reaction was stirred at room temperature for 6h. The reaction was concentrated and EtOAc (10 mL) was added. The aqueous layer was acidified to pH 4. This was then extracted with EtOAc (4 x 10 mL). The combined organic extracts were then washed with brine, dried over  $\text{Na}_2\text{SO}_4$ , and solvent removed *in vacuo* to give the title compound as a white solid (0.26 g, 1.3 mmol, 87%).

$^1\text{H}$  NMR (400 MHz,  $\text{CDCl}_3$ ),  $\delta$  8.44 (bs, 1H, COOH), 4.98 (s, 1H, NH), 4.03 (s, 1H, CH), 2.53 (s, 2H, CH<sub>2</sub>), 1.43 (s, 9H, C(CH<sub>3</sub>)<sub>3</sub>), 1.29 – 1.14 (m, 3H, CH<sub>3</sub>).

$^{13}\text{C}$  NMR (100 MHz,  $\text{CDCl}_3$ )  $\delta$  79.65 (C-1), 43.36 (C-3), 40.70 (C-2), 28.41 (C(CH<sub>3</sub>)<sub>3</sub>), 20.46 (C-4).

ESI-MS, low res,  $m/z$  201.4 ( $\text{M}-\text{H}^+$ ),  $\text{C}_9\text{H}_{17}\text{NO}_4$

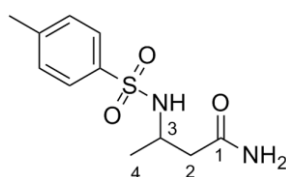
### (*R*)-3-((*tert*-butoxycarbonyl)amino)butanoic acid (**146b**)<sup>5</sup>



Solid (*R*)-3-aminobutyric acid (0.05 g, 0.41 mmol) was added to a solution of dioxane (5 mL), water (2.4 mL), and NaOH (1M, 2.4 mL). Di-*tert*-butyl dicarbonate (0.12 g, 0.58 mmol) was

then added at 0°C. The reaction was stirred at room temperature for 6h. The reaction was concentrated and EtOAc (10 mL) was added. The aqueous layer was acidified to pH 4. This was then extracted with EtOAc (4 x 10 mL). The combined organic extracts were then washed with brine, dried over Na<sub>2</sub>SO<sub>4</sub>, and solvent removed *in vacuo* to give the title compound as a white solid (0.06 g, 0.30 mmol, 61%). The enantiomer was analysed on an OJ-H column; Hex:IPA (90:10 + 0.1% TFA), flow rate 1.0 mL min<sup>-1</sup>, which gave (*R*)-enantiomer t<sub>R</sub> = 4.72 min, where the racemic acid gave t<sub>R</sub> = 4.60 min and t<sub>R</sub> = 4.85 min

### 3-(4-methylphenylsulfonamido)butanamide (147)<sup>8</sup>

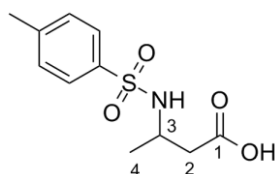


*N*-(1-cyano-2-propanyl)-4-methylbenzenesulfonamide (0.025 g, 0.10 mmol) was dissolved in MeOH (5 mL). Potassium carbonate (0.13 g, 0.94 mmol) and aqueous hydrogen peroxide (35%, 1 mL). The reaction was stirred at room temperature with monitoring. On completion, the MeOH was removed under reduced pressure and the aqueous phase was diluted with water. This was extracted with DCM (3 x 20 mL). The combined organic extracts were dried over Na<sub>2</sub>SO<sub>4</sub> and the solvent removed *in vacuo* to give the title compound as a white solid (0.016g, 0.06 mmol, 59%).

<sup>1</sup>H NMR (400 MHz, ACN-D<sub>3</sub>) δ 7.84 – 7.58 (m, 2H, Ar-H), 7.45 – 7.23 (m, 2H, Ar-H), 6.10 (s, 1H, NH), 5.98 (d, *J* = 7.3 Hz, 1H, CH<sub>2</sub>), 5.63 (s, 1H, CH<sub>2</sub>), 3.59 – 3.44 (m, 1H, CH), 2.39 (s, 3H, CH<sub>3</sub>), 0.98 (d, *J* = 6.5 Hz, 3H, CH<sub>3</sub>).

<sup>13</sup>C NMR (100 MHz, ACN-D<sub>3</sub>) δ 172.57 (C-1), 143.55 (C-Ar), 138.43 (C-Ar), 137.01 (C-Ar), 129.74 (C-Ar), 126.88 (C-Ar), 47.30 (C-3), 41.39 (C-2), 20.57 (C-4), 20.24 (CH<sub>3</sub>)

ESI-MS, low res, *m/z* 278.6 (M+Na<sup>+</sup>), 256.6 (M+H<sup>+</sup>), C<sub>11</sub>H<sub>16</sub>N<sub>2</sub>O<sub>3</sub>S

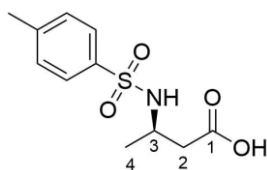
**3-[[4-(4-methylphenyl)sulfonyl]amino]butanoic acid (148)<sup>8</sup>**

*N*-(1-cyano-2-propanyl)-4-methylbenzenesulfonamide (0.16 g, 0.67 mmol) was suspended in concentrated NaOH (10 mL). The mixture was heated to reflux for 24 h. The pH was adjusted with HCl to 5 and the mixture was diluted with water. The mixture was extracted with DCM (3 x 20 mL), dried over Na<sub>2</sub>SO<sub>4</sub>, and the solvent removed *in vacuo*. The product was purified by semi-preparatory HPLC, gradient elution (H<sub>2</sub>O:ACN + 0.1% formic acid), flow rate 5 mL min<sup>-1</sup>, to give the title compound as a white solid (0.10 g, 0.39 mmol, 92%).

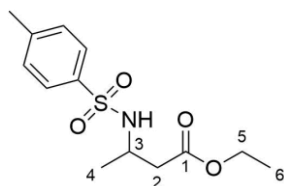
<sup>1</sup>H NMR (400 MHz, ACN-D<sub>3</sub>), δ 7.74 – 7.65 (m, 2H, Ar-H), 7.34 (d, *J* = 7.9 Hz, 2H, Ar-H), 5.69 (bs, 1H, COOH), 3.65 – 3.48 (m, 1H, NH), 2.37 (d, *J* = 4.3 Hz, 3H, Ar-CH<sub>3</sub>), 1.92 (dt, *J* = 5.0, 2.5 Hz, 1H, CH), 0.99 (d, *J* = 5.0 Hz, 3H, CH<sub>3</sub>).

<sup>13</sup>C NMR (100 MHz, ACN-D<sub>3</sub>), δ 172.33 (C-1), 143.60 (C-Ar), 138.43 (C-Ar), 129.76 (C-Ar), 126.87 (C-Ar), 46.94 (C-2), 41.04 (C-3), 20.61 (Ar-CH<sub>3</sub>), 20.21 (C-4)

ESI-MS, low res, *m/z* 280 (M+Na<sup>+</sup>), 257.9 (M+H<sup>+</sup>), C<sub>11</sub>H<sub>15</sub>NO<sub>4</sub>S

**(*R*)-3-[[4-(4-methylphenyl)sulfonyl]amino]butanoic acid (148b)<sup>8</sup>**

Solid (*R*)-*N*-(1-cyano-2-propanyl)-4-methylbenzenesulfonamide (0.05 g 0.21 mmol) was suspended in concentrated NaOH (10 mL). The mixture was heated to reflux for 24 h. The pH was adjusted with HCl to 5 and the mixture was diluted with water. The mixture was extracted with DCM (3 x 20 mL), dried over Na<sub>2</sub>SO<sub>4</sub>, and the solvent removed *in vacuo*. The product was purified by semi-preparatory HPLC, gradient elution (H<sub>2</sub>O:ACN + 0.1% formic acid), flow rate 5 mL min<sup>-1</sup>, to give the title compound as a white solid (0.03 g, 0.12 mmol, 25%). The enantiomer was analysed on an IA column; Hex:IPA (90:10 + 0.1% TFA), flow rate 1.0 mL min<sup>-1</sup>, which gave (*R*)-enantiomer *t<sub>R</sub>* = 35.3 min, where the racemic acid gave *t<sub>R</sub>* = 27.1 min and *t<sub>R</sub>* = 35.9 min

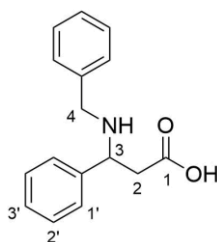
**Ethyl-3-[[4-(4-methylphenyl)sulfonyl]amino]butanoate (164)<sup>9</sup>**

Solid 3-[[4-(4-methylphenyl)sulfonyl]amino]butanoic acid (0.0020 g, 0.01 mmol) was dissolved in mixture of water:ethanol:pyridine (60:32:8). Ethyl chloroformate (120  $\mu$ L) was added and the reaction mixture was stirred for 5 min. The mixture was extracted with chloroform including 1% ethyl chloroformate (2.4 mL). The solvent was removed *in vacuo* to give the title compound as a colourless residue (0.0020 g, 0.01 mmol, 90%).

<sup>1</sup>H NMR (400 MHz, ACN-D<sub>3</sub>),  $\delta$  7.72 – 7.66 (m, 2H, Ar-H), 7.35 (d,  $J$  = 7.9 Hz, 2H, Ar-H), 5.69 (d,  $J$  = 7.6 Hz, 1H, NH), 4.05 – 3.91 (m, 2H, CH<sub>2</sub>-CH<sub>3</sub>), 3.65 – 3.51 (m, 1H, CH), 2.22 (s, 3H, Ar-CH<sub>3</sub>), 1.92 (dq,  $J$  = 5.0, 2.4 Hz, 2H, CH<sub>2</sub>), 1.14 (t,  $J$  = 7.1 Hz, 3H, CH<sub>3</sub>), 0.98 (d,  $J$  = 6.7 Hz, 3H, CH<sub>2</sub>-CH<sub>3</sub>)

<sup>13</sup>C NMR (100 MHz, ACN-D<sub>3</sub>),  $\delta$  129.73 (C-5), 126.83 (C-2), 106.68 (C-3).

ESI-MS, low res,  $m/z$  308.0 (M+Na<sup>+</sup>), 286.0 (M+H<sup>+</sup>), C<sub>13</sub>H<sub>19</sub>NO<sub>4</sub>S

**3-(benzylamino)-3-phenylpropanoic acid (40)<sup>7</sup>**

Benzaldehyde (0.079 g, 76  $\mu$ L, 0.74 mmol,) and 3-amino-3-phenylpropanoic acid (0.15 g, 0.91 mmol) were stirred together in MeOH (10 mL) at room temperature under nitrogen for 3h. Solid NaBH<sub>4</sub> (0.045 g, 1.2 mmol) was added portion-wise and the mixture was stirred for a further 2h. The reaction was quenched with NaOH (1M, 10 mL). The mixture was extracted with diethyl ether (3 x 20 mL). The combined organic extracts were washed with brine (20 mL), dried over Na<sub>2</sub>SO<sub>4</sub>, and the solvent removed *in vacuo*. The product was purified by silica flash chromatography using gradient (100% Hex to 30% EtOAc) to give the title compound as a colourless oil (0.040 g 0.15 mmol, 17%).

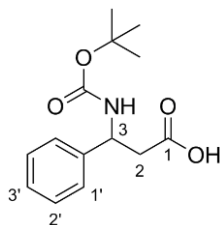


$^1\text{H}$  NMR (400 MHz,  $\text{ACN-D}_3$ )  $\delta$  7.72 – 7.31 (m, 10H, Ar-H), 4.51 (dd,  $J = 8.7, 6.1$  Hz, 1H,  $\text{CH}_2$ ), 4.04 – 4.00 (m, 1H, NH), 3.89 – 3.86 (m, 1H, CH), 3.26 (dd,  $J = 17.7, 8.7$  Hz, 1H,  $\text{CH}_2$ ), 2.92 (dd,  $J = 17.7, 6.2$  Hz, 1H,  $\text{CH}_2$ ).

$^{13}\text{C}$  NMR (100 MHz,  $\text{ACN-D}_3$ )  $\delta$  184.66 (C-1), 174.70 (C-Ar), 133.78 (C-Ar), 131.17 (C-Ar), 129.83 (C-Ar), 129.36 (C-Ar), 129.04 (C-Ar), 128.61 (C-Ar), 58.66 (C-3), 56.37 ( $\text{CH}_2$ ), 48.92 (C-2).

ESI-MS, low res,  $m/z$  255.6 ( $\text{M}+\text{H}^+$ ),  $\text{C}_{16}\text{H}_{17}\text{NO}_2$

### 3-(*tert*-butoxycarbonylamino)-3-phenylpropanoic acid (151)<sup>5</sup>

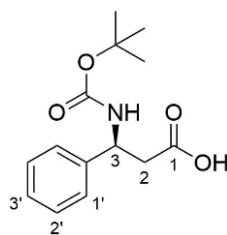


The starting acid 3-amino-3-phenylpropionic acid (0.15 g, 0.91 mmol) was added to a solution of dioxane (2.5 mL), water (1.2 mL), and NaOH (1M, 1.2 mL). Di-*tert*-butyl dicarbonate (0.22 g, 1.0 mmol) was then added at 0°C. The reaction was stirred at room temperature for 6h. Half the solvent was removed *in vacuo* and EtOAc (10 mL) was added. The aqueous layer was acidified to pH 4. This was then extracted with EtOAc (4 x 20 mL). The combined organic extracts were washed with brine, dried over  $\text{Na}_2\text{SO}_4$ , and the solvent removed *in vacuo* to give a white solid (0.17 g, 0.63 mmol, 70%).

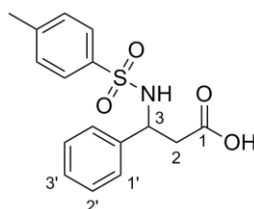
$^1\text{H}$  NMR (400 MHz,  $\text{CDCl}_3$ )  $\delta$  10.32 (s, 1H, COOH), 7.34 – 7.23 (m, 5H, Ar-H), 6.71 (s, 1H, NH), 5.55 (s, 1H,  $\text{CH}_2$ ), 5.02 (d,  $J = 71.1$  Hz, 1H,  $\text{CH}_2$ ), 2.88 – 2.80 (m, 1H, CH), 1.42 – 1.26 (m, 9H,  $\text{C}(\text{CH}_3)_3$ ) (lit.<sup>5</sup>)

$^{13}\text{C}$  NMR (100 MHz,  $\text{CDCl}_3$ )  $\delta$  175.96 (C-1), 155.39 (C-Ar), 141.12 (C-Ar), 128.70 (C-Ar), 127.59 (C-Ar), 126.29 (C-Ar), 80.06 ( $\text{C}(\text{CH}_3)_3$ ), 51.03 (C-3), 40.65 (C-2), 28.36 ( $\text{C}(\text{CH}_3)_3$ ) (lit.<sup>5</sup>)

ESI-MS, low res,  $m/z$  287.6 ( $\text{M}+\text{Na}^+$ ),  $\text{C}_{14}\text{H}_{19}\text{NO}_4$

**(*R*)-3-(*tert*-butoxycarbonylamino)-3-phenylpropanoic acid (151b)<sup>5</sup>**

The starting acid (*R*)-3-amino-3-phenylpropionic acid (0.05 g, 0.30 mmol) was added to a solution of dioxane (2.5 mL), water (1.2 mL), and NaOH (1M, 1.2 mL). Di-*tert*-butyl dicarbonate (0.0087 g, 0.04 mmol) was then added at 0°C. The reaction was stirred at room temperature for 6h. Half the solvent was removed *in vacuo* and EtOAc (10 mL) was added. The aqueous layer was acidified to pH 4. This was then extracted with EtOAc (4 x 20 mL). The combined organic extracts were washed with brine, dried over Na<sub>2</sub>SO<sub>4</sub>, and the solvent removed *in vacuo* to give a white solid (0.05 g, 0.11 mmol, 63%). The enantiomer was analysed on an OJ-H column; Hex:IPA (90:10 + 0.1% TFA), flow rate 1.0 mL min<sup>-1</sup>, which gave (*R*)-enantiomer  $t_R = 6.07$  min, where the racemic acid gave  $t_R = 6.01$  min and  $t_R = 6.85$  min

**3-[[4-(4-methylphenyl)sulfonyl]amino]-3-phenylpropanoic acid (152)<sup>5</sup>**

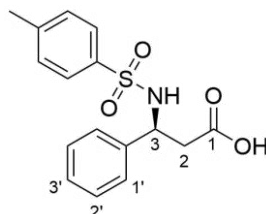
Solid 3-amino-3-phenylpropionic acid (0.30 g, 1.82 mmol) was suspended in concentrated NaOH (2M, 10 mL). Diethyl ether (30 mL) and *p*-toluenesulfonyl chloride (0.55 g, 2.89 mmol) were added. The reaction stirred for 48 h. HCl (1 M, 50 mL) was added and the organic layer was separated. The organic layer was dried (Na<sub>2</sub>SO<sub>4</sub>) and the solvent removed *in vacuo*. The product was purified by silica flash chromatography using gradient (100% Hex to 30% EtOAc) to give the title compound as a white solid (0.02 g, 0.06 mmol, 3%).

<sup>1</sup>H NMR (400 MHz, CDCl<sub>3</sub>) δ 7.59 – 7.57 (m, 4H, Ar-H), 7.20 – 7.08 (m, 5H, Ar-H), 5.78 (s, 1H, NH), 4.72 (d, *J* = 5.2 Hz, 1H, CH), 2.85 (dd, *J* = 16.4, 5.2 Hz, 2H, CH<sub>2</sub>), 2.36 (s, 3H, CH<sub>3</sub>) (lit.<sup>8</sup>)

$^{13}\text{C}$  NMR (100 MHz,  $\text{CDCl}_3$ )  $\delta$  174.96 (C-1), 143.49 (Ar-C), 139.07 (Ar-C), 137.23 (Ar-C), 129.57 (Ar-C), 128.71 (Ar-C), 127.97 (Ar-C), 127.20 (Ar-C), 126.53 (Ar-C), 54.10 (C-3), 40.87 (C-2), 21.55 (Ar- $\underline{\text{C}}\text{H}_3$ ) (lit.<sup>8</sup>)

ESI-MS, low res,  $m/z$  636.6 (2M-H), 317.8 (M-H<sup>+</sup>),  $\text{C}_{16}\text{H}_{17}\text{NO}_4\text{S}$

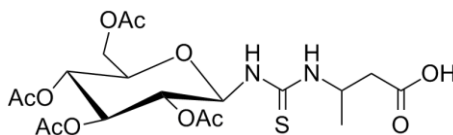
**(R)-3-[[4-(4-methylphenyl)sulfonyl]amino]-3-phenylpropanoic acid (152b)<sup>5</sup>**



Solid (*R*)-3-amino-3-phenylpropionic acid (0.30 g, 1.82 mmol) was suspended in concentrated NaOH (2M, 10 mL). Diethyl ether (30 mL) and *p*-toluenesulfonyl chloride (0.55 g, 2.89 mmol) were added. The reaction stirred for 48 h. HCl (1 M, 50 mL) was added and the organic layer was separated. The organic layer was dried ( $\text{Na}_2\text{SO}_4$ ) and the solvent removed *in vacuo*. The product was purified by silica flash chromatography using gradient (100% Hex to 30% EtOAc) to give the title compound as a white solid (0.04 g, 0.13 mmol, 7%). The enantiomer was analysed on an OJ-H column; Hex:IPA (90:10 + 0.1% TFA), flow rate 1.0 mL  $\text{min}^{-1}$ , which gave (*R*)-enantiomer  $t_{\text{R}} = 24.8$  min, where the racemic acid gave  $t_{\text{R}} = 24.9$  min and  $t_{\text{R}} = 26.9$  min

**7.7.1 GITC Derivatisations**

**GITC-3-aminobutyric acid (158)<sup>10</sup>**

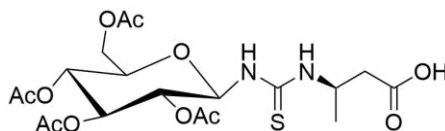


Triethylamine (0.2% w/v) and GITC (0.8% w/v) were added to a solution of 3-aminobutyric acid (0.050 g, 0.48 mmol) in ACN (3 mL). The mixture was left to stir at 40°C for 1 h. The mixture was injected directly into the HPLC. The enantiomers were separated on a C18

Symmetry column; MeOH:H<sub>2</sub>O (35:65 + 0.1% TFA), flow rate 1.0 mL min<sup>-1</sup>, which gave (*R*)-enantiomer  $t_R = 22.1$  min and (*S*)-enantiomer  $t_R = 27.3$  min.

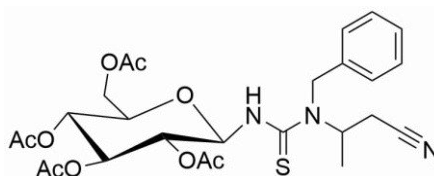
ESI-MS, low res,  $m/z$  1005.2 (2M<sup>+</sup>+Na<sup>+</sup>), 515.1 (M+Na<sup>+</sup>), 493.1 (M+H<sup>+</sup>)

#### GITC-(*R*)-3-aminobutyric acid (158b)<sup>10</sup>



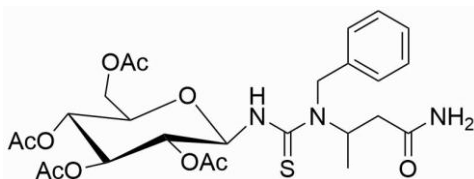
Triethylamine (0.2% w/v) and GITC (0.8% w/v) were added to a solution of (*R*)-3-aminobutyric acid (0.050 g, 0.48 mmol) in ACN (3 mL). The mixture was left to stir at 40°C for 1 h. The mixture was injected directly into the HPLC. The enantiomer was analysed on a C18 Symmetry column; MeOH:H<sub>2</sub>O (35:65 + 0.1% TFA), flow rate 1.0 mL min<sup>-1</sup>, which gave (*R*)-enantiomer  $t_R = 21.9$  min, where the racemic acid gave  $t_R = 17.4$  min and  $t_R = 21.4$  min.

#### GITC-3-(benzylamino)butyronitrile (160)<sup>10</sup>



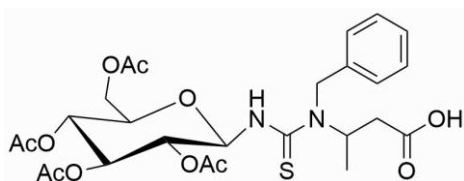
Triethylamine (0.2% w/v) and GITC (0.8% w/v) were added to a solution of 3-(benzylamino)butyronitrile (0.050 g, 0.29 mmol) in ACN (3 mL) was added. The mixture was left to stir at 40°C for 1 h. The mixture was injected directly into the HPLC. The enantiomers were separated on a C18 Symmetry column; MeOH:H<sub>2</sub>O (50:50 + 0.1% TFA), flow rate 1.0 mL min<sup>-1</sup>, which gave  $t_R = 16.6$  min (major) and  $t_R = 22.3$  min (minor).

ESI-MS, low res,  $m/z$  586.2 (M+Na<sup>+</sup>), 564.2 (M+H<sup>+</sup>)

**GITC-3-(benzylamino)butyroamide (161)<sup>10</sup>**

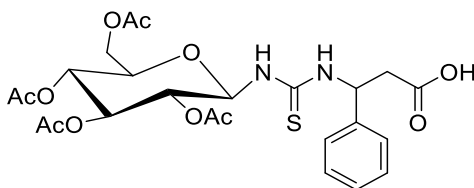
Triethylamine (0.2% w/v) and GITC (0.8% w/v) were added to a solution of 3-(benzylamino)butyroamide (0.050 g, 0.26 mmol) in ACN (3 mL) was added. The mixture was left to stir at 40°C for 1 h. The mixture was injected directly into the HPLC. The enantiomers were separated on a C18 Symmetry column; MeOH:H<sub>2</sub>O (55:45 + 0.1% TFA), flow rate 1.0 mL min<sup>-1</sup>, which gave  $t_R = 20.7$  min (minor) and  $t_R = 24.1$  min (major).

ESI-MS, low res,  $m/z$  604.3 (M+Na<sup>+</sup>), 582.3 (M+H<sup>+</sup>)

**GITC-3-(benzylamino)butyric acid (162)<sup>10</sup>**

Triethylamine (0.2% w/v) and GITC (0.8% w/v) were added to a solution of 3-(benzylamino)butyric acid (0.050 g, 0.26 mmol) in ACN (3 mL) was added. The mixture was left to stir at 40°C for 1 h. The mixture was injected directly into the HPLC. The enantiomers were separated on a C18 Symmetry column; MeOH:H<sub>2</sub>O (45:55 + 0.1% TFA), flow rate 1.0 mL min<sup>-1</sup>, which gave  $t_R = 11.5$  min (minor) and  $t_R = 22.6$  min (major).

ESI-MS, low res,  $m/z$  605.2 (M+Na<sup>+</sup>), 583.3 (M+H<sup>+</sup>)

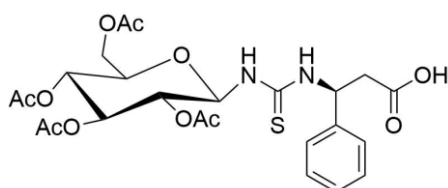
**GITC-3-amino-3-phenylpropionic acid (165)<sup>10</sup>**

Triethylamine (0.2% w/v) and GITC (0.8% w/v) were added to a solution 3-amino-3-phenylpropionic acid (0.050 g, 0.30 mmol) in ACN (3 mL) was added. The mixture was left to

stir at 40°C for 1 h. The mixture was injected directly into the HPLC. The enantiomers were separated on a C18 Symmetry column; MeOH:H<sub>2</sub>O (47:53 + 0.1% TFA), flow rate 1.0 mL min<sup>-1</sup>, which gave  $t_R = 14.9$  min (major) and  $t_R = 19.7$  min (minor).

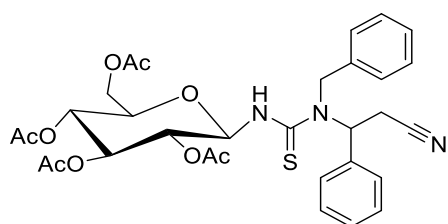
ESI-MS, low res,  $m/z$  552.9 (M-H<sup>+</sup>), C<sub>28</sub>H<sub>38</sub>N<sub>2</sub>O<sub>7</sub>S

### GITC-(*R*)-3-amino-3-phenylpropionic acid (165b)<sup>10</sup>



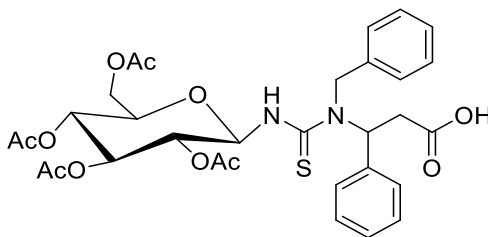
Triethylamine (0.2% w/v) and GITC (0.8% w/v) were added to a solution of (*R*)-3-amino-3-phenylpropionic acid (0.050 g, 0.30 mmol) in ACN (3 mL). The mixture was left to stir at 40°C for 1 h. The mixture was injected directly into the HPLC. The enantiomer was analysed on a C18 Symmetry column; MeOH:H<sub>2</sub>O (35:65 + 0.1% TFA), flow rate 1.0 mL min<sup>-1</sup>, which gave (*R*)-enantiomer  $t_R = 15.1$  min, where the racemic acid gave  $t_R = 14.9$  min and  $t_R = 19.7$  min.

### GITC-3-(benzylamino)-3-phenylpropanenitrile (166)<sup>10</sup>



Triethylamine (0.2% w/v) and GITC (0.8% w/v) were added to a solution of 3-(benzylamino)-3-phenylpropanenitrile (0.050 g, 0.20 mmol) in ACN (3 mL) was added. The mixture was left to stir at 40°C for 1 h. The mixture was injected directly into the HPLC. The enantiomers were separated on a C18 Symmetry column; MeOH:H<sub>2</sub>O (55:45 + 0.1% TFA), flow rate 1.0 mL min<sup>-1</sup>, which gave  $t_R = 22.6$  min (major) and  $t_R = 28.6$  min (minor).

ESI-MS, low res,  $m/z$  648.3 (M+Na<sup>+</sup>), 626.2 (M+H<sup>+</sup>), C<sub>35</sub>H<sub>43</sub>N<sub>3</sub>O<sub>5</sub>S

**GITC-3-(benzylamino)-3-phenylpropanoic acid (167)<sup>10</sup>**

Triethylamine (0.2% w/v) and GITC (0.8% w/v) were added to a solution of 3-(benzylamino)-3-phenylpropanoic acid (0.050 g, 0.20 mmol) in ACN (3 mL) was added. The mixture was left to stir at 40°C for 1 h. The mixture was injected directly into the HPLC. The enantiomers were separated on a C18 Symmetry column; MeOH:H<sub>2</sub>O (35:65 + 0.1% TFA), flow rate 1.0 mL min<sup>-1</sup>, which gave  $t_R = 11.4$  min (major) and  $t_R = 12.6$  min (minor).

ESI-MS, low res,  $m/z$  643.1 (M+H<sup>+</sup>), C<sub>35</sub>H<sub>44</sub>N<sub>2</sub>O<sub>7</sub>S

**7.8 HPLC Analysis of  $\beta$ -aminonitrile Substrates and Products**

HPLC methods were developed to acquire yields and enantioselectivity data from the biotransformations. Separations were achieved on normal phase HPLC with Hex:IPA mobile phase and on reverse phase HPLC with MeOH:H<sub>2</sub>O mobile phase. The columns used to achieve separation were Chiralpak AD-H, IA, and OJ-H, and Symmetry C18. Flow rates were 1 mL min<sup>-1</sup> unless otherwise stated. Methods were isocratic with the exception of the GITC derivatised products whose method development necessitated the need for a gradient method.

**Table 7.1: HPLC analysis conditions for the compounds. Hex: hexane. IPA: isopropanol.**  
<sup>1</sup>Analysis of its Cbz variant. <sup>2</sup>Analysis of its GITC derivative. <sup>a</sup>Analysis of its ethyl ester.

Compound	Column	Mobile Phase	Flow Rate (mL/min)	t <sub>1</sub> (min)	t <sub>2</sub> (min)	
155 <sup>1</sup>	NH <sub>2</sub> aliphatic	OJ-H	Hex:IPA 80:20	1.0	24.3	26.9
158 <sup>2</sup>		C18	MeOH:H <sub>2</sub> O + 0.1% TFA Gradient	1.0	14.1	17.1
		C18	MeOH:H <sub>2</sub> O 35:65 + 0.1% TFA	1.0	20.5	25.4
160 <sup>2</sup>	N-Bn aliphatic	C18	MeOH:H <sub>2</sub> O + 0.1% TFA Gradient	1.0	21.9	29.7
		C18	MeOH:H <sub>2</sub> O 50:50 + 0.1% TFA	1.0	16.6	22.3
161 <sup>2</sup>		C18	MeOH:H <sub>2</sub> O 55:45 + 0.1% TFA	1.0	20.7	24.1
162 <sup>2</sup>		C18	MeOH:H <sub>2</sub> O + 0.1% TFA Gradient	1.0	19.7	22.9
		C18	MeOH:H <sub>2</sub> O 55:45 + 0.1% TFA	1.0	22.9	28.5
145	N-Boc aliphatic	IA	Hex:IPA 97:3 + 0.1% TFA	1.0	23.4	25.6
146		OJ-H	Hex:IPA 90:10 + 0.1% TFA	1.0	4.7	4.9
127	N-Tosyl aliphatic	IA	Hex:IPA 90:10	1.0	30.9	34.9
147		OJ-H	Hex:IPA 90:10 + 0.1% TFA	1.0	34.4	41.3
164 <sup>a</sup>		IA	Hex:IPA 90:10 + 0.1% TFA	1.0	18.2	21.9
122	NH <sub>2</sub> aromatic	AD-H	Hex:IPA 90:10	0.8	16.1	18.9
165		C18	MeOH:H <sub>2</sub> O 47:53 + 0.1% TFA	1.0	14.9	19.7
166	N-Bn aromatic	C18	MeOH:H <sub>2</sub> O 55:45 + 0.1% TFA Gradient	1.0	22.6	28.6
167		C18	MeOH:H <sub>2</sub> O 35:65 + 0.1% TFA	1.0	11.4	12.6
129	N-Boc aromatic	IA	Hex:IPA 90:10	1.0	9.9	11.2
151		OJ-H	Hex:IPA 90:10 + 0.1% TFA	1.0	6.0	6.8
45	N-Tosyl aromatic	IA	Hex:IPA 90:10	1.0	29.3	31.3
152		OJ-H	Hex:IPA 90:10 + 0.1% TFA	1.0	24.7	26.7



## 7.9 Screening of SET1 Towards 3-aminobutyronitrile hydrochloride (124)

### 7.9.1 Initial enantioselectivity screening studies

Isolate SET1 was screened for activity on 3-aminobutyronitrile on a 6 mL scale. The biotransformations were carried out in a suspension of phosphate buffer (0.1 M, pH 7 and 9) containing induced cells ( $OD_{600nm}=1$ ). Racemic 3-aminobutyronitrile (0.0103 g, 0.12 mmol, 10 mM) was added to each flask and the mixture was incubated at 25°C for 3 days with mechanical shaking (200 rpm). The reaction was quenched by removal of the biomass by centrifugation. The supernatant was concentrated *in vacuo* then NaOH (4 mL, 2M) was added. A solution of *N*-carbobenzoxyoxysuccinimide (Cbz-Osu) (0.0598 g, 0.24 mmol) in THF (5 mL) was added at 0°C. The mixture was stirred at room temperature overnight (approximately 16 h minimum).

The pH was adjusted to 12 and the mixture was extracted with EtOAc (3 x 50 mL). The combined organic extracts were dried over Na<sub>2</sub>SO<sub>4</sub> and the solvent removed *in vacuo* to give the crude nitrile. This was diluted with pre-prepared mobile phase (Hex:IPA 80:20) before analysis using Chiral HPLC on the OJ-H column with mobile phase Hex:IPA 80:20 and a flow rate of 1 mL min<sup>-1</sup>.

The pH of the aqueous mixture was subsequently adjusted to 4 and extracted with EtOAc (3 x 50 mL). The combined organic extracts were dried over Na<sub>2</sub>SO<sub>4</sub> and the solvent removed *in vacuo* to give the acid. The presence of acid product was confirmed by LC-MS as an initial screening method.

### 7.9.2 Larger-scale biotransformations

The biotransformation was carried out in a suspension of phosphate buffer (0.1 M, pH 7, 8, or 9) containing induced cells ( $OD_{600nm} = 1$ ). Racemic 3-aminobutyronitrile (0.0500 g, 0.59 mmol, 10 mM) was added to the flask and the mixture was incubated at 25°C for 3 days with mechanical shaking (200 rpm), monitored by TLC. The reaction was quenched by removal of the biomass by centrifugation. A 1 mL aliquot of the supernatant was removed and lyophilised in preparation for GITC derivatisation. The remaining supernatant was concentrated *in vacuo* and NaOH (4 mL, 2M) was added. A solution of Cbz-Osu (0.2941 g, 1.2 mmol) in THF (5 mL) was added at 0°C. The mixture was stirred at room temperature for 24 h. Cell blanks were

conducted as previously described, with the amendment that no cells were added to the reaction mixtures.

The pH was adjusted to 12 and the mixture was extracted with EtOAc (3 x 50 mL). The combined organic extracts were dried over Na<sub>2</sub>SO<sub>4</sub> and the solvent removed *in vacuo* to give the crude nitrile and amide. A solution of pre-prepared mobile phase (Hex:IPA 80:20) was added before analysis by Chiral HPLC on the OJ-H column with mobile phase Hex:IPA 80:20, and a flow rate of 1 mL min<sup>-1</sup>).

The pH of the aqueous mixture was then adjusted to 4 and extracted with EtOAc (3 x 50 mL). The combined organic extracts were dried over Na<sub>2</sub>SO<sub>4</sub> and the solvent removed *in vacuo* to give the acid and subjected to purification by prep TLC (Hex:EtOAc 70:30).

To determine the ee of acid, the lyophilised aliquot of the supernatant, triethylamine (0.2% w/v) and GITC (0.8% w/v) were added, including ACN (3 mL). The mixture was left to stir at 40°C for 1 h. The mixture was injected directly into the HPLC. The acid enantiomers were separated on a C18 Symmetry column with mobile phase MeOH:H<sub>2</sub>O 35:65 + 0.1% TFA and a flow rate of 1 mL min<sup>-1</sup>.

### 7.9.3 *Enantioselectivity screening of other bacterial isolates towards 3-aminobutyronitrile hydrochloride (124)*

A set of five bacterial isolates (isolates 3, 6, 12, 39, 46) acquired from the PMBRC isolate library, were screened for activity on 3-aminobutyronitrile on a 6 mL scale. The biotransformation was carried out in a suspension of phosphate buffer (0.1 M, pH 7 and 9) containing induced cells (OD<sub>600nm</sub>=1). Racemic 3-aminobutyronitrile (0.0103 g, 0.12 mmol, 10 mM) was added to each flask and the mixture was incubated at 25°C for 3 days with mechanical shaking (200 rpm). The reaction was quenched by removal of the biomass by centrifugation. A 1 mL aliquot of the supernatant was removed and lyophilised in preparation for GITC derivatisation to detect acid. The remaining supernatant was concentrated *in vacuo* and NaOH (4 mL, 2M) was added. A solution of *N*-carbobenzoxyoxysuccinimide (Cbz-Osu) (0.0598 g, 0.24 mmol) in THF (5 mL) was added at 0°C. The mixture was stirred at room temperature overnight (approximately 16 h minimum).

The pH was adjusted to 12 if necessary, with NaOH (1M) then the mixture was extracted with EtOAc (3 x 50 mL). The combined organic extracts were dried over Na<sub>2</sub>SO<sub>4</sub> and the solvent removed *in vacuo* to give the nitrile. A solution of the pre-prepared mobile phase (Hex:IPA 80:20) was added before analysis by Chiral HPLC on the OJ-H column with mobile phase Hex:IPA 80:20, and a flow rate of 1 mL min<sup>-1</sup>).

The pH of the aqueous mixture was then adjusted to 4 and extracted with EtOAc (3 x 50 mL). The combined organic extracts were dried over Na<sub>2</sub>SO<sub>4</sub> and the solvent removed *in vacuo* to give the acid.

To determine the ee of acid, triethylamine (0.2% w/v) and GITC (0.8% w/v) along with ACN (3 mL) were added to the lyophilised aliquot of the supernatant. The mixture was left to stir at 40°C for 1 h. The mixture was injected directly into the HPLC. The acid enantiomers were separated on a C18 Symmetry column with mobile phase MeOH:H<sub>2</sub>O 35:65 + 0.1% TFA and a flow rate of 1 mL min<sup>-1</sup>.

#### 7.9.4 Standard curves

Various standard curves were produced to aid in analysis for screening 3-aminobutyronitrile biotransformations, and to assist in high throughput investigations.

##### 7.9.4.1 *N*-Cbz protected 3-aminobutyronitrile and acid standard curves

Stock solutions of both the nitrile and acid standards were made up in Hex:IPA 90:10, with the acid standard containing 0.1% TFA. For the first standard curve for the nitrile, serial dilutions were carried out to give the following concentrations: 0.5 mg mL<sup>-1</sup>, 1 mg mL<sup>-1</sup>, 2 mg mL<sup>-1</sup>, 3 mg mL<sup>-1</sup>, 4 mg mL<sup>-1</sup>, 5 mg mL<sup>-1</sup>, 6 mg mL<sup>-1</sup>, and 7 mg mL<sup>-1</sup>. Serial dilutions were then carried out to give the following concentrations for a second nitrile curve and for the acid standard curve at: 0.03 mg mL<sup>-1</sup>, 0.06 mg mL<sup>-1</sup>, 0.12 mg mL<sup>-1</sup>, 0.3 mg mL<sup>-1</sup>, 0.48 mg mL<sup>-1</sup>, and 0.6 mg mL<sup>-1</sup>. These were analysed in duplicate by HPLC with mobile phase Hex:IPA 90:10 (+ 0.1% TFA for the acid samples) and a flow rate of 1 mL min<sup>-1</sup>. The standard curves are shown in Figure 7.1 to Figure 7.3.

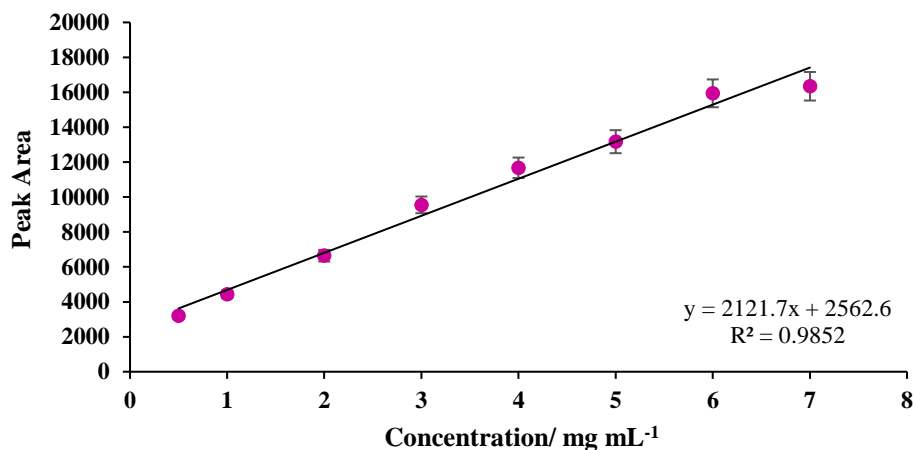


Figure 7.1: First HPLC standard curve of Benzyl (1-cyano-2-propenyl)carbamate. Analysis carried out on an IA column. Mobile phase Hex:IPA 90:10, at a flow rate of 1 mL.min<sup>-1</sup>. Error bars represent the error across the mean of the HPLC duplicates

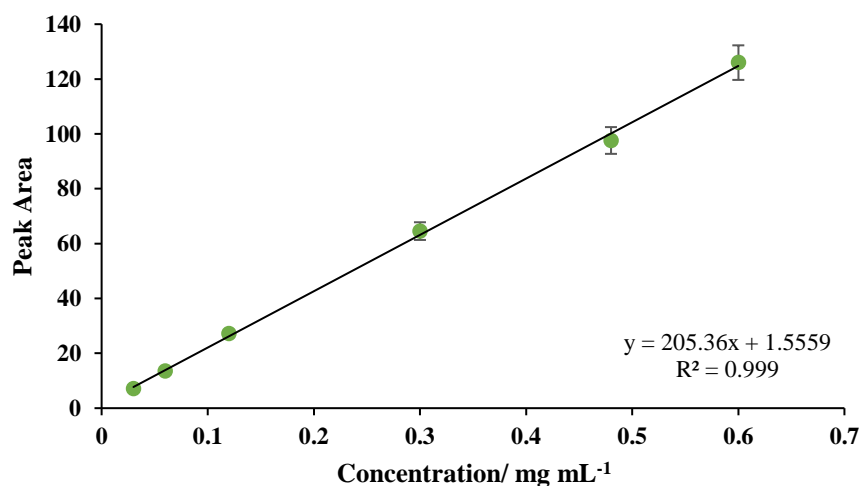


Figure 7.2: Second HPLC standard curve of Benzyl (1-cyano-2-propenyl)carbamate. Analysis carried out on an IA column. Mobile phase Hex:IPA 90:10, at a flow rate of 1 mL.min<sup>-1</sup>. Error bars represent the error across the mean of the HPLC duplicates

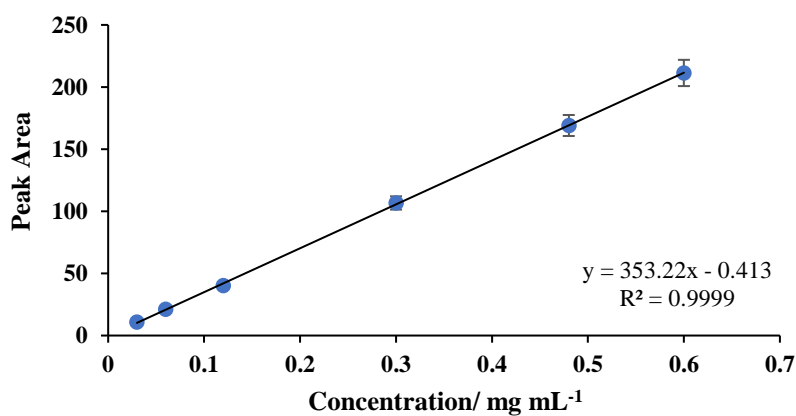


Figure 7.3: HPLC standard curve of 3-[(Benzyloxy)carbonyl]amino}butanoic acid. Analysis carried out on an IA column. Mobile phase Hex:IPA 90:10, + 0.1% TFA at a flow rate of 1 mL.min<sup>-1</sup>. Error bars represent the error across the mean of the HPLC duplicates

### 7.10 Biotransformations of *N*-Benzyl Protected Nitriles with SET1 – General Procedure

The biotransformation was carried out in a suspension of phosphate buffer (0.1 M, pH 7) containing induced cells ( $OD_{600nm}=1$ ). Racemic nitrile (0.0500 g, 10 mM) was added to the flask and the mixture was incubated at 25°C for 3 days with mechanical shaking (200 rpm). Reactions were followed by TLC. The reaction was quenched by removal of the biomass by centrifugation. The supernatant was concentrated *in vacuo* and HCl (1M, 5 mL) was added. This was left to stand at room temperature for 30 min then loaded on a manual cation exchange resin column (Amberlite® IR120, glass column) and eluted with water (200 mL) and 1% aqueous ammonia (200 mL) successively. The ammonia eluant was concentrated and purified on a semi-prep HPLC (Phenomenex Jupiter C18, 10  $\mu$ m), gradient elution (ACN:H<sub>2</sub>O + 0.1% formic acid), 5 mL min<sup>-1</sup>, to give acid and amide products, as well as any nitrile present. These were lyophilised then triethylamine (0.2% w/v) and GITC (0.8% w/v) were added, including ACN (3 mL). The mixture was left to stir at 40°C for 1 h. The mixture was injected directly into HPLC. The enantiomers were separated on a C18 Symmetry column with mobile phase MeOH:H<sub>2</sub>O 35:65 + 0.1% TFA and a flow rate of 1 mL min<sup>-1</sup>. Yields were acquired as isolated yields prior to GITC derivatisation. Products were characterised by NMR.

### 7.11 Biotransformations on *N*-Tosyl and *N*-Boc Protected Nitriles

The biotransformation was carried out in a suspension of phosphate buffer (0.1 M, pH 7) containing induced cells ( $OD_{600nm} = 1$ ). Racemic nitrile (0.0500 g, 10 mM) was added to the flask and the mixture was incubated at 25°C for 3 days with mechanical shaking (200 RPM). The reaction was quenched by removal of the biomass by centrifugation. The pellet was washed with EtOAc (5 mL). The pH of the supernatant was adjusted to 9 with NaOH (1M) and was extracted with dichloromethane (3 x 30 mL). The combined EtOAc and dichloromethane extracts were washed with water, then brine, then dried over Na<sub>2</sub>SO<sub>4</sub>. The solvent was removed *in vacuo* to give the nitrile and amide products.

For the *N*-tosyl nitrile and amide products, these had pre-prepared mobile phase (Hex:IPA 90:10, 1 mL) added to the nitrile samples and pre-prepared mobile phase (Hex:IPA 90:10 + 0.1% TFA, 1 mL) added to the amide samples, before analysis by Chiral HPLC on the IA

(Hex:IPA 90:10, flow rate 1 mL min<sup>-1</sup>) and OJ-H columns (Hex:IPA 90:10 + 0.1% TFA, flow rate 1 mL min<sup>-1</sup>) respectively. The pH of the supernatant was adjusted to 4 with NaOH (1M) and was extracted with dichloromethane (3 x 30 mL). The combined organic extracts were washed with water, then brine, then dried over Na<sub>2</sub>SO<sub>4</sub>. The solvent was removed *in vacuo* to give the acid product. The *N*-tosyl acid product was dissolved in a mixture of water:ethanol:pyridine (60:32:8). Ethyl chloroformate (120 μL) was added and the reaction mixture was stirred for 5 min. The mixture was extracted with chloroform including 1% ethyl chloroformate (2.4 mL). The solvent was removed *in vacuo* to give the ester product then pre-prepared mobile phase was added (Hex:IPA 90:10 +0.1% TFA) before analysis by chiral HPLC on the IA column with mobile phase Hex:IPA 90:10 +0.1% TFA and flow rate of 1 mL min<sup>-1</sup>. Products were characterised by LC-MS and NMR.

The *N*-boc nitrile recovered was hydrolysed to the amide. This was achieved by dissolving the recovered nitrile in methanol (3 mL) and to it, potassium carbonate (5 eq) and hydrogen peroxide (35%, 1 mL) were added. The mixture was stirred at room temperature and monitored by TLC. The product was worked up using extraction, dried over Na<sub>2</sub>SO<sub>4</sub> and the solvent removed *in vacuo*. The product was purified by silica flash chromatography Hex:EtOAc (70:30) and mobile phase (Hex:IPA 97:3 + 0.1% TFA) was added before analysis by Chiral HPLC on the IA column with mobile phase Hex:IPA 97:3 + 0.1% TFA and a flow rate 1.0 mL min<sup>-1</sup>. The same conditions were used to analyse the *N*-boc amide products.

The pH of the supernatant was adjusted to 4 and was extracted with dichloromethane (3 x 30 mL). The combined organic extracts were washed with water, then brine, then dried over Na<sub>2</sub>SO<sub>4</sub>. The solvent was removed *in vacuo* to give the acid product. The *N*-boc acid products had pre-prepared mobile phase (Hex:IPA 90:10 + 0.1% TFA) added before analysis by chiral HPLC on the OJ-H column with mobile phase Hex:IPA 90:10 + 0.1% TFA and a flow rate 1.0 mL min<sup>-1</sup>. Products were characterised by LC-MS.

## 7.12 Purification and Identification of Contaminated Isolates

### 7.12.1 Agar plates preparation and cell culture

M9 agar plates: Deionised water (776 mL) was added to minimal agar (15 g). This was autoclaved and 5X M9 minimal media basis (200 mL), trace elements (1 mL), FeSO<sub>4</sub> (1 mL),

glucose (20 mL), CaCl<sub>2</sub> (1 mL), MgSO<sub>4</sub> (1 mL) and 3-hydroxybutyronitrile (43.6 µL, 5 mM) were added. This was poured into sterile plates and allowed to set.

Nutrient agar plates: Deionised water (1000 mL) was added to nutrient agar (29 g) and this was autoclaved. This was then poured into sterile plates and allowed to set.

These agar plates were used to streak out the bacterial colonies which were then allowed to incubate at 25°C for 3 days (nutrient agar) or 4 days (M9 agar) and then subsequently incubated at 4°C for 2 nights. The plates were visually assessed and if observed to be pure, the selected colonies were stocked in a mixture of M9-minimal media and glycerol 70%.

### 7.12.2 Procedure for PCR

Glycerol stocks of the isolates were thawed and centrifuged. The supernatant was decanted, and sterile deionised water (1 mL) was added. The optical density was adjusted to OD<sub>600nm</sub> = 1. The primer mix was created by adding 5 µL forward primer 63f (5 µL) and reverse primer 1387r (5 µL) to sterile deionised water (30 µL) to give a 25 µM primer mix. The 2X GoTaq Green Master Mix was already pre-optimised and contained; Taq polymerase, buffer, MgCl<sub>2</sub>, and Dntps. The final PCR recipe was composed of 1X GoTaq Master Mix (12.5 µL), primer mix (1 µL, 0.5 µM), sterile de-ionised water (10 µL), and cells at OD<sub>600nm</sub> = 1 (1.5 µL). PCR was performed using the following cycle; initially there was a 5 min hold at 95°C, after which there were 30 cycles of: 95°C for 1 min, 56°C for 1 min, and 72°C for 1.5 min. This was followed by running at 72°C for 8 min and the cycle was ended with a hold step at 4°C.

### 7.12.3 Procedure for electrophoresis

The gel was prepared with agarose (0.4 g, 0.8%) and TAE buffer (50 mL, 1X). This was heated to aid in dissolving the agarose. Ethidium bromide (2.5 µL) was then added and the gel was poured into the well to set. The ladders used were Promega, 100 bp DNA (5 µL) and Promega 1 Kb DNA (5 µL) with blue/orange loading dye. The amplified DNA (5 µL) acquired from the PCR reaction was added to the subsequent wells, including a blank which had sterile deionised

water (5  $\mu\text{L}$ ). The gel was run for 25 min at 180 V, 108 mA, and 19 W. The gel was then visualised.

#### 7.12.4 Procedure for sequencing

To each 20  $\mu\text{L}$  volume of the DNA sample, DNA binding buffer (40  $\mu\text{L}$ ) was added. The mixture was then loaded into a Zymo-Spin column which in turn was then placed into a 2 mL collection tube. This was centrifuged at 15000 rpm for 10 seconds. The flow-through was discarded. Wash buffer (200  $\mu\text{L}$ ) was added to the column and this was centrifuged for 10 seconds. Another 200  $\mu\text{L}$  of wash buffer was added, and the column was centrifuged to 30 seconds. The Zymo-Spin column was placed into a new 1.5 mL tube. Water (10  $\mu\text{L}$ ) was added and the column was centrifuged for seconds to elute the DNA. The concentration of the DNA was determined by the NanoDrop® spectrophotometer ND1000 and the volumes were adjusted with sterile deionised water to give a concentration between 50 – 80 ng/ $\mu\text{L}$  in 5  $\mu\text{L}$  solution. The adjusted DNA samples were then sent off for sequencing at a different location.

### 7.13 Screening of The Purified Enzyme Nit1 with Unprotected and N-Protected Nitriles

#### 7.13.1 Nessler's microscale ammonia assay for determination of Nit1 activity

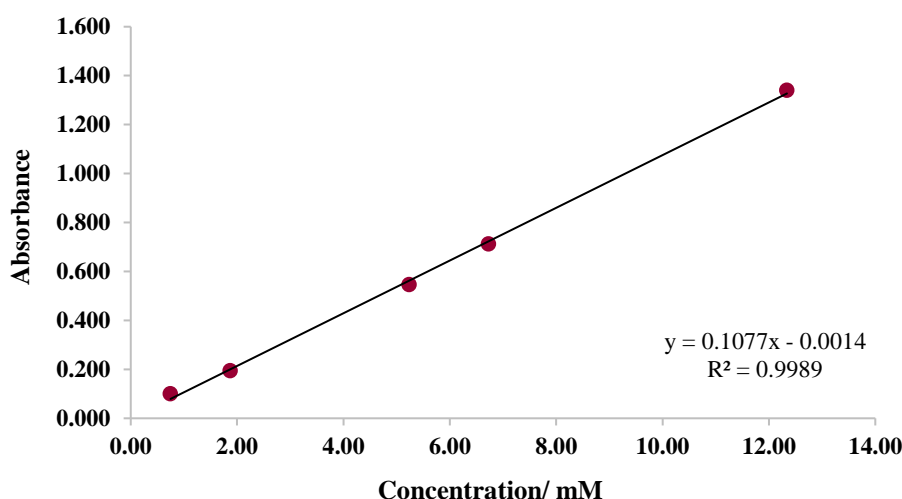
The required concentration of Nit1 enzyme for use in biocatalytic reactions was determined for each batch of purified enzyme using the Nessler's colorimetric assay. A stock solution of 4-HPAN in ethanol (2 mL) was prepared to give a concentration of 200 mM. The biotransformation was carried out in phosphate buffer (1.0 M, pH 7) to which 4-HPAN in ethanol was added was (10 mM), followed by the addition of Nit1. After incubation and shaking for 24 h, the reaction was quenched by the addition of HCl (37.5  $\mu\text{L}$ , 250 mM). The Eppendorf tubes were centrifuged at 15000 rpm for 5 min. The supernatant (20  $\mu\text{L}$ ) was transferred to a microtitre plate and 181  $\mu\text{L}$  of assay mastermix was added (155  $\mu\text{L}$  deionised water, 1  $\mu\text{L}$  NaOH (10 M), 25  $\mu\text{L}$  Nessler's reagent). The reaction was allowed to stand for 10 minutes and the UV absorbance was read at 425 nm. Nessler's blank contained 181  $\mu\text{L}$  of



Nessler's mastermix and 20  $\mu$ L of phosphate buffer (pH 7). The absorbance values were then related back to a standard curve to calculate the concentration of ammonia generated and thus the enzyme activity.

### 7.13.2 Standard curve for Nessler's colorimetric assay for HPAN activity determination

The required amounts of ammonium chloride were weighed on an analytical balance and each was dissolved in potassium phosphate buffer (pH 7, 5 mL). This generated standards with the following concentrations: 1 mM, 2 mM, 3 mM, 4 mM, 5 mM, 7 mM, 10 mM, 12 mM. The absorbance of each solution was then measured at 425 nm using a spectrometer along with a blank sample containing 181  $\mu$ L of Nessler's mastermix and 20  $\mu$ L of phosphate buffer (pH 7). This allowed the standard curve in Figure 7.4 to be produced.



**Figure 7.4:** Representative Nessler's standard curve. \*points at 3, 4, and 10 mM excluded as outliers

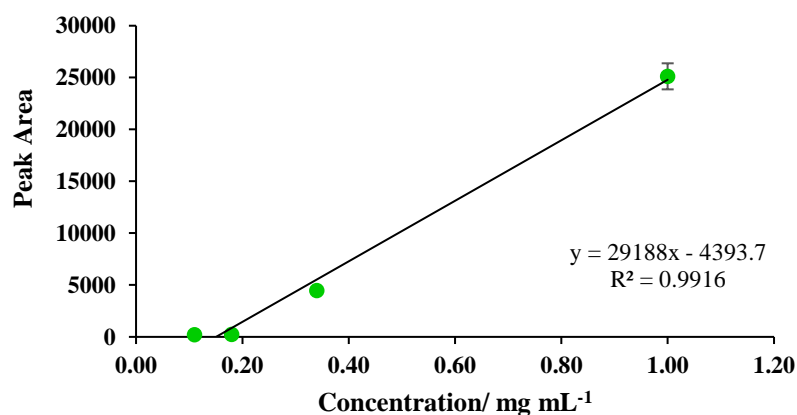
### 7.13.3 Procedure for Nit1 screening with nitriles

Stock solutions of the nitrile were prepared to give a 200 mM concentration in the relevant system (100% phosphate buffer or 100% water). In the case where solvent was required, DMSO or EtOH was added to give a final solvent concentration of 5% in the 200  $\mu$ L reaction. 10  $\mu$ L of the nitrile solution was added to Eppendorf tubes, followed by the calculated volume of purified enzyme from the Nessler's assay, then the relevant solvent system was added (100%

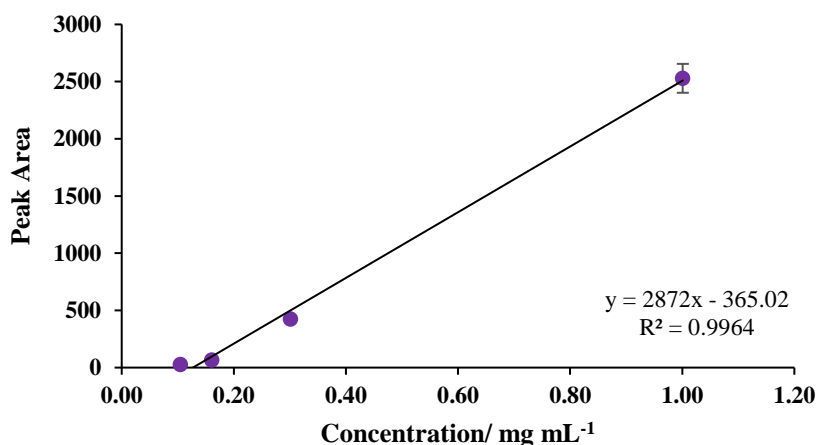
phosphate buffer or 100% water) to bring the total reaction volume to 200  $\mu\text{L}$ . The mixture was incubated at 25°C for 3 days with mechanical shaking (200 rpm). The reaction was quenched by the addition of ACN (600  $\mu\text{L}$ ) then the removal of the biomass by centrifugation. For the unprotected nitrile and the *N*-benzyl nitrile, the supernatant was removed and lyophilised. Triethylamine (0.2% w/v) and GITC (0.8% w/v) were then added, including ACN (3 mL). The mixture was left to stir at 40°C for 1 h. The mixture was then injected directly into the HPLC. The enantiomers were separated on a C18 Symmetry column. For the *N*-boc and *N*-tosyl nitriles, the supernatant was acidified with HCl (1M), extracted with EtOAc, dried and made up in pre-prepared mobile phase for HPLC analysis as described previously. Enzyme blanks were prepared for all the substrates and analysed accordingly.

#### 7.10.1.1 Standard curves of GITC-3-aminobutyronitrile and acid

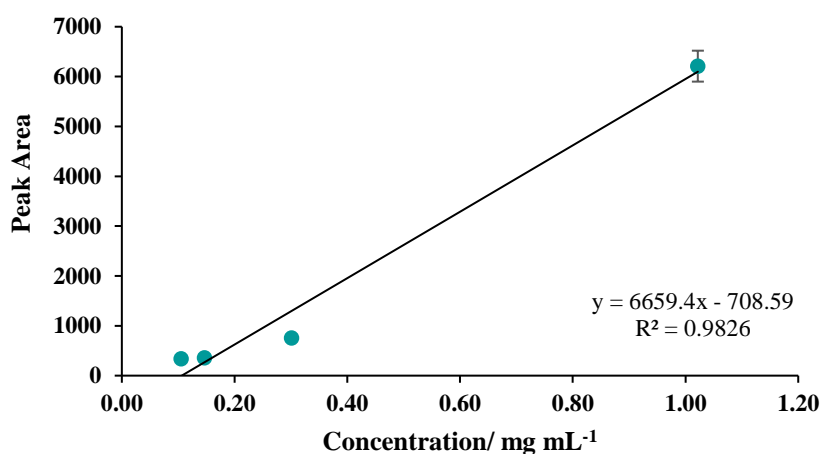
For the studies carried out with Nit1, standard curves were made for GITC-3-aminobutane nitrile and GITC-3-aminobutyric acid. The nitrile and acid standards were taken through the relevant workup to include possible solvent effects. The standards were weighed on an analytical balance to give the following concentrations: 0.05  $\text{mg mL}^{-1}$ , 0.10  $\text{mg mL}^{-1}$ , 0.15  $\text{mg mL}^{-1}$ , 0.30  $\text{mg mL}^{-1}$ , 1.00  $\text{mg mL}^{-1}$ , and 2.50  $\text{mg mL}^{-1}$  and diluted to a final volume of 1 mL in the respective solvent systems (100% phosphate buffer at pH 7, phosphate buffer at pH 7 + 5% DMSO, phosphate buffer at pH 7 + 5% EtOH, 100%  $\text{H}_2\text{O}$ ). These were then lyophilised for 24 h, then derivatised using GITC as outlined previously. The standards were analysed by HPLC in duplicate. The respective curves are shown in Figure 7.5 to Figure 7.12.



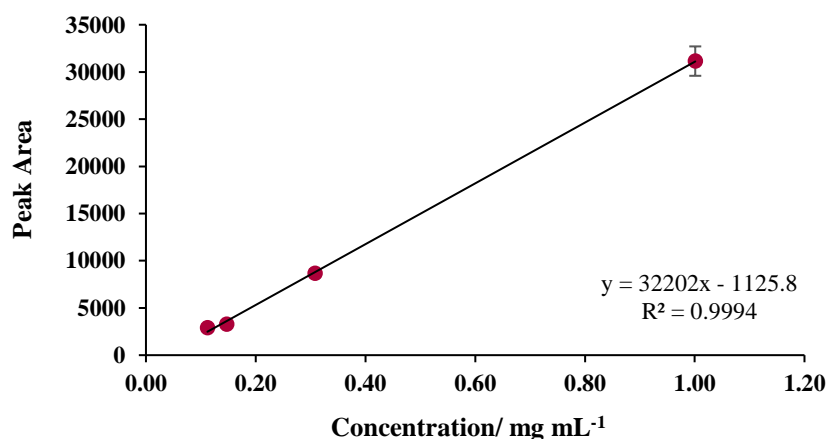
**Figure 7.5:** HPLC standard curve of GITC-3-aminobutyronitrile in 100% phosphate buffer at pH 7. Mobile phase MeOH:H<sub>2</sub>O 35:65 +0.1% TFA, flow rate 1 mL.min<sup>-1</sup>. Error bars represent the error across the mean of the HPLC duplicates



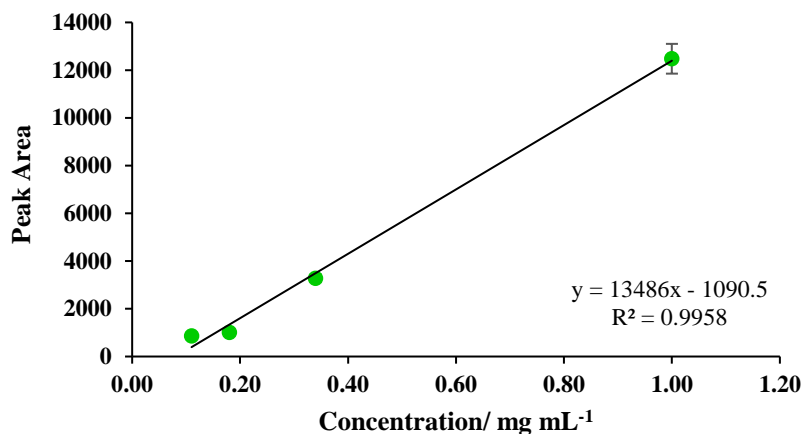
**Figure 7.6:** HPLC standard curve of GITC-3-aminobutyronitrile in phosphate buffer with 5% DMSO at pH 7. Mobile phase MeOH:H<sub>2</sub>O 35:65 +0.1% TFA, flow rate 1 mL.min<sup>-1</sup>. Error bars represent the error across the mean of the HPLC duplicates



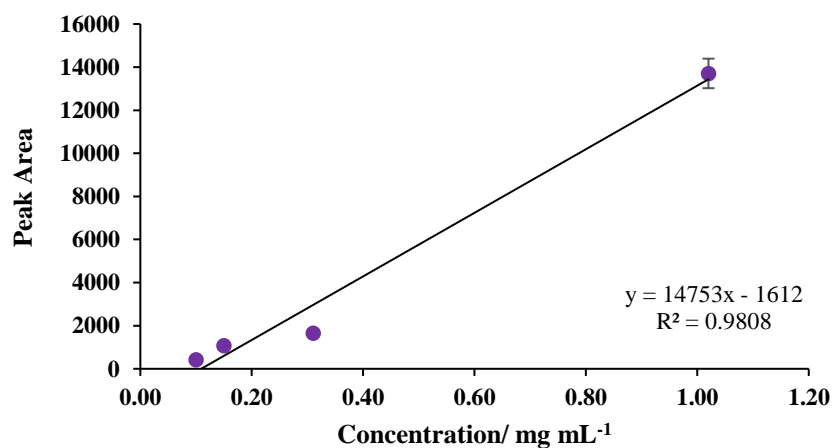
**Figure 7.7:** HPLC standard curve of GITC-3-aminobutyronitrile in phosphate buffer with 5% EtOH at pH 7. Mobile phase MeOH:H<sub>2</sub>O 35:65 +0.1% TFA, flow rate 1 mL.min<sup>-1</sup>. Error bars represent the error across the mean of the HPLC duplicates



**Figure 7.8:** HPLC standard curve of GITC-3-aminobutyronitrile in 100% H<sub>2</sub>O at pH 7. Mobile phase MeOH:H<sub>2</sub>O 35:65 +0.1% TFA, flow rate 1 mL.min<sup>-1</sup>. Error bars represent the error across the mean of the HPLC duplicates



**Figure 7.9:** HPLC standard curve of GITC-3-aminobutyric acid in 100% phosphate buffer at pH 7. Mobile phase MeOH:H<sub>2</sub>O 35:65 +0.1% TFA, flow rate 1 mL.min<sup>-1</sup>. Error bars represent the error across the mean of the HPLC duplicates



**Figure 7.10:** HPLC standard curve of GITC-3-aminobutyric acid in phosphate buffer with 5% DMSO at pH 7. Mobile phase MeOH:H<sub>2</sub>O 35:65 +0.1% TFA, flow rate 1 mL.min<sup>-1</sup>. Error bars represent the error across the mean of the HPLC duplicates

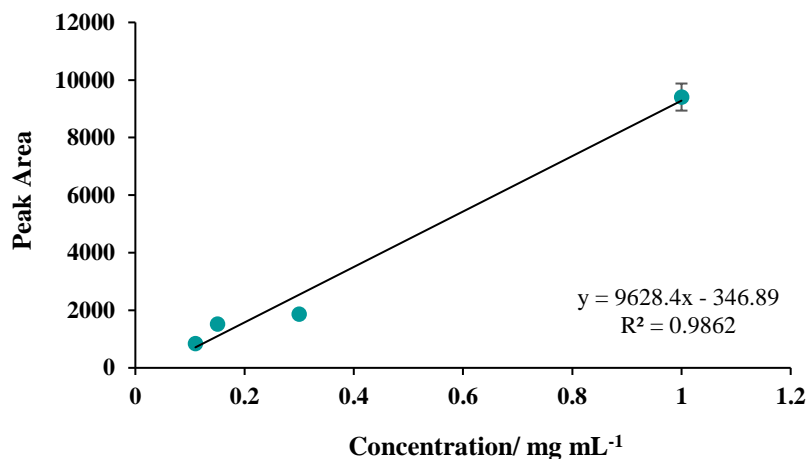


Figure 7.11: HPLC standard curve of GITC-3-aminobutyric acid in phosphate buffer with 5% EtOH at pH 7. Mobile phase MeOH:H<sub>2</sub>O 35:65 +0.1% TFA, flow rate 1 mL.min<sup>-1</sup>. Error bars represent the error across the mean of the HPLC duplicates

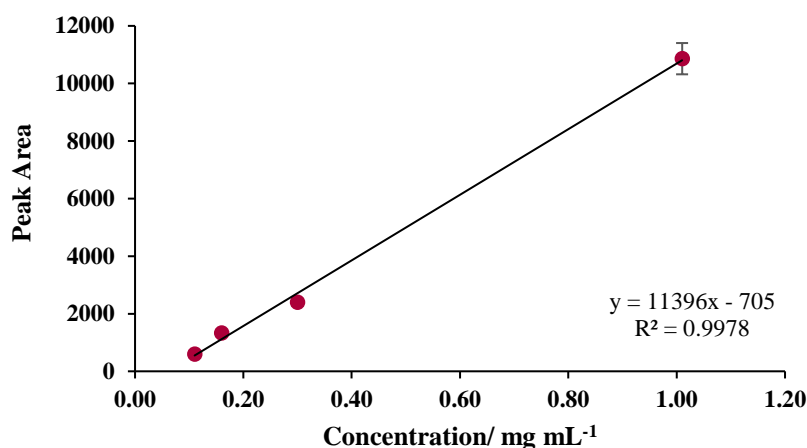


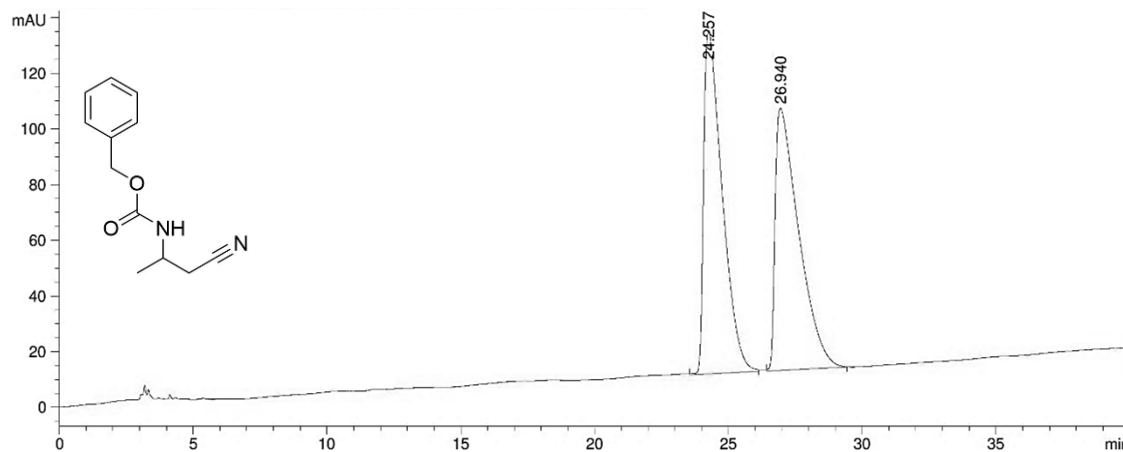
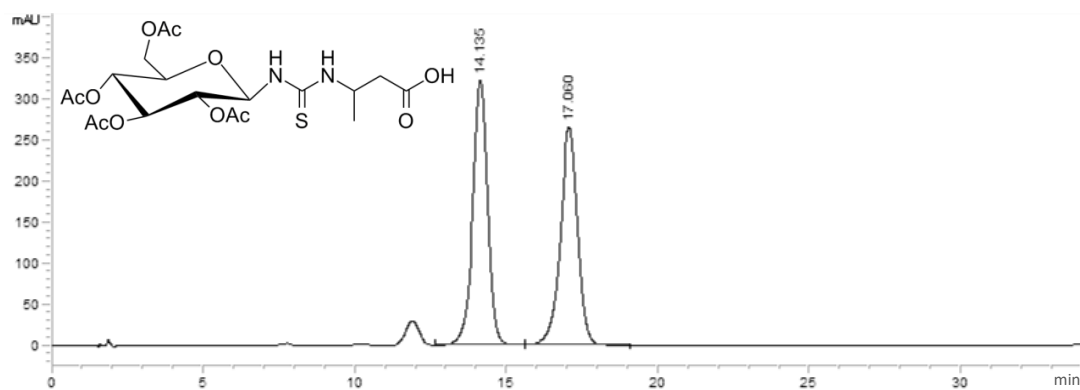
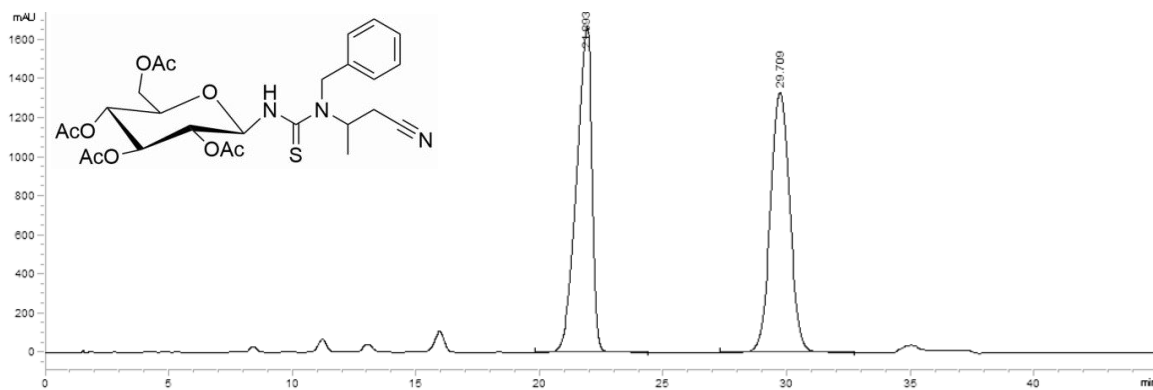
Figure 7.12: HPLC standard curve of GITC-3-aminobutyric acid in 100% H<sub>2</sub>O at pH 7. Mobile phase MeOH:H<sub>2</sub>O 35:65 +0.1% TFA, flow rate 1 mL.min<sup>-1</sup>. Error bars represent the error across the mean of the HPLC duplicates

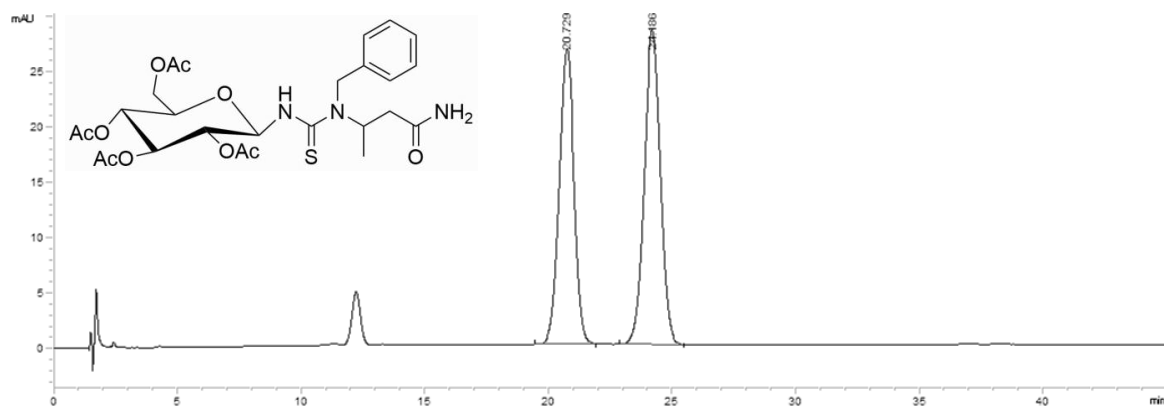
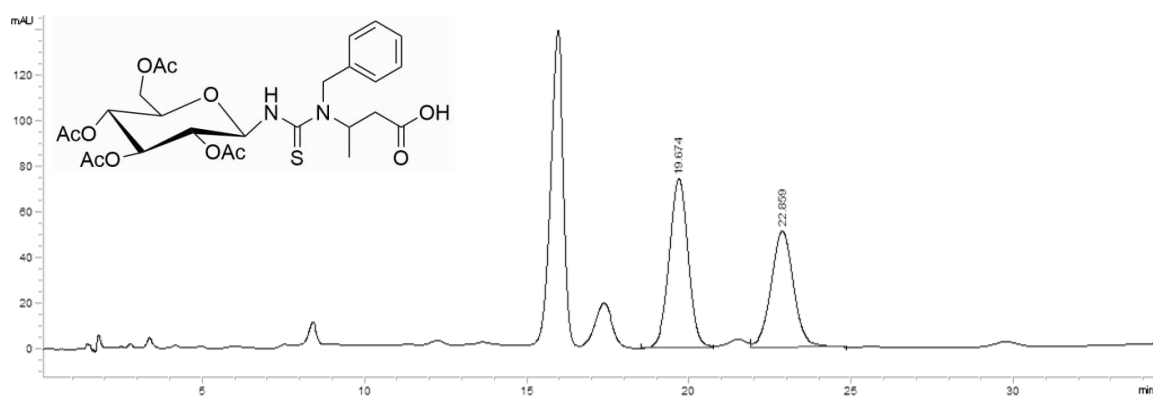
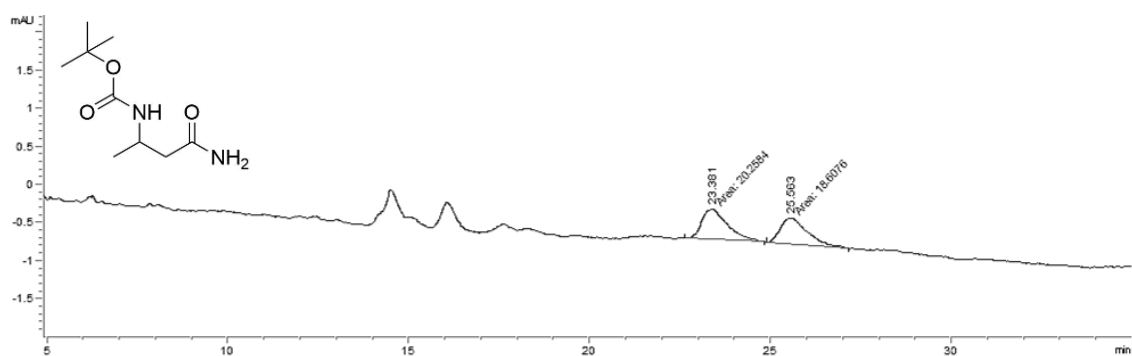
## REFERENCES

1. Coady, Tracey. M. *et al.* *Substrate Evaluation of Rhodococcus erythropolis SET1, a Nitrile Hydrolysing Bacterium, Demonstrating Dual Activity Strongly Dependent on Nitrile Sub-Structure.* European Journal of Organic Chemistry, 2015, **2015**, (5), 1108-1116

2. Bragança, Caio. Roberto. Soares. *Development of Recombinant Enzymes Towards the Production of Pharmaceutical Intermediates Using Biotransformations*, Doctor of Philosophy thesis, Waterford Institute of Technology, (2020).
3. Dooley-Cullinane, Tríona. Marie. *The Identification of Genes and Enzymes in the Aldoxime-nitrile Metabolising Pathway*, PhD thesis, Waterford Institute of Technology, (2019).
4. Ma, Da-You. *et al.* *Nitrile Biotransformations for the Synthesis of Highly Enantioenriched  $\beta$ -Hydroxy and  $\beta$ -Amino Acid and Amide Derivatives*. *Journal of Organic Chemistry*, 2008, **73**, (11), 4087-4091
5. Chhiba, Varsha. *et al.* *Enantioselective Biocatalytic Hydrolysis of  $\beta$ -aminonitriles to  $\beta$ -Amino-amides Using *Rhodococcus rhodochrous* ATCC BAA-870*. *Journal of Molecular Catalysis B: Enzymatic*, 2012, **76**, 68-74
6. Dondoni, Alessandro. *et al.* *A Facile and General Entry to C-Glycosyl (R)- and (S)- $\beta$ -Amino Acid Pairs from Glycosyl Cyanides Through Enamino Ester Intermediates*. *Synlett*, 2006, (4), 0539-0542
7. Abdel-Magid, Ahmed F. *et al.* *Reductive Amination of Aldehydes and Ketones with Sodium Triacetoxyborohydride*. *Journal of Organic Chemistry*, 1996, **61**, (11), 3849-3862
8. Winkler, Margit. *et al.* *Synthesis and Microbial Transformation of  $\beta$ -amino Nitriles*. *Tetrahedron*, 2005, **61**, (17), 4249-4260
9. Husek, Petr. *Rapid Derivatization and Gas Chromatographic Determination of Amino Acids*. *Journal of Chromatography*, 1991, **552**, 289-299
10. Mitsukura, Koichi. *et al.* *Asymmetric Synthesis of Chiral Amine From Cyclic Imine by Bacterial Whole-cell Catalyst of Enantioselective Imine Reductase*. *Organic & Biomolecular Chemistry*, 2010, **8**, (20), 4533-4535

## APPENDIX I

*HPLC chromatograms of synthesised  $\beta$ -aminonitrile substrates and products***Figure 1.1: Benzyl (1-cyano-2-propanyl)carbamate (155)****Figure 1.2: GITC-3-aminobutyric acid (158)****Figure 1.3: GITC-3-(benzylamino)butyronitrile (160)**

**Figure 1.4: GITC-3-(benzylamino)butanamide (161)****Figure 1.5: GITC-3-(benzylamino)butyric acid (144)****Figure 1.6: *tert*-butyl 1-carbanoylpropan-2-ylcarbamate (145)**



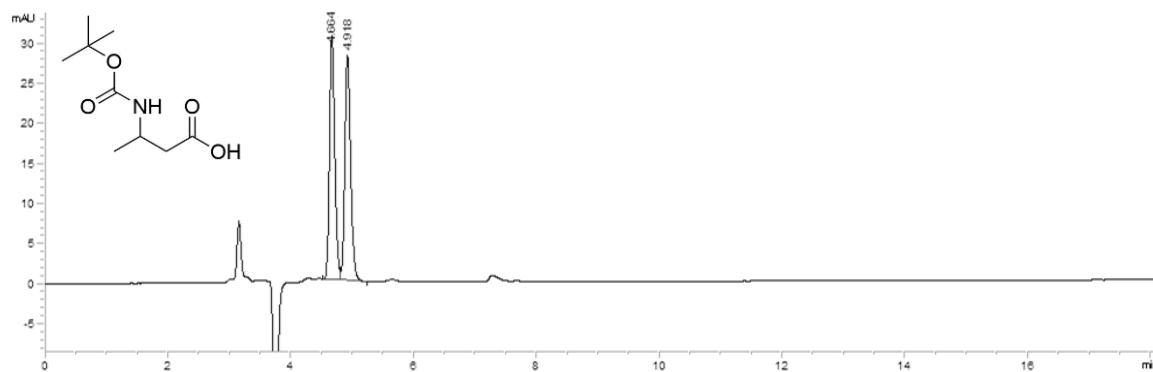


Figure 1.7: 3-((*tert*-butoxycarbonyl)amino)butanoic acid (146)

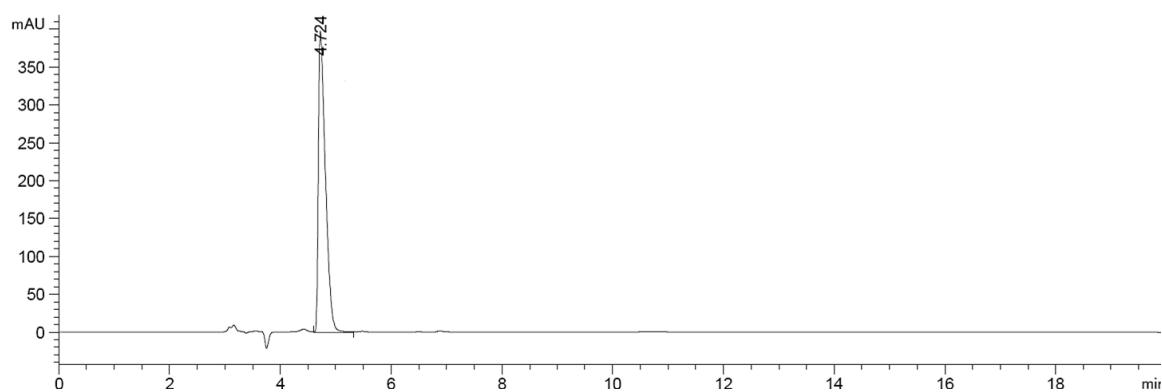


Figure 1.8: (*R*)-3-((*tert*-butoxycarbonyl)amino)butanoic acid (146b)

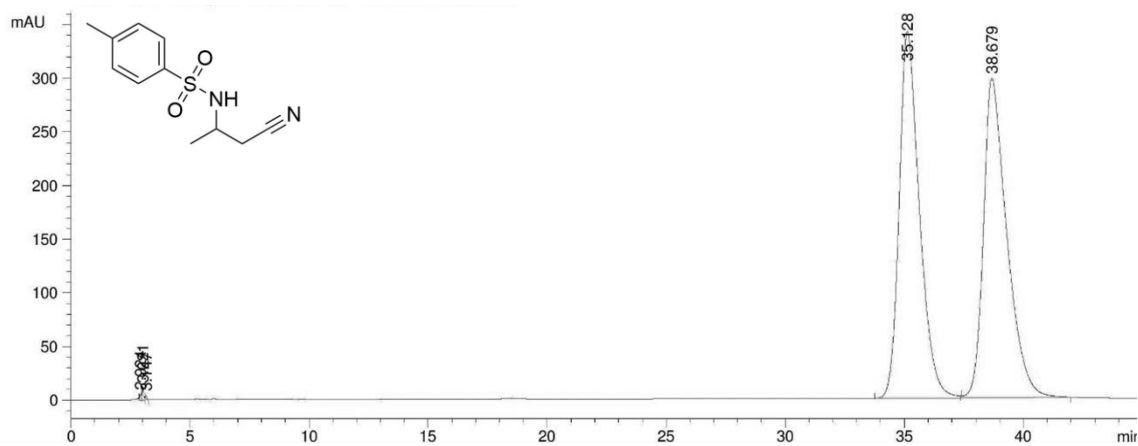


Figure 1.9: *N*-(1-cyano-2-propanyl)-4-methylbenzenesulfonamide (127)

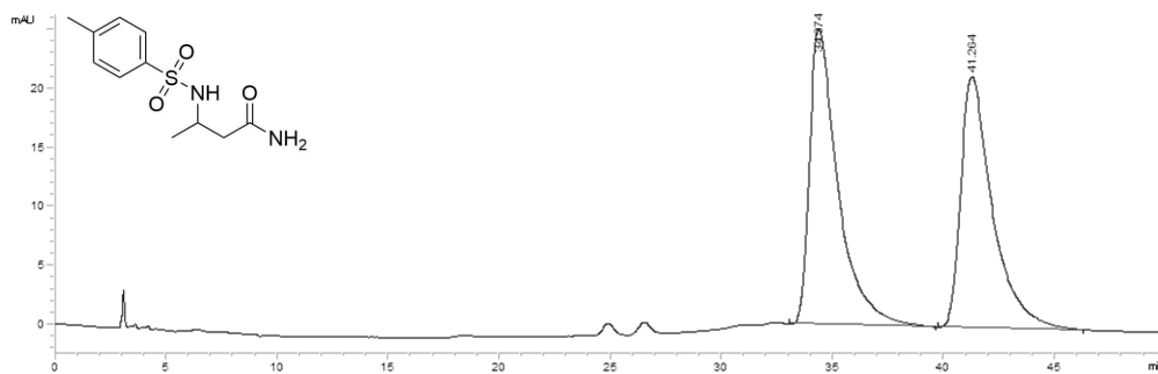


Figure 1.10: 3-(4-methylphenylsulfonamido)butanamide (147)

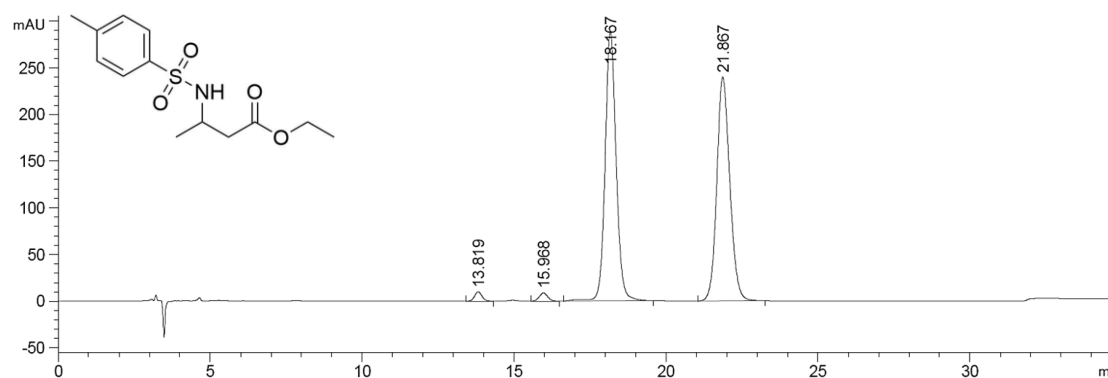


Figure 1.11: Ethyl-3-[[4-(4-methylphenyl)sulfonyl]amino]butanoate (164)

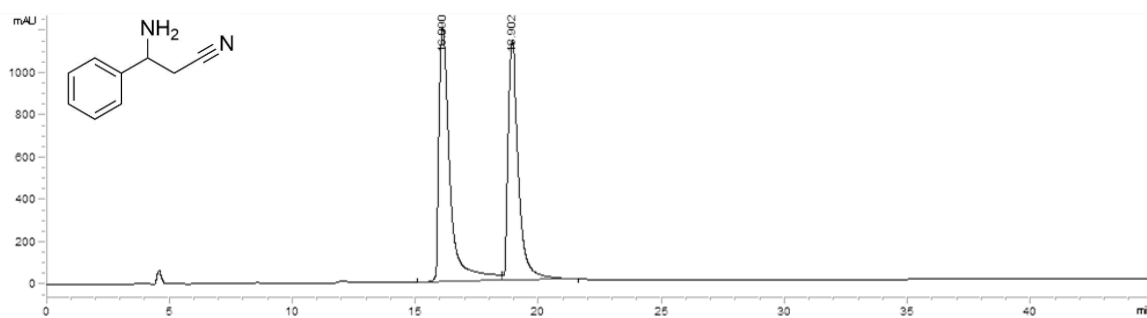


Figure 1.12: 3-amino-3-phenylpropionitrile (122)

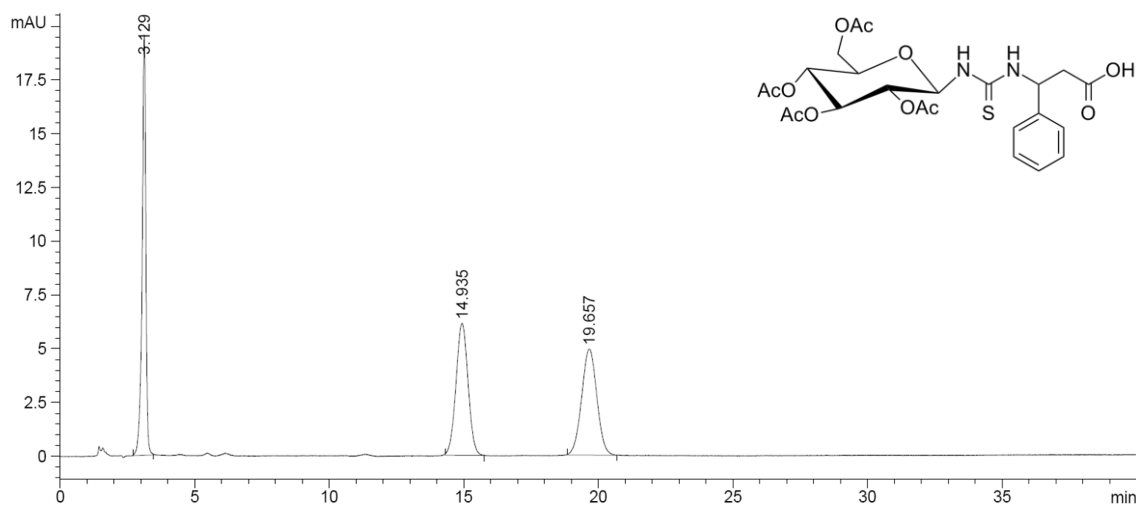


Figure 1.13: GITC-3-amino-3-phenylpropionic acid (165)

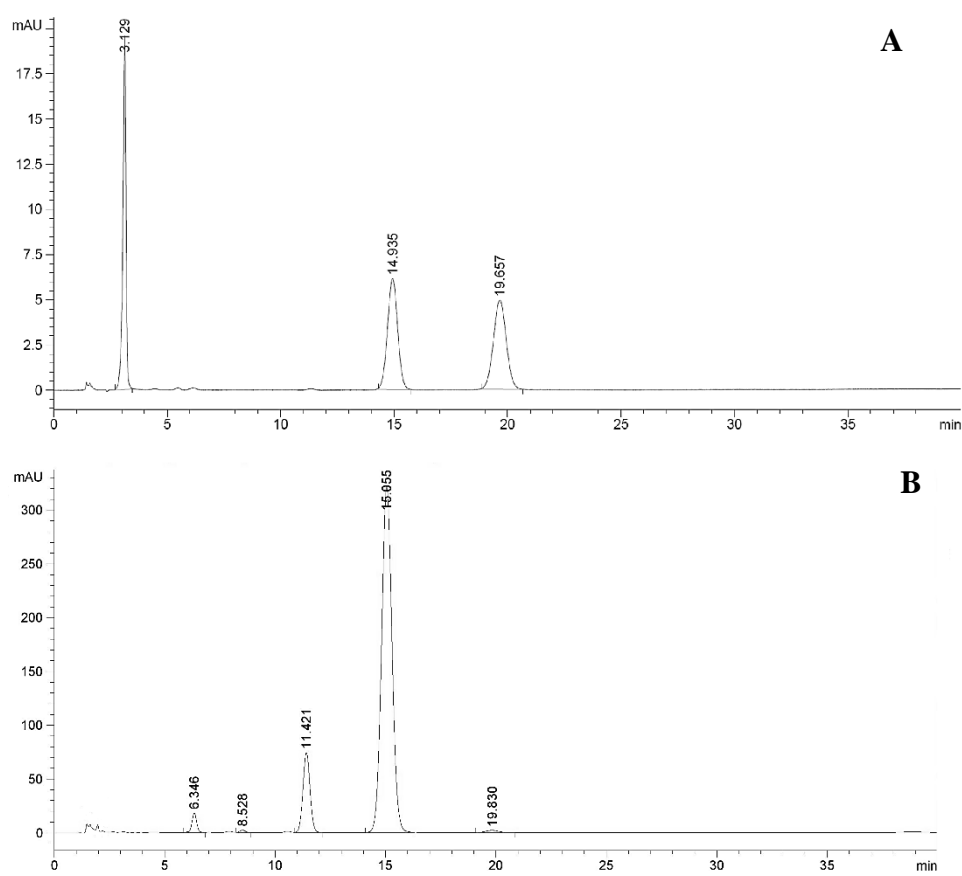


Figure 1.14: A - GITC-3-amino-3-phenylpropionic acid, B - GITC-(R)-3-amino-3-phenylpropionic acid

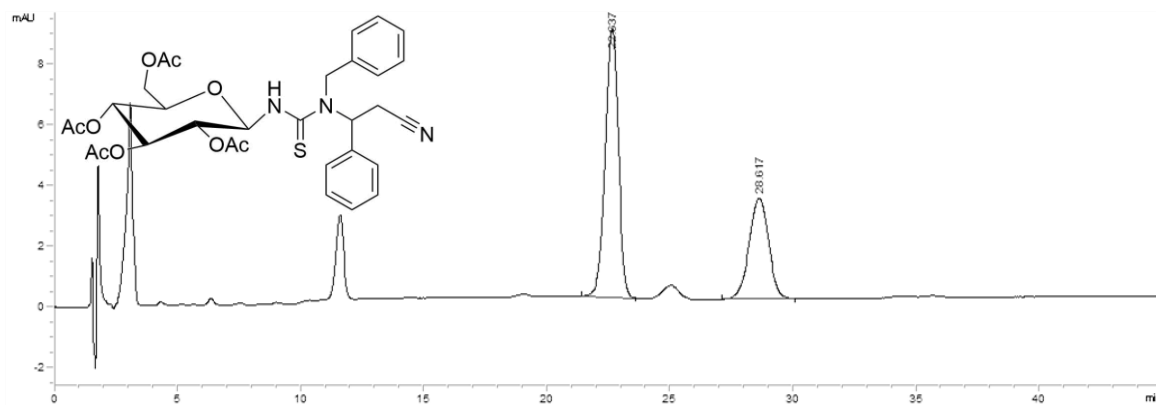


Figure 1.15: GITC-3-(benzylamino)-3-phenylpropanenitrile (166)

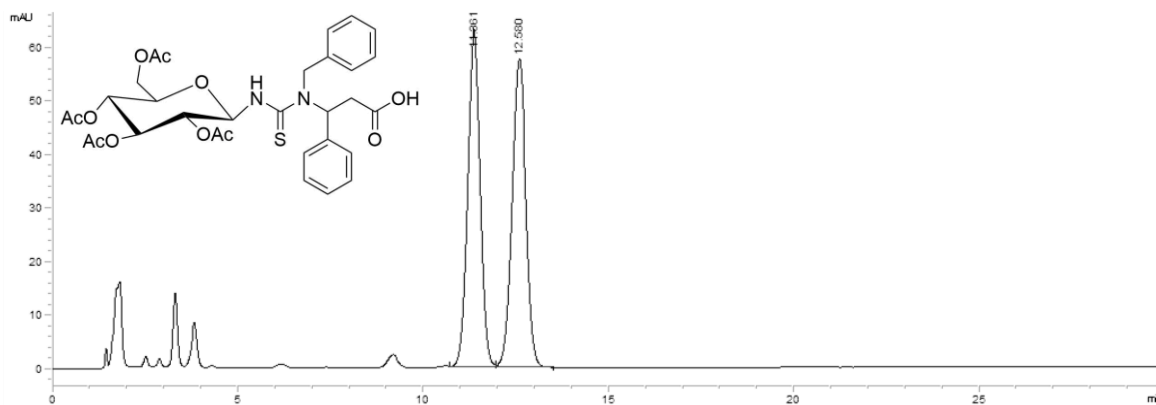


Figure 1.16: GITC-3-(benzylamino)-3-phenylpropanoic acid (167)

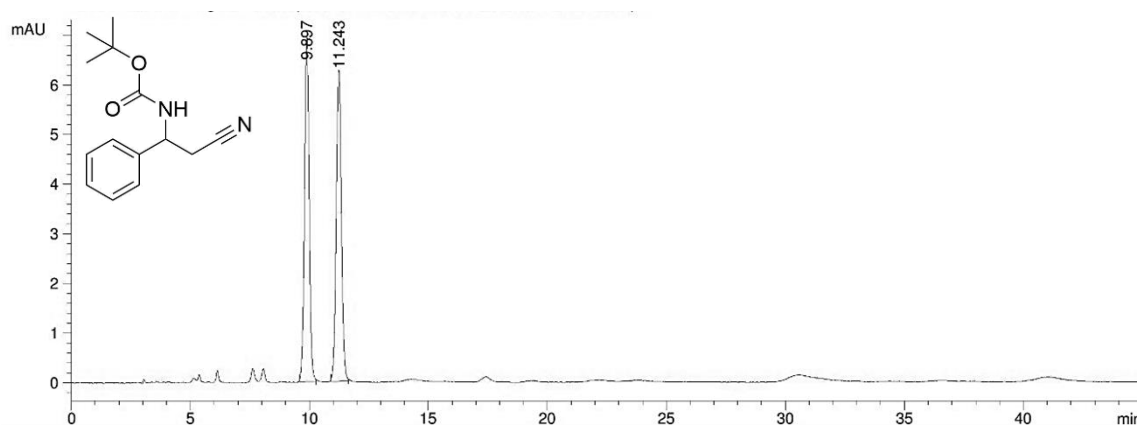


Figure 1.17: *tert*-Butyl (2-cyano-1-phenylethyl)carbamate (129)

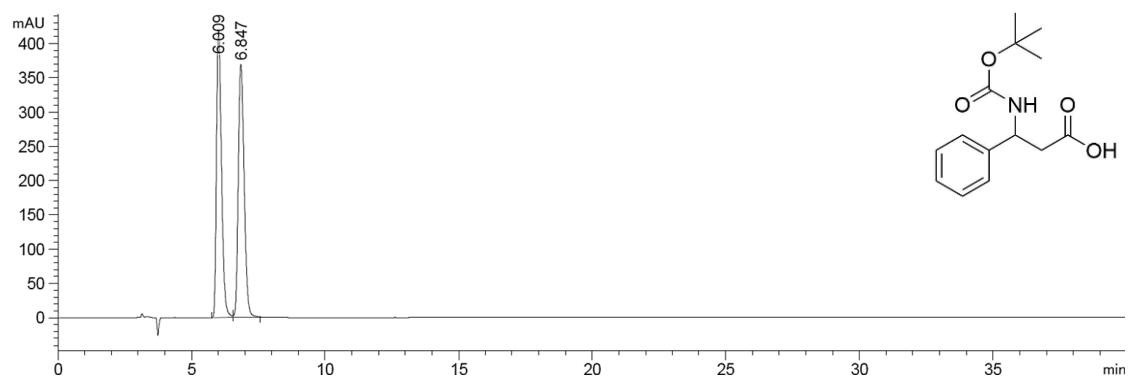


Figure 1.18: 3-(*tert*-butoxycarbonylamino)-3-phenylpropanoic acid (151)

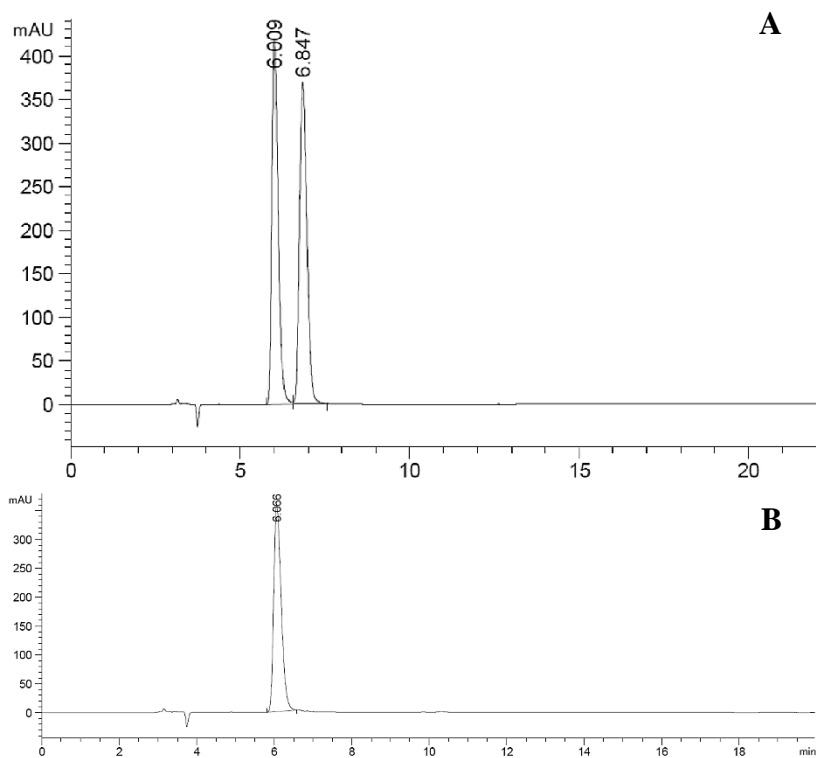


Figure 1.19: A – 3-(*tert*-butoxycarbonylamino)-3-phenylpropanoic acid, B – (*R*)-3-(*tert*-butoxycarbonylamino)-3-phenylpropanoic acid

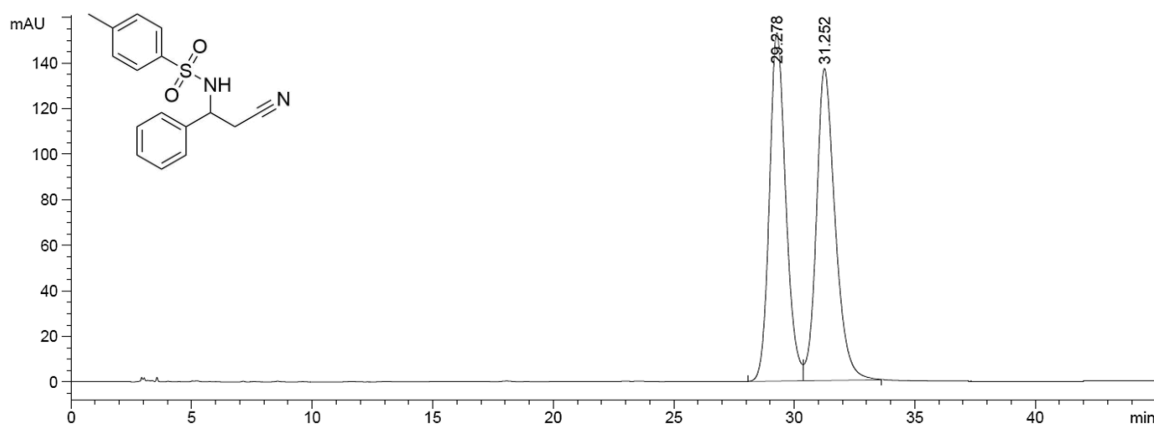


Figure 1.20: *N*-(2-cyano-1-phenylethyl)-4-methylbenzenesulfonamide (45)

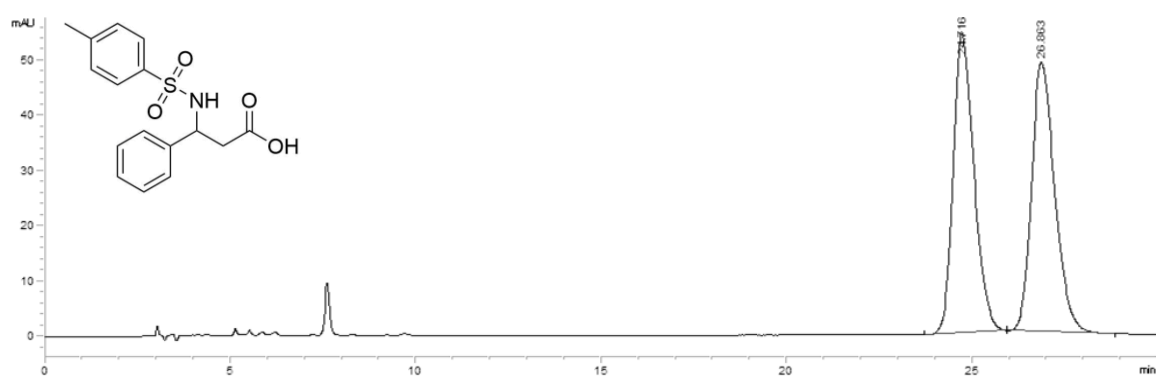


Figure 1.21: 3-[[4-methylphenyl]sulfonyl]amino-3-phenylpropanoic acid (152)

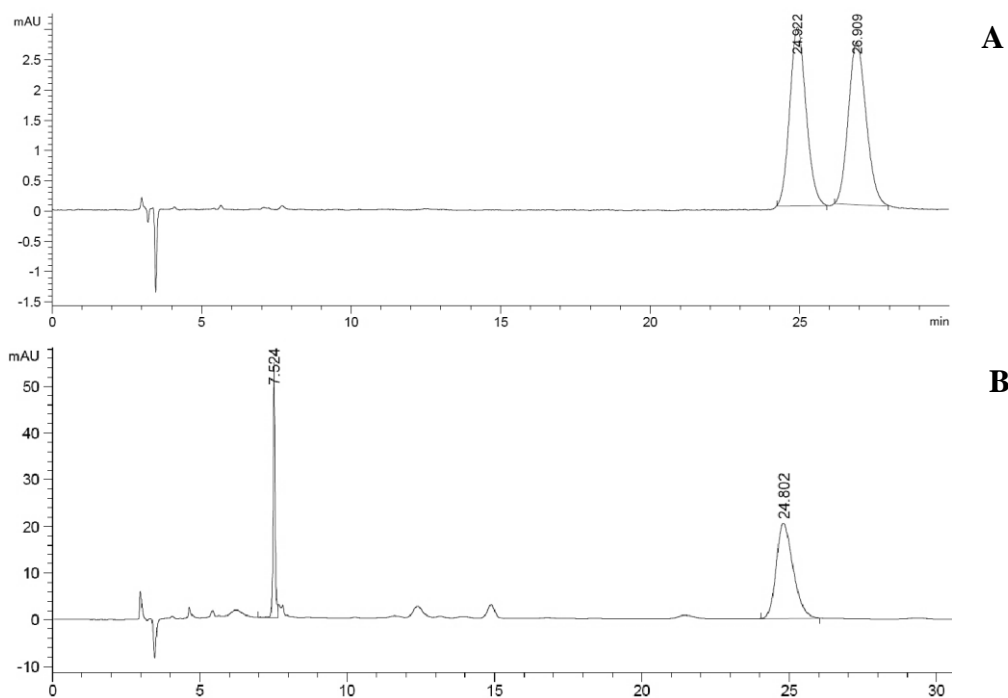
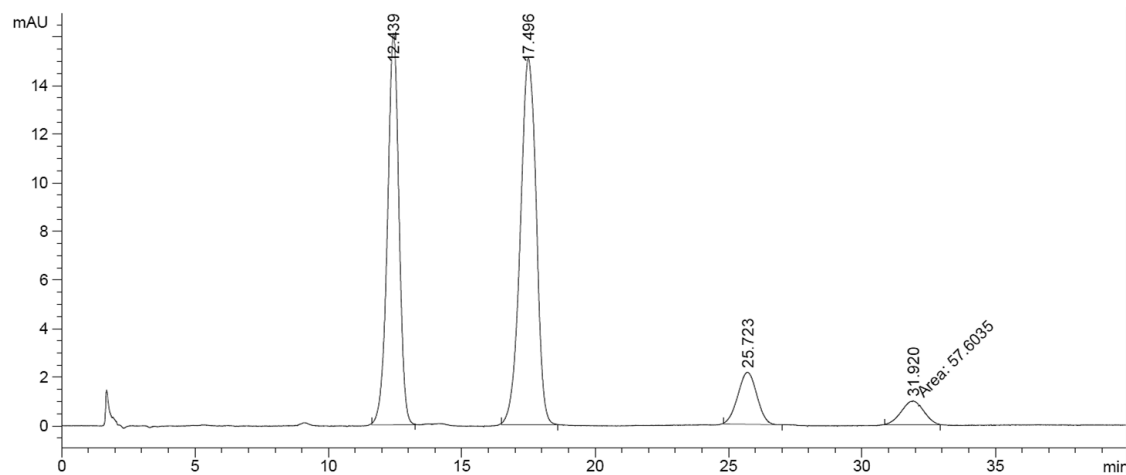
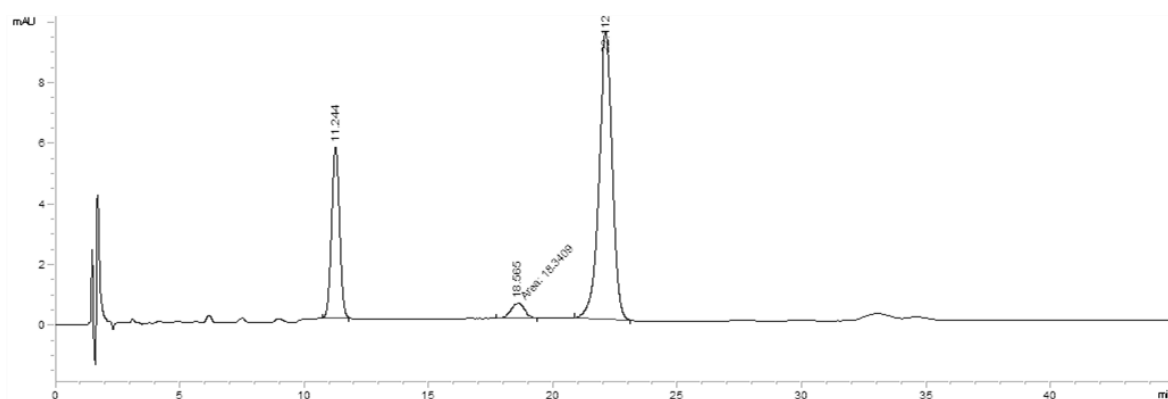


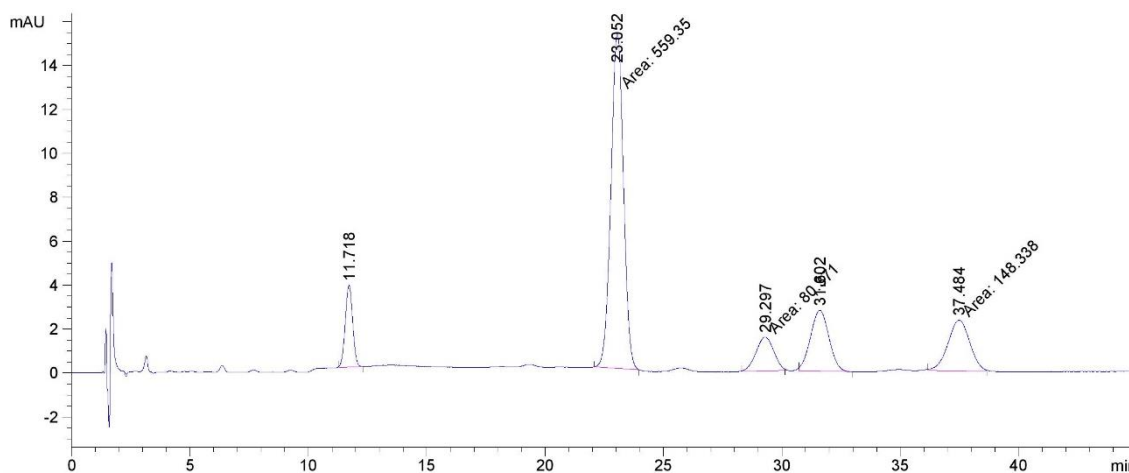
Figure 1.22: **A** – 3-[[4-methylphenyl]sulfonyl]amino-3-phenylpropanoic acid, **B** - (*R*)-3-[[4-methylphenyl]sulfonyl]amino-3-phenylpropanoic acid



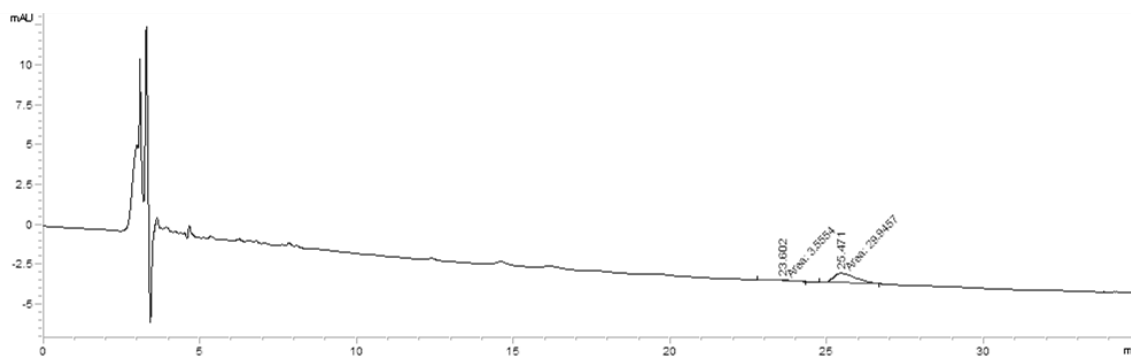
**Figure 1.23:** Representative biocatalytic reaction of SET1 with 3-aminobutyronitrile (124), at pH 7 - acid product, crude reaction mixture



**Figure 1.24:** Representative biocatalytic reaction of SET1 with 3-(benzylamino)butyronitrile (125), at pH 7 - amide product, crude reaction mixture



**Figure 1.25:** Representative biocatalytic reaction of SET1 with 3-(benzylamino)butyronitrile (125), at pH 7 - acid product, crude reaction mixture

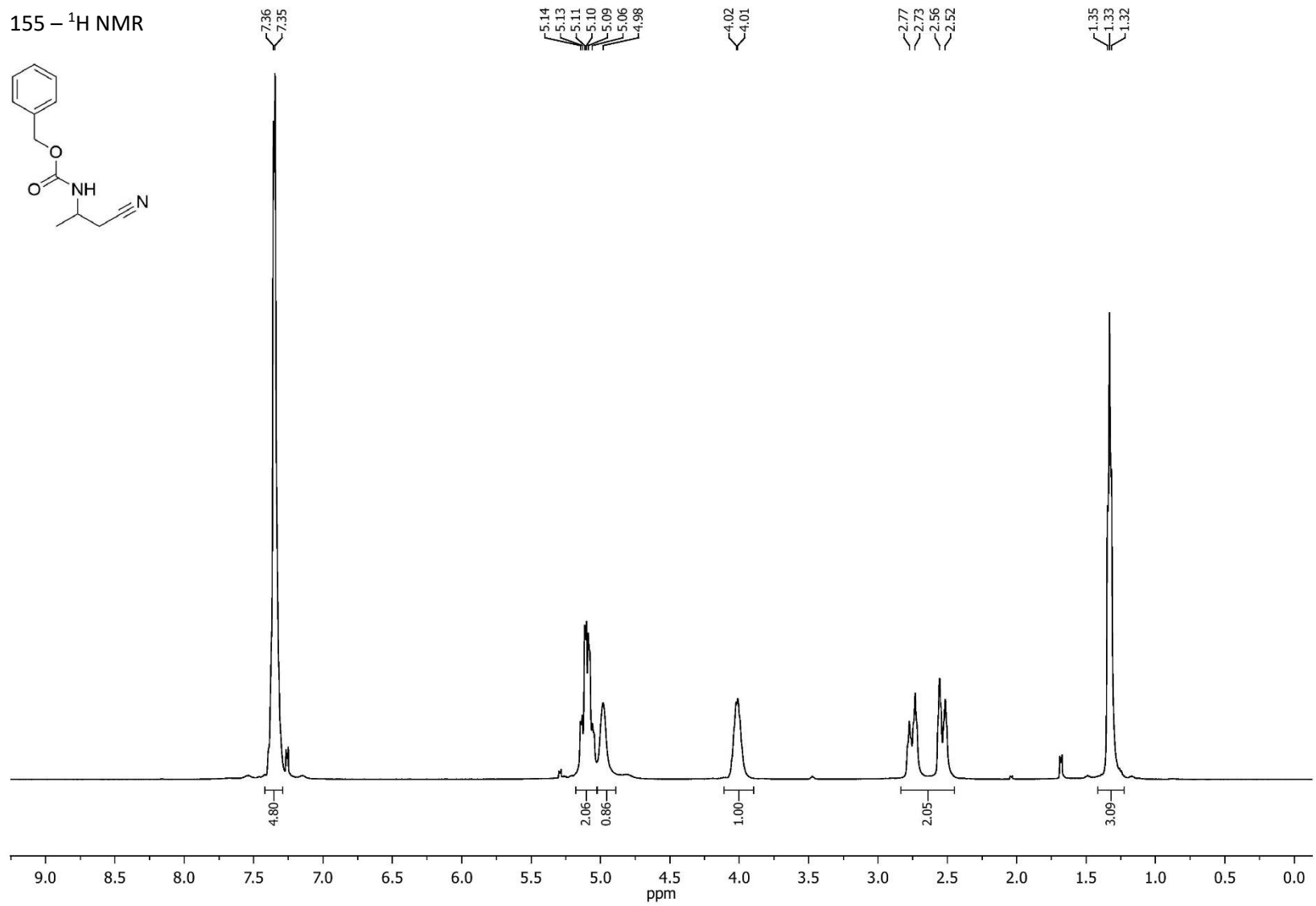
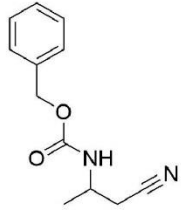


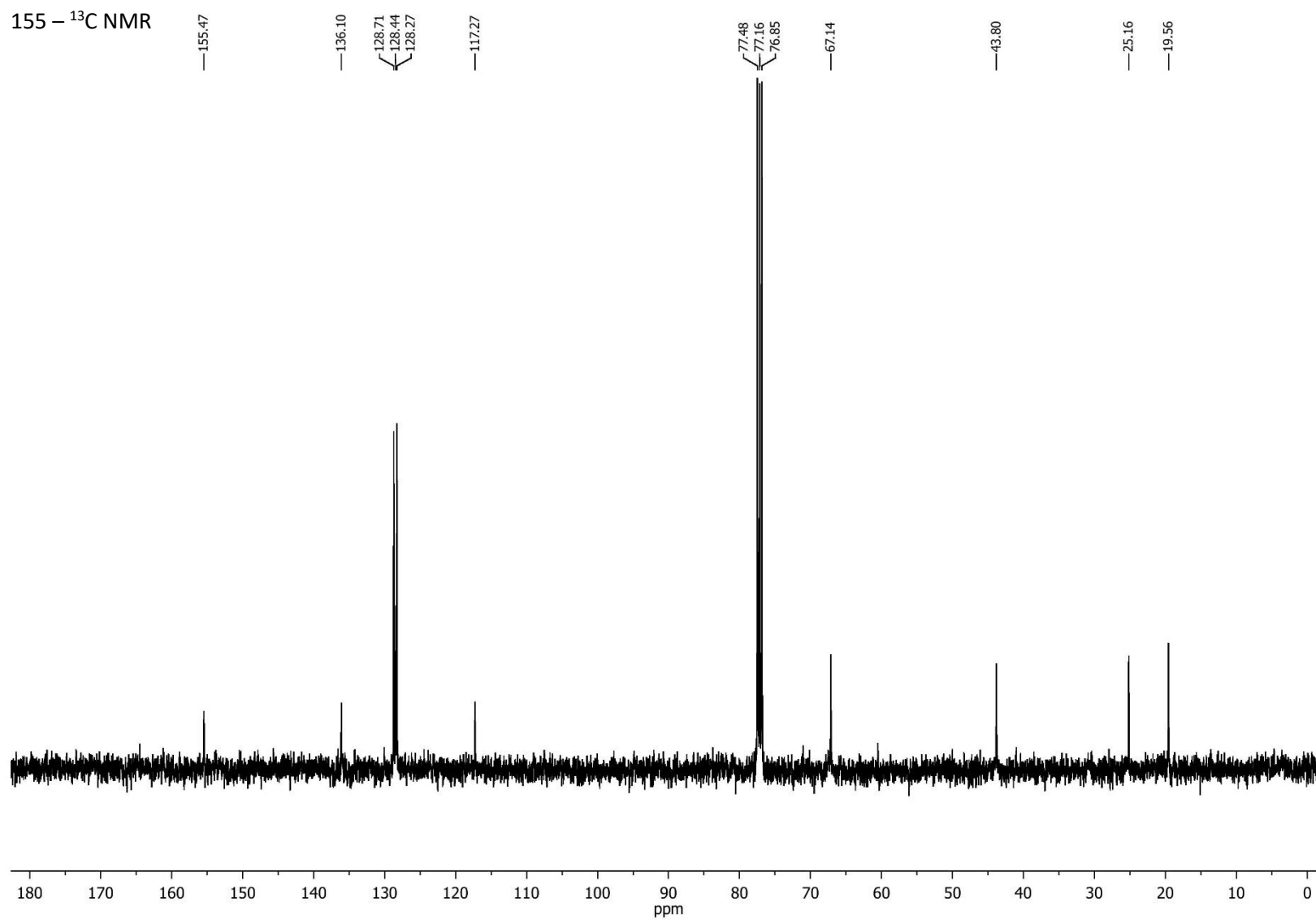
**Figure 1.26:** Representative biocatalytic reaction of SET1 with *tert*-butyl 1-carbanoylpropan-2-ylcarbamate (126), at pH 7 - nitrile hydrolysed to be analysed as amide

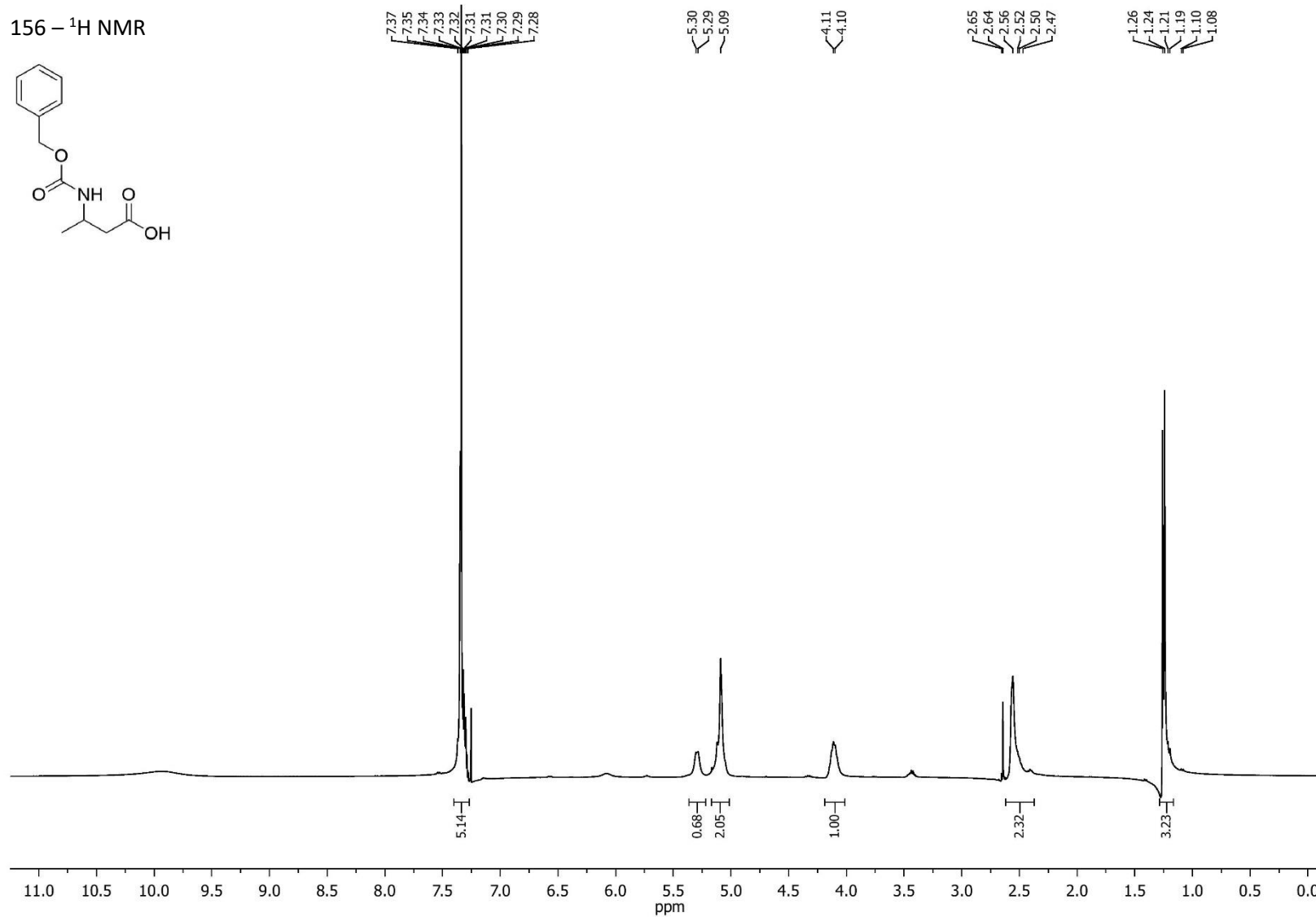
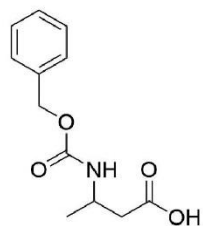
*<sup>1</sup>H and <sup>13</sup>C NMR spectra*

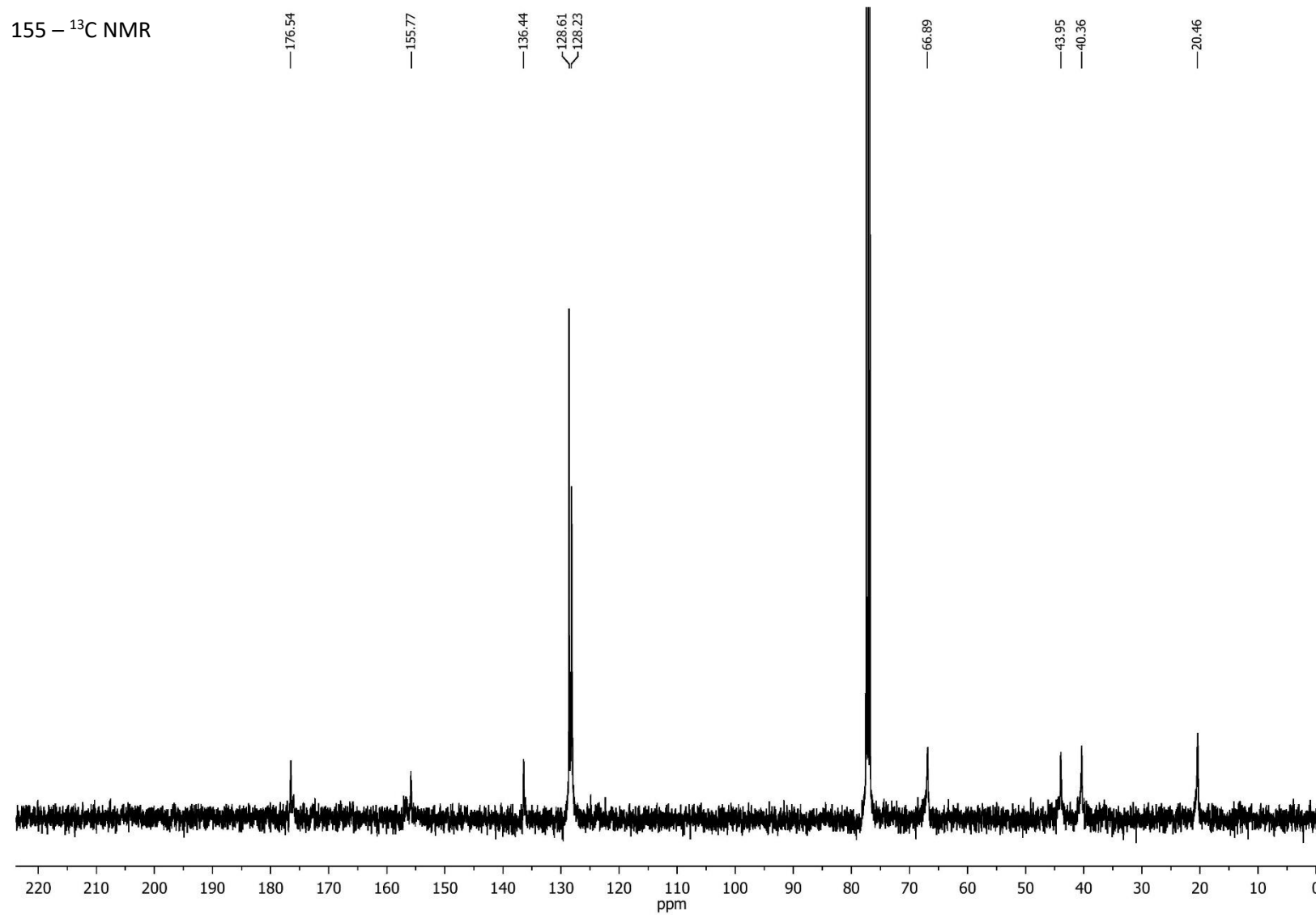


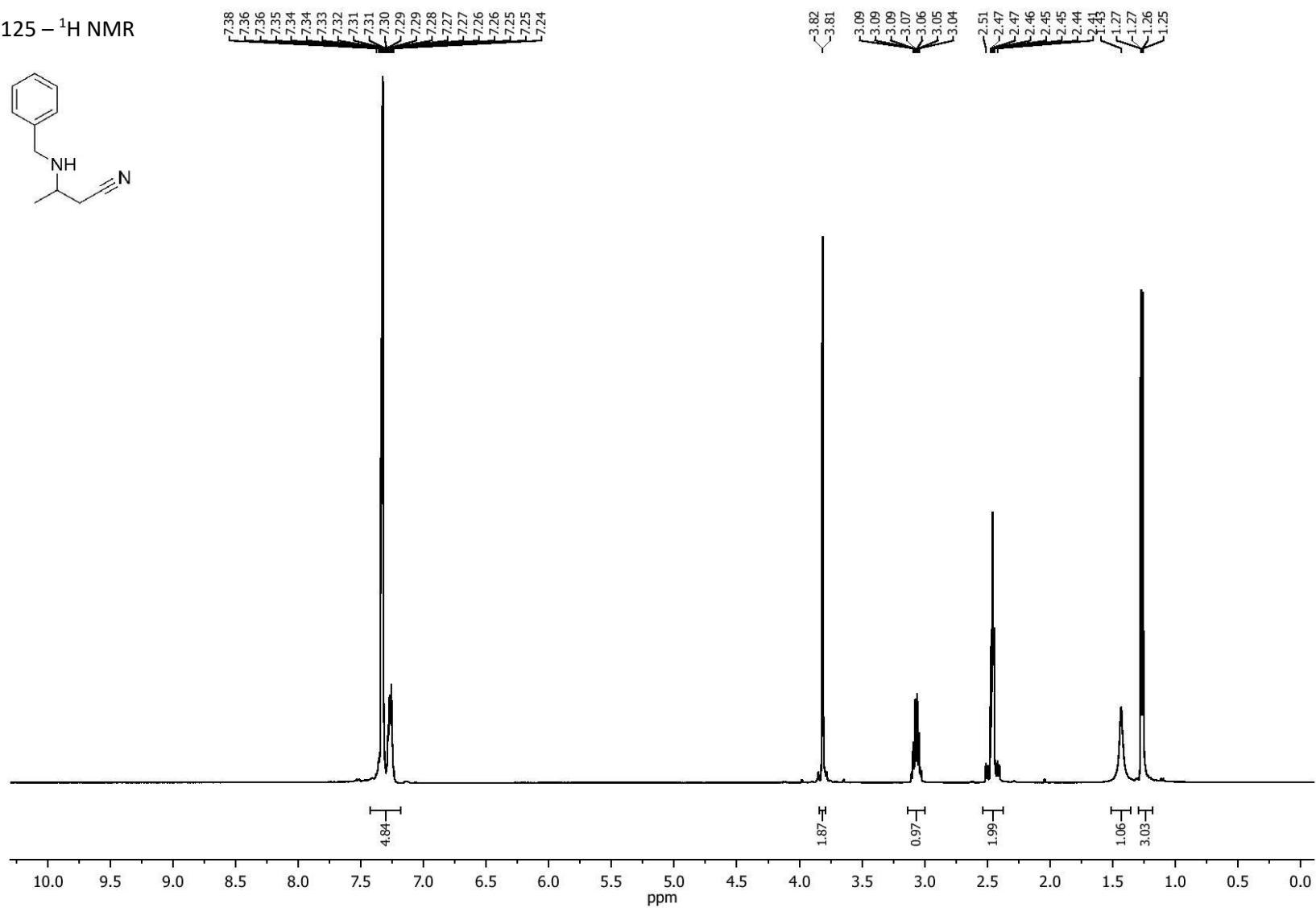
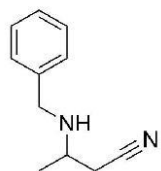
155 -  $^1\text{H}$  NMR

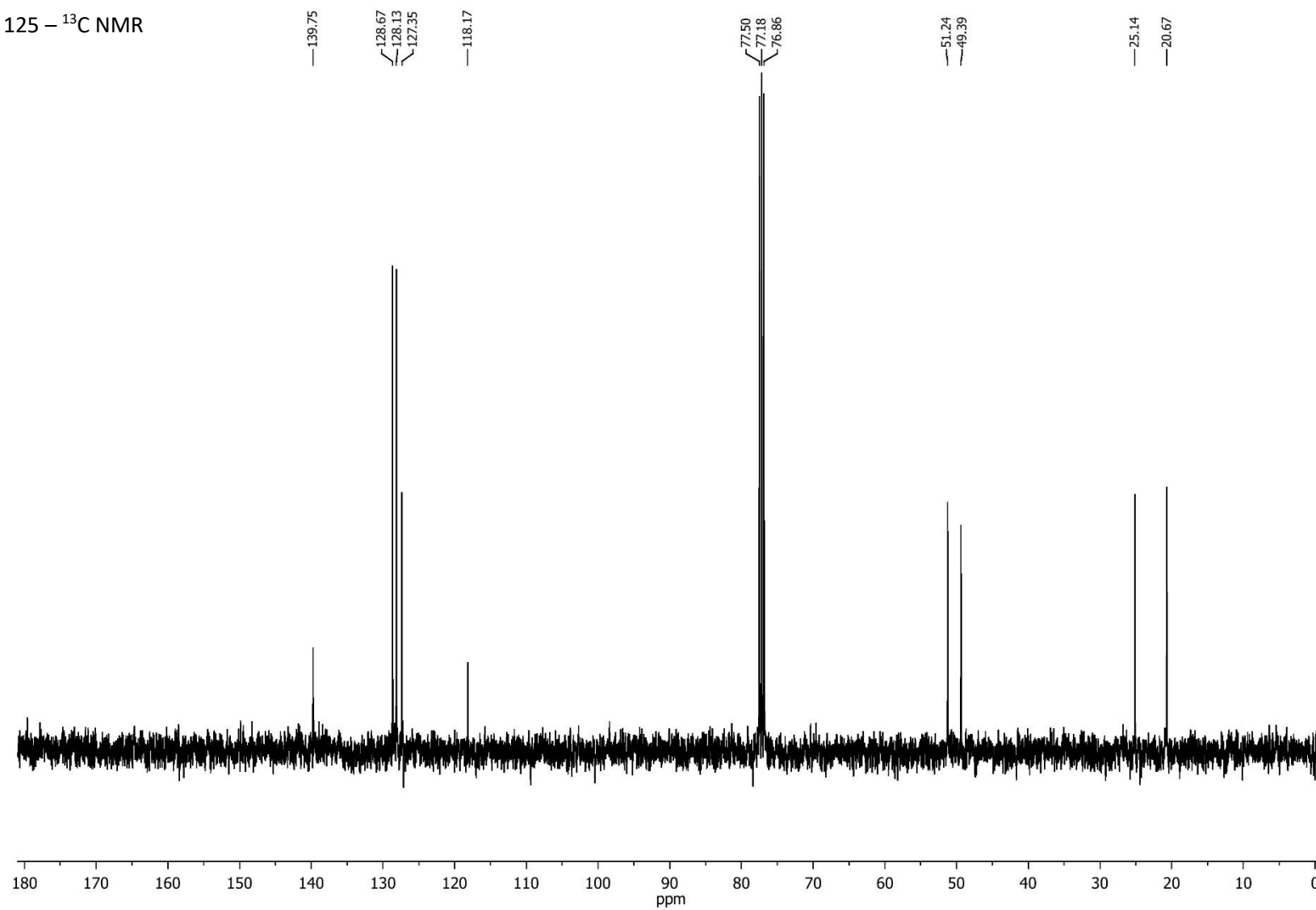


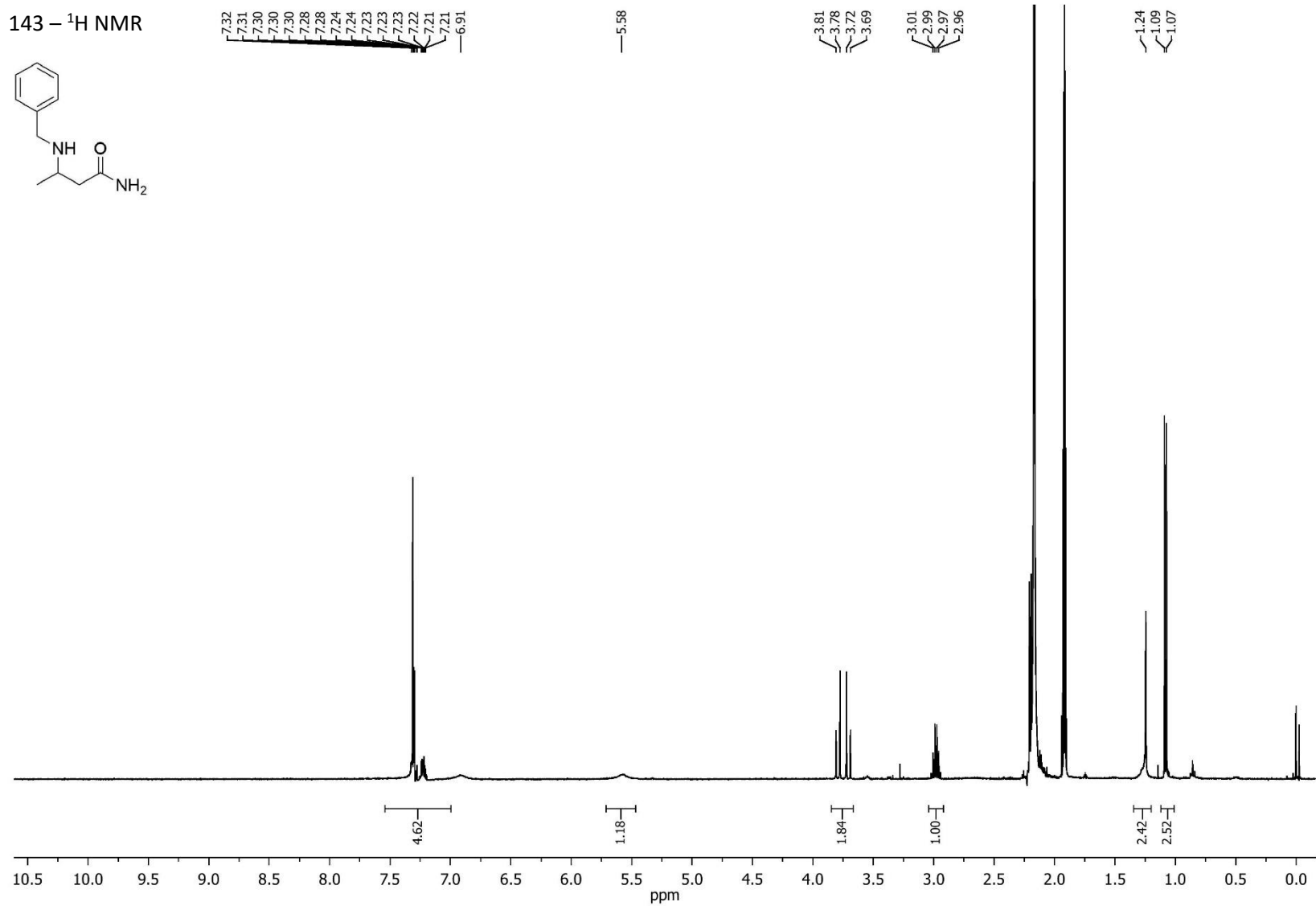
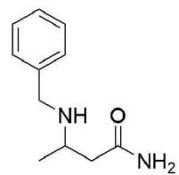


156 –  $^1\text{H}$  NMR

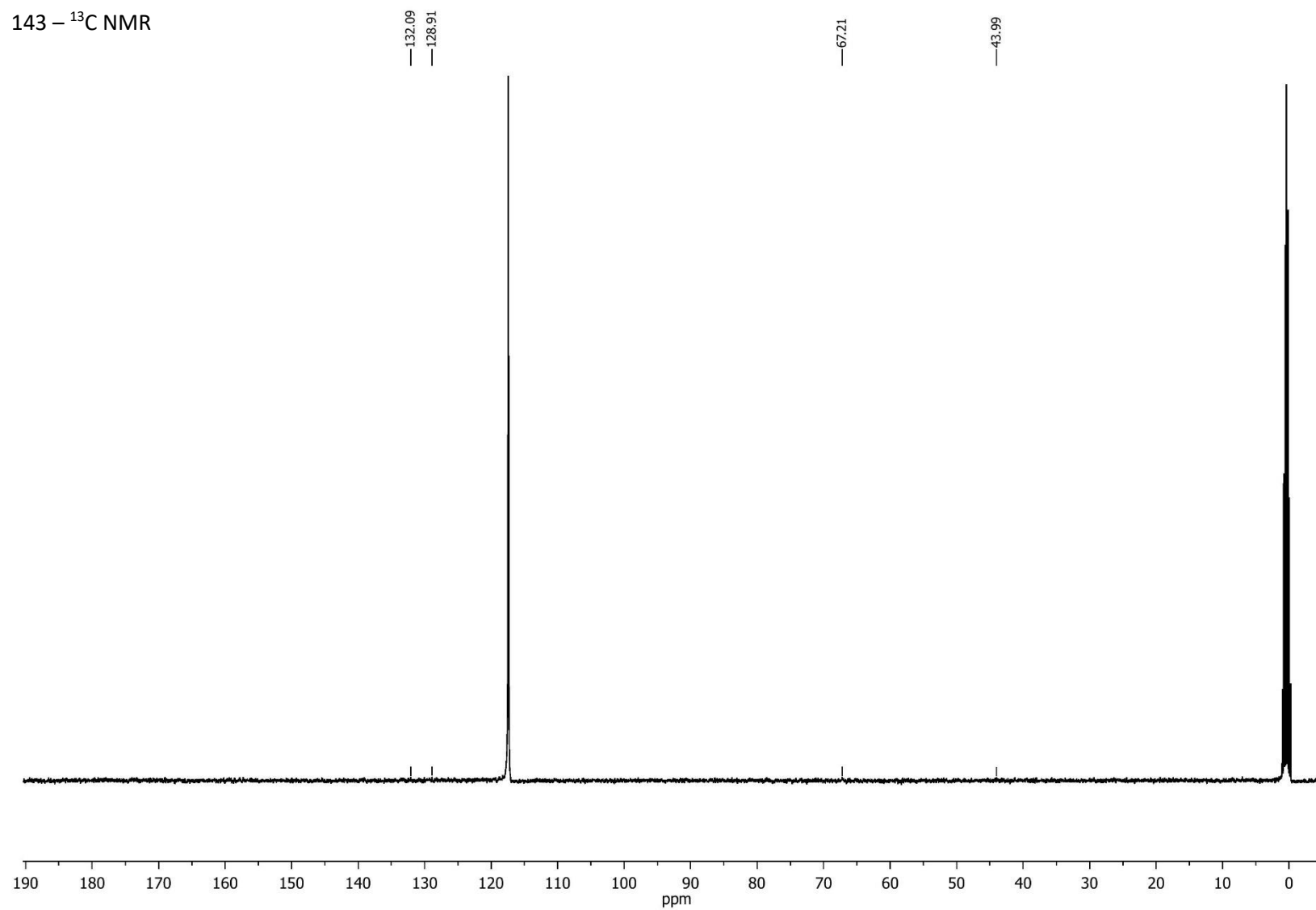


125 –  $^1\text{H}$  NMR

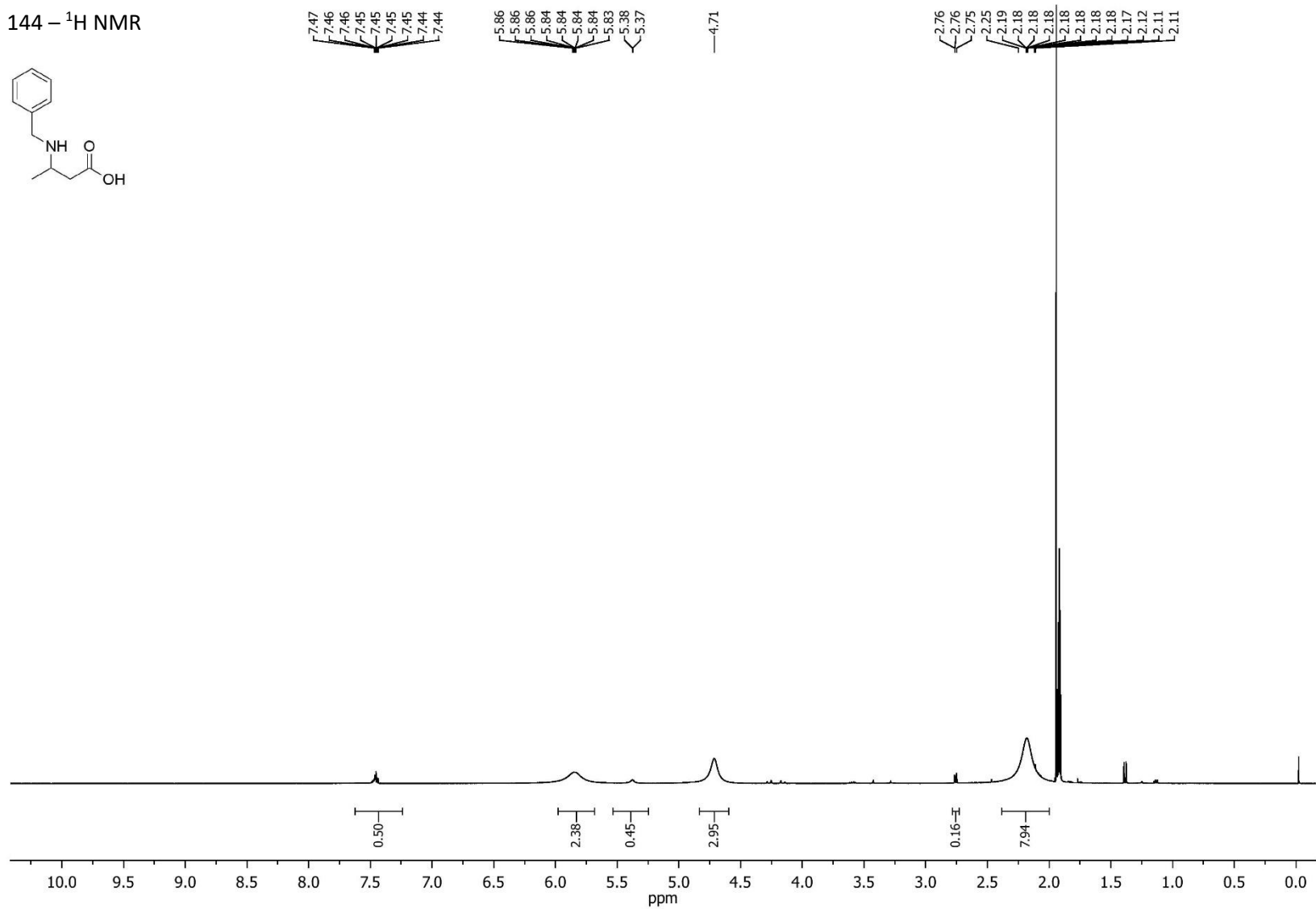
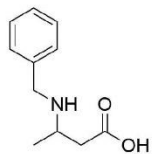
125 –  $^{13}\text{C}$  NMR

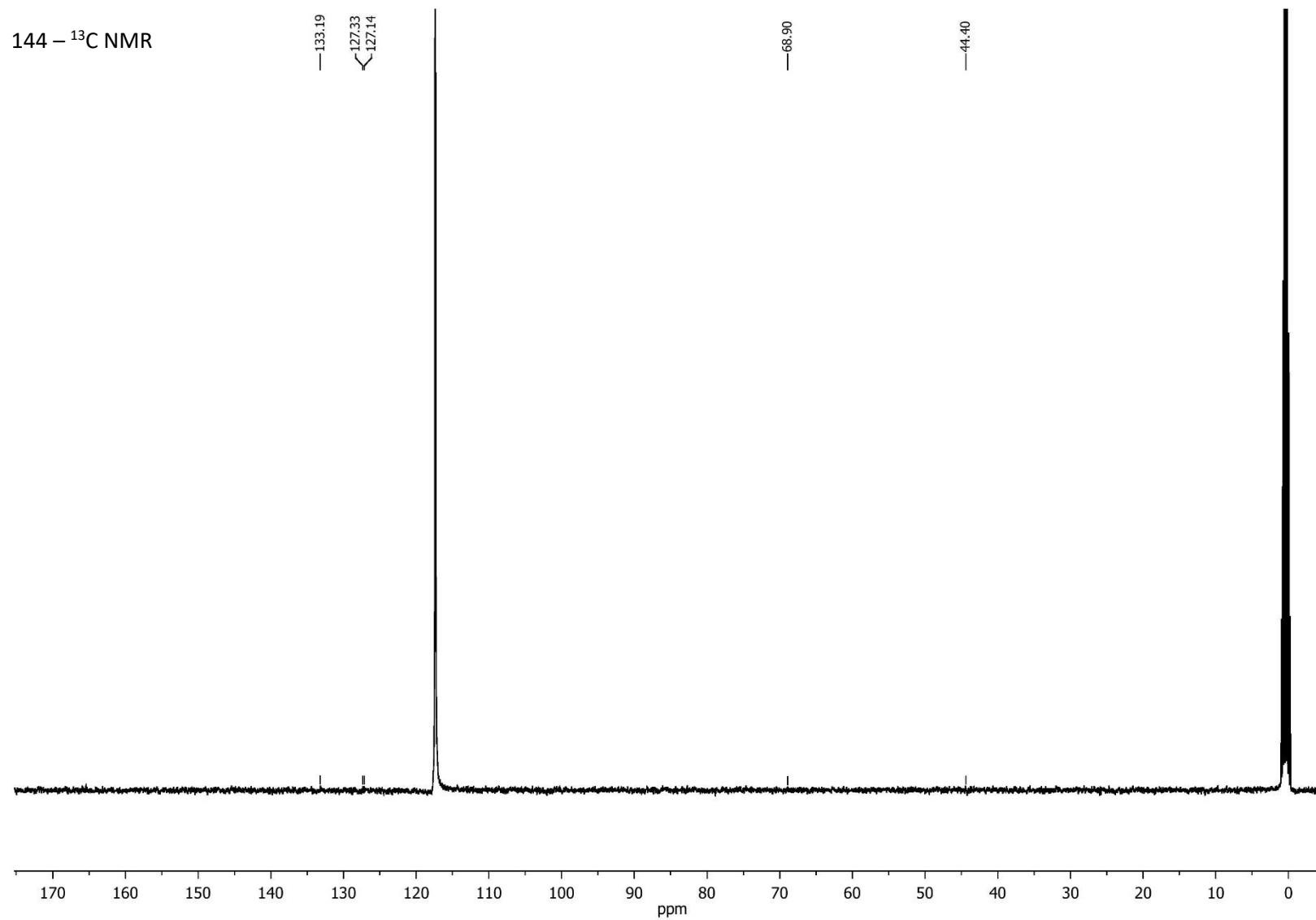
143 -  $^1\text{H}$  NMR

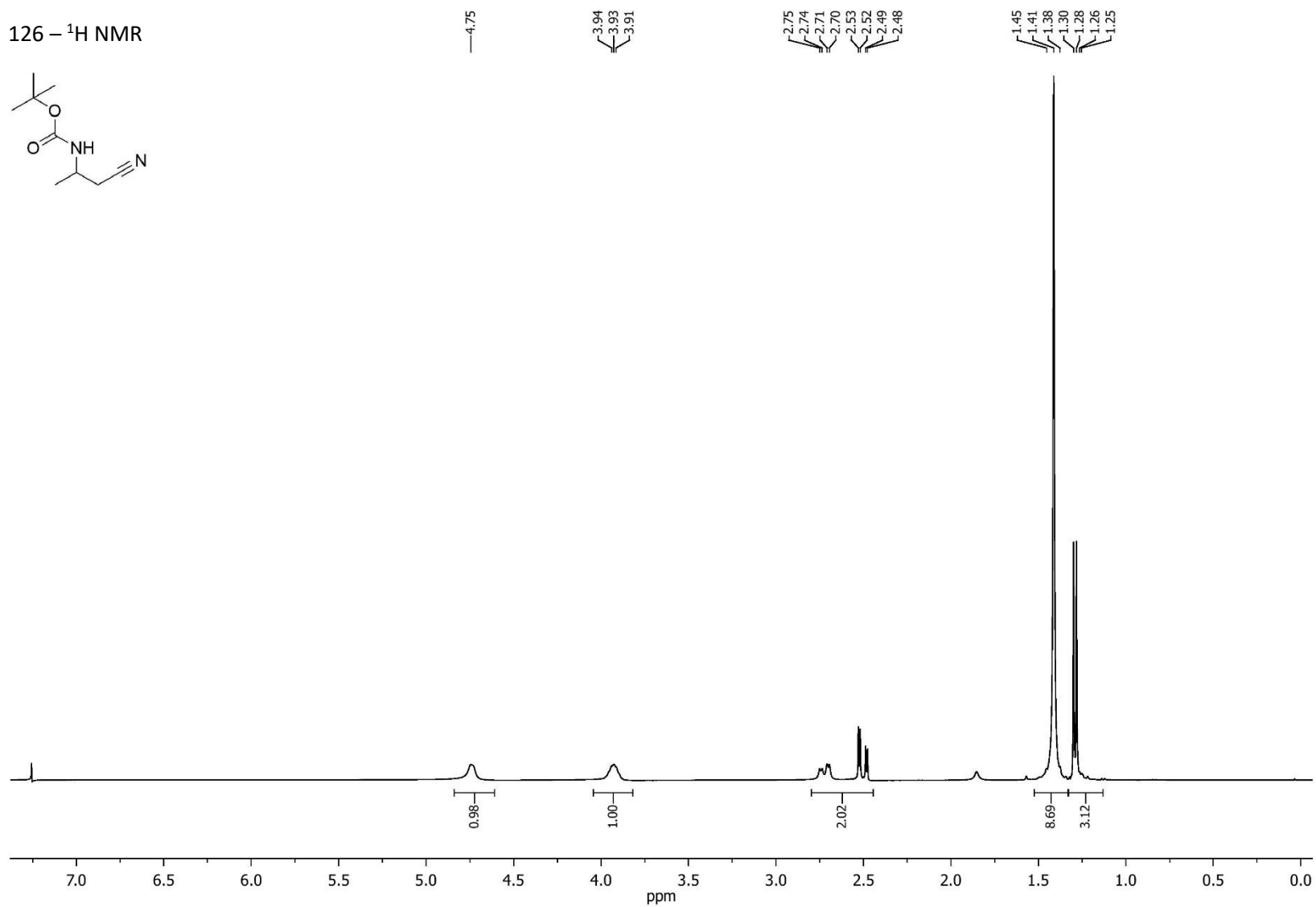
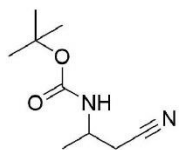
143 – <sup>13</sup>C NMR

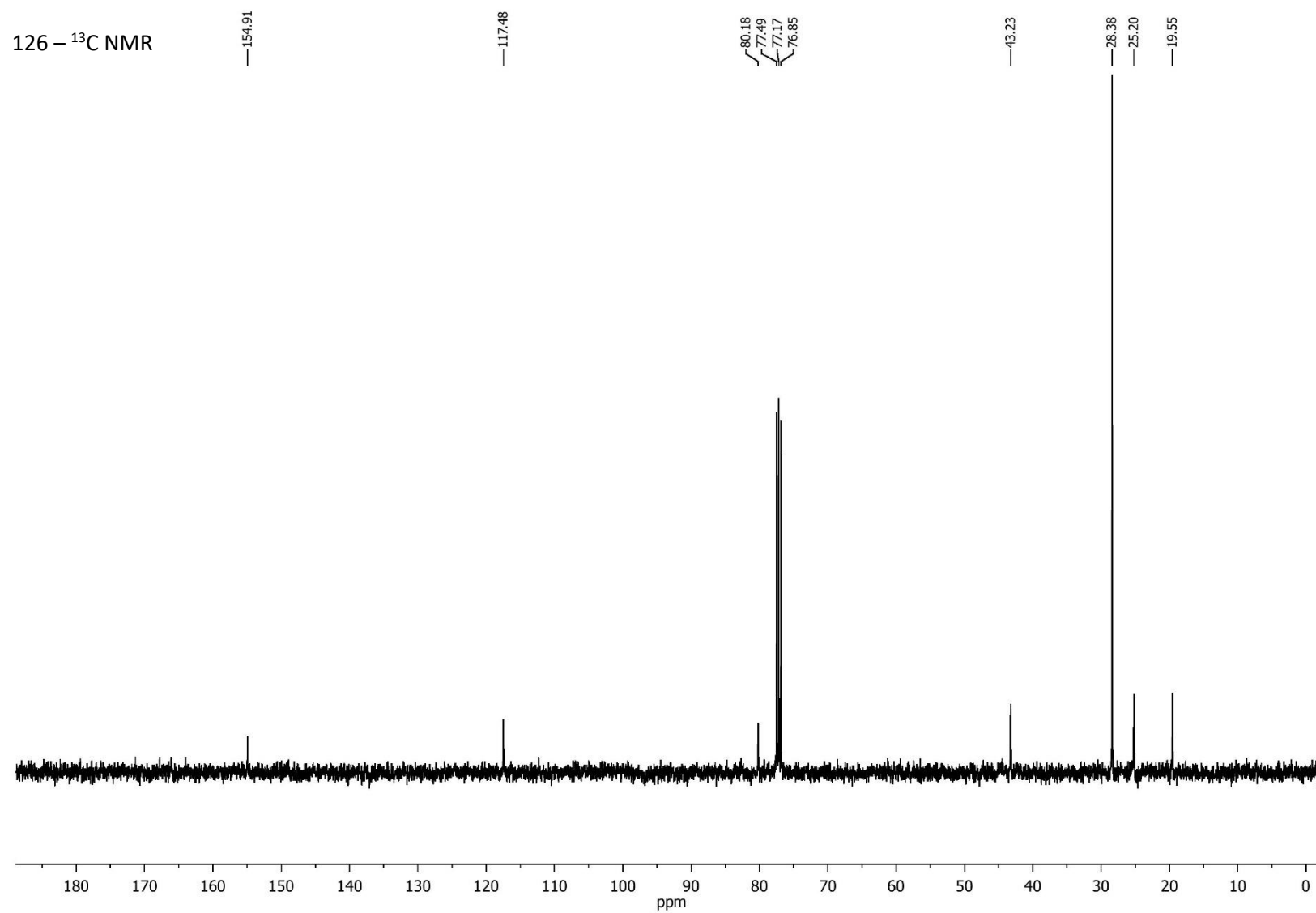


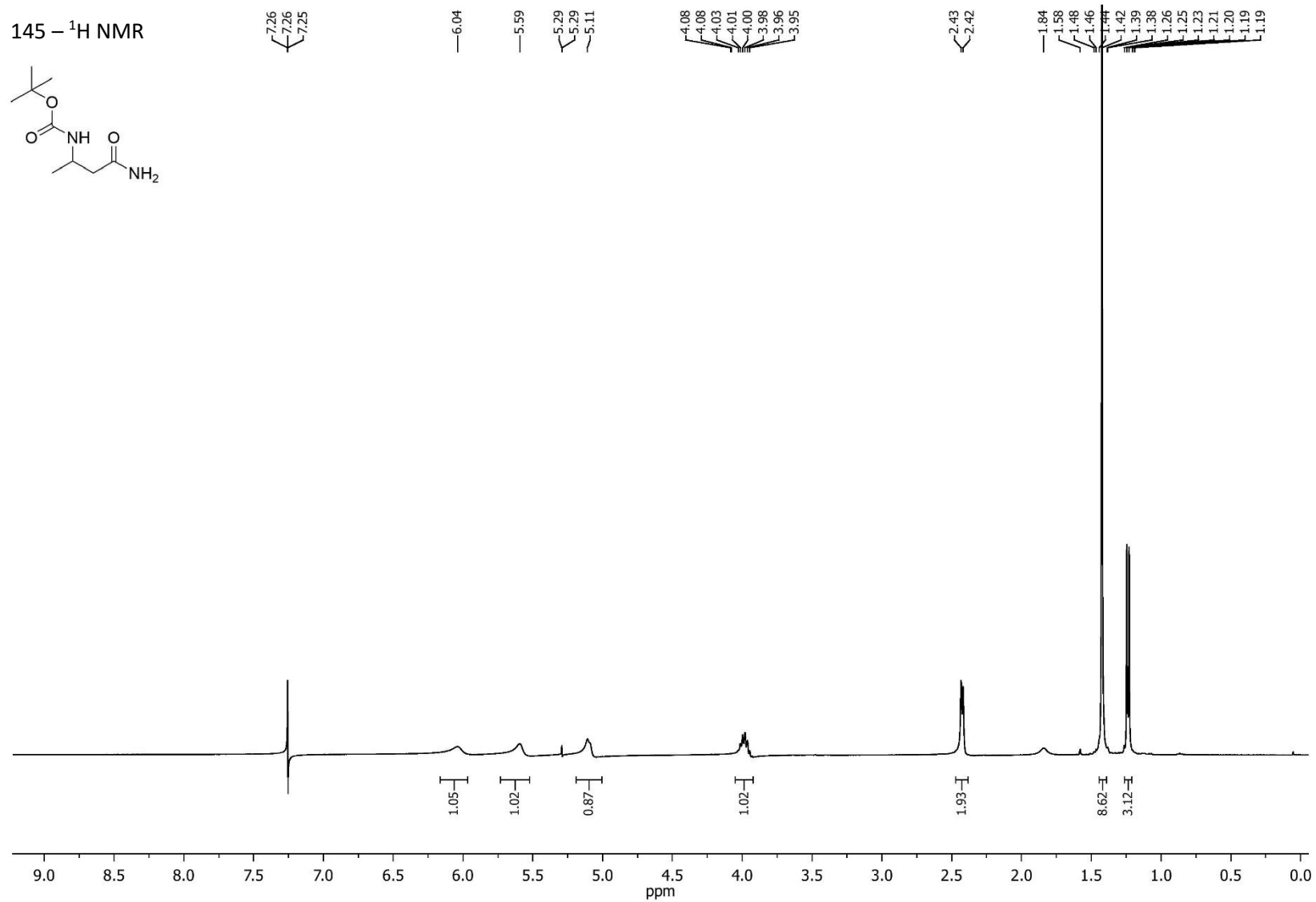


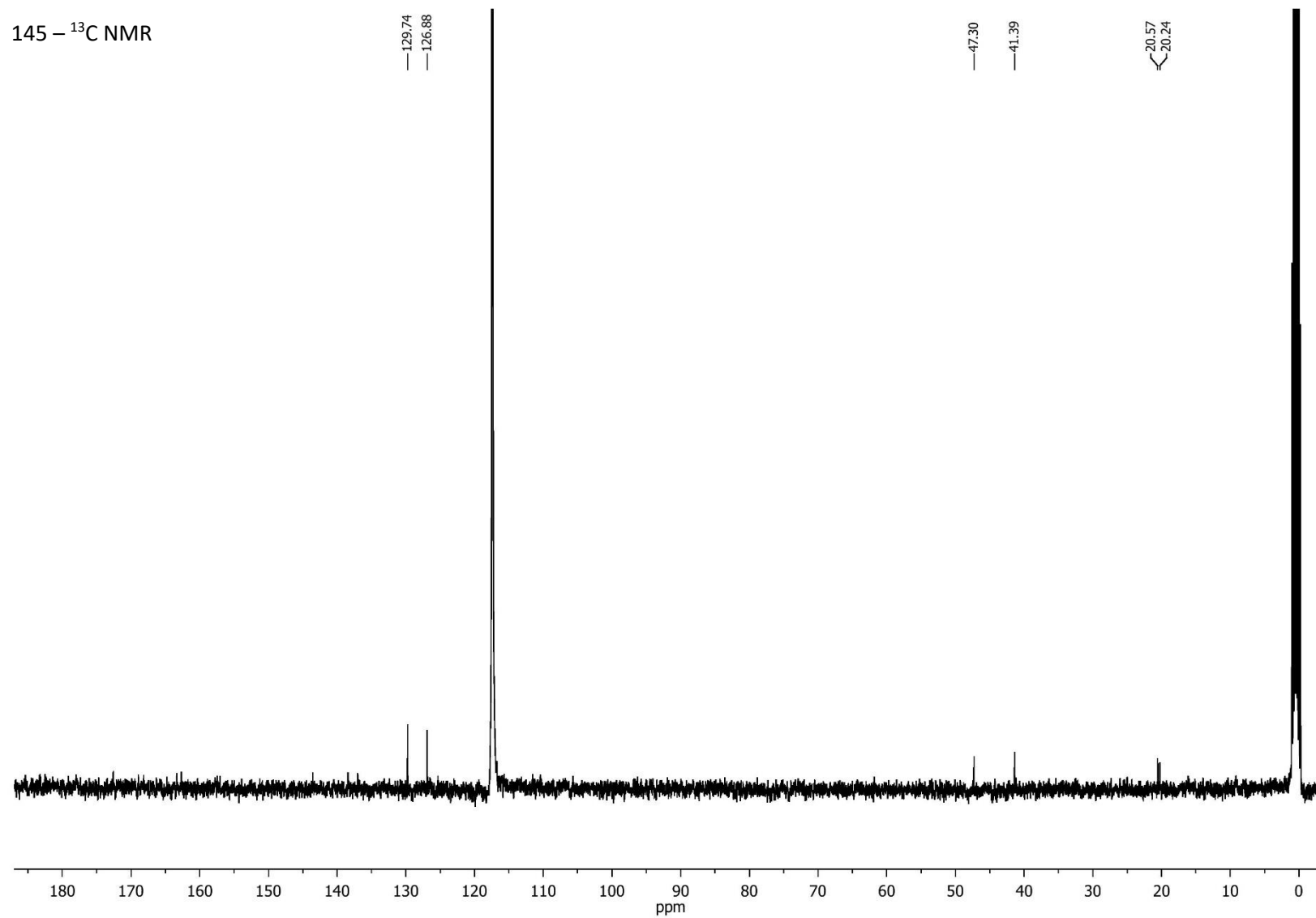
144 -  $^1\text{H}$  NMR

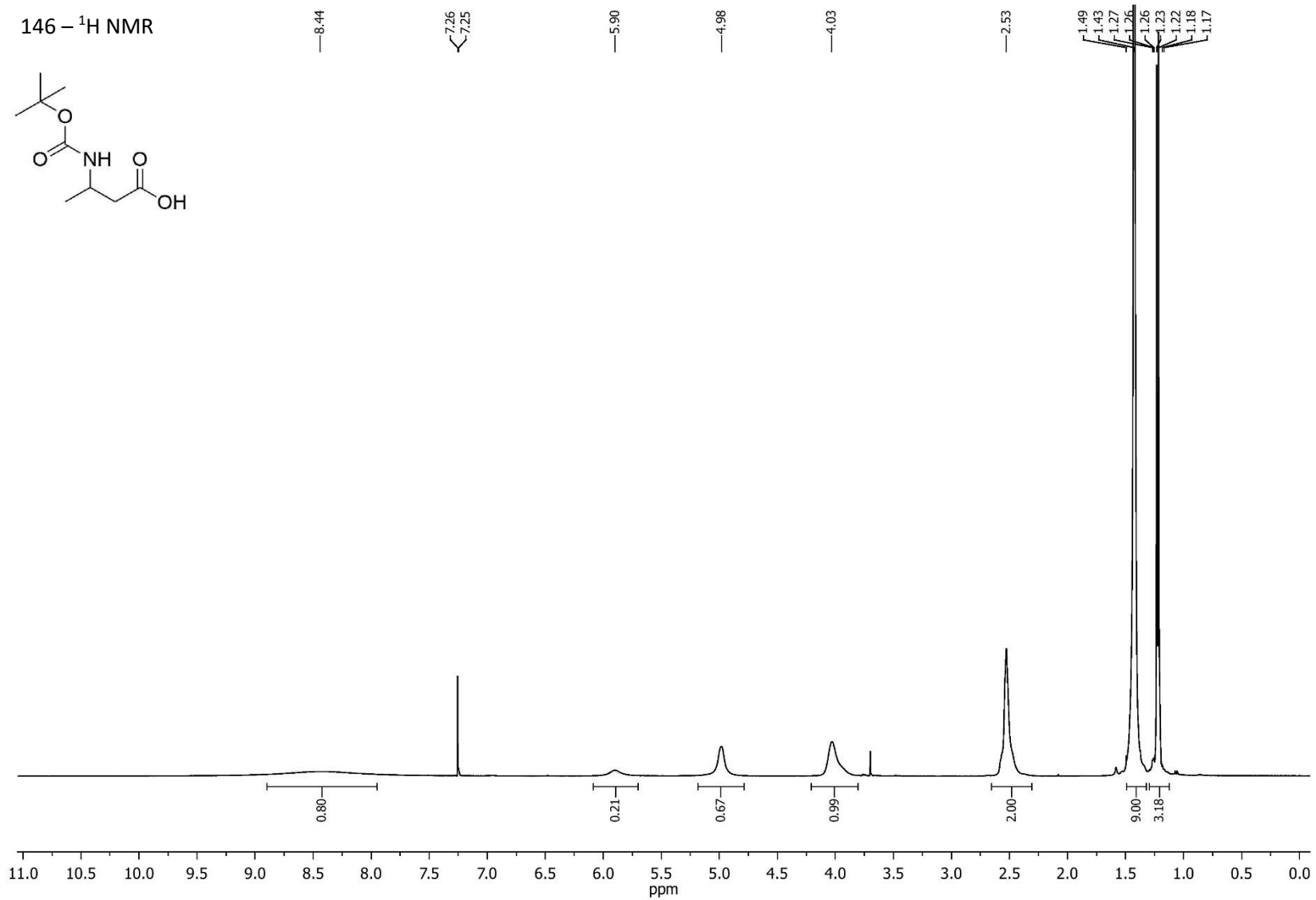


126 -  $^1\text{H}$  NMR

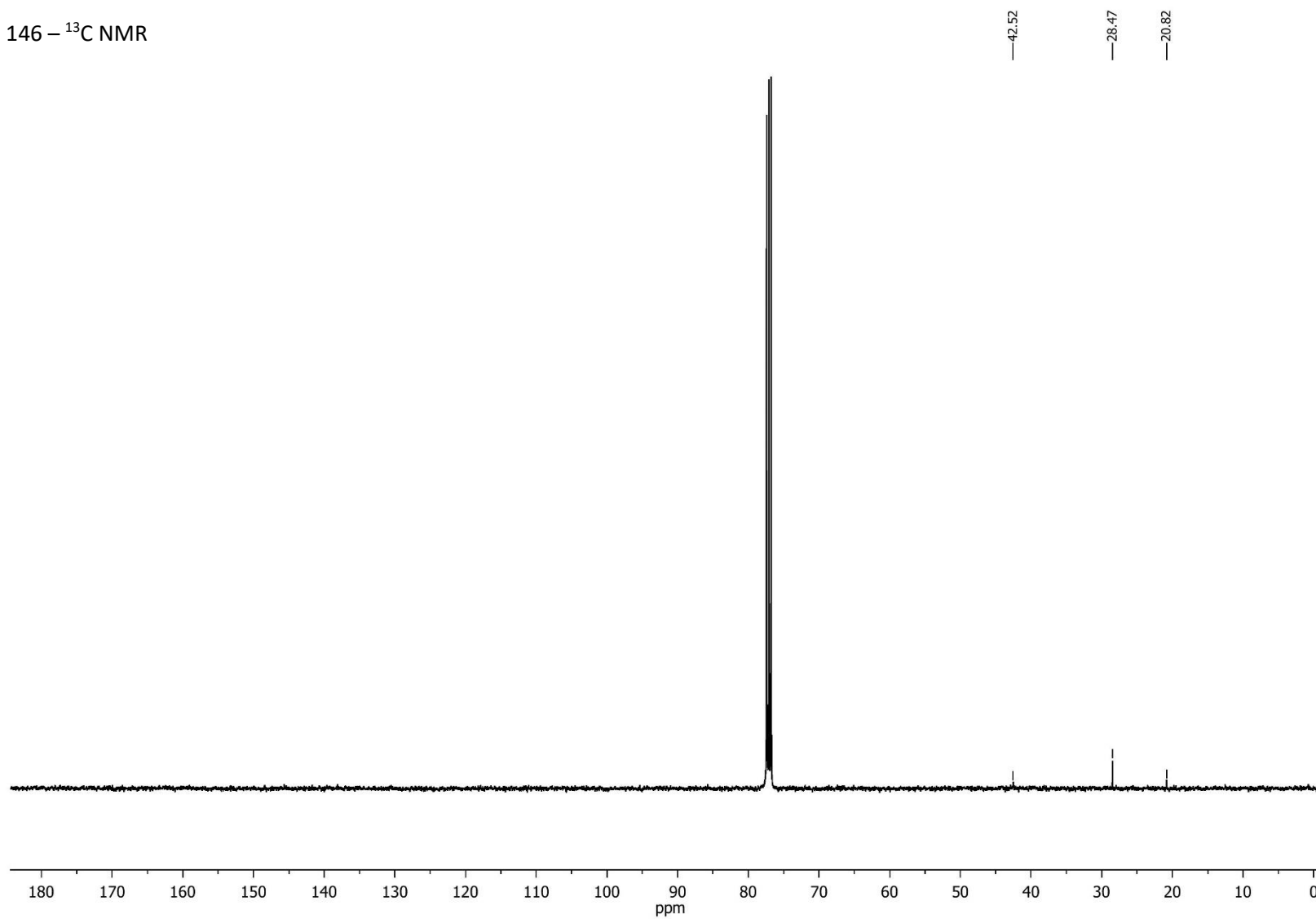




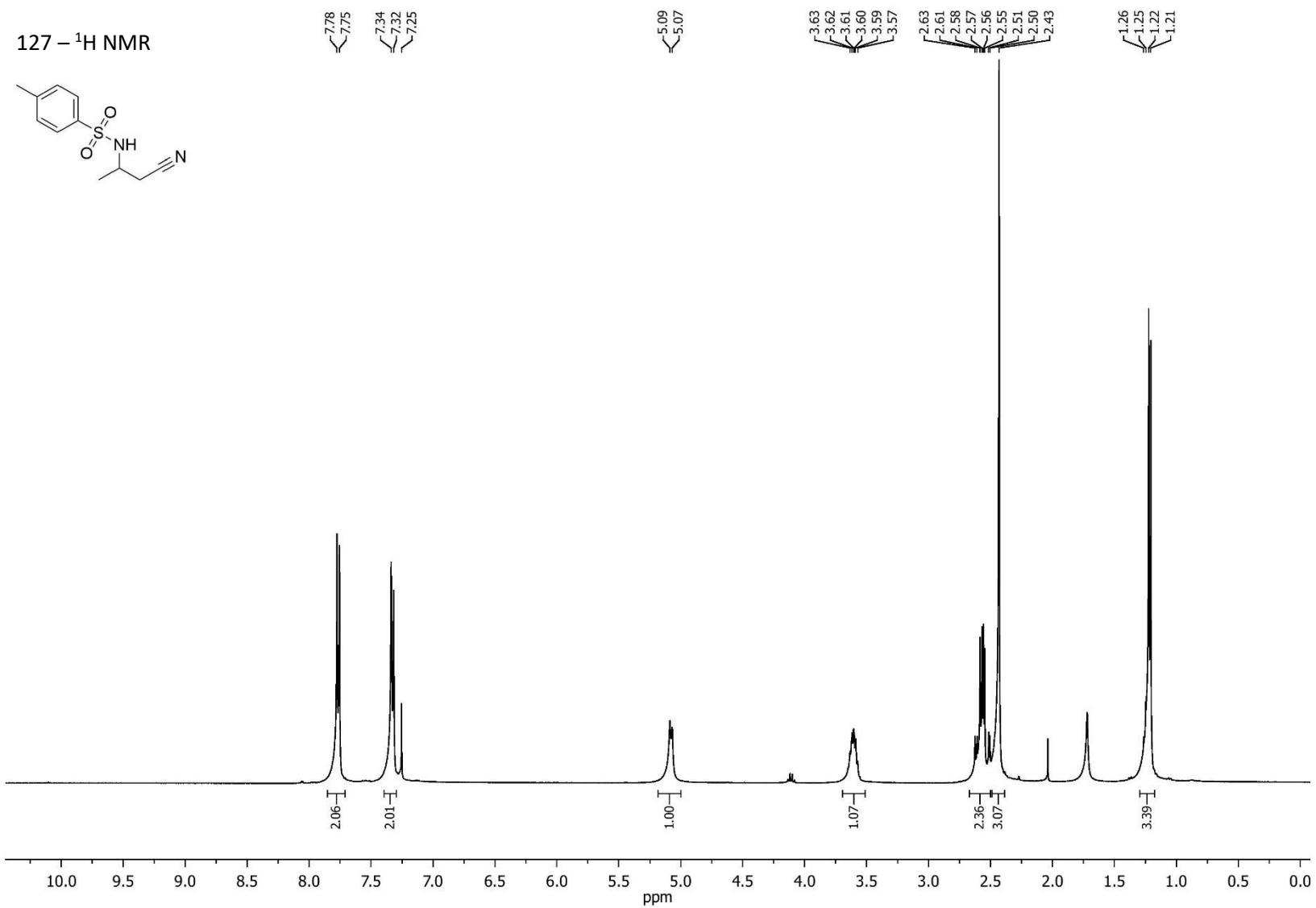


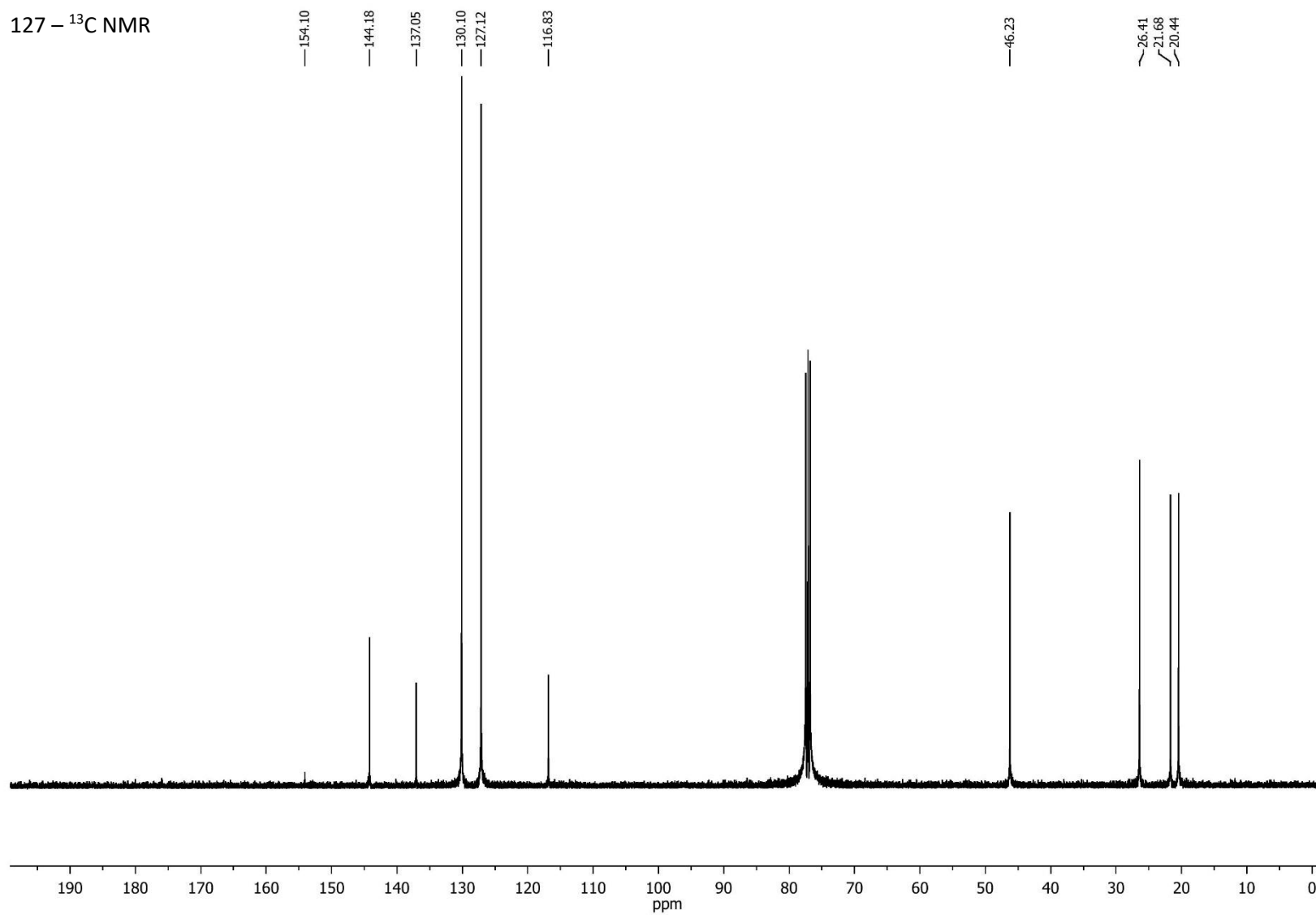


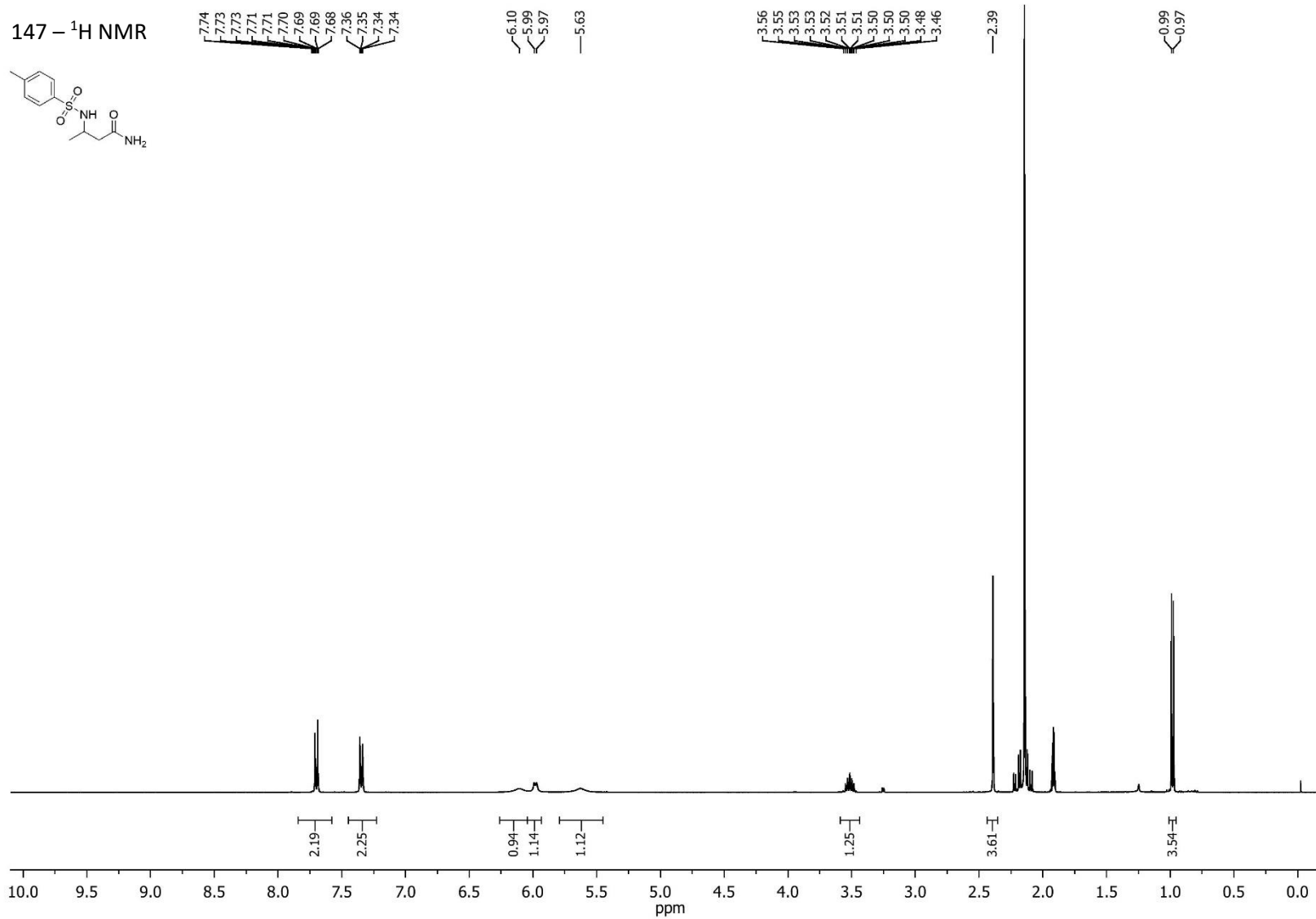
146 -  $^{13}\text{C}$  NMR

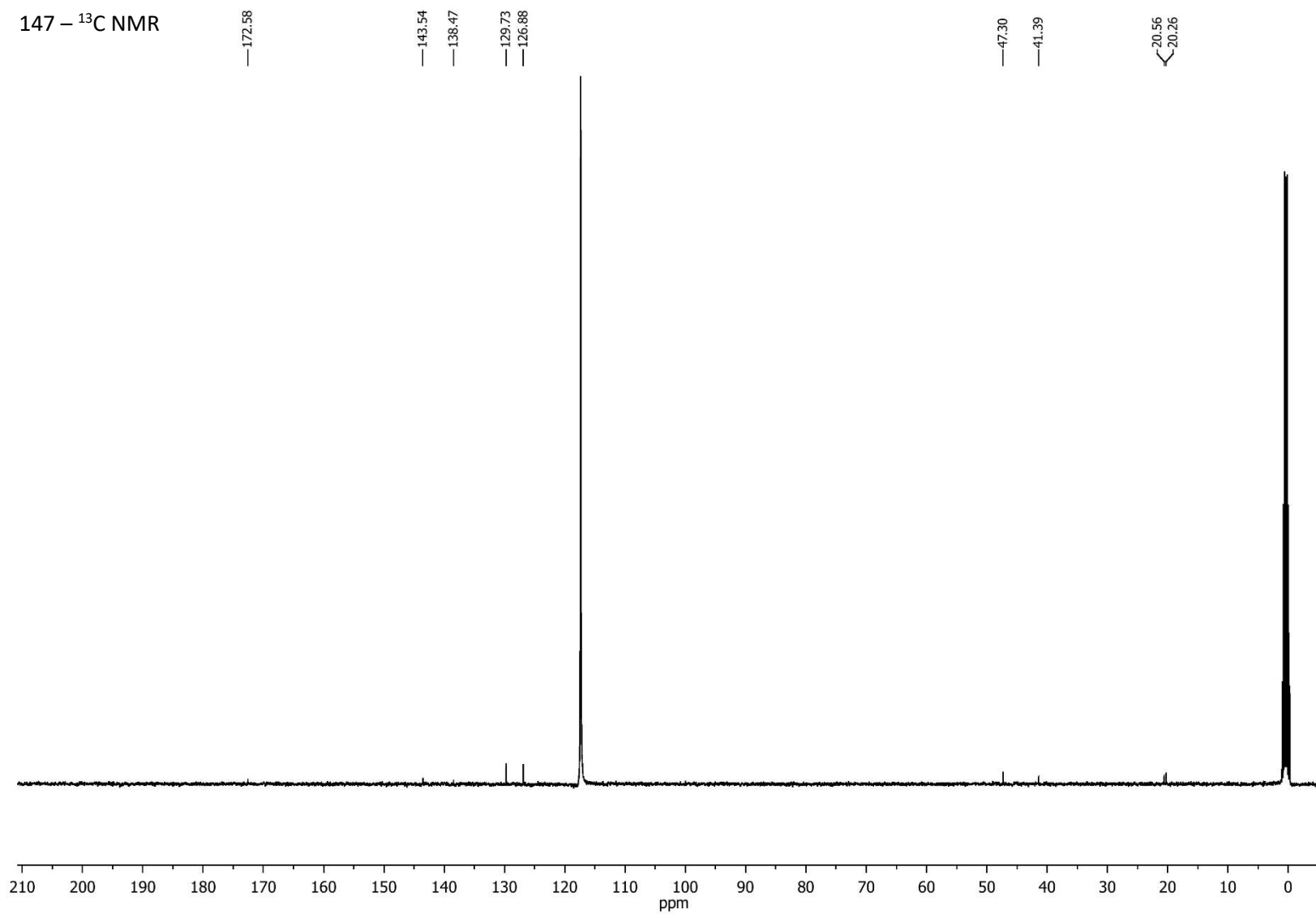


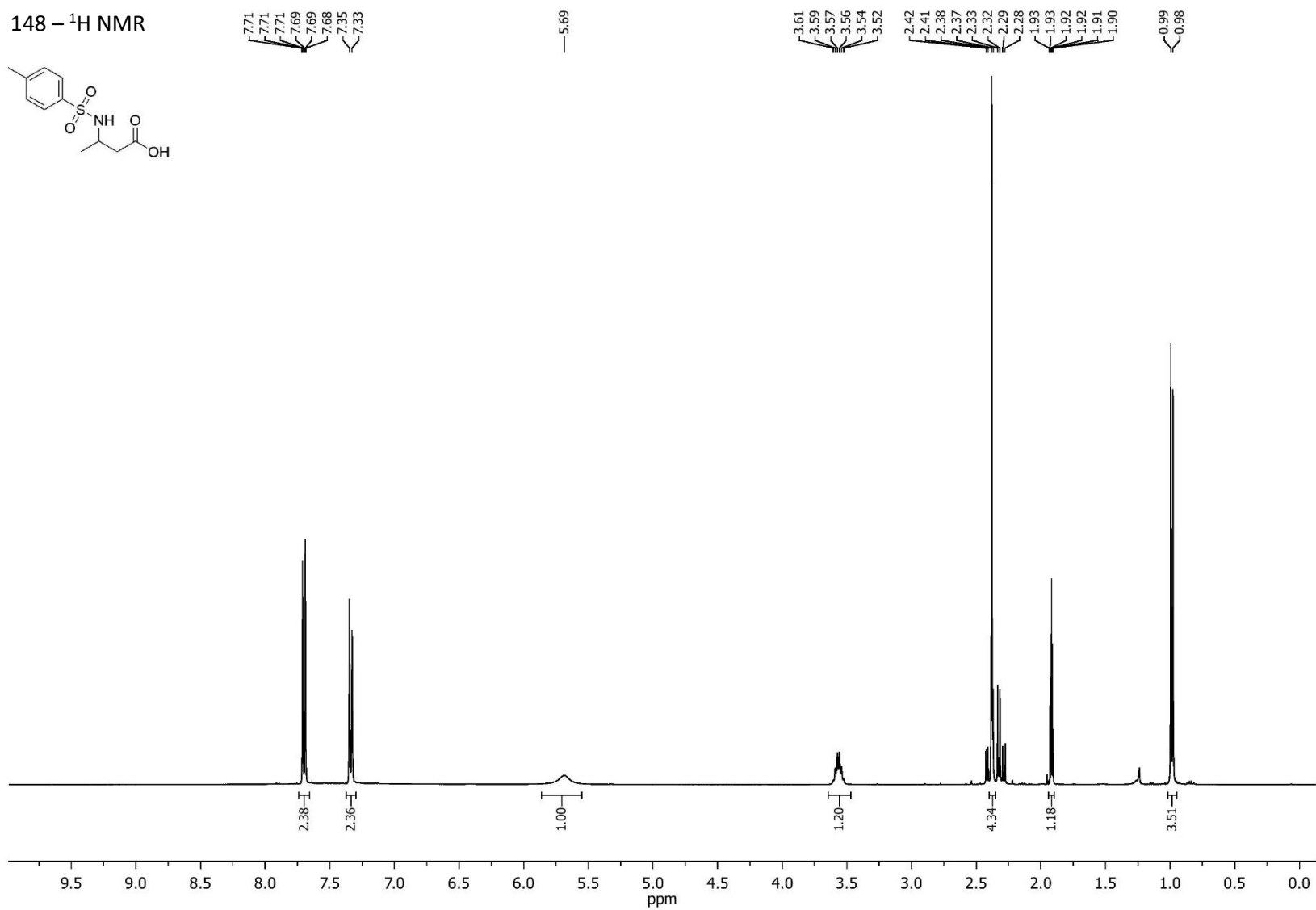


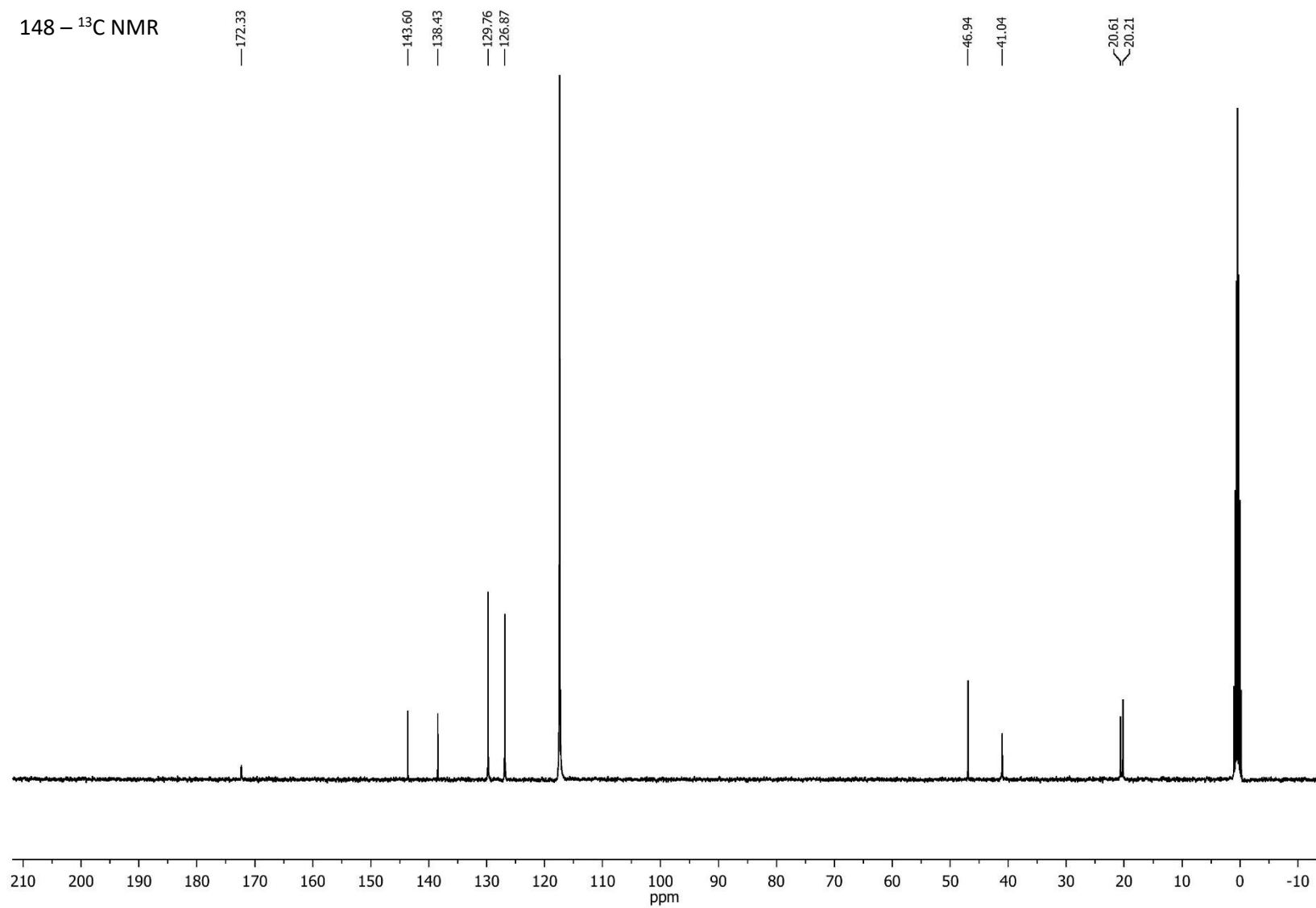


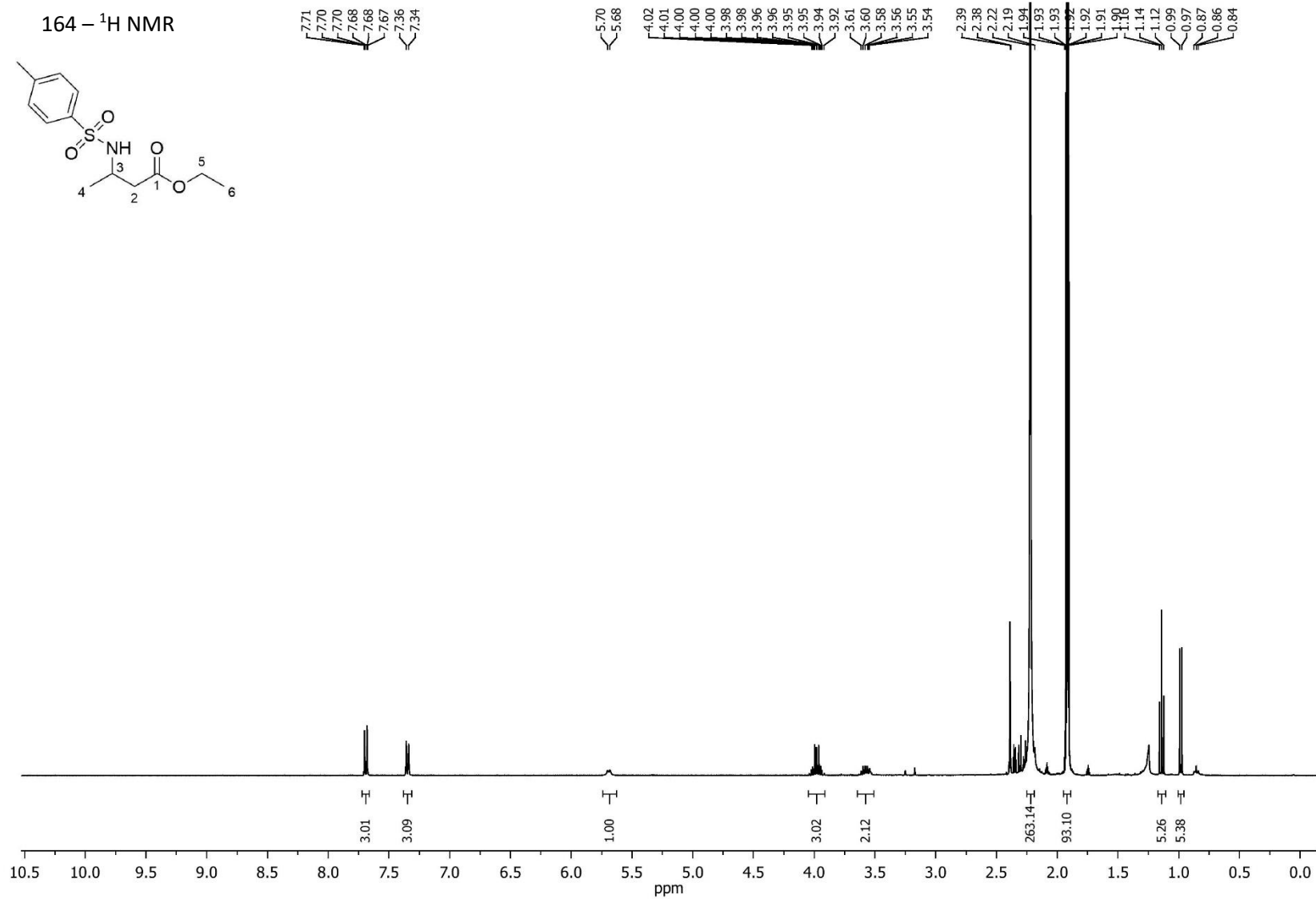


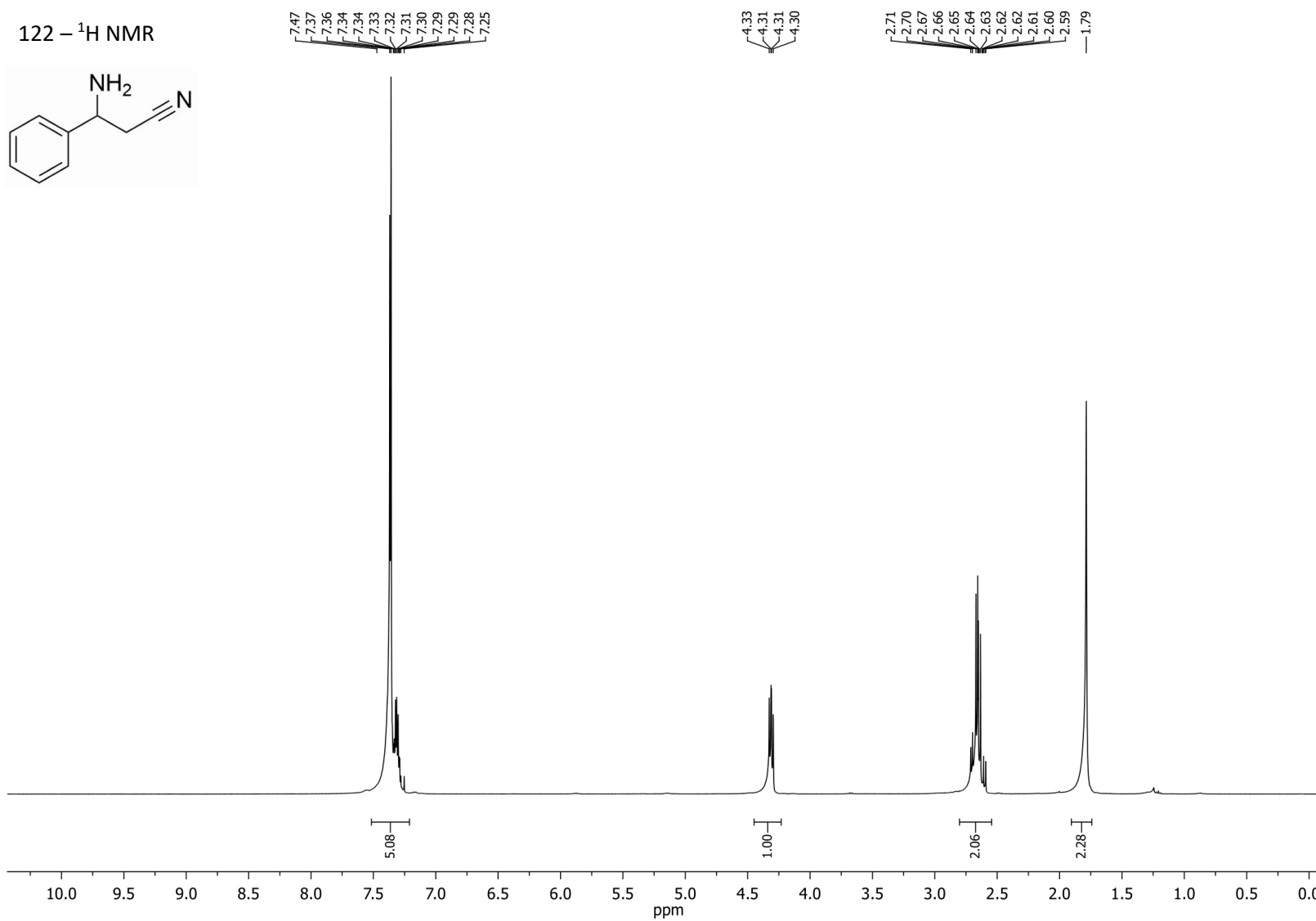




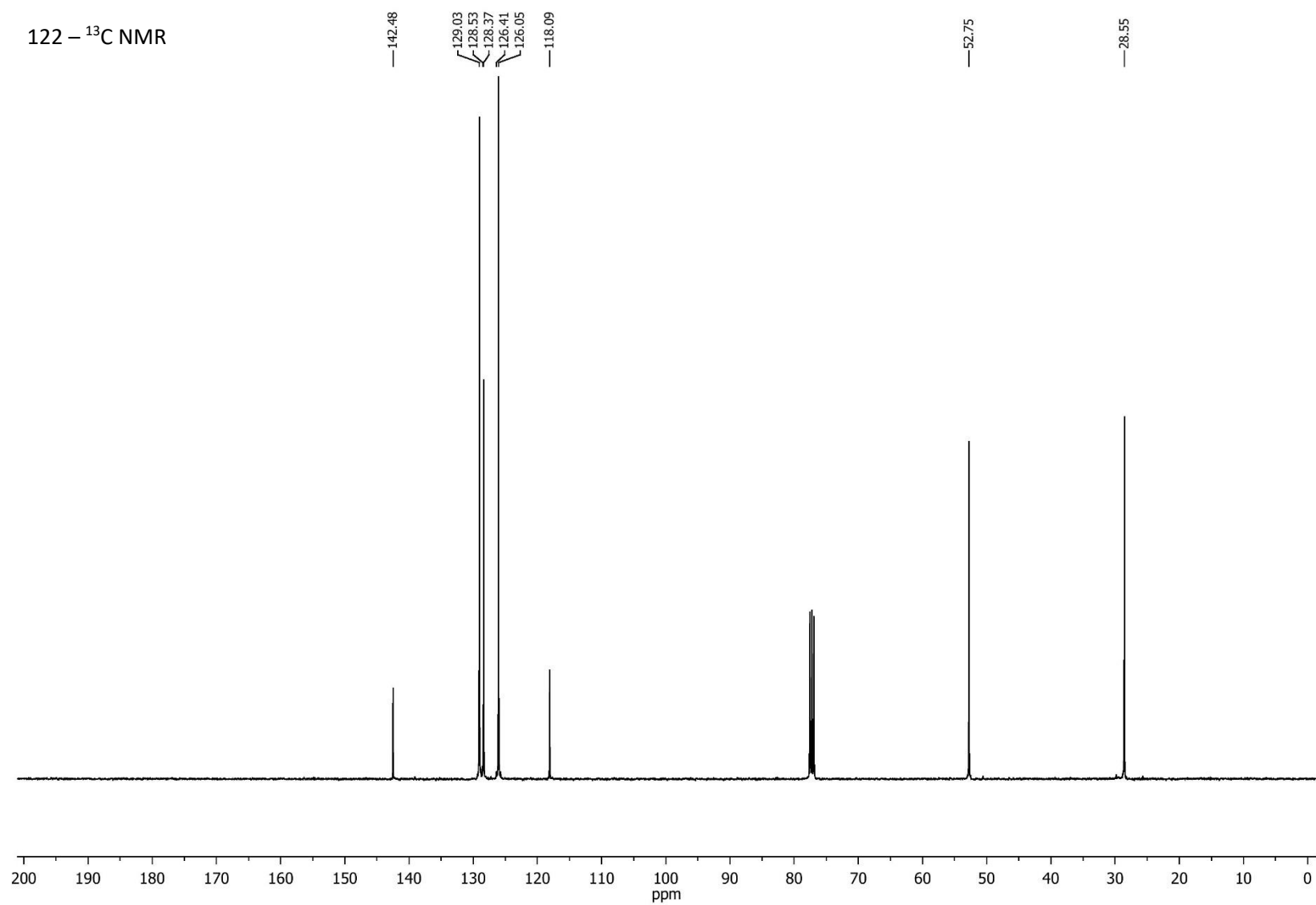
148 -  $^1\text{H}$  NMR

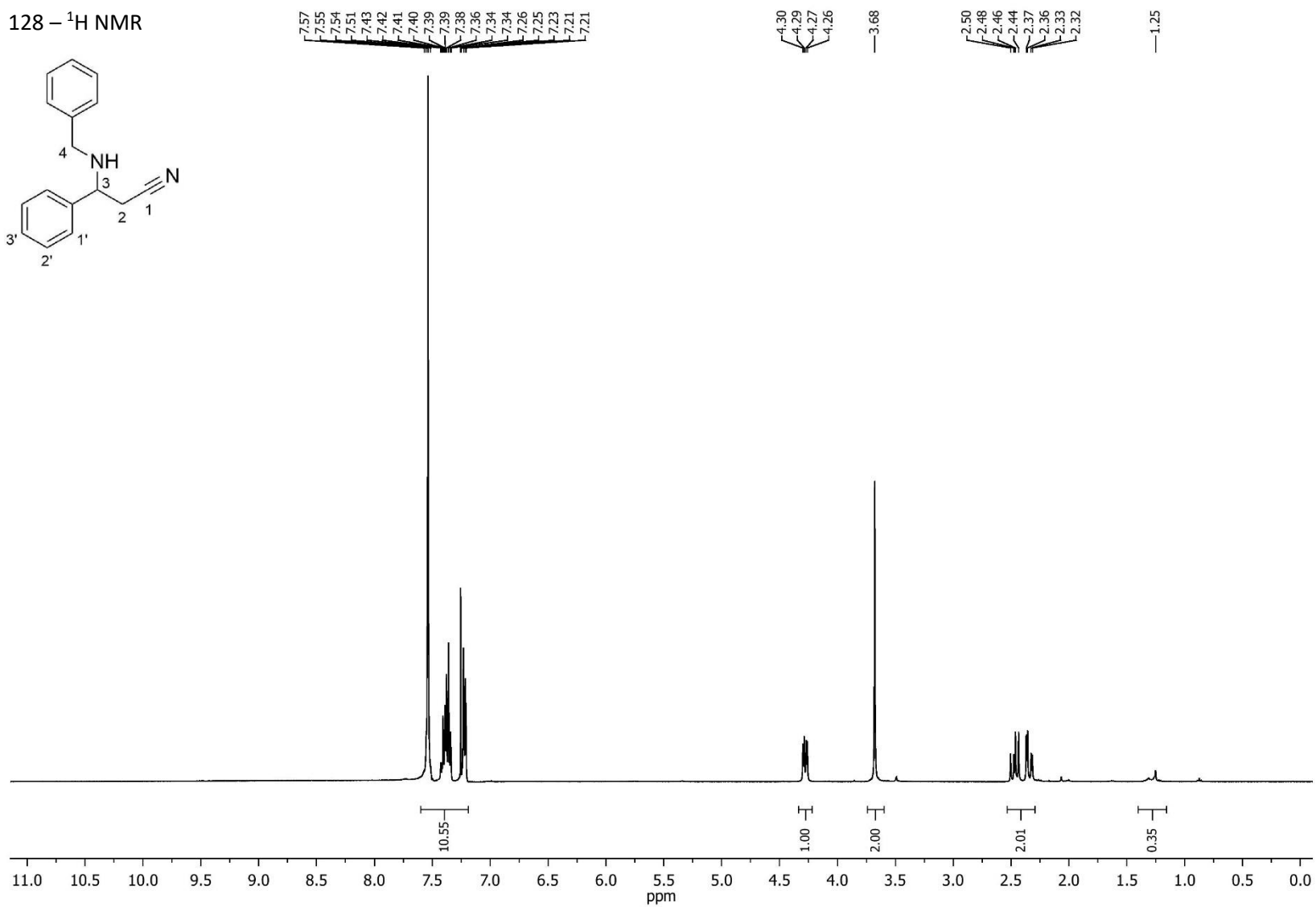
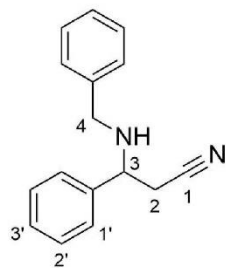


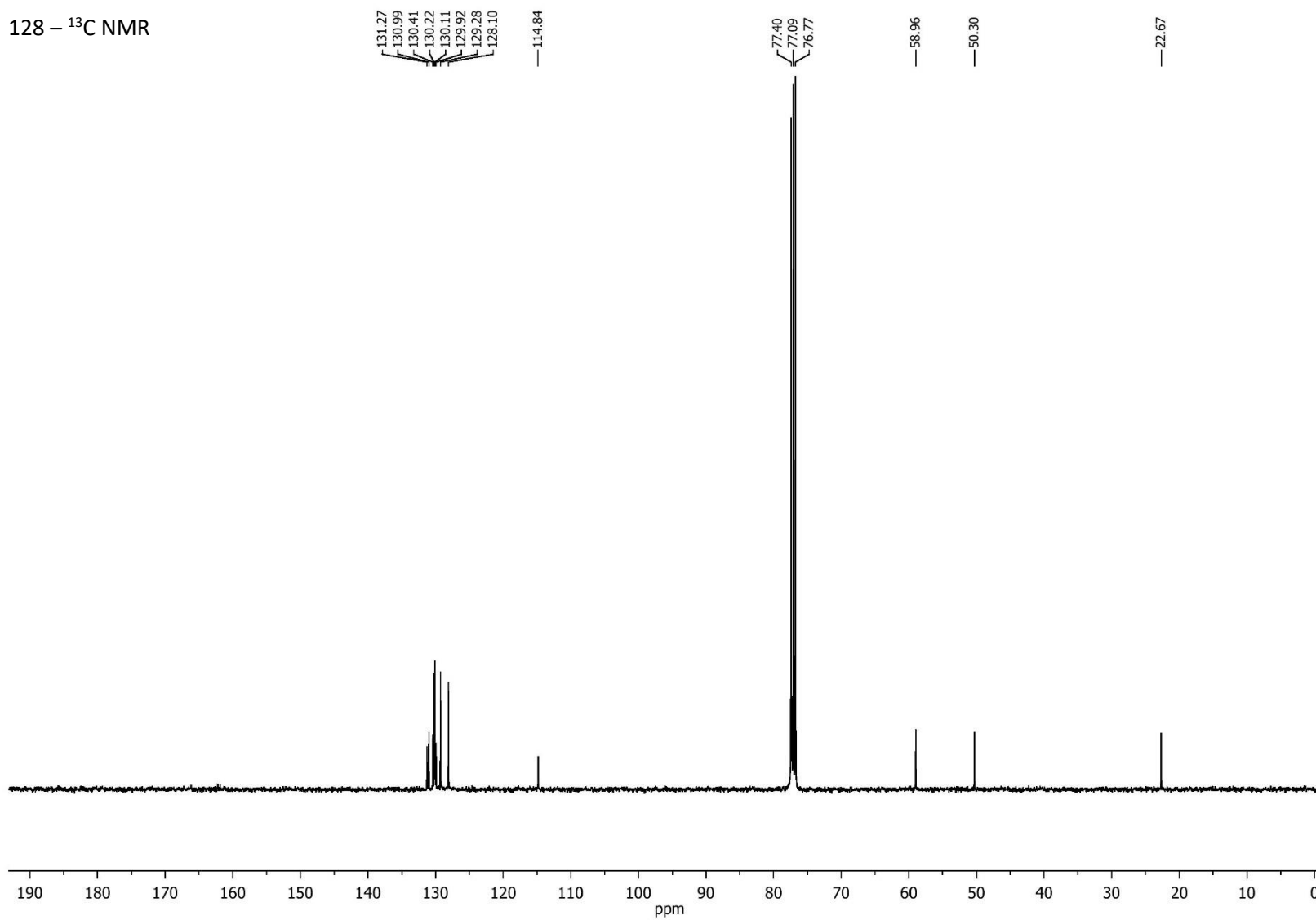


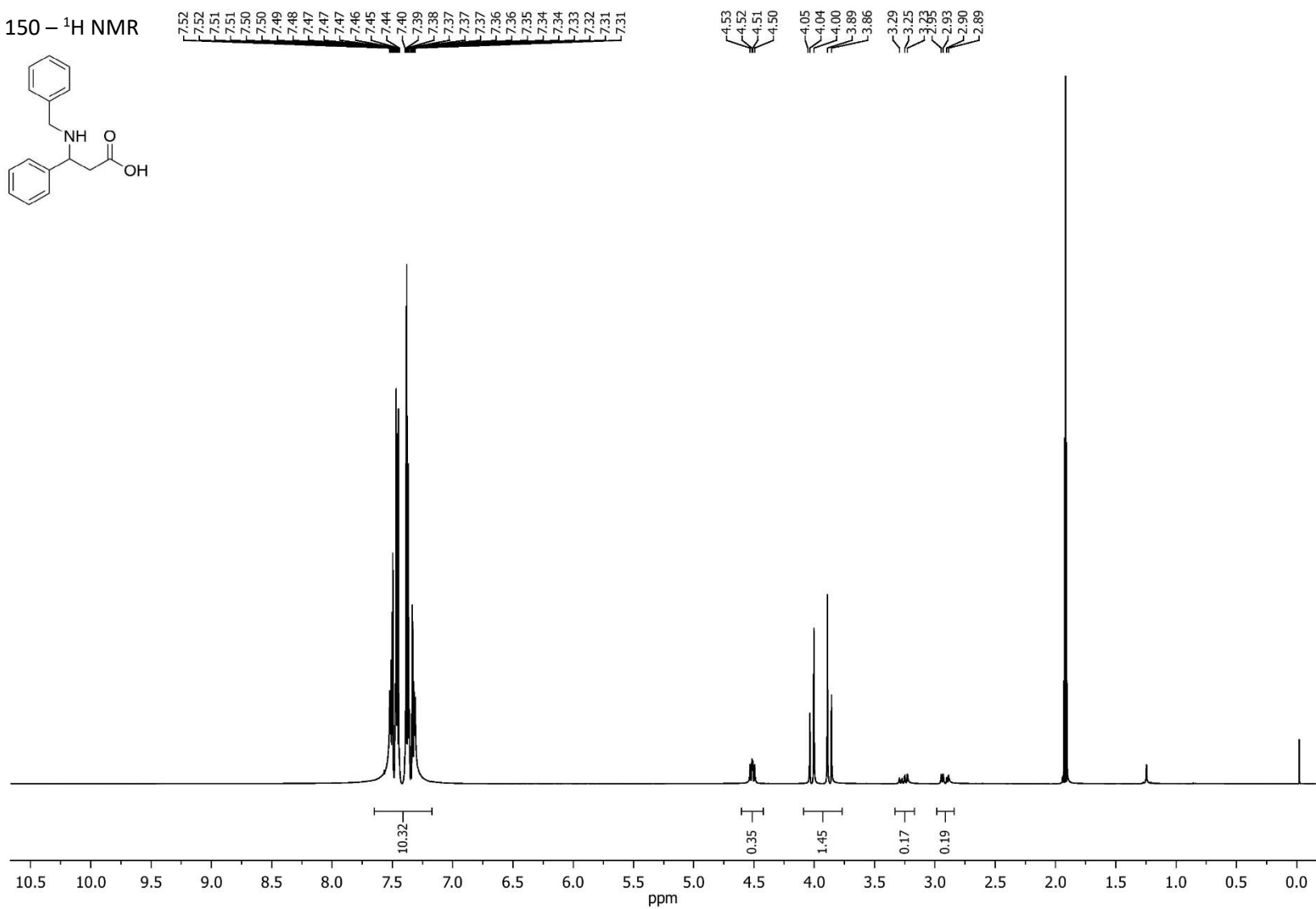
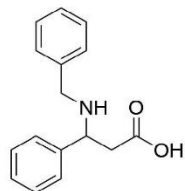


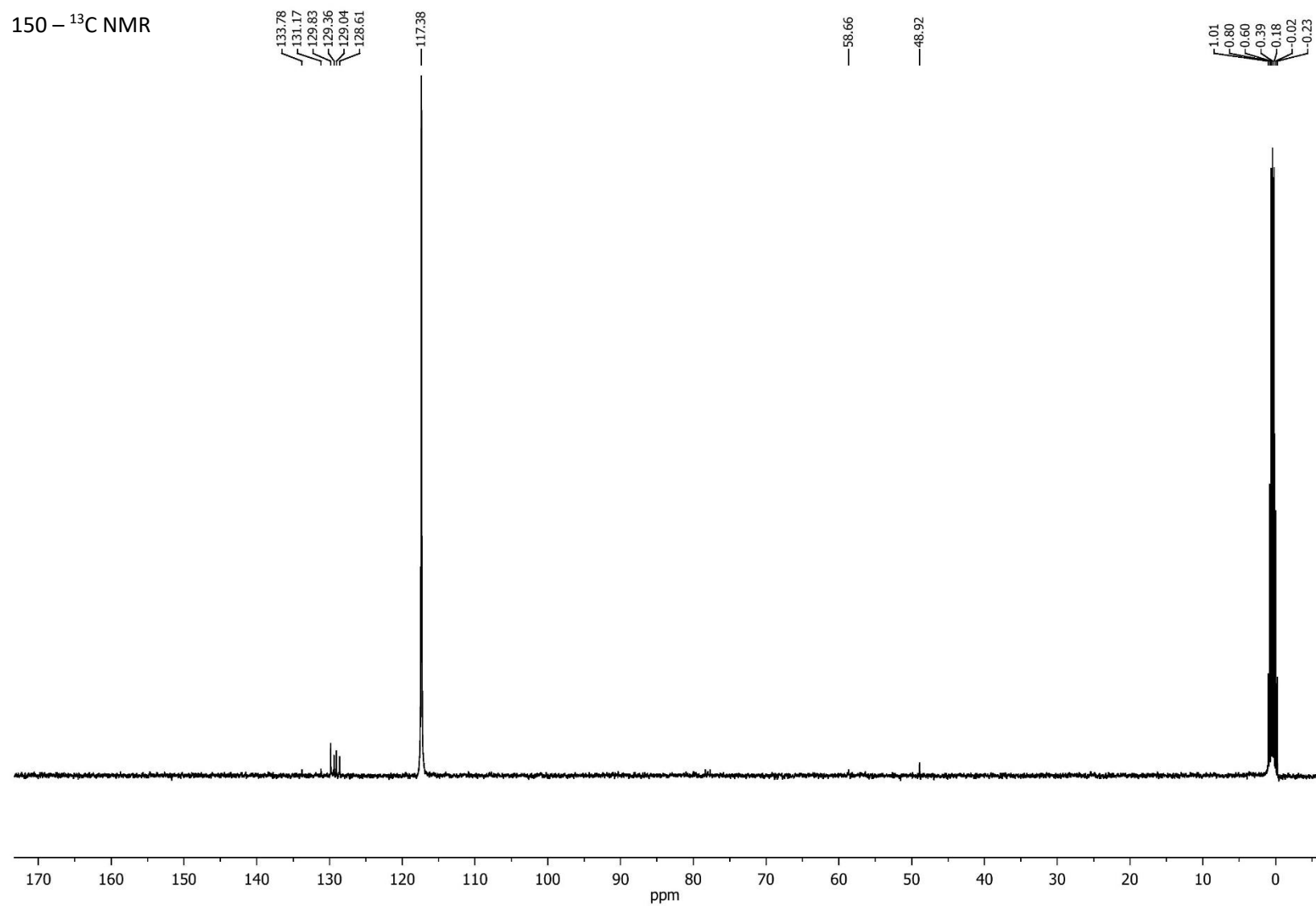


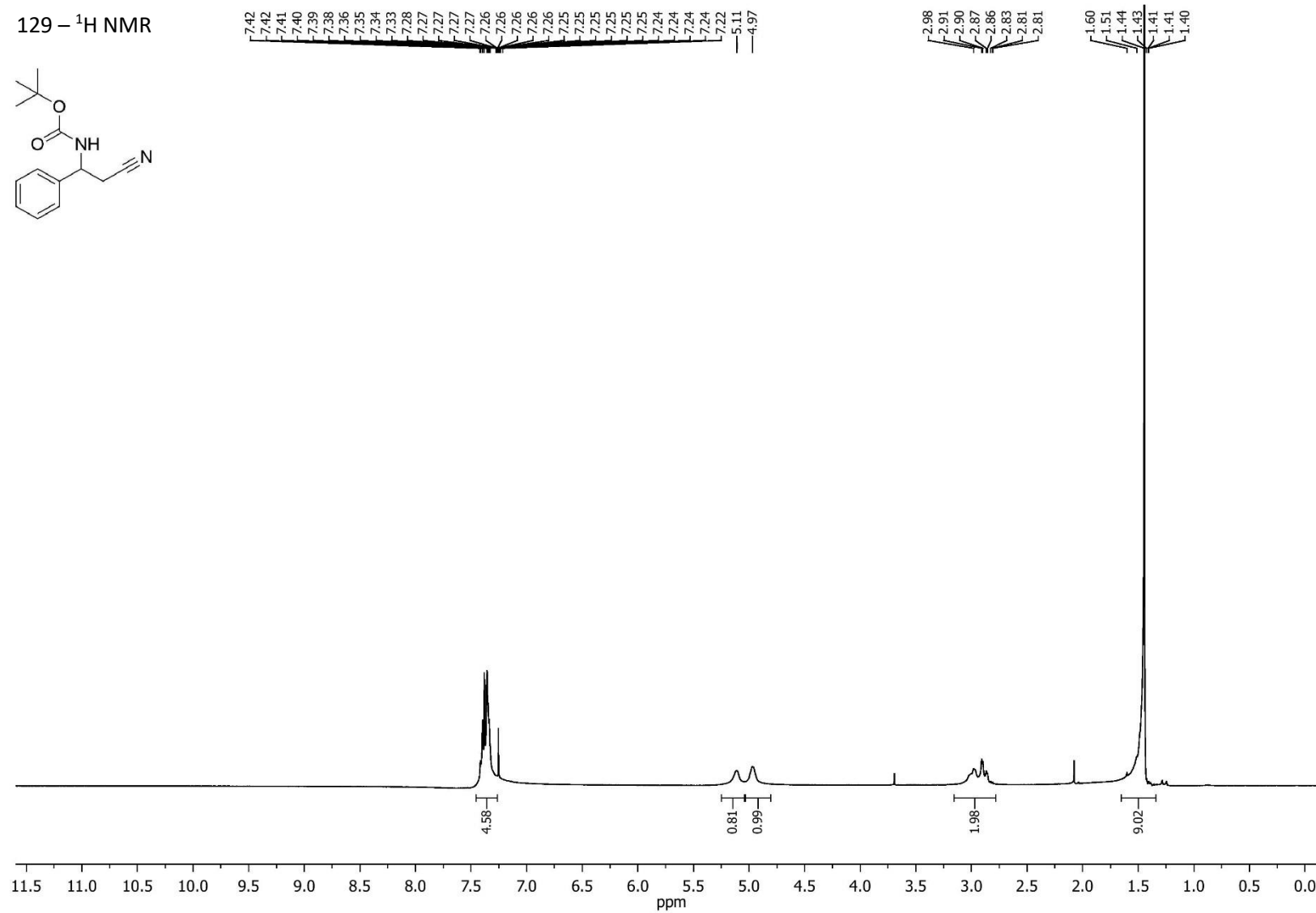
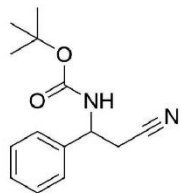


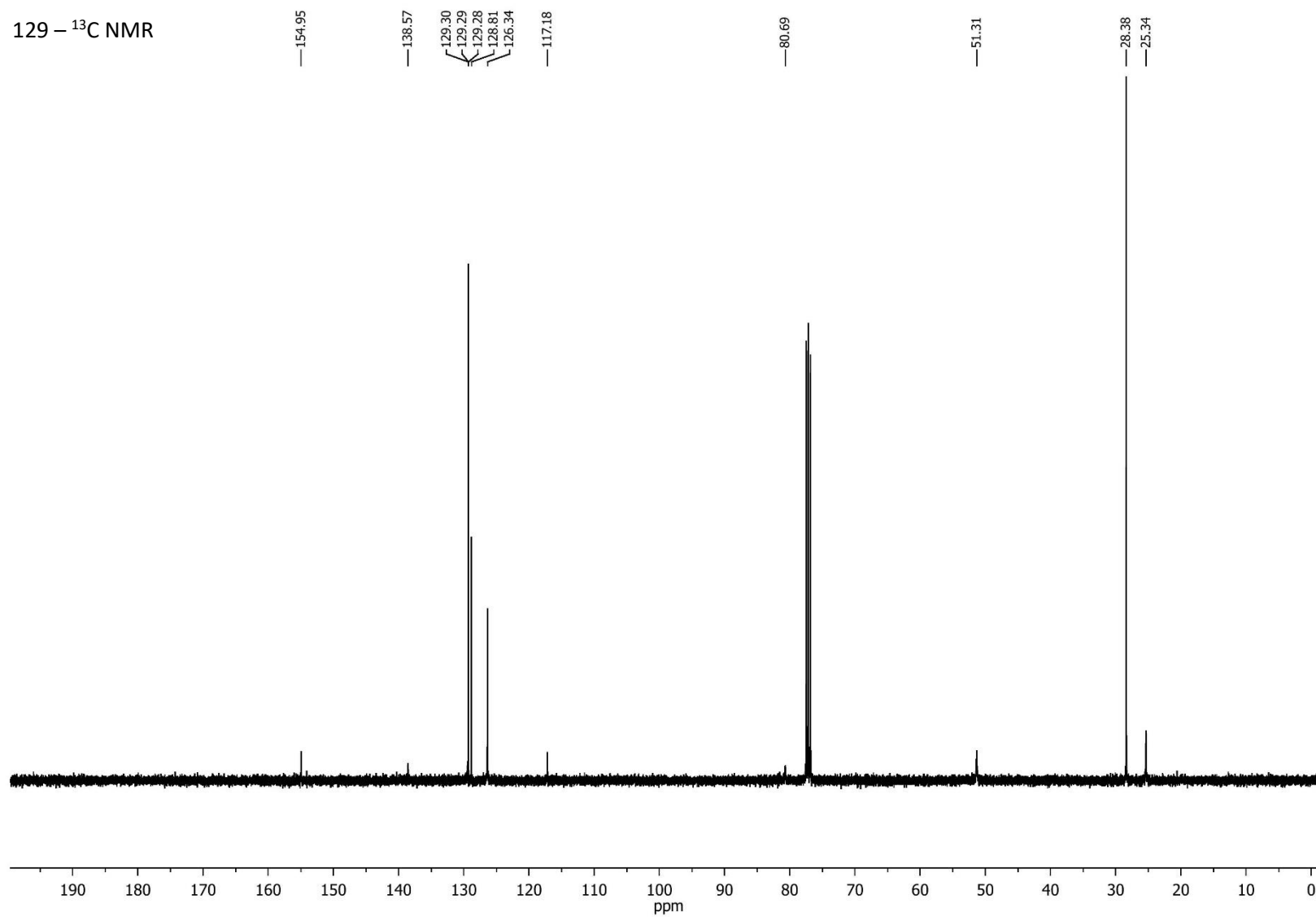
128 -  $^1\text{H}$  NMR

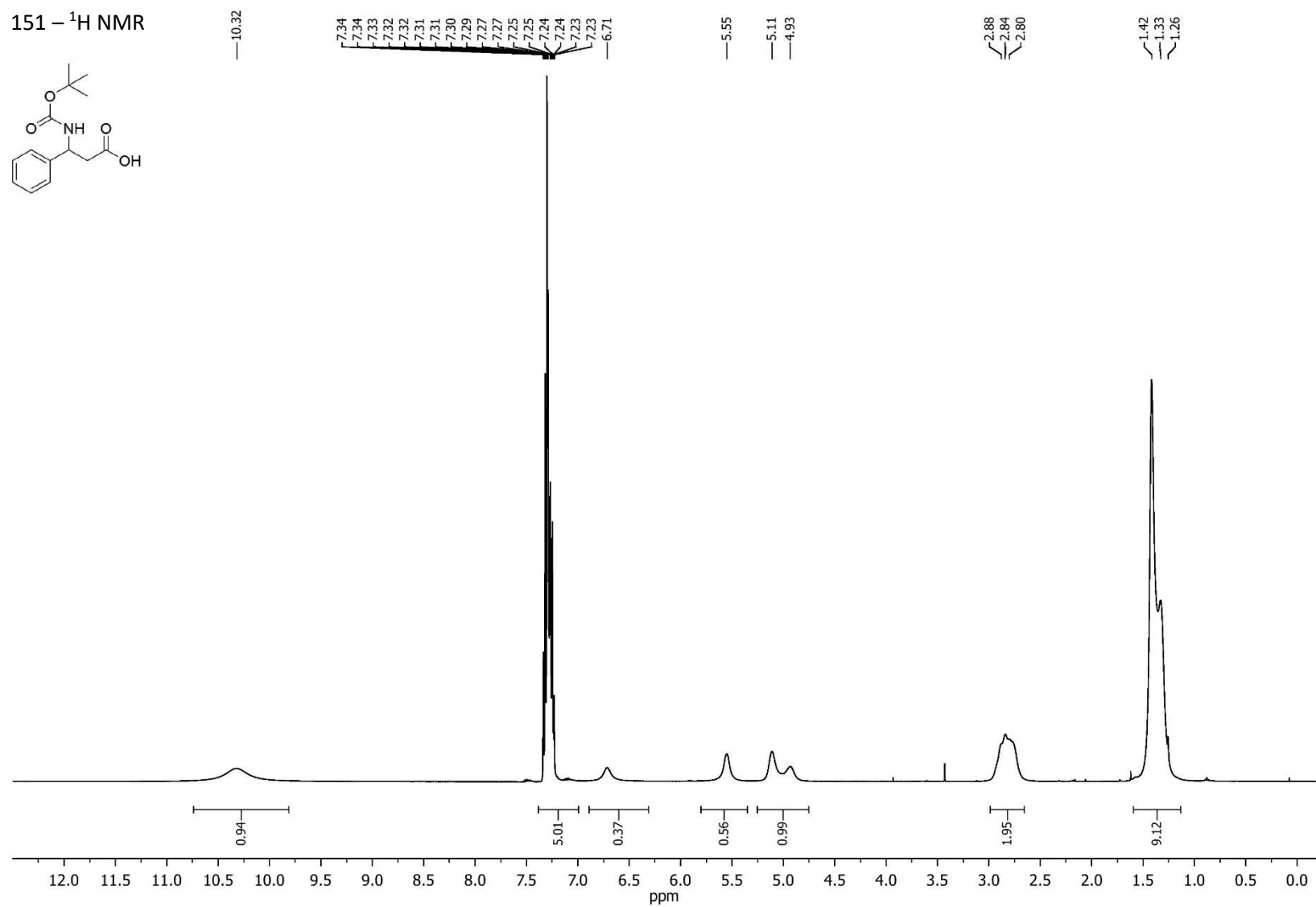
128 -  $^{13}\text{C}$  NMR

150 –  $^1\text{H}$  NMR

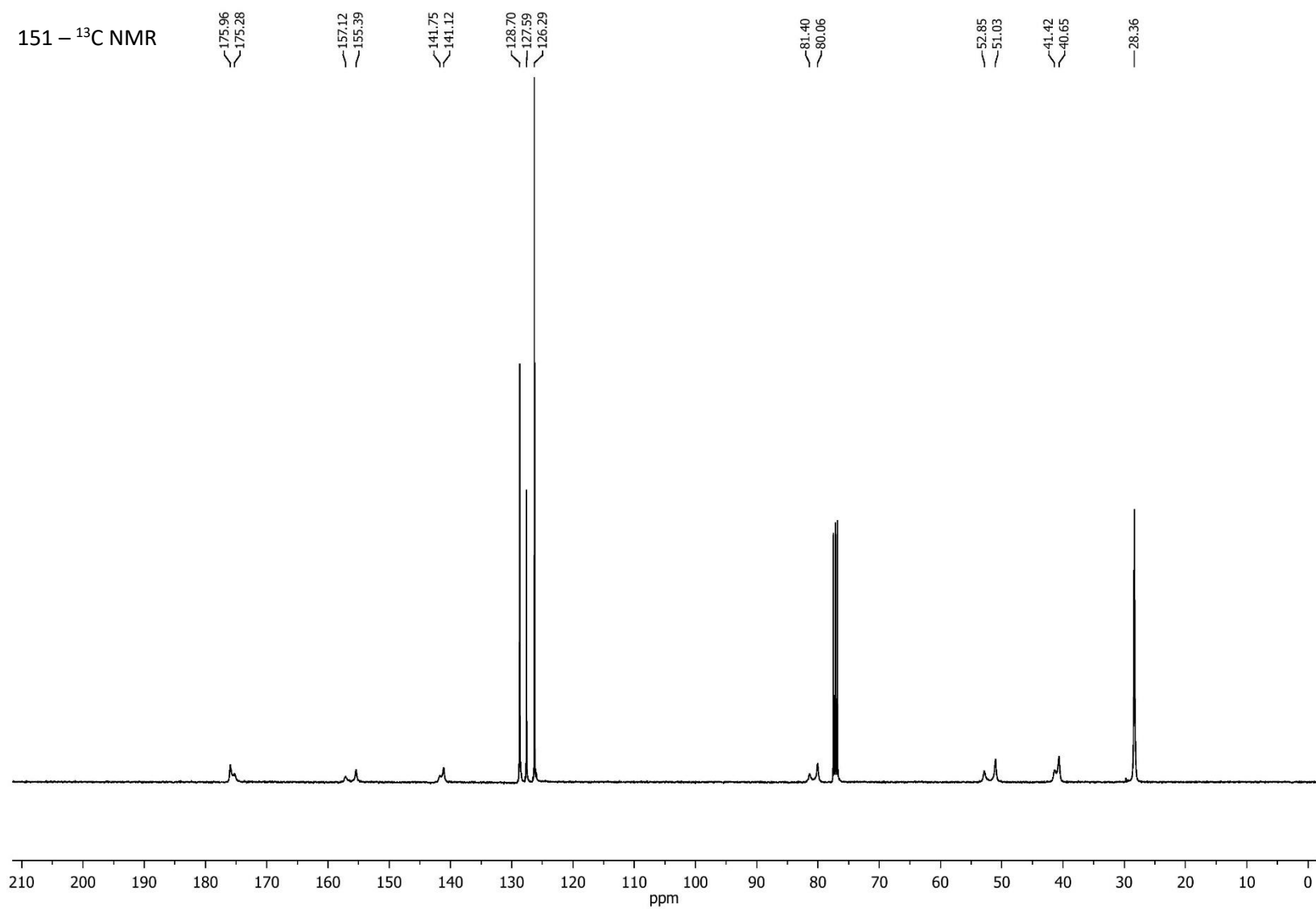


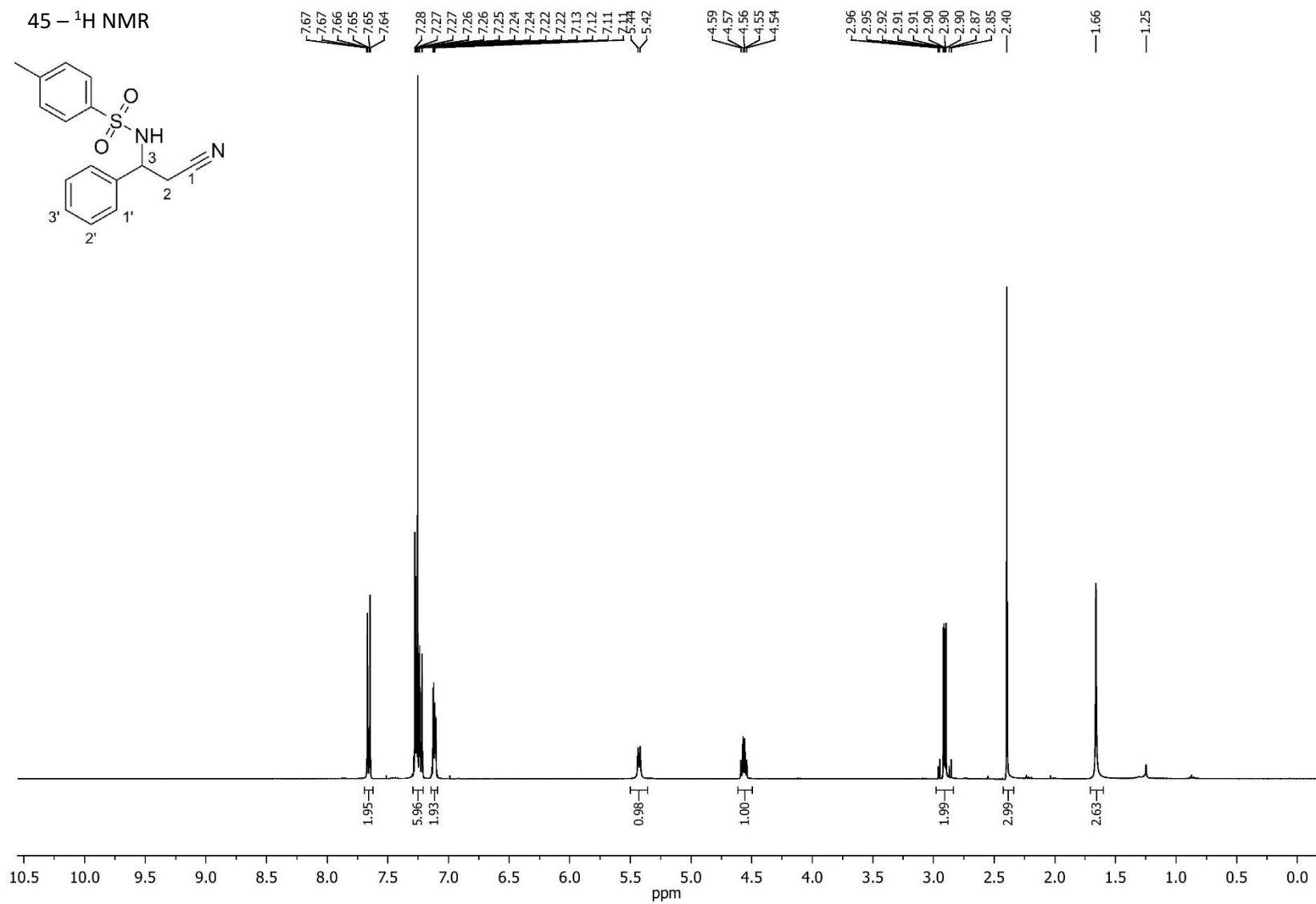
129 -  $^1\text{H}$  NMR

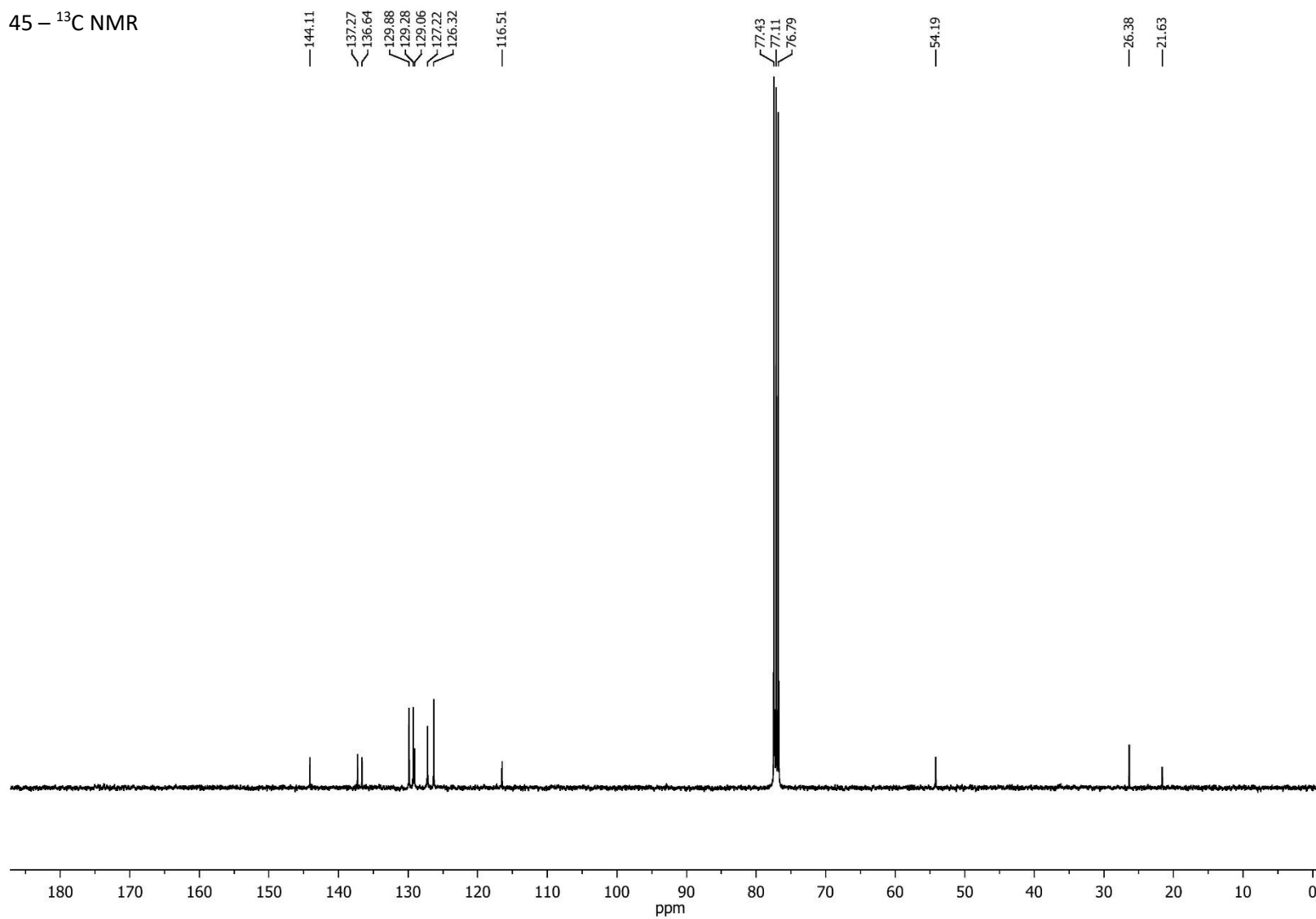


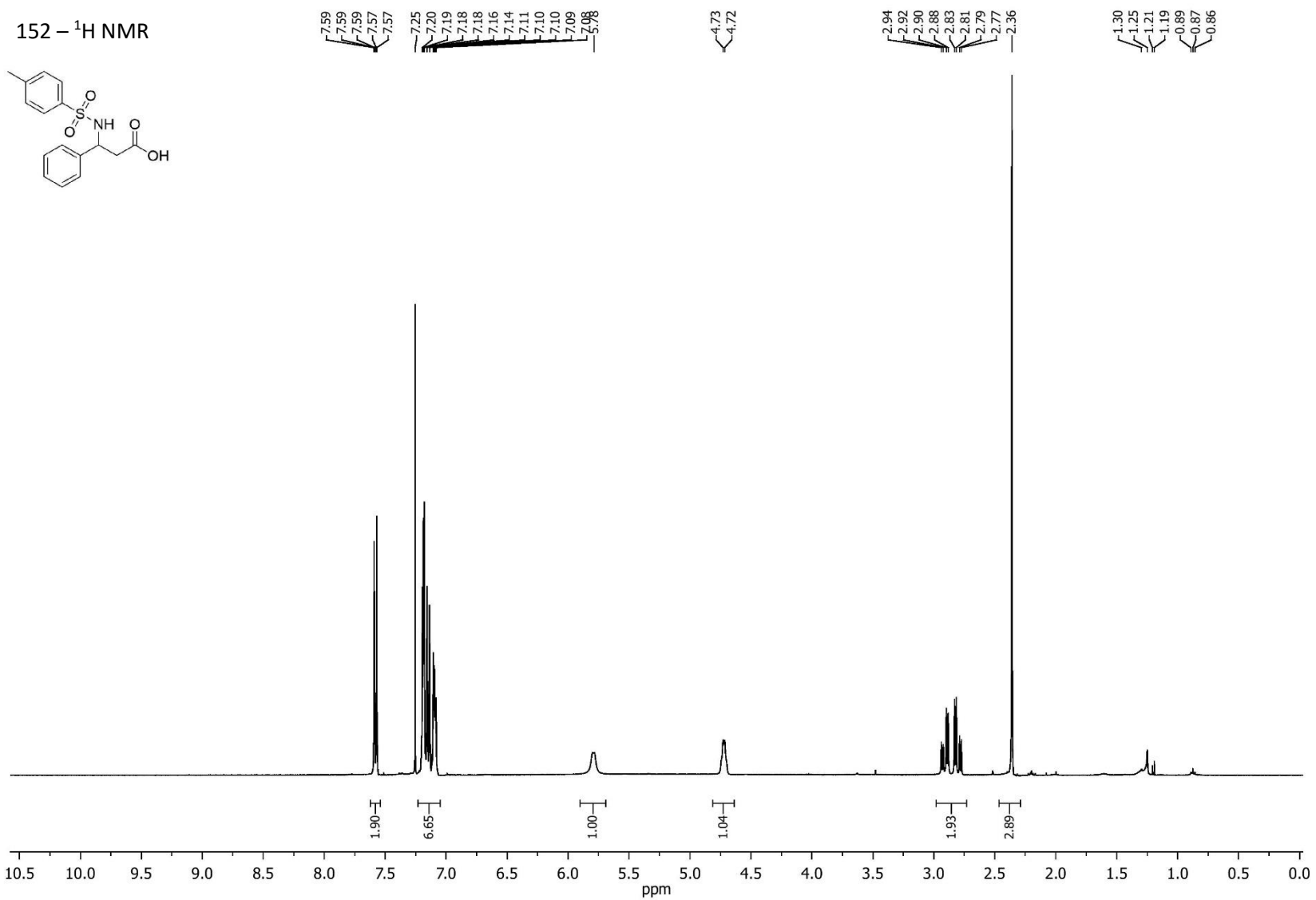


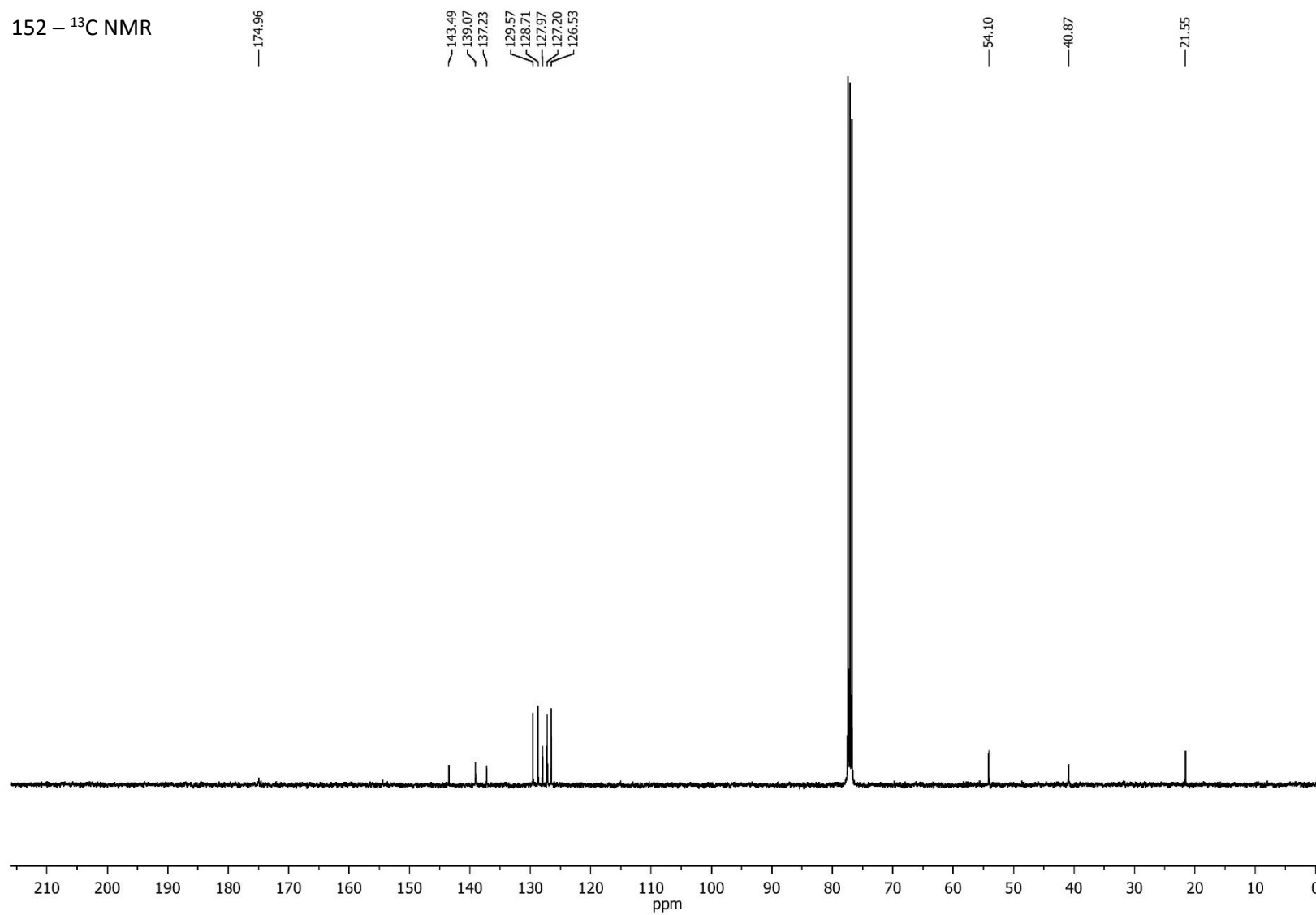






45 -  $^{13}\text{C}$  NMR





## **APPENDIX II**

### *Publications*